

MICROWAVE EFFECTS ON THE CURING, STRUCTURE PROPERTIES AND DECOMPOSITION OF EPOXY RESINS.

A thesis submitted to the University of Manchester for the degree of Doctor of Philosophy in the Faculty of Engineering and Physical Sciences

2010

BABATUNDE BOLASODUN

School of Materials

LIST OF CONTENTS

LIST OF FIGURES	5
LIST OF TABLES	25
LIST OF SYMBOLS	29
LIST OF ABBREVIATIONS	31
ABSTRACT	33
DECLARATION	34
COPYRIGHT STATEMENT	35
ACKNOWLEDGEMENTS	36
1.0 INTRODUCTION	37
2.0 LITERATURE REVIEW	40
2.1 Epoxy Resins.....	40
2.1.2 Properties of Epoxy Resins	40
2.2 Structure of a basic epoxy molecule	42
2.3 Synthesis of a basic epoxy-resin molecule.....	43
2.3.1 Epichlorohydrin.....	43
2.3.2 Bisphenol A.....	44
2.3.2 Diglycidyl ether of bisphenol A.....	47
2.4 Epoxy resin characterization	49
2.5 Amines	51
2.5.1 Aliphatic Amines	53
2.5.2 Aromatic Amines	53
2.5.3 Tertiary and secondary amines.....	54
2.5.4 Amine Hardening Systems.....	54
2.5 Organic Acids Hardening Systems	54
2.7 Araldite LY 5052 epoxy resin.....	58
2.8 4 4 Diphenyl diaminosulfone.....	59
2.9 Microwaves	59
2.9.2 Applications of Microwaves	60
2.9.4 Material Properties	63
2.9.5 Maxwell’s Equations.....	65
2.9.5 Plane Wave.....	66
2.9.5.1 Characteristics of a Plane wave	66
2.9.5.2 Wavelength of a propagating wave.....	67
2.9.6 Basic Concepts of Microwaves.....	67
2.9.7 Microwave Heating Mechanism	69
2.10 Advantages and Disadvantages of Microwave heating over Thermal heating ...	70
2.13 Cure Kinetics.....	71
2.13.1 Isothermal vs Dynamic cure Kinetics	72
2.13.2 Standard (n-th order) and Autocatalyzed Kinetics Reaction.....	72
2.13.3 Modelling of cure kinetics	73
2.13.4 Temperature Dependence of Reaction Rates	76
2.13.5 The Arrhenius parameters	76
2.13.6 Degree of Conversion α and Reaction Rate $\frac{d\alpha}{dt}$	78
2.13.7 Methods of evaluating degrees of conversion and reaction rate.....	79
2.13.8 Dynamic Curing	82

$\ln\left(\frac{d\alpha}{dt}\right) = \ln[k_0f(\alpha)] - \frac{E}{RT}(\alpha=ct)$	84
2.14 Dynamic Kinetic Analysis	87
2.14.1 Kissinger's Method	87
2.15 Previous work on Microwave vs Thermal Curing	89
3.0 EXPERIMENTAL	94
3.1 Materials.....	94
3.2 Resin Characterization	94
3.2.1 Density Measurement.....	94
3.3 Curing Methods.....	96
3.3.1 Microwave Curing	96
3.3.2 Dynamic Scanning Calorimetry	100
3.3.3 DSC System	102
3.3.4 Applications of DSC	104
3.3.5 Calorimetric Measurement.....	104
3.3.6 Microwave curing	107
3.4 Dielectric Properties.....	114
3.4.1 Cavity Perturbation Method.....	114
3.4.2 Dielectric properties measurement.....	114
3.5 Infrared Spectroscopy	116
3.5.1 Uses of Infra-red Spectroscopy	118
3.6 Nuclear Magnetic Resonance Spectroscopy	120
3.6.1 Principles of NMR spectroscopy.....	121
3.7 Dynamic Mechanical Analysis	125
3.7.1 Mechanical Moduli	126
3.7.2 Glass Transition Temperature.....	129
3.7.3 Applications of DMTA	129
3.7.1 Sample preparation and measurement procedure	130
3.8 Flexural Testing	131
3.8.1 Principle of flexural testing.....	131
3.8.1 Sample preparation and measurement procedure	134
3.9 Microwave Acid Digestion	134
3.10 High Performance Liquid Chromatography (HPLC).....	135
3.10.1 Mode of Operation	136
3.10.2 Types of HPLC	137
3.11 Gel Permeation Chromatography.....	139
3.11.1 Applications of Gel Permeation Chromatography.....	141
3.12 Mass Spectrometry.....	142
3.12.1 Ionization methods	143
3.12.2 Ionization of volatile materials.....	143
3.13 RESIN IDENTIFICATION AND CHARACTERISATION	144
3.14 Introduction	144
3.15 Chemical Structure Identification	145
3.16 Araldite DLS 772	145
3.16.1 Molecular weight measurement	145
3.16.2 Chemical structure determination.....	146
3.17 Araldite LY 5052 epoxy resin.....	149
3.17.1 Molecular weight measurement	149
3.17.2 Chemical structure determination	150
3.18 Density Measurement.....	153

4.0 CURE REACTION STUDY.....	154
4.1 Introduction	154
4.2 Determination of Appropriate stoichiometric molar ratio	154
4.3.1 Rheology	159
4.4 Dynamic Conventional Curing	161
4.5 Microwave Curing	173
4.5.1 Comparison of the fractional conversion and reaction rate obtained from DSC and Microwave calorimeter.....	182
4.6 Modelling of cure kinetics	191
4.7 Ozawa's method.....	202
4.8 Kissinger's method	214
4.9 Dielectric Properties measurement	217
4.10 Isothermal Curing.....	226
4.11 Isothermal Conventional Curing.....	226
4.11 Isothermal Microwave Curing	236
4.12 Modelling of cure kinetics	247
5.0 FOURIER TRANSFORM INFRARED SPECTROSCOPY.....	262
5.1 Introduction	262
5.2 Araldite LY 5052 / 4 4' DDS and Araldite DLS 772 / 4 4 epoxy systems.....	262
6.0 EFFECT OF CURING METHOD ON PHYSICAL AND MECHANICAL PROPERTIES	276
6.1 Introduction	276
6.2 Effect of curing on Polymer density	276
6.3 Effect of curing on Dynamic Mechanical Properties.....	281
6.4 Cross- Link density	289
6.5 Average molecular weight between cross-links.....	292
6.6 Effect of curing on flexural properties	296
7.0 DECOMPOSITION AND CHEMICAL ANALYSIS OF CURED EPOXY SYSTEM USING MICROWAVE REACTION SYSTEM.....	302
7.1 Introduction	302
7.2 Decomposition of fully cured Araldite DLS 772 / 4 4' DDS with amine / epoxy ratio of 0.8	302
7.3 Fourier Transform Infrared Spectroscopy.....	307
7.4 Nuclear Magnetic Resonance.....	308
7.5 ¹³ C-NMR and Distortion Enhancement by Polarization Transfer (DEPT).....	310
7.6 Distortion Enhancement Polarisation Transfer	311
7.7 Heteronuclear Multiple-Quantum Correlation.....	313
7.8 Electrospray Ionization Mass Spectroscopy	317
8.0 CONCLUSIONS AND SUGGESTIONS FOR FUTHER WORK.....	319
8.1 Conclusions	319
8.2 Suggestions for further work.....	322
REFERENCES.....	324
APPENDIX	332

Word Count62,148

LIST OF FIGURES

Figure 2.1	Structure of basic epoxy – resin moiety	42
Figure 2.2	Diglycidyl ether of Bisphenol A	42
Figure 2.3	Chemical structure of epichlorohydrin	43
Figure 2.4	Complete reaction from propylene to epichlorohydrin	44
Figure 2.5	Chemical Structure of Bisphenol A	44
Figure 2.6	Formation of Phenol	45
Figure 2.7	Formation of Acetone	46
Figure 2.8	Reaction between phenol and acetone to form Bisphenol A	46
Figure 2.9	Formation of diglycidyl ether of bisphenol A	47
Figure 2.10	Formation of diglycidyl ether of bisphenol A	48
Figure 2.11	First step of the reaction of bisphenol A and epichlorohydrin in the presence of 0.1 and 0.2 percent of a Friedel-Crafts type catalyst	49
Figure 2.12	Second step of the reaction of bisphenol A and epichlorohydrin in the presence of 0.1 and 0.2 percent of a Friedel-Crafts type catalyst.	49
Figure 2.13	Amine curing reaction of epoxy resins	52
Figure 2.14	Reactions of epoxy resins in the presence of organic acids	55
Figure 2.15	Opening of the Anhydride ring.	56
Figure 2.16	Reaction of carboxylic acid with epoxy resin	56
Figure 2.17	Etherification of epoxy groups with hydroxyl groups	56
Figure 2.18	Reaction of the monoester with hydroxyl	57
Figure 2.19	Hydrolysis of the anhydride to give a diacid	57
Figure 2.20	Hydrolysis of anhydride to give an acid and an alcohol	58
Figure 2.21	Chemical Structure of Epoxy Phenol Novalak Resin	58
Figure 2.22	Chemical structure of 1,4-bis(4-epoxyphenyl)butane	58
Figure 2.23	4,4'-diphenyldiaminosulfone	59
Figure 2.24	An electromagnetic spectrum	67
Figure 2.25	An electromagnetic wave	68
Figure 3.1	Different types of volume-calibrated pycnometers	95
Figure 3.2	Simulated electromagnetic field patterns at 2.45GHz for TM ₀₁₀ mode microwave cavity with the presence of sample generated using Ansoft HFSS v8.5 simulation software. The colour scale shows the relative field strength generated inside the cavity	97
Figure 3.3	A schematic diagram of a microwave heating system using a single mode cavity operated in TM ₀₁₀ mode	97
Figure 3.4	Simulated electromagnetic field patterns at 2.45GHz for TM ₀₁₀ mode microwave cavity with the presence of sample	98

	generated using an Ansoft HFSS v8.5 simulation software. The colour scale shows the relative electric field strength generated inside the cavity	
Figure 3.5	The fax paper after exposure to microwave radiation. The line indicates the position of the PTFE mould inside the cavity	100
Figure 3.6	Schematic of the arrangement of power compensated DSC	101
Figure 3.7	Schematic diagram of the sample chamber of a heat flux DSC	101
Figure 3.8	Schematic diagram of DSC apparatus	102
Figure 3.9	Series illustrating different types of DSC and DTA	103
Figure 3.10	A Perkin- Elmer Pyris 1 power compensated DSC	105
Figure 3.11	A schematic diagram of a microwave-heated calorimeter	108
Figure 3.12	Simulated electromagnetic field patterns at a frequency of 2.45 GHz for TE ₁₁₁ mode microwave cavity with the presence of sample generated using Ansoft HFSS V8.5 simulation software	109
Figure 3.13	The vertical plane of the microwave cavity showing the arrangement of sample tube and temperature probe; (1) is the sample tube, (2) indicates the temperature probe and capillary tube while (3) is the PTFE support used to hold the sample tube in the cavity	109
Figure 3.14	Microwave Heated Calorimeter used for research	110
Figure 3.15	Raw data obtained from the exothermic reaction for microwave curing of Araldite DLS 772 / 4 4' DDS epoxy system with an amine / epoxy ratio of 1.1 at a heating rate of 10 K min ⁻¹	111
Figure 3.16	Microwave curing reaction of Araldite DLS 772 / 4 4' DDS epoxy system with an amine / epoxy ratio of 1.1 at a heating rate of 10 K min ⁻¹ after applying Fast Fourier Transform (FFT) Filter	111
Figure 3.17	Raw data obtained from the exothermic reaction for microwave curing of Araldite LY 5052 / 4 4' DDS epoxy system with an amine / epoxy ratio of 0.85 at a heating rate of 100 K min ⁻¹	113
Figure 3.18	Microwave Curing reaction of Araldite LY 5052 / 4 4' DDS epoxy system with an amine / epoxy ratio of 0.85 at a heating rate of 100 K min ⁻¹ after applying Fast Fourier Transform (FFT) Filter	113
Figure 3.19	Stretching and Bending vibration modes	117
Figure 3.20	Schematic Diagram of the FT-IR spectrometer	119
Figure 3.21	The spinning charge on the proton generates a magnetic dipole	121
Figure 3.22	Precession of a rotating particle in a magnetic field, B ₀	122
Figure 3.23	Magnetic moment and energy levels for a nucleus with a	123

	spin quantum number of $\frac{1}{2}$ and $-\frac{1}{2}$	
Figure 3.24	Schematic diagram of NMR spectrometer. The tube is perpendicular to the z-axis of the magnet	124
Figure 3.25	Schematic of different types of deformation	128
Figure 3.26	DMTA of epoxy showing alpha, beta and gamma different transitions	130
Figure 3.27	A Perkin- Elmer Pyris Diamond Dynamic Mechanical Analyser used for this research.	131
Figure 3.28	Effect of load on a test specimen in three point bending	132
Figure 3.29	Stresses present in a test specimen during a three point bending test	132
Figure 3.30	The deflection (D) of the test specimen under load P	133
Figure 3.31	A specimen undergoing three point bending test	134
Figure 3.32	An Anton Paar Microwave reaction system	135
Figure 3.33	Schematic diagram of HPLC pump	136
Figure 3.34	A Gilson Pump Controlled HPLC system	139
Figure 3.35	Schematic apparatus of a GPC set-up	141
Figure 3.36	Schematic representation of an electron ionisation source	143
Figure 3.37	Log weight fraction molar mass distributions for Araldite DLS 772 epoxy resin	145
Figure 3.38	^1H -NMR spectra of Araldite DLS 772 epoxy resin	146
Figure 3.39	^{13}C -NMR spectra of Araldite DLS 772 epoxy resin	148
Figure 3.40	Log weight fraction molar mass distributions for Araldite DLS 772 epoxy resin	149
Figure 3.41	^1H -NMR spectra of Araldite LY 5052 epoxy resin	150
Figure 3.42	Chemical structure of Araldite LY 5052 epoxy resin with lettering indicating the ^1H -NMR peaks in figure 3.41	151
Figure 3.43	^{13}C -NMR spectra of Araldite LY 5052 epoxy resin	152
Figure 3.44	Chemical structure of Araldite LY 5052 epoxy resin with lettering indicating the ^{13}C -NMR peaks in figure 3.43	152
Figure 4.1	Plot of Glass Transition against Molar ratio for different stoichiometric ratios for both conventional and microwave cured samples of Araldite LY 5052 / 4 4' DDS epoxy system.	156
Figure 4.2	Plot of Glass Transition against Molar ratio for different stoichiometric ratios for both conventional and microwave curing for Araldite DLS 772 / 4 4' DDS epoxy system.	158
Figure 4.3	Viscosity development during cure for Araldite LY 5052 / 4 4' DDS epoxy system with amine / epoxy ratio of 0.85 as temperature is ramped from 70 °C (t = 0 min) to 180 °C (t = 30 mins).	159

Figure 4.4	Viscosity development during cure for Araldite LY 5052 / 4 4' DDS epoxy system with amine / epoxy ratio of 1.0 as temperature is ramped from 70 °C (t = 0 min) to 180 °C (t = 30 mins).	160
Figure 4.5	Viscosity development during cure for Araldite LY 5052 / 4 4' DDS epoxy system with amine / epoxy ratio of 0.8 as temperature is ramped from 70 °C (t = 0 min) to 180 °C (t = 30 mins).	160
Figure 4.6	Typical DSC thermograms for Araldite LY 5052 / 4 4' DDS epoxy system with an amine / epoxy ratio of 0.85 at different heating rates using conventional DSC	161
Figure 4.7	Reaction rates for dynamic cure of Araldite LY 5052 / 4 4' DDS epoxy system with an amine / epoxy ratio of 0.85 using conventional heating	162
Figure 4.8	Fractional conversion for dynamic cure of Araldite LY 5052 / 4 4' DDS epoxy system with an amine / epoxy ratio of 0.85 using conventional heating.	163
Figure 4.10	Plot of Reaction rate against Fractional Conversion for the curing reaction of Araldite LY 5052 / 4 4' DDS epoxy system with an amine / epoxy ratio of 0.85 using conventional heating.	164
Figure 4.11	DSC thermograms for Araldite LY5052 / 4 4' DDS epoxy system with an amine / epoxy ratio of 1.0 obtained from conventional DSC at different heating rates	164
Figure 4.12	Reaction rates for dynamic cure of Araldite LY5052 / 4 4' DDS epoxy system with an amine / epoxy ratio of 1.0 at different heating rates using conventional heating	166
Figure 4.13	Fractional conversion for dynamic cure of Araldite LY 5052 / 4 4 ' DDS epoxy system with an amine / epoxy ratio of 1.0 at different heating rates using conventional heating.	166
Figure 4.14	Rate of reaction against fractional conversion for the curing reaction of Araldite LY 5052 / 4 4' DDS epoxy system with an amine / epoxy ratio of 1.0 at different heating rates using conventional heating	167
Figure 4.15	DSC thermograms for Araldite DLS 772 / 4 4' DDS epoxy system with an amine / epoxy ratio of 0.8 obtained from conventional DSC at different heating rates	168
Figure 4.16	Reaction rates for dynamic cure for Araldite DLS 772 / 4 4' DDS epoxy system with an amine / epoxy ratio of 0.8 at different heating rates using conventional heating	169

Figure 4.17	Fractional conversion for dynamic cure of Araldite DLS 772 / 4 4' DDS epoxy system with an amine / epoxy ratio of 0.8 at different heating rates using conventional heating	169
Figure 4.18	Rate of reaction against fractional conversion for the curing reaction of Araldite DLS 772 / 4 4' DDS epoxy system with an amine / epoxy ratio of 0.8 at different heating rates	170
Figure 4.19	DSC thermograms for Araldite DLS 772 / 4 4' DDS epoxy system with an amine / epoxy ratio of 1.1 obtained from conventional DSC at different heating rates	170
Figure 4.20	Reaction rates for dynamic cure of Araldite DLS 772 / 4 4' DDS epoxy system with an amine / epoxy ratio of 1.1 at different heating rates using conventional heating	170
Figure 4.21	Fractional conversion for dynamic cure of Araldite DLS 772 / 4 4' DDS epoxy system with an amine / epoxy ratio of 1.1 at different heating rates using conventional heating	172
Figure 4.22	Rate of reaction against fractional conversion for the curing reaction of Araldite DLS 772 / 4 4' DDS epoxy system with amine / epoxy ratio of 1.1 at different heating rates using conventional heating.	173
Figure 4.23	Microwave thermograms for Araldite LY 5052 / 4 4' DDS epoxy system with an amine / epoxy ratio of 0.85 obtained from microwave heating at different heating rates.	173
Figure 4.24	Fractional conversion of dynamic microwave cure reaction of Araldite LY 5052 / 4 4' DDS epoxy system with an amine / epoxy ratio of 0.85 at different heating rates using microwave heating	175
Figure 4.25	Plot of Reaction rates against temperature for dynamic microwave cure reaction of Araldite LY 5052 / 4 4' DDS epoxy system with an amine / epoxy ratio of 0.85 at different heating rates using microwave heating	175
Figure 4.26	Plot of reaction rates against fractional conversion for the dynamic microwave cure reaction of Araldite LY 5052 / 4 4' DDS epoxy system with an amine / epoxy ratio of 0.85 at different heating rates	176
Figure 4.27	DSC thermograms for Araldite LY 5052 / 4 4' DDS epoxy system with an amine / epoxy ratio of 1.0 obtained from	177

	microwave heating at different heating rates	
Figure 4.28	Fractional conversion for dynamic cure of Araldite LY 5052 / 4 4' DDS epoxy system with an amine / epoxy ratio of 1.0 at different heating rates using microwave heating.	178
Figure 4.29	Reaction rates for dynamic microwave cure of Araldite LY 5052 / 4 4' DDS epoxy system with an amine / epoxy ratio of 1.0 at different heating rates using microwave heating.	179
Figure 4.30	Plot of reaction rates against fractional conversion for the dynamic microwave cure reaction of Araldite LY 5052 / 4 4' DDS epoxy system with an amine / epoxy ratio of 1.0 at different heating rates	179
Figure 4.31	Thermograms obtained for Araldite DLS 772 / 4 4' DDS epoxy system with an amine / epoxy ratio of 0.8 obtained from microwave heating at different heating rates.	180
Figure 4.32	Reaction rates for dynamic microwave cure of Araldite DLS 772 / 4 4' DDS epoxy system with an amine / epoxy ratio of 0.8 at different heating rates using microwave heating	181
Figure 4.33	Fractional conversion for dynamic microwave cure of Araldite DLS 772 / 4 4' DDS epoxy system with an amine / epoxy ratio of 0.8 at different heating rates using microwave heating.	181
Figure 4.34	Rate of reaction against fractional conversion for the curing reaction of Araldite DLS 772 / 4 4' DDS epoxy system with an amine / epoxy ratio of 0.8 at different heating rates for microwave curing	182
Figure 4.35	Temperature dependence of the reaction rate (left), and fractional conversion (right) for the curing of Araldite LY 5052 / 4 4' DDS epoxy system with an amine / epoxy ratio of 0.8 under conventional and microwave curing at heating rates	184
Figure 4.36	Temperature dependence of the reaction rate (left), and fractional conversion (right) for the curing of Araldite LY 5052 / 4 4' DDS epoxy system with an amine / epoxy ratio of 0.8 under conventional and microwave curing, at different	187

	heating rates. The blue curve indicates conventional heating, while the pink curve indicates microwave heating.	
Figure 4.37	Temperature dependence of the reaction rate (left), and fractional conversion (right) for the curing of Araldite DLS 772 / 4 4' DDS epoxy system with an amine / epoxy ratio of 0.8 under conventional and microwave curing, at heating different rates	190
Figure 4.38	Temperature dependence of the reaction rate (left), and fractional conversion (right) for the curing of Araldite DLS 772 / 4 4' DDS epoxy system with an amine / epoxy ratio of 1.1 under conventional and microwave curing, at heating rates.	191
Figure 4.39	Comparison between temperature dependence of experimental reaction rate curves and the curves predicted by means of autocatalytic adjustment for conventional heating of Araldite LY 5052 / 4 4' DDS epoxy system with an amine / epoxy ratio of 0.85 on the left, and microwave heating on the right.	193
Figure 4.40	Comparison between temperature dependence of experimental reaction rate curves and the curves predicted by means of autocatalytic adjustment for conventional heating of Araldite LY 5052 / 4 4' DDS epoxy system with an amine / epoxy ratio of 1.0 on the left, and microwave heating on the right	195
Figure 4.41	Comparison between temperature dependence of experimental reaction rate curves and the curves predicted by means of autocatalytic adjustment for conventional heating of Araldite DLS 772 / 4 4' DDS epoxy system with an amine / epoxy ratio of 0.8 on the left, and microwave heating on the right	197
Figure 4.43	Ozawa plots of logarithm of heating rate against the inverse of temperature at constant fractional conversions for the dynamic cure of Araldite LY 5052 / 4 4' DDS epoxy system with an amine / epoxy ratio of 0.85 using conventional heating. Fractional conversions α of 0.1, 0.2, 0.3, 0.4, 0.5, 0.6, 0.7, 0.8, 0.9, 1.00 are shown	203
Figure 4.44	Ozawa plots of logarithm of heating rate against the inverse of temperature at constant fractional conversions for the dynamic cure of Araldite LY 5052 / 4 4' DDS epoxy system with an amine / epoxy ratio of 0.85 using microwave heating. Fractional conversions α of 0.1, 0.2, 0.3, 0.4, 0.5, 0.6, 0.7, 0.8, 0.9, 1.00 are shown	203
Figure 4.45	Dependence of activation energy, E_a on the fractional conversion for both conventionally and microwave cured samples of Araldite LY 5052 / 4 4' DDS epoxy system with an amine / epoxy ratio of 0.85	204
Figure 4.46	Ozawa plots of logarithm of heating rate against the inverse of temperature at constant fractional conversions for the	205

	dynamic cure of Araldite LY 5052 / 4 4' DDS epoxy system with an amine / epoxy ratio of 1.0 using conventional heating. Fractional conversions α of 0.1, 0.2, 0.3, 0.4, 0.5, 0.6, 0.7, 0.8, 0.9, 1.00 are shown	
Figure 4.47	Ozawa plots of logarithm of heating rate against the inverse of temperature at constant fractional conversions for the dynamic cure of Araldite LY 5052 / 4 4' DDS epoxy system with an amine / epoxy ratio of 1.0 using microwave heating. Fractional conversions α of 0.1, 0.2, 0.3, 0.4, 0.5, 0.6, 0.7, 0.8, 0.9, 1.00 are shown	206
Figure 4.48	Dependence of activation energy, E_a on the fractional conversion for both conventionally and microwave cured samples of Araldite LY 5052 / 4 4' DDS epoxy system with an amine / epoxy ratio of 1.0	206
Figure 4.49	Ozawa plots of logarithm of heating rate against the inverse of temperature at constant fractional conversions for the dynamic cure of Araldite DLS 772 / 4 4' DDS epoxy system with an amine / epoxy ratio of 0.8 using conventional heating. Fractional conversions α of 0.1, 0.2, 0.3, 0.4, 0.5, 0.6, 0.7, 0.8, 0.9, 1.00 are shown	208
Figure 4.50	Ozawa plots of logarithm of heating rate against the inverse of temperature at constant fractional conversions for the dynamic cure of Araldite DLS 772 / 4 4' DDS epoxy system with an amine / epoxy ratio of 0.8 using microwave heating. Fractional conversions α of 0.1, 0.2, 0.3, 0.4, 0.5, 0.6, 0.7, 0.8, 0.9, 1.00 are shown	208
Figure 4.51	Dependence of activation energy, E_a on the fractional conversion for both conventionally and microwave cured samples of Araldite DLS 772 / 4 4' DDS epoxy system with an amine / epoxy ratio of 0.8.	209
Figure 4.52	Ozawa plots of logarithm of heating rate against the inverse of temperature at constant fractional conversions for the dynamic cure of Araldite DLS 772 / 4 4' DDS epoxy system with an amine / epoxy ratio of 1.1 using conventional heating.	210
Figure 4.53	Dependence of activation energy, E_a on the fractional conversion for both conventionally and microwave cured samples of Araldite DLS 772 / 4 4' DDS epoxy system with an amine / epoxy ratio of 1.1	210
Figure 4.54	Plot of $\log \Phi$ against T_p^{-1} for conventional and microwave curing of Araldite LY 5052 / 4 4' DDS epoxy system with an amine / epoxy ratio of 0.85	212
Figure 4.55	Plot of $\log \Phi$ against T_p^{-1} for conventional and microwave curing of Araldite LY 5052 / 4 4' DDS epoxy system with an amine / epoxy ratio of 1.0.	212
Figure 4.56	Plot of $\log \Phi$ against T_p^{-1} for conventional and microwave curing of Araldite DLS 772 / 4 4' DDS epoxy system with an amine / epoxy ratio of 0.8.	213

Figure 4.57	Plot of $\log \Phi$ against T_p^{-1} for conventional and microwave curing of Araldite DLS 772 / 4 4' DDS epoxy system with an amine / epoxy ratio of 0.8	213
Figure 4.58	Plot of $-\ln(\Phi/T_p^2)$ against T_p^{-1} for conventional and microwave curing of Araldite LY 5052 / 4 4' DDS epoxy system with an amine / epoxy ratio of 0.85.	216
Figure 4.59	Plot of $-\ln(\Phi/T_p^2)$ against T_p^{-1} for conventional and microwave curing of Araldite LY 5052 / 4 4' DDS epoxy system with an amine / epoxy ratio of 1.0	215
Figure 4.60	Plot of $-\ln(\Phi/T_p^2)$ against T_p^{-1} for conventional and microwave curing of Araldite DLS 772 / 4 4' DDS epoxy system with an amine / epoxy ratio of 0.8.	216
Figure 4.61	Plot of $-\ln(\Phi/T_p^2)$ against T_p^{-1} for conventional and microwave curing of Araldite DLS 772 / 4 4' DDS epoxy system with an amine / epoxy ratio of 1.1.	216
Figure 4.62	Plot of dielectric constant and dielectric loss factor as a function of reaction temperature for microwave-cured Araldite LY 5052 / 4 4' DDS epoxy system with an amine / epoxy ratio of 0.85 at a heating rate of 5 K min^{-1}	218
Figure 4.63	A plot of dielectric loss factor and reaction exotherm as a function of reaction temperature for microwave cured Araldite LY 5052 / 4 4' DDS epoxy system with an amine / epoxy ratio of 0.85 at a heating rate of 5 K min^{-1}	219
Figure 4.64	Plot of dielectric constant and dielectric loss factor as a function of reaction temperature for microwave-cured Araldite LY 5052 / 4 4' DDS epoxy system with an amine / epoxy ratio of 1.0 at a heating rate of 5 K min^{-1}	220
Figure 4.65	A plot of dielectric loss factor and reaction exotherm as a function of reaction temperature for microwave cured Araldite DLS 772 / 4 4' DDS epoxy system with an amine / epoxy ratio of 1.0 at a heating rate of 5 K min^{-1}	220
Figure 4.66	Plot of dielectric constant and dielectric loss factor as a function of reaction temperature for microwave-cured Araldite DLS 772 / 4 4' DDS epoxy system with an amine / epoxy ratio of 0.8 at a heating rate of 5 K min^{-1}	221
Figure 4.67	A plot of dielectric loss factor and reaction exotherm as a function of reaction temperature for microwave cured Araldite DLS 772 / 4 4' DDS epoxy system with an amine / epoxy ratio of 1.1 at a heating rate of 5 K min^{-1}	221
Figure 4.68	Dielectric constant E' and Dielectric loss factor E'' as a function of reaction temperature for microwave cured Araldite LY 5052 / 4 4' DDS epoxy system with an amine / epoxy ratio of 0.85 at different heating rates	223

Figure 4.69	Dielectric constant E' and Dielectric loss factor E'' as a function of reaction temperature for microwave cured Araldite LY 5052 / 4 4' DDS epoxy system with an amine / epoxy ratio of 1.0 at different heating rates	224
Figure 4.70	Dielectric constant E' and Dielectric loss factor E'' as a function of reaction temperature for microwave cured Araldite DLS 772 / 4 4' DDS epoxy system with an amine / epoxy ratio of 0.8 at different heating rates.	224
Figure 4.71	Dielectric constant E' and dielectric loss factor E'' as a function of reaction temperature for microwave cured Araldite DLS 772 / 4 4' DDS epoxy system with an amine / epoxy ratio of 1.1 at different heating rates.	225
Figure 4.72	DSC thermograms of conventional isothermal cure (left) and subsequent DSC run to test for exotherm for Araldite LY 5052 / 4 4' DDS epoxy system with an amine / epoxy ratio of 0.85	228
Figure 4.73	Typical DSC thermograms for Araldite LY 5052 / 4 4' DDS epoxy system system with an amine / epoxy ratio of 0.85 at different heating rates using conventional DSC.	228
Figure 4.74	Reaction rates for isothermal cure of Araldite LY 5052 / 4 4' DDS epoxy system system with an amine / epoxy ratio of 0.85 using conventional heating.	228
Figure 4.75	Fractional conversion for isothermal cure of Araldite LY 5052 / 4 4' DDS epoxy system with an amine / epoxy ratio of 0.85 using conventional heating at different isothermal temperatures	229
Figure 4.76	Plot of Reaction rate against Fractional Conversion for the curing reaction of Araldite LY 5052 / 4 4' DDS epoxy system system with an amine / epoxy ratio of 0.85 at different isothermal temperatures	230
Figure 4.77	DSC thermograms for isothermal cure of Araldite LY 5052 / 4 4' DDS epoxy system with an amine / epoxy ratio of 1.0 obtained from conventional DSC at different heating rates.	230
Figure 4.78	Fractional conversion for isothermal cure of Araldite LY 5052 / 4 4' DDS epoxy system with an amine / epoxy ratio of 1.0 at different heating rates using conventional heating.	231
Figure 4.79	Reaction rates for isothermal cure of Araldite LY 5052 / 4 4' DDS epoxy system with an amine / epoxy ratio of 1.0 at different heating rates using conventional heating.	231
Figure 4.80	Rate of reaction against fractional conversion for the curing reaction of Araldite LY 5052 / 4 4' DDS epoxy system with an amine / epoxy ratio of 1.0 at different heating rates	232
Figure 4.81	DSC thermograms for Araldite DLS 772 / 4 4' DDS epoxy system system with an amine / epoxy ratio of 0.8 obtained from conventional DSC at a range of isothermal	232

	temperatures	
Figure 4.82	Fractional conversion for isothermal cure of Araldite DLS 772 / 4 4' DDS epoxy system with an amine / epoxy ratio of 0.8 at different isothermal temperatures using conventional heating.	233
Figure 4.83	Reaction rates for isothermal cure of Araldite DLS 772 / 4 4' DDS epoxy system with an amine / epoxy ratio of 0.8 at different isothermal temperatures using conventional heating.	233
Figure 4.84	Rate of reaction against fractional conversion for the isothermal curing reaction of Araldite DLS 772 / 4 4' DDS epoxy system with an amine / epoxy ratio of 0.8 at different heating rates.	234
Figure 4.85	DSC thermograms for Araldite DLS 772 / 4 4' DDS epoxy system with an amine / epoxy ratio of 1.1 obtained from conventional DSC at different isothermal temperatures.	234
Figure 4.86	Fractional conversion for isothermal cure of Araldite DLS 772 / 4 4' DDS epoxy system with an amine / epoxy ratio of 1.1 at different isothermal temperatures using conventional heating	235
Figure 4.87	Reaction rates for isothermal cure of Araldite LY 5052 / 4 4' DDS epoxy system with an amine / epoxy ratio of 1.1 at different isothermal temperatures using conventional heating.	235
Figure 4.88	Rate of reaction against fractional conversion for the isothermal curing reaction of Araldite DLS 772 / 4 4' DDS epoxy system with an amine / epoxy ratio of 1.1 at different isothermal temperatures	236
Figure 4.89	Isothermal thermograms of microwave isothermal cure (left) and subsequent DSC run 10 K min ⁻¹ from 30 to 300 °C (right) to test for exotherm for Araldite LY 5052 / 4 4' DDS epoxy system with an amine epoxy ratio of 0.85	238
Figure 4.90	Fractional conversion of dynamic cure of Araldite LY 5052 / 4 4' DDS epoxy system with an amine / epoxy ratio of 0.85 at different isothermal temperatures using microwave heating.	238
Figure 4.91	Plot of Reaction rates against temperature for dynamic cure of Araldite LY 5052 / 4 4' DDS epoxy system with an amine / epoxy ratio of 0.85 at different isothermal temperatures using microwave heating.	239
Figure 4.92	Plot of reaction rates against fractional conversion for the microwave cure reaction of Araldite LY 5052 / 4 4' DDS epoxy system with an amine / epoxy ratio of 0.85 at different isothermal temperatures	239

Figure 4.93	Fractional conversion for isothermal cure of Araldite LY5052 / 4 4' DDS epoxy system with an amine / epoxy ratio of 1.0 at different isothermal temperatures using microwave heating	240
Figure 4.94	Reaction rates for isothermal cure of Araldite LY 5052 / 4 4' DDS epoxy system with an amine / epoxy ratio of 1.0 at different isothermal temperatures using microwave heating	241
Figure 4.95	Plot of reaction rates against fractional conversion for the microwave cure reaction of Araldite LY 5052 / 4 4' DDS epoxy system with an amine / epoxy ratio of 1.0 at different isothermal temperatures	241
Figure 4.96	Fractional conversion for isothermal cure of 0.8M amine / epoxy ratio for Araldite DLS 772 / 4 4' DDS epoxy system at different isothermal temperatures using microwave heating.	242
Figure 4.97	Reaction rates for dynamic cure of Araldite DLS 772 / 4 4' DDS epoxy system with an amine / epoxy ratio of 0.8 at different isothermal temperatures using microwave heating	242
Figure 4.98	Plot of reaction rates against fractional conversion for the microwave cure reaction of Araldite DLS 772 / 4 4' DDS epoxy system with an amine / epoxy ratio of 0.8 at different isothermal temperatures.	243
Figure 4.99	Time dependence of the fractional conversion (right) and the reaction rate (right) for Araldite LY 5052 / 4 4' DDS epoxy system with an amine / epoxy ratio of 0.85 under conventional and microwave curing, at different isothermal temperatures.	244
Figure 4.100	Time dependence of the fractional conversion (left), and reaction rate (right) for the curing of Araldite LY 5052 / 4 4' DDS epoxy system with an amine / epoxy ratio of 1.0 under conventional and microwave curing, at different isothermal temperatures.	246
Figure 4.101	Comparison between time dependence of experimental reaction rate curves and the curves predicted by means of autocatalytic adjustment for conventional heating of Araldite LY 5052 / 4 4' DDS epoxy system with an amine / epoxy ratio of 0.85 on the left, and microwave heating on the right	248
Figure 4.102	Comparison between time dependence of experimental reaction rate curves and the curves predicted by means of autocatalytic adjustment for conventional heating of Araldite	249

	LY 5052 / 4 4' DDS epoxy system with an amine / epoxy ratio of 1.0 on the left, and microwave heating on the right	
Figure 4.103	Comparison between time dependence of experimental reaction rate curves and the curves predicted by means of autocatalytic adjustment for conventional heating of Araldite DLS 772 / 4 4' DDS epoxy system with an amine / epoxy ratio of 0.8 on the left, and microwave heating on the right.	251
Figure 4.104	Comparison between time dependence of experimental reaction rate curves and the curves predicted by means of autocatalytic adjustment for conventional heating of Araldite DLS 772 / 4 4' DDS epoxy system with an amine / epoxy ratio of 1.1 on the left, and microwave heating on the right.	252
Figure 4.105	Rate constants of curing reaction against temperature for isothermal cure of Araldite LY 5052 / 4 4' DDS epoxy system with an amine / epoxy ratio of 0.85 under conventional curing	256
Figure 4.106	Rate constants of curing reaction against temperature for isothermal cure of Araldite LY 5052 / 4 4' DDS epoxy system with an amine / epoxy ratio of 0.85 under microwave curing	256
Figure 4.107	Rate constants of curing reaction against temperature for isothermal cure of Araldite LY 5052 / 4 4' DDS epoxy system with an amine / epoxy ratio of 1.0 under conventional curing.	257
Figure 4.108	Rate constants of curing reaction against temperature for isothermal cure of Araldite LY 5052 / 4 4' DDS epoxy system with an amine / epoxy ratio of 1.0 under microwave curing	257
Figure 4.109	Rate constants of curing reaction against temperature for isothermal cure of Araldite DLS 772 / 4 4' DDS epoxy system with an amine / epoxy ratio of 0.8 under conventional curing	258
Figure 4.110	Rate constants of curing reaction against temperature for isothermal cure of Araldite DLS 772 / 4 4' DDS epoxy system with an amine / epoxy ratio of 0.8 under microwave curing.	258
Figure 4.111	Rate constants of curing reaction against temperature for isothermal cure of Araldite DLS 772 / 4 4' DDS epoxy	259

	system with amine / epoxy ratio of 1.1 under conventional curing.	
Figure 4.112	Rate constants of curing reaction against temperature for isothermal cure of Araldite DLS 772 / 4 4' DDS epoxy system with an amine / epoxy ratio of 0.85 under microwave curing.	259
Figure 5.1	FT-IR Spectra of uncured Araldite LY 5052 / 4 4' DDS epoxy system with an amine / epoxy ratio of 0.85	262
Figure 5.2	Expanded view of FT-IR Spectra of uncured 0.85M amine / epoxy ratio for Araldite LY 5052 / 4 4' DDS epoxy system	263
Figure 5.3	Overlaid FT-IR Spectra of Araldite LY 5052 / 4 4' DDS with an amine / epoxy ratio of 0.85 after conventional and microwave heating at 180 °C for 240 minutes.	264
Figure 5.4	Expanded view of Overlaid FT-IR Spectra of Araldite LY 5052 / 4 4' DDS with an amine / epoxy ratio of 0.85 after conventional and microwave heating at 180 °C for 240 minutes	264
Figure 5.5	Overlaid FT-IR Spectra of Araldite DLS 772 / 4 4' DDS with an amine / epoxy ratio of 0.8 after conventional and microwave heating at 180 °C for 240 minutes.	265
Figure 5.6	Expanded view of Overlaid FT-IR Spectra of Araldite DLS 772 / 4 4' DDS with an amine / epoxy ratio of 0.8 after conventional and microwave heating at 180 °C for 240 minutes	266
Figure 5.7	Overlaid spectra for conventionally cured Araldite LY 5052 / 4 4' DDS an amine / epoxy ratio of 0.85	266
Figure 5.8	Overlaid spectra for microwave cured Araldite LY 5052 / 4 4' DDS an amine / epoxy ratio of 0.85	267
Figure 5.9	Overlaid spectra for conventionally cured Araldite LY 5052 / 4 4' DDS an amine / epoxy ratio of 1.0	267
Figure 5.10	Overlaid spectra for microwave cured Araldite LY 5052 / 4 4' DDS an amine / epoxy ratio of 1.0	268
Figure 5.11	Overlaid spectra for conventional cured Araldite DLS 772 / 4 4' DDS an amine / epoxy ratio of 0.8.	269
Figure 5.12	Overlaid spectra for microwave cured Araldite DLS 772 / 4	269

	4' DDS an amine / epoxy ratio of 0.8.	
Figure 5.13	Epoxide absorbance normalised against the absorbance for phenyl fo Araldite LY 5052 /4 4' DDS an amine / epoxy ratio of 0.85 at different times at 180 °C during conventional and microwave heating	270
Figure 5.14	Epoxide absorbance normalised against the absorbance for phenyl for Araldite LY 5052 / 4 4' DDS with an amine / epoxy ratio of 1.0 at different times at 180 °C during conventional and microwave heating	271
Figure 5.15	Epoxide absorbance normalised against the absorbance for phenyl for Araldite DLS 772 / 4 4' DDS with an amine / epoxy ratio of 0.8 at different times at 180 °C during conventional and microwave heating	271
Figure 5.16	Epoxide absorbance normalised against the absorbance for phenyl for Araldite DLS 772 / 4 4' DDS with an amine / epoxy ratio of 1.1 at different times at 180 °C during conventional and microwave heating	272
Figure 5.17	Amine absorbance normalised against the absorbance for phenyl for Araldite LY 5052 / 4 4' DDS with an amine / epoxy ratio of 0.85 at different times at 180 °C during conventional and microwave heating	273
Figure 5.18	Amine absorbance normalised against the absorbance for phenyl for Araldite LY 5052 / 4 4' DDS with an amine / epoxy ratio of 1.0 at different times at 180 °C during conventional and microwave heating.	274
Figure 5.19	Amine absorbance normalised against the absorbance for phenyl for Araldite DLS 772 / 4 4' DDS with an amine / epoxy ratio of 0.8 at different times at 180 °C during conventional and microwave heating.	274
Figure 5.20	Amine absorbance normalised against the absorbance for phenyl for Araldite DLS 772 / 4 4' DDS with an amine / epoxy ratio of 1.1 at different times at 180 °C during conventional and microwave heating.	275
Figure 6.1	Plot of Average Density for conventionally and microwave cured samples of Araldite LY 5052 / 4 4' DDS epoxy system with an amine / epoxy ratio of 0.85	277
Figure 6.2	Plot of Average Density for conventionally and microwave cured samples of Araldite LY 5052 / 4 4' DDS epoxy system with an amine / epoxy ratio of 0.8	278
Figure 6.3	Plot of Average Density for conventionally and microwave cured samples of Araldite DLS 772 / 4 4' DDS epoxy system with an amine / epoxy ratio of 1.0	278
Figure 6.4	Plot of Average Density for conventionally and microwave cured samples of Araldite DLS 772 / 4 4' DDS epoxy system with an amine / epoxy ratio of 1.1.	279
Figure 6.5	Dependence of storage modulus (G'), Loss modulus (G'')	281

	and $\tan \delta$ with temperature for a fully cured sample of Araldite LY 5052 / 4 4' DDS epoxy system with an amine / epoxy ratio of 0.85 prepared using microwave heating at 180°C for 240 mins	
Figure 6.6	Dependence of storage modulus (G'), Loss modulus (G'') and $\tan \delta$ with temperature for a fully cured sample of Araldite LY 5052 / 4 4' DDS epoxy system with an amine / epoxy ratio of 0.85 prepared using conventional heating at 180 °C for 240 mins.	282
Figure 6.7	Dependence of storage modulus (G'), Loss modulus (G'') and $\tan \delta$ with temperature for a fully cured sample of Araldite LY 5052 / 4 4' DDS epoxy system with an amine / epoxy ratio of 1.0 prepared using conventional heating at 180 °C for 240 mins.	282
Figure 6.8	Dependence of storage modulus (G'), Loss modulus (G'') and $\tan \delta$ with temperature for a fully cured sample of Araldite LY 5052 / 4 4' DDS epoxy system with an amine / epoxy ratio of 1.0 prepared using microwave heating at 180 °C for 240 mins.	283
Figure 6.9	Dependence of storage modulus (G'), Loss modulus (G'') and $\tan \delta$ with temperature for a fully cured sample of Araldite DLS 772 / 4 4' DDS epoxy system with an amine / epoxy ratio of 0.8 prepared using microwave heating at 180 °C for 240 mins.	284
Figure 6.10	Dependence of storage modulus (G'), Loss modulus (G'') and $\tan \delta$ with temperature for a fully cured sample of Araldite DLS 772 / 4 4' DDS epoxy system with an amine / epoxy ratio of 0.8 prepared using conventional heating at 180 °C for 240 mins.	285

Figure 6.11	Dependence of storage modulus (G'), Loss modulus (G'') and $\tan \delta$ with temperature for a fully cured sample of Araldite DLS 772 / 4 4' DDS epoxy system an amine / epoxy ratio of 1.1 prepared using microwave heating at 180 °C for 240 mins.	285
Figure 6.12	Dependence of storage modulus (G'), Loss modulus (G'') and $\tan \delta$ with temperature for a fully cured sample of Araldite DLS 772 / 4 4' DDS epoxy system an amine / epoxy ratio of 1.1 prepared using conventional heating at 180 °C for 240 mins	286
Figure 6.13	Bar chat of Average T_g values of conventional and microwave cured samples of Araldite LY 5052 / 4 4' DDS epoxy system with an amine / epoxy ratio of 0.85.	287
Figure 6.14	Bar chat of Average T_g values of conventional and microwave cured samples of Araldite LY 5052 / 4 4' DDS epoxy system with an amine / epoxy ratio of 1.0.	288
Figure 6.15	Bar chat of Average T_g values of conventional and microwave cured samples of Araldite DLS 772 / 4 4' DDS epoxy system with an amine / epoxy ratio of 0.8.	288
Figure 6.16	Bar chat of Average T_g values of conventional and microwave cured samples of Araldite DLS 772 / 4 4' DDS epoxy system with an amine / epoxy ratio of 1.1.	289
Figure 6.17	Plot of Bar chart of cross-link density values of conventional and microwave cured samples of Araldite LY 5052 / 4 4' DDS epoxy system with an amine / epoxy ratio of 0.85.	290
Figure 6.18	Plot of Bar chart of cross-link density values of conventional and microwave cured samples of Araldite LY 5052 / 4 4' DDS epoxy system with an amine / epoxy ratio of 1.0.	291
Figure 6.19	Plot of Bar chart of cross-link density values of conventional and microwave cured samples of 0.8M amine / epoxy ratio of Araldite DLS 772 / 4 4' DDS epoxy system.	291

Figure 6.20	Plot of Bar chart of cross-link density values of conventional and microwave cured samples of Araldite DLS 772 / 4 4' DDS epoxy system with an amine / epoxy system of 1.1.	291
Figure 6.21	Plot of average molecular weight between cross-links (M_c) of conventional and microwave cured samples of Araldite LY 5052 / 4 4' DDS epoxy system with an amine / epoxy ratio of 0.85 using Nielsen's equation.	293
Figure 6.22	Plot of average molecular weight between cross-links (M_c) of conventional and microwave cured samples of Araldite LY 5052 / 4 4' DDS epoxy system with an amine / epoxy ratio of 0.85 using Nielsen's equation.	294
Figure 6.23	Plot of average molecular weight between cross-links (M_c) of conventional and microwave cured samples of Araldite LY 5052 / 4 4' DDS epoxy system with an amine / epoxy ratio of 1.0 using Nielsen's equation.	294
Figure 6.24	Plot of average molecular weight between cross-links (M_c) of conventional and microwave cured samples of Araldite DLS 772 / 4 4' DDS epoxy system with an amine / epoxy ratio of 0.8 using Nielsen's equation.	295
Figure 6.25	Plot of average molecular weight between cross-links (M_c) of conventional and microwave cured samples of Araldite LY 5052 / 4 4' DDS epoxy system with an amine / epoxy ratio of 1.1 using Nielsen's equation	295
Figure 6.26	Load vs Displacement plot for conventional and microwave cured samples of Araldite LY 5052 / 4 4' DDS epoxy system with an amine / epoxy ratio of 0.85.	296
Figure 6.27	Load vs Displacement plot for conventional and microwave cured samples of Araldite LY 5052 / 4 4' DDS epoxy system with an amine / epoxy ratio of 1.0.	297
Figure 6.28	Load vs Displacement plot for conventional and microwave cured samples of Araldite DLS 772 / 4 4' DDS epoxy system with an amine / epoxy ratio of 0.8.	297
Figure 6.29	Bar chat of Average flexural strength values of conventional and microwave cured samples of Araldite LY 5052 / 4 4' DDS epoxy system with an amine / epoxy ratio of 0.85.	298
Figure 6.30	Bar chat of Average flexural strength values of conventional and microwave cured samples of Araldite LY 5052 / 4 4'	299

	DDS epoxy system with an amine / epoxy ratio of 1.0.	
Figure 6.31	Bar chat of Average flexural strength values of conventional and microwave cured samples of Araldite DLS 772 / 4 4' DDS epoxy system with an amine / epoxy ratio of 0.8.	299
Figure 6.32	Bar chat of Average flexural strength values of conventional and microwave cured samples of Araldite DLS 772 / 4 4' DDS epoxy system with an amine / epoxy ratio of 1.1.	300
Figure 7.1	Fully cured sample of Araldite DLS 772 / 4 4' DDS with an amine / epoxy ratio of 0.8 before decomposition in Microwave Reaction System	303
Figure 7.2	Product obtained after decomposition of fully cured samples of Araldite DLS 772 / 4 4' DDS with an amine / epoxy ratio of 0.8 after decomposition at 120 °C for a total of 75 minutes in Microwave Reaction System	303
Figure 7.3	HPLC trace results of decomposed product of fully conventionally cured Araldite DLS 772 / 4 4' DDS epoxy system with an amine / epoxy ratio of 0.8 passed through a silica column using 50 : 50 Hexane / Ethyl acetate as solvents and detected at 254 nm.	304
Figure 7.4	HPLC trace results of decomposed product of fully microwave cured Araldite DLS 772 / 4 4' DDS epoxy system with an amine / epoxy ratio of 0.8 passed through a silica column using 50 : 50 Hexane / Ethyl acetate as solvents and detected at 254nm.	305
Figure 7.5	Analytical HPLC trace results of collected isolated compound of decomposed conventional cured Araldite DLS 772 / 4 4' DDS epoxy system with an amine / epoxy ratio of 0.8.	306
Figure 7.6	Analytical HPLC trace results of collected isolated compound of decomposed conventional cured Araldite DLS 772 / 4 4' DDS epoxy system with an amine / epoxy ratio of 0.8.	306
Figure 7.7	Infrared spectra of dried isolated compound collected from the decomposed product of cured Araldite DLS 772 / 4 4'	307

	DDS with an amine / epoxy ratio of 0.8	
Figure 7.8	Expanded view of Infrared spectra of dried isolated compound collected from the decomposed product of cured Araldite DLS 772 / 4 4' DDS with an amine / epoxy ratio of 0.8	308
Figure 7.9	¹ H-NMR spectra of dried isolated compound collected from the decomposed product of cured Araldite DLS 772 / 4 4' DDS with an amine / epoxy ratio of 0.8	309
Figure 7.10	¹³ C-NMR spectra of dried isolated compound collected from the decomposed product of microwave cured Araldite DLS 772 / 4 4' DDS with an amine / epoxy ratio of 0.8	310
Figure 7.11	DEPT with $\theta = 90^\circ$ spectra of dried isolated compound collected from the decomposed product of microwave cured Araldite DLS 772 / 4 4' DDS with an amine / epoxy ratio of 0.8.	312
Figure 7.12	DEPT with $\theta = 135^\circ$ spectra of dried isolated compound collected from the decomposed product of microwave cured Araldite DLS 772 / 4 4' DDS with an amine / epoxy ratio of 0.8.	312
Figure 7.13	HSQC spectra of dried isolated compound collected from the decomposed product of microwave cured Araldite DLS 772 / 4 4' DDS with an amine / epoxy ratio of 0.8.	314
Figure 7.14	Structure of 1, 3 – di(ethyl ester)-5-(diethyl amino)-2-hydroxybenzene	315
Figure 7.15	Electrospray ionization spectra of 1, 3 – di(ethyl ester)-5-(diethyl amino)-2-hydroxybenzene.	317

LIST OF TABLES

Table 2.1	Properties of diphenyl diaminosulfone	59
Table 3.1	The assignment of the peaks for Araldite DLS 772 epoxy resin in the $^1\text{H-NMR}$ spectrum	147
Table 3.2	Assignment of the peaks for Araldite DLS 772 epoxy resin in the $^1\text{H-NMR}$ spectrum	148
Table 3.3	Comparison of manufacturer's density values with experimental density values for Araldite LY 5052 and DLS 772 epoxy resins	153
Table 4.1	Glass transition temperatures of different Amine / Epoxy ratios after a DSC run for Araldite LY 5052 / 4 4' DDS epoxy system	155
Table 4.2	Glass transition temperatures of Araldite LY 5052 / 4 4' DDS with different Amine / Epoxy ratios after curing with a microwave heated calorimeter and subsequently subjected to a DSC run	155
Table 4.3	Glass transition temperatures of Araldite DLS 772 / 4 4' DDS with different Amine / Epoxy ratios after curing with DSC and subjected to a T_g run	156
Table 4.4	Glass transition temperatures of different Amine / Epoxy ratios after curing using microwave calorimetry and subsequently subjected to a DSC run for Araldite DLS 772 / 4 4' DDS epoxy system	157
Table 4.5	Stoichiometric ratios chosen for this research	158
Table 4.6	Exothermic peak temperature, T_p , The total heat of reaction, ΔH_T , and fractional conversion at the exothermic peak temperature, α_p for Araldite LY 5052 / 4 4' DDS epoxy system with an amine / epoxy ratio 0.85.	162
Table 4.7	The exothermic peak T_p , the total heat of reaction, ΔH_T , and fractional conversion at the exothermic peak temperature, α_p for Araldite LY 5052 / 4 4'	165
Table 4.8	The exothermic peak T_p , the total heat of reaction, ΔH_T , and fractional conversion at the exothermic peak temperature, α_p for Araldite DLS 772 / 4 4' DDS epoxy system with an amine / epoxy ratio of 0.8 at different heating rates	168
Table 4.9	The exothermic peak T_p , the total heat of reaction, ΔH_T , and fractional conversion at the exothermic peak temperature, α_p for Araldite DLS 772 / 4 4' DDS epoxy system with an amine / epoxy ratio of 1.1 at different heating rates.	171
Table 4.10	The exothermic peak T_p , the total heat of reaction, ΔH_T , and fractional conversion at the exothermic peak	174

	temperature, α_p for Araldite LY 5052 / 4 4' DDS epoxy system with an amine / epoxy ratio of 0.85 at different heating rates using microwave heating.	
Table 4.11	The exothermic peak T_p , the total heat of reaction, ΔH_T , and fractional conversion at the exothermic peak temperature, α_p for Araldite LY 5052 / 4 4' DDS	177
Table 4.12	Kinetic parameters for dynamic cure of Araldite LY 5052 / 4 4' DDS epoxy system with an amine / epoxy ratio of 0.85 using conventional heating	199
Table 4.13	Kinetic parameters for dynamic cure of Araldite LY 5052 / 4 4' DDS epoxy system with an amine / epoxy ratio of 0.85 using microwave heating.	199
Table 4.14	Kinetic parameters for dynamic cure of Araldite LY 5052 / 4 4' DDS epoxy system with an amine / epoxy ratio of 1.0 using conventional heating	199
Table 4.15	Kinetic parameters for dynamic cure of Araldite LY 5052 / 4 4' DDS epoxy system with an amine / epoxy ratio of 1.0 using microwave heating	200
Table 4.16	Kinetic parameters for dynamic cure of Araldite DLS 772 / 4 4' DDS epoxy system with an amine / epoxy ratio of 0.8 using conventional heating	200
Table 4.17	Kinetic parameters for dynamic cure of Araldite DLS 772 / 4 4' DDS epoxy system with an amine / epoxy ratio of 0.8 using microwave heating	201
Table 4.18	Kinetic parameters for dynamic cure of Araldite DLS 772 / 4 4' DDS epoxy system with an amine / epoxy ratio of 1.1 using microwave heating	201
Table 4.19	Kinetic parameters for dynamic cure of Araldite DLS 772 / 4 4' DDS epoxy system with an amine / epoxy ratio of 1.1 using microwave heating	202
Table 4.20	Kinetic Parameters at different degrees of conversion for conventionally and microwave cured Araldite LY 5052 / 4 4' DDS epoxy system with an amine / epoxy ratio of 0.85 determined by Ozawa's method.	205
Table 4.21	Kinetic Parameters at different degrees of conversion for conventionally and Araldite LY 5052 / 4 4' DDS epoxy system with an amine / epoxy ratio of 1.0 determined by Ozawa's method	207
Table 4.22	Kinetic Parameters at different degrees of conversion for conventionally and microwave cured Araldite DLS 772 / 4 4' DDS epoxy system with an amine / epoxy ratio of 0.8 determined by Ozawa's method	209
Table 4.23	Kinetic Parameters at different degrees of conversion for	211

	conventionally and microwave cured Araldite DLS 772 / 4 4' DDS epoxy system with an amine / epoxy ratio of 1.1 determined by Ozawa's method.	
Table 4.24	Values of Activation energy and pre-exponential factor for different stoichiometric ratios of Araldite LY 5052 / 4 4' DDS and Araldite DLS 772 / 4 4' DDS epoxy systems using conventional and microwave heating	213
Table 4.25	Values of Activation energy and pre-exponential factor for different stoichiometric ratios of Araldite LY 5052 / 4 4' DDS and Araldite DLS 772 / 4 4' DDS epoxy systems using conventional and microwave heating	216
Table 4.26	Kinetic parameters for isothermal cure of Araldite LY 5052 / 4 4' DDS epoxy system with an amine epoxy ratio of 0.85 using conventional heating	252
Table 4.27	Kinetic parameters for isothermal cure of Araldite LY 5052 / 4 4' DDS epoxy system with an amine / epoxy ratio of 0.85 using microwave heating	253
Table 4.28	Kinetic parameters for isothermal cure of Araldite LY 5052 / 4 4' DDS epoxy system with an amine / epoxy ratio of 1.0 using conventional heating	253
Table 4.29	Kinetic parameters for isothermal cure of Araldite LY 5052 / 4 4' DDS epoxy system with an amine / epoxy ratio of 1.0 using microwave heating.	253
Table 4.30	Kinetic parameters for isothermal cure of Araldite DLS 772 / 4 4' DDS epoxy system with an amine / epoxy ratio of 0.8 using microwave heating.	254
Table 4.31	Kinetic parameters for isothermal cure of Araldite DLS 772 / 4 4' DDS epoxy system with an amine / epoxy ratio of 1.1 using conventional heating	254
Table 4.32	Kinetic parameters for isothermal cure of Araldite DLS 772 / 4 4' DDS epoxy system with an amine / epoxy ratio of 1.1 using microwave heating.	254
Table 4.33	K_1 and K_2 activation energy values obtained from figures for both conventional and microwave heating for both Araldite LY 5052 / 4 4' DDS and Araldite DLS 772 / 4 4' DDS epoxy systems.	259
Table 6.1	Table of abbreviations used for amine / epoxy ratios for both Araldite LY 5052 / 4 4' DDS and Araldite DLS 772 / 4 4' DDS epoxy systems	279

Table 6.2	Density values of fully cured samples of Araldite LY 5052 / 4 4' DDS and Araldite DLS 772 / 4 4' DDS epoxy systems	280
Table 6.3	Glass transition values for fully cured samples of Araldite LY 5052 / 4 4' DDS and Araldite DLS 772 / 4 4' DDS epoxy systems at different stoichiometric ratios.	286
Table 6.4	Cross-link density values for fully cured microwave and conventionally cured samples of Araldite LY 5052 / 4 4' DDS and Araldite DLS 772 / 4 4' DDS epoxy systems.	292
Table 6.5	Flexural Strength values for fully cured samples of Araldite LY 5052 / 4 4' DDS and Araldite DLS 772 / 4 4' DDS epoxy systems at different stoichiometric ratios.	297
Table 7.1	Assignment of peaks of the ¹ H-NMR spectrum of 1, 3 – di(ethyl ester)-5-(diethyl amino)-2-hydroxybenzene	315
Table 7.2	Assignment of peaks of the ¹ H-NMR spectrum of 1, 3 – di(ethyl ester)-5-(diethyl amino)-2-hydroxybenzene	316

LIST OF SYMBOLS

ρ	Density
ω	Angular frequency of microwaves
α	Fractional conversion
μ	Magnetic dipole
γ	Magnetogyric ratio
Φ	Linear heating rate
ν	Cross-link density
ρ_ν	Depolarization ratio
ϵ^*	Complex dielectric constant
ϵ'	Dielectric constant
ϵ''	Dielectric loss factor
μ'	Relative permeability of the medium
D	Electric flux density
H	Magnetic field
α_d	Dipolar polarization
α_e	Electronic polarization
Δf	Half power bandwidth
σ_f	Flexural stress
ϵ_f	Flexural strain
ΔH_{dyn}	Total heat of reaction
ΔH_{iso}	Isothermal heat of reaction
ΔH_{res}	Residual heat of reaction
ΔH_T	Total heat of reaction released during the reaction
B	Magnetic Flux density
ϵ_0	Permittivity of free space
μ_0	Permeability of free space
α_p	Fractional conversion at the exothermic peak temperature
J	Current density
q	Charge density
α_t	Total dielectric polarization
B_0	External magnetic field
C_p	Specific heat of material
E	Electric field strength
E_a	Activation energy
f	Frequency
G'	Storage (or elastic) modulus
G''	Loss (or viscous) modulus
I	Nuclear spin quantum number
m	Magnetic quantum number
M_c	Average molecular weight between cross-links
M_n	Number-average molecular weight
M_w	Weight-average molecular weight
P	Power absorption per unit volume
p	Angular momentum

Q_c	Quality factor of the empty cavity
Q_s	Quality factor of the perturbed cavity
R	Gas constant
Tan δ	Loss tangent
T_{end}	Temperature at completion of reaction
T_g	Glass transition temperature
T_{on}	Onset temperature
T_p	Exothermic peak temperature
m/z	Mass-to-charge ratio
h	Planck constant
c	Speed of light
ν	Stretching vibration mode of a molecule in infrared radiation
δ	Bending vibrations mode of a molecule in infrared radiation
A	Preexponential factor
Q	Quality Factor

LIST OF ABBREVIATIONS

¹³ C-NMR	Carbon 13 nuclear magnetic resonance spectroscopy
¹ H-NMR	Proton nuclear magnetic resonance spectroscopy
A/E	Amine / Epoxy
DDM	4,4'-Diaminodiphenyl methane
4,4'-DDS	4,4'-Diamino diphenylsulphone
DGEBA	Diglycidyl ether of Bisphenol A
DGEBF	Diglycidyl ether of Bisphenol F
DEPT	Distortion Enhancement Polarisation Transfer
DMTA	Dynamic mechanical thermal analysis
DSC	Differential scanning calorimetry
FCC	Federal communication commission
FT-IR	Fourier transform infrared spectroscopy
GPC	Gel permeation chromatography
HMQC	Heteronuclear Multiple Quantum Correlation
NMR	Nuclear magnetic resonance spectroscopy
NWCC	North West Composites Centre
PID	Proportional integral derivative
PTFE	Polytetrafluoroethylene
SEC	Size exclusion chromatography
THF	Tetrahydrofuran
TMA	Thermal mechanical analysis
TMS	Tetramethylsilane
CA85	Conventional cured Araldite LY 5052 /4 4 DDS epoxy system with an amine / epoxy ratio of 0.85
MA85	Microwave cured Araldite LY 5052 /4 4 DDS epoxy system with an amine / epoxy ratio of 0.85
CA 100	Conventional cured Araldite LY 5052 /4 4 DDS epoxy system with an amine / epoxy ratio of 1.0
MA100	Microwave cured Araldite LY 5052 /4 4 DDS epoxy system with an amine / epoxy ratio of 1.0
CD80	Conventional cured Araldite DLS 772 /4

	4 DDS epoxy system with an amine / epoxy ratio of 0.85
MD80	Microwave cured Araldite DLS 772 /4 4 DDS epoxy system with an amine / epoxy ratio of 0.8
CD110	Conventional cured Araldite DLS 772 /4 4 DDS epoxy system with an amine / epoxy ratio of 1.1
MD110	Microwave cured Araldite DLS 772 /4 4 DDS epoxy system with an amine / epoxy ratio of 1.1

The University of Manchester
Babatunde O Bolasodun
PhD

Microwave effects on the curing, structure properties and decomposition of epoxy resins.
01-11-2010

ABSTRACT

Comparative studies were carried out on the curing kinetics, physical and mechanical properties of conventionally and microwave cured epoxy resins. Epoxy resins Araldite LY 5052 and DLS 772 were used for this study. 4,4'-Diaminodiphenyl sulfone was used as a hardener in the preparation of both systems. Nuclear magnetic resonance and gel permeation chromatography were used to identify the chemical structure of the resins. Differential scanning calorimetry was used to monitor the curing kinetics of conventionally cured epoxy samples while a microwave heating calorimeter was used to monitor the curing kinetics of microwave cured epoxy samples "*in situ*". These studies were carried out under non-isothermal and isothermal conditions. For both conditions, there was a significant increase in the fractional conversion of the microwave cured samples compared to the conventionally cured samples. The curing reactions for samples cured using microwave heating took place over a smaller temperature range. Higher reaction rates were observed in the samples cured using microwave heating. There were some differences in the kinetic parameters of the non-isothermal curing reactions of samples cured using microwave and conventional heating. For the Araldite LY 5052 / 4,4'-DDS epoxy system, the microwave cured samples had higher activation energy than conventionally cured samples, while for the Araldite DLS 772 / 4,4'-DDS epoxy system, the microwave cured samples had lower activation energy. The activation energies of the microwave isothermal curing of both Araldite LY 5052 / 4,4'-DDS and Araldite DLS 772 / 4,4'-DDS epoxy systems were lower than the activation energies of the conventionally cured samples. Infrared spectroscopy showed that the curing reaction followed the same path during conventional and microwave heating. It also revealed that the reaction rate of the microwave cured samples was higher than the conventionally cured samples. For both epoxy systems, the microwave cured samples had a higher glass transition temperature (T_g), higher cross-link density (ν) and lower molecular weight between cross-links. These showed that the microwave cured samples had a more compact network structure than the conventionally cured samples, which is an indication of better mechanical properties. A microwave reaction system was used to successfully dissolve conventional and microwave cured samples of Araldite DLS 772 / 4,4'-DDS epoxy system. The chemical structure of the decomposed product was determined.

DECLARATION

I hereby declare that no portion of this work referred to in this thesis has been submitted in support of an application for another degree or qualification of this or any other university or institution of learning.

BABATUNDE O BOLASODUN

COPYRIGHT STATEMENT

- i) The author of this thesis (including any appendices and/or schedules to this thesis) owns certain copyright or related rights in it (the “copyright”) and he has given the University of Manchester certain rights to use such Copyright, including for administrative purposes.
- ii) Copies of this thesis, either in full or in extracts and whether in hard or electronic copy may be made **only** in accordance with the copyright, Designs and Patents Act 1988 (as amended) and regulations issued under it or, where appropriate, in accordance with licensing agreements which the university has from time to time. This page must form part of any such copies made.
- iii) The ownership of certain Copyright, patents, designs, trademarks and other intellectual property (the “Intellectual Property”) and any reproductions of copyright works in the thesis, for example graphs and tables (“Reproductions”), and which may be described in the thesis, may not be owned by the author and may be owned by third parties. Such Intellectual Property and reproductions cannot and must not be made available for use without the prior and written permission of the owner of the relevant Intellectual property and/or Reproductions.
- iv) Further information on the conditions under which disclosure, publication and commercialisation of this thesis, the Copyright and any Intellectual Property and/or Reproductions described in it may take place is available in the university IP Policy (see <http://www.campus.manchester.ac.uk/medialibrary/policies/intellectual-property.pdf>), in any relevant Thesis restriction declarations deposited in the University Library, the University Library’s regulations (see <http://www.manchester.ac.uk/library/aboutus/regulations>) and in The University’s policy on presentation of Theses.

ACKNOWLEDGEMENTS

I would first give Glory, Thanks and Praise to God for his Protection, Guidance and Blessings.

Special thanks goes to my family (Dr and Mrs Bolasodun, Bolanle, Bukola, Bolatito) for their endless love, support, encouragement and Prayers right from as long as I can possibly remember.

I would like to thank my supervisor, Professor Richard Day for his encouragement, guidance and support throughout the duration of my research studies.

I will also thank Dr Arthur Wilkinson for his useful advice and support throughout my research.

Special thanks also go to Mr and Mrs Julius. A. Akinsanya for their love and unflinching support, and to my cousins Bimbo, Femi, Segun, and Afolabi for their support.

I will forever be grateful to Mr Micheal Olumide Ogunmola for his priceless support. My sincere thanks go to the Late Mr M.O. Ogunlowo, Mr Jimba, Dr Ajayi, Mr Durowoju, and Mr Adebayo, Mr Olatunji, Yetunde Adepeju for all their love and prayers.

I would like to thank all the members of the Northwest Composite Centre especially Dr Alan Nesbitt for their selfless technical assistance throughout my research. I owe a lot of thanks to Rehana Sung for her assistance and help in chemical analysis. Andy Zadoroshnyi, Polly Crook, gave me a lot of technical assistance and I would like to say a very big thank you to them all.

I would like to thank Mayokun Ogundare for her Love, support and encouragement, and last but not least, I would like to say a very big thank you to myself for all my hardwork and perseverance.

CHAPTER ONE

1.0 INTRODUCTION

An epoxy is a thermosetting resin which usually starts out as a liquid and is converted into a solid by a chemical reaction only. When cured, epoxies become irreversibly rigid. An epoxy based polymer is mechanically strong, and in its solid form, it is chemically resistant to degradation. They are also highly adhesive during conversion from liquid to solid. These properties when put together, make epoxy materials very versatile [1].

Epoxy systems are made up of two essential components, a resin and a hardener. Sometimes there is a third component which is an accelerator. The resin component is the epoxy while the hardener is what the epoxy reacts with chemically and it is often a type of amine. When the epoxy and amine are added together and mixed in a specific way and then heated, they will react chemically and link together irreversibly. When the full reaction is complete, the resulting product is a rigid plastic polymer material [1]

Due to increasing applications of epoxy materials as high performance structural adhesive systems in the aerospace and the microelectronic industries, the demand for epoxies is on the rise. This rise has led to the exploration of faster and more efficient methods of manufacturing epoxy materials [2]

Although thermal curing increases the rate at which the material cures and lowers the time taken for it to cure, it is limited by the fact that for any given system, the maximum rate of reaction has an optimum temperature. If a resin or a material is heated to a temperature higher than its optimum temperature, there would not be an increase in its reaction rate, but instead the material would start to degrade thermally [2].

Alternatives to thermal curing which can accelerate the rate of reaction, reduce the cure time or provide a more energy efficient method for curing epoxy resins have been looked into. These alternatives were the use of ultraviolet light, electron beams, gamma rays and microwave energy [2, 3]

Ultraviolet light has a poor ability to penetrate into the material. It also has a restricted close rate. Due to this, application of ultraviolet light in curing materials is only possible in very limited circumstances [2, 3]

Gamma rays are usually delivered from naturally radiating sources such as cobalt-60, but there are several health and environmental concerns which are associated with the radiation hazards from gamma rays. Due to these concerns, they are hardly used[2].

Curing with electron beams has proven to be an efficient and a quick method of curing, however, its disadvantage is that high costs are involved with the operation using this method [2, 3].

Microwaves have been found to be a good alternative method for curing thermoset polymers. Compared to conventional heating techniques which are based on conduction of heat through a material, microwave heating is a direct form of heating. Microwaves generate heat within the materials. Microwave radiation enables sample temperatures to be potentially changed or controlled more readily [4]. Any increase or decrease in the microwave input power leads to a corresponding increase or decrease in the temperature of the material undergoing cure. Unlike conventional heating which heats the material being processed, along with the walls of the oven and the air surrounding the process material, microwave heating affects only the material being processed. This makes microwave heating a more energy efficient method of heating materials being processed, and this translates into lower production costs for microwave heating [3]. Microwaves do not have any intrinsic difficulties associated with their use, as a result of this, microwave cured products are applied to many diverse industries [4].

Plastics and polymers are very beneficial to our society. They have played significant roles in the advancements of satellites aircrafts and missiles. As beneficial as these plastics and polymers are, they also cause a lot of environmental problems [5, 6]. They are non organic substances and hence, various microorganisms that decay matter can not act upon the plastics. As a result of this, they very slowly decay in nature. As they slowly decay, they release hydrocarbons which are added to the carbon cycle. They also have long half-lives in landfills. Burning them will also create pollution which releases toxic gases.

Chemical recycling of plastics and polymers is being explored as an interesting route for converting plastic wastes back into its original constituents, or into other usable substances [7, 8]. Chemical recycling is a very effective and promising method for plastics. It has advantages for the industry especially in the recycling of thermosetting resins.

Amine cured epoxy resins have been successfully dissolved in nitric acid solution. This is because they have a low resistance to nitric acid solution. This successful dissolution has increased the possibility of recycling thermosetting resins [5, 6].

CHAPTER TWO

2.0 LITERATURE REVIEW

2.1 *Epoxy Resins*

Epoxy resins were first synthesized in the 1930's by Castan in Switzerland and Greenlee in the United States[9]. Epoxy resins are thermosetting materials. Thermosetting materials are resins that become hard and infusible systems when converted by a curing agent. Some phenolics however can self crosslink. They cure on heating and then become infusible. Examples of thermosetting materials are phenolic, unsaturated polyester and epoxy resins [9].

Thermoplastic resins on the other hand are composed of long, linear chains which lie together in three dimensions, but are not chemically interconnected with each other.

Practically, as heat or pressure is applied to the materials, thermoplastic materials will soften progressively while thermoset materials will retain their dimensional stability throughout their temperature range. This classification is based on their structure; and should not be considered as criterion of performance. This is because some thermosetting resins are designed for use at a very limited range and they will distort more readily than high-heat-resistant thermoplastic compounds [9].

2.1.2 Properties of Epoxy Resins

Thermoset epoxy resins have a number of peculiar and valuable properties. These properties are immediately amenable to use in the formulation of sealing liquids, castings, laminates and coatings. Some of these valuable properties are

- (1) **Versatility:-** There are a lot of curing agents available for epoxies. These epoxies are compatible with a wide range of modifiers. As a result, the properties of a cured epoxy-resin system can be engineered to widely diverse specifications [9, 10].

- (2) **Good Handling Characteristics:-** Many epoxy systems can be worked at room temperature, and those which can not be worked require just little heat during mixing. Without the curing agent, epoxy resins have an indefinite shelf life; as long as they are made properly and they do not contain any caustic compound [9, 11].
- (3) **High Adhesive Properties:-** As a result of the polarity of the aliphatic hydroxyl and ether (C-O-C) groups present in the initial resin chain and the cured system, epoxy resins have high adhesive strengths. The polarity of these epoxy groups serve to create electromagnetic bonding forces between the epoxy molecule and adjacent surface. Likewise, the epoxy groups will react to provide chemical bonds with surfaces such as metals where active hydrogens may be formed. The chemical bonds established are usually preserved. This is because the resin passes relatively undisturbed (with low shrinkage) [9].
- (4) **Toughness:-** Cured epoxy resins are about seven times tougher than cured phenolic resins. This relative toughness has been attributed to the presence of integral aliphatic chains, and the distance between crosslinking points [9, 10].
- (5) **Low Shrinkage:-** Unlike many thermosetting resins, epoxy resins do not give off any by-products during cure; and in the state, they are highly associated. Shrinkage is on the order of <2 percent for an unmodified system. This indicates that minor internal rearrangement of the molecules is necessary. On the other hand, the condensation and crosslinking of phenolic and polyester resins yield considerably higher shrinkage values [9].
- (6) **Inertness:-** In a cured epoxy resin, the ether groups, the benzene rings and the aliphatic hydroxyl (where present) are almost invulnerable to attack by caustic substances and extremely resistant to acids. This makes cured epoxy resins very inert chemically. The dense, closely packed structure of the resinous mass in the cured epoxy system is extremely resistant to solvent action, and this enhances the chemical inertness of the cured epoxy resin [9].

2.2 Structure of a basic epoxy molecule

The epoxy resin is characterised by the reactive epoxy or ethoxyline groups [9, 10, 12].

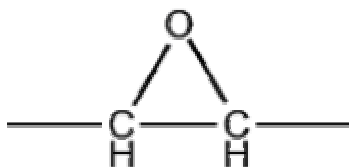


Figure 2.1 Structure of basic epoxy – resin moiety

These groups serve as terminal linear polymerization points. An extremely adhesive and highly inert solid is formed when crosslinking is accomplished through these groups. In its simplest form, the epoxy molecule is represented by the diglycidyl ether of bisphenol A.

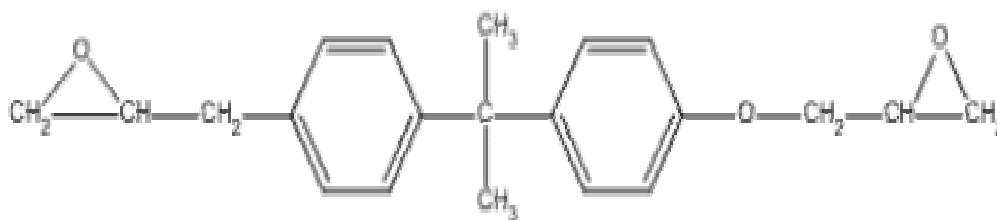


Figure 2.2 Diglycidyl ether of Bisphenol A

The most widely used liquid epoxy resins are predominantly of the above structure. Commercial resins are not molecularly distilled, and because of this, they contain some percentages of higher weight homologs, branched chain molecules, isomers and occasionally monoglycidyl ethers in combination with the basic structure. The high-viscosity and the solid commercial resins are predominantly comprised of more highly polymerized products which are considered as homologs of diglycidyl ether of bisphenol A [9].

2.3 Synthesis of a basic epoxy-resin molecule

The raw materials for the synthesis of the diglycidyl ether of bisphenol A are epichlorohydrin and bisphenol A. These are obtained from natural gas, or by coking by-products.

2.3.1 Epichlorohydrin

Epichlorohydrin is a mobile liquid which is colourless and has irritating chloroform like odour. Epichlorohydrin is represented by the formula below [12, 13].

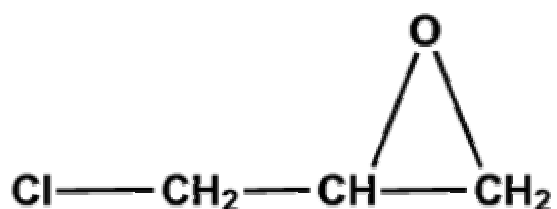


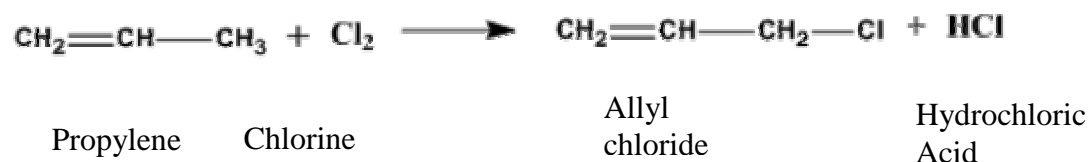
Figure 2.3 Chemical structure of epichlorohydrin

Epichlorohydrin is extremely reactive and it usually combines through the epoxy group with a substance which contains an active hydrogen atom. Epichlorohydrin is commercially available at 98 percent purity.

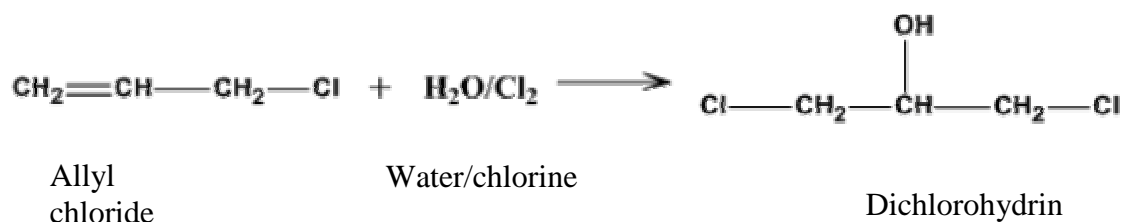
Epichlorohydrin is commonly produced by the chlorination of propylene. This results in allyl chloride being formed, and this is reacted with hypochlorous acid to produce dichlorohydrin, which is exposed to sodium hydroxide at elevated temperatures to strip off one hydrogen and one chlorine atom [9].

These steps are similar to those involved in the preparation of glycerol.

The complete reaction of the formation of epichlorohydrin from propylene is expressed in the equation below.



ii)



iii)

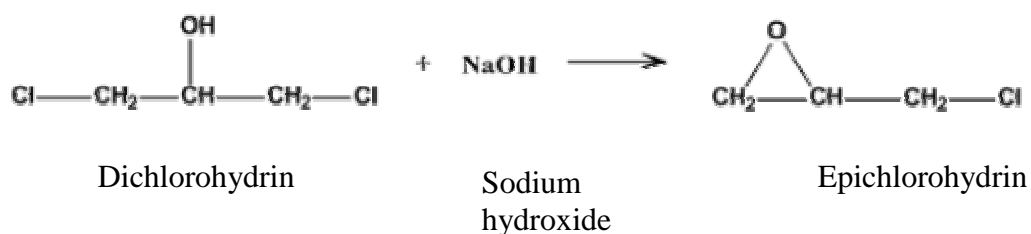


Figure 2.4 Complete reaction from propylene to epichlorohydrin

2.3.2 Bisphenol A

Bisphenol A or bis (4-hydroxyphenyl) dimethylmethane requires two fundamental intermediates for synthesis; phenol and acetone.

Bisphenol A is based on the very stable benzene ring. It is the most easily prepared of the dihydric phenols. It is available commercially as a flaked solid in relatively pure form with a melting point of 153 °C [9, 11-13].

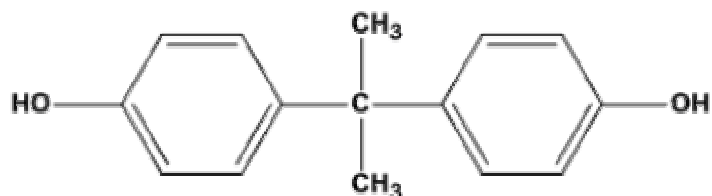
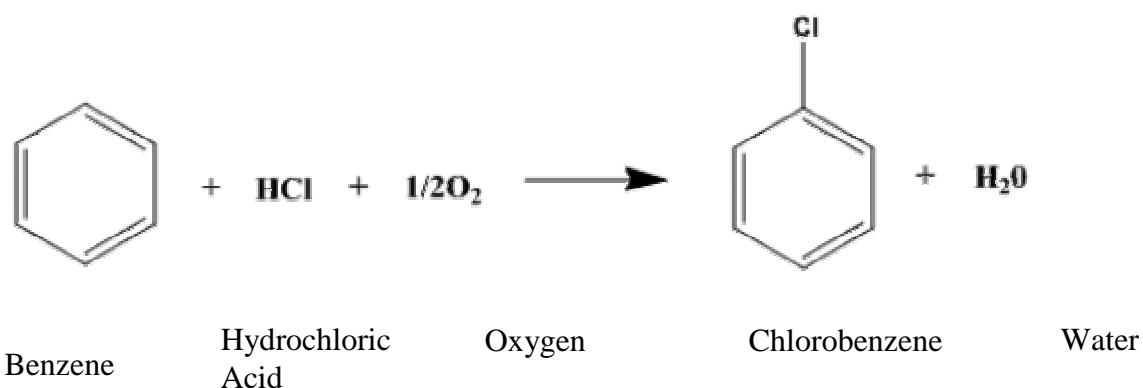


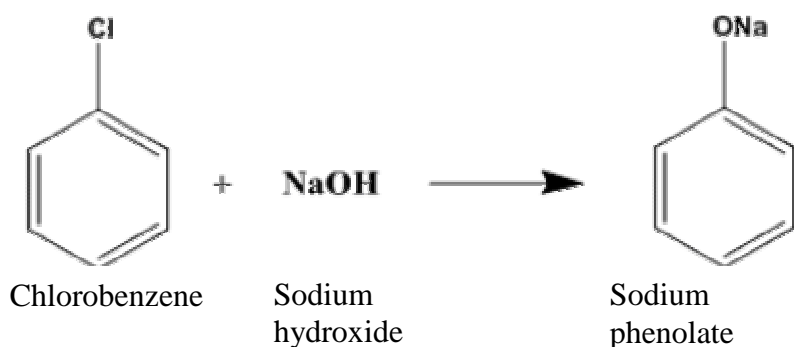
Figure 2.5 Chemical Structure of Bisphenol A

A commercial process of manufacturing bisphenol A would involve benzene, which is obtained from coal gas or water gas, as a starting point. First, benzene is treated with hydrochloric acid and oxygen to produce chlorobenzene. Sodium hydroxide then added to yield sodium phenolate, and phenol is released by the addition of carbon dioxide [9].

i)



ii)



iii)

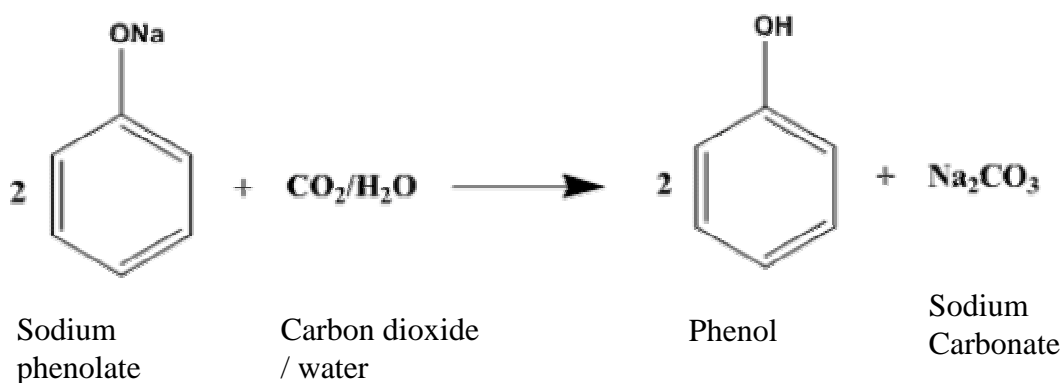
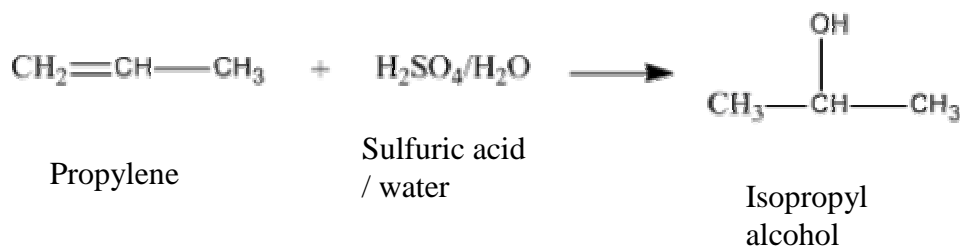


Figure 2.6 Formation of Phenol

Acetone is formed by treating propylene with sulphuric acid to produce isopropyl alcohol. This is then oxidized under mild conditions to acetone. A combination of acetone and phenol gives bisphenol A [9, 12, 13].

i)



ii)

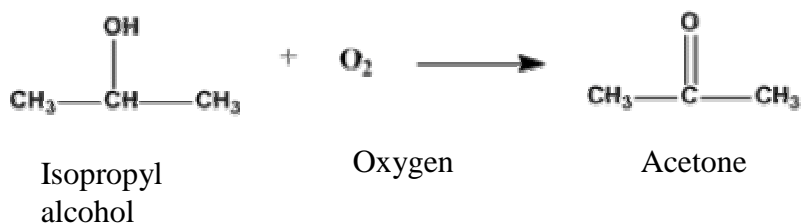


Figure 2.7 Formation of Acetone

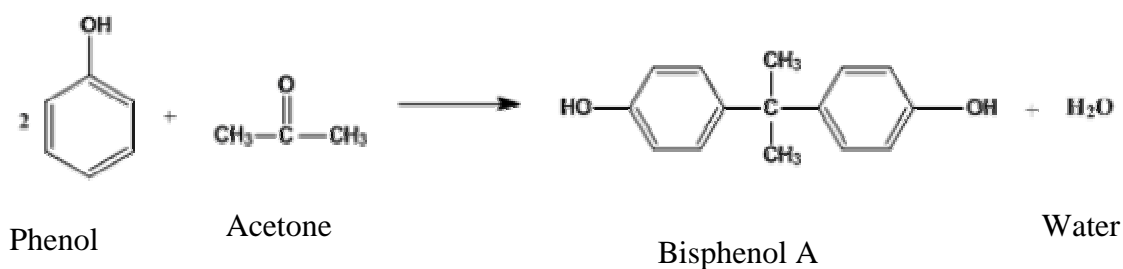


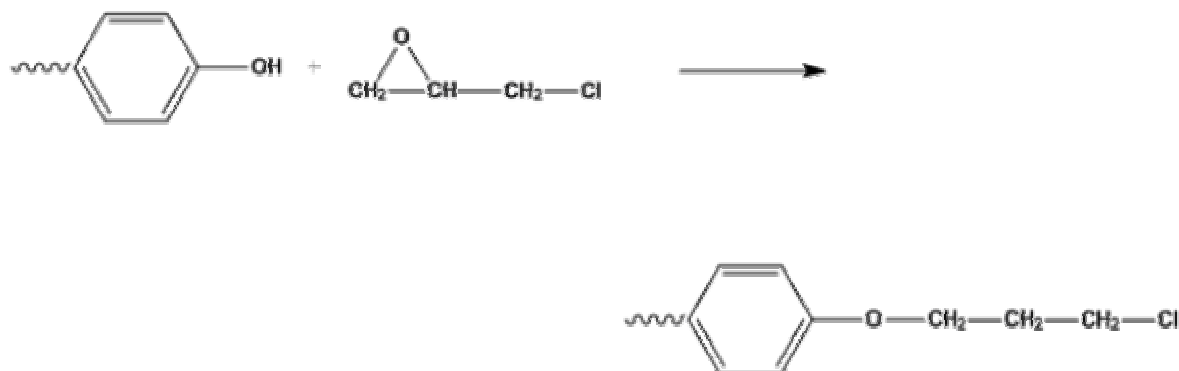
Figure 2.8 Reaction between phenol and acetone to form Bisphenol A

Bisphenol A has been the chief dihydric phenol used in epoxy-resin manufacture. This is because acetone and phenol are easily available, and they are easily manufactured.

2.3.2 Diglycidyl ether of bisphenol A

Diglycidyl Ether of bisphenol A is formed by the reaction of epichlorohydrin and bisphenol A in the presence of sodium hydroxide [9, 10, 13].

i)



ii)

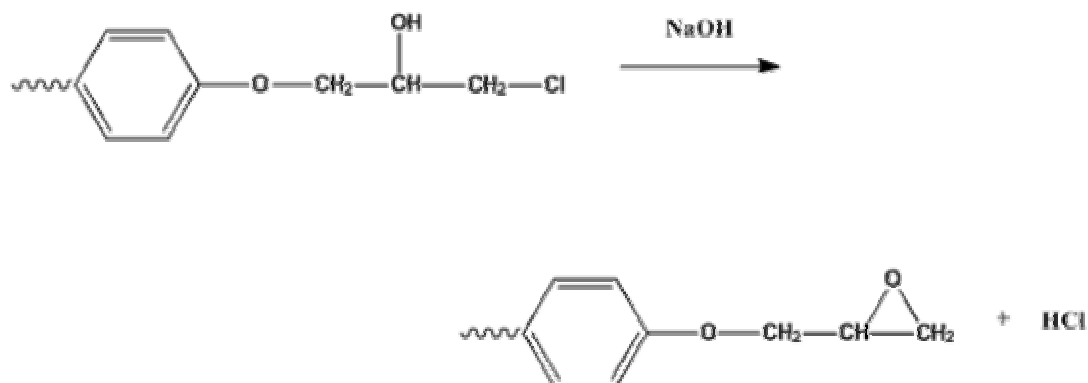


Figure 2.9 Formation of diglycidyl ether of bisphenol A

There have been suggestions that some of the caustic forms phenolate and water as an intermediate step in the reaction. The caustic also serves to neutralize the hydrochloric acid formed as a by-product [9].

Theoretically, in order to obtain diglycidyl ether of bisphenol A, 2 mols of epichlorohydrin are required for each mole of bisphenol A.

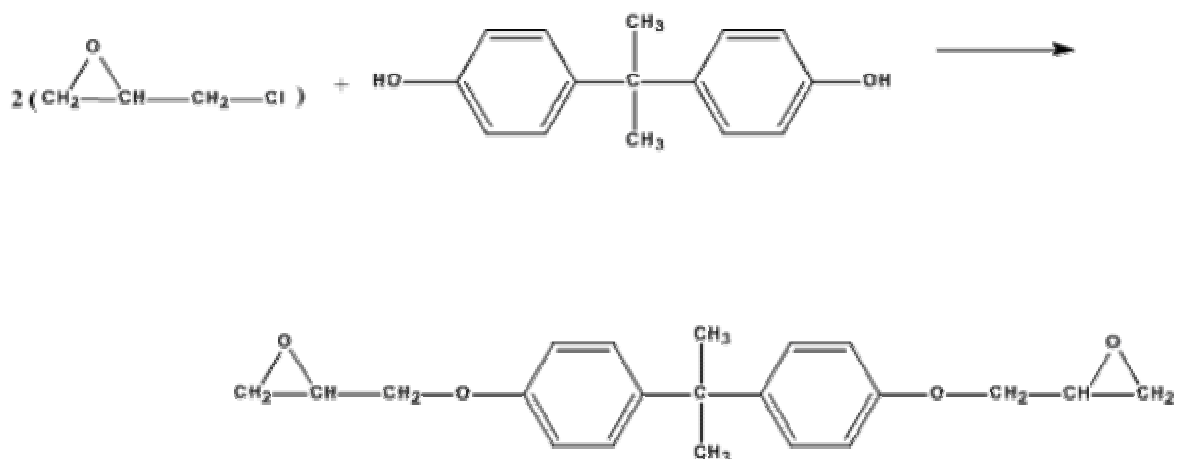


Figure 2.10 Formation of diglycidyl ether of bisphenol A

However, when the stoichiometric ratio of 2:1 is employed, the monomeric yield is less than 10 per cent, with the remaining material being higher-molecular-weight condensation and polymerization products. Excess epichlorohydrin is employed in order to obtain high yields of the monomeric product, and the stoichiometric amount is doubled or tripled. This gives yields of 70 percent or more. There is an additional advantage in the use of excess epichlorohydrin. The epichlorohydrin serves as a reaction medium, making it unnecessary to employ a foreign solvent in the synthesis. The reaction is conducted in an inert atmosphere, and the alkalinity of the solution is carefully controlled by stepwise addition of caustic as necessary [9, 11].

There have also been suggestions of an alternate procedure in the manufacture of epoxy resins, and this involves a two-step process. First, bisphenol A and epichlorohydrin are reacted in the presence of 0.1 to 0.2 percent of a Friedel-Crafts type catalyst.

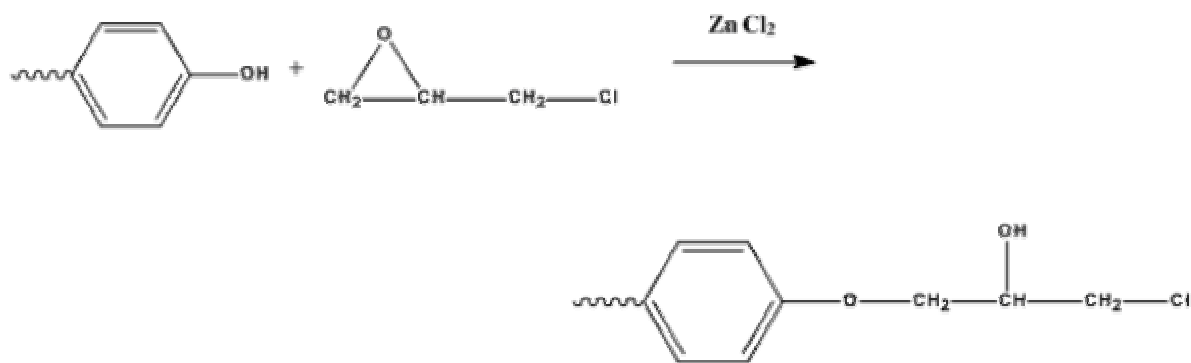


Figure 2.11 First step of the reaction of bisphenol A and epichlorohydrin in the presence of 0.1 and 0.2 percent of a Friedel-Crafts type catalyst.

A dehydrohalogenating compound, such as the aluminates, silicates, and zincates is used to treat the monomeric material in a substantially or completely nonaqueous medium [9].

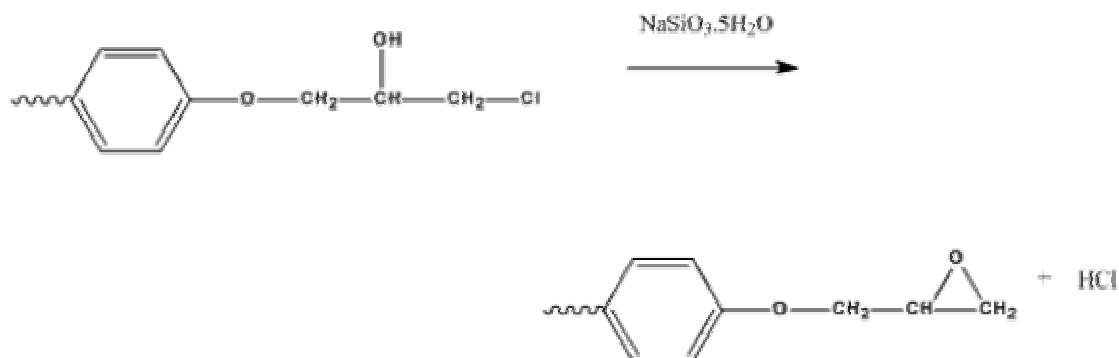


Figure 2.12 Second step of the reaction of bisphenol A and epichlorohydrin in the presence of 0.1 and 0.2 percent of a Friedel-Crafts type catalyst.

2.4 Epoxy resin characterization

There are some characteristics of epoxy resins which may be used as guides to their structure and their usefulness. They are

1. **Epoxy Equivalent:-** The epoxy equivalent can be defined as the weight of resin in grams which contains one gram chemical equivalent of epoxy. Low-

molecular-weight resins have an epoxide equivalent in the range of 175 – 200 g/eq; while higher-weight resins have correspondingly higher values, since in each molecule there are long chains between the epoxy groups [9]. If the resin chains are assumed to be linear with no side branching, and if it also assumed that an epoxy group terminates each end, then the epoxide equivalent (weight) is one half of the average molecular weight of the resin. Epoxy value can be defined as the fractional number of epoxy groups contained in 100 grams of resin. Dividing the epoxy value into 100 gives the epoxide equivalent. Epoxy equivalents are determined by reacting a known quantity of resin with a known quantity of hydrochloric acid and back-titrating the remaining acid to determine its consumption [9].

2. **Hydroxyl Equivalent:-** Hydroxyl equivalent is the weight of the resin containing one equivalent weight of hydroxyl group. It can also be expressed as equivalents per 100 grams[11]. There are several methods of determining hydroxyl equivalents. The methods are (i) esterification with acids, which involves esterifying the resin with about twice the theoretical amount of linseed oil acids necessary to react with all the hydroxyl groups and epoxy groups at a temperature of 225 °C, until a constant acid value is obtained, and then back-titrating the unreacted linseed acids and calculating the hydroxyl groups including epoxy content, one epoxy group being taken as equivalent to two hydroxyl groups. (ii) reaction with acetyl chloride (iii) reaction with lithium aluminium hydride (iv) infrared spectroscopy [11].
3. **Good Handling Characteristics:-** Many epoxy systems can be worked at room temperature and those which cannot be worked require moderate heat during mixing .Before the curing agent is incorporated, the resins have an indefinite shelf life, provided they are not properly made. Cure can be accomplished in almost any specified time period by regulating the cure cycles and properly selecting the curing agent[9].
4. **Toughness:-** Cured epoxy resins are approximately seven times tougher than cured phenolic resins. This toughness has been attributed to the distance between crosslinking points and the presence of integral aliphatic chains [9].

2.5 Amines

Amines are important curing agents for epoxy resins. Amine compounds are classified into primary, secondary, and tertiary amines, depending on whether one, two or three hydrogen molecules of ammonia (NH_3) have been substituted for hydrocarbon, respectively[14].

Depending on their number in one molecule, amines are called monoamine, diamine, triamine, or polyamine. Amines are also classified into aliphatic, alicyclic and aromatic amines according to the types of hydrocarbons involved. These are all important curing agents for the epoxy resins [14].

Aliphatic amines can be used for room temperature cure. The heat resistance of the cured resin is generally about 100°C , and it has excellent bonding properties. Resins cured with aromatic amines have been used to attain greater heat and chemical resistance than those cured using aliphatic amines[14].

The curing of epoxy resin by amine curing agents is expressed by the formula shown in figure below. The epoxy moieties of the DGEBA can react with either the primary or secondary amine to form an OH in the main chain as in (i) and (ii) which, later on, can react with another epoxide ring to further crosslink the resin. The relative rates of those three reactions are important for the final structure and properties of the cured resin[14].

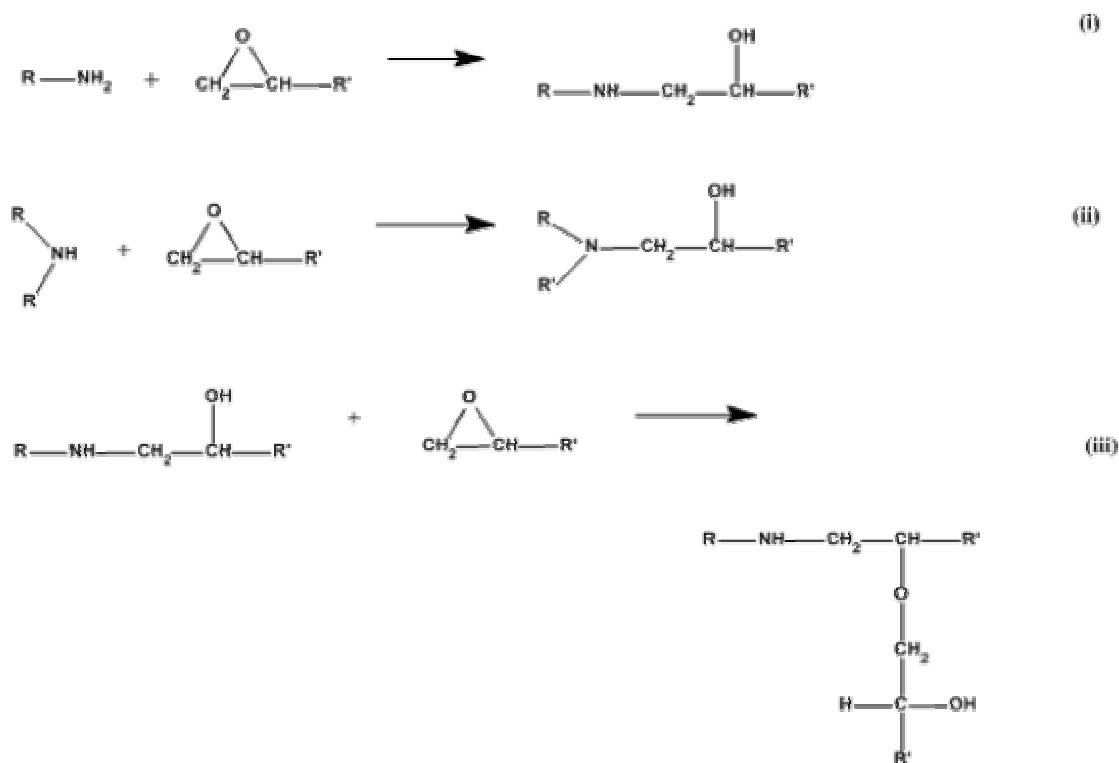


Figure 2.13 Amine curing reaction of epoxy resins

Referring to figure 2.13, in order for the cured resin to become a cross-linked polymer, the curing agent must have more than three active hydrogen atoms and two amino groups in a molecule above. When the number of moles in epoxy groups is equal to that of the active hydrogen, the loading of the curing agent in epoxy resin becomes optimal [14].

The curing speed of individual amines depends on the type and loading of amine. It also depends on the type of epoxy resin. The most commonly used glycidyl-ether type resins easily cure at room temperature, but inner epoxy types such as cyclohexene oxide and epoxidized polybutadiene hardly cure. Glycidyl-ester type cures quite faster than the glycidyl-ether type.

Diglycidyl ether of bisphenol A (DGEBA), which is a condensation product of bisphenol A and epichlorohydrin, is primarily cured by aliphatic amines at room temperature, but with aromatic amines, DGEBA is slowly cured and this requires thermal curing [14].

2.5.1 Aliphatic Amines

Aliphatic amines are room temperature curing agents. They rapidly react with epoxy resins. A large quantity of heat is generated, and they have a short pot life (usable time). If curing of tertiary amines is performed at high temperature, the properties of curing agents that cure at the room temperature are improved. The heat deformation temperature of cured object of DGEBA is 120 °C at the highest [14].

Resins cured with aliphatic amines are strong. They also have excellent bonding properties. In addition, they have resistance to alkalis and some inorganic acids, and they have good resistance to water and solvents, but they are not really good to many organic solvents[14].

Aliphatic amines irritate the skin. Aliphatic amines having high molecular weight and low vapour pressure are less toxic, but they still need to be handled with care[14].

2.5.2 Aromatic Amines

In comparison to aliphatic amines, aromatic amines are weaker bases, and they slowly cure at room temperature. This is as a result of steric hindrance caused by the aromatic ring. The curing virtually stops in the B-stage of a linear polymer solid due to the large differences in the reaction of primary and secondary amines [14].

There are usually two steps involved in the curing of aromatic amines. The first step is heating to a temperature of about 80 °C in order to lessen the heat being generated. This helps to slow cure in order to reduce the exotherm remaining. The second heating is carried out at a high temperature of about 150 to 170 °C [14].

Aromatic amines provide excellent heat resistance, they yield heat distortion temperatures of 150 to 160 °C, with good mechanical properties and the cured resins are strong. In addition, aromatic amines have good electrical properties and excellent chemical resistance, particularly against alkalis, and because of this, it is a curing agent that is highly resistant to solvents [14].

2.5.3 Tertiary and secondary amines

Tertiary amines, the active hydrogen in which has been completely replaced with carbon hydroxide, do not cause an additional reaction with epoxy resin, but work as a polymerisation catalyst [14].

The curing temperature significantly influences the curing speed, the heat generation, and the properties of the cured resin. Thus, this amine is rarely used alone, particularly in large castings, because the properties at the centre and the outer region are different due to the large quantity of heat generated. They are often used in the field of paints and adhesives where the material used is thin [14].

Although tertiary amines are less useful as a curing agent, they are very important compounds as accelerators for acid anhydrides, and they are useful as accelerators or co-curing agents for polyamine and polyamide curing agents[14].

2.5.4 Amine Hardening Systems

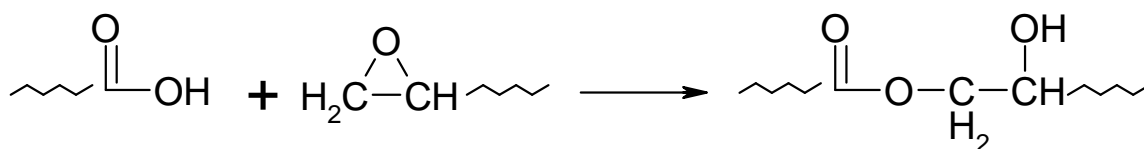
Polyfunctional primary RNH_2 and secondary R_2NH amines are widely used as curing agent for epoxy resins. Theoretically, each primary amine group is capable of reacting with two epoxy groups. Hence a polyamine such as ethylene diamine $\text{H}_2\text{N}-\text{CH}_2-\text{CH}_2-\text{NH}_2$ is capable of reacting with four epoxy groups because of the four active hydrogen atoms attached to the nitrogen atom [14].

2.5 Organic Acids Hardening Systems

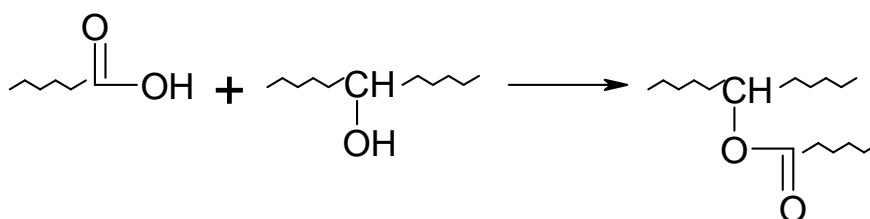
The anhydrides of organic acids are widely used as cross-linkers for liquid epoxy resins. It should also be noted that some organic acids are used to esterify high molecular weight resins for use in surface-coating formulations.

Figure 2.14 describes the reactions of epoxy resins in the presence of organic acids [15].

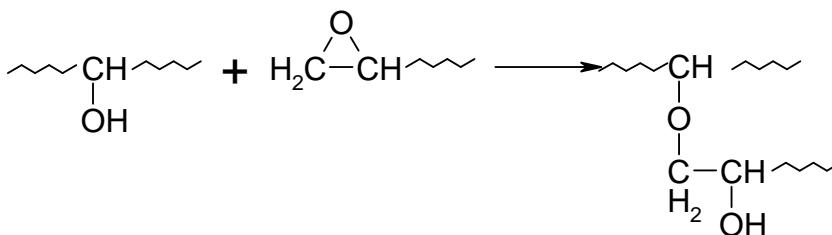
(i) Esterification via epoxy/acid reaction



(ii) Esterification via hydroxyls present in the resin or via the nascent hydroxyls produced in previous reaction



(iii) Reaction of epoxy with aliphatic hydroxyl groups



(iv) Hydration of epoxy groups

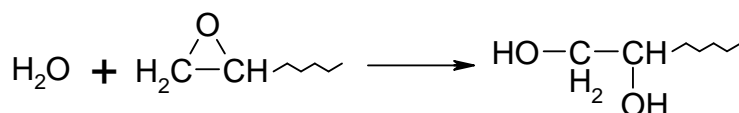


Figure 2.14 Reactions of epoxy resins in the presence of organic acids.

Acid anhydrides react in a manner similar to organic acids, but this reaction is more complex because of the absence of water in the molecule and the necessity for activating the anhydride ring by an alcoholic hydroxyl (or salt or a trace of water). First a hydroxyl group of the epoxy resin open the anhydride, as shown in figure 2.15

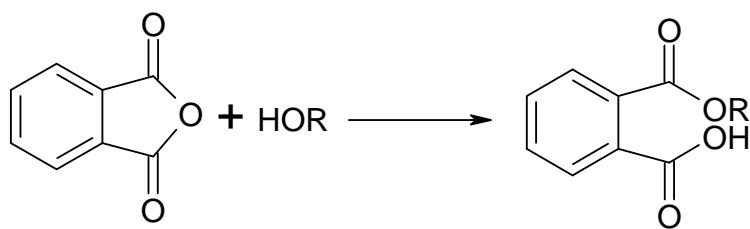


Figure 2.15 Opening of the Anhydride ring.

This opening of the anhydride ring leads to the formation of the carboxylic acid group. This newly formed carboxylic acid can react with the epoxy resin, thus enabling the reaction to go further [15].

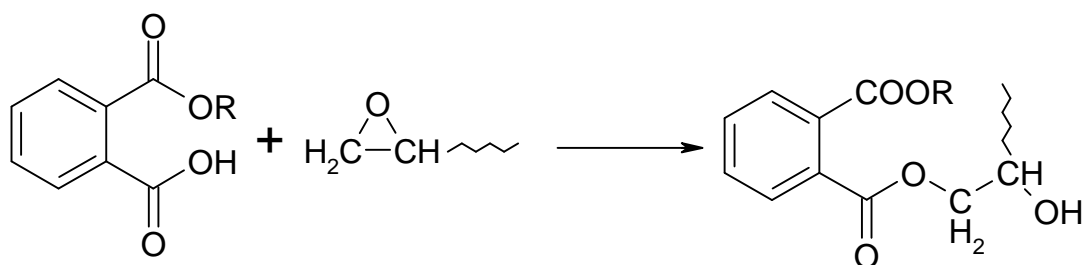


Figure 2.16 Reaction of carboxylic acid with epoxy resin

The etherification of the epoxy groups with hydroxyl groups can occur at this point. This is shown in figure 2.17

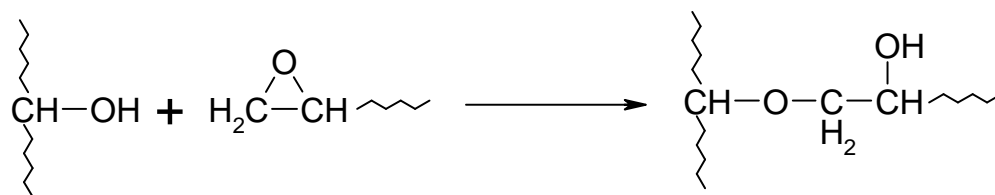


Figure 2.17 Etherification of epoxy groups with hydroxyl groups

Then, reaction of the monoester with the hydroxyls takes place, as shown in figure 2.18

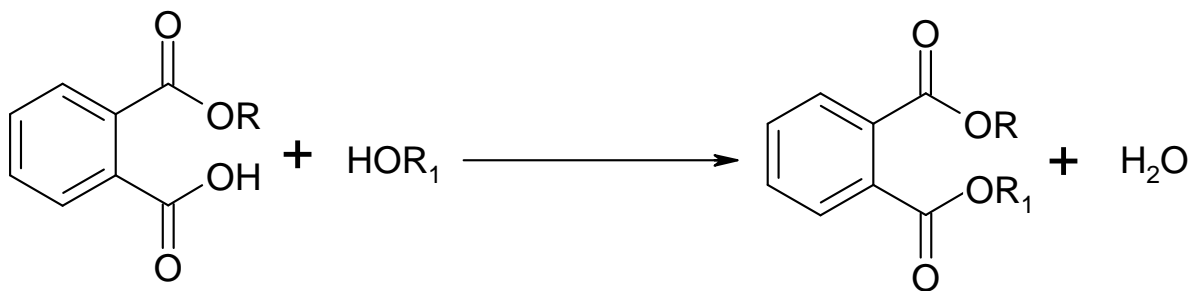


Figure 2.18 Reaction of the monoester with hydroxyl

The water released from the reaction of the monoester with the hydroxyl group can hydrolyse the anhydride to give a diacid as indicated in figure 2.19 below

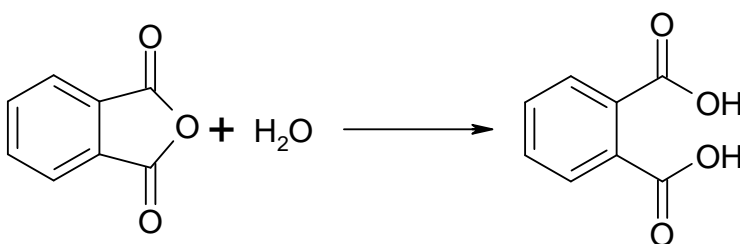


Figure 2.19 Hydrolysis of the anhydride to give a diacid.

Finally the monoester formed during reaction described in figure 2.19 above is again hydrolysed by water to give an acid and an alcohol as shown in figure 2.20 [15].

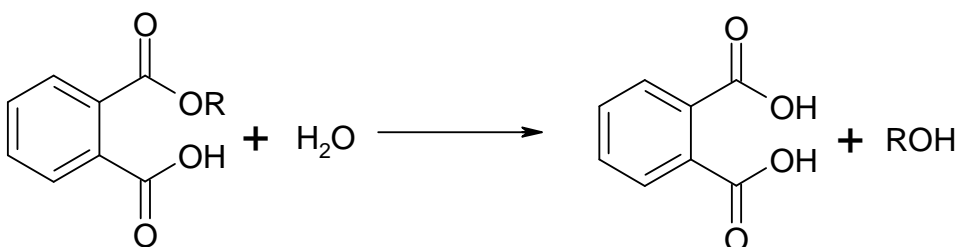


Figure 2.20 Hydrolysis of anhydride to give an acid and an alcohol

2.7 Araldite LY 5052 epoxy resin

Araldite LY 5052 consists of two chemical components. An epoxy phenol novalok resin (38 – 42% composition), and 1, 4 butanediol diglycidyl ether (55 – 68%) composition. The epoxy phenol novalak resin has a functionality of 4, and a molecular weight of 345 g mol⁻¹. 1, 4 butanediol diglycidyl ether has a functionality of 2, and a molecular weight of 202.3 g/mol. The chemical structures of epoxy phenol novalak and 1 4 butanediol doglycidyl ether are shown in the figures 2.21 and 2.22

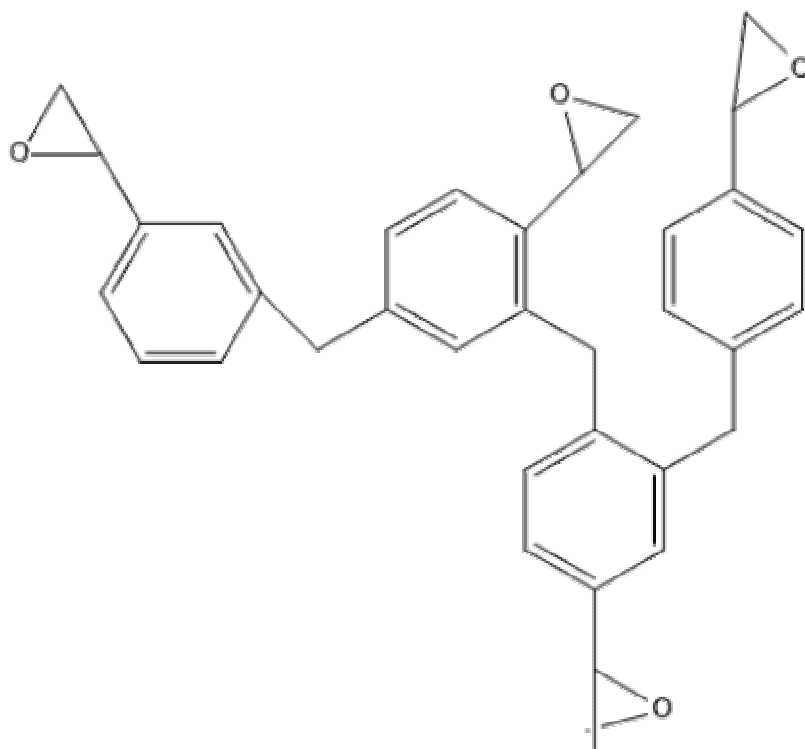


Figure 2.21 Chemical Structure of Epoxy Phenol Novalak Resin

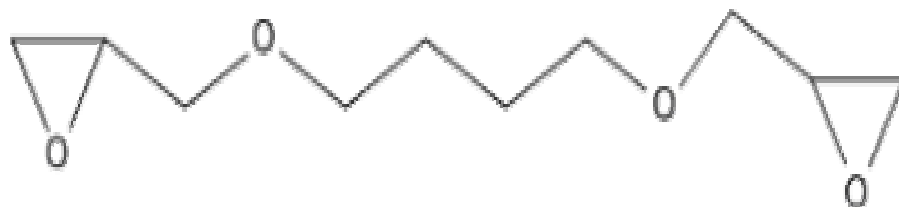


Figure 2.22 Chemical structure of 1 4, butanedioldiglycidyl ether

2.8 4,4' Diphenyl diaminosulfone

4,4' Diphenyl diaminosulfone is an aromatic amine powdered curing agent, light pink in colour. It has to be melted before being used in order to enable cure reaction to proceed with the epoxy resin [16].

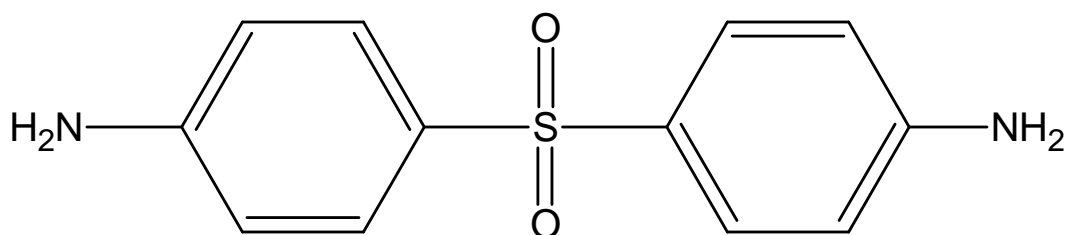


Figure 2.23 4,4' diphenyldiaminosulfone [4]

The table below shows the properties of diphenyl diaminosulfone [16]. The weight of active hydrogen (g mol^{-1}) is determined by calculating the molecular weight and dividing by the number of active hydrogen.

Table 2.1 Properties of diphenyl diaminosulfone [16]

Melting Point Peak ($^{\circ}\text{C}$)	175
Weight of active hydrogen (g mol^{-1})	57
Molecular weight (g mol^{-1})	248

2.9 Microwaves

Microwaves are electromagnetic waves which arise as radiation from electrical disturbances at high frequency [17]. The radiation aspects of electromagnetic power distribution are negligible at low frequencies, and it is necessary to consider electric charges, stored or flowing as currents, and potential difference. Increasing the frequency of the operation makes the radiation more important. The relative importance of radiation depends on the size of the circuit or system under consideration [17]. Any system of electric charges gives rise to electric and magnetic fields in the surrounding

space. The effects of these fields are generally ignored at low frequencies. However, at higher frequencies, the effect of these fields becomes more pronounced [17]. This is seen by the introduction of “stray” capacitance into circuit theory. At high frequencies, even a short length of wire acts as a radiation element, dissipating its electrical signals into surrounding space. The electromagnetic fields become the dominant factor in the study of electrical theory at high frequencies [17-19].

The characteristic wavelength of radiation is related to the frequency of the electrical signals by $\lambda = c / f$ where f is the frequency and c is the speed of light [17-19].

Microwave techniques are considered to cover those applications of electrical technology where the characteristic wavelength is smaller than the dimensions of the system or circuit and yet where it is not so small that only ray optical need to be considered. Microwaves are normally prominent in the range of frequencies between 10^9 to 10^{12} Hz, or a characteristic wavelength of 30cm to 0.3 mm. The components of conventional electronic circuits at this wavelength tend to behave like individual antenna, and dissipate their electrical signals as radiation [17].

2.9.2 Applications of Microwaves

Microwaves are becoming more and more widely used. Microwaves possess certain useful characteristics, among the most vital of these characteristics is the fact that microwave wavelengths are the same size as any structure which is used to enclose or guide them. Microwave pulses can be very short so they can be used for time or distance measurements. This makes them compatible with high speed computers. Microwaves can be used for heating and drying [17]. This is because microwave power is absorbed by water or any material containing water. Many molecular and atomic resonances occur at microwave frequencies and as a result, they are a necessary part of some scientific measurements. Some other applications of microwaves are given below [17].

- 1) **Broadcasting.** Television and radio originally used frequencies below the microwave range. However, reception has been made difficult for some listeners because of increasing congestion of the radio spectrum. There are no frequencies available for any large increase in broadcasting at radio frequencies.

Consequently, any further increase must occur at higher frequencies, which will be in the microwave region. Currently, 12 GHz is being used either for local television stations or for satellite television broadcasting. The domestic consumer has a microwave receiver on the roof as part of a small aerial and a radio frequency signal is transmitted along the aerial cable to the television set [17].

- 2) ***Microwave Heating.*** In most materials, the rate of microwave power absorption is proportional to its water content. This property can be used to provide microwave heating. Microwave power provides a most efficient means of applying heat uniformly throughout a body. This is because microwave signal penetrates most non-conductors. Microwave heating also reduces the time needed for heating a body to uniform temperature. This is because heat does not have to be conducted through the body but is generated through the body [17]. The rate of heating usually depends on the water content, thus microwave heating is a most efficient method of drying. Microwave heating is used in many process industries for heating, drying, sterilizing and curing. Microwave ovens are in use in many homes and catering establishments [17, 20, 21].
- 3) ***Moisture measurement.*** Microwave absorption by water means that moisture content measurement by microwaves is possible. The attenuation of a microwave signal in passing through the specimen is measured [17].
- 4) ***Radar.*** Radar is derived from the initial letters Radio Detection and Ranging. Radar is the traditional use of Microwaves. It started at the beginning of the Second World War. Microwave radiation penetrates fogs and clouds, travels in straight lines and gives distinct shadows and reflections. This enables it to be used for direction and distance measurements and in radar systems [17, 19, 22]. The simplest form of radar is the pulse radar giving a plan position indication (ppi) ; it measures the time for an echo to return. It operates by echo sounding with a narrow beam like a searchlight, and it is used for navigation. The Doppler radar or Carrier Wave (CW) gives a velocity indication; it is used in military operations because it is more difficult for an enemy to jam. The Carrier Wave also has many industry and consumer uses; it is used in industrial controls for

flow or velocity measurement. It can also be used for motion detection [17]. Microwave radiometry uses microwave radiation in the same way that photography uses light, and can give useful information about the object being observed such as the moisture content of soils and vegetation [17].

- 5) **Communication.** Microwave frequencies have to be used for satellite communications and for communications with satellites. This is because the microwave frequencies can pass through the ionosphere which is opaque to lower frequencies. The microwave communication channel has a very large bandwidth and it can accommodate thousands of telephone conversations or dozens of television channels at once [17, 22, 23].
- 6) **Microwave Power Transmission.** Since microwaves can be used directly for heating and exciting fluorescent lights, They have been advocated for electrical power distribution. This possibility is being actively investigated by using microwave transmission to generate satellite power to the earth. The satellite is powered with solar cells, and the microwave power generating valves operate in high vacuum without any glass envelope. The microwave power is then beamed to the earth where it is collected and rectified [20].

2.9.3 Electromagnetic fields

Any system of charges gives rise to its corresponding potential differences and to electric and magnetic fields. The precise mathematical relationships between the different electromagnetic field components and the electric charges and currents enable us to derive expressions for every precisely defined situation [17, 19]. Since the fields, currents and charges exist in the body of a medium, they are all defined in terms of some space distribution. The electromagnetic field components, together with their notation and their units of measurement are:

Electric field	E	volt/metre
Electric Flux density	D	coulomb/metre ²
Magnetic Field	H	ampere/metre

Magnetic Flux Density	B	tesla = weber/metre ²
Charge Density	ρ	coulomb/metre ³
Current Density	J	ampere/metre ²

2.9.4 Material Properties

Some of the field components are related by the properties of the medium in which they exist [17, 18]:

$$\mathbf{B} = \mu\mathbf{H} \quad 2.1$$

$$\mathbf{D} = \epsilon\mathbf{E} \quad 2.2$$

$$\mathbf{J} = \sigma\mathbf{E} \quad 2.3$$

Equation 2.1 is the relationship between the applied magnetic field and the resultant magnetic flux density. The constant μ is usually called the permeability of the medium [17]. In the S.I system of units, this is a dimensional constant. Its dimensions are given by the relationship

$$\mu = \frac{B}{H} = \frac{\text{weber}}{\text{metre}^2} \times \frac{\text{metre}}{\text{ampere}} \quad 2.4$$

$$\mu = \frac{(\text{volt})(\text{second})}{(\text{ampere})(\text{metre})} = \text{henry} / \text{metre} \quad 2.5$$

The permeability is a measure of both the relative effect of having a particular material in the field and also a dimensional constant, so that it can be divided into two parts [5]:

$$\mu = \mu_0\mu_r \quad 2.6$$

μ_0 is the permeability constant and this is dimensional. It is defined to be of the value $4\pi \times 10^{-7}$ henry / metre. It is also sometimes called the permeability of free space.

μ_r is the relative permeability. This is dimensionless and it makes allowance for the effect of the material relative to vacuum for free space.

A similar relationship between the applied electric field and the electric flux density **D** is shown in equation 2.2. ϵ is the permittivity of the medium [17-19]. It is also a dimensionless constant, and its dimensions are given by

$$\epsilon = \frac{D}{E} = \frac{\text{coulomb}}{\text{metre}^2} \times \frac{\text{metre}}{\text{volt}} \quad 2.7$$

$$= \frac{(\text{ampere})(\text{second})}{(\text{volt})(\text{metre})} = \text{farad / metre} \quad 2.8$$

The permittivity can be divided into two parts:

$$\epsilon = \epsilon_0 \epsilon_r \quad 2.9$$

ϵ_0 is the permittivity constant. It is also known as the permittivity of free space. Its definition is from the relationship for the speed of light and from the value of the permeability constant, which is approximately $(36\pi \times 10^9)^{-1}$. ϵ_r is the relative permittivity which is dimensionless. It takes account of the effect of the medium on the electric fields. This is the same as the dielectric constant of the medium [17].

In the solutions of the equations for the electromagnetic fields, the permeability constant and the permittivity constant are usually combined to provide a further two dimensional constants. They are

$$\text{The velocity of light } c = \frac{1}{\sqrt{(\mu_0 \epsilon_0)}} \approx 3 \times 10^8 \text{ m s}^{-1} \quad 2.10$$

$$\text{The impedance of free space } \eta = \sqrt{\left(\frac{\mu_0}{\epsilon_0}\right)} \approx 120\pi = 377\Omega \quad 2.11$$

The expression for the velocity of light is used in the definition for the permittivity constant given above.

Equation 2.3 is the conductivity relationship for the material. σ is the conductivity of the material. When the conductivity is a constant, it is an expression of Ohm's law. It is the reciprocal of the resistivity. With reference to equation 2.3, its dimensions are given by the relationship [23].

$$\sigma = \frac{J}{E} = \frac{\text{ampere}}{\text{metre}^2} \times \frac{\text{metre}}{\text{volt}} = \text{Siemens / metre} \quad 2.12$$

2.9.5 Maxwell's Equations

The relationships between the components of any electromagnetic field are given by Maxwell's Equations 2.13 to 2.16, and by the equations which represent the properties of the medium in which the electromagnetic field exists.

$$\nabla \cdot \mathbf{D} = \rho \quad 2.13$$

$$\nabla \cdot \mathbf{B} = 0 \quad 2.14$$

$$\nabla \times \mathbf{E} = -j\omega\mu\mathbf{H} \quad 2.15$$

$$\nabla \times \mathbf{H} = j\omega\epsilon\mathbf{E} \quad 2.16$$

Equation 2.13 is based on the fact that any stored electric charge gives rise to an electric field or conversely, any discontinuous electric field gives rise to electric charge. This is a mathematical statement of Gauss's law which states that the integration of the perpendicular component of the flux density over any closed surface is equal to the total charge enclosed by that surface [17, 18, 21].

Equation 2.14 is the magnetic form of Gauss's law in which there are no isolated magnetic charges. It states that magnetic field must exist in closed loops. There are no magnetic charges or single magnetic poles in nature. Most of the fundamental particles appear to be magnetic dipoles, but the total magnetic flux integrated over a surface enclosing a dipole is zero; hence equation 2.14 is valid.

Faradays law of electromagnetic induction, which states that the electromagnetic frequency induced in a closed circuit (the curl of the electric field) is proportional to the

rate of change of the magnetic flux threading the circuit [17]. This law is represented in equation 2.15.

Equation 2.16 is partly a statement of Biot – Savart law; which is also known as Ampere’s law. A current gives rise to a closed loop of magnetic field. It has also been found that a magnetic field exists around the air gap between the plates of a parallel plate capacitor which has a time – varying current flowing in its leads. Hence, the conduction current is not the only source of magnetic field. Maxwell solved this difficulty by postulating that the circuit which contains the capacitor must have a continuous series of current flowing around it [17, 19].

2.9.5 Plane Wave

A plane wave is the electromagnetic wave that propagates in unbounded free space. It starts from infinity, it goes to infinity, and it extends to infinity all round. A plane wave can not exist when any boundary conditions have to be considered. Practically, a plane wave is obtained when the source is a long distance away, and when any boundaries to the space are a long distance away [17]. Usually, light may be considered to be a plane wave in most practical situations, but at microwave frequencies, a true plane wave would only exist for signals which originate from a satellite or from another planet.

2.9.5.1 Characteristics of a Plane wave

A plane wave has the following characteristics [17, 21]

- i) It has no fields acting in the direction of the propagation
- ii) There is no variation of field in the plane perpendicular to the direction of propagation.
- iii) It has an electric field normal to the magnetic field.
- iv) Both fields act in a direction along the plane of the wave that is in a direction perpendicular to the direction of propagation;

Also, the electric and magnetic fields are in phase with one another and are directly related by the intrinsic impedance.

2.9.5.2 Wavelength of a propagating wave.

For any periodic waveform, the distance in which it repeats itself is the wavelength of the waveform. The field strength of a propagating wave is a function of both time and distance. It is therefore necessary to establish that the distance is measured at any instant of time [17]. The period of a wave can be defined as the time taken for the waveform to repeat itself at any one position in space.

Wavelength is the distance (measured in the direction of the propagation) between two points which are in the same phase in consecutive cycles of a wave. Wavelength is denoted by λ .

2.9.6 Basic Concepts of Microwaves

Microwaves are a form of electromagnetic radiation. The electromagnetic radiation spectrum covers a very wide range of frequencies in the region of 300 to 300,000 MHz. Two frequencies are commonly used for microwave heating. The frequencies are reserved by The Federal Communications Commission (FCC) for Industrial, Scientific, and Medical Purposes. The frequencies used for microwave heating are 0.915 and 2.45 GHz and they do not interfere with the frequencies used for telecommunications purposes.

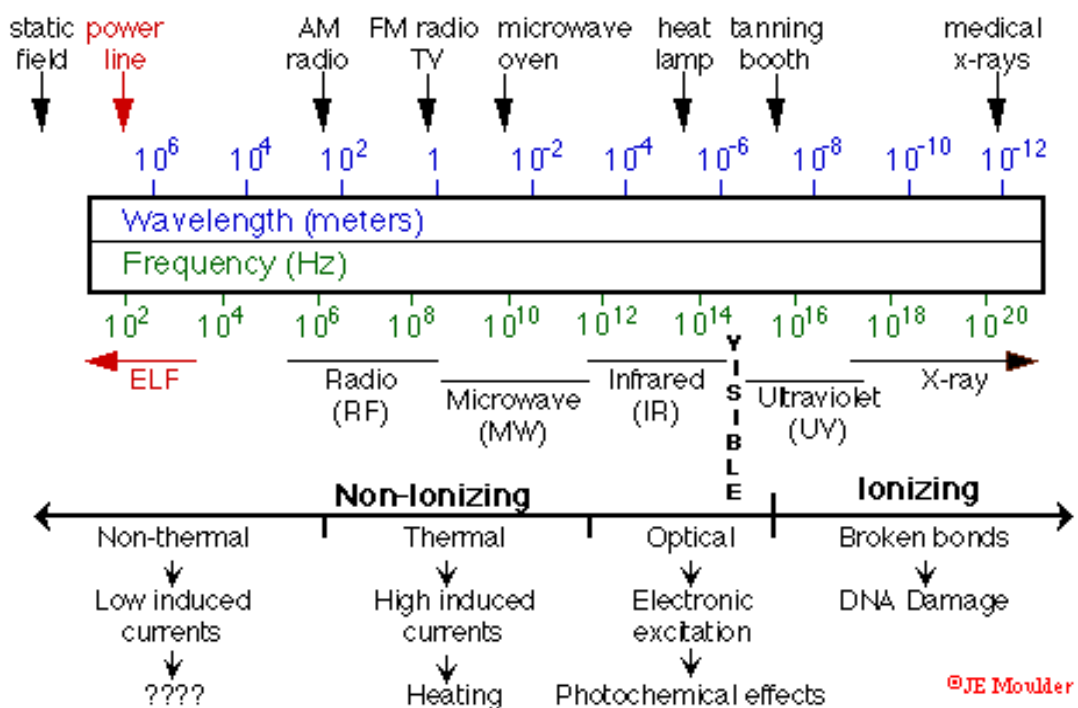


Figure 2.24 An electromagnetic spectrum [15]

Microwave heating uses the ability of some liquids and solids to convert electromagnetic energy into heat. It is based on the principle that a material can be heated by applying energy to it in the form of high frequency electromagnetic waves. An electromagnetic radiation consists of an electric field whose plane is perpendicular to the plane of a magnetic field. The microwave heating effect originates from the interaction of the electric field component of the microwaves with charged particles in the materials. A current will be induced through the material if the charged particles are able to move through the electric field. If the particles can not move because they are bonded to the material, they will simply rearrange themselves in phase with the electric field. This mechanism is called dielectric polarisation [21].

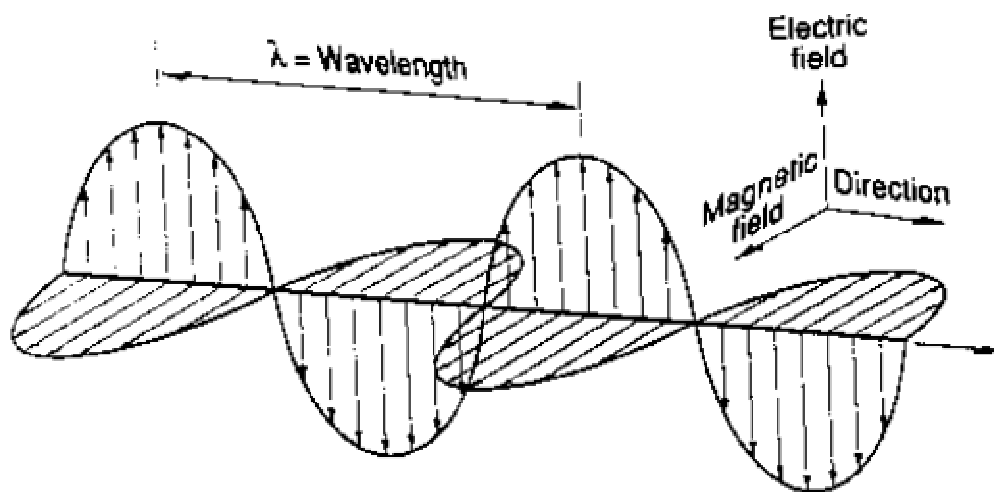


Figure 2.25 An electromagnetic wave [15].

Microwave ovens are used in a general frequency of 2.45GHz (12.3 cm wavelength) so they do not interfere with any other usual radiation [21, 24].

Microwaves are used for melting, drying, polymerisation, sintering, pasteurising. They are the main carriers of high-speed telegraphic data transmissions between stations on the earth and also between ground-based stations and satellites and space probes.

2.9.7 Microwave Heating Mechanism

There are two mechanisms through which materials respond to microwave processing. Depending on the material, the response mechanism can either be through Dipole rotation or Ionic conduction or a combination of both mechanisms.

-Dipole Rotation works on electrically neutral polar molecules with spatially separated positive and negative electric charges. The amplitude of the microwave field increases from zero in one direction, reaches a maximum, decreases to zero and then increases and reaches a maximum in the opposite direction. The molecules in the field respond by rotating their respective polar ends in the direction of the increasing amplitude. The resulting molecular friction generates heat, instantaneously and uniformly throughout the compound [15, 21].

In 2.45GHz microwaves, the oscillation of the electric field of the radiation occurs 4.9×10^9 times per second. The time scale in which the field changes is about the same as the response time (relaxation time) of permanent dipoles present in most organic and inorganic molecules. This fact represents a basic characteristic for an efficient interaction between electromagnetic field of microwaves and a chemical system [15].

-Ionic Conduction is the second mechanism for microwave heating. It generates heat through an induction phenomenon. The microwaves electrical field attracts the free ions of the compound. Collisions with non-ionised molecules occur, which gives up kinetic energy in the form of heat. The phenomenon is not dependent to any great degree on the temperature or microwave frequency [15, 21].

Materials differ in their reaction to the microwave field. Metals tend to reflect microwaves, a quality that enables them to be used as conduits or waveguides and as containers to hold, direct and apply microwave energy. Some non-polar compounds are transparent to microwaves and will not heat with, nor reflect microwave energy. These materials are often used as processing containers, particularly for liquids and as control windows [21, 25].

Materials that respond to and can be processed by microwave energy are composed of polar, ionised or conductive compounds. The key to the effectiveness of microwave heating is that the process is one of direct energy conversion. Treated material converts the microwave energy to heat within itself, eliminating the need to heat an oven as required in conventional processing.

Unlike thermal heating which involves heat conduction and thermal lag associated with it, microwave heating generates heat directly within the sample and because of this can offer possible advantages of higher efficiency, a faster production rate, lower capital cost, more uniform cure, and improved physical/mechanical properties over thermal heating [8].

The heating provided by microwave processing is more selective, more volumetric, faster and it is more controllable than thermal heating [26]. This higher process controllability removes the exothermic temperature excursion that occurs during the curing of thermosets.

Epoxy resins have been most widely looked into mainly because of their industrial importance, and also because their dielectric properties predispose them to effective microwave induced curing [27]. Amazingly, investigations have shown that the rate of curing depends more in the way microwave pulses are applied than in the total power applied. There have been results from experiments which indicate that the curing rate is not directly related to the sample temperature either [2, 28].

2.10 Advantages and Disadvantages of Microwave heating over Thermal heating

Microwave processing is able to quickly and controllably absorb energy for either cooking, dehydration or curing. The advantages microwave heating has over other heating methods are as follows [29].

- 1) Microwave offers fast heating rates, especially at temperatures higher than its glass transition temperature.

- 2) Microwave energy is directed at the material, and not through the containing vessels. As a result, microwave has minimal thermal lag effects[29].
- 3) Microwave heating minimizes thermal gradients. This results in more homogeneous cure, smaller thermal stresses, and minimal material degradation.
- 4) The microwave equipment takes up less floor space than conventional thermal equipment [29].

There are some limitations to the use of microwaves in the processing of polymers. These limitations are

- 1) Some materials are not transparent to microwaves. Materials that are susceptible to microwaves contain dipoles that are active in the applied frequency [29]. There are some materials such as polyolefins which are not active in the microwave field. This can be remedied by adding microwave susceptors to the material.
- 2) There must be further developments in the equipment design and manufacture of microwave equipment, especially for use in large scale production [29].
- 3) There are safety and lack of training issues in the use of microwave energy for materials processing.

2.13 Cure Kinetics

Chemical kinetics is the study of how quickly reactants are consumed and how products are formed [30]. It also looks into how rates of reaction respond to the presence of a catalyst, or to changes in the reaction conditions. This study of reaction rates enables us to understand the mechanism of the reaction [30]. Kinetics can also be defined as the modelling of the effects of temperature and time on the degree of cure of a thermosetting resin [31]. The scientist or the process engineer obtains important information from the cure kinetics of a resin. This information can be used to predict the

shelf lifetime of a thermosetting resin or composite. It can also be used to optimize processing conditions [31].

2.13.1 Isothermal vs Dynamic cure Kinetics

Using the differential scanning calorimeter, there are three different ways of determining the cure kinetics of a thermoset resins [31]. They are

- 1) Single Dynamic Heating experiment
- 2) Multiple Dynamic Heating experiments. This usually involves three or more heating rates.
- 3) Isothermal Heating experiments. This also usually involves three or more different temperatures [31].

Dynamic DSC measurements are in general, less time consuming and as a result they are more attractive than isothermal measurements, which have the disadvantage of being time consuming however, the highest degree of accuracy of can be obtained using the isothermal approach [31]. This is because isothermal conditions remove probable problems such as the occurrence of temperature gradients. Furthermore, the isothermal approach is acceptable for both standard (nth order) and autocatalyzed resins. Also, isothermal heating have a tendency to best simulate and copy the real processing conditions which are used to produce the final thermoset product [31]. Highly erroneous results can be obtained if the dynamic DSC approach is used to study the cure kinetics for autocatalyzed resins [31].

2.13.2 Standard (n-th order) and Autocatalyzed Kinetics Reaction

n-th order kinetics means that the material shows its maximum rate of cure at the start of the experiment (time=0) [31]. A reaction which follows nth order kinetics obeys the general rate equation:

$$\frac{d\alpha}{dt} = k(T) [1-\alpha]^n \quad 2.17$$

where $\frac{d\alpha}{dt}$ = reaction rate (sec⁻¹)
 α = fractional conversion
 $k(T)$ = specific rate constant at temperature T
 n = reaction order. (K)

Autocatalyzed systems are distinguished by the formation of some intermediate species which markedly accelerates the reaction. An autocatalyzed material will have its maximum heat of evolution at 30-40% of the reaction [32]. Epoxy systems used in the industry are an example of autocatalyzed systems.

An autocatalyzed reaction will follow the relationship below [32].

$$\frac{d\alpha}{dt} = k \alpha^m (1-\alpha)^n \quad 2.18$$

$$k = Z e^{-E_a/RT} \quad 2.19$$

Where $\frac{d\alpha}{dt}$ = reaction rate (sec⁻¹)
 K = rate constant (sec⁻¹)
 α = fractional conversion
 m, n = reaction orders (K)

2.13.3 Modelling of cure kinetics

A crucial step in the study of cure kinetics by DSC is fitting of the reaction rate profile obtained from either isothermal or dynamic experiments, to a kinetic model. There are essentially two forms of kinetic models used to describe thermoset curing reactions; empirical and mechanistic models [33]. Due to the complexity of the mechanistic models, the empirical kinetic method is more preferable for practical and comparison purposes. In empirical models, the whole reaction is considered as a single kinetic process, regardless of the different reactive processes or the different stages evolving within the system [34].

Empirical models are based on the assumption that the over all reaction rate, $\frac{d\alpha}{dt}$ can be expressed as [34]:

$$\frac{d\alpha}{dt} = kf(\alpha) \quad 2.20$$

where α is fractional conversion, $f(\alpha)$ is a function of fractional conversion, and k is the rate constant which obeys the Arrhenius relationship:

$$k = A \exp\left(\frac{-E_a}{RT}\right) \quad 2.21$$

where A is pre-exponential rate constant (i.e. also known as the collision frequency factor), E_a is the activation energy, R is the gas constant, and T is the absolute temperature.

The simplest empirical model corresponds to an n th-order equation:

$$\frac{d\alpha}{dt} = k(1-\alpha)^n \quad 2.22$$

where n is the reaction order. This model is applied to a curing system showing no autocatalytic phenomena and no complexity in the reaction mechanism [35].

In the case where the curing system exhibits autocatalytic effect, i.e. a maximum of the reaction rate is observed at some point other than the beginning of the reaction in an isothermal cure, the kinetic model given by equation 5.8 cannot be applied and consequently, the so-called autocatalytic model must be used. For an autocatalytic reaction in which the initial reaction rate is zero, the following equation is applied [36].

$$\frac{d\alpha}{dt} = k\alpha^m(1-\alpha)^n \quad 2.23$$

If the initial reaction rate is not zero, the autocatalytic model is given by [134]:

$$\frac{d\alpha}{dt} = (k_1 + k_2)\alpha^m(1-\alpha)^n \quad 2.24$$

where m and n are the reaction orders.

K_1 is the rate constant associated with the non-catalytic reaction, while K_2 is the rate constant associated with the autocatalytic reactions. K_1 and K_2 usually obey the Arrhenius relation. K_1 and K_2 are functions of temperature. m and n represent the reaction orders. m indicates how much of the curing reaction follows the autocatalytic path, while n indicates how much of the curing reactions follow the non-catalytic path. The introduction of these four parameters enable us to obtain a good fit to the experiment data. The values of m and n are found to vary from experiment to experiment. It is quite usual to assign a value of $m + n = 2$ when using the autocatalytic model. Some researchers have used this value [37] whereas others allowed it to float and the reaction orders were adjusted until the best optimisation of the kinetic parameters were obtained and the value of $m + n$ were reported to vary, for instance, from 1.0 [38] to 7.2 [39]. The autocatalytic model has been widely used by many researchers to study the reaction kinetics of various thermoset polymers including epoxy resins [35, 40], and urethane acrylate resins [41].

Although the empirical models are based on the isothermal experiments, several authors [34, 35] have demonstrated that these models are also valid in dynamic experiments with a simple modification of the rate equation (Equation 5.6) and that;

$$\frac{d\alpha}{dt} = \Phi \frac{d\alpha}{dT} \quad 2.25$$

where Φ is the linear heating rate.

2.13.4 Temperature Dependence of Reaction Rates

The rates of most chemical reactions increase as the temperature increases [30].

2.13.5 The Arrhenius parameters

The Arrhenius equation is named after the Swedish chemist Svante Arrhenius. In the 19th century, when data on reaction rates were accumulated, he noticed that there was a similar dependence temperature for almost all of the data [30]. He observed that a graph of $\ln k$ against $1/T$, where k is the rate constant for the reaction and T is the absolute temperature at which k is measured, gives a straight line with a slope which is typical of the reaction [30]. It was concluded that the rate constant varies with temperature. This conclusion can be represented mathematically as

$$\ln k = \text{intercept} + \text{slope} \times \frac{1}{T} \quad [30] \quad 2.26$$

This expression is normally written as the Arrhenius equation

$$\ln k = \ln A - \frac{E_a}{RT} \quad [30] \quad 2.27$$

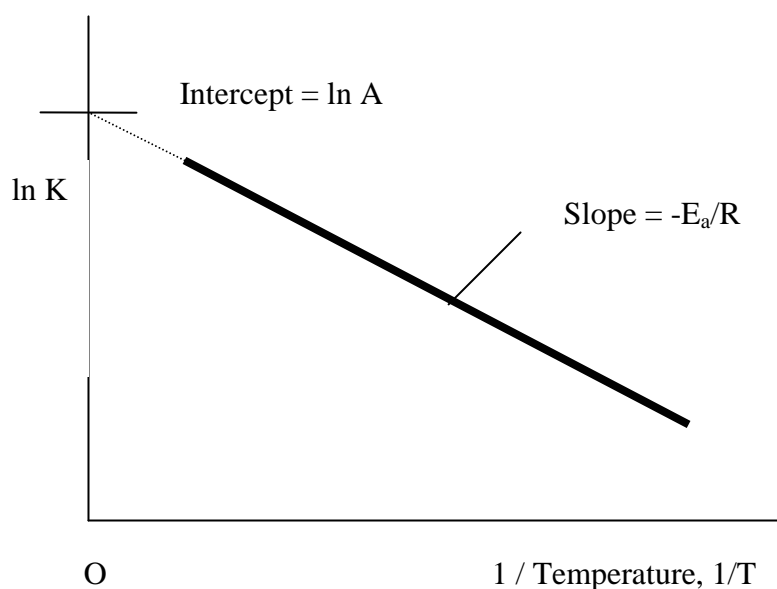


Figure 2.26 General form of Arrhenius plot

The figure above is the general form of an Arrhenius plot of $\ln k$ against $\frac{1}{T}$. The slope of the plot is equal to $-E_a/RT$, while $\ln A$ is the intercept at $\frac{1}{T} = 0$ [30].

Alternatively, the Arrhenius equation can be rewritten as

$$K = Ae^{-E_a/RT} \quad 2.28$$

Arrhenius defended the equation above by arguing that the temperature dependence of rate constants may be similar to the temperature dependence of rate constants [42].

E_a is known as the activation energy of the reaction, while A is the pre-exponential factor [30]. The activation energy of a reaction is the minimum amount of energy required for a chemical reaction to take place. It is a molar energy, and it has the units of kilojoules per mole. Practically, a reaction rate that is very sensitive to temperature will have a high activation energy, while a reaction rate with a low activation energy will only vary slightly with temperature [30]. Reactions with zero activation energy have a rate that hardly depends on temperature [30].

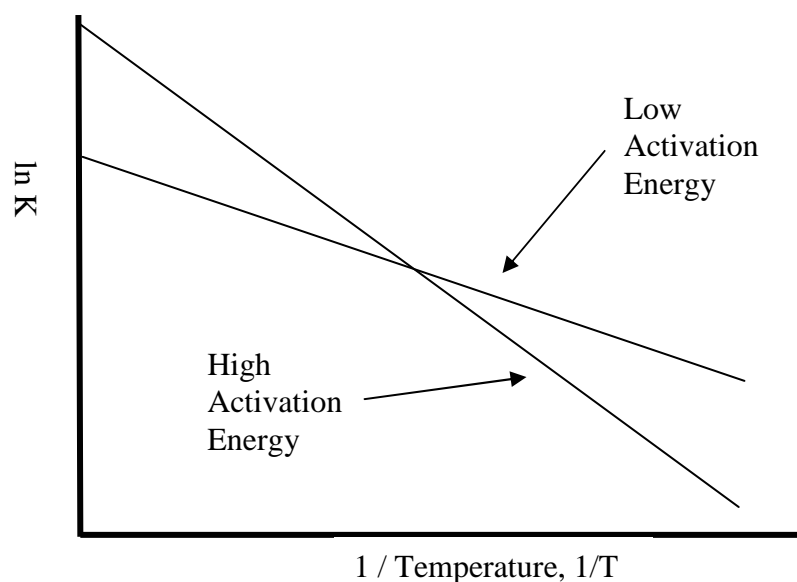


Figure 2.27 Arrhenius plots with different activation energies

The figure above shows two Arrhenius plots which have different activation energies. The plot with higher activation energy is steeper, and this is an indication that the rate of reaction is more sensitive to temperature [30].

It can also be noted that a low activation energy signifies a fast reaction, while a high activation energy is indicative of a slow reaction. As T increases, there is a rapid increase in k . This is mainly because there is an increase in the number of collisions whose energy exceeds the activation energy [12].

The pre-exponential factor A is defined as the constant of proportionality between the concentrations of the reactants and the rate at which the reactant molecules collide [12].

2.13.6 Degree of Conversion α and Reaction Rate $\frac{d\alpha}{dt}$

Epoxy resin curing is an exothermic reaction. For an exothermic reaction, if we assume that [34]

- 1) During curing the exothermic heat generated is proportional to the number of double bonds which have reacted in the system.
- 2) that maximum conversion is attained when all the bonds that can react have reacted
- 3) the rate of reaction during cure is directly proportional to the rate of heat generation,

At time t , it becomes possible to determine the degree of conversion α , and the reaction rate $\frac{d\alpha}{dt}$ at time t [15]. This can be determined by the following expressions.

$$\alpha = \frac{\Delta H_t}{\Delta H_R} \quad 2.29$$

$$\frac{d\alpha}{dt} = \frac{(dH/dt)_t}{\Delta H_R} \quad 2.30$$

Where $(\frac{dH}{dt})_t$ is the rate of heat generation and is directly related to the calorimetric signal at time t, and ΔH_R is the total reaction heat associated with the complete conversion of all the reactive groups, and ΔH_t is the heat released until time t. This can be obtained directly by integrating the calorimetric signal $\frac{dH}{dt}$ until the time t [15].

In order to calculate the reaction rate and the degree of conversion, it is important for us to understand how the calorimetric signal changes according to temperature or time. This depends on whether the experiment is dynamic or isothermal. It is also essential to quantify the reaction heat perfectly [15].

2.13.7 Methods of evaluating degrees of conversion and reaction rate

From a reaction's experimental heat of isothermal experiments, there are four different ways of ascertaining the degrees of conversion and reaction rates [34]. In the methods, α and $\frac{d\alpha}{dt}$ are defined according to equations 2.23 and 2.24. Also, α and $\frac{d\alpha}{dt}$ are obtained for the entire duration of the reaction. This allows us to use differential forms for the rate equation [34].

2.13.7.1 Method A

By integrating the calorimetric signal, the total reaction heat can be measured directly from the isothermal experiments. This is done at temperatures greater than those of complete curing, as long as all the heat generated during the reactive process can be detected by the calorimeter [15]. In this situation, α and $\frac{d\alpha}{dt}$ are expressed from equations 2.23 and 2.24 as

$$\alpha = \frac{\Delta H_t}{\Delta H_{iso}} \quad 2.31$$

$$\frac{d\alpha}{dt} = \frac{(dH/dt)_t}{\Delta H_{iso}} \quad 2.32$$

ΔH_{iso} is equivalent to the heat generated in an isothermal experiment. This can be evaluated by integrating the calorimetric signal until the process recovers the base line [15].

This method is not applicable if the material does not cure thoroughly at the cure temperature. If this is the case for the material after isothermal cure, a temperature scan detects a residual heat [15].

2.13.7.2 Method B

If a dynamic postcure up to high temperatures is carried out on a sample already cured isothermally, and a residual heat ΔH_{res} is obtained, this means that the isothermal reaction heat ΔH_{iso} is not the total reaction heat [15]. The total heat becomes the sum of the isothermal heat and the residual heat $\Delta H_{iso} + \Delta H_{res}$. Hence α and $\frac{d\alpha}{dt}$ will be recalculated with the following expressions [15].

$$\alpha = \frac{\Delta H_t}{\Delta H_{iso} + \Delta H_{res}} \quad 2.33$$

$$\frac{d\alpha}{dt} = \frac{(dH/dT)_t}{\Delta H_{iso} + \Delta H_{res}} \quad 2.34$$

2.13.7.3 Method C

If the sum of the isothermal and residual heat is less than the heat detected for the same reaction in a dynamic cure process, then method B can not be applied [34]. Since we can not know the total reaction heat by other procedures, then the dynamic heat ΔH_{dyn} can be taken as the total reaction heat, since experimentally, this is the maximum heat that can be detected [15]. Hence the degree of conversion and the reaction rate are defined as

$$\alpha = \frac{\Delta H_t}{\Delta H_{dyn}} \quad 2.35$$

$$\frac{d\alpha}{dt} = \frac{(dH/dt)_t}{\Delta H_{dyn}} \quad 2.36$$

2.13.7.4 Method D

If the sum of the isothermal reaction heat and the residual heat is lower than the dynamic heat, this means that either the isothermal heat or the residual heat detected is not correct, since their sum should be equal to the dynamic heat. This can be ascribed to that part of the heat that not be registered isothermally by the calorimeter at the beginning and the end of the reaction because it falls below the sensitivity of the apparatus, or because part of the heat is lost during the stabilization of the calorimeter [15] If the ΔH_{iso} calculated by the integration of the calorimetric signal is not correct, ΔH_t and $(\frac{d\alpha}{dt})_t$ will not be correct either. In this case, the dynamic heat will be taken as the total reaction heat, and ΔH_t and $(\frac{d\alpha}{dt})_t$ will be corrected, considering the part of the heat that has not been registered isothermally [15]. Taking into account these considerations, α and $\frac{d\alpha}{dt}$ are defined as

$$\alpha = \frac{\Delta H_t (\Delta H_{dyn} - \Delta H_{res})}{\Delta H_{iso} \Delta H_{dyn}} \quad 2.37$$

$$\frac{d\alpha}{dt} = \frac{(dH/dT)_t (\Delta H_{dyn} - \Delta H_{res})}{\Delta H_{iso} \Delta H_{dyn}} \quad 2.38$$

When this method is applied to the calculation of the last degree of conversion reached isothermally, that is to say when ΔH_t is equal to ΔH_{iso} , the degree of conversion has the value [34]:

$$\alpha = 1 - \frac{\Delta H_{res}}{\Delta H_{dyn}} \quad 2.39$$

2.13.8 Dynamic Curing

For dynamic curing, α and $\frac{d\alpha}{dt}$ can be directly calculated from equations 2.21 and 2.22.

The dynamic heat ΔH_{dyn} is used as the total reaction heat [34]. As curing is made at a constant linear heating rate, the heating rate relates the curing time and temperature [34].

2.13.8.1 Isothermal Kinetic Analysis

$$\frac{d\alpha}{dt} = kf(\alpha) \quad 2.40$$

Equation is the isothermal with which the kinetic study begins. α is the degree of conversion, the rate constant that depends on the temperature is k . $f(\alpha)$ is a function of the degree of conversion [34]. The dependence of the rate constant on the temperature is taken to follow the arrhenius law.

$$k = k_o \exp\left[-\frac{E}{RT}\right] \quad 2.41$$

where k_o arrhenius frequency factor, E is the activation energy, R is the universal gas constant, and T is the curing temperature.

2.13.8.2 Autocatalytic Model

The autocatalytic model follows the assumption that the whole reactive process can be integrated into a single reaction. This reaction has a single activation energy which is

maintained constantly throughout the curing process, and $f(\alpha)=(1-\alpha)^n\alpha^m$ [15]. Substituting $f(\alpha)$ in equation 2.40,

$$\frac{d\alpha}{dt}=k(1-\alpha)^n\alpha^m \quad 2.42$$

Taking logarithms,

$$\ln\left[\frac{d\alpha}{dt}\right] = \ln k + n \ln(1-\alpha) + m \ln \alpha \quad 2.43$$

In order to use an autocatalytic model to establish the cure kinetics, Isothermal cure is carried out at several temperatures using the DSC machine.

In order to use the autocatalytic model to establish the cure kinetics, isothermal DSC is carried out at several temperatures. The conversion and reaction rates are determined for the complete course of the reaction. The experimental results are finally adjusted with the kinetic equation. For each temperature, the rate constant and the reaction orders are obtained [15]. The activation energy and the frequency factor are obtained from the Arrhenius equation for the dependence of the rate constant on the temperature [15].

2.13.8.3 Isoconversional Adjustment

$$\ln t = A + E/RT \quad (\alpha=ct)$$

If we substitute the Arrhenius equation into the rate equation, and the equation is reordered and integrated between a curing time $t = 0$ where $\alpha = 0$ and time is t , with a degree of conversion α . If we take logarithms, we obtain

$$\ln t = A + \frac{E}{RT} \quad 2.44$$

Where A is a constant for each degree of conversion and it takes the following value

$$A = \ln \left[\int_0^d \frac{d\alpha}{f(\alpha)} \right] - \ln k_0 \quad 2.45$$

According to equation 2.44, the slope and intercept of the linear relationship $\ln t$ against T^{-1} gives us the activation energy and the constant A.

2.13.8.4 Isoconversional Adjustment

$$\ln \left(\frac{d\alpha}{dt} \right) = \ln [k_0 f(\alpha)] - \frac{E}{RT} \quad (\alpha=ct)$$

If we substitute the arrhenius equation 2.28 into equation and take the logarithms, we obtain the relationship below for a given degree of conversion.

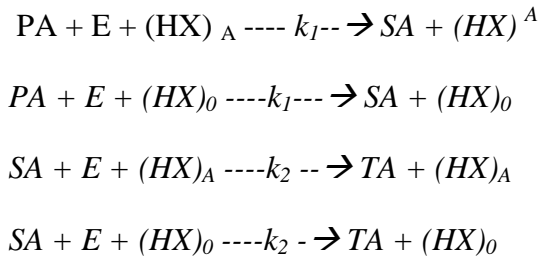
$$\ln \left[\frac{d\alpha}{dt} \right] = \ln [k_0 f(\alpha)] - \frac{E}{RT} \quad 2.46$$

According to the equation 2.46, we can obtain the activation energy E, and the constant $\ln [k_0 f(\alpha)]$ from the slope and the intercept of the linear relationship $\ln \left(\frac{d\alpha}{dt} \right)$ against T^{-1} for a constant conversion [15].

The advantages of the two isoconversional methods over the autocatalytic model are that

- 1) For a given degree of conversion, it is possible to determine the activation energy without the need to know $f(\alpha)$, since it has been assumed that regardless of the curing temperature, $f(\alpha)$ takes the same form for a given degree of conversion.
- 2) Isoconversional methods can be applied to different degrees of conversion to see how the reactive process evolves, and also to know if a single activation energy can describe the entire curing process, as is assumed in the autocatalytic model [15]

Generally, the kinetic models used with epoxy/amine resin systems were derived from a curing kinetics scheme which was proposed by Horie *et al* [43]. The scheme is shown below.



Where PA, SA, and TA are primary, secondary and tertiary amines. E is epoxide, $(HX)_0$ represents a hydroxyl group in the system as it is formed in the amine - epoxide addition reactions. At any time t, the rate of epoxide consumed is derived as;

$$\frac{dx}{dt} = (k_1'c_0 + k_1'x)(e_0 - x)(a_1 - ka_2) \quad 2.47$$

Where x is the concentration of epoxide consumed at a given time, c_0 and e_0 are the initial concentration of $(HX)_0$ and epoxide, a_1 and a_2 are the concentrations of primary amine and secondary amine and $K = k_2/k_1 = k_2'/k_1'$, the relative of reaction rate of secondary amine and primary amine with epoxide.

Sourour *et al* [44, 45] later proposed a kinetic model using Horie's reaction scheme and they assumed that under homogenous reaction conditions, the primary and the secondary amine were of approximately equal reactivity, and the concentration of (HX) was constant. The equation below expresses the total rate of consumption of epoxide.

$$\frac{dx}{dt} = k_1C(1-\alpha)(B-\alpha) + k_2\alpha(1-\alpha)(B-\alpha) \quad 2.48$$

In the equation 2.48, α is the degree of cure of epoxide reacted at time t, B is the initial ratio of diamine equivalents to epoxide equivalents, C is the concentration of (HX) molecules while k_1 and k_2 are the rate constants. If (HX) is assumed to be constant

throughout the reaction, then the product of k_1 and C is a constant, k_1 . Equation 2.48 can thus be rearranged as

$$dx/dt=(k_1 + k_2\alpha)(1-\alpha)(B-\alpha) \quad 2.49$$

which can also be rearranged as

$$\frac{d\alpha / dt}{(1-\alpha)(B-\alpha)} = k_1 + k_2\alpha \quad 2.50$$

Where $\frac{d\alpha}{dt}$ assumed to be $\frac{dx}{dt}$. Equation 2.48 predicts a linear relationship of the left side term with the degree of cure. Hence, parameters k_1 and k_2 can be determined by plotting $\frac{d\alpha / dt}{(1-\alpha)(B-\alpha)}$ against α . A cure study of DDR 332 / m-PDA was used to investigate the validity of this model . The results obtained showed that the model was consistent with isothermal DSC and rheological experiment data at the early stages of cure, after that, the model was noticed to deviate from the experiment data. This deviation was ascribed to the effect of diffusion control which occurred in the later stages of the reaction. Later on, equation was modified into equation 2.49 which is now known as the autocatalytic model which can be used to describe the cure of both bifunctional and multifunctional epoxy resins.

$$\frac{d\alpha}{dt} =(k_1 + k_2\alpha^m)(1-\alpha)^n \quad 2.51$$

k_1 is the rate constant associated with the non-catalytic reaction, while k_2 is the rate constant associated with the autocatalytic reactions.

2.14 Dynamic Kinetic Analysis

Dynamic Kinetic analysis involves three types of procedures. In the first type, the degree of conversion and the rate of reaction are obtained from a single experiment, and they are adjusted to some kinetic model, and all the kinetic parameters are obtained [15]. Although this procedure has the benefit of being fast, it is not usually recommended in complex reactions such as curing of thermosets. This is because it normally overestimates the value of the kinetic parameters [15]. Malek and Criado [46, 47] proved that if the real value of the activation energy is not known previously, the kinetic analysis from a single dynamic experiment.

The second procedure involves the determination of the variation in the temperature at a given conversion. In the third procedure, the peak exotherm temperature is varied according to the heating rate [15].

2.14.1 Kissinger's Method

Kissinger's method is another method which is applied to the curing kinetic analysis. [48]. Kissinger's method is based on the assumption that the exothermic peak coincides with the maximum reaction rate and uses an nth-order equation to describe curing kinetics. Equations 2.21, 2.22, and 2.25 were used to express an nth-order equation for dynamic curing. The expression is described below

$$r = \frac{d\alpha}{dt} = \Phi \frac{d\alpha}{dT} = A \exp\left(\frac{-E_a}{RT}\right) (1-\alpha)^n \quad 2.52$$

where r is the reaction rate. Since the maximum rate occurs when $\frac{dr}{dt} = 0$, differentiating Equation 2.52 with respect to time and equating the resulting expression with zero gives;

$$\Phi \frac{E_a}{RT_p^2} = An(1-\alpha_p)^{n-1} \exp\left(\frac{-E_a}{RT_p}\right) \quad 2.53$$

If we rearrange equation 2.53, and take the natural logarithms, we get;

$$-\ln\left(\frac{\Phi}{T_p^2}\right) = \ln\left(\frac{E_a}{RAn}\right) - (n-1)\ln(1-\alpha_p) + \frac{E_a}{RT_p} \quad 2.54$$

The activation energy can be determined from the slope of the straight line of a plot of $-\ln(\Phi/T_p^2)$ against $\frac{1}{T_p}$

2.14.2 Ozawa's method

Ozawa's method [49] was used to carry out a kinetic analysis of the epoxy systems. This method is based on isoconversional procedure and it does not require knowledge of the reaction rate equation, $f(\alpha)$. Ozawa's method is based on the assumption that regardless of the reaction temperature, the reactive process has the same mechanism of reaction for a given fractional conversion.

Researchers claim that this method has lead to a better understanding of the study of curing [50]. The autocatalytic model method studies the whole curing reaction as a single kinetic process. It does not take into account the different reactive processes or the different stages through which the system evolves. isoconversional kinetic method, on the other hand determines the activation energy for a given fractional conversion, which shows the different stages through which the reactive process proceeds [51].

For the kinetic analysis in dynamic curing experiments, the integral form of the rate equation is expressed as [20];

$$g(\alpha) = \int_0^\alpha \frac{d\alpha}{f(\alpha)} = \frac{A}{\Phi} \int_0^T e^{-(E_a/RT)} dT \quad 2.55$$

The value of the right-hand side of Equation 2.55 can be expressed by means of a polynomial function $P(E/RT)$ as;

$$\frac{E_a}{R} P\left(\frac{E_a}{RT}\right) = \int_0^T e^{-(E_a/RT)} dT \quad 2.56$$

Doyle's approximation for the polynomial function $P(E/RT)$, which is valid in the range $20 < E/RT < 60$ is expressed as [52];

$$\log P\left(\frac{E_a}{RT}\right) = -2.315 - 0.4567 \frac{E_a}{RT} \quad 2.57$$

In order to determine kinetic parameters in dynamic experiments, Equations 2.56 and 2.57 may be combined and rearranged as [53];

$$\log \Phi = \log\left(\frac{AE_a}{g(\alpha)R}\right) - 2.315 - 0.4567 \frac{E_a}{RT} \quad 2.58$$

Equation 2.58 which is also known as Ozawa's method is, for a given degree of conversion, a linear relationship between the logarithm of the heating rate and the inverse of the curing temperature. The activation energy, E_a , and the constant $[\log(AE_a/g(\alpha)R) - 2.315]$ can be determined from the slope and the intercept, respectively, of the linear relationship $\log \Phi$ against T^{-1} for a constant fractional conversion. For the kinetic analysis of the curing process equation 2.58 can be applied to different fractional conversion and can also be expressed as;

$$\log \Phi = A' - 0.4567 \frac{E_a}{RT} \quad 2.59$$

where $A' = [\log(AE_a/g(\alpha)R) - 2.315]$.

2.15 Previous work on Microwave vs Thermal Curing

Wei *et al* used microwave and thermal energy to cure diglycidyl ether of bisphenol A (DGEBA) / diaminodiphenyl sulfone (DDS) and a DGEBA / meta phenylene diamine (mPDA) [26]. They used Fourier Transform Infrared (FTIR) to measure the extent of cure, and thermal mechanical analysis (TMA) to determine the glass transition temperature (T_g). Their findings show that the reaction rate constants of the primary amine-epoxy reaction are equal to those of the secondary amine-epoxy reaction, and the

etherification reaction is negligible for both microwave and thermal cure for the DGEBA / mPDA system [26]. For the DGEBA / DDS system, the reaction rate constants of the primary amine-epoxy reaction are greater than those of the secondary amine- epoxy reaction; and etherification reaction is only negligible at low cure temperatures for both thermal and microwave cure [26]. They also found that particularly at higher isothermal cure temperatures, the vitrification time is shorter in microwave cure than in thermal cure for both the DGEBA / mPDA and DGEBA / DDS systems [26].

Navabpour *et al* used dynamic and isothermal curing methods to study the cure kinetics of a commercial epoxy resin system RTM6 using a microwave heated calorimeter and a conventional differential scanning calorimeter [54]. The resins cured isothermally using microwave heating were found to have larger values of preexponential factor and higher values of activation energy than resins cured using thermal heating [15]. It was observed that the reaction orders were similar for both microwave and thermal heating. This suggested that the mechanisms of curing were similar. For the dynamic curing, the data revealed that microwave cured resin had higher preexponential factor and activation energy than thermal curing. The two heating methods gave different reaction orders [15]. This result implied that the curing mechanisms using microwave and thermal heating are different [15].

Navabpour *et al* also carried out near – infrared spectra during dynamic curing of the resin, and they found out that there was more rapid reaction of the amine groups in microwave curing than in conventional curing of the epoxy resin [15].

Nesbitt *et al* also used dynamic and isothermal curing methods to compare the curing kinetics of diglycidyl ether of bisphenol-A (DGEBA) with HY917 (an acid anhydride hardener) and DY073 (an amine-phenol complex acting as an accelerator) using a conventional differential scanning calorimetry and a microwave heated power compensated calorimeter [55]. They found that dynamic microwave curing of the resin produced higher reaction rates and shorter cure times than conventional heating. Also, microwave cured samples had higher values of preexponential factor and activation energy than conventional curing [16]. The orders of the reaction for microwave and conventional heating methods were similar. The glass transition temperatures of the

resin cured using conventional heating was higher than resins cured using microwave heating for each heating rate used in curing the resin [16]. The activation energy obtained during isothermal curing of the resin using microwaves was lower than the activation energy obtained during conventional curing [16]. They also found that the glass transition temperature of the conventionally cured resin was higher than that of the microwave-cured resin [16].

Hill *et al* used fiber-optic FT-NIR spectroscopy to study the thermal and microwave cure process for the epoxy resin diglycidyl ether of bisphenol A DGEBA with 4,4'-diaminodiphenyl sulfone (DDS) and 4,4'-diaminodiphenyl methane (DDM) [4]. They found the rates of reaction of primary amine and secondary amine to be similar for microwave and thermal cure processes. They also concluded that there was no special effects of microwave radiation on the kinetic parameters of either the primary amine or the secondary amine reactions [17]. They also found both systems to be characterized by a negative substitution effect [17].

Wei *et al* used electromagnetic radiation and conventional heating using thin film sample configurations to cure stoichiometric mixtures of DGEBA / DDS and DGEBA / mPDA isothermally. The extent of cure was measured by Fourier transform infrared spectroscopy (FTIR), while the glass transition temperatures were measured directly from the cured thin film samples using Thermal Mechanical Analysis(TMA) [56]. Microwave radiation was observed to have stronger effects on the DGEBA / DDS system than the DGEBA / mPDA system. Compared to conventional heating, it was observed that there were significant increases in microwave cured DGEBA / DDS samples, while there were only slight increases in the microwave cured DGEBA / mPDA samples. After gelation, the microwave cured samples had higher glass transition temperatures than the thermally cured samples [18]. The magnitude of increase of glass transition temperature between microwave and thermally cured samples was much more significant in DGEBA / DDS system than in DGEBA / mPDA system [18].

Mijovic *et al* carried out an investigation into the cure kinetics of an epoxy formulation diglycidyl ether of bisphenol A and diaminodiphenyl sulfone (DDS) as curing agent. This investigation was carried out using microwave and thermal energy. They used

dynamic scanning calorimetry to measure and compare both the degree of cure, and the glass transition of samples cured in the thermal and microwave fields at the same temperature [28]. They found out that cure proceeded slightly faster in the thermal field than in the microwave field. They also observed that the glass transition temperature range was broader in the microwave field, initiating a probability that there is a difference in the cure mechanism of epoxy systems in the microwave and thermal fields [9].

Marand *et al* used in-situ measurements of microwave dielectric properties and infrared spectroscopy to compare reaction mechanisms of a DGEBA / DDS epoxy system undergoing isothermal cure at different temperatures using thermal and microwave heating [57]. Their findings revealed that the rate of cross-linking was much higher in samples cured by microwave radiation than samples cured thermally. At higher temperatures especially, this higher cross-linking rate appeared to lead to an entrapment of the unreacted epoxy and amine groups within the resin matrix, and in the microwave cured samples, this led to an overall lower degree of cure [19]. Marand stressed that his conclusions were limited to the epoxy systems he examined, and that in other molecular systems, acceleration of reactions by microwave energy may lead to overall faster reaction rates, void of the possibility of cross-linking reactions [19].

Wallace *et al* cured PR500 epoxy resin using a conventional oven and a commercial microwave oven. Modulated Differential Scanning Calorimetry MDSC, Dynamic Thermal Analysis, Infrared Spectroscopy, and solid-state NMR spectroscopy were used to compare the cured resins [58]. Their investigations showed that in microwave-cured samples, the epoxy-amine reaction is more dominant than the other possible curing reactions, including the epoxy-hydroxyl reaction. At the same degree of cure, Infrared spectroscopy revealed that the intensity of the hydroxyl and the amine bands was more in the thermally cured sample [58]. This indicated that during microwave cure, the amine-epoxy reaction was more dominant under these conditions. $-CH_2OH$ group is formed in the epoxy-hydroxyl reaction. Solid State NMR spectroscopy showed that there were a larger number of $-CH_2OH$ groups in the thermally cured sample, hence, the epoxy-hydroxyl reaction must be more dominant during the thermal curing process [20].

Wallace *et al* inferred that from the results of the IR spectroscopy, solid-state NMR and DMA, microwave curing of epoxy samples under these conditions lead to the increase of the amine-epoxy reaction compared to the epoxy-hydroxyl reaction, leading to a different network structure revealed by DMA. Wallace suggested that this could be responsible for the widening of the glass transition temperature which is commonly observed in microwave cured epoxy resins [20].

CHAPTER THREE

3.0 EXPERIMENTAL

3.1 Materials

Two commercial epoxy resins were used for this study. Araldite LY 5052 supplied by Huntsman UK and DLS 772 supplied by Hexcel UK. Araldite LY5052 has an epoxide weight equivalent of 148.33, while DLS 772 has an epoxy equivalent of 192.33. 4,4'-Diaminodiphenylsulfone (4,4'-DDS) was used as the curing agent for both epoxy resins. The resin and the curing agent were mixed with a magnetic bar in a beaker using a hot plate, and stirred with a stirrer until the 4,4'-diaminodiphenylsulfone dissolved in the resin.

The mixtures were blended at different stoichiometric ratios. Eight stoichiometric ratios were initially prepared. They were 0.5, 0.6, 0.7, 0.8, 0.9, 1.0, 1.1 and 1.2. The epoxy resin systems were cured using a DSC and a microwave heated calorimeter. The stoichiometric ratios which produced the highest glass transition temperature were used for subsequent experiments.

3.2 Resin Characterization

3.2.1 Density Measurement

Density is defined as how much mass is contained in a given unit volume. It is a measure of how “tightly” a material is packed together.

Absolute density (ρ) is defined as;

$$\rho = \frac{W}{V} \quad 3.1$$

Where W is the mass and V volume of the object [59].

The pycnometer method is one of the most common methods used for measuring the absolute density of macromolecule substances. The density is measured by determining the weight of a volume-calibrated pycnometer which is filled with a liquid of known density in which a certain quantity of the polymer sample is immersed. The sample volume equals the pycnometer volume minus the undispersed volume of liquid of known density [59].

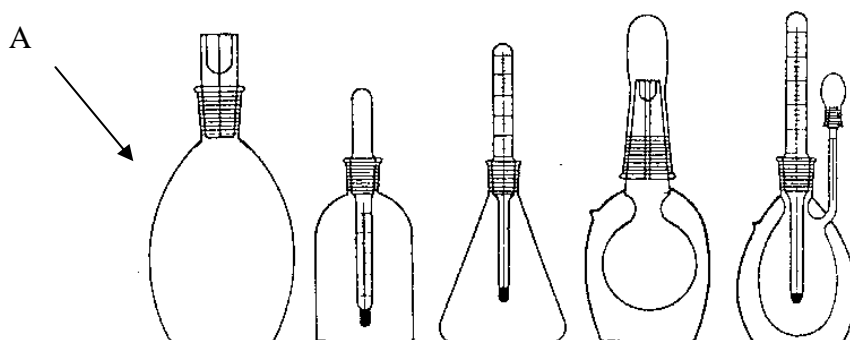


Figure 3.1 Different types of volume-calibrated pycnometers [59].

Pycnometer A in figure 3.1 was used for this research. The density measurements using the pycnometer method were carried out as follows [60].

- (i) The pycnometer was cleaned, dried and weighed to obtain dry weight (W_1). The pycnometer was then filled with distilled water and reweighed (W_2). The volume of the pycnometer (V_p) was calculated from the equation below.

$$V_p = (W_2 - W_1) / \rho_w \quad 3.2$$

Where ρ_w is the density of water.

- (ii) The pycnometer was then dried again and weighed (W_1). The pycnometer was again filled with the sample and reweighed (W_3).

$$\text{Mass of sample} = W_3 - W_1 \quad 3.3$$

- (iii) The pycnometer filled with sample and water was weighed (W_4)

$$\text{Mass of water} = W_4 - W_3 \quad 3.4$$

$$\text{Volume of water (V}_w) = (W_4 - W_3) / \rho_w \quad 3.5$$

$$\text{Volume of sample (V}_s) = V_p - V_w \quad 3.6$$

$$\text{Density of sample (}\rho_s) = (W_3 - W_1) / V_s \quad 3.7$$

Since the density measurements were carried out at room temperature (25°C), the density of water (ρ_w) used in this study was taken as 1.0 g/cm³. Several measurements were conducted on each sample to ensure that reliable results were obtained.

3.3 Curing Methods

A series of samples of stoichiometric ratios of epoxy resin systems Araldite LY 5052 / 4 4' DDS and Araldite DLS 772 / 4 4' DDS were cured using conventional and microwave heating techniques. Fully cured samples were prepared for the purpose of investigating the physical properties (e.g density, glass transition temperature) and also the mechanical properties. Also partially prepared samples were also prepared for Fourier Transform Infrared (FT-IR) analysis. The conventional and the microwave curing techniques are explained below.

3.3.1 Microwave Curing

A single mode cavity was used to carry out microwave curing of the epoxy resin system. Microwave curing was performed in a cylindrical brass, single mode cavity having a radius of 46.9 mm, and a length of 265.0mm. The cavity was at a frequency of 2.45 GHz in the resonant TM₀₁₀ mode. As shown in the figure 3.2 below, this cavity is designed to have its maximum electric field strength along the centre of the cavity axis. Figure 3.3 shows the schematic diagram of the microwave heating system. The microwaves are generated by a network analyser (Hewlett Packard 8714ET). A solid state amplifier (Microwave Amplifier Limited) was used to amplify the generated microwaves. This Amplifier has a maximum output of 200W. A GPIB interface between the network analyser and the computer was used to adjust the source power and the microwave frequency. The sample temperature was monitored using an Opsens

fluoroptic thermometer which was inserted through a small hole drilled at the top of the cavity. A small glass tube was used to protect the tip of the temperature probe. The thermometer was connected to a PID temperature controller manufactured by CAL Control Ltd., with a model number CAL 9500. This temperature controller was designed to give it the desired heating rate.

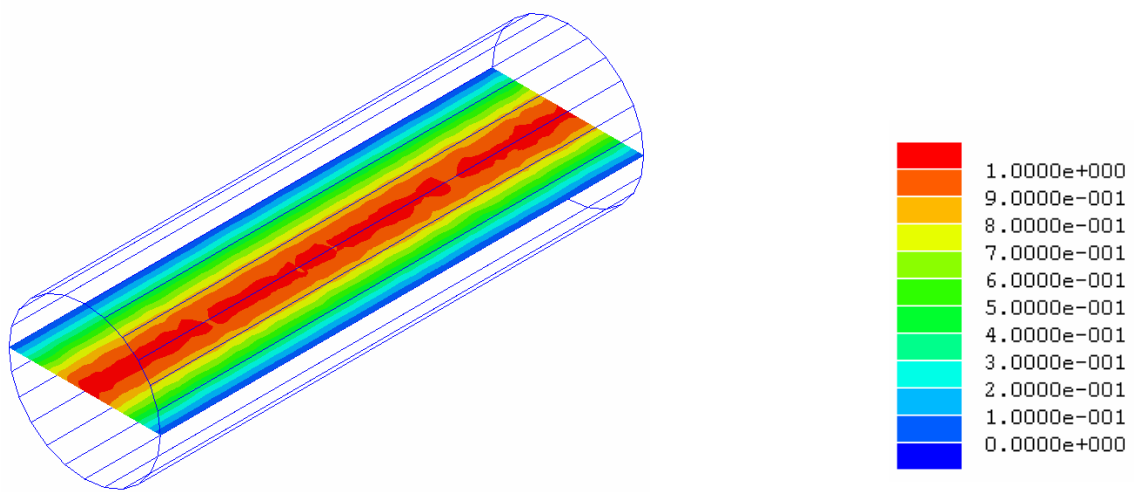


Figure 3.2 Simulated electromagnetic field patterns at 2.45GHz for TM010 mode microwave cavity with the presence of sample generated using Ansoft HFSS v8.5 simulation software. The colour scale shows the relative field strength generated inside the cavity [61]

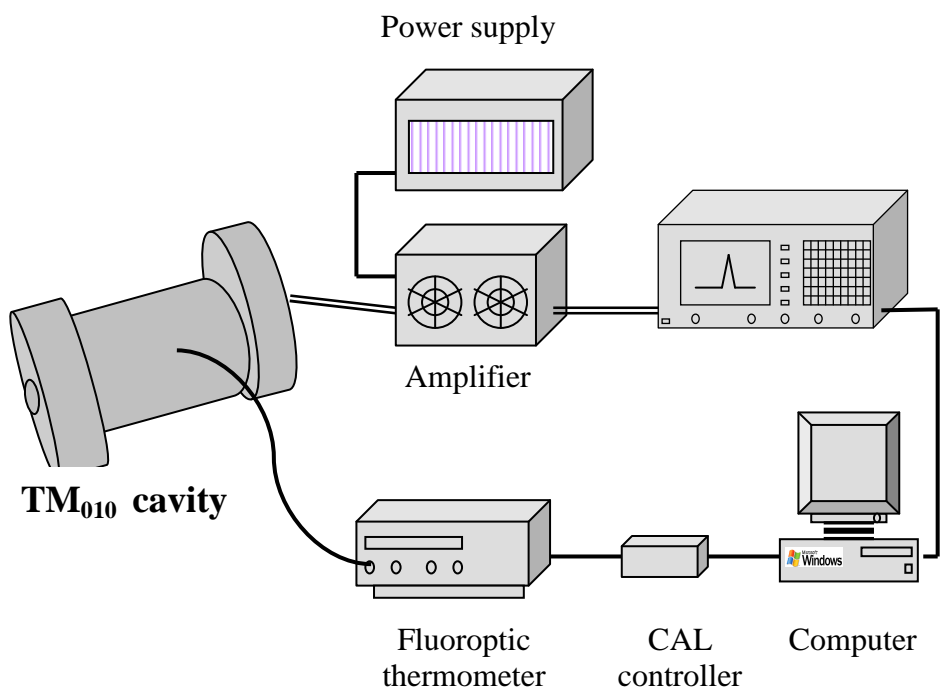
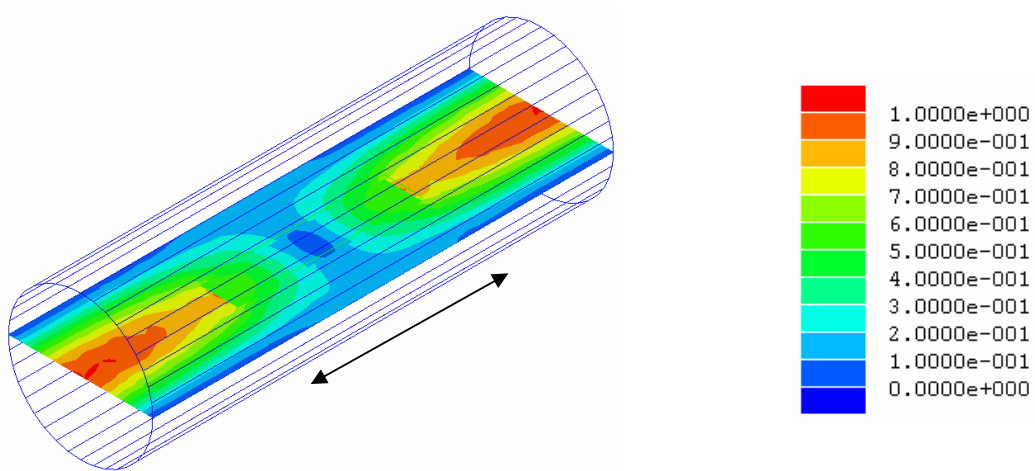
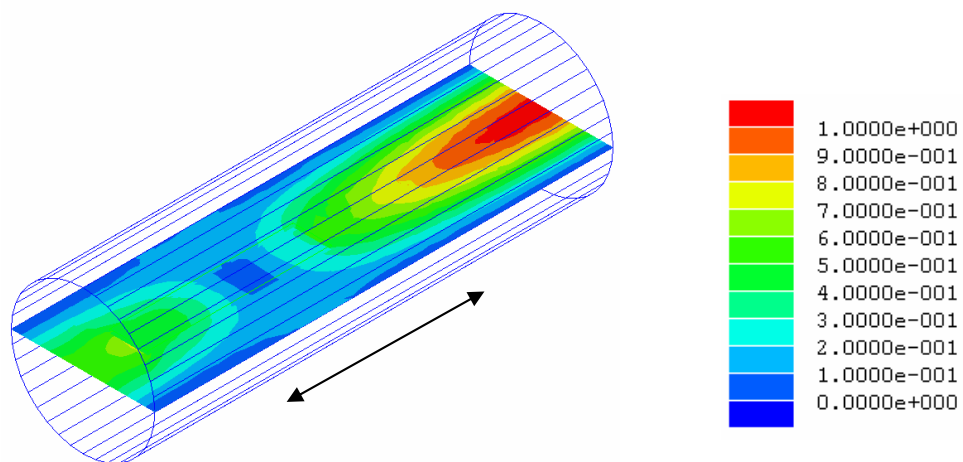


Figure 3.3 A schematic diagram of a microwave heating system using a single mode cavity operated in TM_{010} mode [61].

A sample was placed in the cavity, and a computer was used to numerically simulate the distribution of the electromagnetic field in the cavity (Ansoft; high frequency Structure Simulation, HFSS v.8.5). The simulated results showed that the sample placed in the cavity affected the electromagnetic field distribution. This is shown in figure 3.4 below [61]



a) The sample was placed in the centre of the cavity as indicated by the arrow

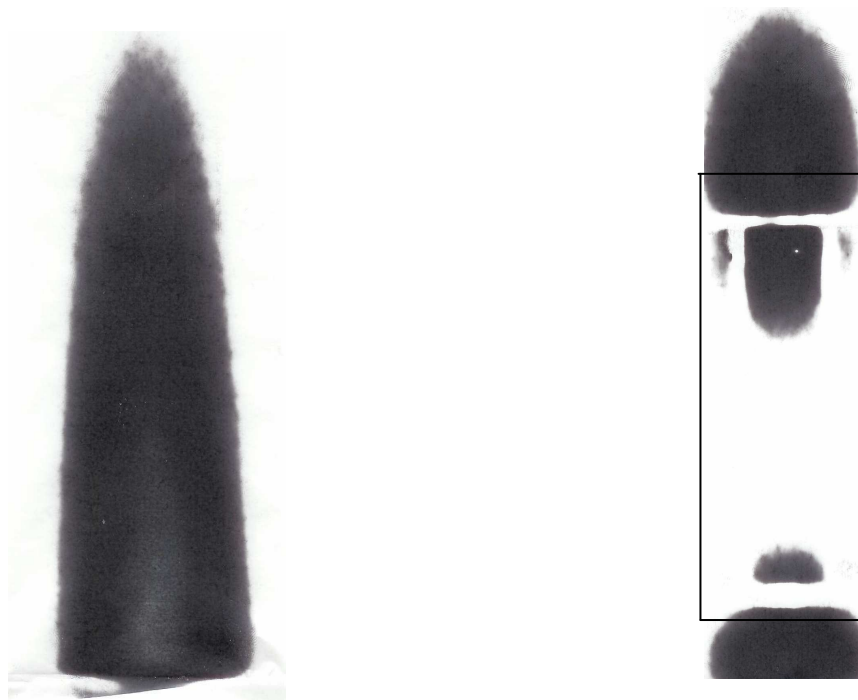


b) The sample was placed in the front area of the cavity as indicated by the arrow.

Figure 3.4 Simulated electromagnetic field patterns at 2.45GHz for TM010 mode microwave cavity with the presence of sample generated using an Ansoft HFSS v8.5 simulation software. The colour scale shows the relative electric field strength generated inside the cavity [61].

From figure 3.4 , we can see that the electromagnetic field distribution in the cavity was affected by the location of the sample. The distribution was uneven. Both ends of the sample mould were subjected to higher E field strength. The middle region of the sample mould was exposed to a lower E field. At the centre of the sample mould, there was very little or no electric field. This would suggest that it would be impossible to prepare a fully cured sample. The sample would be fully cured at both ends of the mould, but not at the centre of the mould.

In order to confirm the changes in the field distribution with the E field pattern obtained from the simulation software, the E field in the microwave cavity was investigated experimentally. The experiment was performed using a fax paper which turns black when it is exposed to heat. This attribute was used as an indicator to show the E field in the microwave cavity. The fax paper was cut into the dimensions of 46.9 x 265.0mm and placed in the cavity. The experiments were performed with and without the PTFE mould. The results are shown in the figure. The patterns shown on the fax paper after exposure to microwave radiation are in good agreement with the electromagnetic field pattern obtained from the simulation software. The E field distribution was altered by the presence of the PTFE mould. Figure 6(b) clearly shows that only the ends of the PTFE mould were exposed to significant electric field [61].



a) The cavity without the PTFE mould b) The cavity with the PTFE mould

Figure 3.5 The fax paper after exposure to microwave radiation. The line indicates the position of the PTFE mould inside the cavity [61].

A PTFE mould with dimensions 120mm length x 30mm breath x and 5mm height was designed to fit into the cylindrical cavity. Samples were prepared and poured into the mould. The PTFE mould was then placed in the centre of the cavity. The samples were programmed to heat from room temperature to 180 °C at 10 K min⁻¹. It was found that the sample exothermed before it attained its programmed temperature. This was attributed to the high heating rate used. At a much lower heating rate of 2 K min⁻¹, the sample fully cured without any exotherm.

3.3.2 Dynamic Scanning Calorimetry

Dynamic Scanning Calorimetry is a method of thermal analysis whereby power (heat flow) is applied to a sample pan and a reference pan, and the difference in power is monitored against temperature or time while the temperature of the sample is

programmed in a specified atmosphere [42]. DSC is one of the easiest ways of determining the cure kinetics of a resin [31].

There are two types of DSC:

1. **Power – Compensated DSC**:- In power compensated DSC, the sample and the reference are heated by separate heaters. The temperature difference is kept close to zero, while the electrical power which is required to maintain equal temperatures ($\Delta p = \frac{d(\Delta q)}{dt}$) is measured [42]

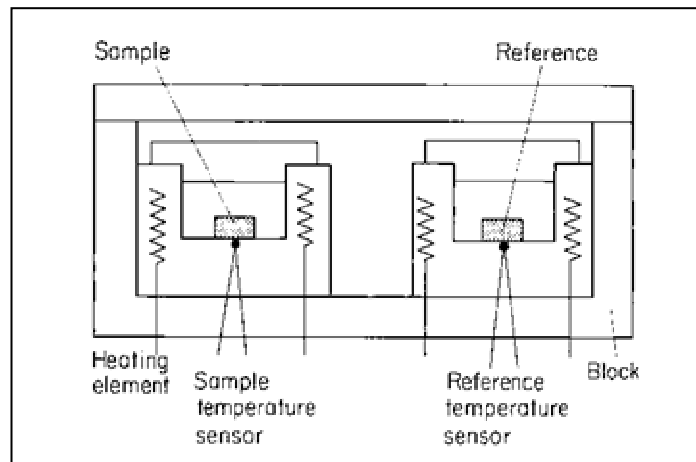


Figure 3.6 Schematic of the arrangement of power compensated DSC [61].

2. **Heat Flux DSC**:- Unlike the power compensated DSC, the sample and the reference are heated from the same source and the difference in temperature ΔT is measured. A calorimetric sensitivity is used to convert the temperature difference into a power difference Δp [42].

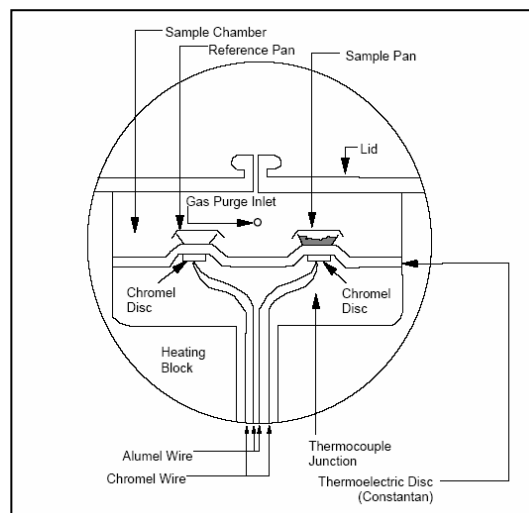


Figure 3.7 Schematic diagram of the sample chamber of a heat flux DSC [61]

The power compensation DSC is more ideal for carrying out isothermal cure studies of thermosetting resins. This is because the low mass furnaces provide low thermal inertia and a fast response time [31]. This enables the uncured resin to be heated ballistically to the target temperature from room temperature at a heating rate of 400 – 500 K per minute. This quick response time enables the power compensation DSC to quickly “lock in” on the isothermal target temperature and equilibrate [31]. This gives the best possible isothermal cure peak and it minimizes the risk that the cure data will be lost, especially at the very crucial beginning portions of the isothermal experiments which is very crucial [31]. Also, the sample temperature is maintained constant, rather than it being at a higher temperature than the control temperature because of the exotherm during cure.

Compared to the power compensation DSC, Heat flux DSC devices have a very slow and apathetic responsiveness. This is due to their larger furnace, which does not allow the heat flux DSC to heat up and bring to equilibrium as rapidly as power compensation DSC. As a result of this, important data will be lost when performing isothermal cure studies with heat flux DSC.

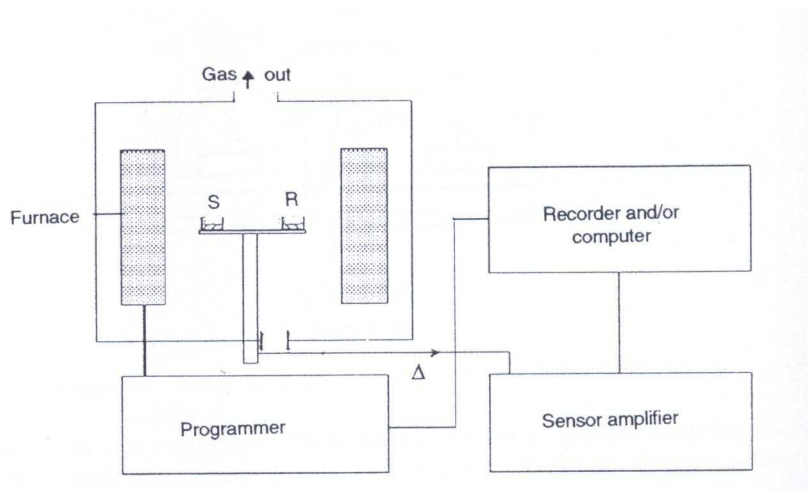


Figure 3.8 Schematic diagram of DSC apparatus [42]

3.3.3 DSC System

The major parts of a DSC system are

1. The DSC sensors plus amplifier.
2. The furnace and temperature sensor
3. The programmer or computer
4. The recorder, plotter or data acquisition device.

3.3.3.1 DSC Sensors

Many DSC units use thermocouples as sample and reference sensors. This is shown in figure 3.9 [42]. Copper-constantan or Chromel –Aluminium have been used for low temperatures, while Pt-Pt/13% Rh also has been employed [42]. In diagrams (a) and (b), single thermocouples are in contact with the sample, but in types (c) to (e), they are outside the sample. As shown in (d) and (e), multiple thermocouples are sometimes used to increase the signal. Sometimes, heat is conducted to the pans through a conducting metal disc. The power compensated DSC is an exception because the sensors are platinum resistors, and power is separately supplied to the sample and the reference [42].

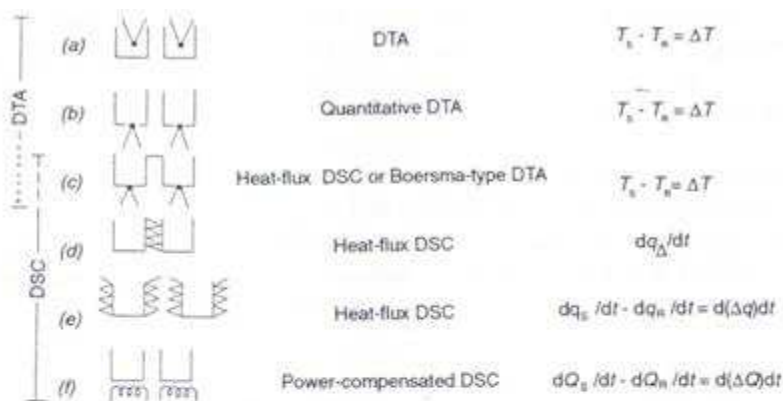


Figure 3.9 Series illustrating different types of DSC and DTA [42]

Aluminium pans are commonly used for DSC measurements. Care should be taken to ensure that they are used below the melting point of aluminium which is about 660°C, and they are not attacked by the samples [42].

3.3.3.2 The Furnace and controller

A resistance heated furnace enclosure of silver is used in many small DSC systems. Silver is used because it has a very high thermal conductivity, and this ensures that there is uniform temperature [42].

A range of between 0 – 500 K min⁻¹ is used as heating rates, but 10 K min⁻¹ is normally used. DSC is also used below room temperature. For this purpose, a cooling accessory or a refrigeration unit is fitted around the cell. The system can then be cooled directly with liquid nitrogen or other coolants. It is important that dry purge gas is passed through the cell assembly during cooling, otherwise ice may condense onto the cells [42].

3.3.4 Applications of DSC

DSC has a wide range of applications. DSC applications may be divided into physical changes and measurements, such as melting, crystalline phase changes, phase diagrams, heat capacity, thermal conductivity, glass transitions, liquid crystalline states, diffusivity and emissivity. Chemical reaction applications are dehydrations, polymer curing, glass formation, oxidative attack [42].

3.3.5 Calorimetric Measurement

Conventional curing of the epoxy resin systems Araldite LY 5052 / 4 4' Diaminodiphenylsulfone and DLS 772 / 4 4' Diaminodiphenylsulfone were conducted “*in-situ*” using a Perkin- Elmer Pyris 1 power compensation DSC.



Figure 3.10 A Perkin- Elmer Pyris 1 power compensated DSC

Dynamic heating was performed from 40 to 330 °C at heating rates of 2, 5, 8, 10 and 15 K min⁻¹. Samples with weights in the range 1-5 mg were sealed in aluminium sample pans. These pans contained a small hole in the lid. This small hole was designed to prevent large pressures from building up in the pan.

The differential scanning calorimetry (DSC) technique is the most widely used approach for measuring reaction kinetics of thermoset polymers. DSC has the advantages of being simple to use and it has few limitations. It can also provide simultaneous information regarding the kinetics, heat of reaction and thermal properties [62]. Generally, the reaction kinetics can be studied under both isothermal and dynamic conditions. In this research, both were used to investigate the two epoxy systems

3.3.5.1 The overall conversion and reaction rate

During the study of the curing kinetics of thermosetting resins with the use of DSC, the reaction rate $\frac{d\alpha}{dt}$ is assumed to be directly proportional to the rate of evolution of heat,

$$\frac{dh}{dt}$$

The expression below is used to determine the reaction rate [63].

$$\frac{d\alpha}{dt} = \frac{1}{\Delta H_T} \frac{dH}{dt} \quad 3.8$$

Where the rate of heat generation, $\frac{dH}{dt}$ is the ordinate of a DSC trace and ΔH_T is the total heat of reaction.

At any temperature during dynamic curing, and at any time during isothermal curing, the fractional conversion is given by [64]

$$\alpha = \frac{1}{\Delta H_T} \int_{T_0}^T \frac{dH}{dt} \delta t \quad 3.9$$

The lower bound of the integration is the lowest temperature at which the evolution of heat begins. If the total area enclosed under the DSC thermogram is integrated, the total heat of reaction released during the reaction (ΔH_T) will be obtained. The total heat of reaction which is obtained as the area of the DSC thermogram is assumed to represent the total heat of polymerisation. Hence, for dynamic conversion, a 100% conversion is achieved in all curing reactions performed using different heating rates [64].

Before equation 3.8 can be integrated, the baseline from which the integration has to be performed needs to be established. The problem of sample background correction arises from the fact that the specific heat of the system changes continuously during the thermal event (i.e., melting or curing) from the level of the initial substances (reactants) to the level of the final product. In order to obtain the net effect due to the thermal event, the course of the heat capacity changes should be subtracted from the data corrected for the instrument baseline. An expression which includes the changes in the specific heat due to the degree of cure using the thermal response of the material before and after any thermal event was constructed by Bandera et al [65]. The expression is written below

$$F(t) = \alpha\{P_2(t) - P_1(t)\} + P_1(t) \quad 3.10$$

From the expression above, $F(t)$ is the sample background which is to be calculated, t is the time coordinate, which is proportional to temperature for constant heating rate; α is the current fractional conversion. It is also the partial concentration of the product. $P_1(t)$ is the DSC signal for the initial substance in the absence of the event which can be estimated through linear extrapolation of the portion of the total curve before the thermal event; while $P_2(t)$ is the DSC signal for the product alone which can be estimated through linear extrapolation of the portion of the total curve after the thermal event.

The current fractional conversion is defined by the expression [65]

$$\alpha = \frac{\int_0^t \{G(t) - F(t)\} dt}{\int_0^{t_{end}} \{G(t) - F(t)\} dt} \quad 3.11$$

Where $G(t)$ is the total signal corrected for the instrument background and t_{end} is the time of the termination of the thermal event.

If we substitute equation 3.11 into equation 3.10, we will get

$$F(t) = \frac{\int_0^t \{G(t) - F(t)\} dt}{\int_0^{t_{end}} \{G(t) - F(t)\} dt} \{P_2(t) - P_1(t)\} + P_1(t) \quad 3.12$$

3.3.6 Microwave curing

For microwave curing, the calorimetric measurements were conducted in a microwave heated calorimeter. Figure 3.11 shows the schematic diagram of the microwave heated calorimeter. The microwaves were generated by a network analyser (Hewlett Packard 8714ET). A solid state amplifier (Microwave Amplifier Ltd) was used to amplify the generated microwaves. The microwave frequency and the source power were adjusted by a GPIB interface between the network analyser and a computer. A directional coupler was used to feed the output from the amplifier to a microwave cavity. The directional coupler also enabled the reflected signal to be monitored. A power sensor

(Anritsu, MA2472B) measured the transmitted and reflected powers. The transmitted and reflected powers were measured by a computer through a GPIB interface. The sample temperature was measured using a fluoro optic fibre sensor and thermometer (Luxtron Corp. Ltd, Model 790). The thermometer was connected to a PID temperature controller (CAL Control Ltd., Model CAL 9500), which was programmed to give the desired heating rate

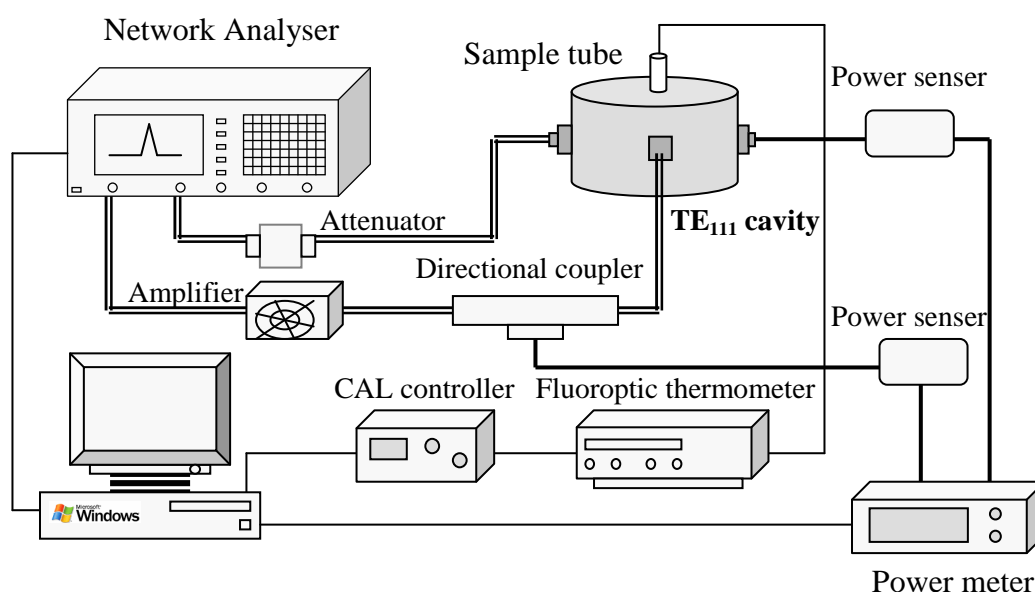


Figure 3.11 A schematic diagram of a microwave-heated calorimeter [61]

A cylindrical brass, single mode microwave cavity with a radius of 58mm and height of 77 mm was used as the heating cell of the calorimeter. The cavity was operated at a frequency of 2.45 GHz in the TE₁₁₁ mode, which was designed to have the maximum electric field strength at the centre of the cavity as shown in the figure 3.12. The samples were placed in 10 mm diameter Pyrex test tubes and inserted in the centre of the cavity. This location gave the highest electrical field strength. The sample tube was held in place with a PTFE support on the top of the cavity. A relatively small volume (approx 0.3ml) of sample was used for each microwave cure. This amount was used in order to prevent an excessive build up of heat in the sample leading to a highly exothermic reaction [61]. The Opsens fibre optic temperature probe was inserted in a 1.5mm diameter capillary tube and placed into the centre of the sample. The

arrangement of the sample tube and temperature probe inside the microwave cavity is illustrated in Figure 3.9. For calorimetric analysis, the sample was dynamically cured in the microwave-heated calorimeter from ambient temperature to 330°C at heating rates of 2, 5, 8, 10, 15 K min⁻¹

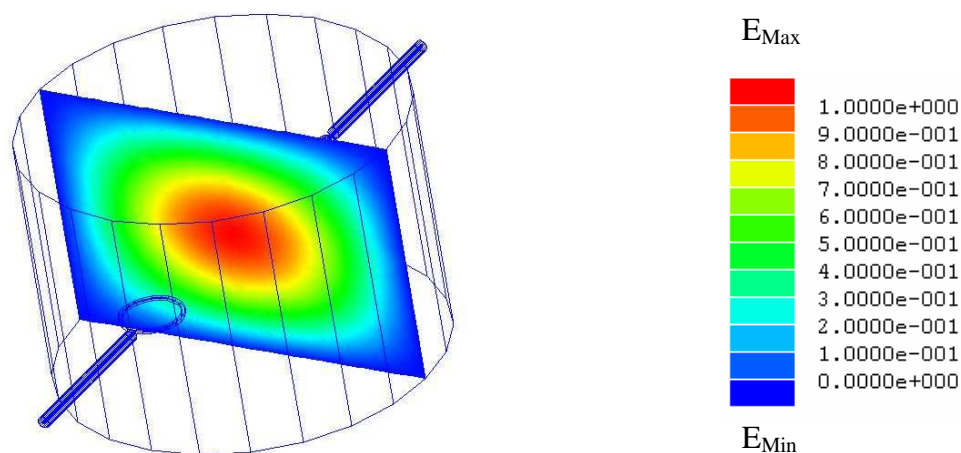


Figure 3.12 Simulated electromagnetic field patterns at a frequency of 2.45 GHz for TE₁₁₁ mode microwave cavity with the presence of sample generated using Ansoft HFSS V8.5 simulation software. The colour scale shows the relative electric field strength generated inside the cavity [61].

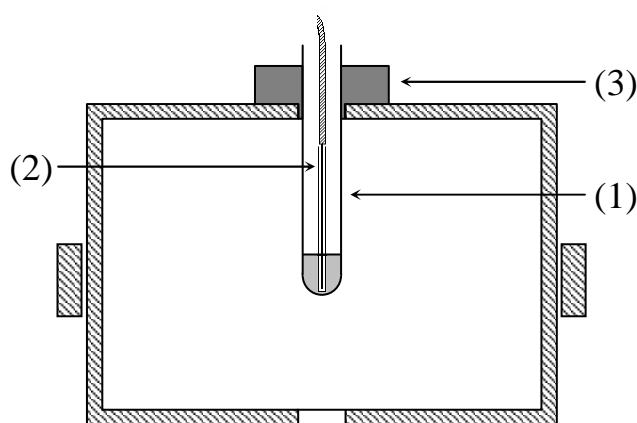


Figure 3.13 The vertical plane of the microwave cavity showing the arrangement of sample tube and temperature probe; (1) is the sample tube, (2) indicates the temperature probe and capillary tube while (3) is the PTFE support used to hold the sample tube in the cavity [61].

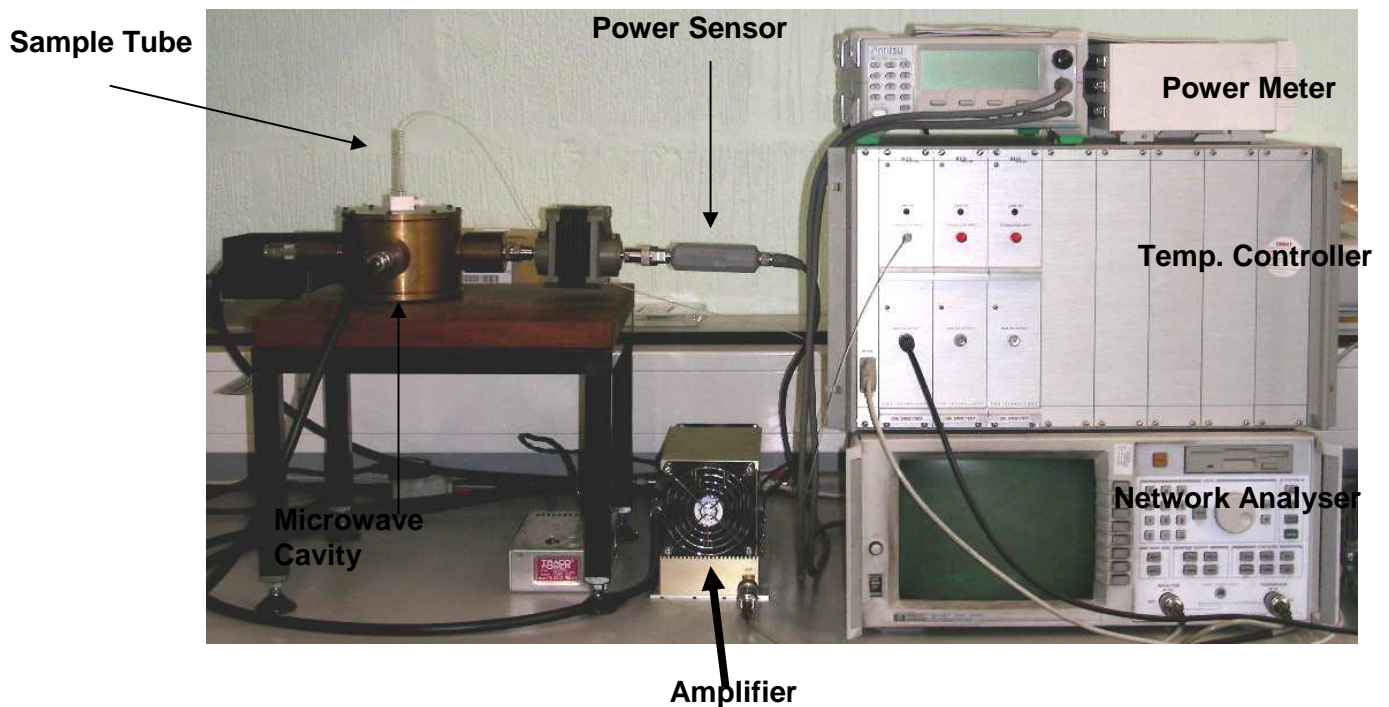


Figure 3.14 Microwave Heated Calorimeter used for research.

During the microwave curing, the variation of the amount of power required to maintain a particular heating rate is related to the changes in enthalpy which are associated with some processes such as chemical reactions. During an exothermic reaction, a lower amount of energy will be needed to maintain the temperature of the sample at its program set point. As a result of this, the power required for heating the sample will decrease. On the other hand, during an endothermic reaction where energy is needed to be absorbed in order to maintain the temperature of the sample at its program set point, the power required for heating the sample will increase [66]. An exothermic reaction will be expected for the curing of an epoxy resin because the free radical cross-linking reaction of an epoxy thermoset polymer involves the release of a large amount of heat. Figure 3.15 shows a typical data obtained from the microwave-heated calorimeter.

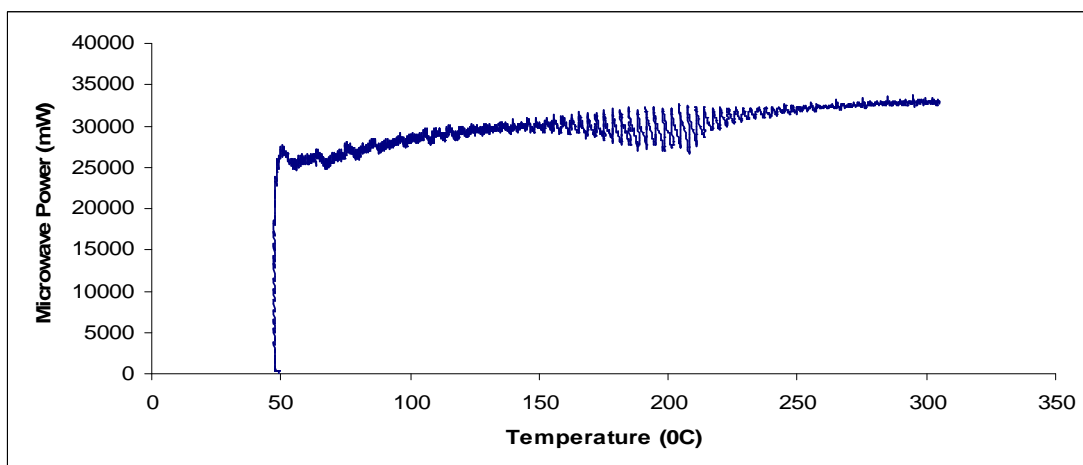


Figure 3.15 Raw data obtained from the exothermic reaction for microwave curing of Araldite DLS 772 / 4 4' DDS epoxy system with an amine / epoxy ratio of 1.1 at a heating rate of 10 K min^{-1}

The raw data shows a lot of noise, and because of this distortion, it is not possible to carry out kinetics analysis in on the raw data. A fast Fourier Transform filter (FFT Filter) developed by Navapour [54, 55, 66] was used to remove the noise in the raw data. After applying FFT filter, the data obtained is shown in figure 3.16.

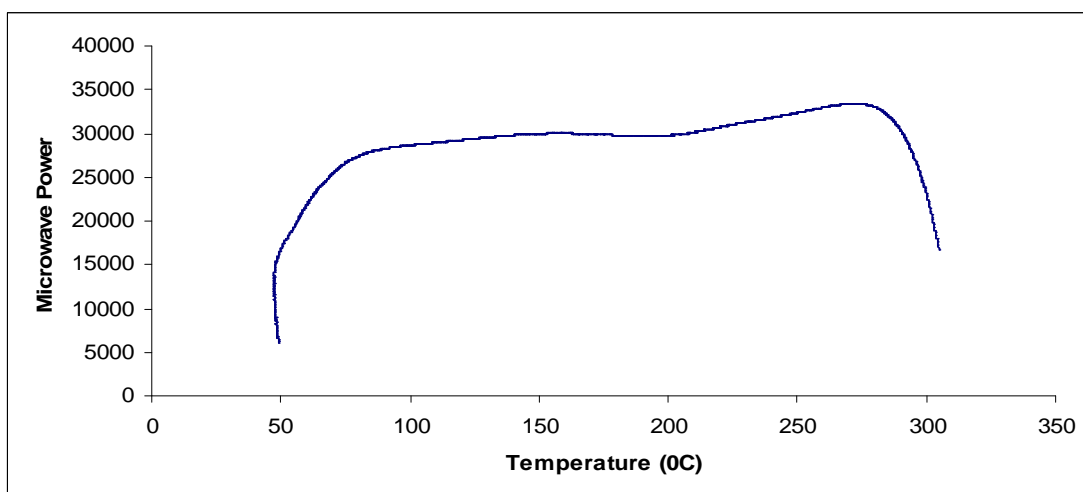


Figure 3.16 Microwave curing reaction of Araldite DLS 772 / 4 4' DDS epoxy system with an amine / epoxy ratio of 1.1 at a heating rate of 10 K min^{-1} after applying Fast Fourier Transform (FFT) Filter.

The filtered data obtained from the microwave-heated calorimeter which is shown in figure 3.16 is comparable to conventional power compensated DSC measurements. The effect of sample background affects the appearance of the two measurements (conventional and microwave). For conventional DSC measurements, during curing, a small difference is observed in the background before and after the exothermic peak. This is a result of changes in the specific heat capacity of the material during the curing reaction. In the microwave calorimeter data, however, a large change was observed in the background during curing. In addition to the changes in the specific heat capacity, changes in the dielectric loss and the extent of cure as the sample temperature increases affect the sample. As the sample cured, the dielectric loss factor decreased. This led to a decrease in the power dissipated within the sample, resulting in an increase in the microwave power required to maintain the heating rate [66].

Because some quantity of sample was used for isothermal curing (about 3 grams), a lot of microwave power was needed to heat the sample very quickly to the desired isothermal cure temperature. At the desired isothermal temperature, the power becomes too high and then it drops in an attempt to stabilise itself. As a result of these attempts by the power to stabilise itself in the initial part of the experiment, some data may be lost, or may become too noisy to be interpreted. Figure 3.17 shows a typical data obtained from the microwave-heated calorimeter.

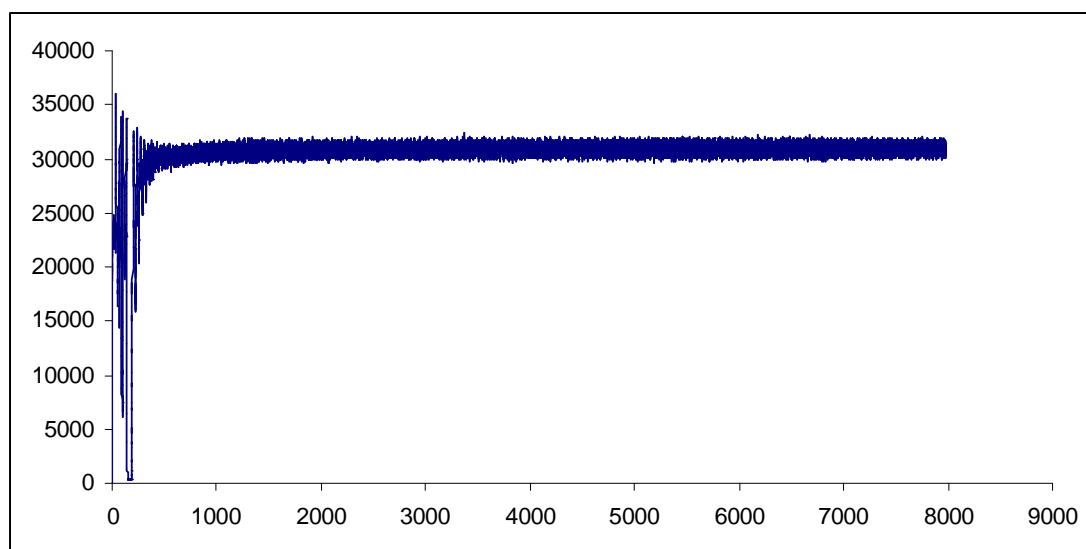


Figure 3.17 Raw data obtained from the exothermic reaction for microwave curing of Araldite LY 5052 / 4 4' DDS epoxy system with an amine / epoxy ratio of 0.85 at a heating rate of 100 K min^{-1} .

We can see from the figure 3.17 above that the raw data was observed. A fast Fourier Transform filter (FFT Filter) developed by Navapnour [54, 55, 66] was used to remove the noise in the raw data. After applying FFT filter, the data obtained is shown in figure 3.18 below.

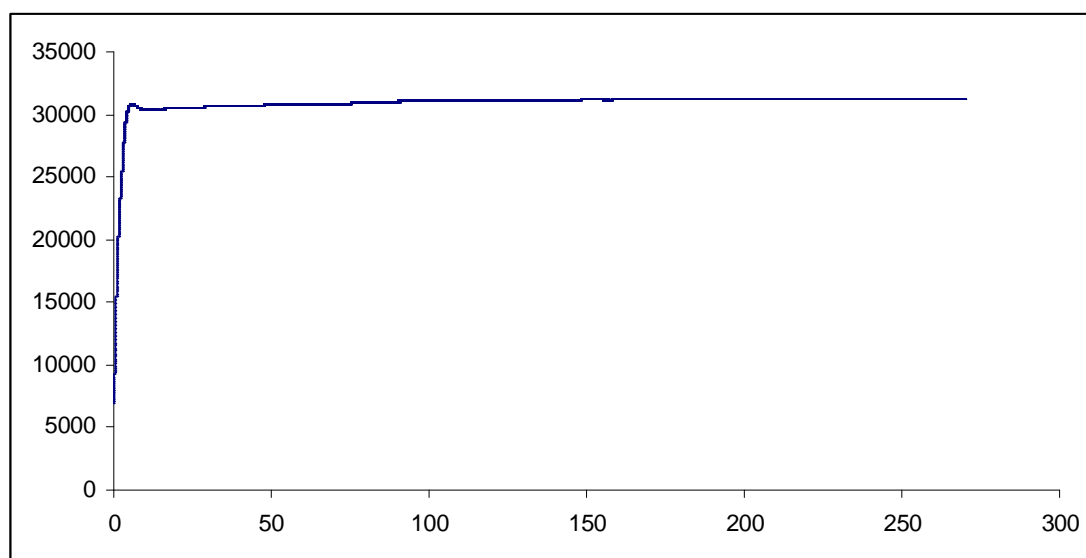


Figure 3.18 Microwave Curing reaction of Araldite LY 5052 / 4 4' DDS epoxy system with an amine / epoxy ratio of 0.85 at a heating rate of 100 K min^{-1} after applying Fast Fourier Transform (FFT) Filter.

The microwave-heated calorimeter was used to prepare microwave-cured samples for FT-IR analysis. The sample was heated from ambient temperature at a heating rate of 100 K min^{-1} to $180 \text{ }^\circ\text{C}$. Curing of samples in the microwave-heated calorimeter was carried out for different curing time intervals, thus providing a series of cured samples. For FT-IR analysis, the microwave curing of samples was carried out at $180 \text{ }^\circ\text{C}$ and held at time increments of 30 minutes. At the prescribed time, each sample tube was then quickly removed from the microwave cavity and quenched in liquid nitrogen to ensure that the reaction did not continue due to the residual heat within the sample.

3.4 Dielectric Properties

It is possible to predict the heating efficiency of a material placed in a microwave field. This can be done with the knowledge of the dielectric properties of the material in question. The microwave consists of magnetic and electric fields. The permittivity (ϵ) and permeability (μ) are used to describe the interaction of a material with an electric field and magnetic field. The interaction between the material and the magnetic and electric fields of the microwave occurs in two ways:- storage and loss. Storage explains the lossless part of the exchange of energy between the field and the material. This loss happens when energy is absorbed by the material during its interaction with the microwave field. These electromagnetic parameters can be measured using several methods, among which is the cavity perturbation technique. This method is explained briefly in the section 3.4.1.

3.4.1 Cavity Perturbation Method

The cavity perturbation technique has been widely used extensively to measure the dielectric properties of a material at microwave frequencies. When a small quantity of sample is introduced into a resonant cavity, the resonant frequency (f) and the quality factor (Q) inside the cavity are slightly perturbed. The quality factor is defined as a measure of how efficient the cavity is in storing electromagnetic energy.

$$Q = 2\pi \frac{\text{Total Energy Stored}}{\text{Energy Dissipated per cycle}} \quad 3.13$$

The changes in the resonant frequency and the quality factor between an empty cavity a cavity with sample yield the dielectric constant and the dielectric loss, respectively. The basic assumption of the cavity perturbation technique is that the sample must be very small compared to the cavity itself, so that a frequency shift produced by the insertion of the sample is small compared to the resonant frequency [55].

3.4.2 Dielectric properties measurement

The cavity perturbation technique was used to monitor the dielectric properties of the samples during microwave heating. The measurements were conducted in the TE₁₁₁

cylindrical cavity. Different heating rates of 10 K min^{-1} were used. The calorimetric measurement and the dielectric measurement were performed simultaneously. The experiment set-up in figure 3.11 was used to measure the dielectric measurements. In order to monitor the dielectric measurements, the peak frequency (f) and the quality factor (Q) were measured periodically during heating. The equations below were used to calculate the dielectric constant (ϵ') and the dielectric loss factor (ϵ'')

$$\epsilon' = 1 + \frac{(f_c - f_s)}{f_c} \frac{V_c}{V_s} \frac{1}{A} \quad 3.14$$

$$\epsilon'' = \frac{1}{B} \left(\frac{1}{Q} - \frac{I}{Q_c} \right) \frac{V_c}{V_s} \quad 3.15$$

Where f_c is the peak frequency of the empty cavity, f_s is the peak frequency of the perturbed cavity. That is after the sample has been introduced into the cavity. V_c is the volume of the cavity while V_s is the volume of the sample.

A and B are independent of the dielectric properties of the sample material. They depend on the cavity and sample geometries and the resonance mode. A and B can be determined analytically only for a few specific configuration of the cavity, sample and resonance mode. In other cases, the value of A and B can be determined experimentally by calibration using materials with known dielectric properties [28].

To obtain the parameters involved in the equations above, the transmission peak frequency and the Q value of the empty cavity (without the sample) were first measured. Other components such as the sample tube, fluoroptic temperature probe, and capillary tube were assumed to contribute a constant value to the measurements as the temperature was varied. A 1.0 ml syringe was used to fill the sample tube with 0.3 ml which was used to measure the transmission peak frequency and the quality factor of the empty cavity. The tube was then re-inserted into the cavity. The transmission peak frequency and the Q value of the perturbed cavity were measured as the sample was heated.

3.5 Infrared Spectroscopy

Infrared spectroscopy is the study of the identification of chemical compounds observing how infrared radiation is absorbed by the chemical bonds within the compounds [67]. When applied to a molecule, infrared radiation encourages transitions between vibrational and rotational energy levels of the ground (lowest) electronic energy state [21]. Atoms in molecules are constantly vibrating with respect to one another. This happens as long as the temperature of the molecule is above zero [68]. When infrared radiation is directed on a molecule, and the frequency of a specific vibration is equal to the frequency of the infra-red radiation, the molecule absorbs the radiation. This absorption will be represented on the infrared spectrum as a peak [22].

There are two types of vibration modes; the stretching and the bond vibration modes. When infrared radiation is absorbed, the energy associated with the absorption is converted to either of the vibration modes [22]. The only vibration that can occur in a simple diatomic molecule A-B is the periodic stretching along the A-B bond [21]. A stretching vibration resembles the to and fro movements of two bodies which are connected by a spring. The vibrational frequency ν (cm^{-1}) required to stretch a bond A-B is given by the equation

$$\nu = \frac{1}{2\pi c} \left(\frac{f}{\mu} \right)^{1/2} \quad 3.16$$

Where f is the force constant of the bond, μ is the reduced mass of the system, and c is the velocity of light. μ is defined by the equation below.

$$\mu = \frac{m_A m_B}{m_A + m_B} \quad 3.17$$

Where m_A and m_B are the individual masses of A and B.

Bond vibrations modes are divided into two types:- the stretching and the deformation (bending) vibrations. As defined earlier, the stretching vibration is the periodic stretching of the bond A-B along the bond axis [21]. Bending vibrations are

displacements which occur at right angles to the bond axis of the bond A-B. Stretching and deformation vibration frequencies are differentiated by spectroscopists using the symbols ν and δ . τ is used to symbolize twisting vibration frequencies and π for out-of-plane deformation.

Each atom has three degrees of freedom. This corresponds to motions along any of the three Cartesian coordinate axes (x, y, z) [22]. A molecule containing n number of atoms which is non-linear will have $3n$ degrees of freedom. These degrees of freedom are distributed as 3 rotational, 3 translational, and $3n-6$ vibrational motions. Each motion has a distinctive fundamental band frequency [21]. When a molecule is exposed to infrared radiation, and the dipolar character of the molecule changes, it is only then that absorption will occur. Total symmetry about a bond will eliminate certain absorption bands. It has been confirmed by spectroscopists that specific absorption bands for particular bonds or groups occur within a molecule at or around the expected frequencies [21].

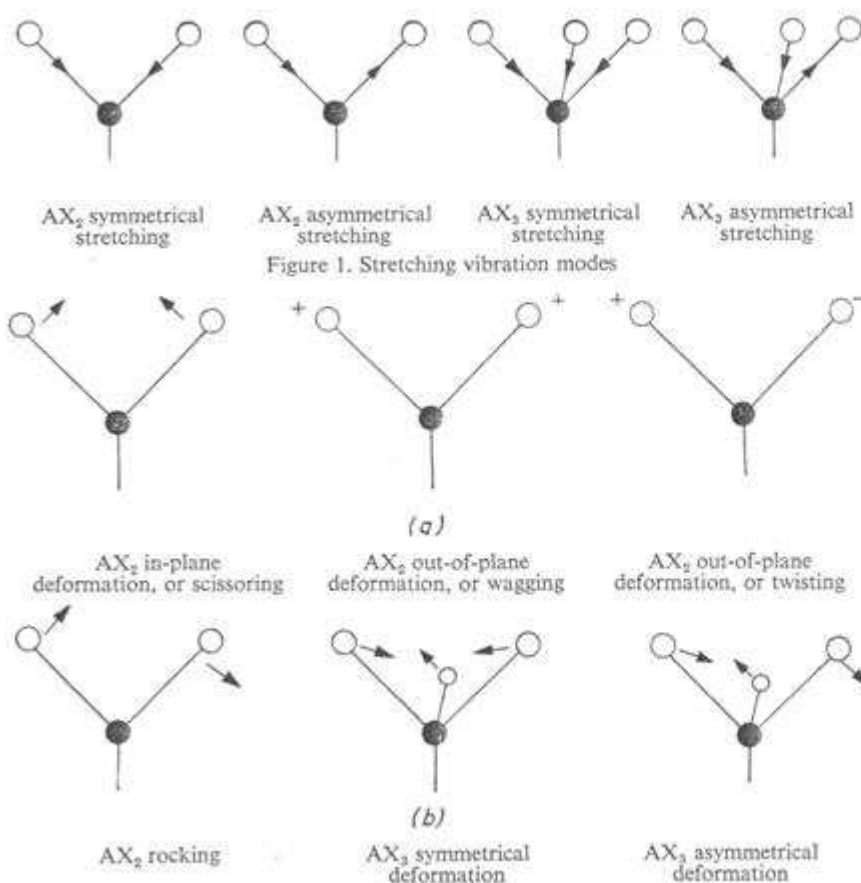


Figure 3.19 Stretching and Bending vibration modes [21].

Wavenumbers (ν) or wavelengths (λ) are usually used to represent infra-red absorption. Wavenumbers define the number of waves per unit length, and they are directly proportional to the energy of the infra-red absorption, and also the frequency [22]

When a specimen is exposed to infrared radiation, radiant power is transmitted by the sample [22]. The ratio of this radiant power transmitted by the sample to the radiant power incident (I_0) on the sample is known as the transmittance T . If the value of the transmittance is reciprocated, and its logarithm of base 10 is taken, we will get the absorbance (A) [68]. The transmittance spectrum ranges from 0 to 100% T , while the range of absorbance spectra is from infinity to zero. As a result, the transmittance spectrum provides a better contrast between the intensities of strong and weak bands [25].

3.5.1 Uses of Infra-red Spectroscopy

The primary aim of infra-red spectroscopy is the determination of functional groups in the sample [22]. Other uses of infra-red spectroscopy are;

- i) Identifying all types of organic compounds. Compounds can be identified by matching the spectrum of the unknown compound with a reference spectrum.
- ii) Identification of many inorganic compounds.
- iii) It is used to determine the molecular composition of surfaces.
- iv) Chromatographic effluents can be identified using infra-red spectroscopy.
- v) The molecular orientation of polymers and solutions can be determined using infra-red spectroscopy [22].
- vi) It is used for the determination of purity, production control, and quantitative analysis.

vii) Reaction kinetic studies.

Two types of instruments are generally used for recording infrared spectra. They are the Fourier Transform Infrared spectrometer (FT-IR), and the classical dispersive spectrometer. Most modern instruments are of the Fourier Transform Infrared Spectrometer type. This is because the FT-IR has several advantages over the classical dispersive spectrometer; some of which are having the ability to record complete spectra in a much shorter timescale [69]. FT-IR also has better signal-to-noise ratios. The figure 3.15 shows the basic construction of the FT-IR spectrometer

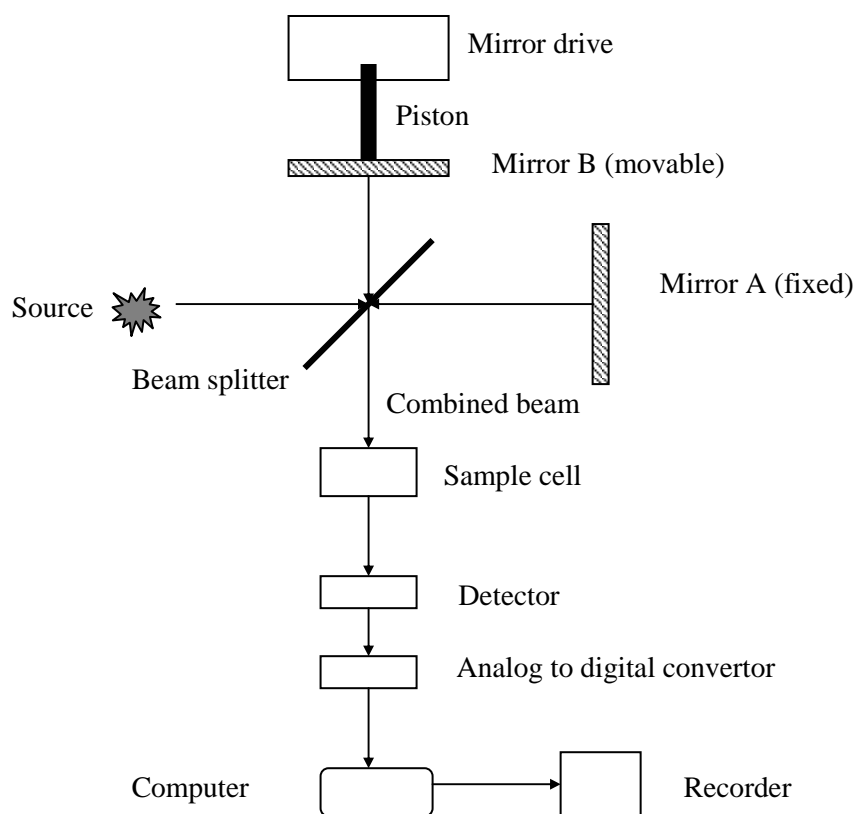


Figure 3.20 Schematic Diagram of the FT-IR spectrometer [70].

The infrared radiation is generated from a source; which is usually a globar or a Nernst filament. This generated infrared radiation passes into the Michelson interferometer. The interferometer consists of two mirrors which are at 90 degrees to each other. It also consists of a beam splitter which is at an angle of 45 degrees to both mirrors. One mirror is fixed, while the other mirror is movable in a direction which is perpendicular to its front surface at a constant velocity.

The beam splitter partially transmits and partially reflects the beam. The transmitted and the reflected beams are incident normal to the two mirrors and after reflection, they recombine at the beam splitter, and there they produce interference effect. When the optical path difference is an integral number of wavelengths, the reflected beams are in phase and hence produce constructive interference. In contrast, when the optical path is an odd number of half wavelengths, then destructive interference will occur. This will result in an oscillatory pattern or interferogram, which represents the spectral distribution of the absorption signal. Fourier transformation derives the true absorption spectrum from the interferogram [70].

A Thermo Nicolet 5700 FT-IR spectrometer with single bounce Diamond ATR crystal was used for this study. KBR discs were used for measuring the infrared spectra of the uncured Araldite DLS 772 / 4 4' DDS and Araldite LY 5052 / 4 4' DDS epoxy systems in order to prevent the resin from sticking to the sampling plate. The microwave cured samples were broken into pieces and a few pieces were extracted and placed on the sampling plate for infrared measurements. Infrared spectroscopy was taken using the Attenuated Total Reflectance (ATR) method. DSC pans were used to conventionally cure the samples in an oven, and the single point diamond FT-IR was used to take the infrared spectra via the ATR method.

3.6 Nuclear Magnetic Resonance Spectroscopy

Nuclear Magnetic Resonance (NMR) spectroscopy is a very powerful technique used for the identification of chemicals. It can also be used to measure chemical substituents or mixture components. NMR technique is very important in structure analysis because it is able to obtain signals from specific atoms along the backbone and the side chains of the polymer molecules. The magnetic environment of the NMR active nuclei and the local field that they experience influence the properties of the NMR signal. In this research, ^1H and ^{13}C -NMR were used to study the chemical structure of as-received resins. ^1H and ^{13}C -NMR were also used to determine the chemical structure of the products obtained as a result of the decomposition of cured Araldite DLS 772 / 4 4' DDS epoxy system with amine / epoxy ratio of 0.8.

3.6.1 Principles of NMR specteroscropy

Nuclear magnetic resonance spectroscopy originates from the interaction of the applied electromagnetic radiation with nuclear spin where the energy level in the nuclear spin have been split by an external magnetic field [71]. Atoms or Isotopes with nuclei having an odd number of proton or neutron have nuclear spin and can thus be detected by NMR. Nuclear spin is defined by a non-zero value of the nuclear spin quantum number (I). This value can either be integral or half integral. The most simple situation of interest in polymers involve nuclei for which $I=1/2$ such as ^1H and ^{13}C . These nuclei carry a charge and a spin on the nuclear axis, and this creates a magnetic dipole along the axis as shown in the figure 3.21.

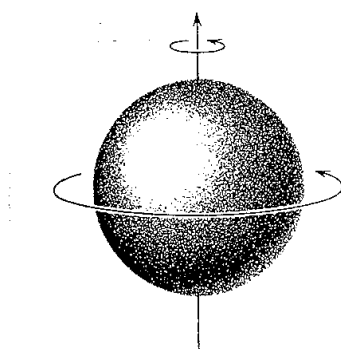


Figure 3.21 The spinning charge on the proton generates a magnetic dipole [70].

The resulting magnetic dipole, μ is oriented along the axis of the spin and is proportional to the angular momentum, p . Thus,

$$\mu = \gamma p \quad 3.18$$

where γ = Proportionality constant. It is also known as the magnetogyric ratio, γ and it has a different value for each nucleus [72].

When the magnetic nuclei are brought into an external magnetic field B_0 , they are inclined to orient themselves along the same direction as the applied field [72]. This

action is similar to that of a compass needle exposed to a magnetic field. The nuclei cannot be completely aligned parallel to the B_0 [73]. However, because of the angular momentum and the thermal motion, the force applied to the magnetic field to the axis of rotation causes the plane which is perpendicular to the field direction to move. As a result, the axis of the rotating particle moves in a circular path around the magnetic field as shown in the figure 3.22.

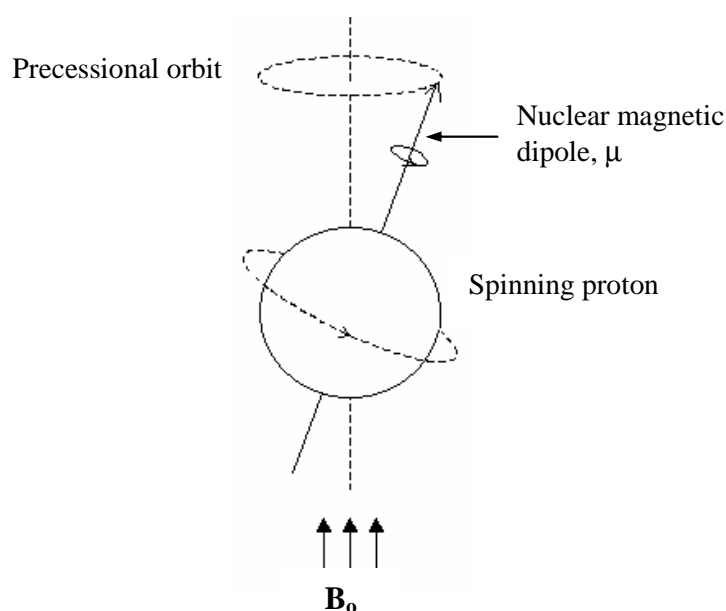


Figure 3.22 Precession of a rotating particle in a magnetic field, B_0 [70]

According to the quantum theory, only certain orientations of magnetic moment with respect to the magnetic field are permitted. These permitted orientations are given by the values of the magnetic quantum number, m which is given by [71];

$$m = I, I-1, I-2, \dots, -I$$

In instances of ^1H and ^{13}C where $I = \frac{1}{2}$, the nuclear quantum number can take only two values, $m = \frac{1}{2}$ and $m = -\frac{1}{2}$. These may be taken to represent instances where the

nuclear spins are aligned either in a low energy state (parallel) or a high energy state (anti-parallel) to the magnetic field direction. This is shown schematically in the figure 3.23 [26]

The potential energy E of a nucleus in these two orientations is given by equation 2.50 [72]

$$E = -\frac{\gamma h}{2\pi} B_0 \quad 3.19$$

Where h is the Plank's constant

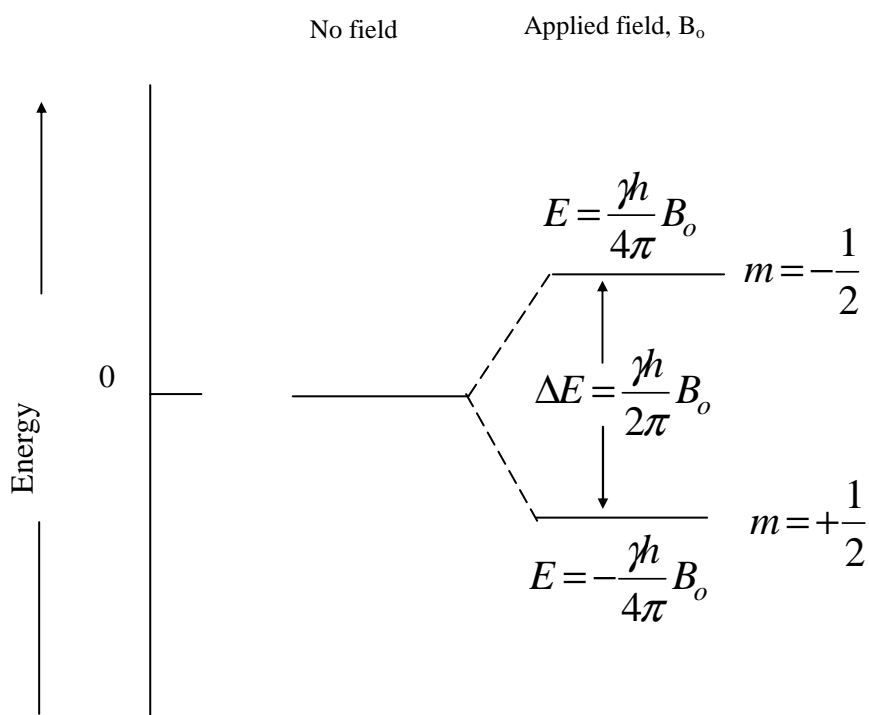


Figure 3.23 Magnetic moment and energy levels for a nucleus with a spin quantum number of $\frac{1}{2}$ and $-\frac{1}{2}$ [72]

An NMR spectrum is obtained by inducing transitions from the lower energy spin state to the higher energy spin state. This transition leads to absorption of energy. In order to achieve this, the radio frequency passing through the processing frequency, ν_0 , of the nuclei at the constant magnetic field strength is varied. When the radio frequency

matches ν_0 , the energy is absorbed by the nuclei and transition is induced from the lower state to the higher state. This condition is known as nuclear magnetic resonance. In another method, the applied radio frequency is fixed and the B_0 is swept over ν_0 until the resonance condition is satisfied. The energy absorbed during this transition is detected, and then amplified by a receiver coil as the NMR signal, which subsequently is transformed into a NMR spectrum. The figure 3.24 below shows the schematic diagram of a NMR spectrometer [70].

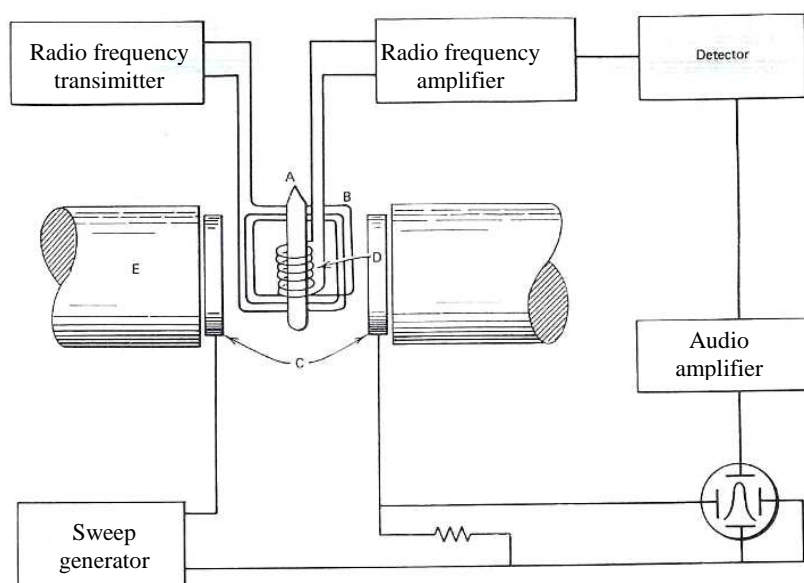


Figure 3.24 Schematic diagram of NMR spectrometer. The tube is perpendicular to the z-axis of the magnet [70].

In figure 3.24, A is the Sample tube, B is the Transmitter coil, C is the Sweep coil, D is the Receiver coil and E is the Magnet.

The precessing frequency (ν_0) of all nuclei in an applied magnetic field (B_0) depends on their chemical environment. The field experienced by the nucleus is modified due to magnetic shielding by the electron orbiting the nucleus. Induced electric currents produce a magnetic field [70]. This magnetic field opposes the applied magnetic field. The higher the electron density, the greater the extent of shielding, and thus lower the ν_0 . This effect changes with the chemical environment of the nuclei. The variation, gives rise to small differences in the absorption positions. This results in different positions of

the peaks in the NMR spectrum. The position of the peak is expressed relative to a reference peak. This is known as the chemical shift (δ) [70]

$$\delta = \frac{10^6 (\nu^{sample} - \nu^{ref})}{\nu^{ref}} \quad 3.20$$

The resonance frequencies of the sample and the reference are denoted as ν^{sample} and ν^{ref} respectively.

Tetramethylsilane ($\text{Si}(\text{CH}_3)_4\text{TMS}$) is the most widely accepted and widely used compound used as reference in NMR analysis. This is because it is chemically inert and it is also soluble in most organic solvents. This makes it very advantageous. Additionally, it gives a single, sharp peak. Also its protons are more “shielded” than almost all other organic protons. Most ^1H absorptions occur in the range 0-12 ppm, while ^{13}C absorptions occur over the range 0-250 ppm. As a result, ^{13}C -NMR spectroscopy gives a greater resolution than ^1H -NMR spectroscopy [25].

^1H -NMR is the most sensitive to observe and to use for quantitative application. This is because of the massive abundance of ^1H in nature (99.98 % of hydrogen atom). The ^{13}C isotope unlike the ^1H has a natural abundance of 1.11 %. This makes the ^{13}C less sensitive than ^1H . [74, 75]. Thus, the intensities of resonance lines for ^1H are more than 5000 times greater than those for ^{13}C . That notwithstanding, if adequate amounts are used, (100-500mg), a good resolution ^{13}C can be obtained. The ^{13}C is much more sensitive to the chemical environment. This makes the chemical shift range for ^{13}C NMR about 20 times larger than the chemical shift for ^1H NMR. Consequently, the peaks overlap less, and a more detailed information on the chemical structure can be obtained [71].

3.7 Dynamic Mechanical Analysis

The mechanical properties of a material are a useful guide to determine how suitable it may be for a particular application [42]. It can also show how the material has been treated prior to testing [69]. The most important factor in determining the mechanical properties of a material is its molecular nature. For instance, the chemical structure of a

plastic, its blending and the way it has been fabricated will greatly influence its behaviour [69].

In dynamic mechanical analysis, the storage modulus and the loss modulus of the sample are monitored against time, temperature or frequency of oscillation under oscillating load while the temperature of the sample in a specified atmosphere is programmed [42]. Usually the experiment is carried out in such a way that the dynamic strain constant is maintained. Sometimes, constant stress experiments are also used [42].

3.7.1 Mechanical Moduli

If force is applied on a sample, it will behave in a number of ways. If the applied force is large, often times the material will break. Application of a small force will deform the material. Depending on their viscosity η , liquids will flow when subjected to force. The deformation caused by the application of a small force may be elastic, whereby if the force is taken back, the material will return to its precise shape and size [42]. The deformation of other materials may be viscoelastic, and the material will show characteristics of elastic and flow deformation [69]. If a force is applied on a material beyond its elastic limit, the material will become permanently distorted. This phenomenon is known as plastic deformation. The parameters which are used for studying the mechanical properties are explained below.

Stress is defined as the force applied per unit area. This may be

$$\text{A normal stress:} \quad \sigma = \frac{F}{A} \quad 3.21$$

$$\text{A tangential, shearing stress} \quad \tau = \frac{F}{A} \quad 3.22$$

$$\text{A pressure change} \quad \delta p = \frac{F}{A} \quad 3.23$$

N/m^2 or Pa are the units used for the above definitions [12].

Application of stress on a material will cause a deformation. This deformation is measured by the strain. It is defined as the deformation per unit dimension. Strain has no units. It may be expressed as

Tensile strain or elongation	$\epsilon = \frac{\delta l}{l}$	3.24
------------------------------	---------------------------------	------

Shear strain	$\gamma = \frac{\delta x}{y}$	3.25
--------------	-------------------------------	------

Volume or bulk strain	$\theta = \frac{\delta v}{V}$	3.26
-----------------------	-------------------------------	------

Hooke's law states that in an elastic material, the strain is proportional to stress. Its constant is the modulus [42].

Modulus = $\frac{\text{Stress}}{\text{Strain}}$. There are several types of modulus.

Tensile, or Young's Modulus	$E = \frac{\sigma}{\epsilon}$	3.27
-----------------------------	-------------------------------	------

Shear Modulus	$G = \frac{\tau}{\gamma}$	3.28
---------------	---------------------------	------

Bulk (or compression) modulus	$K = \frac{\Delta p}{(\Delta v/v)}$	3.29
-------------------------------	-------------------------------------	------

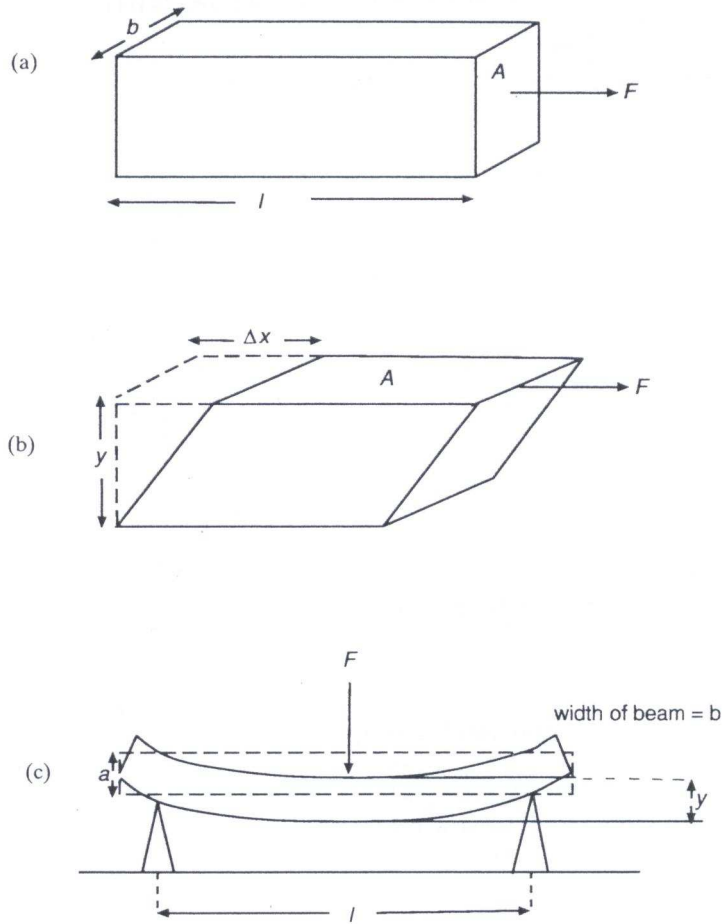


Figure 3.25 Schematic of different types of deformation [42]

In the case of an ideal elastic material, the deformations are exactly reversible. Should there be any viscoelasticity, the moduli will become complex, and it will contain two parts. In the case of the tensile modulus for instance, one is the storage modulus E' , and the other is the loss Modulus E'' [42, 69].

$$E^* = E' + iE'' \quad 3.30$$

Where $i = \sqrt{-1}$

The ratio of the storage and the loss modulus will give the loss tangent $\tan(\delta)$

$$\tan(\delta) = \frac{E''}{E'} \quad 3.31$$

If an oscillatory sine-wave stress is applied to a perfectly elastic solid, the deformation and the strain will be exactly in phase with the stress [42]. When the same oscillatory stress is applied to a viscoelastic solid, the strain lags behind the stress and becomes out-of-phase by an angle δ . The complex dynamic modulus (E^* in extension mode) must be used [12]:

$$E^* = E' + iE'' \quad 3.32$$

3.7.2 Glass Transition Temperature

The glass transition temperature of a polymer is the temperature at which it changes from a hard and brittle material into a soft and pliable one. Below the glass transition temperature T_g , the polymer segments do not have enough energy to rotate or to rearrange themselves [42]. Such a material is brittle and glassy. When heat is applied to the sample, there is a minor increase in its energy and its volume, the chains become more mobile and the polymer becomes more rubbery until at the glass transition. If the sample is heated further, the polymer will crystallize and melt [69]. At glass transition temperature, the chains will have an increased freedom of movement. This is as a result of an increase in the heat capacity of the sample. Thus, at glass transition, we will notice a step, an increase in heat capacity and also a change in expansion [42].

3.7.3 Applications of DMTA

3.7.3.1 Glass Transition Temperatures

When a polymer passes through its glass transition T_g , the storage modulus decreases by two or three orders of magnitude. The decrease in modulus happens when there is a main chain molecular motion. The $\tan \delta$ also goes through a maximum as the polymer passes through its glass transition. This occurs when the frequency of the forced vibration happens simultaneously with the frequency of the diffusional motion of the main chain. Compared to DSC and other thermal techniques, DMA is a much more sensitive method of studying the glass transition temperatures.

$\tan \delta$ is a measure of the ratio of energy dissipated as heat to the maximum energy stored in the material during one cycle of oscillation. Hence, any two of the quantities

G' , G'' and $\tan \delta$ can describe the stiffness and damping properties of the material [42, 69].

3.7.3.2 Beta and other transitions

At much lower temperatures, there are secondary transitions occurring in most polymers. The glass transition temperature is referred to as the alpha transition. The beta and gamma transitions are found at much lower temperatures. The alpha transition is associated with the relaxation of the main chain backbone. The beta transition gives a $\tan \delta$ which is usually broad. This is due to the motion of the small groups [42]. Further below is the gamma peak. This peak is also broad and it is as a result of the motion of small chain segments.

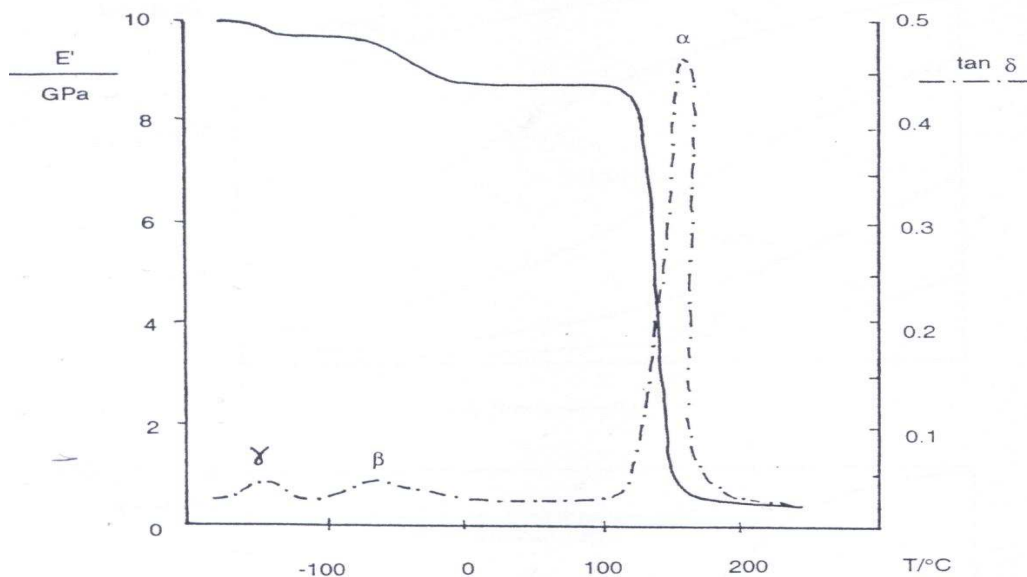


Figure 3.26 DMTA of epoxy showing alpha, beta and gamma different transitions [42]

3.7.1 Sample preparation and measurement procedure

In this research, the dynamic mechanical analysis tests were carried out on the cured samples using a Pyris Diamond Dynamic Mechanical Analyzer in a temperature sweep mode. This test mode provides a sensitive means for measuring glass transitions. During the test, the glass transition is detected as a sudden and an obvious change in the storage

modulus and consequently a peak in the $\tan \delta$ curve. The temperature at which this transition occurs is known as the glass transition temperature, T_g [42].



Figure 3.27 A Perkin- Elmer Pyris Diamond Dynamic Mechanical Analyser used for this research.

Conventional and microwave cured samples were prepared using the technique described in the earlier section. The samples were cut into dimensions of 50mm x 10mm x 2mm. In order to get a smooth, flat surface, the samples were polished with silicon carbide paper. A minimum of five rectangular specimens was prepared for each sample. The specimens were tightly fitted between two fixtures located in a temperature controlled chamber. The lower fixture was driven in oscillatory mode by an actuator at the frequency of 1 Hz. The upper fixture was connected to a transducer, which measured the stress. The specimen was heated from -120 to 300°C at a heating rate of 5 K min⁻¹. The temperature dependence of $\tan \delta$, G' , and G'' were measured.

3.8 Flexural Testing

3.8.1 Principle of flexural testing

Flexural stress-strain testing measures the load required to produce a given level of strain in a specimen under bending conditions. Fundamentally, flexural testing involves the bending of a long, flat specimen of a rectangular cross section using either a three-point or four-point conditions. Three point bending conditions was utilized for this research. In three-point bending, the maximum stress occurs in the specimen where the centre support is. figure 3.28 shows the effect of the load on the test specimen in three point bending.

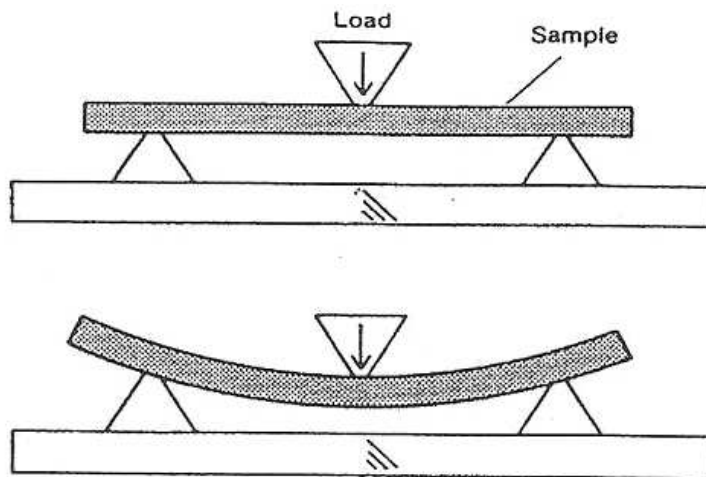


Figure 3.28 Effect of load on a test specimen in three point bending [76]

Figure 3.29 illustrates the stresses which are present within a specimen during a three point bending test. Tensile and compressive stresses act on a specimen undergoing a three point bending test. Tensile stresses act on the outer surface of the specimen while compressive stresses usually dominate the inner surface. There is a region in the specimen which neither experiences tensile nor compressive stress. This region is known as the neutral axis [27].

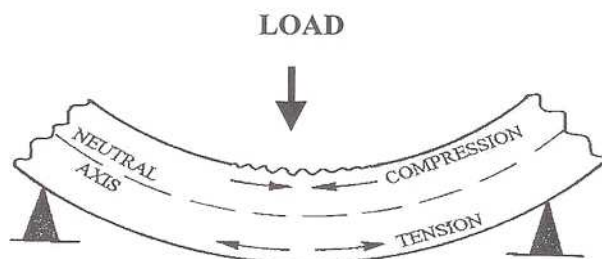


Figure 3.29 Stresses present in a test specimen during a three point bending test [27]

Flexural strength is the maximum stress developed when a test specimen is subjected to a bending force which is acting perpendicular to the specimen. The load is applied at a specified crosshead speed. Hence the flexural stress (σ_f) is given by [27]

$$\sigma_f = \frac{3PL}{2WT^2} \quad 3.33$$

P is the load at a given point on the load-deflection curve (N), L is the support span (mm), W is the width of the specimen (mm), and T is the specimen thickness (mm).

The flexural strain (ϵ_f) of the specimen under testing can be obtained from the following expression;

$$\epsilon_f = \frac{6DT}{L^2} \quad 3.34$$

D is the deflection under load.

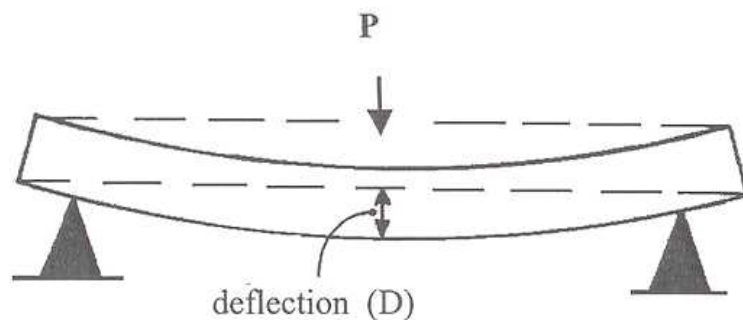


Figure 3.30 The deflection (D) of the test specimen under load P [27]

The flexural modulus (E) is a measure of bending stiffness, and it can be obtained from the initial slope of the load-deflection curve.

$$E = \frac{PL^3}{4WDT^3} \quad 3.35$$

3.8.1 Sample preparation and measurement procedure

An Instron Universal Testing machine model 4500 was used to perform the three point bending test. The conventional and microwave cured samples were prepared using the technique described in the earlier section. The samples were ground using a grinding machine with a 400 silicon carbide to get a smooth, flat surface and then cut into a dimension of approximately 60 mm x 10 mm x 2.5 mm. A minimum of five rectangular specimens was prepared for each sample. The flexural properties were determined at a crosshead speed of 2 mm min⁻¹ with a support span of 40mm.

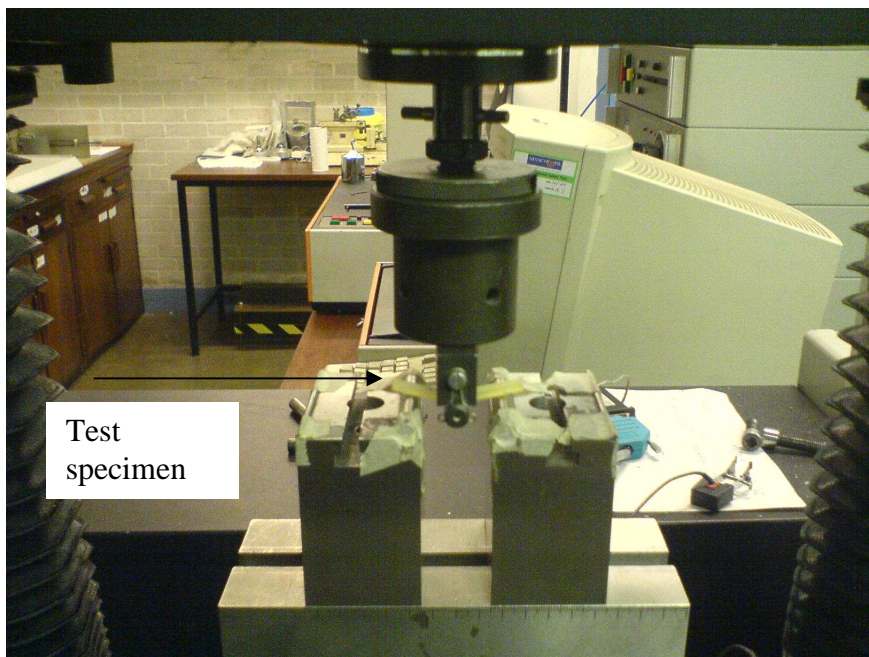


Figure 3.31 A specimen undergoing three point bending test

3.9 Microwave Acid Digestion

An Anton – Paar microwave reaction system was used to decompose the cured epoxy resin in nitric acid. It consists of sixteen vessels. A diagram of the Microwave reaction system is shown in figure 3.32.



Figure 3.32 An Anton Paar Microwave reaction system.

About 1 – 2 grammes of the specimen were put in each reaction vessel, and 15 ml of 4M Nitric Acid was added into the vessels.

3.10 High Performance Liquid Chromatography (HPLC)

High Performance Liquid HPLC is a chromatography technique used to separate a mixture of compounds. It is used in biochemistry and in analytical chemistry to identify, quantify and also purify the individual components of the mixture [77].

A schematic diagram of the HPLC pump is shown in figure 3.33.

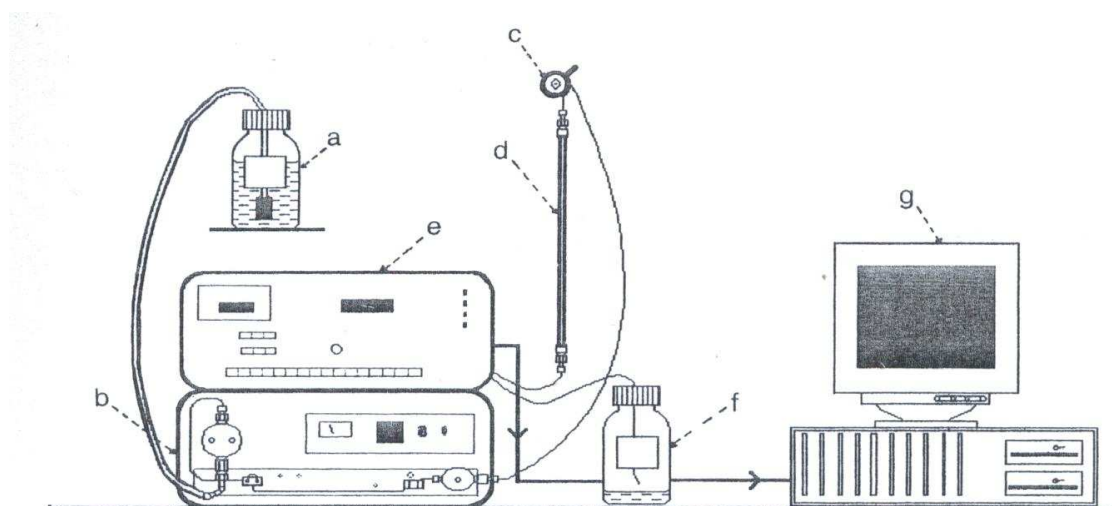


Figure 3.33 Schematic diagram of HPLC pump [77].

Figure 3.33 shows the schematic diagram of HPLC pump. The label a is the mobile phase reservoir, b is the pump which is capable of delivering pulse-free flow at pressures of up to 6000 psi. c is the injection valve, d is the column. e is the detector; the most popular of which is the UV absorbance. F is the labelled waste mobile phase reservoir [77]

With HPLC, a pump is used to provide the pressure needed to impel the mobile phase and the analyte through the densely packed column. The increased density arises from the smaller particle sizes. This enables a better separation on columns of shorter lengths [77].

3.10.1 Mode of Operation

A small volume of the sample which is to be analysed is injected to a stream of mobile phase. Movement of the injected sample through the column is slowed down by its interactions (either physical or chemical) with the stationary phase as it moves through

the column. The nature of the sample to be analysed and the composition of the mobile and stationary phase influence the speed of the sample through the column. The retention time is the time at which a specific analyte comes out the end of the column. The use of smaller particle size column packing creates higher back pressure and consequently increases the linear velocity. This gives the components less time to diffuse within the column, leading to an improved resolution in the resulting chromatogram [78].

3.10.2 Types of HPLC

Partition Chromatography:- It is the first kind of chromatography which was developed by chemists. Partition Chromatography either uses a retained solvent on the surface or within the grains or fibres of an “inert” solid supporting matrix; or it takes advantage of some additional hydrogen donor interaction with the solid support. The molecules balance between a liquid stationary phase and the element. This is known as Hydrophilic Interaction Chromatography (HILIC) in HPLC, and in this method, analytes are separated based on their polar differences. One of the advantages of HILIC is that acidic, basic and neutral solutes can be separated in a single chromatogram [78].

Normal - Phase Chromatography:- This is also known as Normal Phase HPLC or adsorption chromatography. In this method, the analytes are separated based on polarity and by adsorption to a stationary surface chemistry. NP-HPLC uses a polar stationary phase and a non – polar, non- aqueous mobile phase. It is very effective in separating analytes which are readily soluble in non-polar solvents [78]. The analyte is retained by the polar stationary phase. As the analyte polarity increases, the adsorption strength. Also , the interaction of the polar analyte and the polar stationary phase increases the elution time. The strength of the interaction depends on both the functional groups in the analyte molecule and also on the steric factors [78].

Displacement Chromatography:- In Displacement chromatography, a molecule with a high affinity for the chromatography matrix will compete effectively for binding sites, and will thus displace all the molecules with lesser affinities.

Reverse – Phase Chromatography :- Reversed phase HPLC has a non-polar stationary phase and an aqueous, moderately polar mobile phase. Silica which has been treated with $R\text{me}_2\text{SiCl}$, where R is a straight chain alkyl group such as $\text{C}_{18}\text{H}_{37}$ or C_8H_{17} is a commonly used stationary phase. For molecules which are non-polar, the retention time is longer when they pass through stationary phases such as silica. Polar molecules, on the other hand elute more readily. Addition of more water to the mobile phase makes the affinity of the hydrophobic analyte for the hydrophobic stationary phase stronger relative to the mobile phase which has become more hydrophilic. This increases the retention time. Adding more organic solvent to the element decreases the retention time [78].

Ion Exchange Chromatography:- In ion exchange chromatography, retention of the analyte is based on the attraction between solute ions and charged sites which are bonded to the stationary phase. Ions of the same charge are excluded. The types of ion exchanges include [78]

- i) Polyester resins
- ii) Cellulose ion exchanges
- iii) Controlled – pore glass or porous silica

Generally, ion exchanges favour the binding of ions higher charge and smaller radius. With respect to the functional groups in the resins, an increase in counter ion concentration reduces the retention time. An increase in PH reduces the retention time in cation exchange while a decrease in PH reduces the retention time in anion exchange. Ion exchange chromatography is widely used in water purification, higher exchange chromatography [78].

In this research, 100 mg of the decomposed resin was put in a small tube and methanol was used to dissolve the sample. A small syringe was then used to inject about 100 microlitres into a Gilson pump controlled system through the rheodyne. Figure 3.34 shows the diagram of the Gilson pump controlled system.

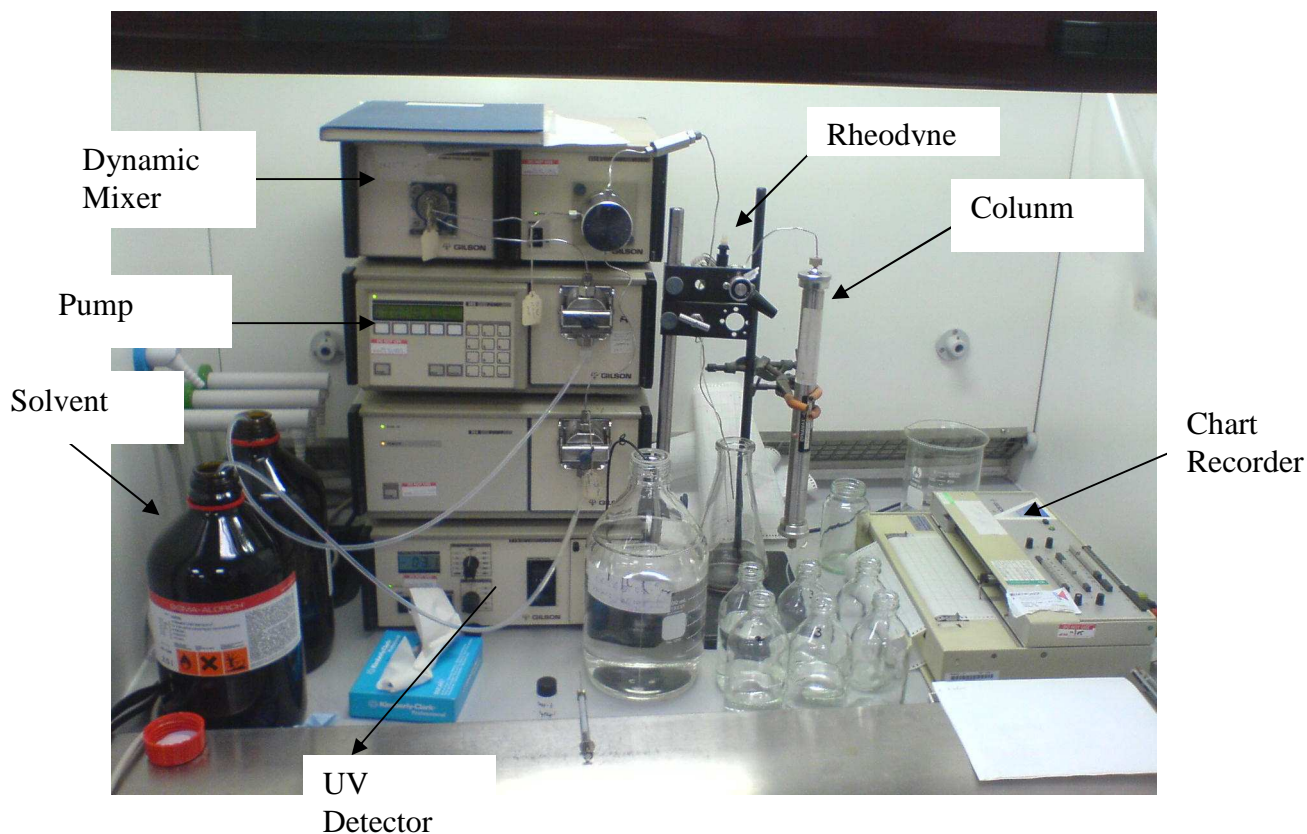


Figure 3.34 A Gilson Pump Controlled HPLC system.

The Gilson pump controlled system consists of a chart recorder which indicates when an analyte is being eluted from the column. A pump is used to pump the solvents (hexane and ethyl acetate) through the column, and through the UV which is connected to the chart recorder. When the absorbance of the UV detector rises, it sends a signal to the chart recorder. The the sample is injected through the rheodyne, and it goes through the column, coming out through the UV. The dynamic mixer mixes the solvents A and B.

3.11 Gel Permeation Chromatography

Gel Permeation Chromatography is one of the most useful techniques used to establish both the molecular mass distributions and the average molecular masses of polymers. Gel Permeation Chromatography is a form of liquid chromatography which involves the separation of molecules according to their molecular size, or their hydrodynamic volume in solution. In Gel Permeation Chromatography, a dilute solution of polydisperse polymer is injected into a continuous flow of solvents passing through a column which contains tightly packed microporous gel particles. In order to give

efficient packing, The sizes of the gel particles are in the range of 5-10 μ m. This is in order to give efficient packing, and it usually has a variety of pore sizes from 0.5-10⁵ nm, which corresponds to effective size range of polymer molecules [71].

When the molecules pass through the pores, they are separated according to their sizes, with the smaller sized particles able to pass through more easily than the larger sizes. As a result, their rate of passage through the column is slower. This continuous flow of solvents enables the molecules to be separated according to the sizes, with the larger molecules eluted first. The smaller molecules require longer elution times. This is because they penetrate more deeply into the pores, as a result of their small sizes. From this, *it* follows that the volume of elution is inversely proportional to the molecular size. There would be little or no separation of the molecules if the pore size is so small that the molecules can not penetrate it. Also, if the pore size is so large that all the molecules can pass through easily, there would also be little or no separation of the molecules [71].

Therefore, it is important for the column packing material to have the appropriate pore size distribution, and different columns are usually needed for polymers which have widely different molecular mass distributions. There are now an availability of columns which has gels of mixed pore sizes. These pore sizes can operate over four decades of molecular mass. The size of a polymer molecule or its hydrodynamic volume in solution will influence its ability to enter a pore. Solvent and temperature changes can affect the hydrodynamic volume [71, 79]. This can consequently influence the polymer molecule's ability to be retained by the column. Different molecular mass fractions are characterized by the elution volume, or the peak retention volume (V_R). This is the volume of the solution eluted from the time of injection of the polydisperse sample into the GPC column to the peak of the chromatogram for the particular fraction. Empirically, there is a relationship between V_R , the interstitial volume V_0 , and the volume of liquid within the pores, V_1 .

$$V_R = V_0 + kV_1$$

Where k is the distribution coefficient. K signals the relative ease or otherwise of the solute molecules into the pore structure. When k is 0, there is no penetration, and when k is 1, there is total unrestricted penetration.

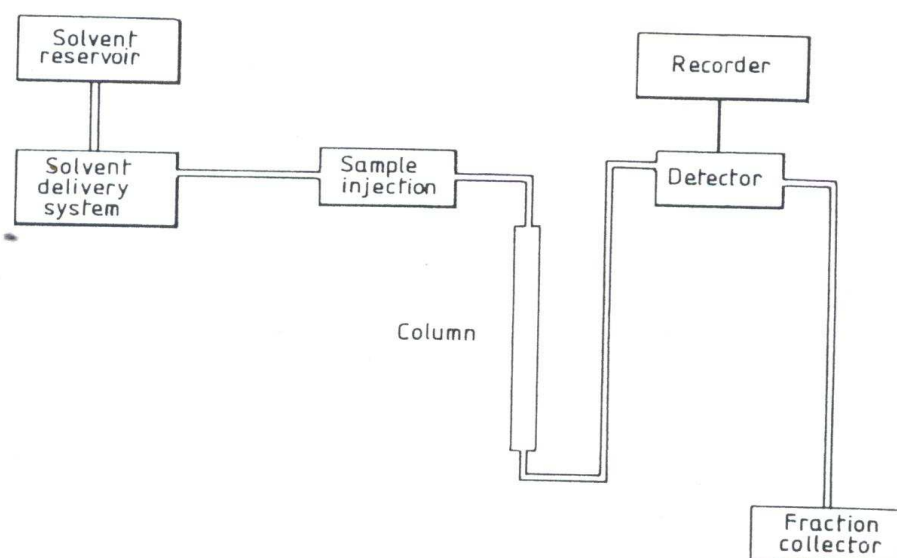


Figure 3.35 Schematic apparatus of a GPC set-up.

The fundamental requirements for a GPC chromatograph are

- 1) Solvent delivery system: capable of maintaining a constant linear velocity flow;
- 2) Column(s) containing suitable microporous gel particles to produce the necessary size separation; They are typically, about 300 – 600 mm long and 7.5 mm in diameter. They are constructed of stainless steel and threaded to permit ready assembly.
- 3) Injection system: capable of delivering accurately small volumes of sample solutions without disturbing the solvent flow;
- 4) Detection system to monitor output from the columns and to provide continuous quantitative and possibly qualitative data on the fractions being eluted;
- 5) Recorder to give continuous output traces.

The ability of GPC to produce molecular mass distribution curves directly and to enable calculation of the average molecular masses makes this an invaluable technique for polymer characterization.

3.11.1 Applications of Gel Permeation Chromatography

- 1) GPC is applied in various areas in polymer science and technology. This is because GPC is able to separate and identify low molecular mass fractions such as monomers and oligomers. GPC is also able to separate and identify additives such as plasticizers, and stabilizers [71].
- 2) GPC is also used increasingly for quality control.
- 3) It is also employed in polymer synthesis and polymer processing.

3.12 Mass Spectrometry

In mass spectral analysis, gaseous ions are formed from an analyte (M) and the mass to charge ratio (m/z) of these ions are measured. The sample is either converted to molecular or quasimolecular ions and their fragments. This depends on the method of ionization used. The molecular ions are generally radical cations (M^+) which are formed by the removal of electron from M. M^- is formed when an electron is added to M, and this is often used for electromagnetic samples [80]. Quasimolecular ions are formed by adding or subtracting an ion to M. “Soft” ionization methods basically generate molecular or quasimolecular ions, while “hard” ionization methods give rise to fragment ions. The ions which are generated by ionization are separated by the mass spectrometer according to their mass-to-charge (m/z) ratio to give a graph of abundance vs m/z . Prior to mass spectrometry, the mixtures are often separated by gas or liquid chromatography. A mass spectrum can be obtained for each individual component and thereby make the characterization of the sample easier [80].

The exact value of (m/z) of the molecular or the quasimolecular ion reveals the elemental composition of the ion. This enables us to analyse the composition of the sample being studied. If the molecular ions are unstable and they decompose completely, the resulting fragmentation patterns can be used as a fingerprint for sample identification. The fragment ions also provide important information about the primary structure of the sample molecule.

Mass spectrometry has an increasing use in polymer analysis because they are very sensitive. Minor components can be analyzed within a mixture. It is also a speedy process; mass spectrometry data can be acquired within seconds [80].

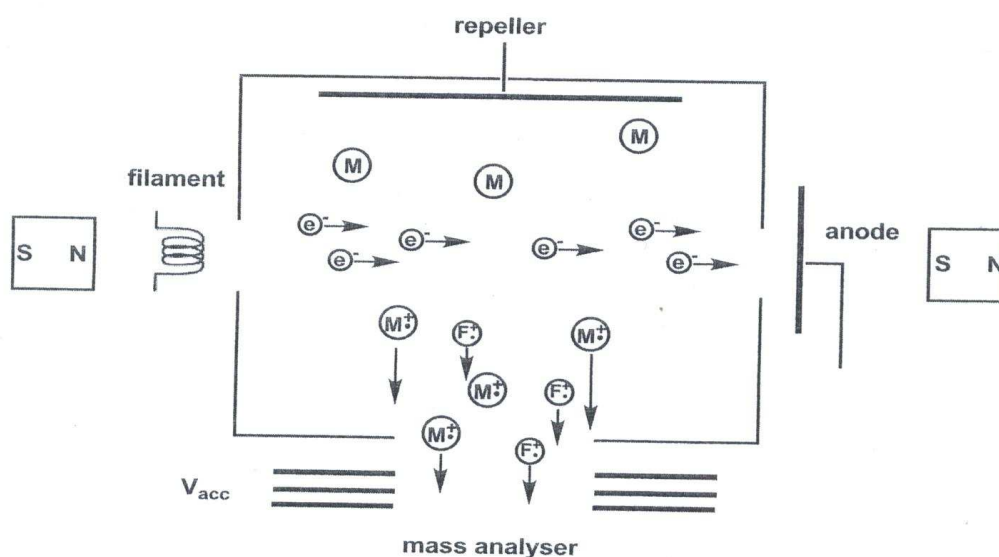


Figure 3.36 Schematic representation of an electron ionisation source [80].

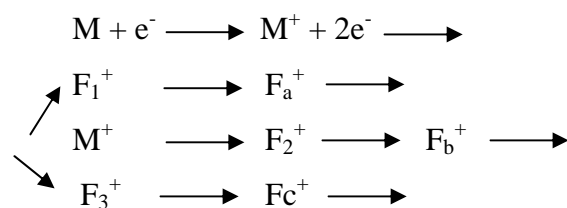
3.12.1 Ionization methods

Gaseous ions can be prepared by three major methods.

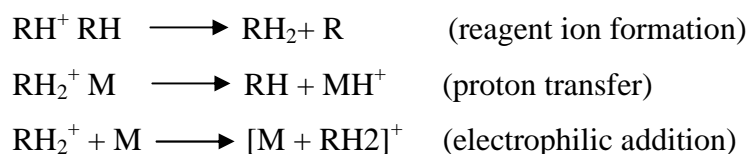
- i) The ionization of volatile materials occurs when their vapours interact with electrons, ions or strong electric fields.
- ii) Non-volatile materials are ionized by strong electric fields.
- iii) Liquid solutions of the analyte may be directly converted to gas phase ions via spray techniques [80].

3.12.2 Ionization of volatile materials

Electron Ionization (EI):- Here, the sample is thermally vaporised and approximately 10^{-5} Torr of its vapour enter the ion source volume. Here, ionization takes place by collision with an electron beam of 70eV kinetic energy. In electron ionization, an electron is ejected from the sample molecule, leading to the production of intact molecular radical cations M^+ . This process gives a wide distribution of internal energies to the newly formed molecular ions, resulting in the formation of many M^+ ions which are excited enough to yield a number of fragment ions through competitive (F_1^+ , F_2^+ , F_3^+) and consecutive (f_a^+ , f_b^+ , f_c^+) decompositions [80].



Chemical Ionization:- In chemical ionization, the gaseous analyte molecules are ionised by ion molecule reactions with reagent ions, which are formed by electron ionization from the appropriate reagent gas. The chemical ionization source is similar to the electron source, but is operated at a higher pressure. (0.1- 0.2 Torr). A proton transfer reaction illustrates the chemical ionization process. This is the most common ionization mode. The reagent molecules are ionised by electron impact, and they react with other reagent molecules to form the reactant ions, RH_2^+ , which protonate the sample [80].



Field Ionization (FI) : - In FI, gaseous analyte molecules (M) approach a surface of high curvature that is maintained at a high positive potential, giving rise to a strong electric field near the surface (of the order of 10^7 V cm^{-1}). A M^+ is created under the influence of the field by the quantum tunnelling of a valence electron from M to the anode surface. This can take place in about 10-12 s. $[M+H]^+$ may also form with polar analytes by hydrogen abstraction from near the anode. FI produces molecular ions which have lower energies than molecular ions produced by EI due to the lower internal energies possessed by FI, they fragment less [80].

3.13 RESIN IDENTIFICATION AND CHARACTERISATION

3.14 Introduction

The chemical structures of the epoxy resins Araldite DLS 772 and Araldite LY 5052 used in this research are confirmed. The molecular weights of the resins are also

investigated. The resins were characterized to determine thermal behaviour. $^1\text{H-NMR}$, $^{13}\text{C-NMR}$ and GPC were used to identify and characterise the resins.

3.15 Chemical Structure Identification

It is important to determine the chemical composition of a resin. This is because it plays a crucial role in the properties of the final product. The cure chemistry of the resin can be studied with the knowledge of its chemical structure. Also, since microwave energy is transferred to the material through dipolar polarisation, the interaction between the microwave and the material is affected by its chemical composition. The reaction can also be controlled in order to determine its optimum properties.

3.16 Araldite DLS 772

3.16.1 Molecular weight measurement

Gel Permeation Chromatography was used to determine the average molecular weight of the Araldite DLS 772 epoxy resin. A molecular weight distribution curve for the resin is shown in figure 4.1 The results show that the number average molecular weight (M_n) of Araldite DLS 772 was 72460g mol^{-1} . The weight average molecular weight (M_w) was 142100 g mol^{-1} . The polydispersity index was 1.96. Polystyrene was used as the standard for this measurement.

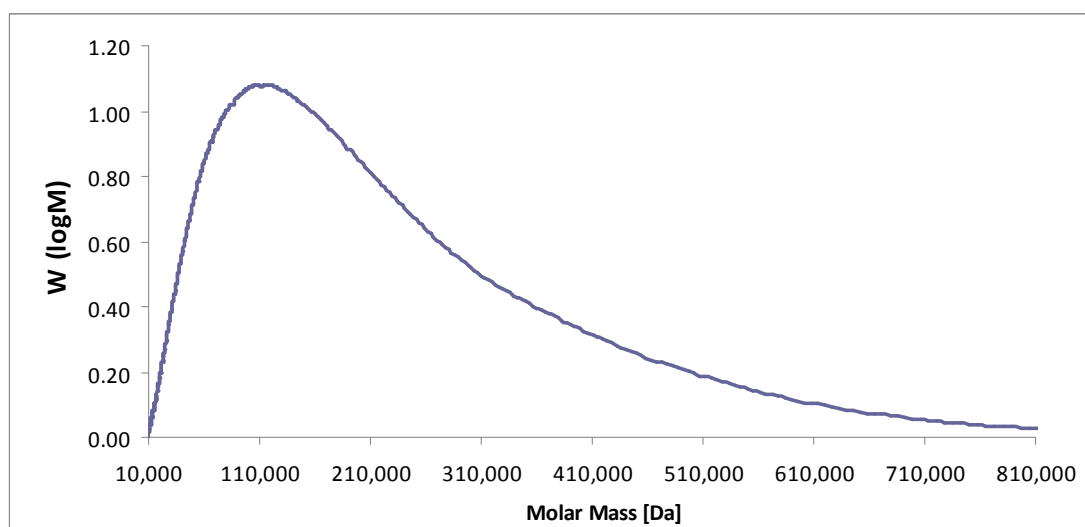


Figure 3.37 Log weight fraction molar mass distributions for Araldite DLS 772 epoxy resin

3.16.2 Chemical structure determination

$^1\text{H-NMR}$ and $^{13}\text{C-NMR}$ were used to identify the chemical structure of Araldite DLS 772 epoxy resin. Figure 3.38 shows the $^1\text{H-NMR}$ spectrum of Araldite DLS 772. The peaks at 6.8 ppm and 7.1 ppm correspond to the aromatic protons [81-83]. The presence of these aromatic peaks is due to the bisphenol A moiety [81]. The methyl protons give rise to a peak at 1.6 ppm. There are five peaks in the range of 2.5 – 3.5 ppm which are characteristic of the glycidyl terminal group [1-3].

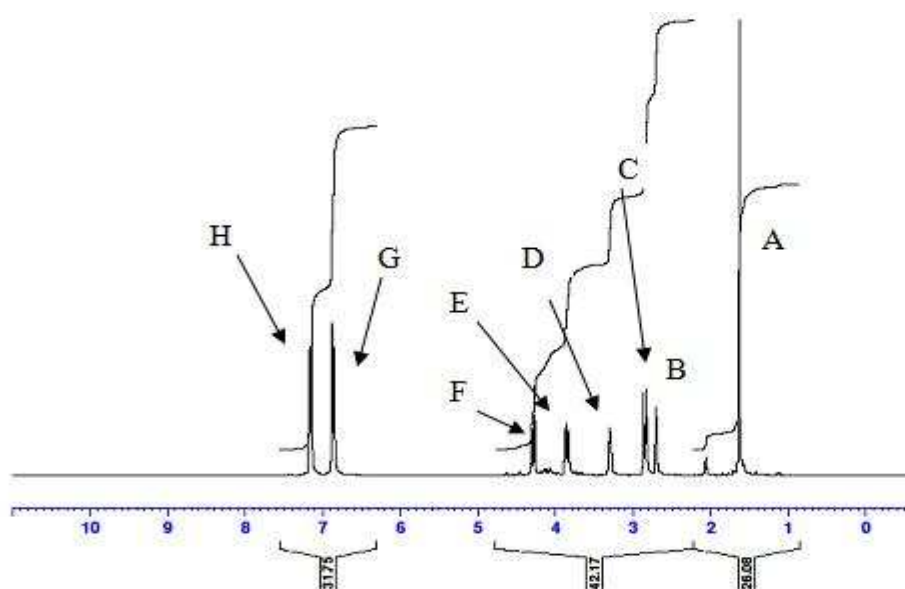
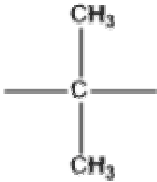

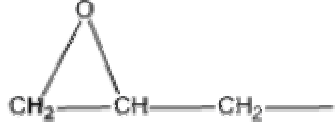


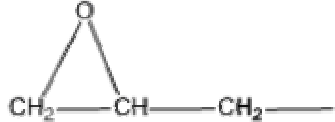
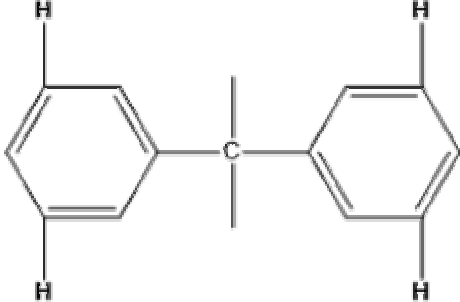
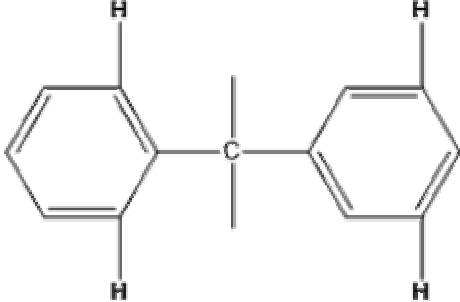


Figure 3.38 $^1\text{H-NMR}$ spectra of Araldite DLS 772 epoxy resin.

The assignment of the peaks for Araldite DLS 772 is shown in the table 3.1 below.

Table 3.1 The assignment of the peaks for Araldite DLS 772 epoxy resin in the $^1\text{H-NMR}$ spectrum

Peak	Chemical Shift, ppm	Assignment
A	1.70	
B	2.38	
C	2.63	
D	3.04	
E	3.95	
F	4.20	
G	6.91	
H	7.19	

^{13}C -NMR analysis was used to obtain more information about the backbone structure of the Araldite DLS 772 epoxy resin. The ^{13}C -NMR spectrum of the Araldite DLS 772 epoxy resin is shown in figure 3.39

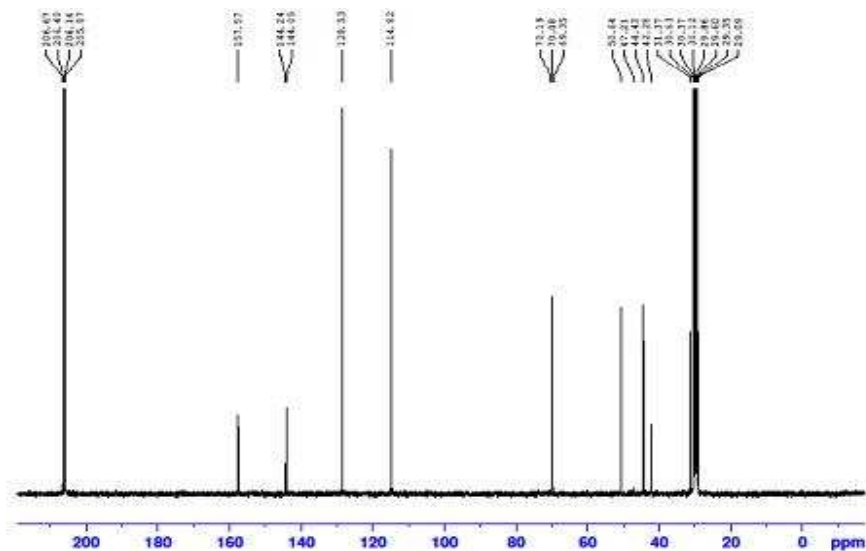


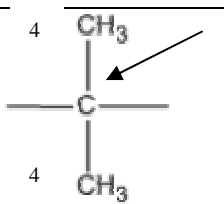
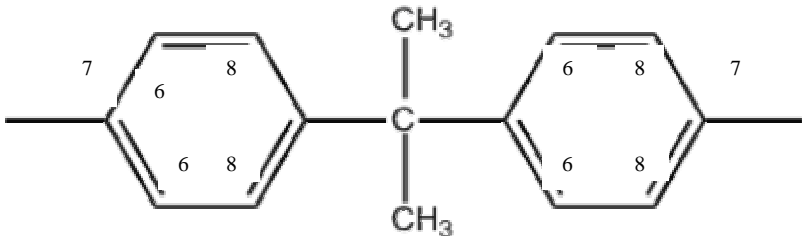
Figure 3.39 ^{13}C -NMR spectra of Araldite DLS 772 epoxy resin.

The aromatic carbons of DGEBA gave rise to five peaks at 114, 128, 140, 144 and 157.6 ppm [70]. The triplet peak at 69-70 ppm and 44.4 ppm are due to the methylene carbons (CH_2) of the epoxy resin. The peaks at 30.9 and 42.4 ppm are due to the carbon atoms present in the methyl (CH_3) and quaternary carbon in the epoxy resin. The peaks around 205 – 207 ppm and 29 - 32 ppm are assigned to the carbon atoms within the acetone, the solvent used in the NMR analysis [4].

The peak at 51.9 ppm was assigned to the methane (CH) carbon of the epoxy resin. Details of the interpretation of the ^{13}C -NMR spectrum of Araldite DLS 772 epoxy resin are shown in table 3.2 below.

Table 3.2 Assignment of the peaks for Araldite DLS 772 epoxy resin in the ^1H -NMR spectrum

Peak	Chemical Shift	Assignment
C1	44.2	
C2	51.9	

C3	69.4	
C4	30.9	
C5	47.3	
C6	114.9	
C7	156.9	
C8	127.7	
C9	146.3	

3.17 Araldite LY 5052 epoxy resin

3.17.1 Molecular weight measurement

Gel Permeation Chromatography was used to determine the average molecular weight of the Araldite LY 5052 epoxy resin. A molecular weight distribution curve for the resin is shown in figure 4.4. The results show that the number average molecular weight (M_n) of Araldite LY 5052 was 72890 g mol^{-1} . The weight average molecular weight (M_w) was $140200 \text{ g mol}^{-1}$. The polydispersity index was 1.92. Polystyrene was the standard used for this measurement.

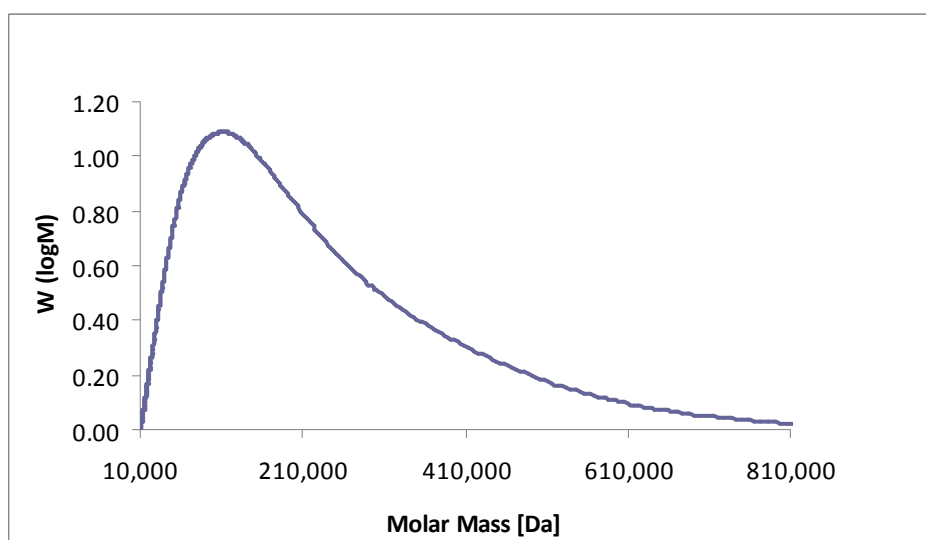


Figure 3.40 Log weight fraction molar mass distributions for Araldite DLS 772 epoxy resin

3.17.2 Chemical structure determination

$^1\text{H-NMR}$ and $^{13}\text{C-NMR}$ were used to identify the chemical structure of Araldite LY 5052 epoxy resin. Figure 3.41 shows the $^1\text{H-NMR}$ spectrum of Araldite LY 5052 epoxy resin.

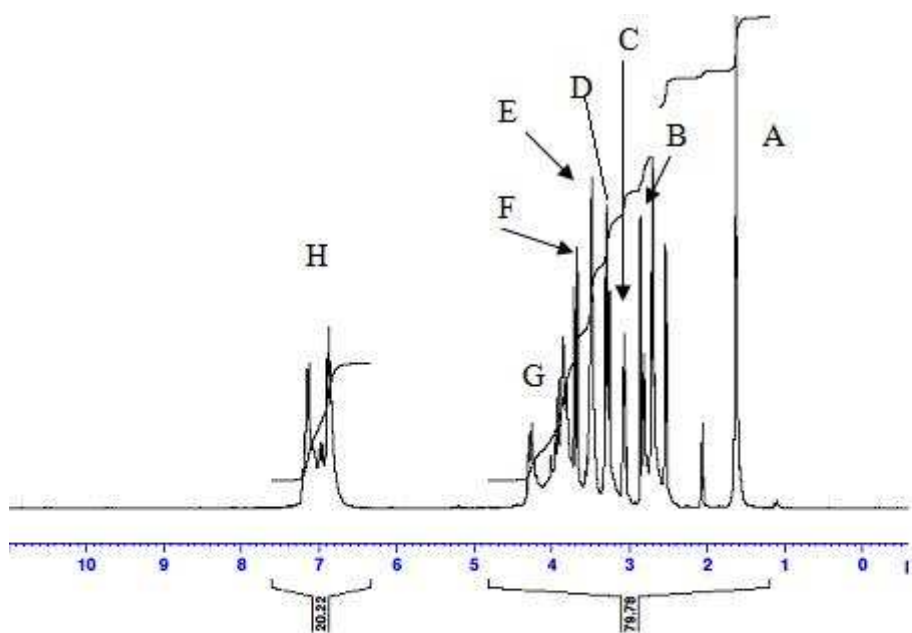


Figure 3.41 $^1\text{H-NMR}$ spectra of Araldite LY 5052 epoxy resin

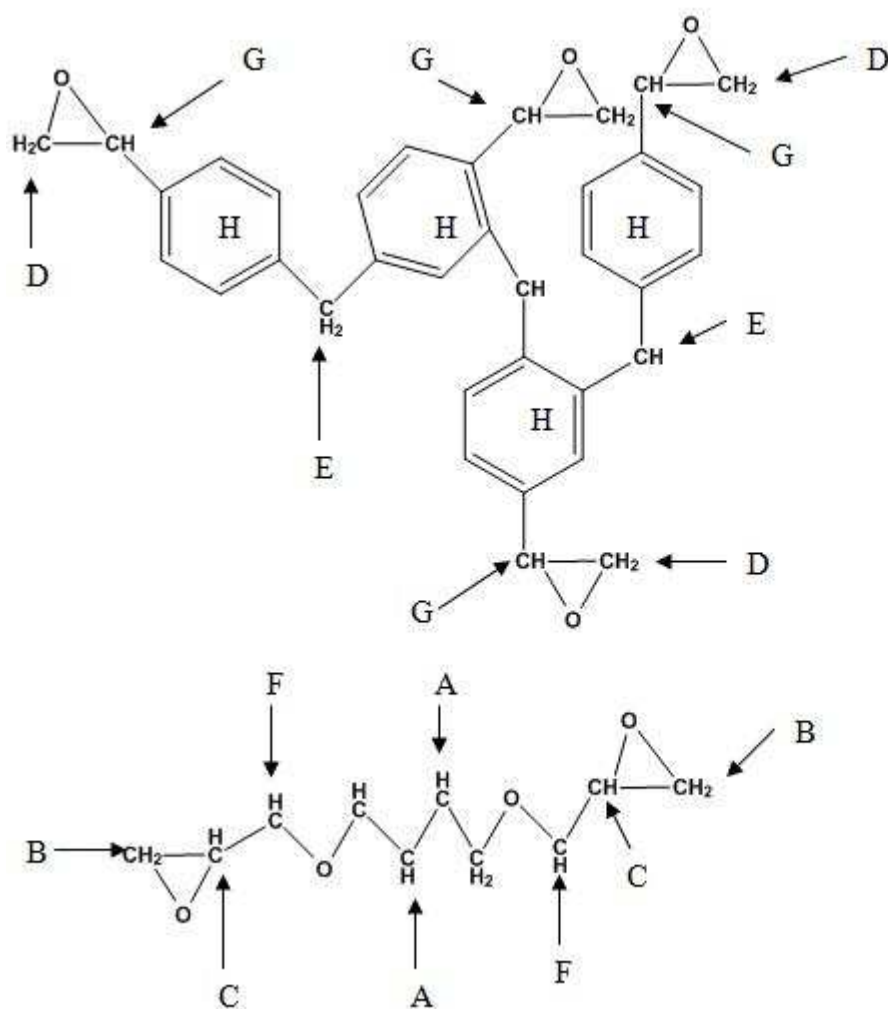


Figure 3.42 Chemical structure of Araldite LY 5052 epoxy resin with lettering indicating the ¹H-NMR peaks in figure 3.41.

¹³C-NMR analysis was again used to obtain more information about the backbone structure of Araldite LY 5052 epoxy resin. The ¹³C-NMR spectrum of Araldite LY 5052 epoxy resin is shown in figure 3.43

Figure 3.44 Chemical structure of Araldite LY 5052 epoxy resin with lettering indicating the ^{13}C -NMR peaks in figure 3.43.

3.18 Density Measurement

The pycnometer technique described in section 3.4 was used to determine the density values of the as-received resins. The results are tabulated in table 3.3. The values obtained from the density measurements are in agreement with the values quoted by the manufacturers [84].

Table 3.3 Comparison of manufacturer's density values with experimental density values for Araldite LY 5052 and DLS 772 epoxy resins.

Material	Manufacturer Value (g/cm³)	Density (g/cm³)
Araldite LY 5052 epoxy resin	1.17	1.19 ± 2
Araldite DLS 772 epoxy resin	1.15 – 1.20	1.17 ± 2

CHAPTER FOUR

4.0 CURE REACTION STUDY

4.1 Introduction

The curing reactions of two epoxy resin systems of Araldite LY 5052, Araldite DLS 772 and the hardener 4,4'-Diaminodiphenylsulfone were studied "in situ" using microwave and conventional curing methods. This was done by the means of differential scanning calorimetry (DSC) and a microwave calorimeter. Isothermal and non-isothermal runs were performed, and the overall fractional conversion and reaction rate were determined from the DSC data. Different methods were used to calculate the kinetic parameters of the curing reactions such as the rate constants, activation energy E_a , reaction orders, and the pre-exponential factor (A). Fourier-transform infrared spectroscopy was used to investigate the fractional conversion profiles of the epoxy chemical groups involved in the curing reactions. During microwave curing, the dielectric properties of the samples were measured using perturbation theory from the changes in resonant frequency and quality factor of the microwave cavity.

4.2 Determination of Appropriate stoichiometric molar ratio

In order to choose the appropriate stoichiometric amine / epoxy (A/E) ratio value to be used for this research, Araldite LY 5052 / 4,4'-DDS epoxy systems were prepared with amine / epoxy stoichiometric ratios of 0.5, 0.6, 0.7, 0.8, 0.9, 1.0, 1.1, 1.2. DSC scans were carried out on these systems. The systems were heated at 10 K min^{-1} from 30 to $350 \text{ }^\circ\text{C}$ in order to cure the sample. It was then cooled back to $0 \text{ }^\circ\text{C}$, and reheated at a heating rate of 10 K min^{-1} in order to determine the glass transition temperature value. The epoxy amine / epoxy ratio with the highest T_g was chosen for this research.

Similar samples of Araldite LY 5052 / 4,4'-DDS epoxy system with amine / epoxy ratios of 0.5, 0.6, 0.7, 0.8, 0.9, 1.0, 1.1, 1.2 were prepared for microwave curing. A heating rate of 10 K min^{-1} was used to cure the sample from 30 to $310 \text{ }^\circ\text{C}$, and allowed to cool. Pieces of the cured samples were extracted from the microwave sample tube, and a DSC scan was carried out on the extracted piece from 30 to $350 \text{ }^\circ\text{C}$ at a heating rate of 10 K min^{-1} in order to determine its glass transition temperature. The glass

transition values of Araldite LY 5052 / 4 4' DDS samples are shown in tables 4.1 and 4.2 and figure 4.1 below.

Table 4.1 Glass transition temperatures of different Amine / Epoxy ratios after a DSC run for Araldite LY 5052 / 4 4' DDS epoxy system

Amine / Epoxy Ratio	T _g run 1 (°C)	T _g run 2 (°C)	T _g run 3 (°C)	T _g run 4 (°C)	T _g run 5 (°C)	Average (°C)	Standard Deviation
0.5	130.1	135.4	135.4	126.1	130.7	130.3	3.4
0.6	169.0	146.7	156.7	148.0	150.8	152.1	9.6
0.7	161.1	160.1	159.9	164.7	164.6	162.6	2.4
0.8	176.9	175.5	164.5	178.0	176.4	174.3	5.5
0.85	183.4	185.3	191.6	195.0	190.7	189.2	4.7
0.9	174.9	177.6	173.7	179.4	175.8	176.3	2.3
1.0	169.2	173.3	175.8	167.5	168.6	170.9	3.5
1.1	164.5	164.1	165.4	165.3	163.2	164.5	0.9
1.2	155.9	150.5	154.2	149.6	153.8	152.8	2.7

Table 4.2 Glass transition temperatures of Araldite LY 5052 / 4 4' DDS with different Amine / Epoxy ratios after curing with a microwave heated calorimeter and subsequently subjected to a DSC run.

A/E Ratio	T _g run 1 (°C)	T _g run 2 (°C)	T _g run 3 (°C)	T _g run 4 (°C)	T _g run 5 (°C)	Average (°C)	Standard Deviation
0.5	86.8	77.2	83.9	82.6	84.7	83.0	3.6
0.6	88.8	91.9	96.5	92.4	93.5	92.6	2.8
0.7	115.1	136.4	134.4	128.7	133.1	129.6	8.5
0.8	139.2	125.3	127.2	130.6	136.8	131.8	6.0
0.9	170.5	176.7	175.3	174.0	175.0	174.3	2.3
1.0	194.7	191.2	190.7	193.2	192.9	192.4	1.6
1.1	156.4	172.0	158.5	165.4	162.3	162.9	6.2
1.2	145.6	154.2	147.6	151.0	148.1	149.3	3.4

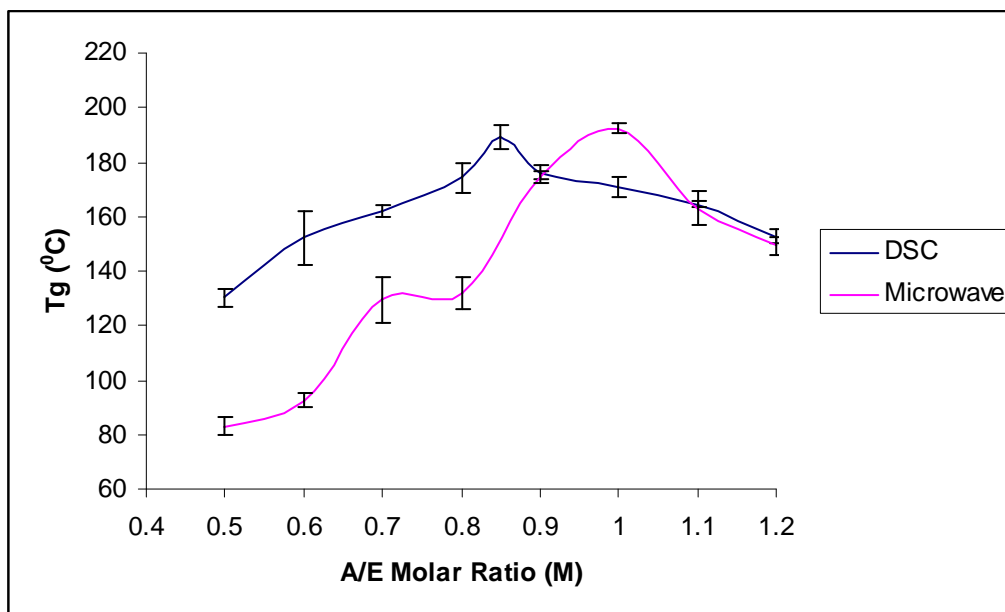


Figure 4.1 Plot of Glass Transition against Molar ratio for different stoichiometric ratios for both conventional and microwave cured samples of Araldite LY 5052 / 4 4' DDS epoxy system.

A similar “heat / cool / heat” DSC scan was performed on Araldite DLS 772 / 4 4' DDS epoxy system with amine / epoxy stoichiometric ratios ranging from 0.5 to 1.2 for conventional cure, and 0.5 to 1.2 for microwave cure. The T_g values for the different molar ratios are shown in the tables 4.3 and 4.4 and figure 4.2 below.

Table 4.3 Glass transition temperatures of Araldite DLS 772 / 4 4' DDS with different Amine / Epoxy ratios after curing with DSC and subjected to a T_g run.

Amine / Epoxy Ratio	T _g run 1 (°C)	T _g run 2 (°C)	T _g run 3 (°C)	T _g run 4 (°C)	T _g run 5 (°C)	Average (°C)	Standard Deviation
0.5	107.0	110.4	114.11	105.2	107.4	108.8	3.5
0.6	128.6	132.5	128.4	127.8	130.2	129.1	2.3
0.7	144.4	146.3	146.7	148.5	145.4	146.2	1.5
0.8	164.6	169.9	168.5	165.9	168.3	167.5	2.1
0.9	150.8	156.1	157.7	159.1	155.4	155.8	3.2
1.0	151.1	147.5	152.6	148.6	149.5	149.8	2.0
1.1	149.7	142.5	150.3	147.3	146.5	147.3	3.1
1.2	140.2	138.4	143.8	139.1	140.6	140.4	2.1

Table 4.4 Glass transition temperatures of different Amine / Epoxy ratios after curing using microwave calorimetry and subsequently subjected to a DSC run for Araldite DLS 772 / 4 4' DDS epoxy system

Amine / Epoxy Ratio	T _g run 1 (°C)	T _g run 2 (°C)	T _g run 3 (°C)	T _g run 4 (°C)	T _g run 5 (°C)	Average (°C)	Standard Deviation
0.5	65.2	67.15	71.0	69.5	66.2	67.8	2.4
0.6	104.9	94.7	102.9	101.4	105.8	101.9	4.4
0.7	121.4	121.1	118.0	122.4	123.8	121.3	2.1
0.8	133.4	144.5	138.0	139.4	138.6	138.8	4.0
0.9	167.1	157.6	166.6	165.3	162.4	163.8	3.9
1.0	172.2	161.59	165.8	170.4	168.8	167.5	4.2
1.1	149.7	142.5	150.3	147.3	146.5	147.3	3.1
1.2	140.2	138.3	143.8	139.1	140.6	140.4	2.1

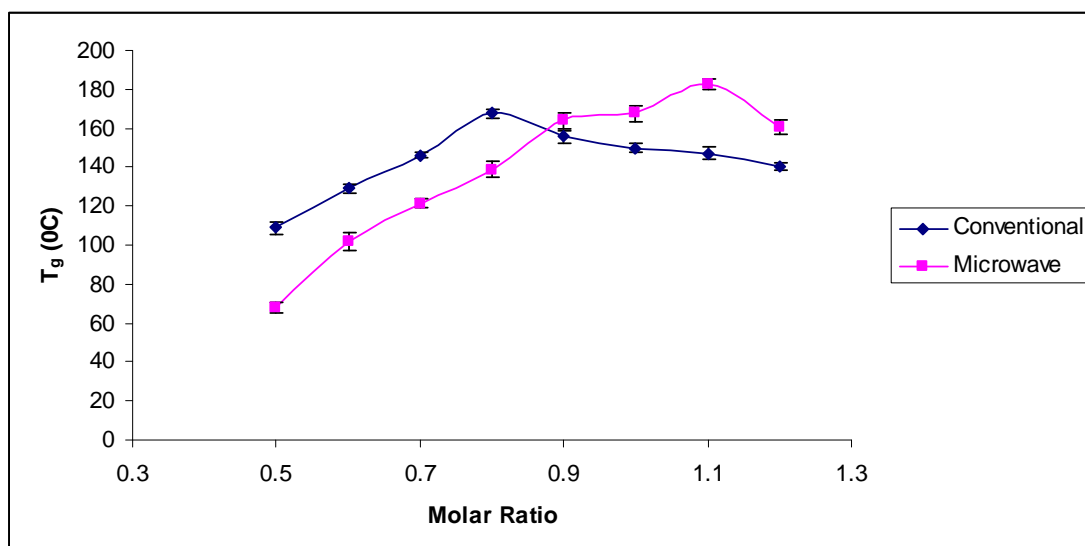


Figure 4.2 Plot of Glass Transition against Molar ratio for different stoichiometric ratios for both conventional and microwave curing for Araldite DLS 772 / 4 4' DDS epoxy system.

Both plots show an increase in T_g values as the Amine / Epoxy ratio increases up to a maximum, and then the T_g starts to decrease. The highest T_g values of conventional and microwave heated samples occur at different stoichiometric ratios. The highest T_g value of the microwave cured sample occurs at a higher Amine / Epoxy Molar ratio than conventional heating. This is an early indication that the curing mechanisms for conventional and microwave curing are different. For both epoxy systems, the Amine / Epoxy ratio with the highest T_g for both microwave and conventionally cured samples was selected and used for all subsequent experiments in this research. Table 4.5 below shows the selected Amine / Epoxy ratio from the conventionally and microwave cured samples which were used in this research.

Table 4.5 Stoichiometric ratios chosen for this research.

Epoxy system	Conventional (amine / epoxy ratio)	Microwave (amine / epoxy ratio)
Araldite LY 5052 / 4 4 DDS	0.85	1.0
Araldite DLS 772 / 4 4 DDS	0.8	1.1

4.3.1 Rheology

Figure 4.3 shows the rheology results of Araldite LY 5052 / 4 4' DDS epoxy system with an amine / epoxy ratio of 0.85.

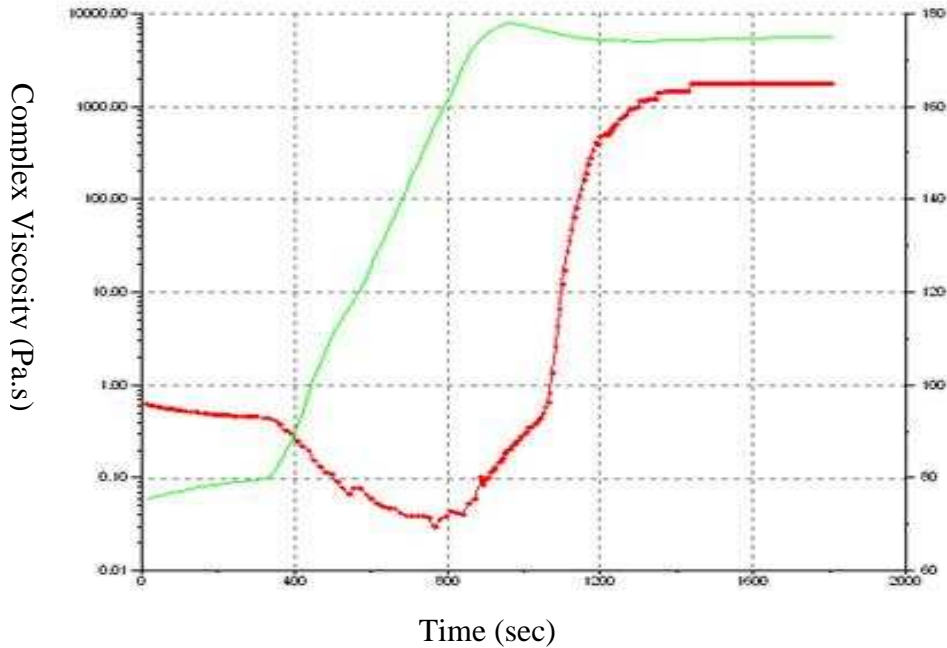


Figure 4.3 Viscosity development during cure for Araldite LY 5052 / 4 4' DDS epoxy system with amine / epoxy ratio of 0.85 as temperature is ramped from 70 °C (t = 0 min) to 180 °C (t = 30 mins).

Figure 4.3 shows the an experimental data for the viscosity of Araldite LY 5052 / 4 4' DDS epoxy system with amine / epoxy ratio of 0.85 as temperature is ramped up with time. The viscosity decreases as the temperature increases. As the time progresses, the viscosity starts to increase. This increase in viscosity is as a result of the progression of the curing reaction. The experimental data for the viscosity of Araldite LY 5052 / 4 4' DDS epoxy system with amine / epoxy ratio of 1.0 and Araldite DLS 772 / 4 4' DDS with amine / epoxy ratio of 0.8 are shown in figures 4.4 and 4.5 below. The curves all show a similar trend. The viscosity drops as the temperature increases, and then starts to rise as the time increases as a result of the progression of the curing reaction.

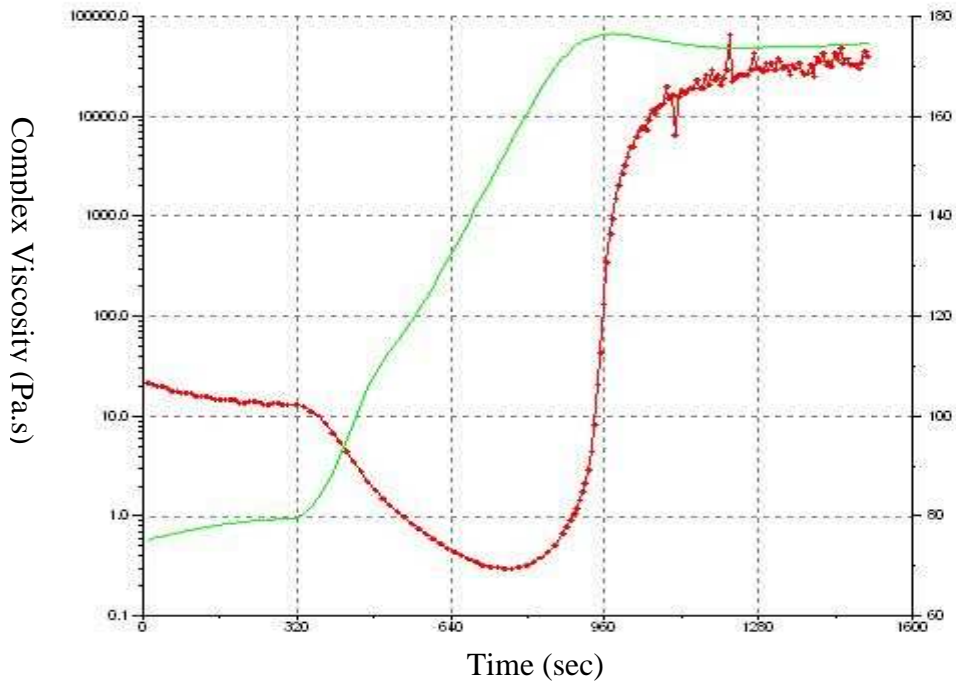


Figure 4.4 Viscosity development during cure for Araldite LY 5052 / 4 4' DDS epoxy system with amine / epoxy ratio of 1.0 as temperature is ramped from 70 °C (t = 0 min) to 180 °C (t = 30 mins).

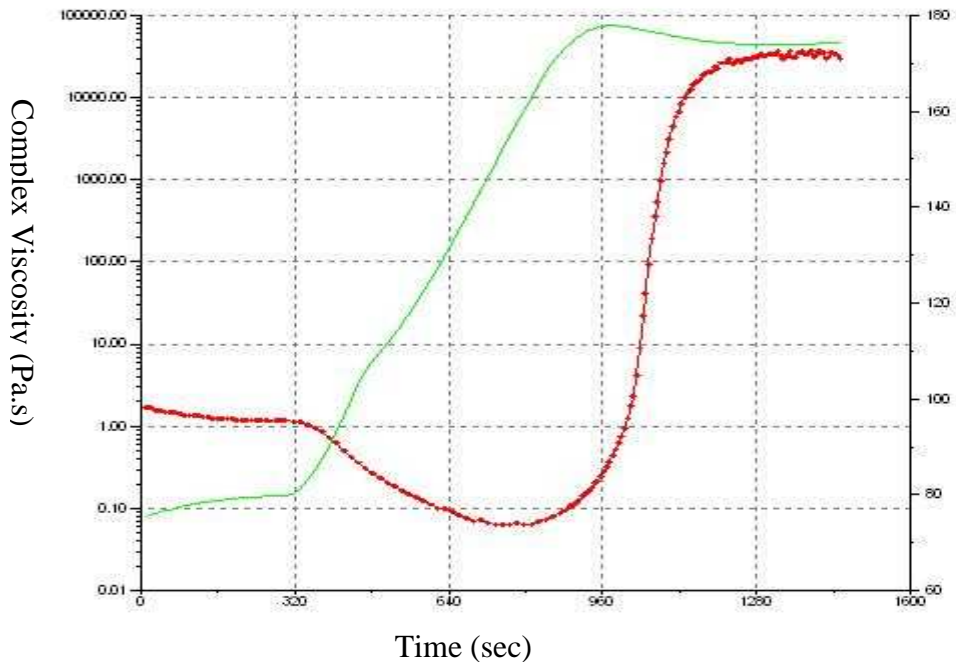


Figure 4.5 Viscosity development during cure for Araldite LY 5052 / 4 4' DDS epoxy system with amine / epoxy ration of 0.8 as temperature is ramped from 70 °C (t = 0 min) to 180 °C (t = 30 mins).

4.4 Dynamic Conventional Curing

A conventional power compensation DSC was used to study the conventional curing reactions of all the stoichiometric mixtures. The typical DSC thermograms for the cure of the Araldite LY 5052 / 4 4' DDS epoxy system with amine / epoxy ratio of 0.85 at different heating rates are shown in the figure 4.3. It was observed that the temperature at which the exothermic peak occurred depended on the heating rate. The exothermic peak moved to a slightly higher temperature at higher heating rates. This is because a thermal lag increases with heating rate, and as a result of this increase, the material starts to react at a higher temperature. The temperature at which the curing reactions were completed also depended on the heating rate. As the heating rate increased, the curing reactions were completed at a higher temperature. The total heat of reaction was calculated by integrating the area under the DSC thermogram. Table 4.6 summarises the exothermic peak temperature, T_p , and the total heat of reaction, ΔH_T . The total heat of reaction is independent of the heating rates. This could be an indication that the reaction mechanisms remains constant over the range of heating rates used in this research.

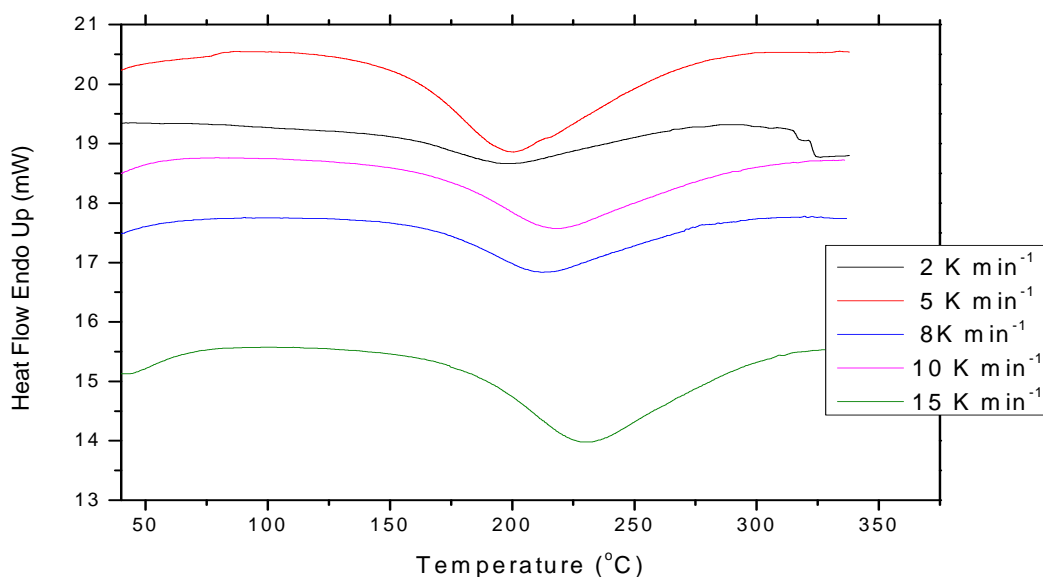


Figure 4.6 Typical DSC thermograms for Araldite LY 5052 / 4 4' DDS epoxy system with an amine / epoxy ratio of 0.85 at different heating rates using conventional DSC.

Table 4.6 Exothermic peak temperature, T_p , The total heat of reaction, ΔH_T , and fractional conversion at the exothermic peak temperature, α_p for Araldite LY 5052 / 4 4' DDS epoxy system with an amine / epoxy ratio 0.85

Heating Rate (K min ⁻¹)	T_p (°C)	ΔH_T (J g ⁻¹)	α_p
2	178	-266	0.38
5	201	-421	0.43
8	212	-272	0.44
10	218	-417	0.45
15	230	-240	0.47

Equations 2.30 and 2.29 in page 80 were used to obtain the values of the reaction rate $\frac{d\alpha}{dt}$, and the fractional conversion, α from the data obtained from the DSC thermogram.

Sections 2.13.6 and 2.13.7 explain how the reaction reaction rate and degree of conversion were obtained. The thermograms were standardized for the purpose of comparison by dividing the calorimetric signal by the sample weight.

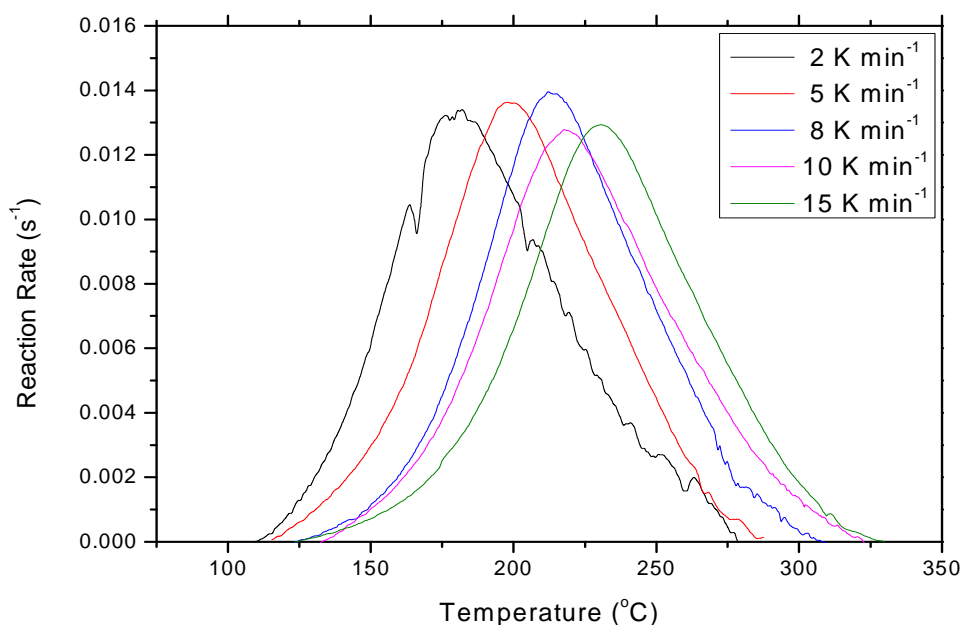


Figure 4.7 Reaction rates for dynamic cure of Araldite LY 5052 / 4 4' DDS epoxy system with an amine / epoxy ratio of 0.85 using conventional heating.

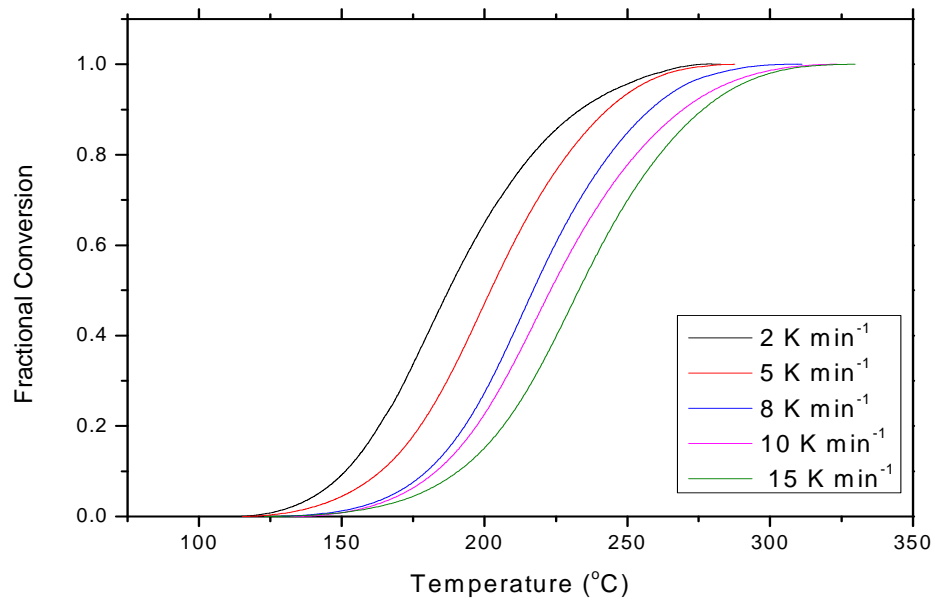


Figure 4.8 Fractional conversion for dynamic cure of Araldite LY 5052 / 4 4' DDS epoxy system with an amine / epoxy ratio of 0.85 using conventional heating.

Figure 4.10 shows a plot of reaction rate against fractional conversion for all the heating rates. Changes can be observed to occur in the reaction rate over the whole range of conversion. For all the heating rates used, the reaction rate increases and reaches a maximum in the fractional conversion range of 0.4-0.5. Beyond this range, the reaction rate started to decrease. This decrease is attributed to the increase in the viscosity of the reaction medium as the curing material gelled [51]. There was a significant reduction in molecular mobility of the reactants at this stage. The reaction became diffusion controlled, and it eventually stopped [37].

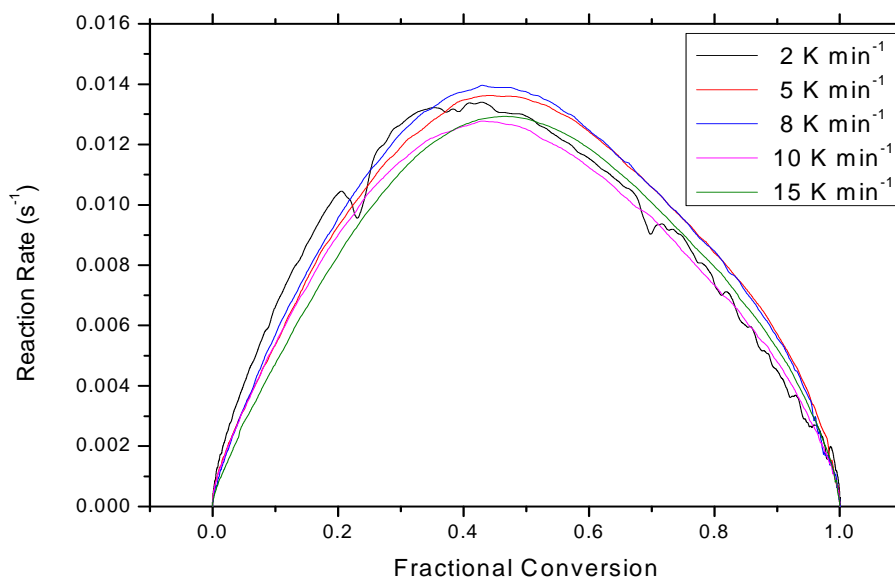


Figure 4.10 Plot of Reaction rate against Fractional Conversion for the curing reaction of Araldite LY 5052 / 4 4' DDS epoxy system with an amine / epoxy ratio of 0.85 using conventional heating.

Typical DSC thermograms for the cure of Araldite LY 5052 / 4 4' DDS epoxy system with an amine / epoxy ratio of 1.0 are shown in figure 4.11 below. As with the Araldite LY 5052 / 4 4' DDS epoxy system with an amine / epoxy ratio of 0.85, the exothermic peak temperature was found to increase with the increasing rate.

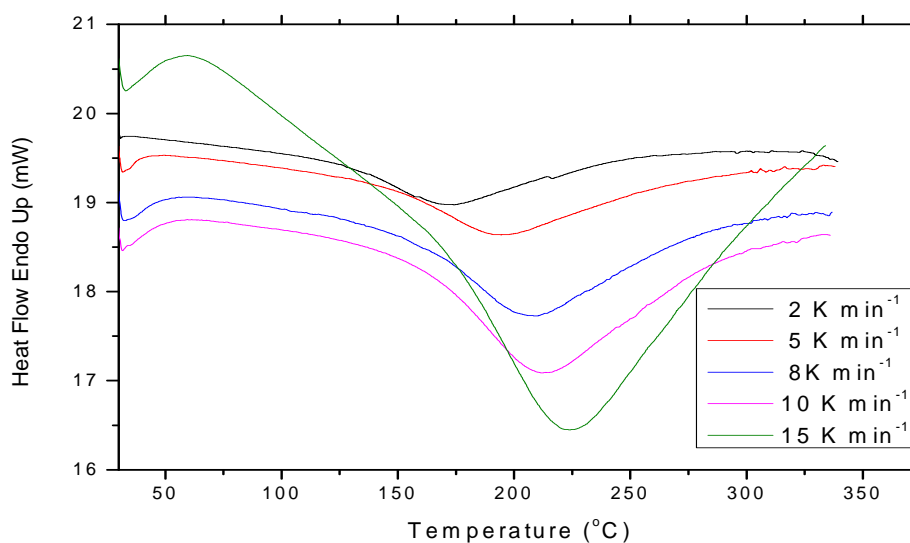


Figure 4.11 DSC thermograms for Araldite LY5052 / 4 4' DDS epoxy system with an amine / epoxy ratio of 1.0 obtained from conventional DSC at different heating rates.

Table 4.7 Summarises the total heat of reaction, ΔH_T , the exothermic peak temperature, T_p and the fractional conversion at the exothermic peak temperature, α_p .

Table 4.7 The exothermic peak T_p , the total heat of reaction, ΔH_T , and fractional conversion at the exothermic peak temperature, α_p for Araldite LY 5052 / 4 4' DDS epoxy system with an amine epoxy ratio of 1.0 at different heating rates.

Heating Rate (K min ⁻¹)	T_p (°C)	ΔH_T (J g ⁻¹)	α_p
2	174	-325	0.43
5	194	-403	0.45
8	210	-415	0.42
10	214	-408	0.46
15	225	-476	0.43

The total heat of reaction seems to be independent of the heating rate. This again suggests that the reaction mechanism remains constant over the range of heating rates used in this study. The temperature dependence of the reaction rates and the temperature dependence on the fractional conversion at different heating rates of Araldite LY 5052 / 4 4' DDS with amine / epoxy ratio of 1.0 are shown in figures 4.11 and 4.12. The plot of reaction rate against fractional conversion for the curing reaction is shown in figure 4.13

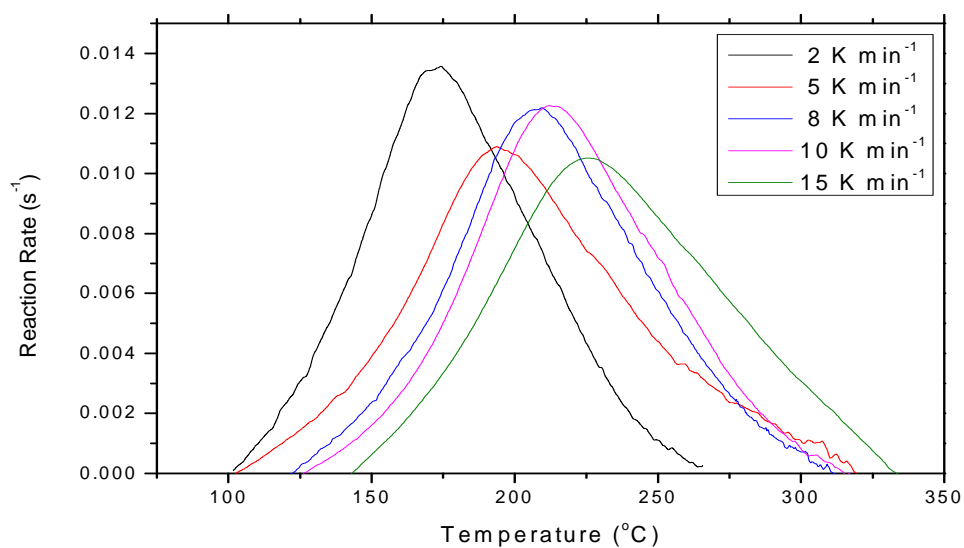


Figure 4.12 Reaction rates for dynamic cure of Araldite LY5052 / 4 4' DDS epoxy system with an amine / epoxy ratio of 1.0 at different heating rates using conventional heating.

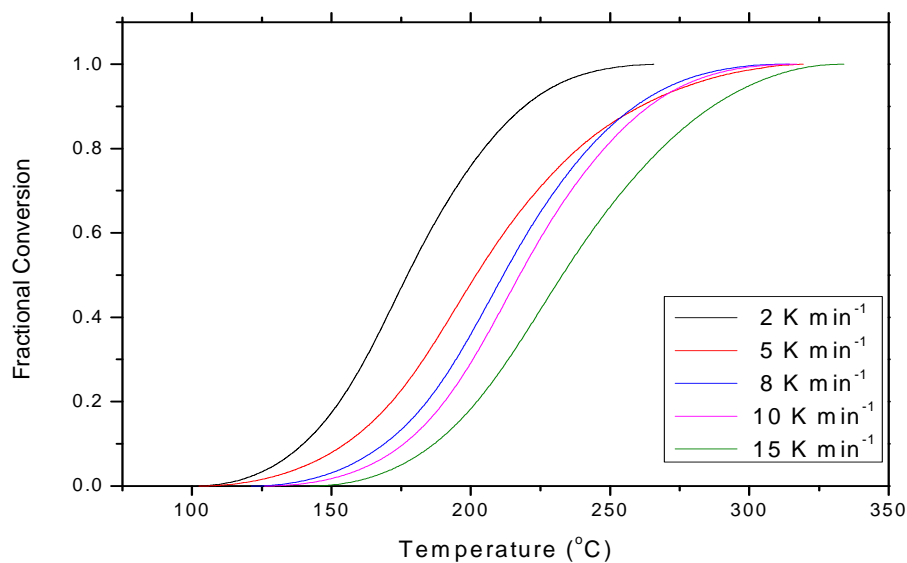


Figure 4.13 Fractional conversion for dynamic cure of Araldite LY 5052 / 4 4' DDS epoxy system with an amine / epoxy ratio of 1.0 at different heating rates using conventional heating.

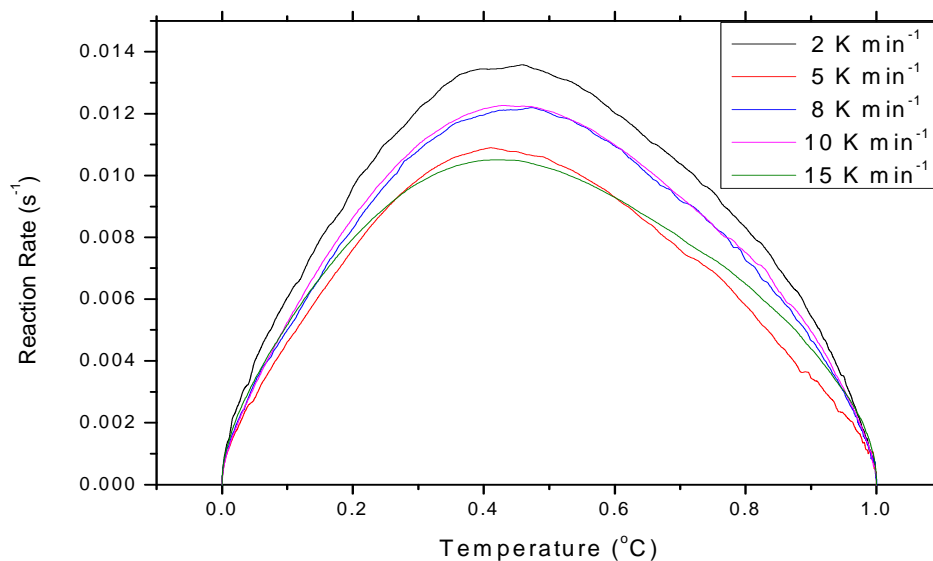


Figure 4.14 Rate of reaction against fractional conversion for the curing reaction of Araldite LY 5052 / 4 4' DDS epoxy system with an amine / epoxy ratio of 1.0 at different heating rates using conventional heating.

Figure 4.14 shows the typical changes in the rate of reaction of Araldite LY5052 / 4 4' DDS epoxy system with an amine / epoxy ratio of 1.0 over the whole range of conversion. For all the heating rates used, the reaction rates reached their maximum values at conversion in the range 0.4 to 0.46. As the reaction proceeded, the viscosity of the reaction medium increased, allowing diffusion controlled termination process to take place [51]. This diffusion controlled termination process leads to a decrease in the reaction rate until the curing reaction eventually stopped [37].

The DSC thermograms, reaction rate plots, fractional conversion plots and plots of reaction rates against fractional conversion for Araldite DLS 772 / 4 4' DDS epoxy systems with amine / epoxy ratios of 0.8 and 1.1 are shown in figure 5.15 to 5.22 below. The total heats of reaction, ΔH_T , the exothermic peak temperatures, T_p and the fractional conversions at the exothermic peak temperature, α_p for Araldite DLS 772 / 4 4' DDS epoxy systems with amine / epoxy ratios of 0.8 and 1.1 are summarised in tables 4.8 and 4.9.

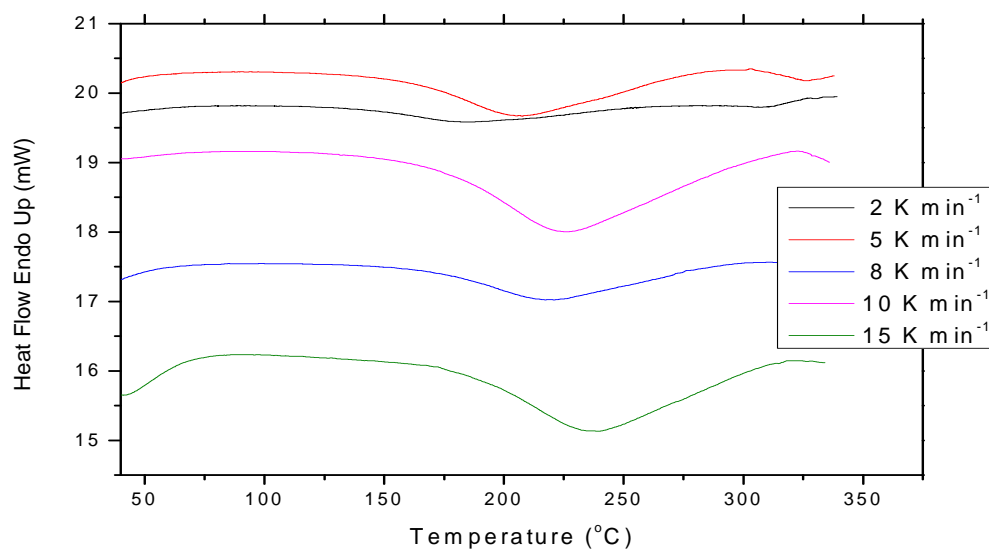


Figure 4.15 DSC thermograms for Araldite DLS 772 / 4 4' DDS epoxy system with an amine / epoxy ratio of 0.8 obtained from conventional DSC at different heating rates.

Table 4.8 The exothermic peak T_p , the total heat of reaction, ΔH_T , and fractional conversion at the exothermic peak temperature, α_p for Araldite DLS 772 / 4 4' DDS epoxy system with an amine / epoxy ratio of 0.8 at different heating rates.

Heating Rate (K min ⁻¹)	T_p (°C)	ΔH_T (J g ⁻¹)	α_p
2	174	-259	0.41
5	194	-324	0.43
8	210	-194	0.46
10	214	-279	0.45
15	225	-224	0.45

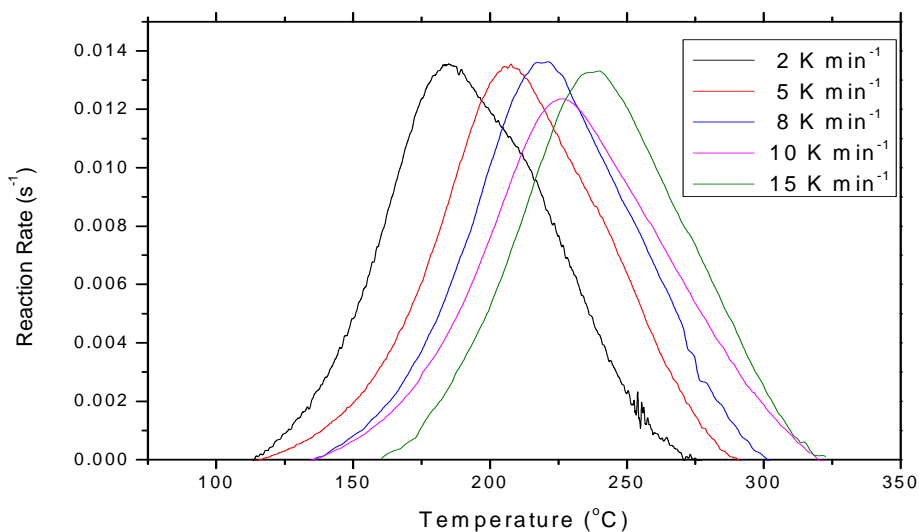


Figure 4.16 Reaction rates for dynamic cure for Araldite DLS 772 / 4 4' DDS epoxy system with an amine / epoxy ratio of 0.8 at different heating rates using conventional heating

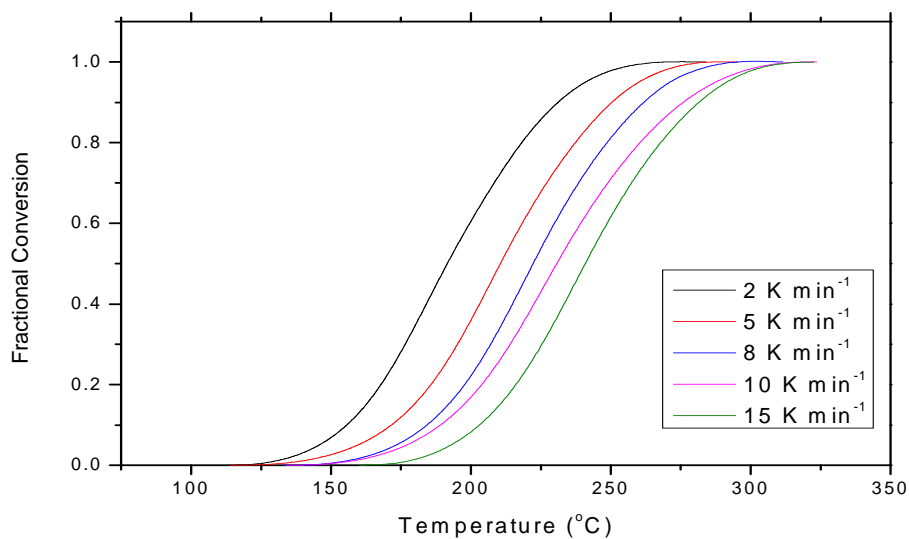


Figure 4.17 Fractional conversion for dynamic cure of Araldite DLS 772 / 4 4' DDS epoxy system with an amine / epoxy ratio of 0.8 at different heating rates using conventional heating

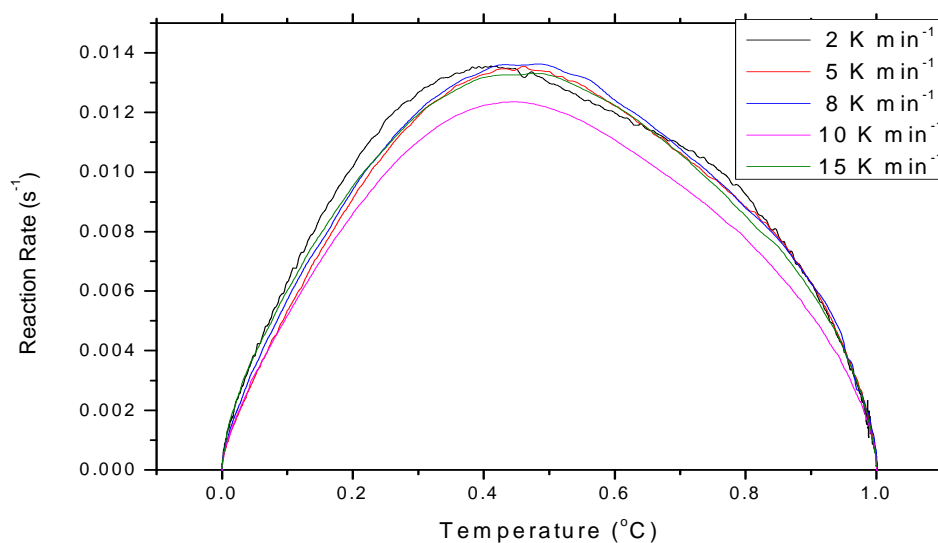


Figure 4.18 Rate of reaction against fractional conversion for the curing reaction of Araldite DLS 772 / 4 4' DDS epoxy system with an amine / epoxy ratio of 0.8 at different heating rates

For all the heating rates used, the reaction rates reached their maximum values at a conversion in the range of 0.4 to 0.5. As the reaction proceeded, the viscosity of the medium increased. Cross-linking became controlled by diffusion and a drop in the reaction rate occurs until the curing reaction eventually stopped [85]

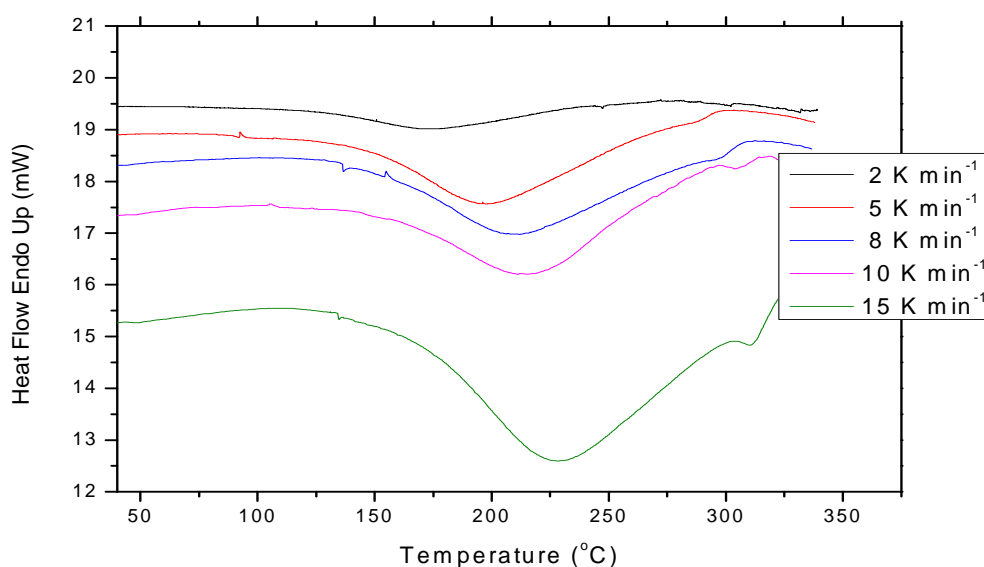


Figure 4.19 DSC thermograms for Araldite DLS 772 / 4 4' DDS epoxy system with an amine / epoxy ratio of 1.1 obtained from conventional DSC at different heating rates.

Table 4.9 The exothermic peak T_p , the total heat of reaction, ΔH_T , and fractional conversion at the exothermic peak temperature, α_p for Araldite DLS 772 / 4 4' DDS epoxy system with an amine / epoxy ratio of 1.1 at different heating rates.

Heating Rate	T_p ($^{\circ}\text{C}$)	ΔH_T (J/g)	α_p
2	174	-212	0.40
5	194	-202	0.42
8	210	-225	0.42
10	214	-213	0.44
15	225	-189	0.46

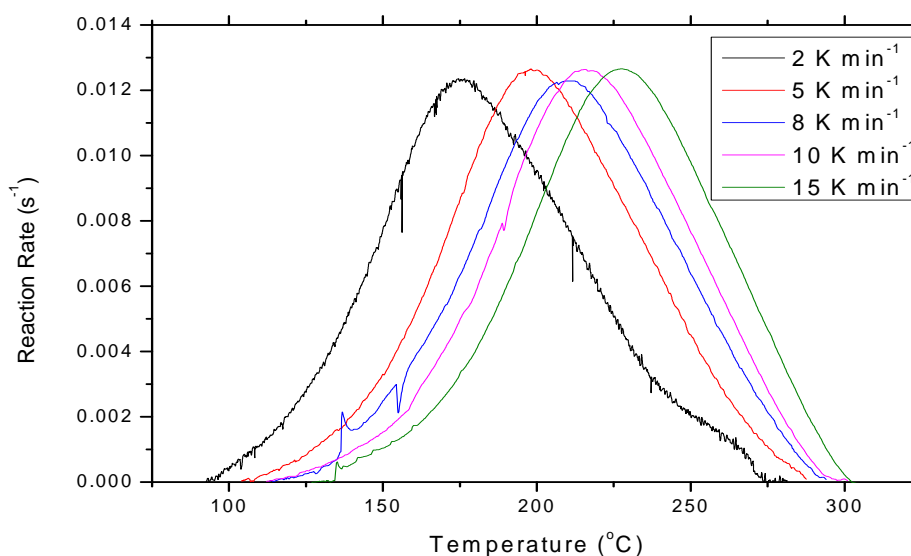


Figure 4.20 Reaction rates for dynamic cure of Araldite DLS 772 / 4 4' DDS epoxy system with an amine / epoxy ratio of 1.1 at different heating rates using conventional heating

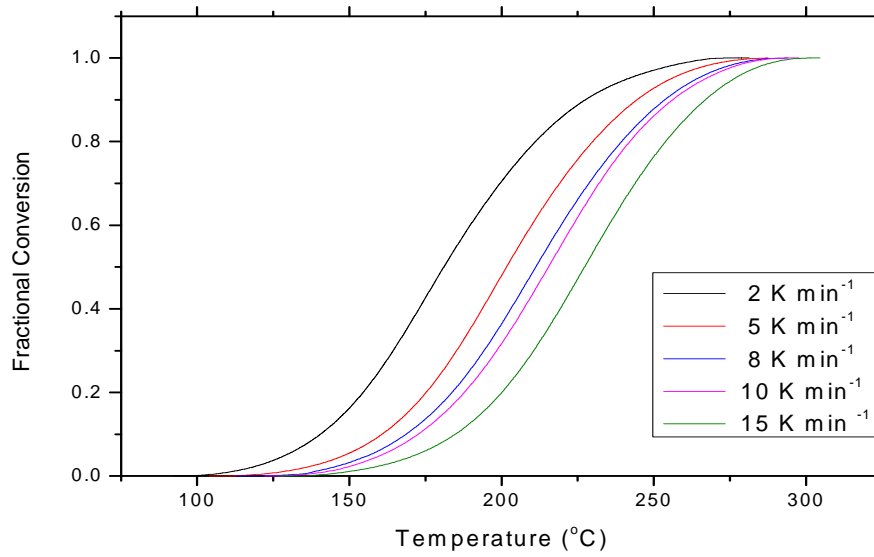


Figure 4.21 Fractional conversion for dynamic cure of Araldite DLS 772 / 4 4' DDS epoxy system with an amine / epoxy ratio of 1.1 at different heating rates using conventional heating

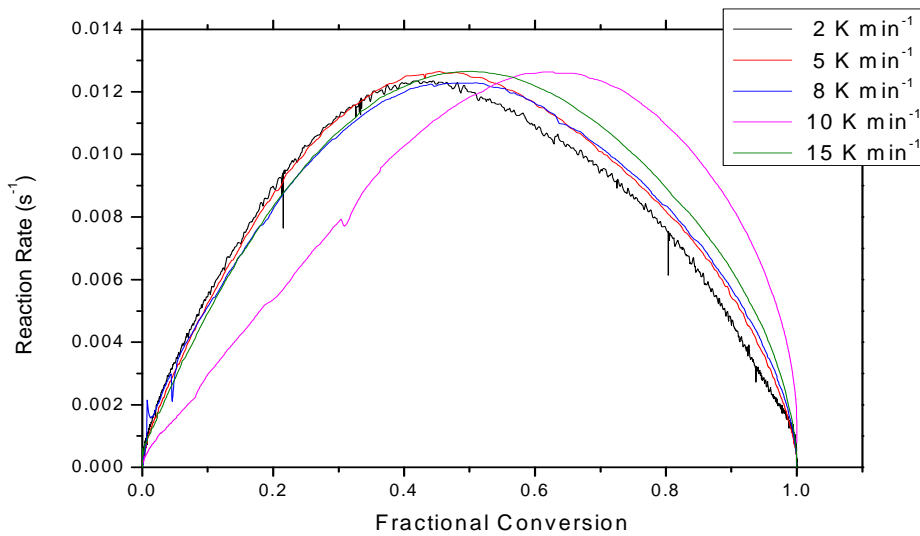


Figure 4.22 Rate of reaction against fractional conversion for the curing reaction of Araldite DLS 772 / 4 4' DDS epoxy system with amine / epoxy ratio of 1.1 at different heating rates using conventional heating.

Figure 4.22 shows the typical changes in the rate of reaction of Araldite DLS 772 / 4 4' DDS epoxy system with an amine / epoxy ratio of 1.1 over the whole range of

conversion. For the heating rates used, the reaction rates reached their maximum values at a conversion of between 0.4 and 0.5. As the reaction proceeded, the viscosity of the reaction medium increases, allowing diffusion controlled termination process to take place. This diffusion controlled termination process led to a decrease in the reaction rate until the curing reaction eventually stopped [37].

4.5 Microwave Curing

A microwave-heated calorimeter was used to cure the samples with microwave heating. The curing procedure is described in section 3.3.3. The microwave thermal analysis measurements were carried out by monitoring the microwave power level as a function of sample temperature during the controlled heating programs.

The measurements of the reaction exotherm for Araldite DLS 772 / 4 4' DDS epoxy system with an amine / epoxy ratio of 0.85 cured at different heating rates is shown in figure 4.23. The values of the exothermic peak temperature, and the fractional conversion value at the exothermic peak temperature are summarised in table 4.10

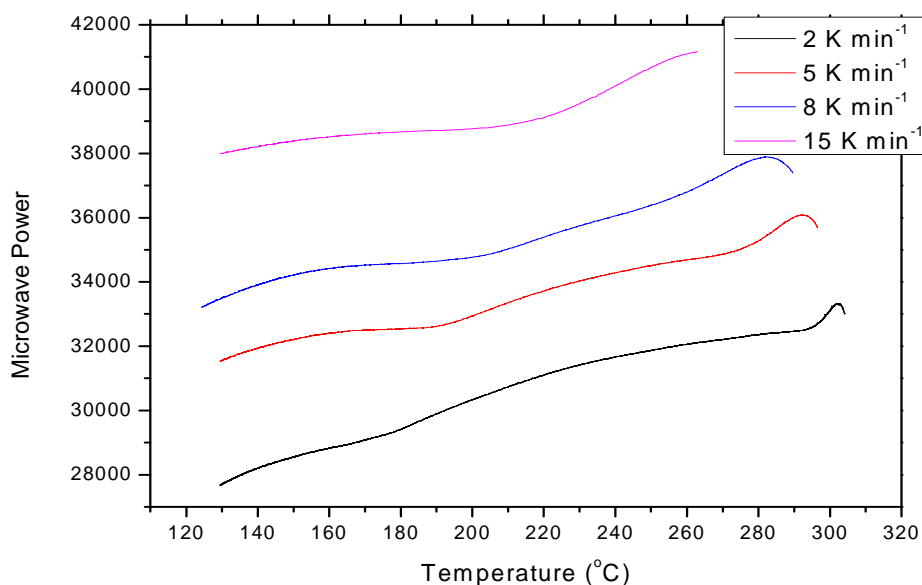


Figure 4.23 Microwave thermograms for Araldite LY 5052 / 4 4' DDS epoxy system with an amine / epoxy ratio of 0.85 obtained from microwave heating at different heating rates.

Table 4.10 The exothermic peak T_p , the total heat of reaction, ΔH_T , and fractional conversion at the exothermic peak temperature, α_p for Araldite LY 5052 / 4 4' DDS epoxy system with an amine / epoxy ratio of 0.85 at different heating rates using microwave heating

Heating Rate ($K \text{ min}^{-1}$)	T_p ($^{\circ}C$)	α_p
2	173	0.58
5	191	0.49
8	200	0.52
10	203	0.52
15	211	0.49

The total heat of reaction ΔH_T for the microwave cured sample can not be determined because although it is possible to convert the microwave power to absolute values, it is extremely time consuming, and it was not within the scope of my study.

Just like conventional heating, we observe that the temperature at which the exothermic peak temperature occurred increased with increasing heating rate. Compared to conventional heating, the exothermic peak temperature was slightly lower in samples cured with microwave heating than samples cured with conventional heating. Also, the onset temperatures were found to be slightly lower in samples cured in microwave heating than samples cured in conventional heating. These observations suggest that the curing reactions under the microwave influence occurred at slightly lower temperatures.

Equations 5.1 and 5.2 were used to determine the reaction rate $\frac{d\alpha}{dt}$ and the fractional conversion, α from the data obtained from the filtered data obtained from microwave heating. The temperature dependence of the fractional conversion and the reaction rates at different heating rates are shown in figures 4.24 and 4.25.

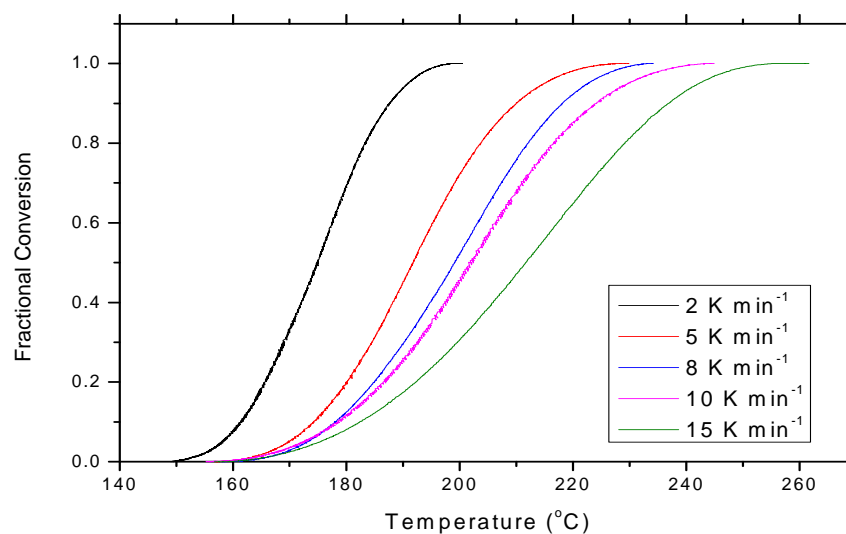


Figure 4.24 Fractional conversion of dynamic microwave cure reaction of Araldite LY 5052 / 4 4' DDS epoxy system with an amine / epoxy ratio of 0.85 at different heating rates using microwave heating.

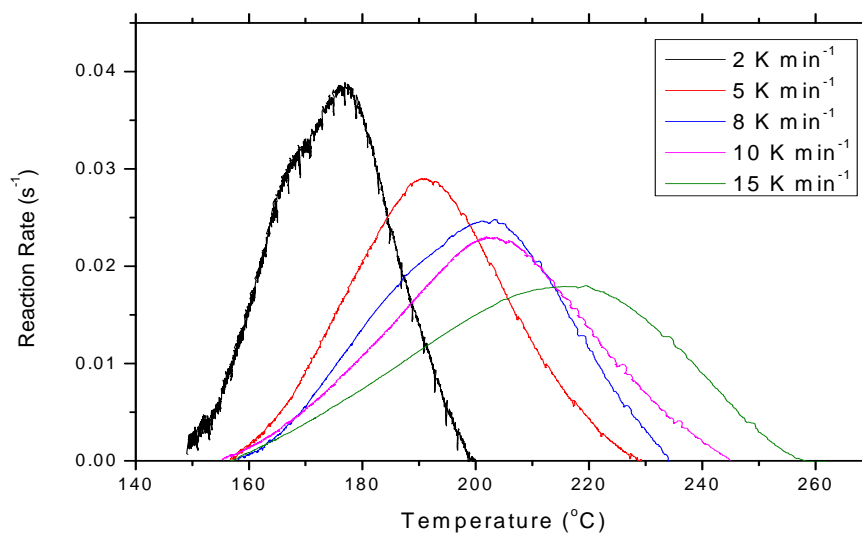


Figure 4.25 Plot of Reaction rates against temperature for dynamic microwave cure reaction of Araldite LY 5052 / 4 4' DDS epoxy system with an amine / epoxy ratio of 0.85 at different heating rates using microwave heating.

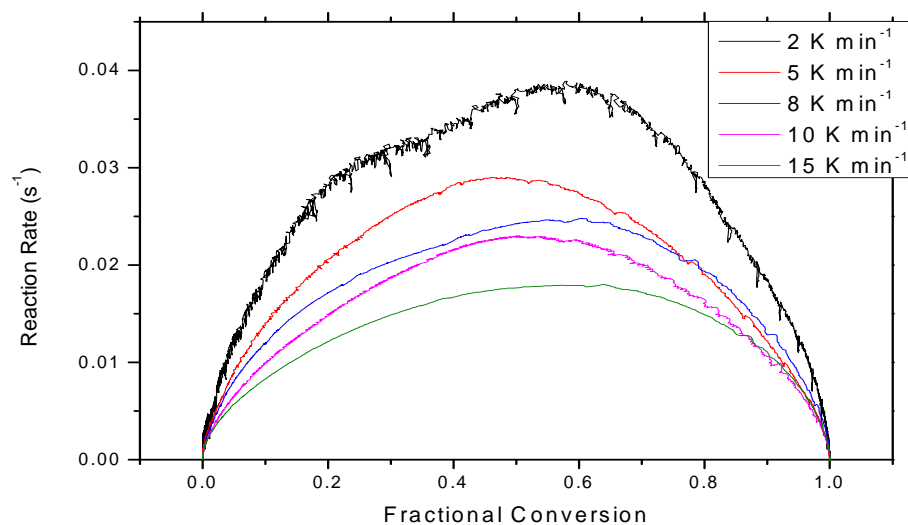


Figure 4.26 Plot of reaction rates against fractional conversion for the dynamic microwave cure reaction of Araldite LY 5052 / 4 4' DDS epoxy system with an amine / epoxy ratio of 0.85 at different heating rates.

Figure 4.26 Shows the typical changes in the rates of reaction over the whole range of conversion of microwave cured Araldite LY 5052 / 4 4' DDS epoxy system with an amine / epoxy ratio of 0.85. The reaction rates reached a maximum values and beyond the maximum points, the reaction rates began to decrease. This is because the viscosity of the reaction medium starts to increase, and this enables the diffusion control of the termination process to become the controlling factor. These factors initiate a decrease in the reaction rates until curing eventually stops. Also, the value of the maximum reaction rate was found to be at approximately 10% higher conversion, than the corresponding value observed in thermal curing.

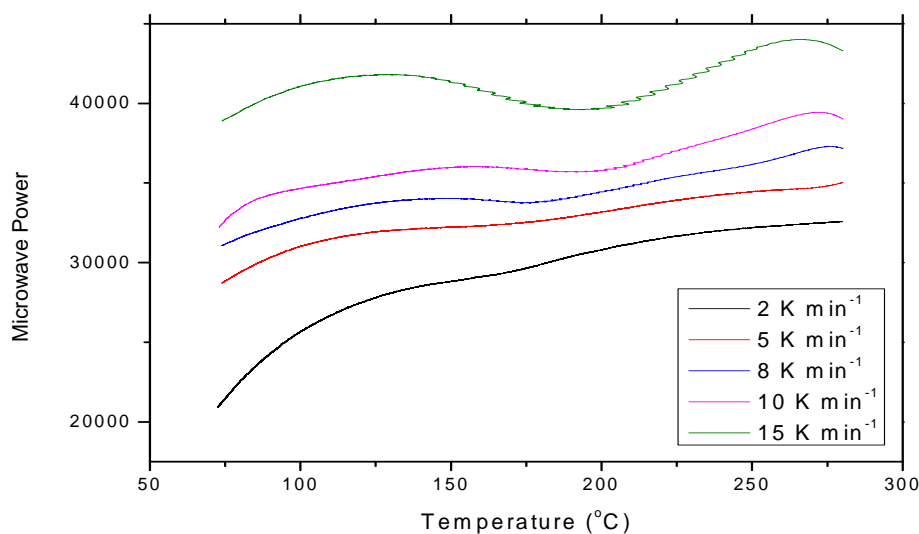


Figure 4.27 DSC thermograms for Araldite LY 5052 / 4 4' DDS epoxy system with an amine / epoxy ratio of 1.0 obtained from microwave heating at different heating rates

Table 4.11 The exothermic peak T_p , the total heat of reaction, ΔH_T , and fractional conversion at the exothermic peak temperature, α_p for Araldite LY 5052 / 4 4' DDS epoxy system with an amine / epoxy ratio of 1.0 at different heating rates using microwave heating.

Heating Rate ($K\ min^{-1}$)	T_p ($^{\circ}C$)	α_p
2	170	0.56
5	178	0.48
8	182	0.43
10	200	0.44
15	205	0.61

Figure 4.27 shows the measurements of reaction exotherm for the curing of 1.0M amine/epoxy ratio for Araldite LY 5052 / 4 4' DDS epoxy system with an amine / epoxy ratio of 1.0 at five different heating rates with the microwave-heated calorimetry. The values of the exothermic peak temperature, T_p and the fractional conversion, α_p at the exothermic peak temperature are shown in table 4.11. As with the microwave curing

of Araldite LY 5052 / 4 4' DDS epoxy system with an amine / epoxy ratio of 0.85, the exothermic peak temperature increased as the heating rate increases. At the same heating rate, the exothermic peak temperature was slightly lower in microwave heating as compared to the conventional heating. Also, the curing reaction of Araldite LY 5052 / 4 4' DDS epoxy system with an amine / epoxy ratio of 1.0 is observed to begin at a lower temperature in microwave heating. This conclusion was arrived at because the onset temperature was found to be lower in microwave heating than in conventional heating.

Figures 4.28 and 4.29 show the plots of the temperature dependence of the fractional conversion and the reaction rates of cured microwave cured samples of Araldite LY 5052 / 4 4' DDS epoxy system with an amine / epoxy ratio of 1.0

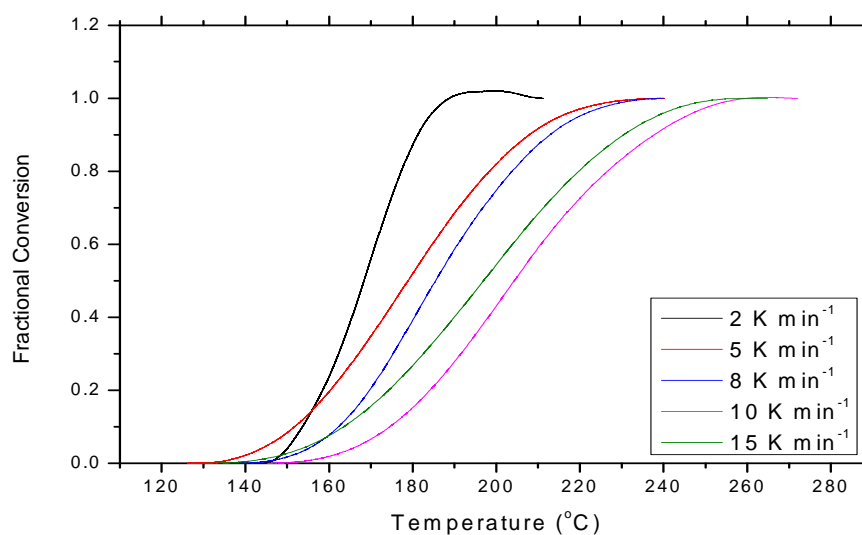


Figure 4.28 Fractional conversion for dynamic cure of Araldite LY 5052 / 4 4' DDS epoxy system with an amine / epoxy ratio of 1.0 at different heating rates using microwave heating.

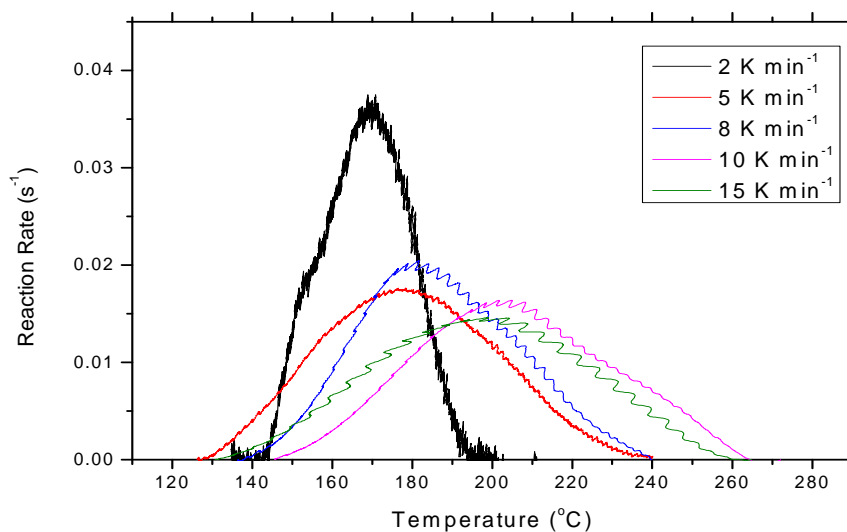


Figure 4.29 Reaction rates for dynamic microwave cure of Araldite LY 5052 / 4 4' DDS epoxy system with an amine / epoxy ratio of 1.0 at different heating rates using microwave heating.

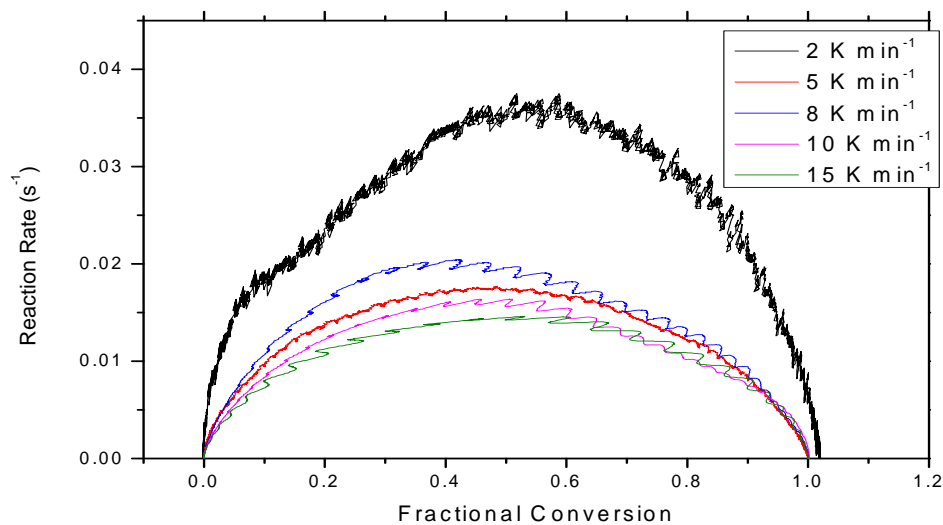


Figure 4.30 Plot of reaction rates against fractional conversion for the dynamic microwave cure reaction of Araldite LY 5052 / 4 4' DDS epoxy system with an amine / epoxy ratio of 1.0 at different heating rates.

At a specific temperature, the fractional conversion is higher for microwave curing at a lower heating rate. The fractional conversion increased with increasing heating rate.

The changes in the rate of reaction over the range of conversion of microwave cured Araldite LY 5052 / 4 4' DDS epoxy system with an amine / epoxy ratio of 1.0 is shown in figure 4.32. The reaction rates reached a maximum at conversion range of 0.4 - 0.55 for all the heating rates used. These values suggested that the same curing reactions occurred regardless of the heating rates. Also, the value of the fractional conversion at the maximum reaction rate was found to be slightly higher, about 10% higher than the corresponding value which was observed in thermal curing of Araldite LY 5052 / 4 4' DDS epoxy system with an amine / epoxy ratio of 1.0.

The thermograms for the dynamic microwave cure of Araldite DLS 772 / 4 4' DDS with an amine / epoxy ratio of 0.8 is shown in figure 4.31.

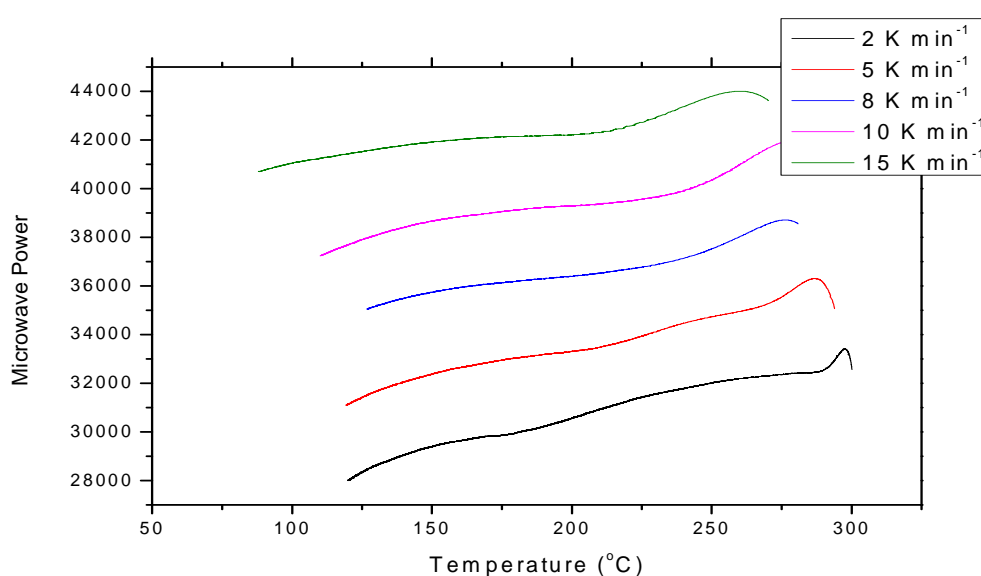


Figure 4.31 Thermograms obtained for Araldite DLS 772 / 4 4' DDS epoxy system with an amine / epoxy ratio of 0.8 obtained from microwave heating at different heating rates.

Figures 4.32 and 4.33 show the plots of fractional conversion, and reaction rate against temperature at different heating rates under microwave curing.

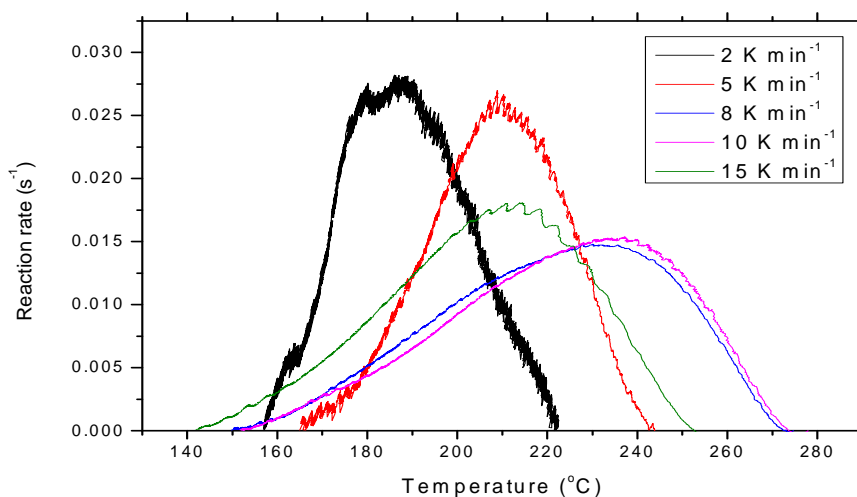


Figure 4.32 Reaction rates for dynamic microwave cure of Araldite DLS 772 / 4 4' DDS epoxy system with an amine / epoxy ratio of 0.8 at different heating rates using microwave heating

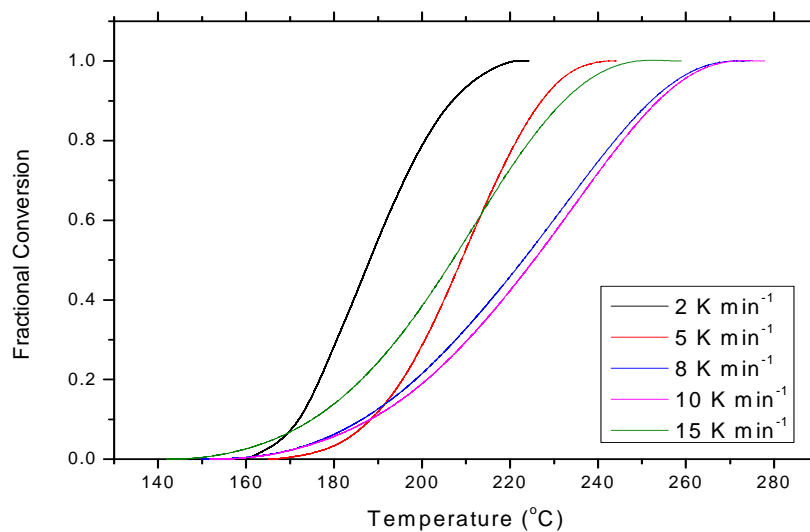


Figure 4.33 Fractional conversion for dynamic microwave cure of Araldite DLS 772 / 4 4' DDS epoxy system with an amine / epoxy ratio of 0.8 at different heating rates using microwave heating.

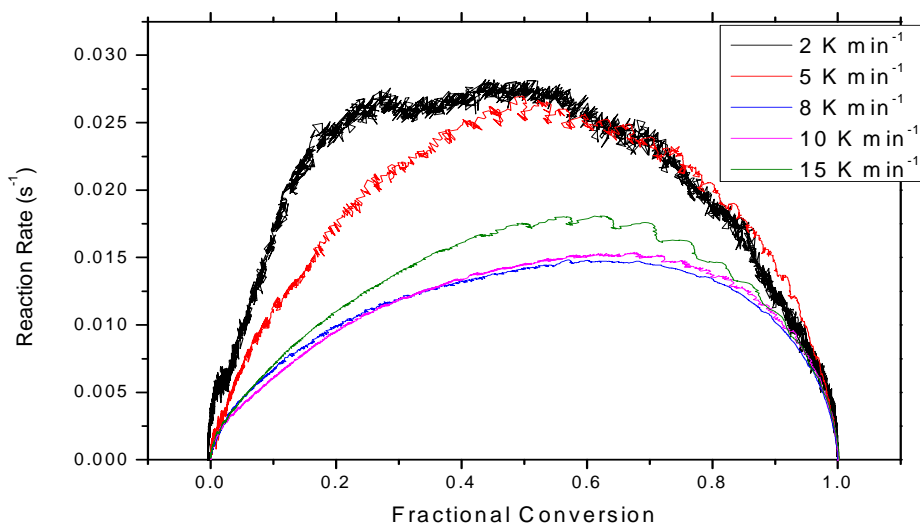


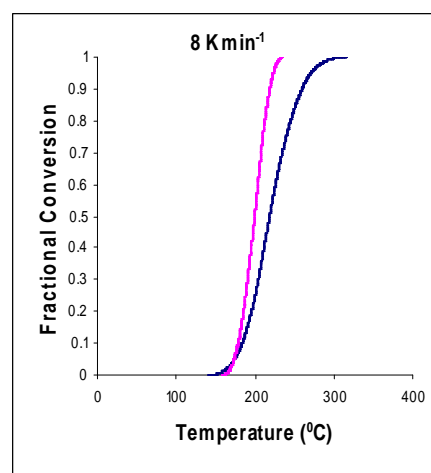
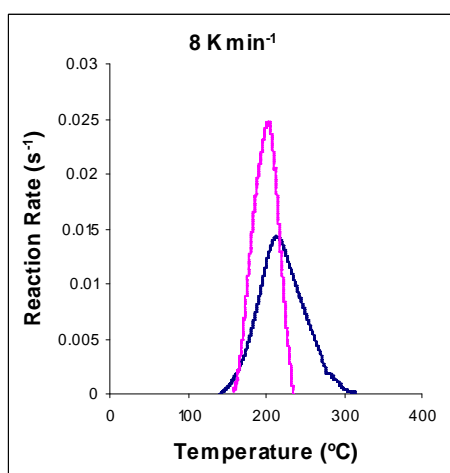
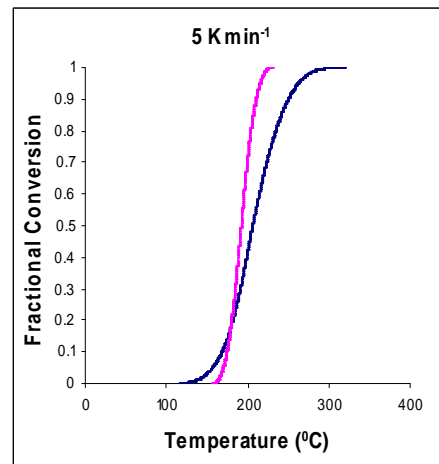
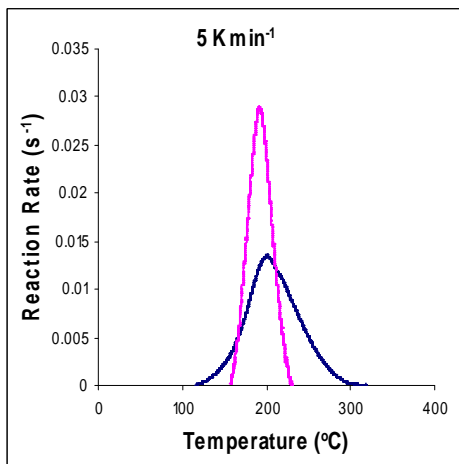
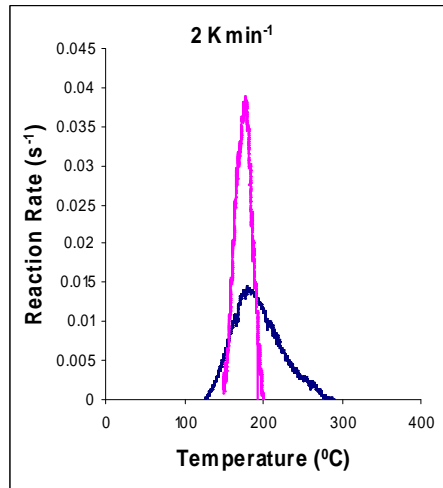
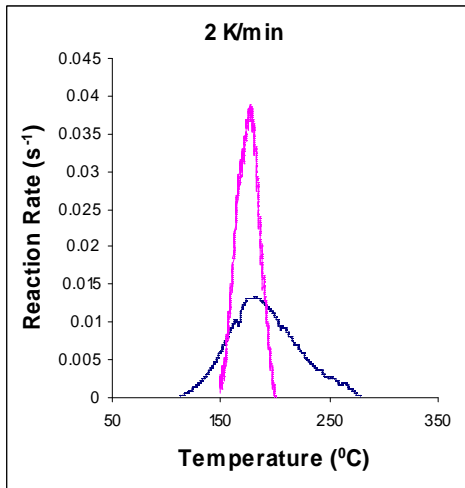
Figure 4.34 Rate of reaction against fractional conversion for the curing reaction of Araldite DLS 772 / 4 4' DDS epoxy system with an amine / epoxy ratio of 0.8 at different heating rates for microwave curing

4.5.1 Comparison of the fractional conversion and reaction rate obtained from DSC and Microwave calorimeter

Some differences can be observed in the curing characteristics of samples undergoing conventional and microwave heating. Some of these differences include

- i) The temperature at which the reaction rate begins and the exothermic peak temperature are slightly lower in microwave heating method.
- ii) The fractional conversion at the maximum reaction rate where the diffusion-controlled reaction starts are lower for microwave cured samples.

The temperature dependence of the reaction rate and fractional conversion for the curing of Araldite LY 5052 / 4 4' DDS epoxy system with amine / epoxy ratio of 0.85 at different heating rates are shown below individually. The blue curve indicates the conventionally cured sample, while the red curve indicates the microwave cured sample.



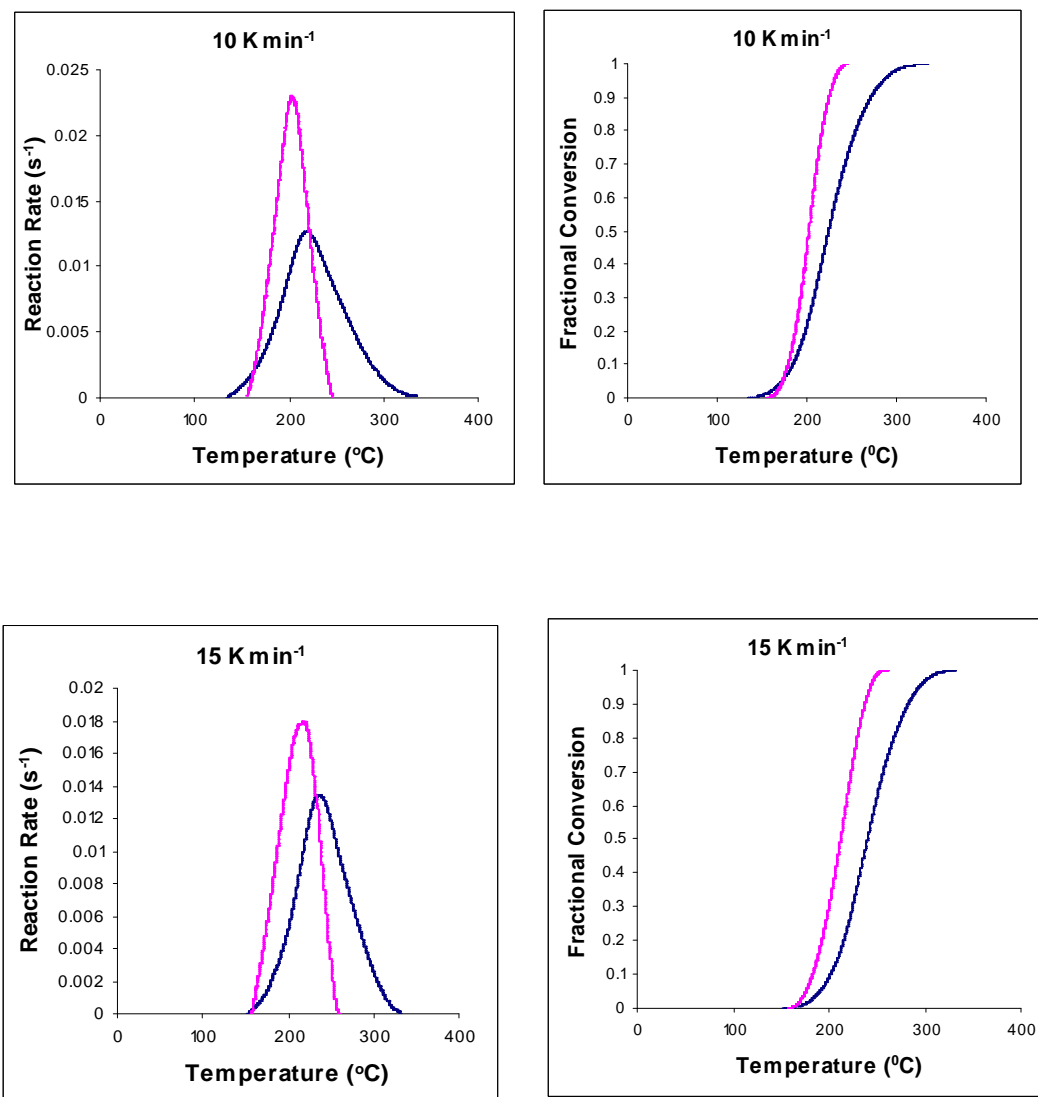


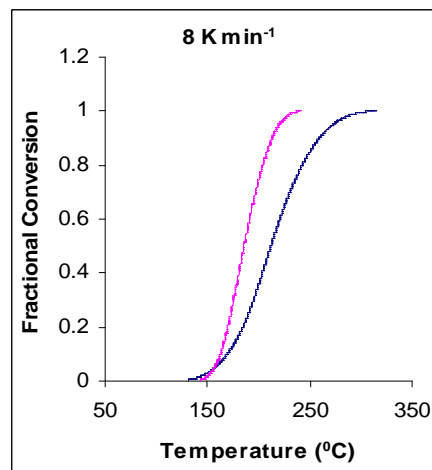
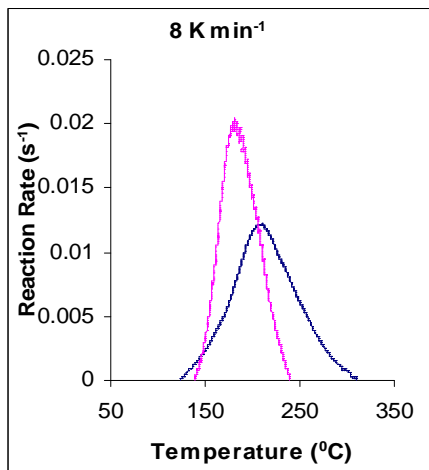
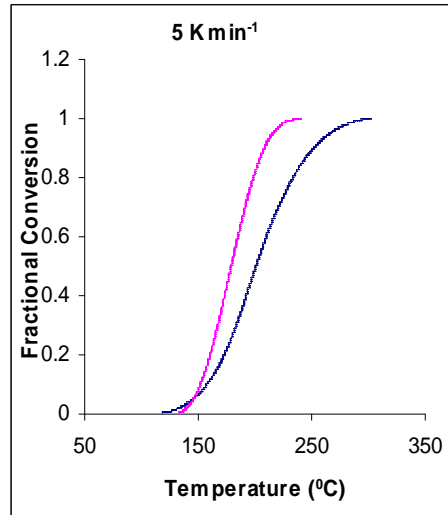
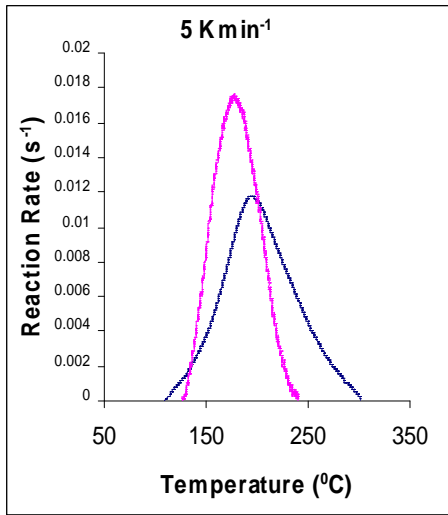
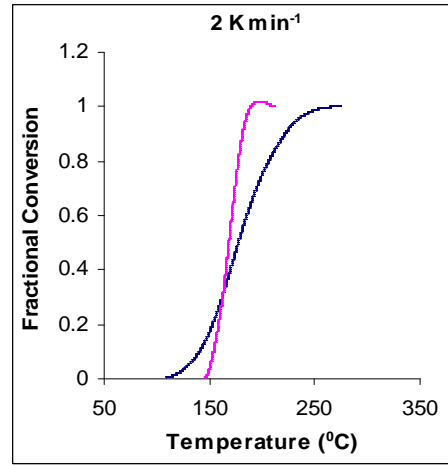
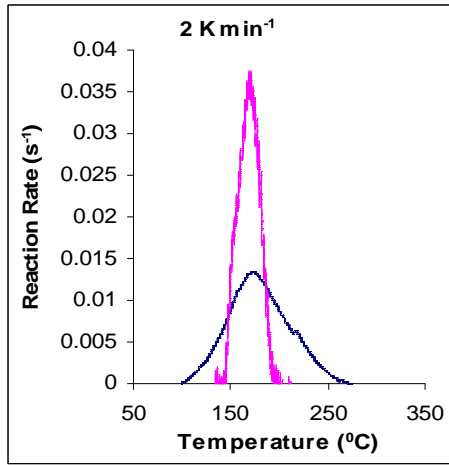
Figure 4.35 Temperature dependence of the reaction rate (left), and fractional conversion (right) for the curing of Araldite LY 5052 / 4 4' DDS epoxy system with an amine / epoxy ratio of 0.85 under conventional and microwave curing at heating rates.

Figure 4.35 illustrates the temperature dependence of the reaction rate and the fraction conversion at different heating rates using microwave and conventional curing. It shows the comparison of the temperature dependence of the fractional conversion and the reaction rates at different heating rates for both conventional and microwave cured Araldite LY 5052 / 4 4' DDS epoxy system with amine / epoxy ratio of 0.85. For all the heating rates, the curing of the Araldite LY 5052 / 4 4' DDS epoxy system with amine / epoxy ratio of 0.85 occurred over a smaller temperature range during microwave curing. The microwave heated samples had a higher peak reaction rate than the conventionally

cured samples for all the heating rates used. We also observe that the reaction rate peak occurred at a lower temperature using microwave energy than in the case of conventional. When compared to the conventionally cured samples, there was a significant increase in the reaction rate of the microwave cured samples. For all the heating rates, a higher onset temperature, and a higher reaction rate were observed in microwave cured samples.

These differences are all as a result of an improved efficiency in the transfer of energy for the microwave heating. Microwave heating involves the direct delivery of energy to the material as a result of an interaction of molecules with the electromagnetic field. This interaction causes heat to be generated internally throughout the volume of the material [86], whereas in conventional heating, energy is transferred from the surface of the material into the material via conduction or convection. Polymer molecules are heated in the microwave field directly as a result of the relaxation of the dipole polarization along the electromagnetic field. Microwaves are absorbed selectively by the reactive polar molecules, and this greatly enhances the reaction, unlike conventional heating which requires the entire molecule to first be heated before the reaction can take place.[57, 87]. The higher fractional conversion for the microwave cured samples can be as a result of an increase in the reactant mobility after gelation. This is as a result of the induced polarization of the polymer and monomer molecules along the applied electromagnetic field [56], enabling more reactants to be consumed to form a more rigid network.

Figure 4.36 shows the temperature dependence of the reaction rate (left), and fractional conversion (right) for the curing of Araldite LY 5052 / 4 4' DDS epoxy system with an amine / epoxy ratio of 1.0 under conventional and microwave curing, at different heating rates. The blue curve indicates conventional heating, while the pink curve indicates microwave heating.



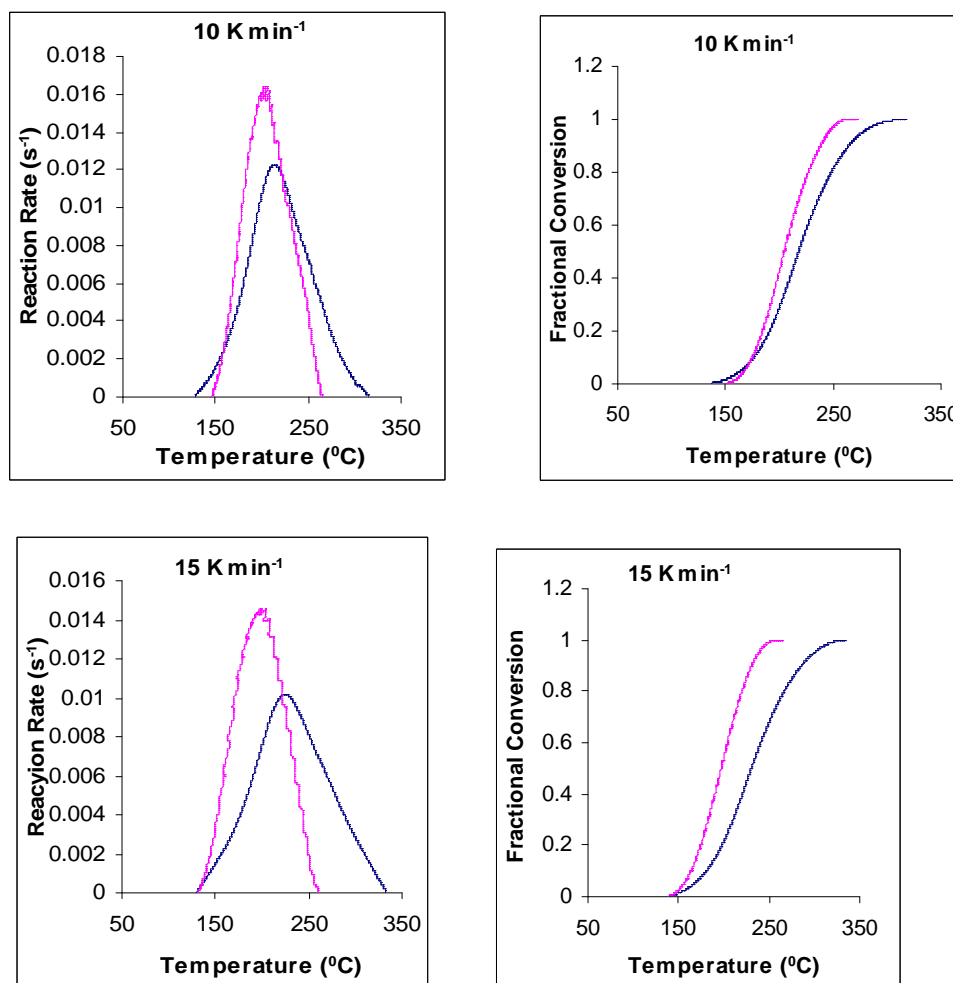
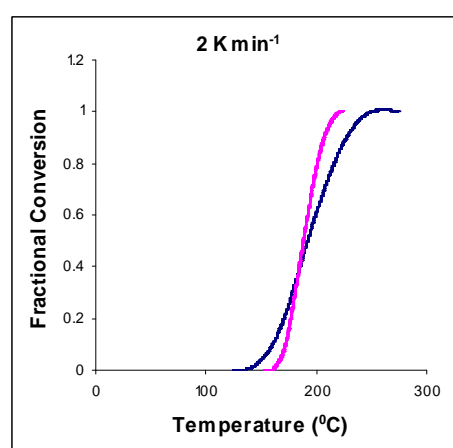
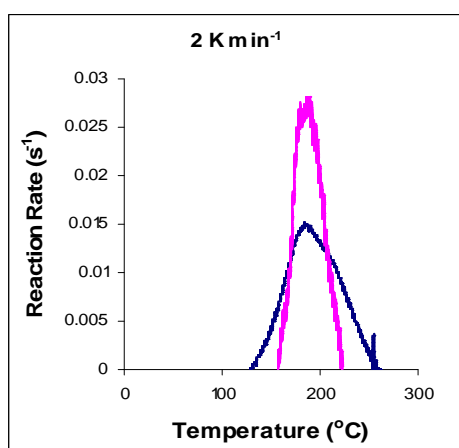


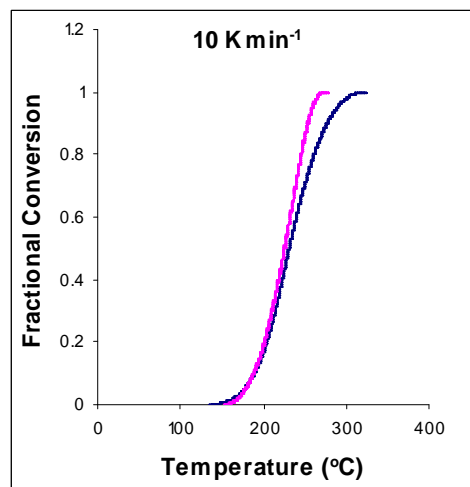
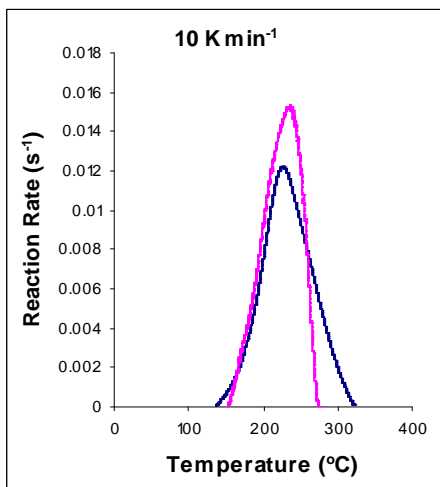
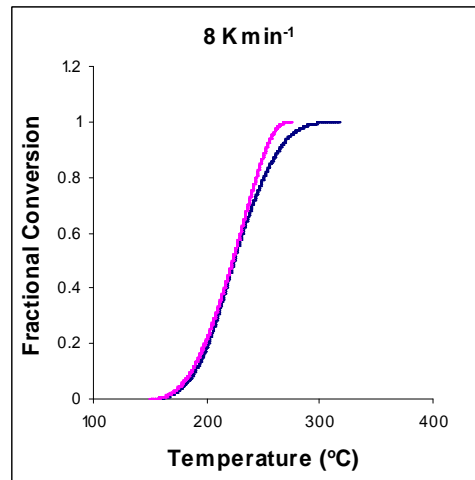
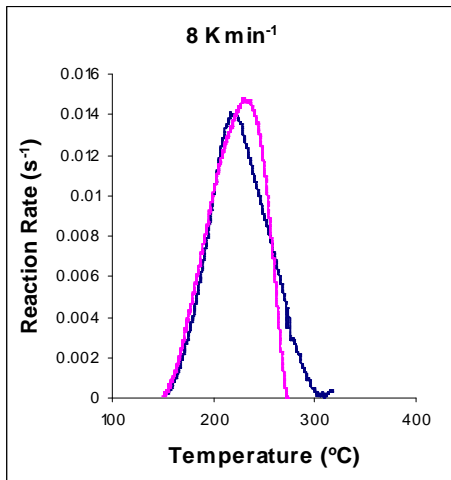
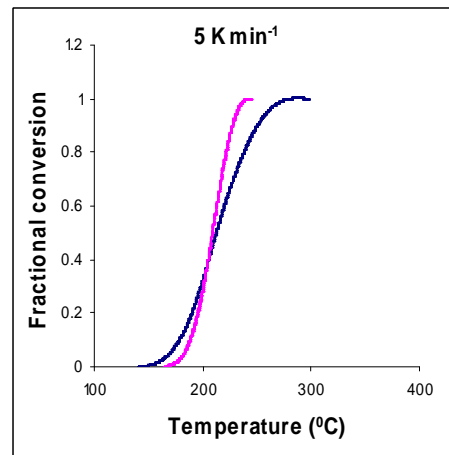
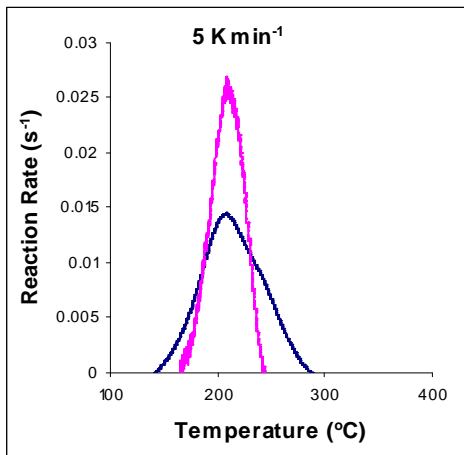
Figure 4.36 Temperature dependence of the reaction rate (left), and fractional conversion (right) for the curing of Araldite LY 5052 / 4 4' DDS epoxy system with an amine / epoxy ratio of 1.0 under conventional and microwave curing, at different heating rates. The blue curve indicates conventional heating, while the pink curve indicates microwave heating.

Figure 4.36 shows the comparison of the temperature dependence of the fractional conversion and the reaction rates at different heating rates for both conventional and microwave cured 1.0M amine / epoxy ratio for Araldite LY 5052 / 4 4' DDS epoxy system. The observations of the plots are very similar to those of Araldite LY 5052 / 4 4' DDS epoxy system with amine / epoxy ratio of 0.85. The curing of Araldite DLS 772 / 4 4' DDS epoxy system with an amine / epoxy ratio of 1.0 occurred over a smaller temperature range during microwave curing for all the heating rates. A higher peak of reaction was observed in the microwave cured samples than the conventionally cured

samples. The reaction rate peak occurred at a lower temperature using microwave energy than in the case of conventional heating. There was a significant increase in the reaction rate of the microwave cured samples in comparison to the conventionally cured samples. A higher onset temperature, and a higher reaction rate were observed in microwave cured samples at all the heating rates.

As explained above, microwave heating has led to an improved efficiency in the transfer of energy. Microwave heating involves the direct delivery of energy to the material as a result of an interaction of molecules with the electromagnetic field; which causes heat to be generated internally throughout the volume of the material [86], whereas in conventional heating, energy is transferred from the surface of the material into the material via conduction or convection. Polymer molecules are heated in the microwave field directly as a result of the relaxation of the dipole polarization along the electromagnetic field. Microwaves are absorbed selectively by the reactive polar molecules, and this greatly enhances the reaction, unlike conventional heating which requires the entire molecule to first be heated before the reaction can take place [57, 87]. An increase in the reactant mobility after gelation is probably the reason why there is a higher fractional conversion for the microwave cured samples. This is as a result of the induced polarization of the polymer and monomer molecules along the applied electromagnetic field [56], which enables more reactants to be consumed to form a more rigid network. These same observations were made for the temperature dependence on the reaction rate curves and the fractional conversion of the curing of Araldite DLS 772 / 4 4' DDS epoxy system with amine / epoxy ratios of 0.8 and 1.1 in figures 4.37 and 4.38





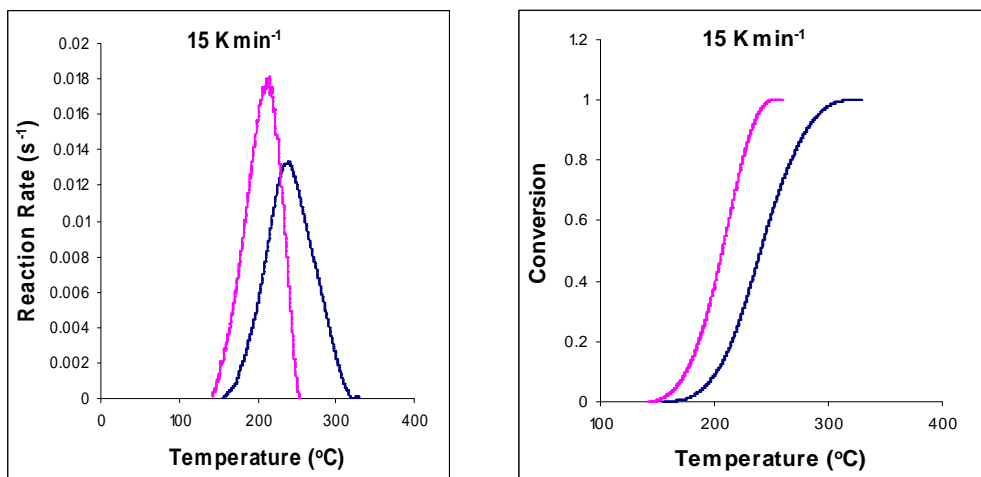
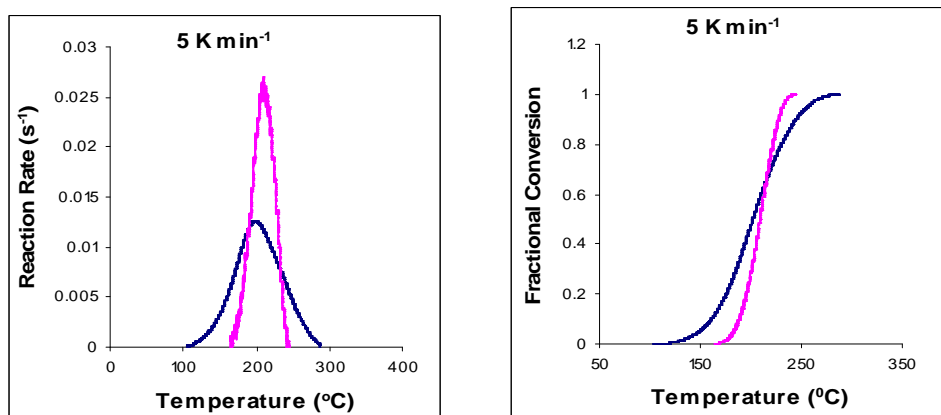
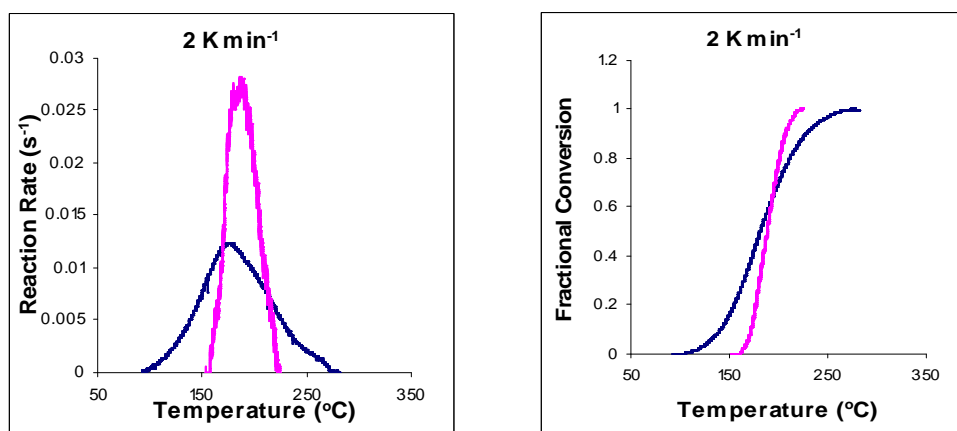


Figure 4.37 Temperature dependence of the reaction rate (left), and fractional conversion (right) for the curing of Araldite DLS 772 / 4 4' DDS epoxy system with an amine / epoxy ratio of 0.8 under conventional and microwave curing, at heating different rates. The blue curve indicates conventional heating, while the pink curve indicates microwave heating.



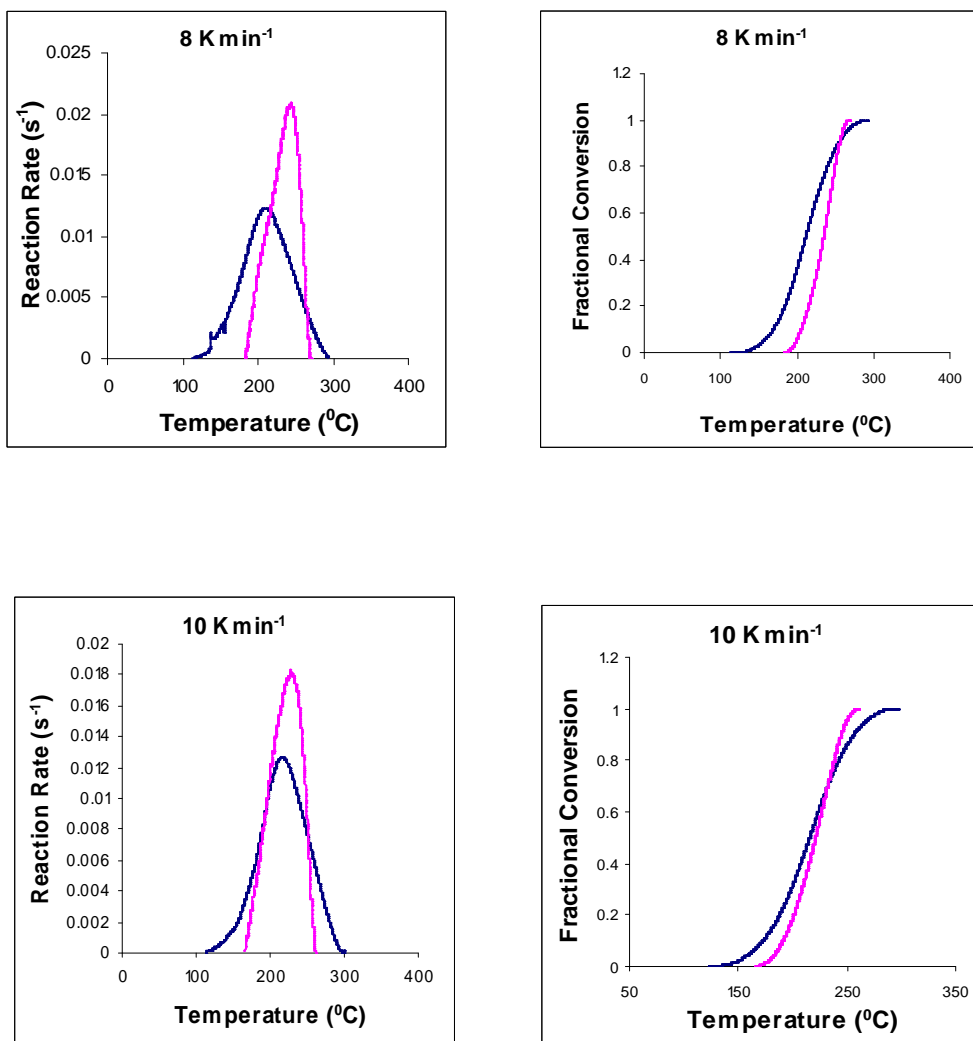
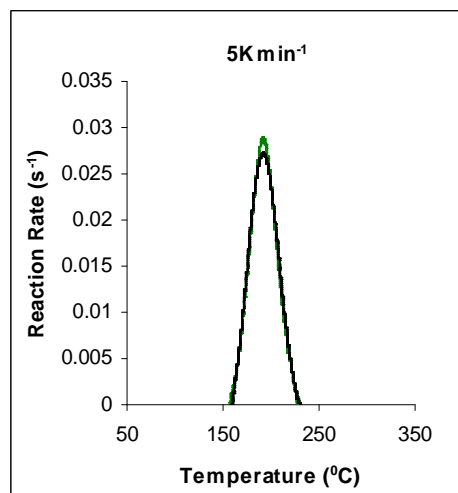
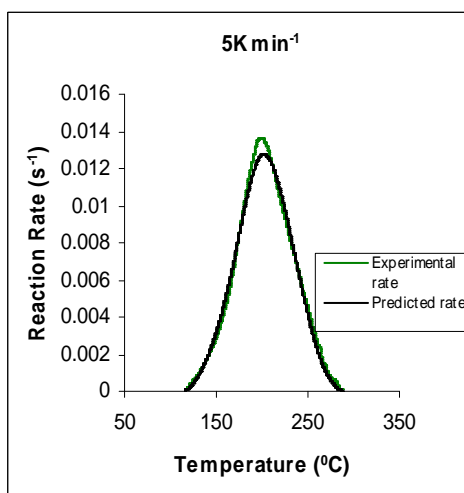
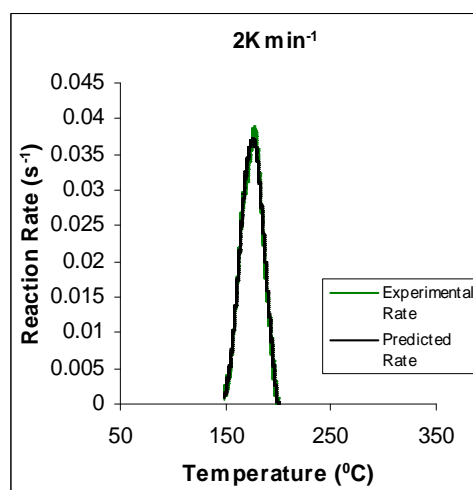
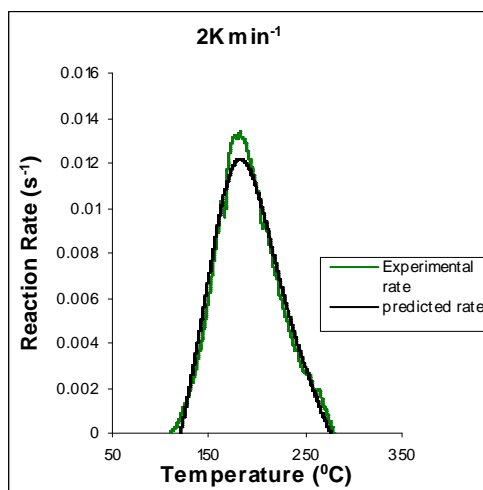


Figure 4.38 Temperature dependence of the reaction rate (left), and fractional conversion (right) for the curing of Araldite DLS 772 / 4 4' DDS epoxy system with an amine / epoxy ratio of 1.1 under conventional and microwave curing, at heating rates.

4.6 Modelling of cure kinetics

The autocatalytic model of equation 2.24 was used for this research. The experimental data was fitted into equation 2.24. The optimisation of the kinetic parameters (K_1 , K_2 , m , n) was obtained using a non-linear regression analysis by a minimization of the sum of squares of the weighted difference between the experimental reaction rate profile and the model prediction.

Figures 4.39 to 4.42 below compares the reaction rate profile of both conventionally (Left) and microwave cured (Right) Araldite LY 5052 / 4 4' DDS epoxy system with amine / epoxy ratio of 0.85 obtained experimentally and the reaction rate profile predicted by the autocatalytic model. The green curve indicates experimental rate, while the black curve indicates the predicted rate.



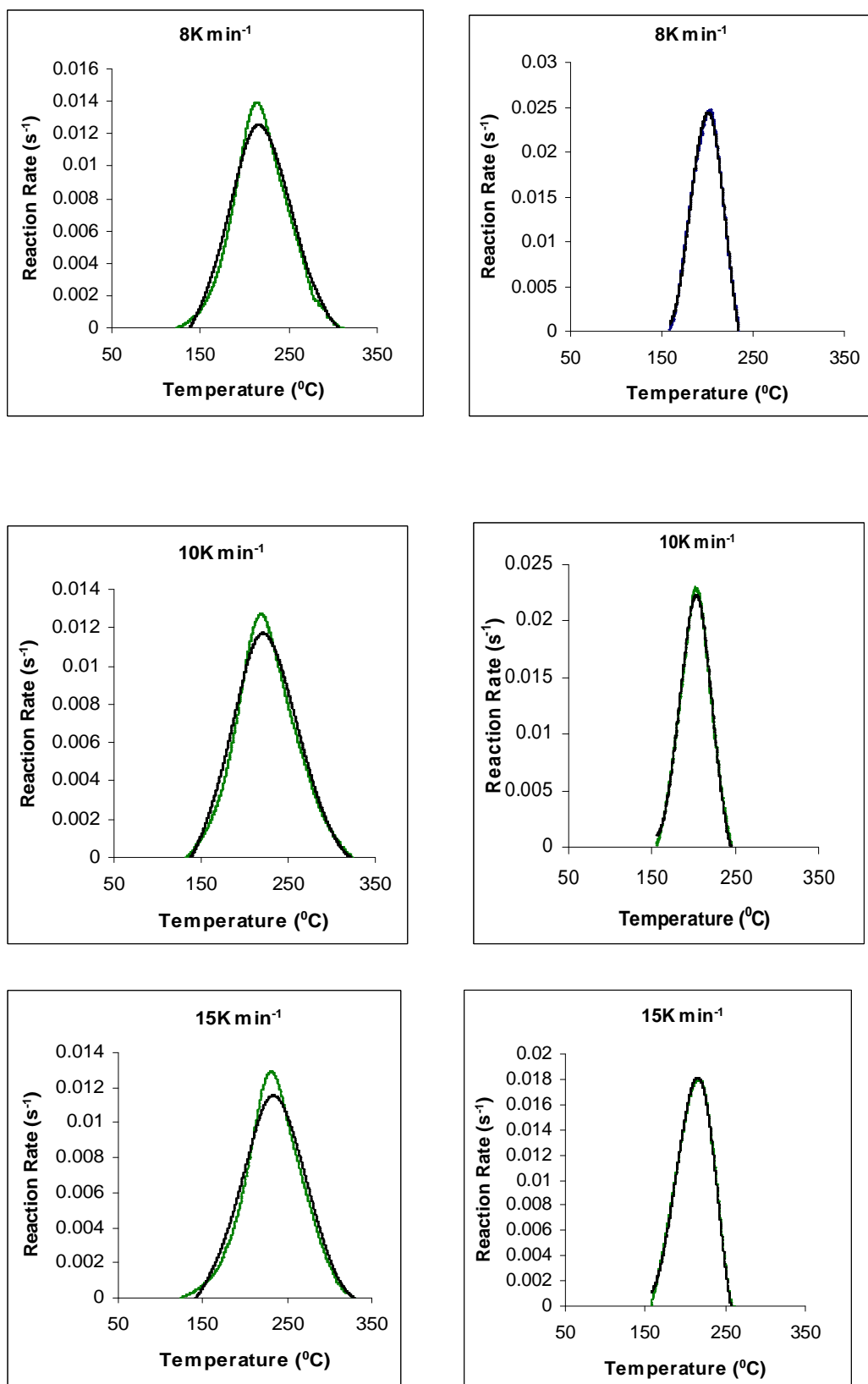
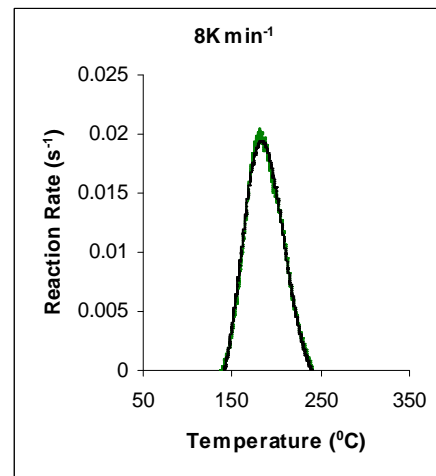
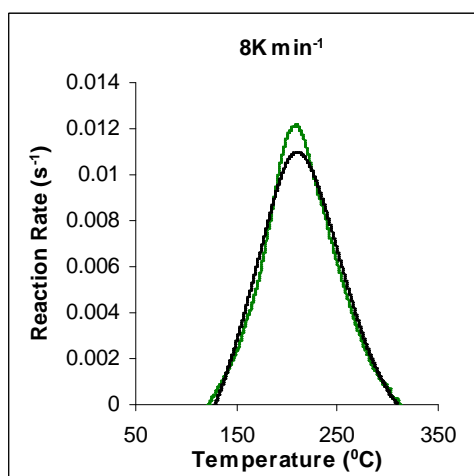
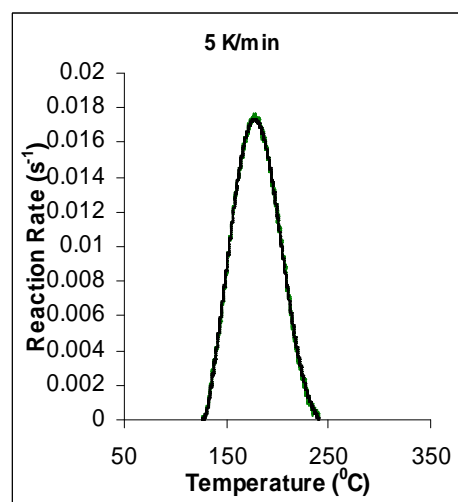
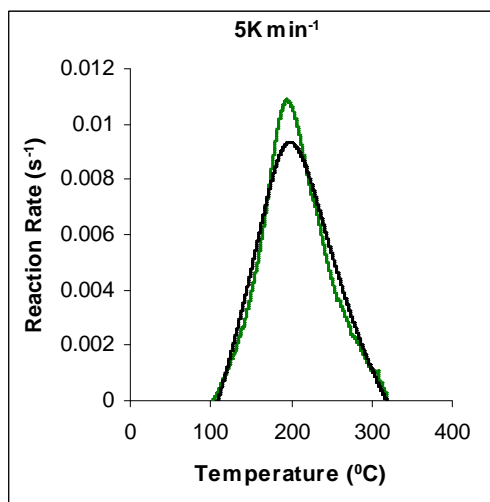


Figure 4.39 Comparison between temperature dependence of experimental reaction rate curves and the curves predicted by means of autocatalytic adjustment for conventional

heating of Araldite LY 5052 / 4 4' DDS epoxy system with an amine / epoxy ratio of 0.85 on the left, and microwave heating on the right.



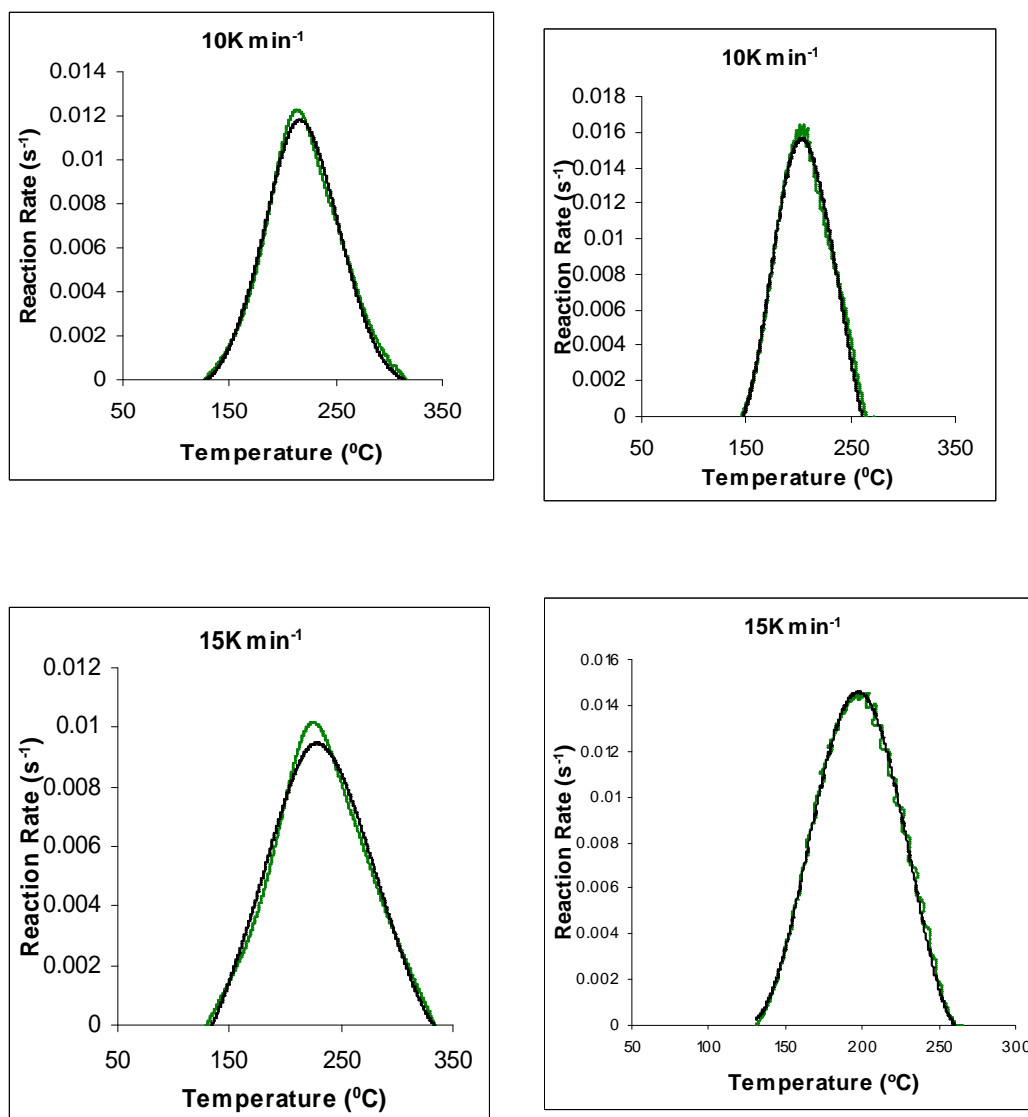
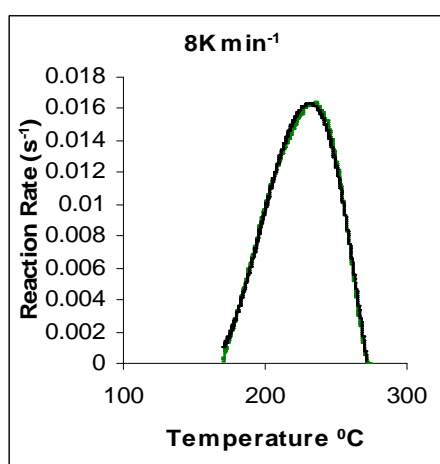
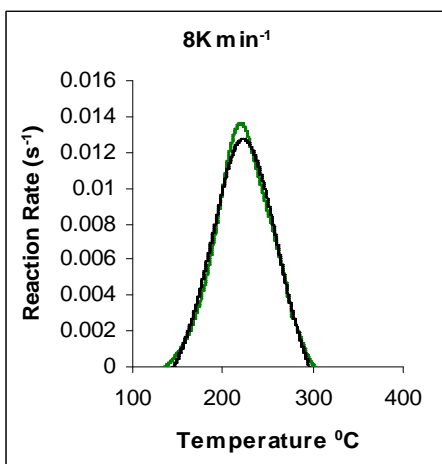
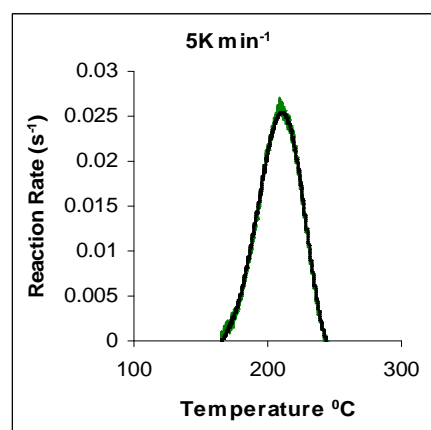
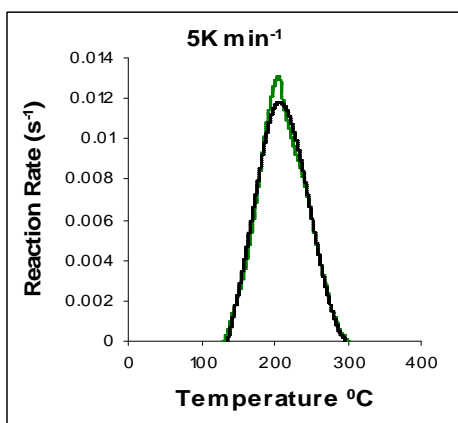
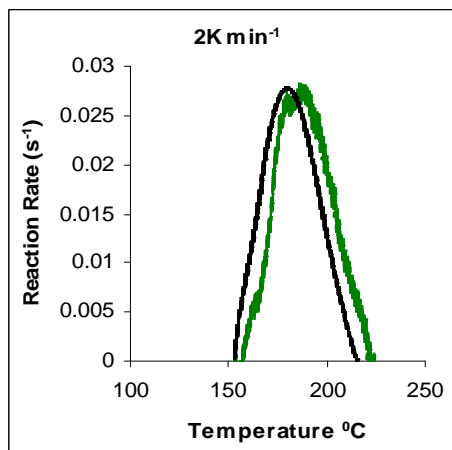
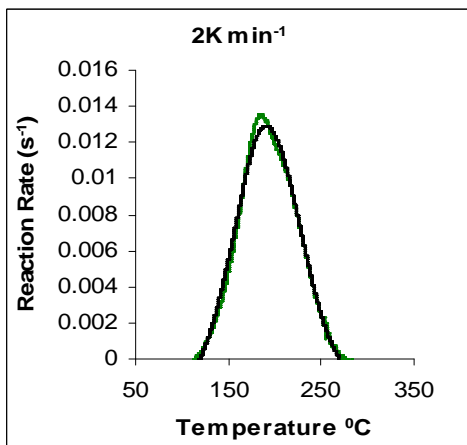


Figure 4.40 Comparison between temperature dependence of experimental reaction rate curves and the curves predicted by means of autocatalytic adjustment for conventional heating of Araldite LY 5052 / 4 4' DDS epoxy system with an amine / epoxy ratio of 1.0 on the left, and microwave heating on the right. The green curve indicates experimental rate, while the black curve indicates the predicted rate



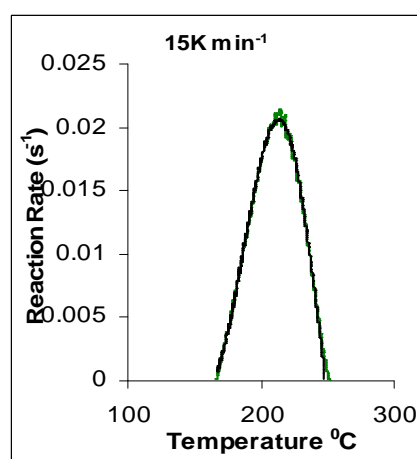
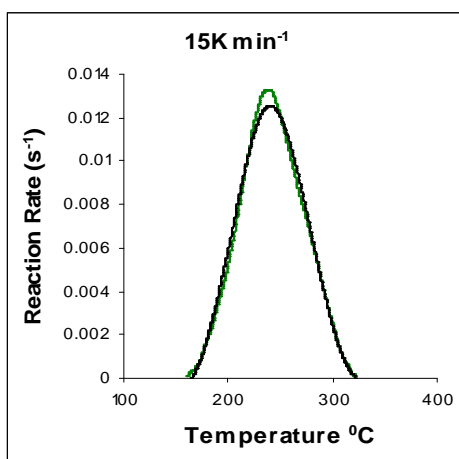
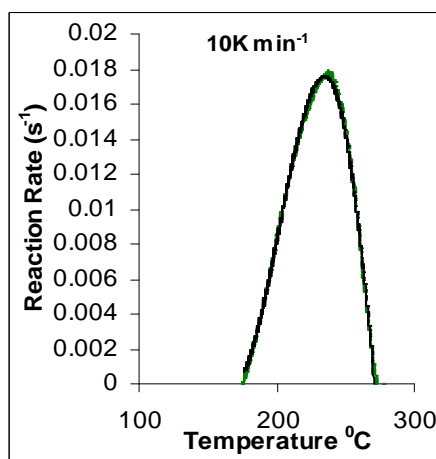
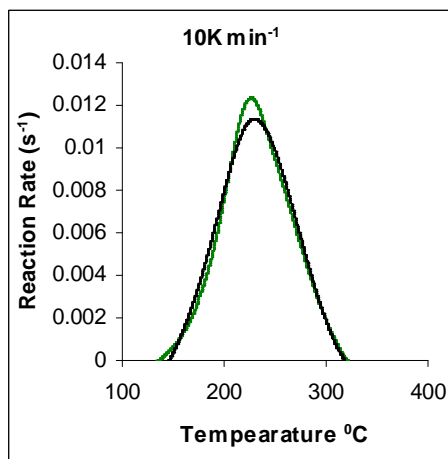
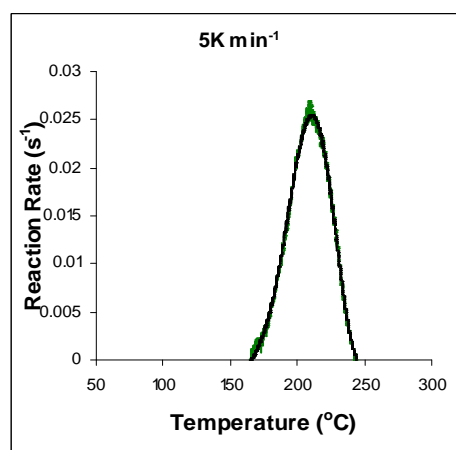
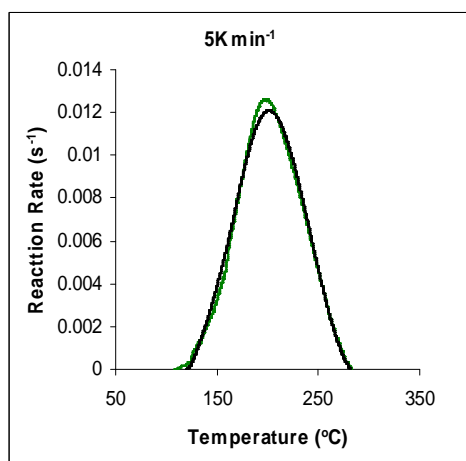


Figure 4.41 Comparison between temperature dependence of experimental reaction rate curves and the curves predicted by means of autocatalytic adjustment for conventional heating of Araldite DLS 772 / 4 4' DDS epoxy system with an amine / epoxy ratio of 0.8 on the left, and microwave heating on the right.



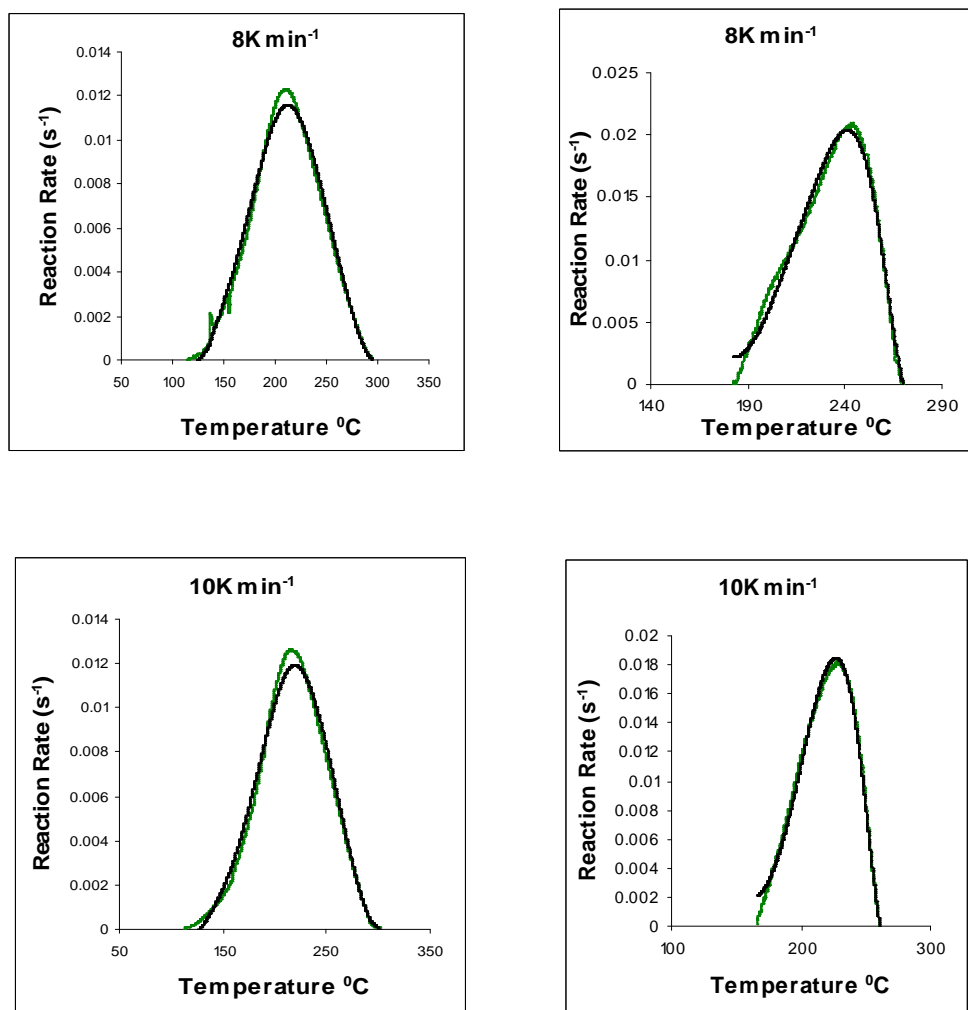


Figure 4.42 Comparison between temperature dependence of experimental reaction rate curves and the curves predicted by means of autocatalytic adjustment for conventional heating of Araldite DLS 772 / 4 4' DDS epoxy system with an amine / epoxy ratio of 1.1 on the left, and microwave heating on the right.

From the figures 4.39 and 4.42 above, we observe that the result of the mathematical simulations compare well with experimental results. The good agreement between the experimental and the model results enforces the proposition that the autocatalytic model is able to predict the curing path of the epoxy system.

The kinetic parameters obtained from fitting the predicted reaction rate with the experimental reaction rate are tabulated below.

Table 4.12 Kinetic parameters for dynamic cure of Araldite LY 5052 / 4 4' DDS epoxy system with an amine / epoxy ratio of 0.85 using conventional heating.

Heating Rate (K min ⁻¹)	K ₁	K ₂	$k = \frac{K_1}{K_2}$	<i>m</i>	<i>n</i>	<i>m+n</i>
2	0.001202	0.03680	0.0327	0.499	0.745	1.244
5	0.000545	0.03402	0.01601	0.678	0.733	1.411
8	0.000523	0.02885	0.01812	0.648	0.641	1.289
10	0.000782	0.03291	0.0238	0.636	0.763	1.399
15	0.000922	0.0290	0.0318	0.616	0.643	1.259

Table 4.13 Kinetic parameters for dynamic cure of Araldite LY 5052 / 4 4' DDS epoxy system with an amine / epoxy ratio of 0.85 using microwave heating.

Heating Rate (K min ⁻¹)	K ₁	K ₂	$k = \frac{K_1}{K_2}$	<i>m</i>	<i>n</i>	<i>m+n</i>
2	0.000738	0.0937	0.0079	0.698	0.656	1.354
5	0.000757	0.06839	0.011	0.613	0.679	1.292
8	0.000798	0.0601	0.0133	0.718	0.620	1.338
10	0.000972	0.0628	0.0155	0.810	0.726	1.536
15	0.00113	0.0444	0.025	0.777	0.591	1.368

Table 4.14 Kinetic parameters for dynamic cure of Araldite LY 5052 / 4 4' DDS epoxy system with an amine / epoxy ratio of 1.0 using conventional heating.

Heating Rate (K min ⁻¹)	K ₁	K ₂	$k = \frac{K_1}{K_2}$	<i>m</i>	<i>n</i>	<i>m+n</i>
2	0.0000608	0.0349	0.0017	0.686	0.783	1.469
5	0.00221	0.0209	0.106	0.413	0.833	1.246
8	0.0619	0.178	0.348	0.634	0.680	1.314
10	0.01729	0.547	0.0316	0.685	0.760	1.445
15	0.000267	0.0241	0.0111	0.608	0.685	1.293

Table 4.15 Kinetic parameters for dynamic cure of Araldite LY 5052 / 4 4' DDS epoxy system with an amine / epoxy ratio of 1.0 using microwave heating.

Heating Rate (K min ⁻¹)	K ₁	K ₂	$k = \frac{K_1}{K_2}$	<i>m</i>	<i>n</i>	<i>m+n</i>
2	0.00261	0.0280	0.0932	0.300	0.310	0.61
5	0.000313	0.0424	0.0014	0.612	0.679	1.291
8	0.00112	0.0479	0.0234	0.561	0.701	1.262
10	0.00238	0.0386	0.0617	0.612	0.681	1.293
15	0.002792	0.0360	0.078	0.673	0.649	1.326

Table 4.16 Kinetic parameters for dynamic cure of Araldite DLS 772 / 4 4' DDS epoxy system with an amine / epoxy ratio of 0.8 using conventional heating.

Heating Rate (K min ⁻¹)	K ₁	K ₂	$k = \frac{K_1}{K_2}$	<i>m</i>	<i>n</i>	<i>m+n</i>
2	0.00044	0.0321	0.014	0.607	0.672	1.297

5	0.00074	0.0308	0.024	0.628	0.663	1.291
8	0.00070	0.0300	0.0233	0.646	0.656	1.302
10	0.00067	0.0284	0.0235	0.605	0.655	1.260
15	0.00013	0.0267	0.0049	0.663	0.663	1.326

Table 4.17 Kinetic parameters for dynamic cure of Araldite DLS 772 / 4 4' DDS epoxy system with an amine / epoxy ratio of 0.8 using microwave heating.

Heating Rate (K min ⁻¹)	K ₁	K ₂	$k = \frac{K_1}{K_2}$	<i>m</i>	<i>n</i>	<i>m+n</i>
2	0.000073	0.0679	0.00108	0.587	0.708	1.295
5	0.000274	0.0641	0.0043	0.718	0.612	1.330
8	0.000942	0.0369	0.026	0.669	0.485	1.154
10	0.000652	0.0370	0.0176	0.657	0.471	1.128
15	0.000584	0.0463	0.0126	0.652	0.548	1.200

Table 4.18 Kinetic parameters for dynamic cure of Araldite DLS 772 / 4 4' DDS epoxy system with an amine / epoxy ratio of 1.1 using microwave heating.

Heating Rate (K min ⁻¹)	K ₁	K ₂	$k = \frac{K_1}{K_2}$	<i>m</i>	<i>n</i>	<i>m+n</i>
2	0.0000965	0.0360	0.0268	0.759	0.861	1.62
5	0.000591	0.0297	0.0199	0.622	0.654	1.276
8	0.00039	0.0288	0.0135	0.649	0.637	1.286
10	0.000495	0.0299	0.0165	0.663	0.632	1.295

15	0.00463	0.0305	0.1518	0.688	0.620	1.308
----	---------	--------	--------	-------	-------	-------

Table 4.19 Kinetic parameters for dynamic cure of Araldite DLS 772 / 4 4' DDS epoxy system with an amine / epoxy ratio of 1.1 using microwave heating.

Heating Rate (K min ⁻¹)	K ₁	K ₂	$k = \frac{K_1}{K_2}$	<i>m</i>	<i>n</i>	<i>m+n</i>
2	0.000073	0.06789	0.00107	0.587	0.708	1.295
5	0.00027	0.0641	0.0042	0.718	0.612	1.330
8	0.00094	0.0345	0.0272	0.669	0.485	1.154
10	0.00065	0.0369	0.018	0.657	0.471	1.128
15	0.00058	0.0462	0.0126	0.652	0.548	1.200

4.7 Ozawa's method

Equation 2.59 was used to follow the reaction kinetic parameters during the curing reaction of Araldite LY 5052 / 4 4' DDS and Araldite DLS 772 / 4 4' DDS epoxy systems with both conventional and microwave heating.

The experimental curves of log Φ against T⁻¹ for various fractional conversions for conventionally and microwave cured Araldite LY 5052 / 4 4' DDS epoxy system with an amine / epoxy ratio of 0.85 are shown in figures 4.43 and 4.44 respectively.

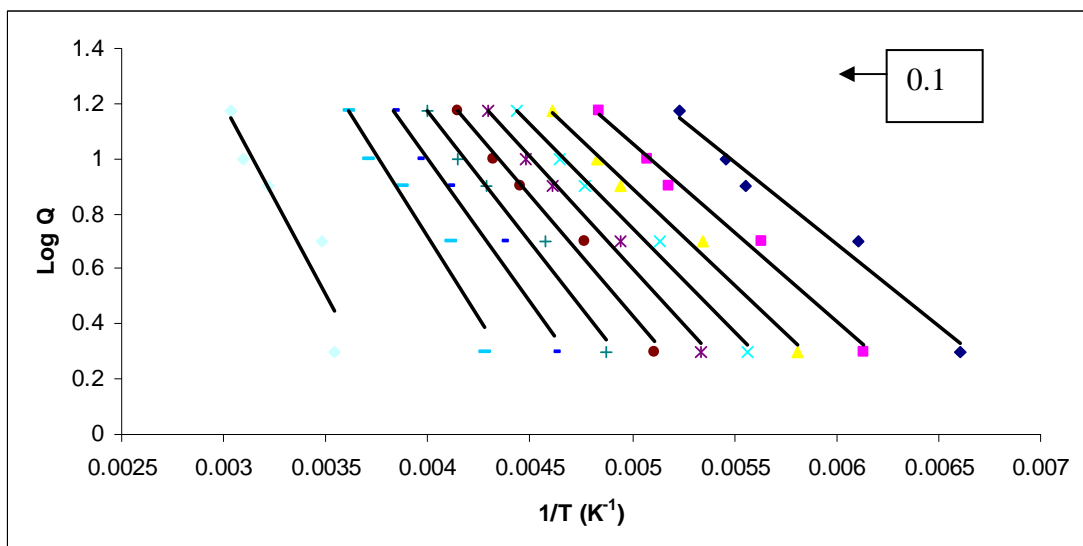


Figure 4.43 Ozawa plots of logarithm of heating rate against the inverse of temperature at constant fractional conversions for the dynamic cure of Araldite LY 5052 / 4 4' DDS epoxy system with an amine / epoxy ratio of 0.85 using conventional heating. Fractional conversions α of 0.1, 0.2, 0.3, 0.4, 0.5, 0.6, 0.7, 0.8, 0.9, 1.00 are shown.

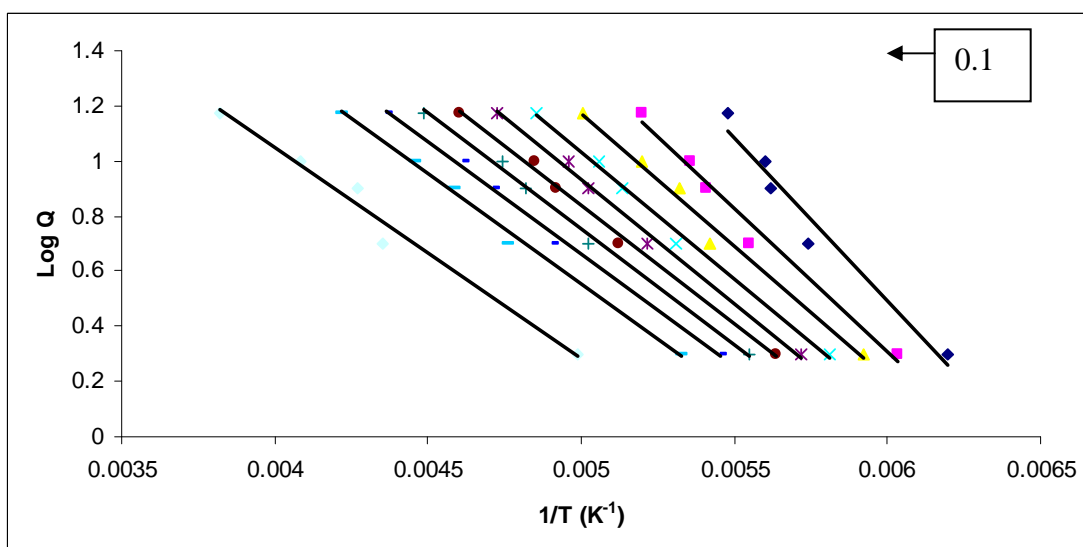


Figure 4.44 Ozawa plots of logarithm of heating rate against the inverse of temperature at constant fractional conversions for the dynamic cure of Araldite LY 5052 / 4 4' DDS epoxy system with an amine / epoxy ratio of 0.85 using microwave heating. Fractional conversions α of 0.1, 0.2, 0.3, 0.4, 0.5, 0.6, 0.7, 0.8, 0.9, 1.00 are shown.

For both conventionally and microwave cured samples, the activation energy was determined at fractional conversions of 0.1, 0.2, 0.3, 0.4, 0.5, 0.6, 0.7, 0.8, 0.9, 1.0. A plot showing the activation energies as the fractional conversion increases for conventionally and microwave cured samples of Araldite LY 5052 / 4 4' DDS epoxy system with an amine / epoxy ratio of 0.85 is shown in figure 4.45.

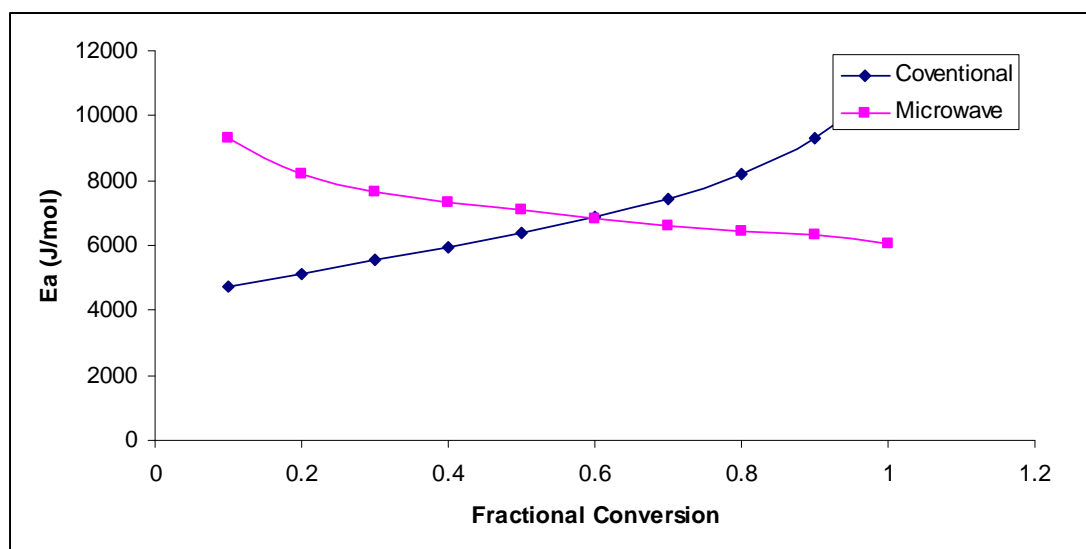


Figure 4.45 Dependence of activation energy, E_a on the fractional conversion for both conventionally and microwave cured samples of Araldite LY 5052 / 4 4' DDS epoxy system with an amine / epoxy ratio of 0.85.

Figure 4.45 shows the values of activation energy at various fractional conversions of microwave and conventionally cured samples. The activation energies and the constants A' for conventional and microwave cured Araldite LY 5052 / 4 4' DDS epoxy system with an amine / epoxy ratio of 0.85 are summarised in table 4.20 below. In all the cases, the regression coefficients obtained were between $0.97 < r < 1.00$.

Table 4.20 Kinetic Parameters at different degrees of conversion for conventionally and microwave cured Araldite LY 5052 / 4 4' DDS epoxy system with an amine / epoxy ratio of 0.85 determined by Ozawa's method.

Fractional Conversion (α)	Activation Energy (E_a) Conventional	Activation Energy (E_a) Microwave	A' Conventional	A' Microwave
0.1	47.07	93.11	4.26	7.56
0.2	51.31	82.22	4.30	6.55
0.3	55.51	76.40	4.40	6.01
0.4	59.46	73.01	4.50	5.65
0.5	63.76	70.77	4.63	5.40
0.6	68.73	68.22	4.78	5.15
0.7	74.49	66.19	4.94	4.94
0.8	81.84	64.29	5.13	4.73
0.9	93.02	63.42	5.43	4.56
1.0	109.56	60.38	5.35	4.10
Average	70.475	71.801	4.772	5.465
Std. Dev	19.69	9.93	0.427	1.027

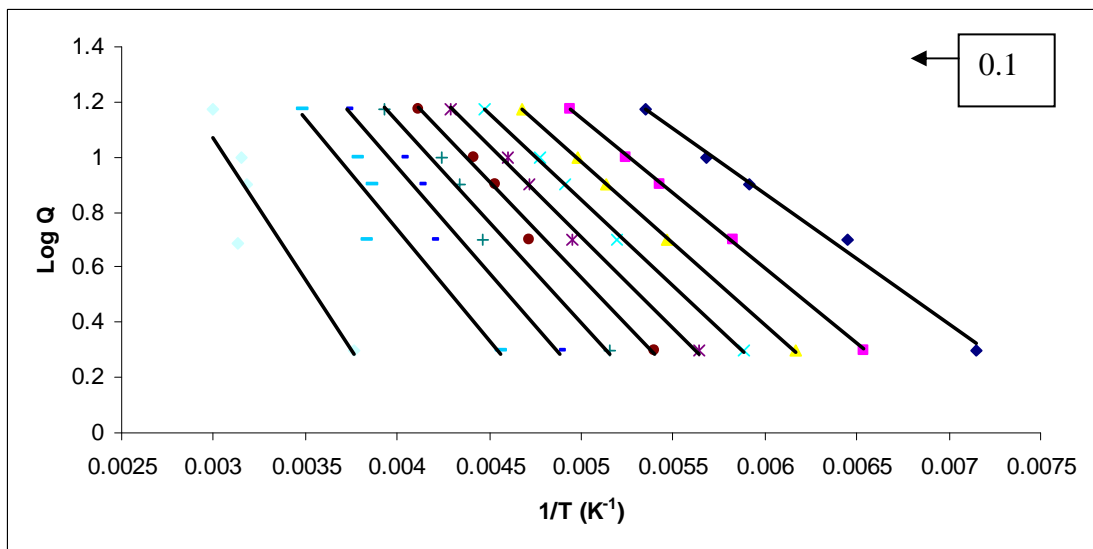


Figure 4.46 Ozawa plots of logarithm of heating rate against the inverse of temperature at constant fractional conversions for the dynamic cure of Araldite LY 5052 / 4 4' DDS epoxy system with an amine / epoxy ratio of 1.0 using conventional heating. Fractional conversions α of 0.1, 0.2, 0.3, 0.4, 0.5, 0.6, 0.7, 0.8, 0.9, 1.00 are shown.

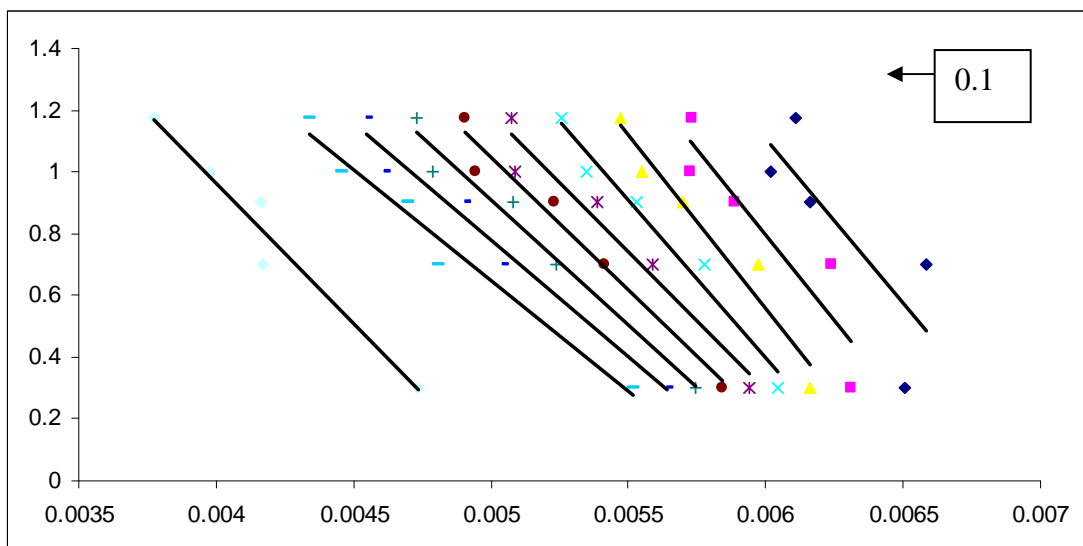


Figure 4.47 Ozawa plots of logarithm of heating rate against the inverse of temperature at constant fractional conversions for the dynamic cure of Araldite LY 5052 / 4 4' DDS epoxy system with an amine / epoxy ratio of 1.0 using microwave heating. Fractional conversions α of 0.1, 0.2, 0.3, 0.4, 0.5, 0.6, 0.7, 0.8, 0.9, 1.00 are shown.

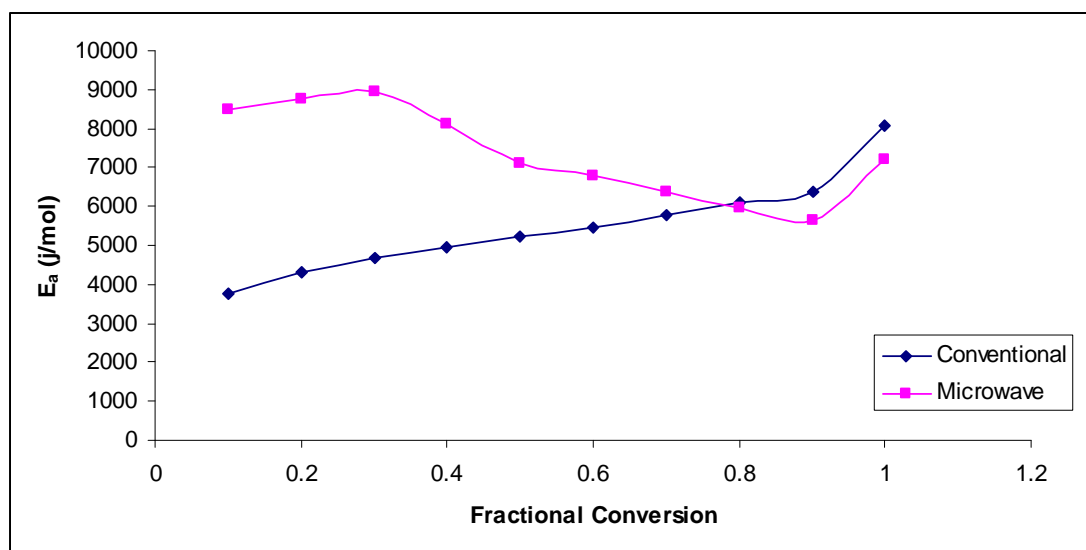


Figure 4.48 Dependence of activation energy, E_a on the fractional conversion for both conventionally and microwave cured samples of Araldite LY 5052 / 4 4' DDS epoxy system with an amine / epoxy ratio of 1.0.

Figure 4.48 shows the values of activation energy at various fractional conversions of microwave and conventionally cured samples. Table 4.21 summarizes the activation

energies and the constants A' for conventional and microwave cured Araldite LY 5052 / 4 4' DDS epoxy system with an amine / epoxy ratio of 1.0. In all the cases, the regression coefficients obtained were between $0.97 < r < 1.00$ in all the cases.

Table 4.21 Kinetic Parameters at different degrees of conversion for conventionally and Araldite LY 5052 / 4 4' DDS epoxy system with an amine / epoxy ratio of 1.0 determined by Ozawa's method.

Fractional Conversion (α)	Activation Energy (Ea) Conventional	Activation Energy (Ea) Microwave	A' Conventional	A' Microwave
0.1	39.39	84.80	3.71	7.55
0.2	43.00	87.49	3.86	7.43
0.3	46.64	89.49	3.94	7.35
0.4	49.42	81.27	3.97	6.56
0.5	52.10	71.28	4.01	5.7
0.6	54.76	67.98	4.03	5.35
0.7	57.69	63.98	4.05	4.96
0.8	60.82	59.84	4.04	4.56
0.9	63.64	56.58	3.96	4.23
1.0	80.81	72.17	4.13	4.62
Average	54.827	73.488	3.97	5.831
Std. Dev	11.92	11.74	0.12	1.29

Figures 4.49 and 4.50 below show the Ozawa plots of logarithm of heating rate against the inverse of temperature at constant fractional conversions for the dynamic cure of Araldite DLS 772 / 4 4' DDS epoxy system with an amine / epoxy ratio of 0.8 using conventional and microwave heating.

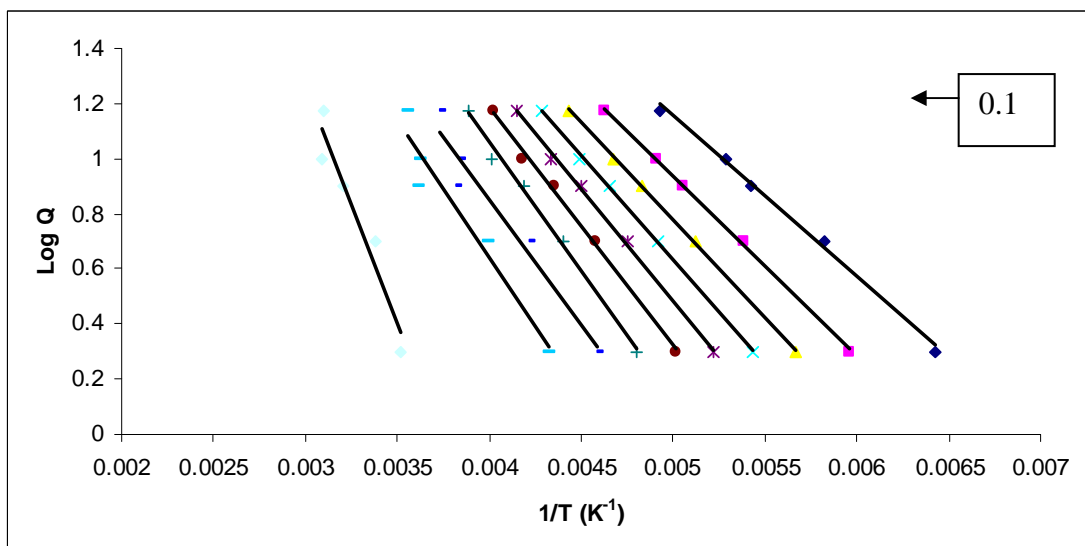


Figure 4.49 Ozawa plots of logarithm of heating rate against the inverse of temperature at constant fractional conversions for the dynamic cure of Araldite DLS 772 / 4 4' DDS epoxy system with an amine / epoxy ratio of 0.8 using conventional heating. Fractional conversions α of 0.1, 0.2, 0.3, 0.4, 0.5, 0.6, 0.7, 0.8, 0.9, 1.00 are shown.

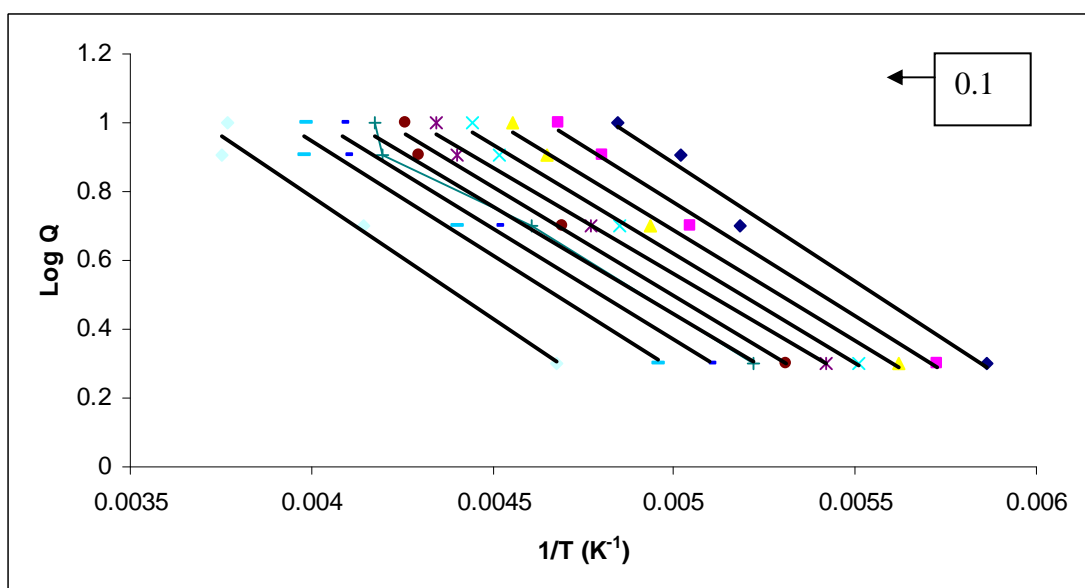


Figure 4.50 Ozawa plots of logarithm of heating rate against the inverse of temperature at constant fractional conversions for the dynamic cure of Araldite DLS 772 / 4 4' DDS epoxy system with an amine / epoxy ratio of 0.8 using microwave heating. Fractional conversions α of 0.1, 0.2, 0.3, 0.4, 0.5, 0.6, 0.7, 0.8, 0.9, 1.00 are shown.

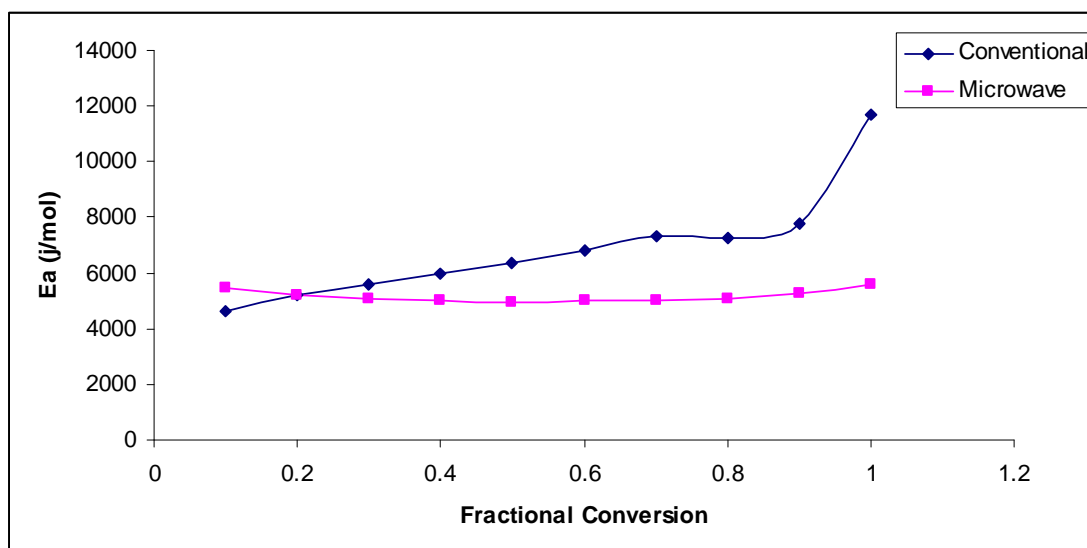


Figure 4.51 Dependence of activation energy, E_a on the fractional conversion for both conventionally and microwave cured samples of Araldite DLS 772 / 4 4' DDS epoxy system with an amine / epoxy ratio of 0.8.

Table 4.22 Kinetic Parameters at different degrees of conversion for conventionally and microwave cured Araldite DLS 772 / 4 4' DDS epoxy system with an amine / epoxy ratio of 0.8 determined by Ozawa's method,

Fractional Conversion (α)	Activation Energy (E_a) Conventional	Activation Energy (E_a) Microwave	A' Conventional	A' Microwave
0.1	46.18	54.53	4.07	4.33
0.2	51.89	52.33	4.22	4.08
0.3	55.83	50.69	4.31	3.89
0.4	59.70	50.08	4.41	3.78
0.5	63.69	49.52	4.51	3.70
0.6	68.32	49.94	4.64	3.66
0.7	73.30	49.94	4.77	3.60
0.8	72.39	50.95	4.51	3.59
0.9	77.89	52.49	4.58	3.60
1.0	116.58	55.80	6.45	3.61

Average	68.58	51.63	4.65	3.78
Std. Dev	19.64	4.64	0.67	0.25

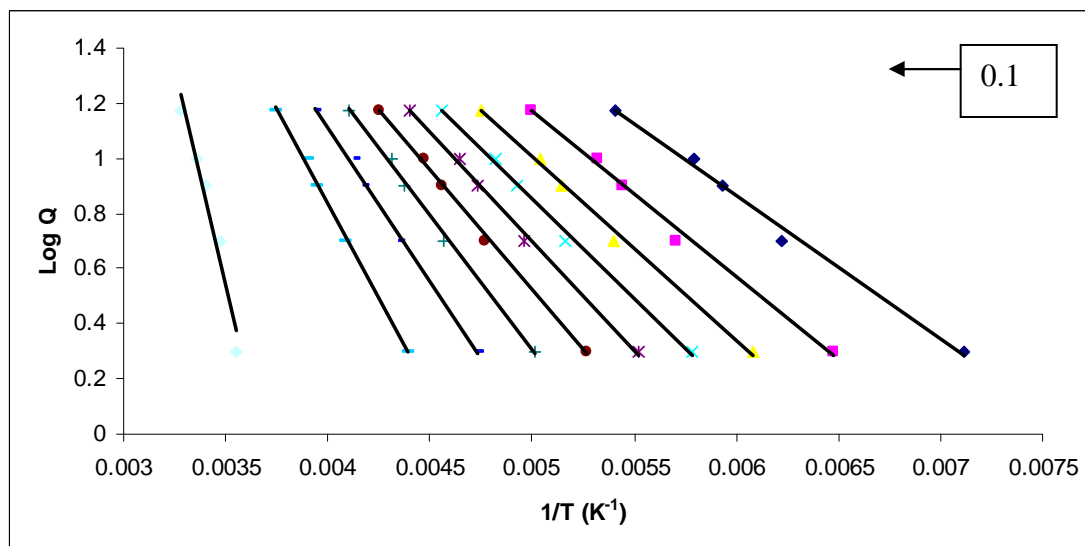


Figure 4.52 Ozawa plots of logarithm of heating rate against the inverse of temperature at constant fractional conversions for the dynamic cure of Araldite DLS 772 / 4 4' DDS epoxy system with an amine / epoxy ratio of 1.1 using conventional heating.

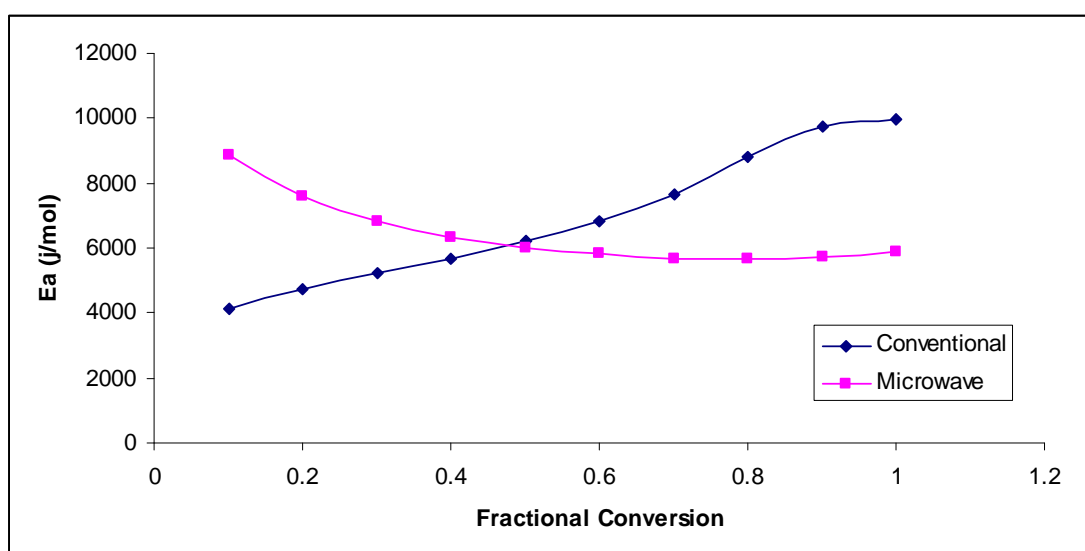


Figure 4.53 Dependence of activation energy, E_a on the fractional conversion for both conventionally and microwave cured samples of Araldite DLS 772 / 4 4' DDS epoxy system with an amine / epoxy ratio of 1.1.

Table 4.23 Kinetic Parameters at different degrees of conversion for conventionally and microwave cured Araldite DLS 772 / 4 4' DDS epoxy system with an amine / epoxy ratio of 1.1 determined by Ozawa's method.

Fractional Conversion (α)	Activation Energy (E_a) Conventional	Activation Energy (E_a) Microwave	A' Conventional	A' Microwave
0.1	41.11	88.85	3.98	6.85
0.2	47.47	76.18	4.17	5.73
0.3	52.40	68.36	4.31	5.07
0.4	56.93	63.56	4.45	4.65
0.5	62.02	60.09	4.62	4.34
0.6	68.35	58.34	4.84	4.15
0.7	76.70	56.97	5.15	3.99
0.8	87.84	56.67	5.56	3.89
0.9	97.65	57.31	6.28	3.83
1.0	99.73	58.80	9.27	3.66
Average	69.02	64.51	5.26	4.62
Std. Dev	20.79	10.56	1.57	1.01

Ozawa's method can also be used to determine the activation energy through the exothermic peak temperature. In this method, the exothermic peak temperature can be obtained directly from the dynamic DSC thermograms at different heating rates. This procedure gave us a single activation energy for the entire reaction process. If we plot a graph of the logarithm of the heating rate against the inverse of peak temperatures, we can obtain the activation energy and the constant A' from the slope and the intercept respectively. Plots of $\log \Phi$ against T_p^{-1} for Araldite LY 5052 / 4 4' DDS and DLS 772 / 4 4' DDS epoxy systems using both conventional DSC and microwave calorimeter.

The activation energies and constants A' for epoxy systems are shown in the tables above. In all cases, the regression coefficients obtained were between $0.98 < r < 1.00$.

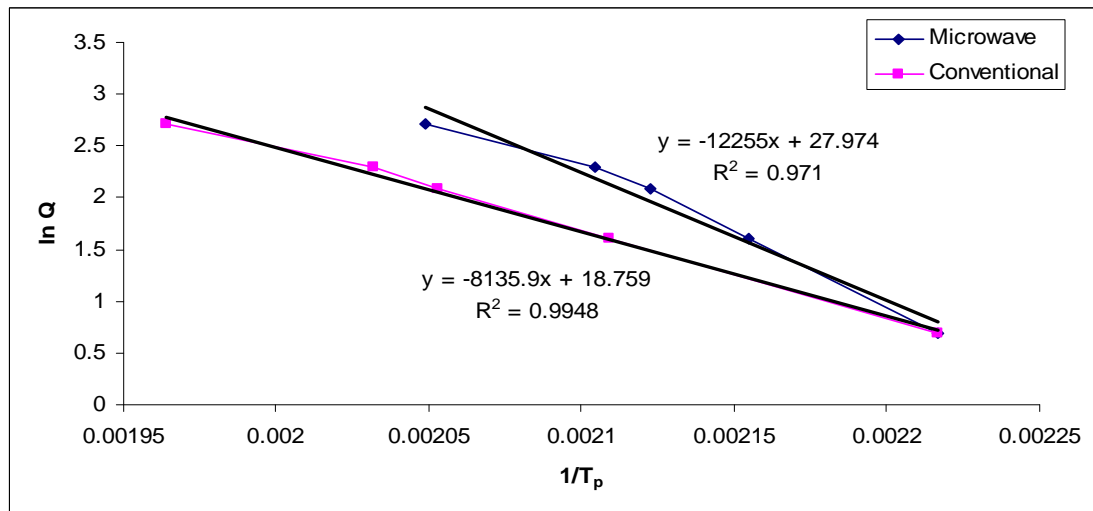


Figure 4.54 Plot of $\log \Phi$ against T_p^{-1} for conventional and microwave curing of Araldite LY 5052 / 4 4' DDS epoxy system with an amine / epoxy ratio of 0.85.

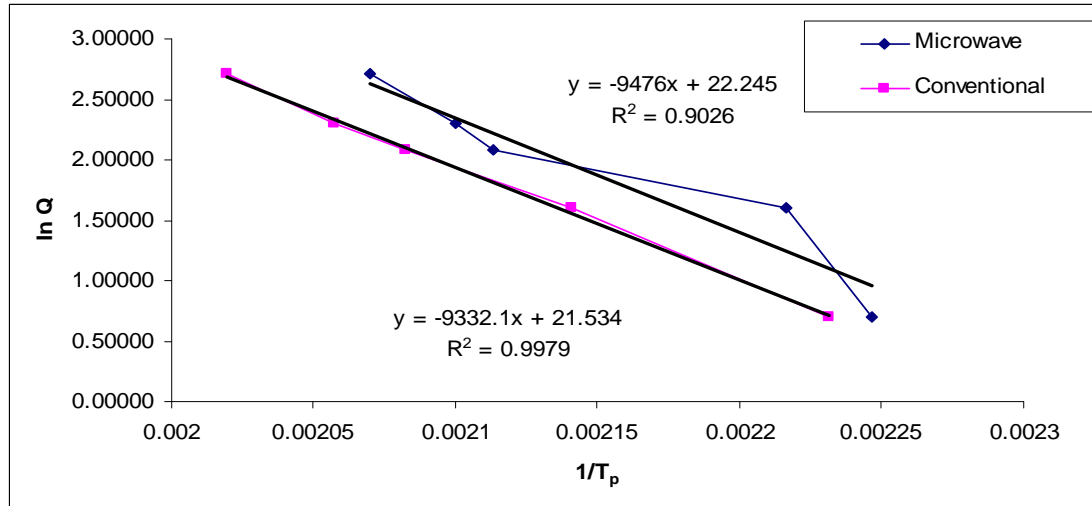


Figure 4.55 Plot of $\log \Phi$ against T_p^{-1} for conventional and microwave curing of Araldite LY 5052 / 4 4' DDS epoxy system with an amine / epoxy ratio of 1.0.

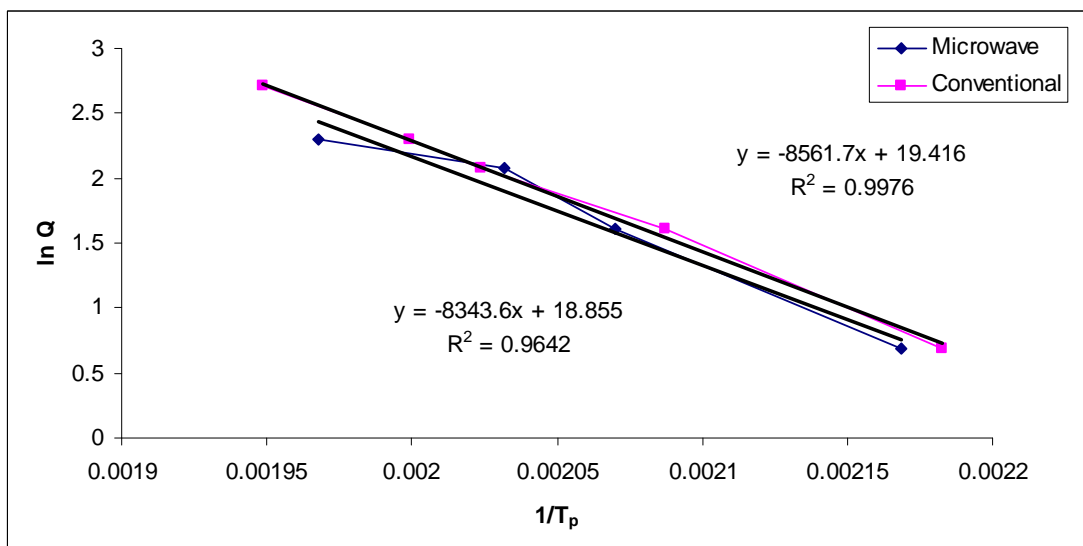


Figure 4.56 Plot of $\log \Phi$ against T_p^{-1} for conventional and microwave curing of Araldite DLS 772 / 4 4' DDS epoxy system with an amine / epoxy ratio of 0.8.

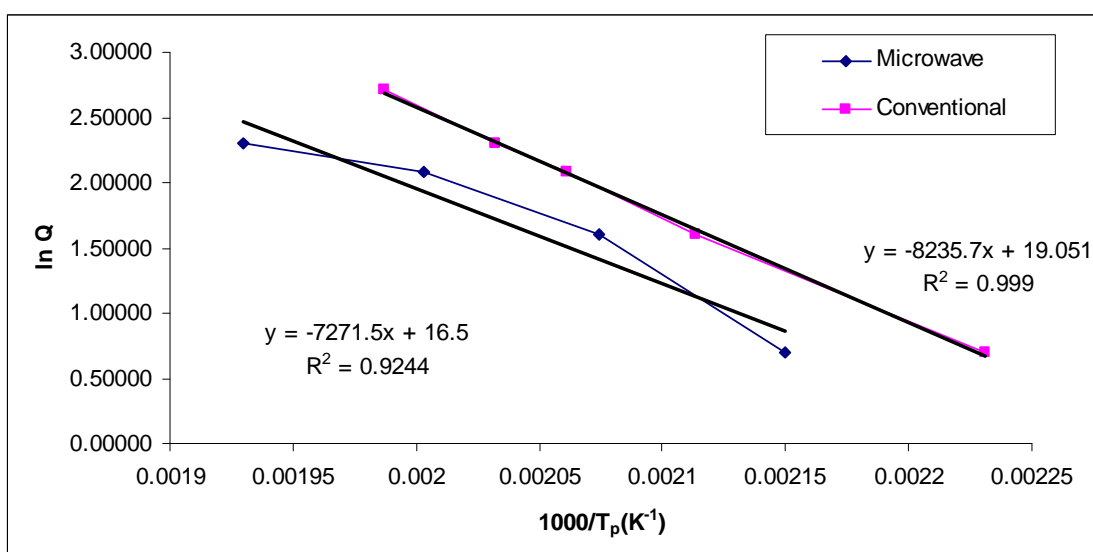


Figure 4.57 Plot of $\log \Phi$ against T_p^{-1} for conventional and microwave curing of Araldite DLS 772 / 4 4' DDS epoxy system with an amine / epoxy ratio of 0.8.

Table 4.24 Values of Activation energy and pre-exponential factor for different stoichiometric ratios of Araldite LY 5052 / 4 4' DDS and Araldite DLS 772 / 4 4' DDS epoxy systems using conventional and microwave heating.

Sample	Conventional Heating		Microwave Heating	
	A' (s ⁻¹)	E _a (KJ/mol)	A' (s ⁻¹)	E _a (KJ/mol)
LY 5052 0.85M	18.76	64.3	27.97	96.9
LY 5052 1.0 M	7.23	73.8	7.97	77.5
DLS 772 0.8 M	19.42	67.6	18.85	60.9
DLS 772 1.1 M	19.05	65.1	16.50	57.5

From table 4.24, for the Araldite LY 5052 / 4 4' DDS epoxy systems, the activation energies of all microwave-cured samples were higher than those of conventionally cured samples. While for the Araldite DLS 772 / 4 4' DDS epoxy systems, the activation energies of the conventionally cured samples were higher than the activation energies of the microwave cured samples. This result was consistent with those obtained using Ozawa's method based on the isoconversion procedure as well as the results obtained from the autocatalytic model method.

4.8 Kissinger's method

Figures 4.58 to 4.61 show the example of the plots of $-\ln(\Phi/T_p^2)$ against T_p^{-1} for the Araldite LY 5052 / 4 4' DDS epoxy system cured using conventional DSC and microwave calorimeter. The values of the activation energy for the all resins and blends are summarised in Table 4.25. In all cases, the regression coefficients obtained were between $0.90 < r < 1.00$. Again, the activation energies of all microwave-cured samples were also found to be higher than those of conventionally cured sample for Araldite LY 5052 / 4 4' DDS epoxy system, but they were lower than the activation energy for the conventionally cured samples of Araldite DLS 772 / 4 4' DDS epoxy systems. For both epoxy systems, the activation energies increased as the stoichiometric ratio increased for conventionally cured samples, but it decreased as the stoichiometric ratio increased for microwave cured samples. Interestingly, Kissinger's method gave a value of activation energy that was similar to the value obtained by Ozawa's method when applied to the

exothermic peak. A major difference between Ozawa and Kissinger's method for the determination of activation energy is that in addition to the determination of the activation energy of the entire reaction process, Ozawa's method can be used to determine the activation energy at any specific extent of fractional conversion, while Kissinger's method can only be used to measure the activation energy for the entire reaction process.

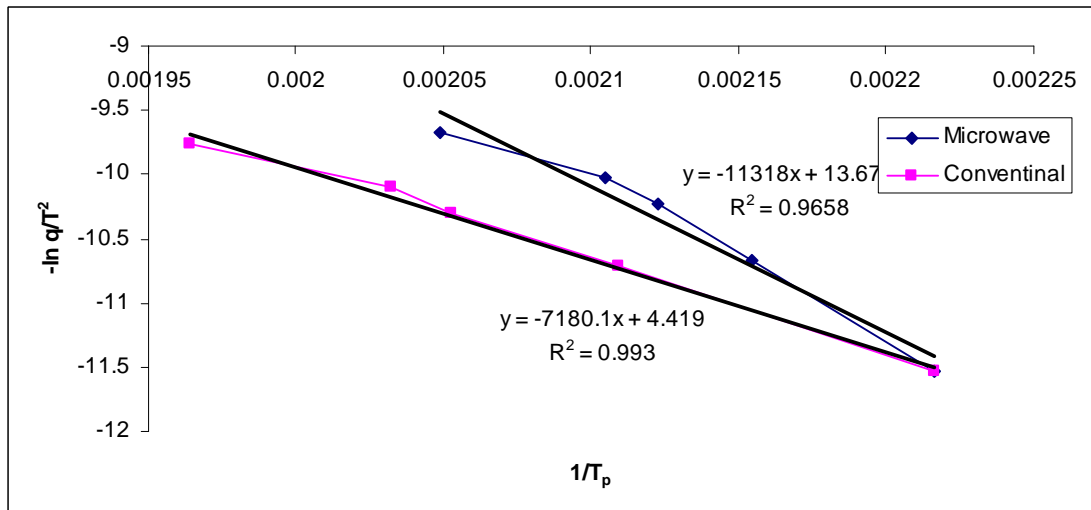


Figure 4.58 Plot of $-\ln(\Phi/T_p^2)$ against T_p^{-1} for conventional and microwave curing of Araldite LY 5052 / 4 4' DDS epoxy system with an amine / epoxy ratio of 0.85.

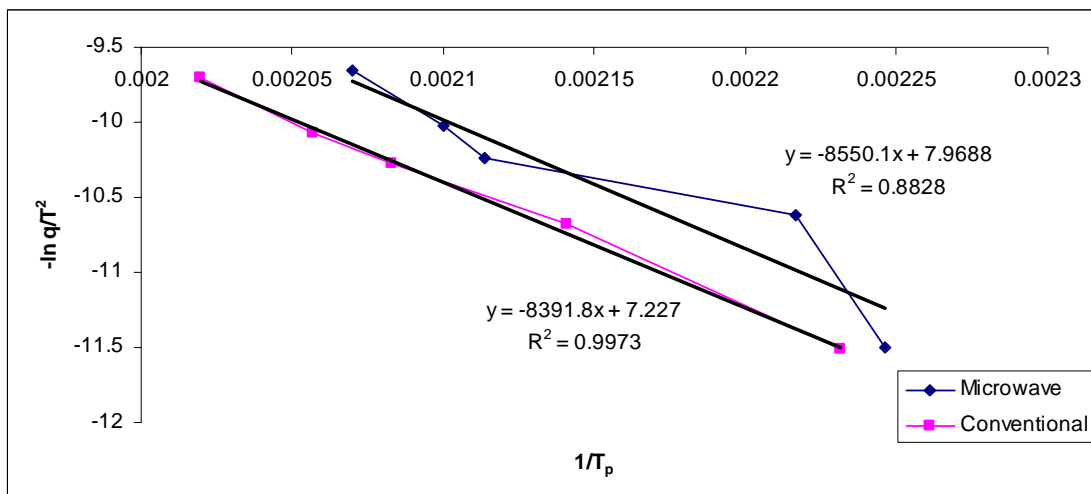


Figure 4.59 Plot of $-\ln(\Phi/T_p^2)$ against T_p^{-1} for conventional and microwave curing of Araldite LY 5052 / 4 4' DDS epoxy system with an amine / epoxy ratio of 1.0.

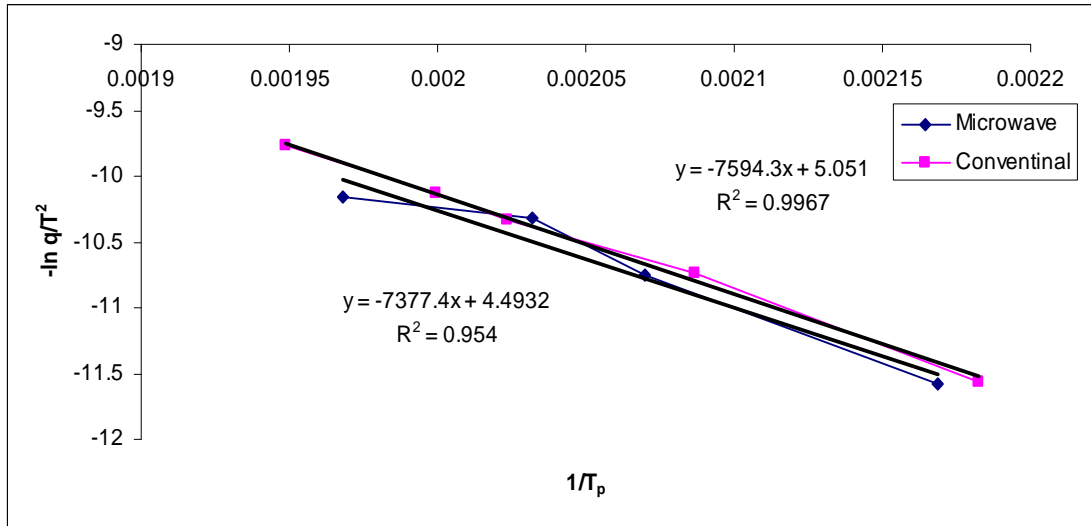


Figure 4.60 Plot of $-\ln(\Phi/T_p^2)$ against T_p^{-1} for conventional and microwave curing of Araldite DLS 772 / 4 4' DDS epoxy system with an amine / epoxy ratio of 0.8.

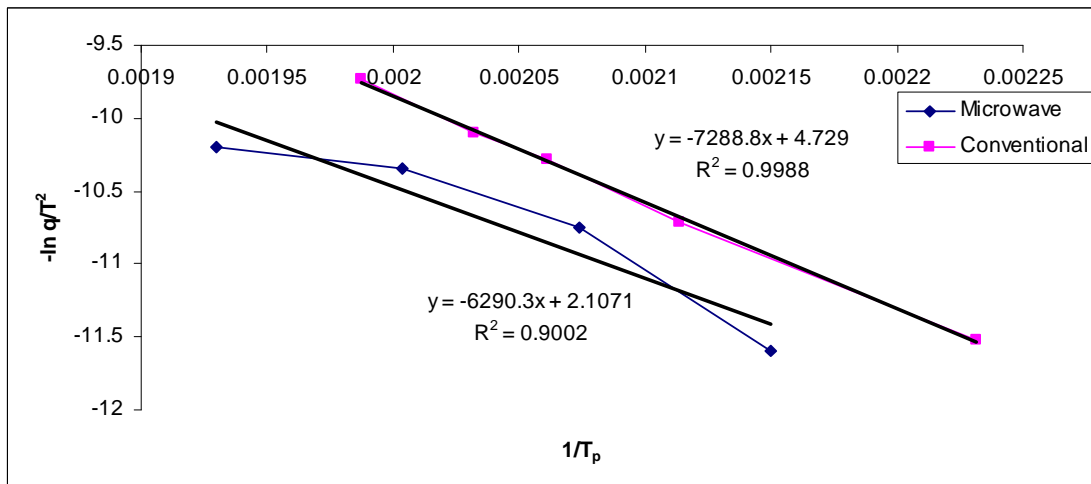


Figure 4.61 Plot of $-\ln(\Phi/T_p^2)$ against T_p^{-1} for conventional and microwave curing of Araldite DLS 772 / 4 4' DDS epoxy system with an amine / epoxy ratio of 1.1.

Table 4.25 Values of Activation energy and pre-exponential factor for different stoichiometric ratios of Araldite LY 5052 / 4 4' DDS and Araldite DLS 772 / 4 4' DDS epoxy systems using conventional and microwave heating.

Sample	Conventional Heating		Microwave Heating	
	A' (s ⁻¹)	E _a (KJ mol ⁻¹)	A' (s ⁻¹)	E _a (KJ mol ⁻¹)
Araladite LY 5052 0.85M	4.42	59.7	13.67	94.1
AralditeLY 5052 1.0 M	21.53	69.8	22.25	71.1
DLS 772 0.8 M	5.50	63.1	4.49	59.3
DLS 772 1.1 M	9.76	60.6	12.76	52.3

The activation energies of conventionally and microwave cured samples of Araldite LY 5052 / 4 4' DDS and Araldite DLS 772 / 4 4' DDS epoxy systems fall within the range of activation energies of chemical reactions (30 to 100 KJ mol⁻¹) [16]

4.9 Dielectric Properties measurement

The cavity perturbation technique was used to measure the dielectric properties of the epoxy systems as the microwave curing reactions proceeded. The experimental procedure is described in section 3.4 The changes in dielectric properties of samples undergoing microwave cure were monitored *in situ* with the cavity perturbation technique. We could not obtain any data for the dielectric properties for conventionally cured samples. A method for the *in situ* monitoring for changes in dielectric properties of samples undergoing thermal cure using cavity perturbation technique has been developed, but this technique is a specialised technique and expensive to purchase. The curing mechanism of the samples during microwave cure can be explained with the knowledge of the dielectric properties of the samples during microwave curing. It is important to know the dielectric properties since the rate of heating when exposed to microwave radiation depends on the loss factor of material being heated.

The dielectric constant, ϵ' and dielectric loss factor, ϵ'' , indicate the ability of the molecular dipole moments in the materials to follow the oscillations of an applied electric field [57, 66, 85, 88]. The dielectric constant represents the component of

immediate alignment of the dipole moments in the direction of the electric field, while the dielectric loss factor shows the retardation incurred in the arrangement. Thus, the changes in the dielectric properties would not only represent the alternation in molecular dipole moments as a result of the chemical reaction taking place but also show the rapid decrease in molecular mobility that occurs during the formation of a cross-linked network. [11].

Figure 4.62 shows the dielectric constant and dielectric loss factor as a function of reaction temperature for microwave curing of Araldite LY 5052 / 4 4' DDS epoxy system with an amine / epoxy ratio of 0.85. The dielectric constant and dielectric loss factor exhibited similar trends as the curing proceeded. The dielectric properties increased as the curing temperature increased until they reached a maximum value and then gradually decreased with increasing temperature. The dielectric constant and dielectric loss factor reached the maximum values at a similar temperature. Figure 4.63 shows a plot of the dielectric loss factor and the reaction exotherm of microwave-cured Araldite LY 5052 / 4 4' DDS epoxy system with an amine / epoxy ratio of 0.85 against temperature.

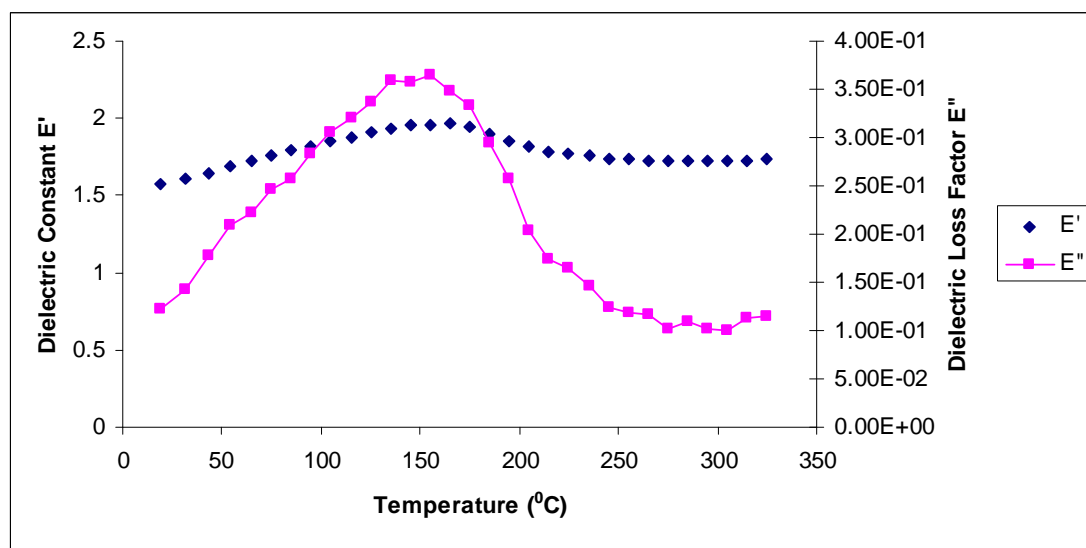


Figure 4.62 Plot of dielectric constant and dielectric loss factor as a function of reaction temperature for microwave-cured Araldite LY 5052 / 4 4' DDS epoxy system with an amine / epoxy ratio of 0.85 at a heating rate of 5 K min⁻¹

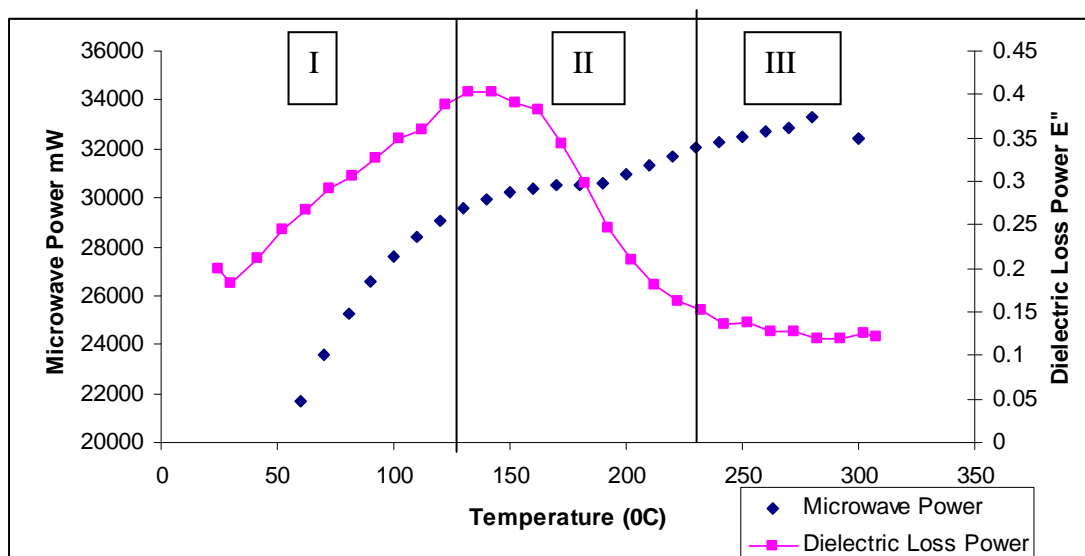


Figure 4.63 A plot of dielectric loss factor and reaction exotherm as a function of reaction temperature for microwave cured Araldite LY 5052 / 4,4'-DDS epoxy system with an amine / epoxy ratio of 0.85 at a heating rate of 5 K min⁻¹

From figure 4.63, the cure process can be divided into three stages. The first stage (Stage I) is the liquid prepolymer heating stage. In this stage the dipoles can rotate freely. This leads to an increase in dielectric loss factor as the temperature increases. As a result of the curing reaction and subsequent decrease in the number of both the functional polar groups and also in the molecular mobility, there will be a significant decrease in the dielectric loss factor [21]. This is shown in stage II. A highly cross-linked structure is formed in stage III. The formation of this crosslinked structure leads to a further decrease in the dielectric properties. Jow *et al* made a similar observation [89]. It is also observed from figure 4.63 that the temperature at the maximum value of dielectric loss factor corresponded to the onset temperature of the exothermic peak.

The dielectric constant, ϵ' and dielectric loss factor, ϵ'' , as a function of reaction temperature for microwave curing Araldite LY 5052 / 4,4'-DDS epoxy system with an amine / epoxy ratio of 1.0 is shown in figure 4.64. Again, the dielectric properties increased with temperature to the maximum value and decreased with increasing temperature.

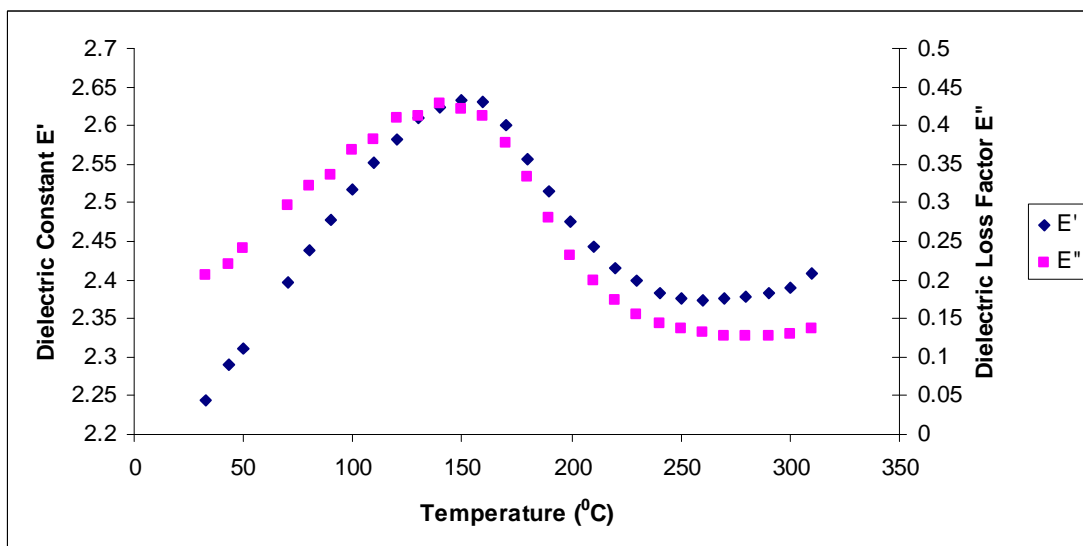


Figure 4.64 Plot of dielectric constant and dielectric loss factor as a function of reaction temperature for microwave-cured Araldite LY 5052 / 4,4'-DDS epoxy system with an amine / epoxy ratio of 1.0 at a heating rate of 5 K min⁻¹

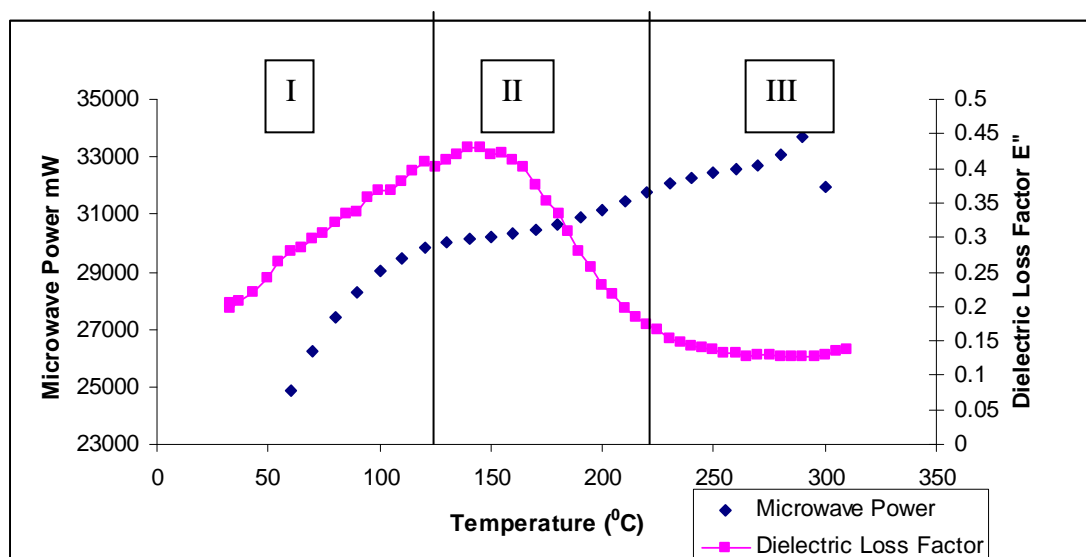


Figure 4.65 A plot of dielectric loss factor and reaction exotherm as a function of reaction temperature for microwave cured Araldite DLS 772 / 4,4'-DDS epoxy system with an amine / epoxy ratio of 1.0 at a heating rate of 5 K min⁻¹

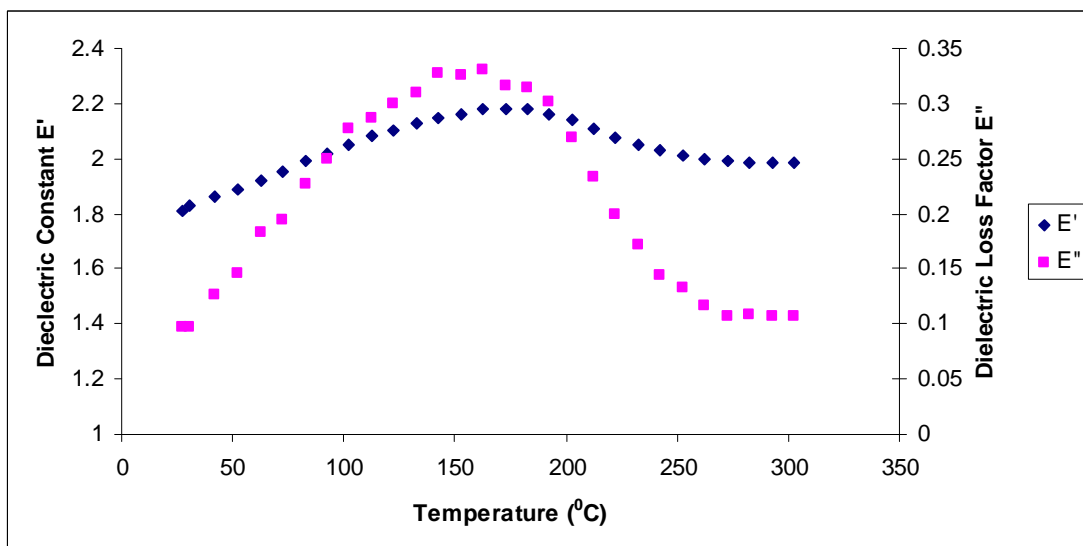


Figure 4.66 Plot of dielectric constant and dielectric loss factor as a function of reaction temperature for microwave-cured Araldite DLS 772 / 4 4' DDS epoxy system with an amine / epoxy ratio of 0.8 at a heating rate of 5 K min⁻¹

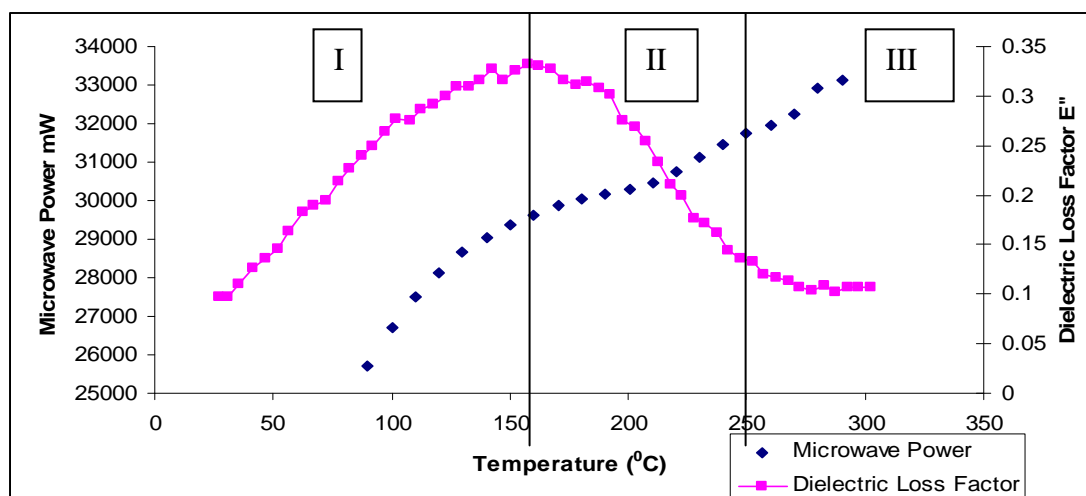
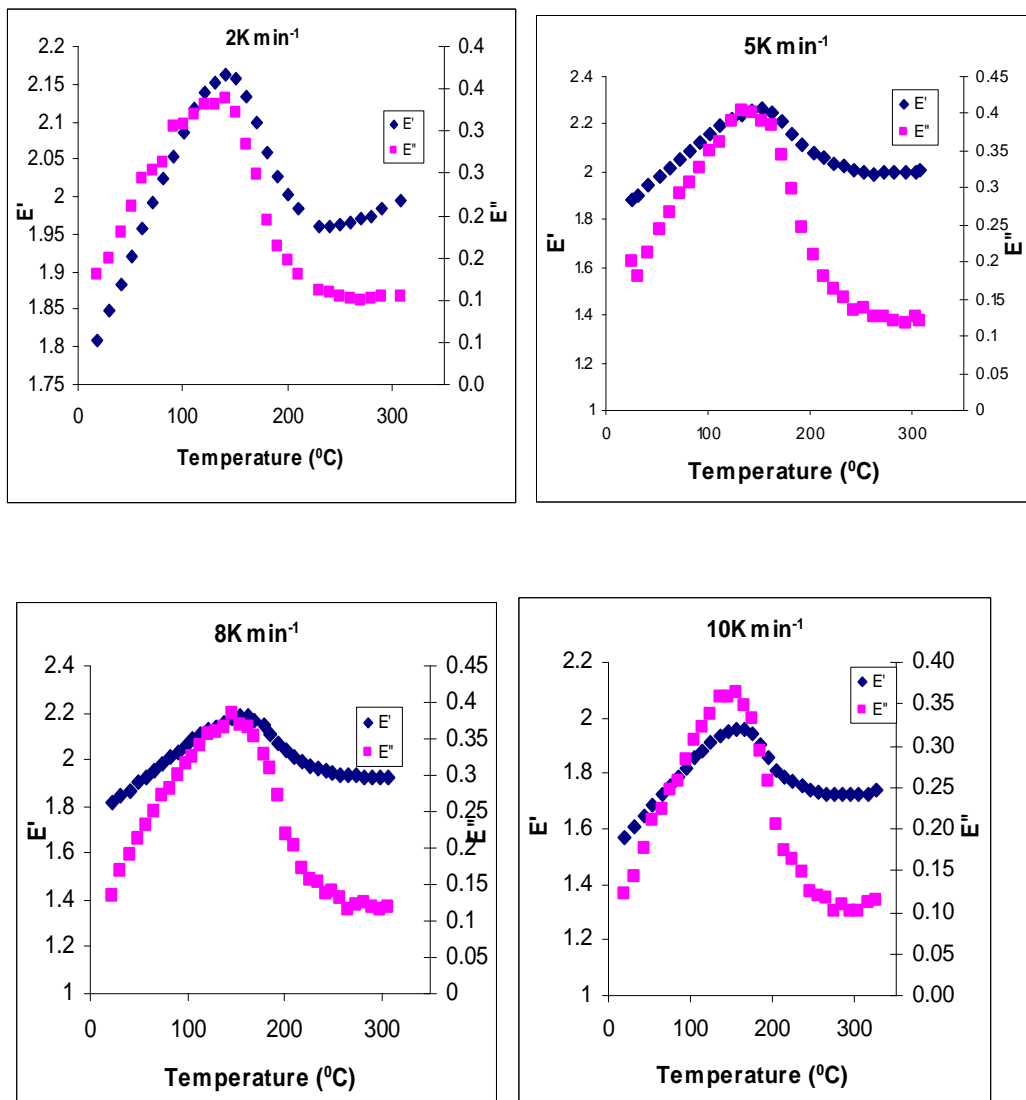


Figure 4.67 A plot of dielectric loss factor and reaction exotherm as a function of reaction temperature for microwave cured Araldite DLS 772 / 4 4' DDS epoxy system with an amine / epoxy ratio of 1.1 at a heating rate of 5 K min⁻¹

In accordance to the dielectric loss factor, just as in the microwave curing of Araldite LY 5052 / 4 4' DDS epoxy system, the microwave curing of Araldite DLS 772 / 4 4' DDS epoxy systems can be divided into three stages. At the temperature which curing of the epoxy system began, the dielectric loss factor started to deplete. As explained

above, this decrease is attributed to the formation of a cross-linked network which occurs as a result of the decrease in the number of functional polar groups as well as a decrease in molecular mobility [57]

The dielectric properties measurements of the epoxy systems at different heating rates are shown in figure 4.68 – 4.71 All the results show a similar trend whereby there was an increase in the dielectric properties as the temperature increased up to a maximum, and as the temperature kept increasing, the dielectric properties started to decrease.



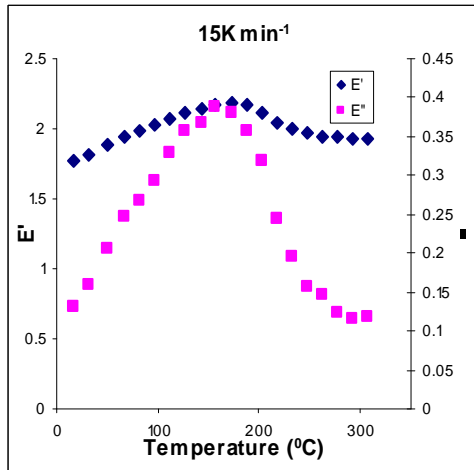
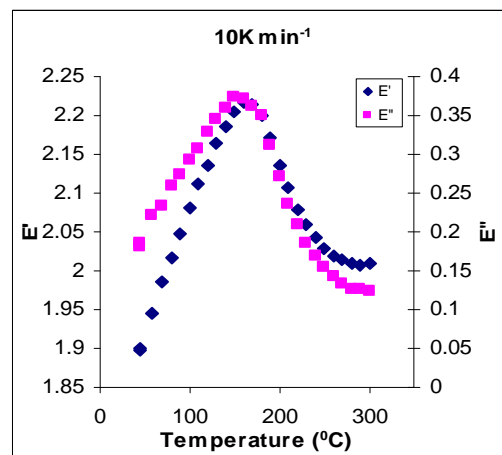
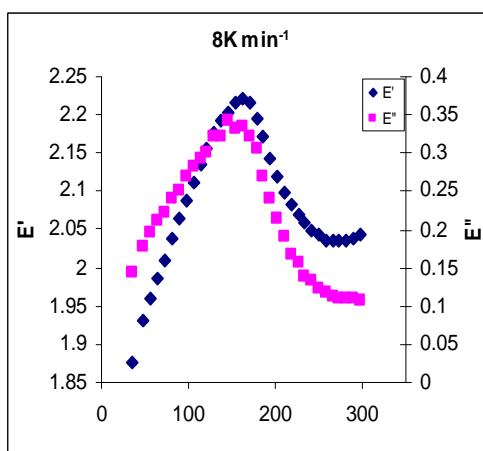
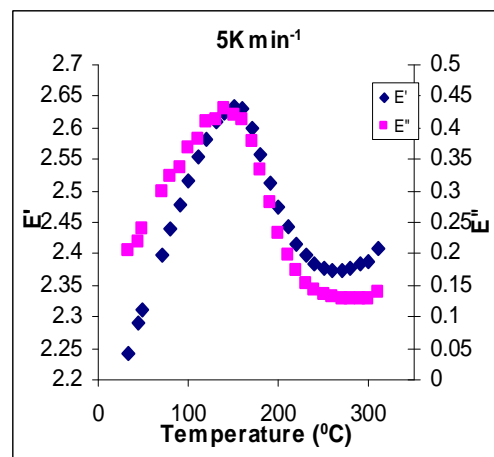
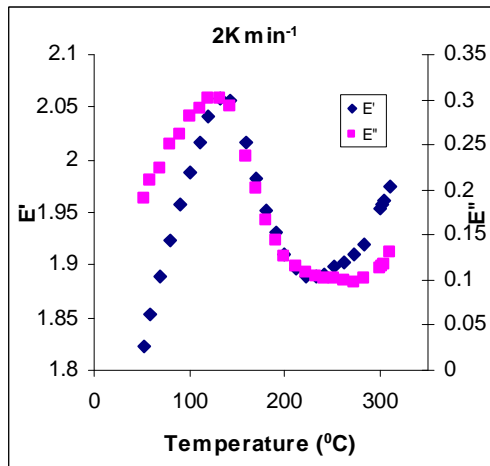


Figure 4.68 Dielectric constant E' and Dielectric loss factor E'' as a function of reaction temperature for microwave cured Araldite LY 5052 / 4 4' DDS epoxy system with an amine / epoxy ratio of 0.85 at different heating rates.



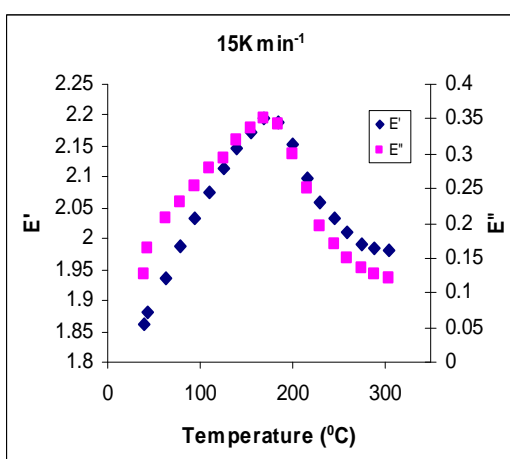


Figure 4.69 Dielectric constant E' and Dielectric loss factor E'' as a function of reaction temperature for microwave cured Araldite LY 5052 / 4 4' DDS epoxy system with an amine / epoxy ratio of 1.0 at different heating rates.

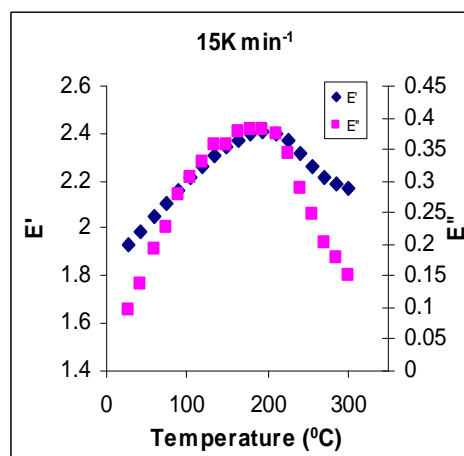
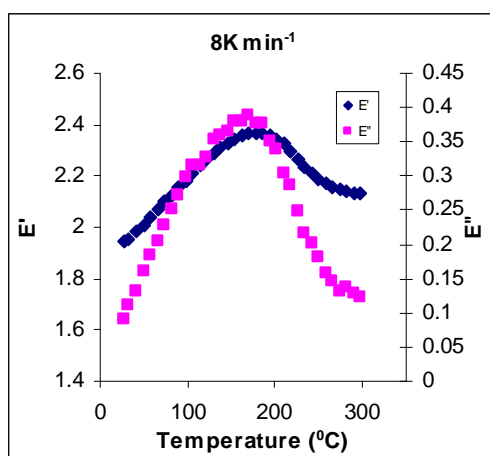
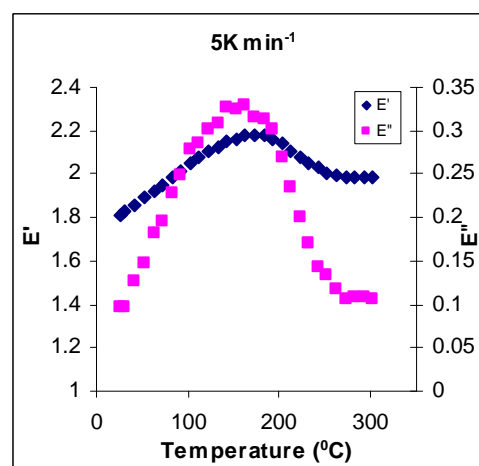
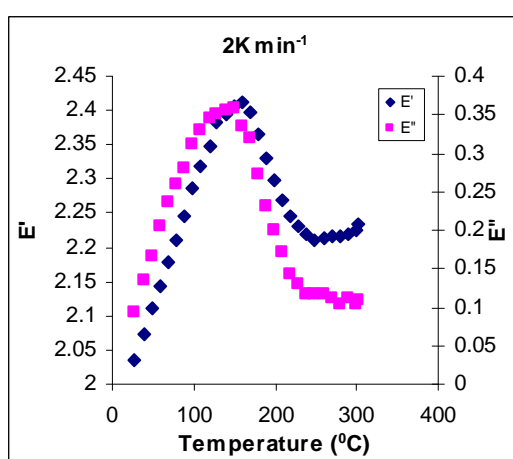


Figure 4.70 Dielectric constant E' and Dielectric loss factor E'' as a function of reaction temperature for microwave cured Araldite DLS 772 / 4 4' DDS epoxy system with an amine / epoxy ratio of 0.8 at different heating rates.

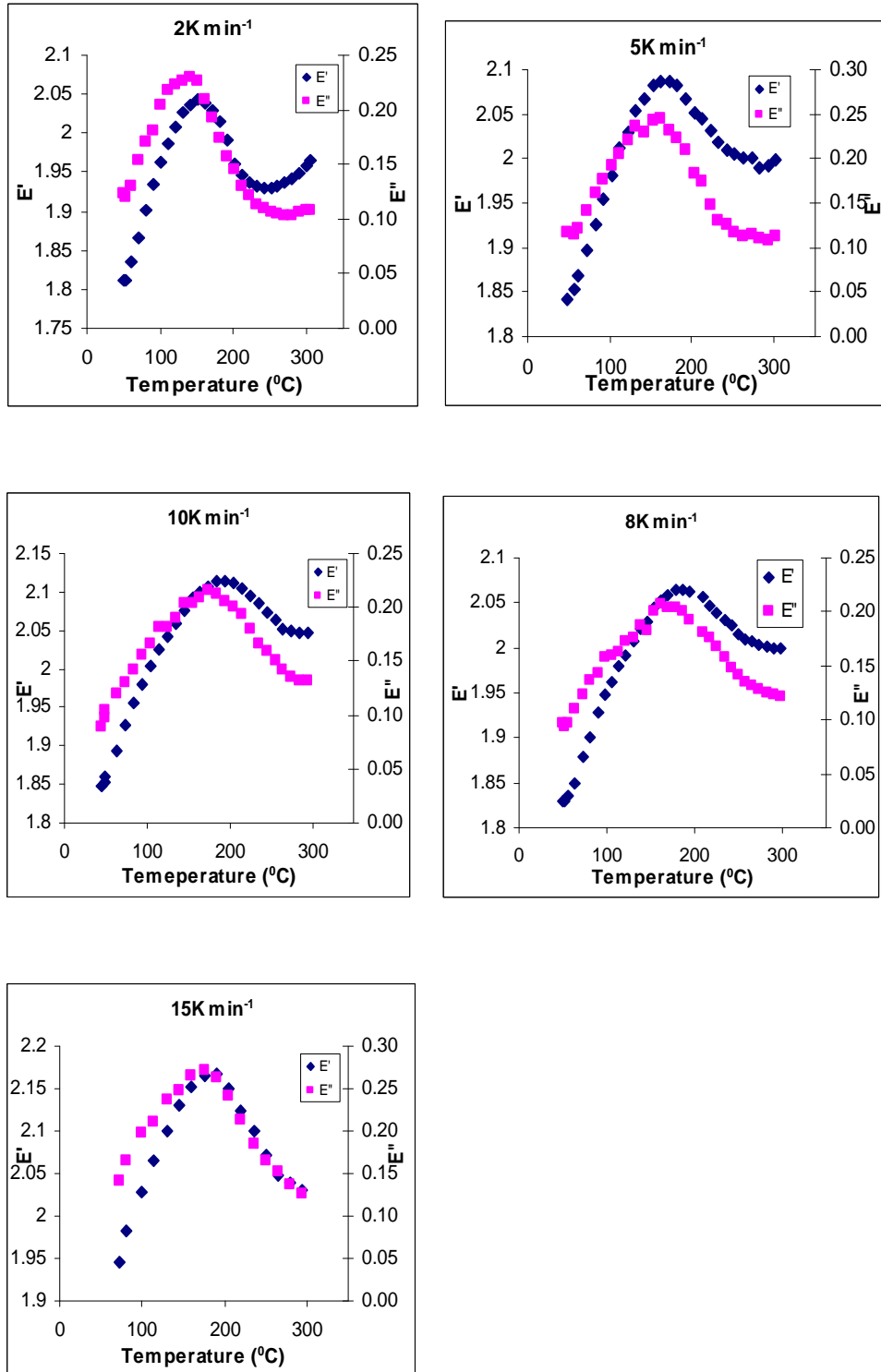
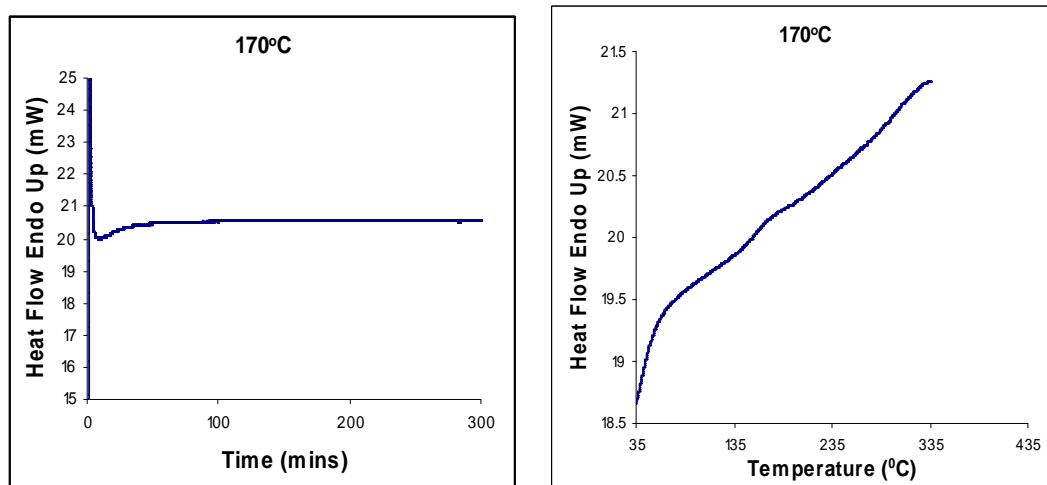


Figure 4.71 Dielectric constant E' and dielectric loss factor E'' as a function of reaction temperature for microwave cured Araldite DLS 772 / 4 4' DDS epoxy system with an amine / epoxy ratio of 1.1 at different heating rates.

4.10 Isothermal Curing

4.11 Isothermal Conventional Curing

The DSC machine was used to cure samples of both epoxy systems at a heating rate of 100 K min^{-1} up to temperatures of 170, 180, 190 and 200 °C. The samples were held at these temperatures for 300, 240, 200 and 200 minutes respectively. At the end of each cure cycle, another DSC scan was carried out on the material at a heating rate of 10 K min^{-1} to 350 °C. The results of the dynamic DSC scan showed a T_g curve and no exotherm. This was taken as an indication that the sample fully cured under the above isothermal curing conditions.



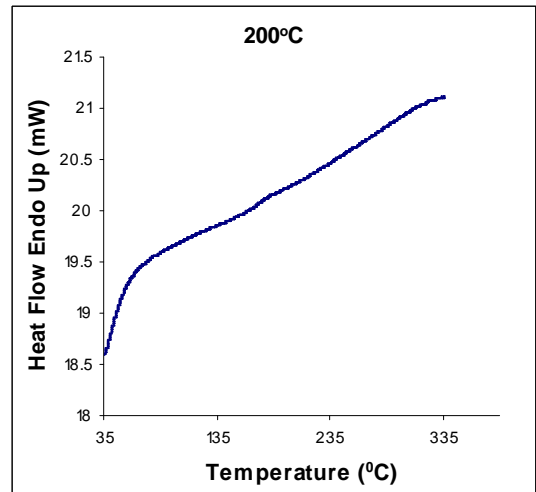
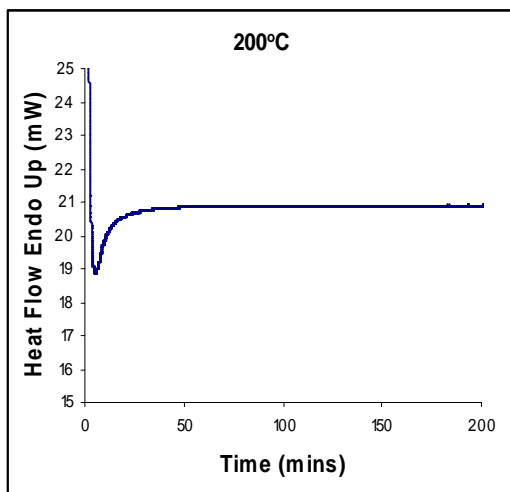
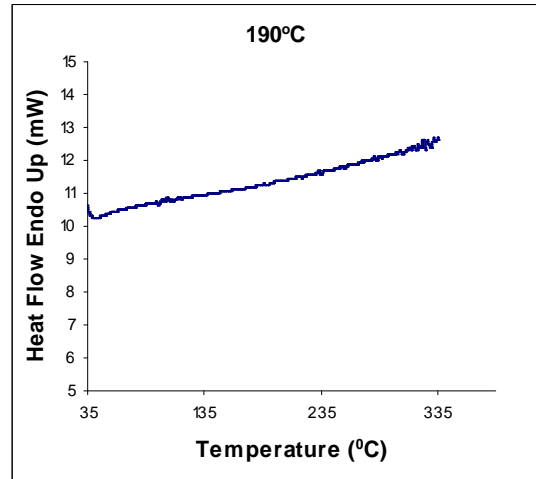
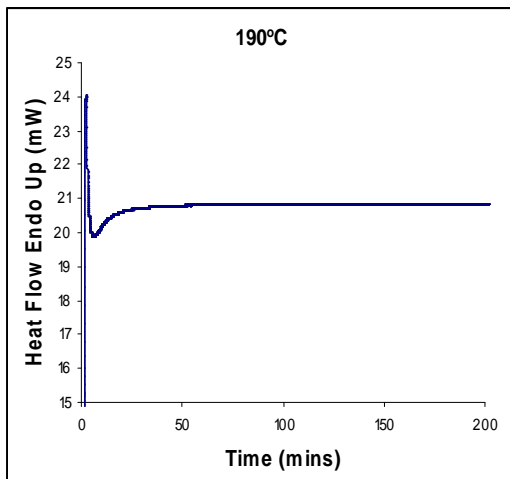
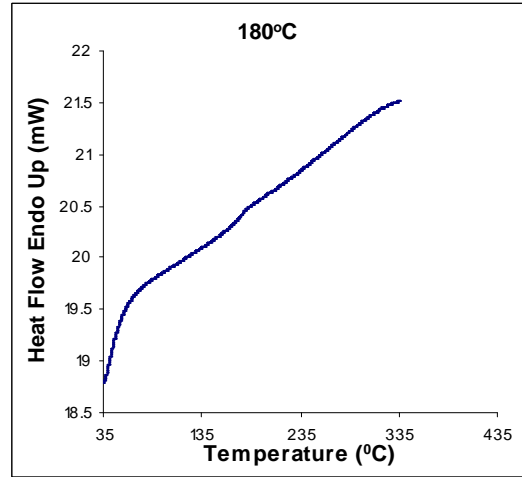
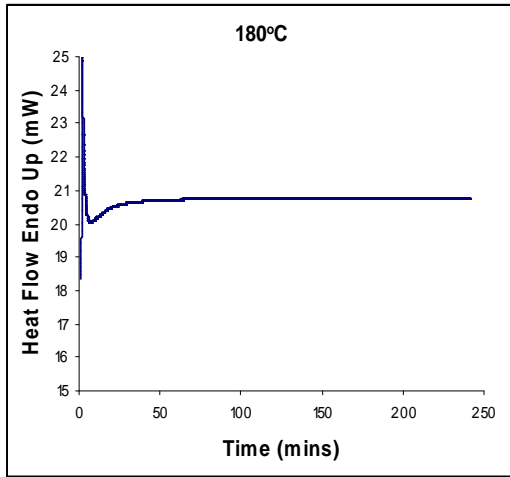


Figure 4.72 DSC thermograms of conventional isothermal cure (left) and subsequent DSC run to test for exotherm for Araldite LY 5052 / 4 4' DDS epoxy system with an amine / epoxy ratio of 0.85.

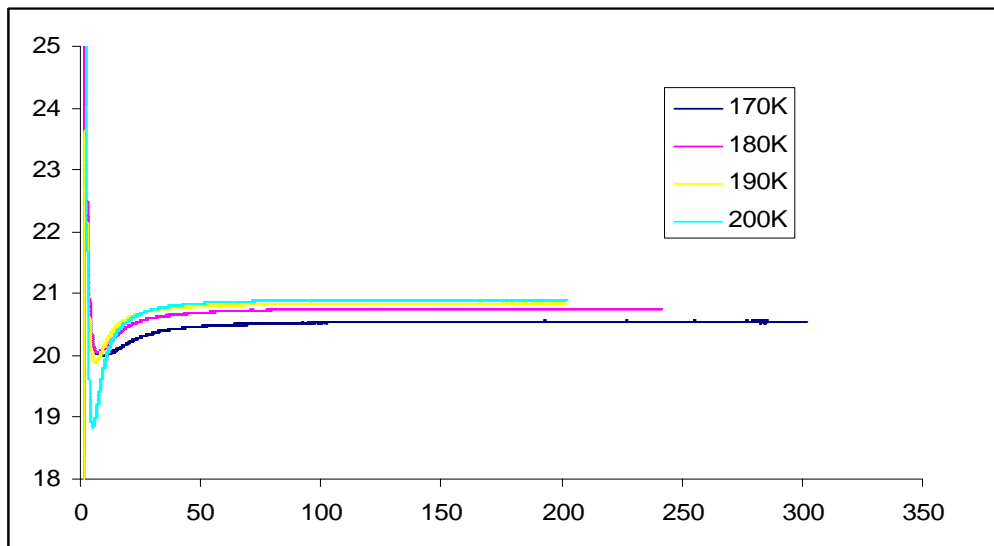


Figure 4.73 Typical DSC thermograms for Araldite LY 5052 / 4 4' DDS epoxy system system with an amine / epoxy ratio of 0.85 at different heating rates using conventional DSC.

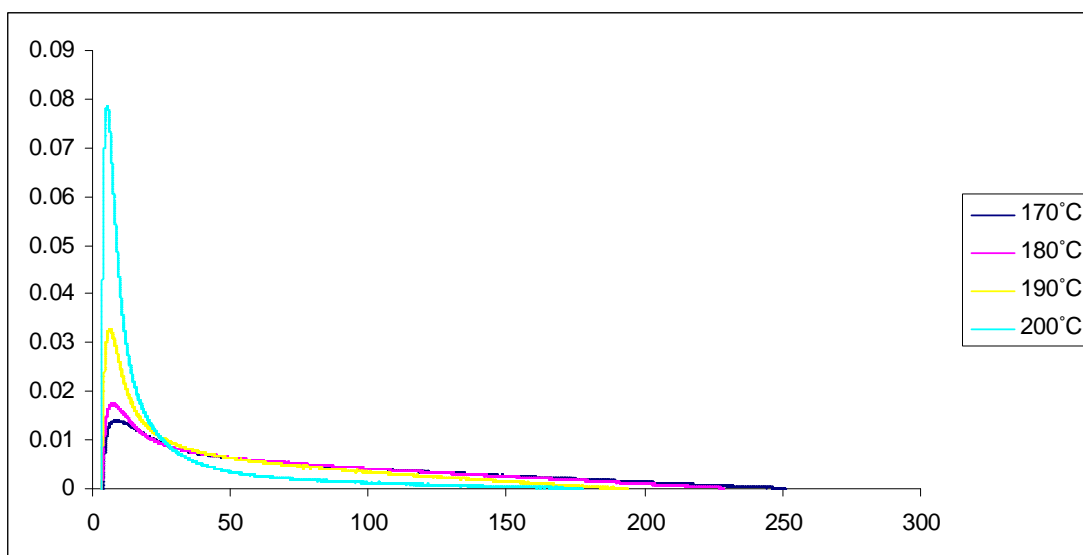


Figure 4.74 Reaction rates for isothermal cure of Araldite LY 5052 / 4 4' DDS epoxy system system with an amine / epoxy ratio of 0.85 using conventional heating.

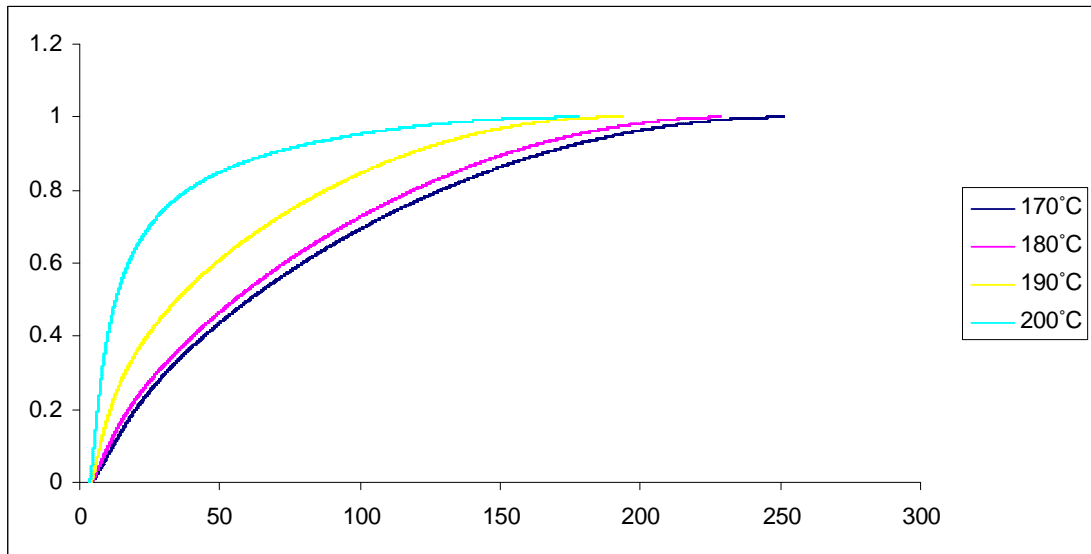


Figure 4.75 Fractional conversion for isothermal cure of Araldite LY 5052 / 4 4' DDS epoxy system with an amine / epoxy ratio of 0.85 using conventional heating at different isothermal temperatures.

Figure 4.74 shows the reaction rate increasing as the reaction temperature increases. The increase in the reaction temperature causes a distinct distribution of molecular speeds and energies followed by an increase in the average value of energy from the reactant molecules. As a result, a larger number of molecules have enough activation energy to surpass the activation barrier, and this leads to an increase in the reaction rate [16, 90, 91].

A plot of fractional conversion against reaction rate for all the heating rates is shown in the figure 4.76 below. Typical changes are found to occur in the reaction rate over the whole range of conversion. For isothermal cure, the reaction rate increases and it quickly reaches a maximum at the early stages of the reaction, in the fractional conversion range of 0 – 0.15. Beyond this range, the reaction rate started to decrease. This decrease is ascribed to the increase in the viscosity of the reaction medium as the curing material gelled [57]. There was a significant reduction in molecular mobility of the reactants at this stage. The reaction became diffusion controlled, and it eventually stopped. It was also observed that the reaction rate increased as the curing temperature increased. Also, at higher temperatures, the time taken to attain full cure becomes lower.

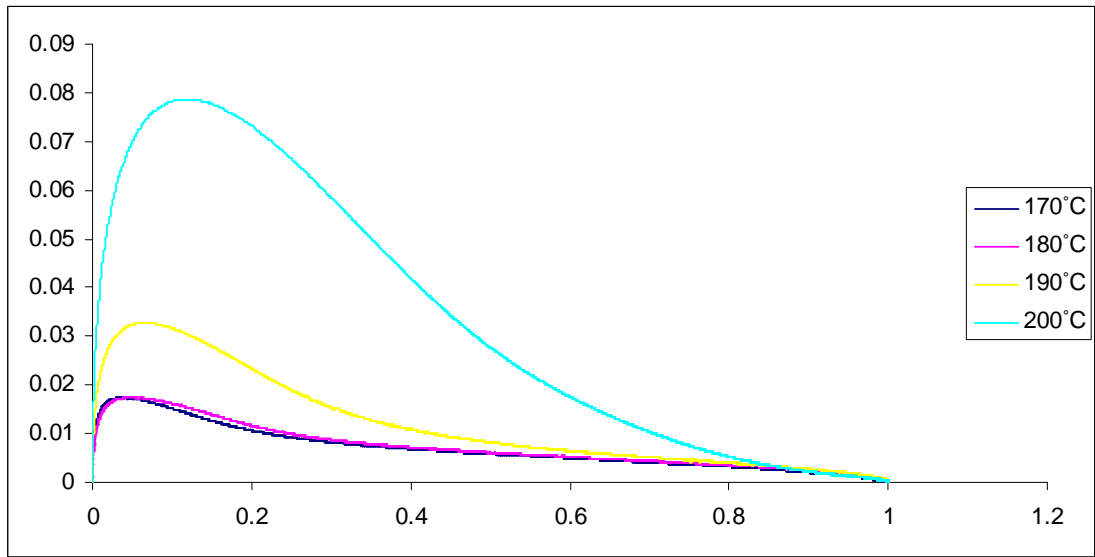


Figure 4.76 Plot of Reaction rate against Fractional Conversion for the curing reaction of Araldite LY 5052 / 4 4' DDS epoxy system system with an amine / epoxy ratio of 0.85 at different isothermal temperatures.

Typical DSC thermograms for the cure of Araldite LY 5052 / 4 4' DDS epoxy system with amine / epoxy ratio of 1.0 are shown in figure 4.81 below.

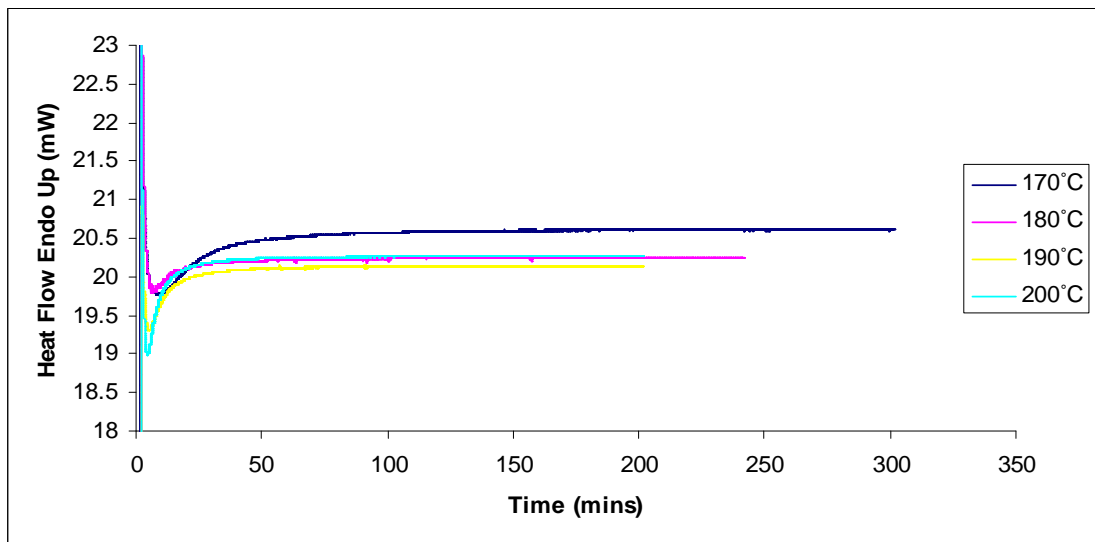


Figure 4.77 DSC thermograms for isothermal cure of Araldite LY 5052 / 4 4' DDS epoxy system with an amine / epoxy ratio of 1.0 obtained from conventional DSC at different heating rates.

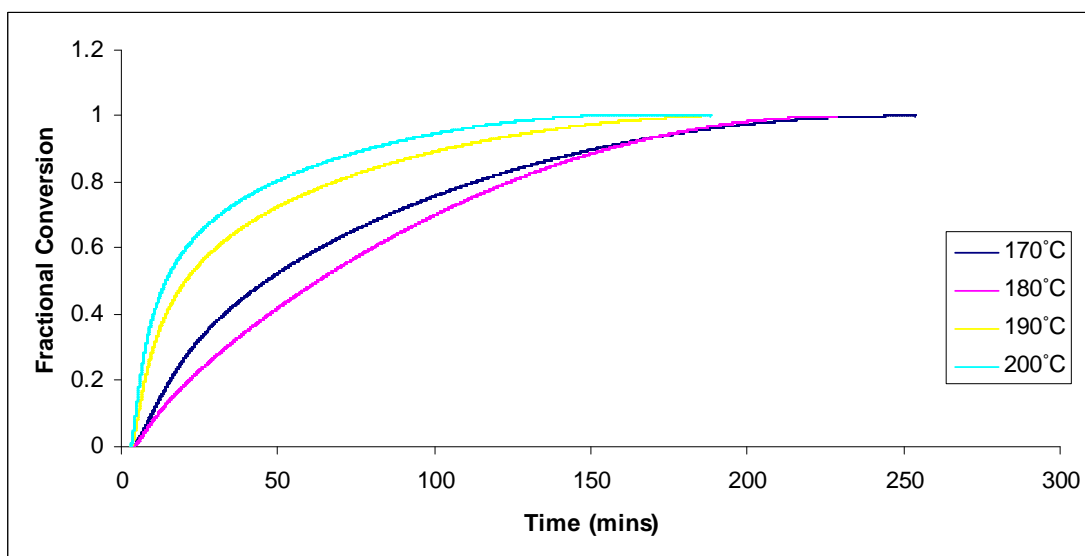


Figure 4.78 Fractional conversion for isothermal cure of Araldite LY 5052 / 4 4' DDS epoxy system with an amine / epoxy ratio of 1.0 at different heating rates using conventional heating.

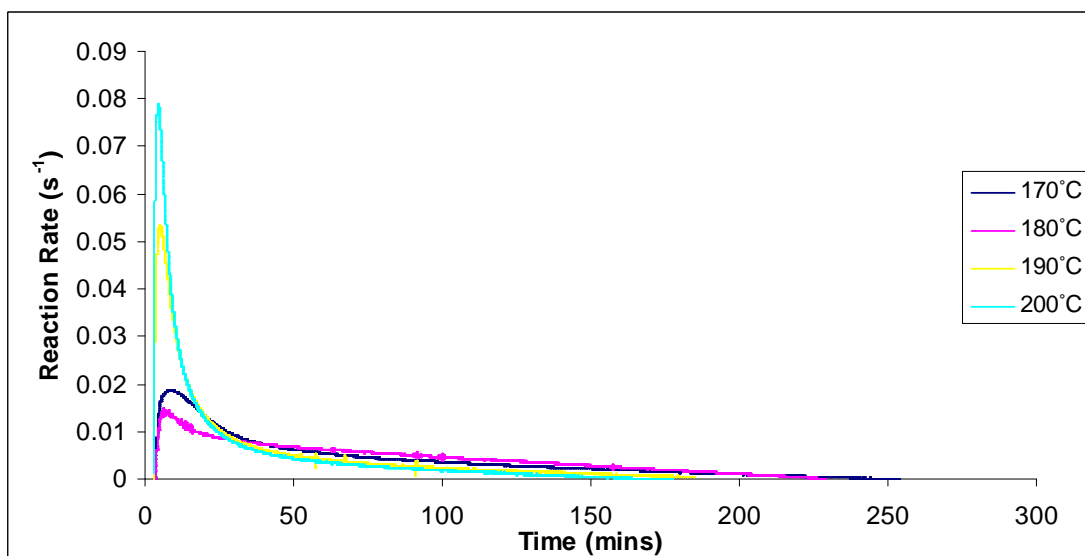


Figure 4.79 Reaction rates for isothermal cure of Araldite LY 5052 / 4 4' DDS epoxy system with an amine / epoxy ratio of 1.0 at different heating rates using conventional heating.

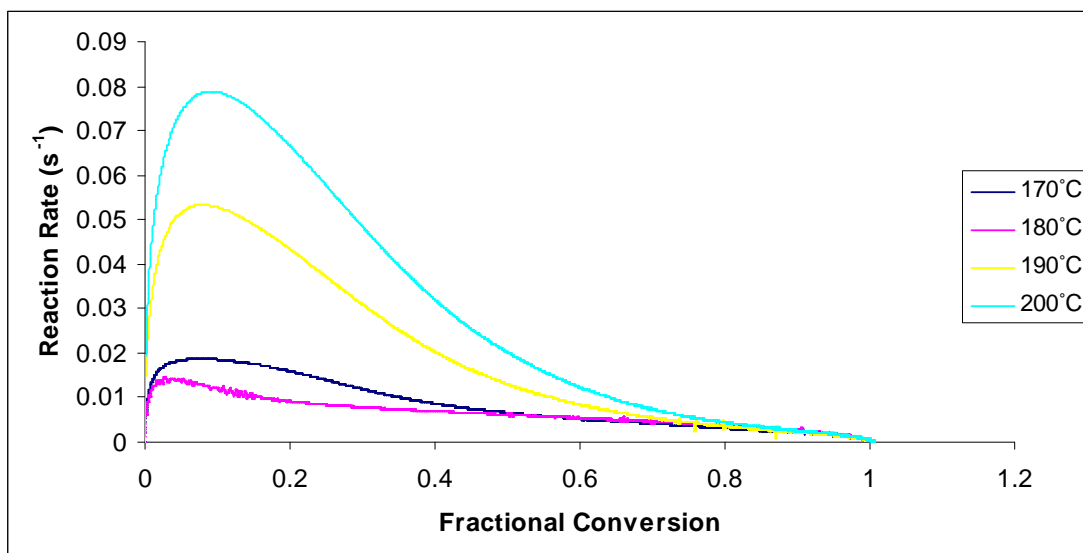


Figure 4.80 Rate of reaction against fractional conversion for the curing reaction of Araldite LY 5052 / 4 4' DDS epoxy system with an amine / epoxy ratio of 1.0 at different heating rates.

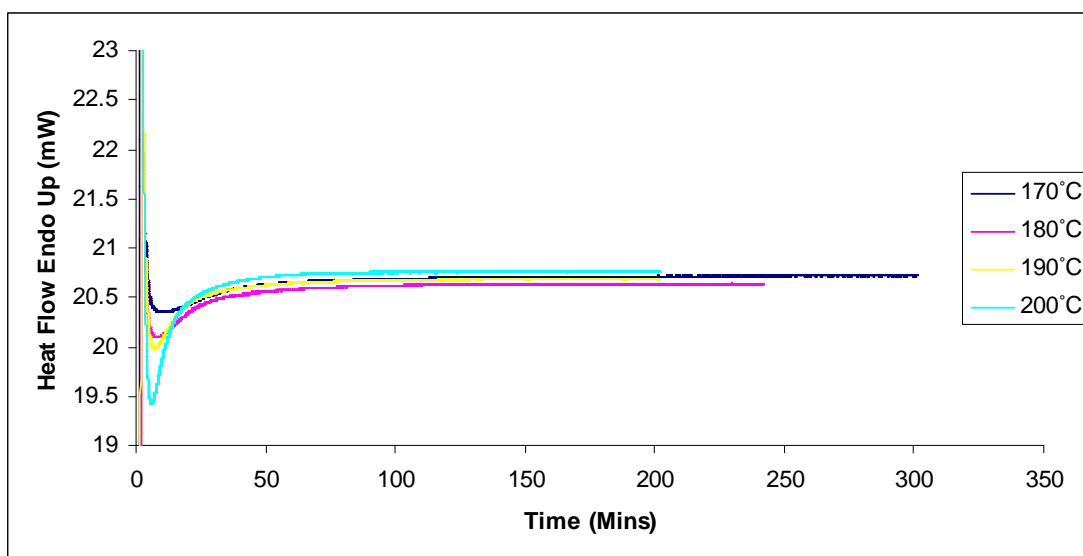


Figure 4.81 DSC thermograms for Araldite DLS 772 / 4 4' DDS epoxy system system with an amine / epoxy ratio of 0.8 obtained from conventional DSC at a range of isothermal temperatures.

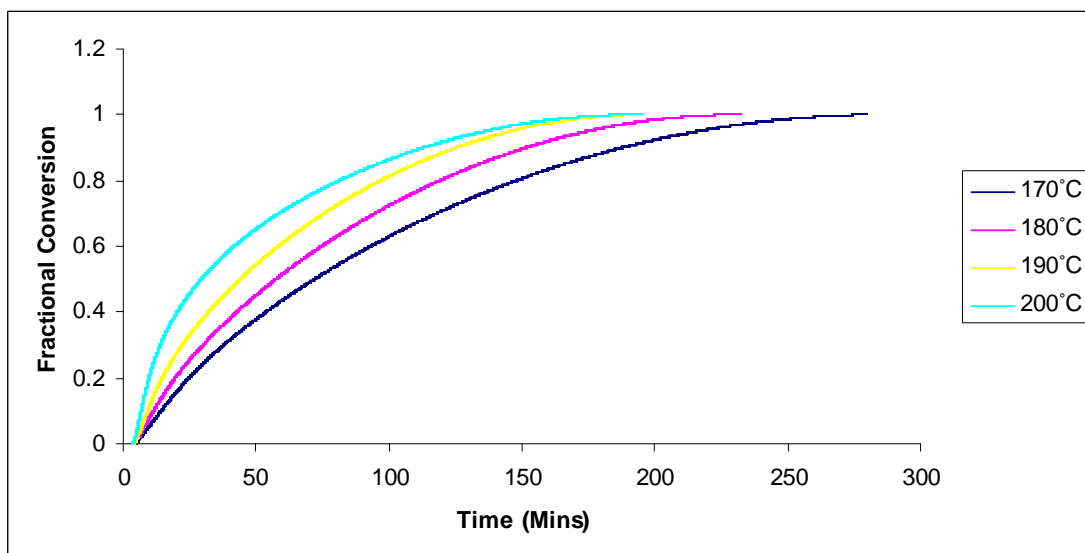


Figure 4.82 Fractional conversion for isothermal cure of Araldite DLS 772 / 4 4' DDS epoxy system with an amine / epoxy ratio of 0.8 at different isothermal temperatures using conventional heating.

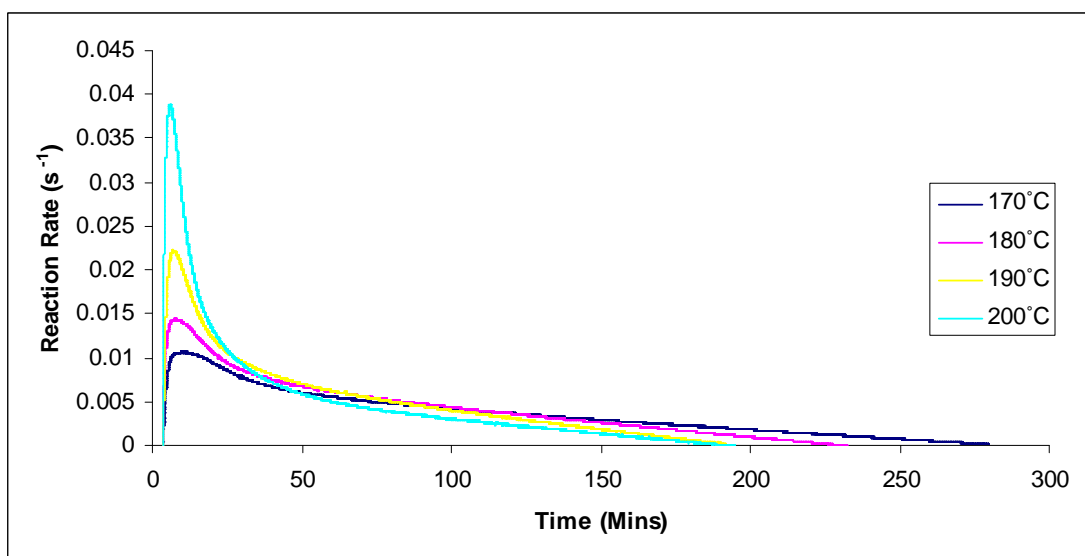


Figure 4.83 Reaction rates for isothermal cure of Araldite DLS 772 / 4 4' DDS epoxy system with an amine / epoxy ratio of 0.8 at different isothermal temperatures using conventional heating.

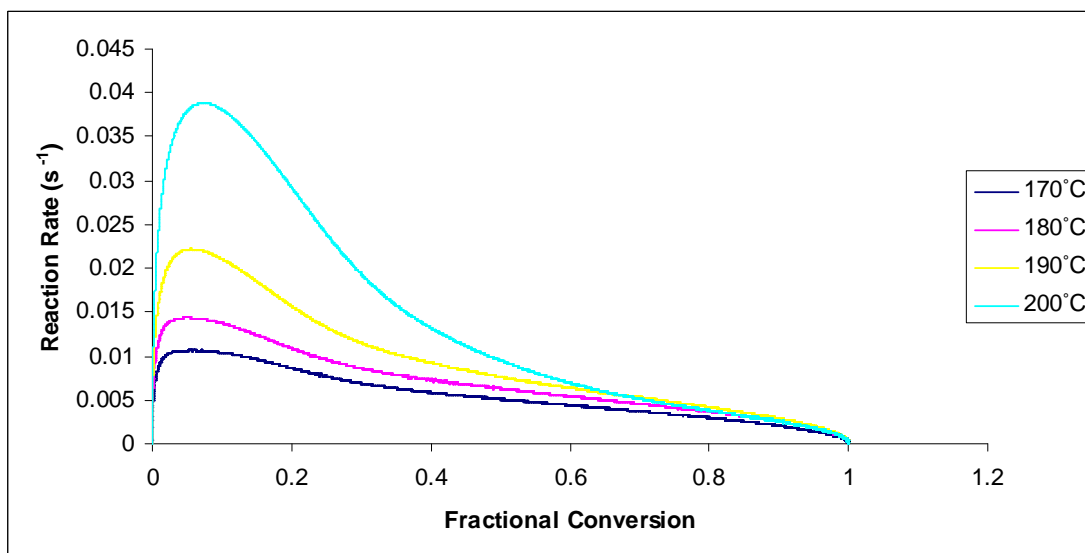


Figure 4.84 Rate of reaction against fractional conversion for the isothermal curing reaction of Araldite DLS 772 / 4 4' DDS epoxy system with an amine / epoxy ratio of 0.8 at different heating rates.

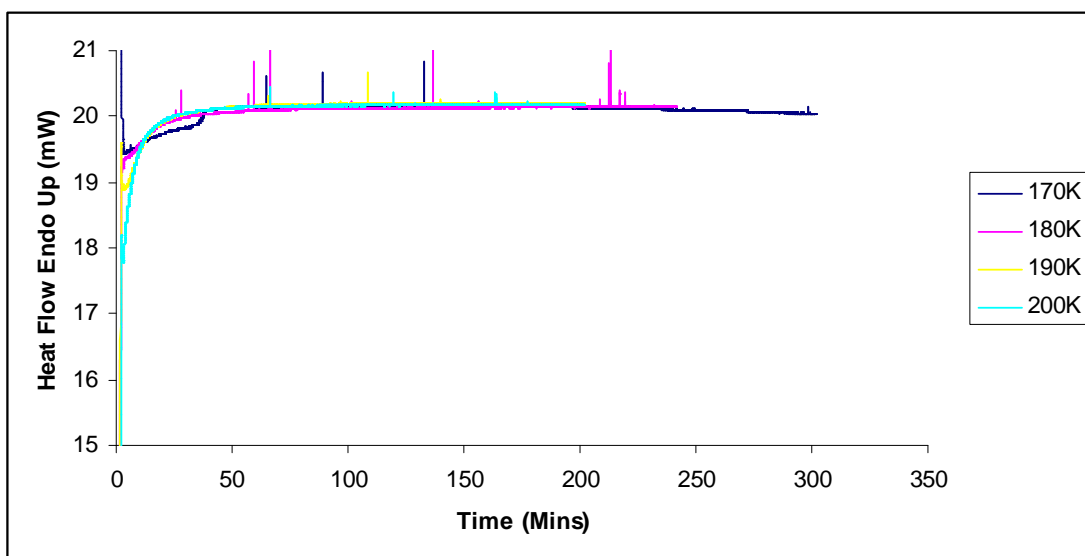


Figure 4.85 DSC thermograms for Araldite DLS 772 / 4 4' DDS epoxy system with an amine / epoxy ratio of 1.1 obtained from conventional DSC at different isothermal temperatures.

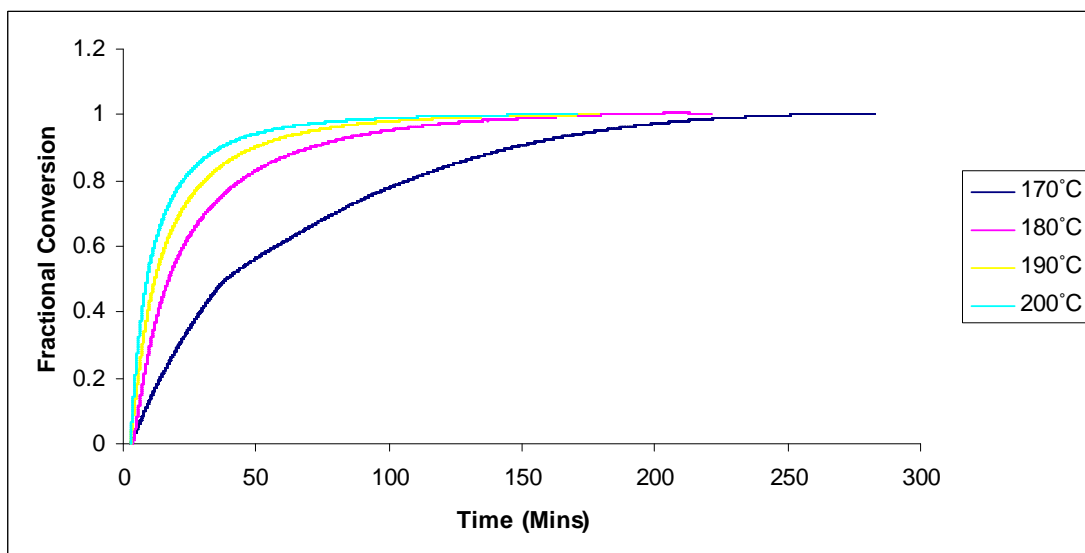


Figure 4.86 Fractional conversion for isothermal cure of Araldite DLS 772 / 4 4' DDS epoxy system with an amine / epoxy ratio of 1.1 at different isothermal temperatures using conventional heating.

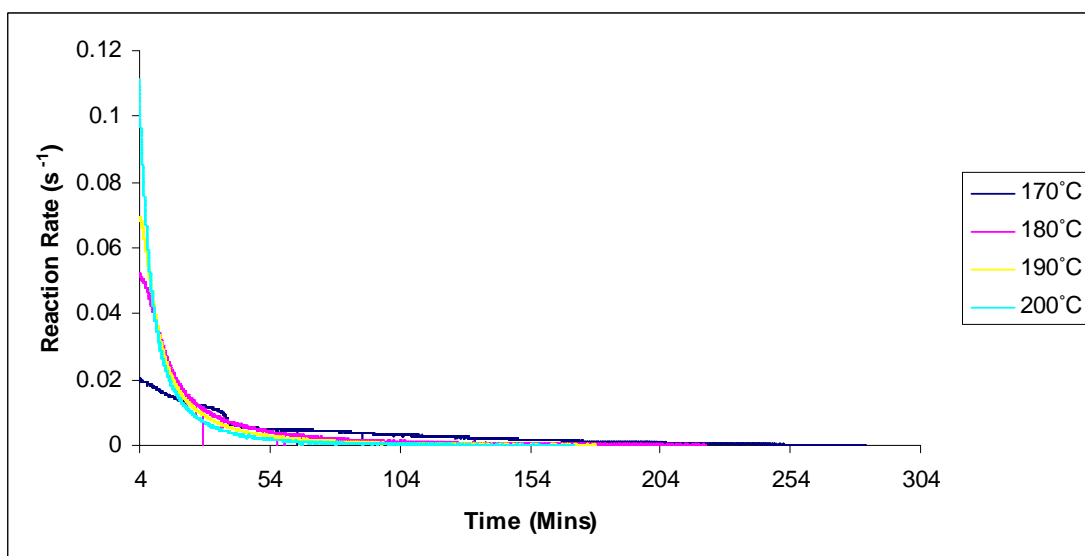


Figure 4.87 Reaction rates for isothermal cure of Araldite LY 5052 / 4 4' DDS epoxy system with an amine / epoxy ratio of 1.1 at different isothermal temperatures using conventional heating.

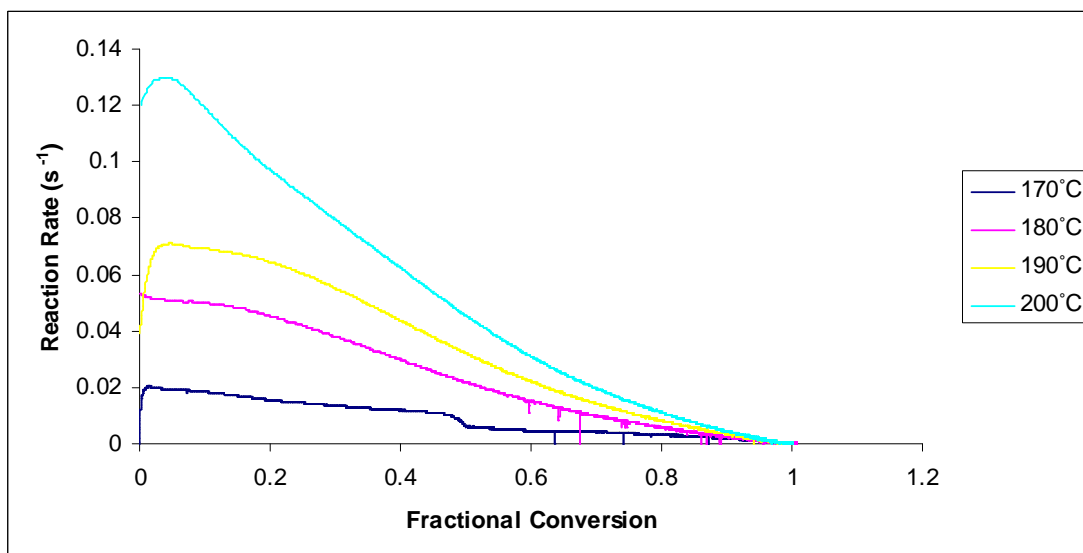


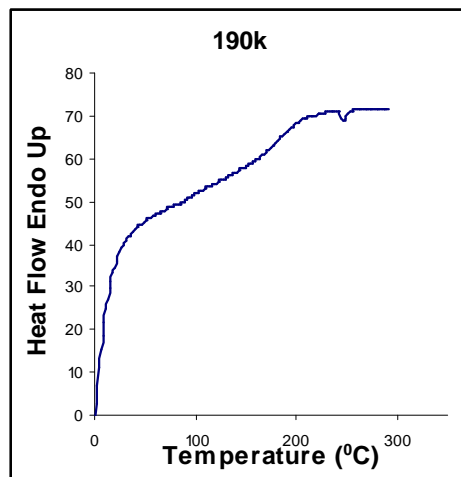
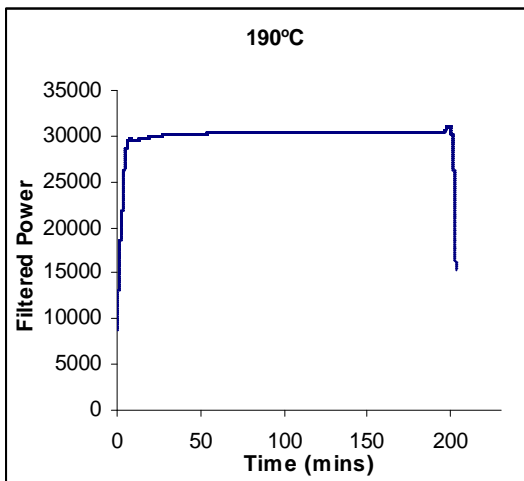
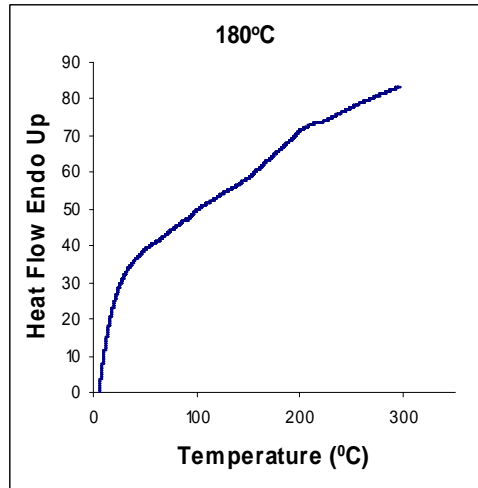
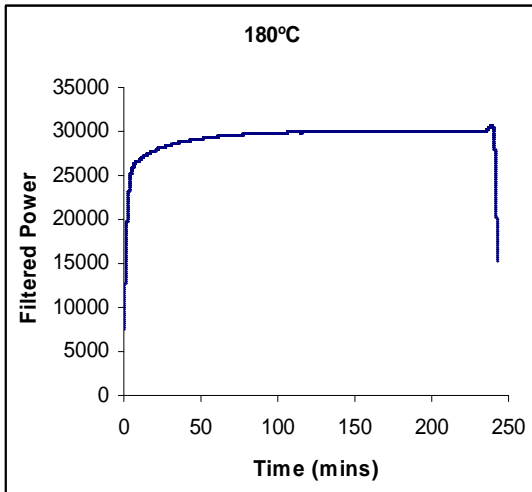
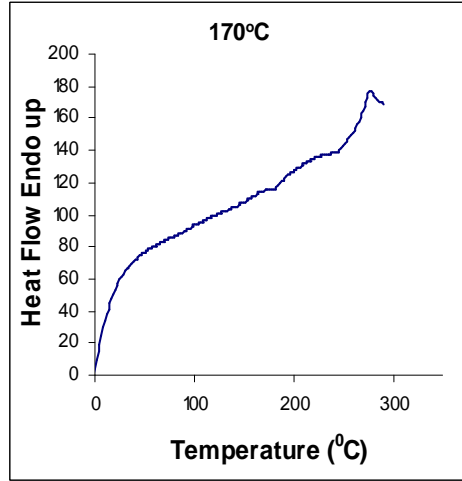
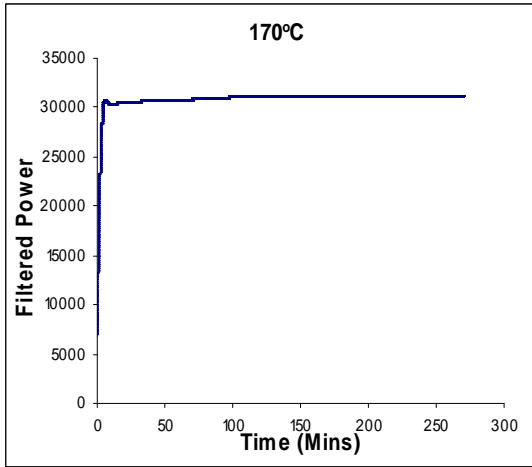
Figure 4.88 Rate of reaction against fractional conversion for the isothermal curing reaction of Araldite DLS 772 / 4 4' DDS epoxy system with an amine / epoxy ratio of 1.1 at different isothermal temperatures.

The results from the reaction rate plots and plots of reaction rates against fractional conversion for Araldite LY 5052 / 4 4' DDS epoxy system system with an amine / epoxy ratio of 1.0 and Araldite DLS 772 / 4 4' DDS epoxy system system with an amine / epoxy ratios of 0.8 and 1.1 all follow a similar path. Higher reaction rates are observed at higher cure temperatures. For all the curing temperatures, the reaction rates reached a maximum value at the start of the reaction (0-.15), after which the reaction rate began to decrease.

4.11 Isothermal Microwave Curing

A microwave-heated calorimeter was used to cure the samples with microwave heating using the same isothermal conditions as for conventional heating.

After each isothermal cure, the pieces of the cured sample were extracted from the glass tube and a DSC run was carried on the samples in order to ensure they were fully cured. The figures below show the microwave thermograms on the left side, and the corresponding T_g run on the right side for each epoxy system.



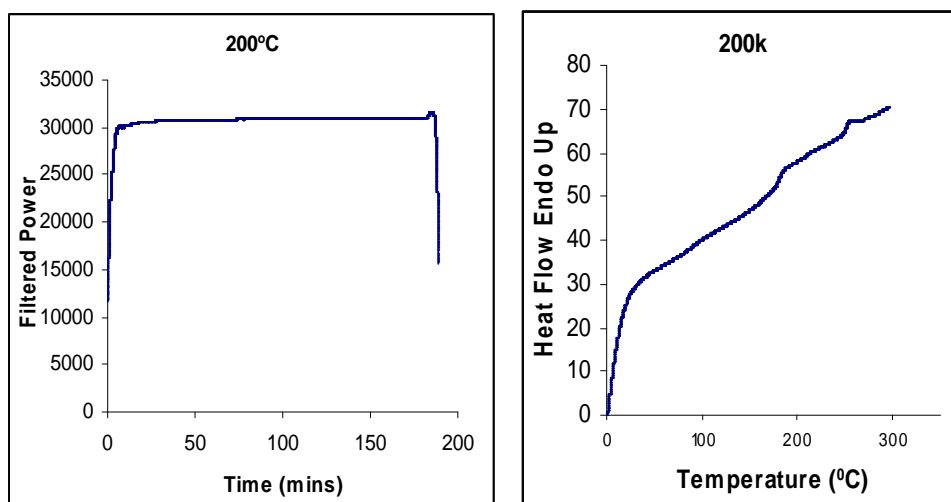


Figure 4.89 Isothermal thermograms of microwave isothermal cure (left) and subsequent DSC run 10 K min^{-1} from 30 to $300\text{ }^{\circ}\text{C}$ (right) to test for exotherm for Araldite LY 5052 / 4 4' DDS epoxy system with an amine epoxy ratio of 0.85

The temperature dependence of the fractional conversion and the reaction rates at different heating rates are shown in figures 4.99 and 4.100 below.

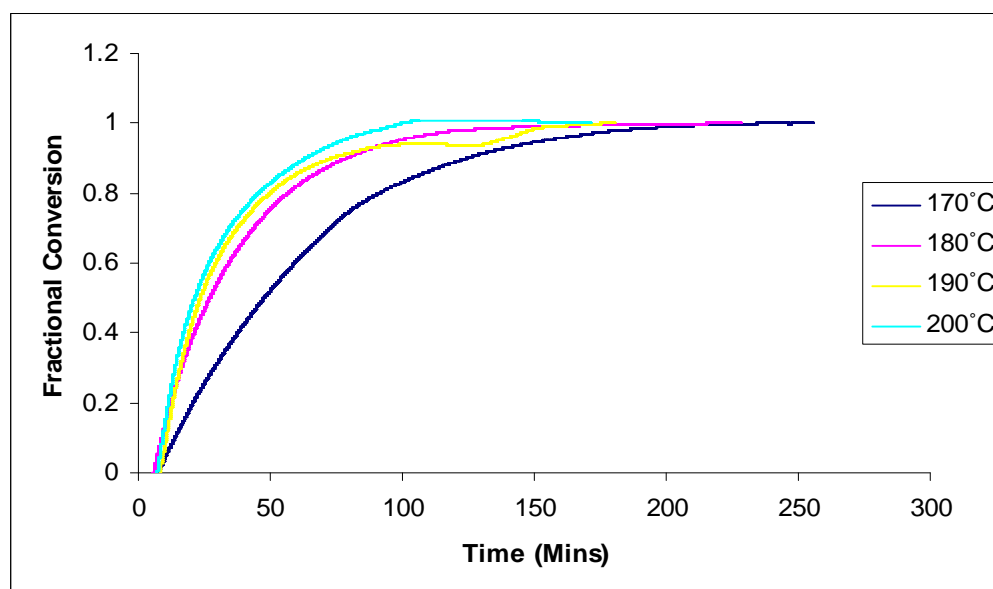


Figure 4.90 Fractional conversion of dynamic cure of Araldite LY 5052 / 4 4' DDS epoxy system with an amine / epoxy ratio of 0.85 at different isothermal temperatures using microwave heating.

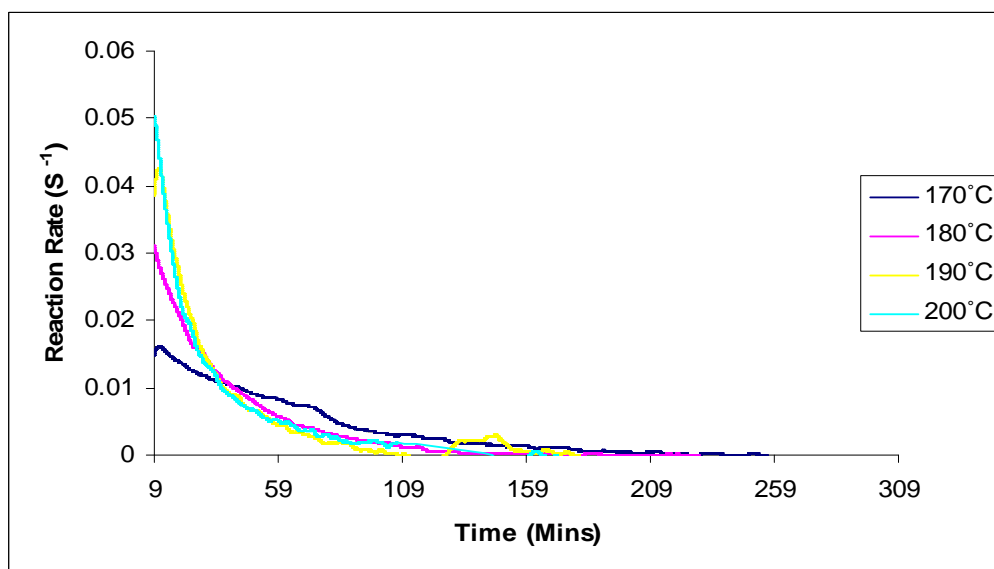


Figure 4.91 Plot of Reaction rates against temperature for dynamic cure of Araldite LY 5052 / 4 4' DDS epoxy system with an amine / epoxy ratio of 0.85 at different isothermal temperatures using microwave heating.

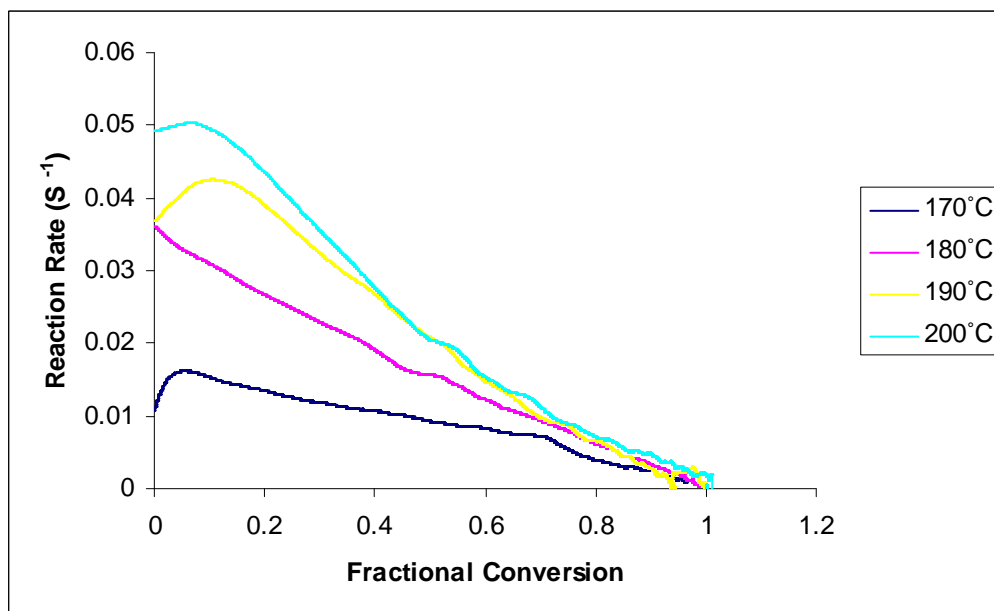


Figure 4.92 Plot of reaction rates against fractional conversion for the microwave cure reaction of Araldite LY 5052 / 4 4' DDS epoxy system with an amine / epoxy ratio of 0.85 at different isothermal temperatures.

Figure 4.92 shows a plot of fractional conversion against reaction rate for all the isothermal temperatures. Typical changes are found to occur in the reaction rate over the whole range of conversion. Just as in conventional curing, the reaction rate increases and it quickly reaches a maximum at the early stages of the reaction within the fractional conversion range of 0 – 0.15 after which the reaction rate started to decrease. This decrease is ascribed to the increase in the viscosity of the reaction medium as the curing material gelled [57]. The reaction rate increased as the curing temperature increased.. The curing times are lower at higher temperatures.

Figures 4.93 and 4.94 shows the plots of the temperature dependence of the fractional conversion and the reaction rates of cured microwave cured samples of Araldite LY 5052 / 4 4' DDS epoxy system with an amine / epoxy ratio of 1.0.

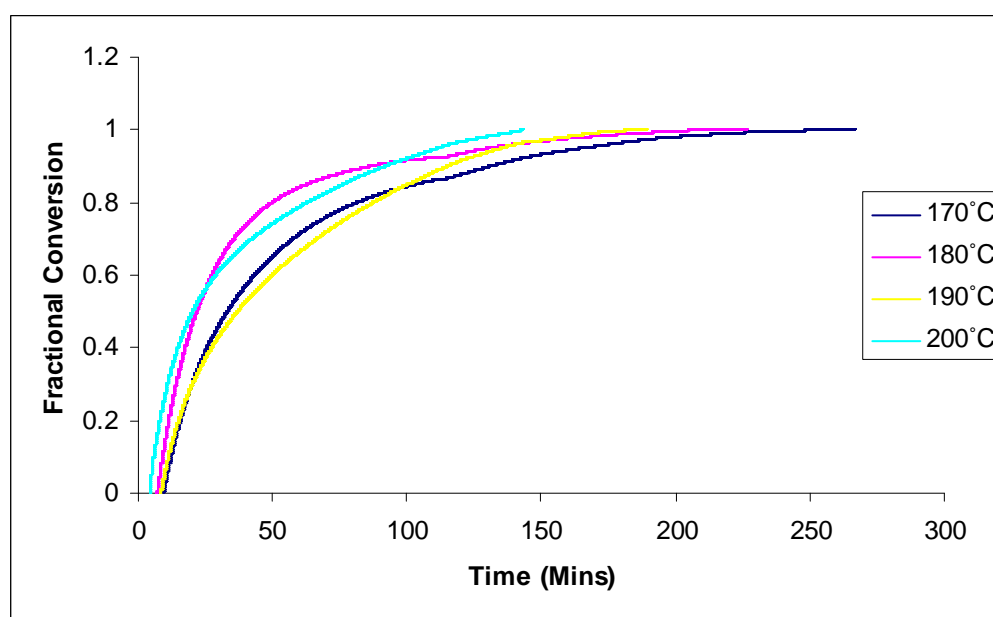


Figure 4.93 Fractional conversion for isothermal cure of Araldite LY 5052 / 4 4' DDS epoxy system with an amine / epoxy ratio of 1.0 at different isothermal temperatures using microwave heating.

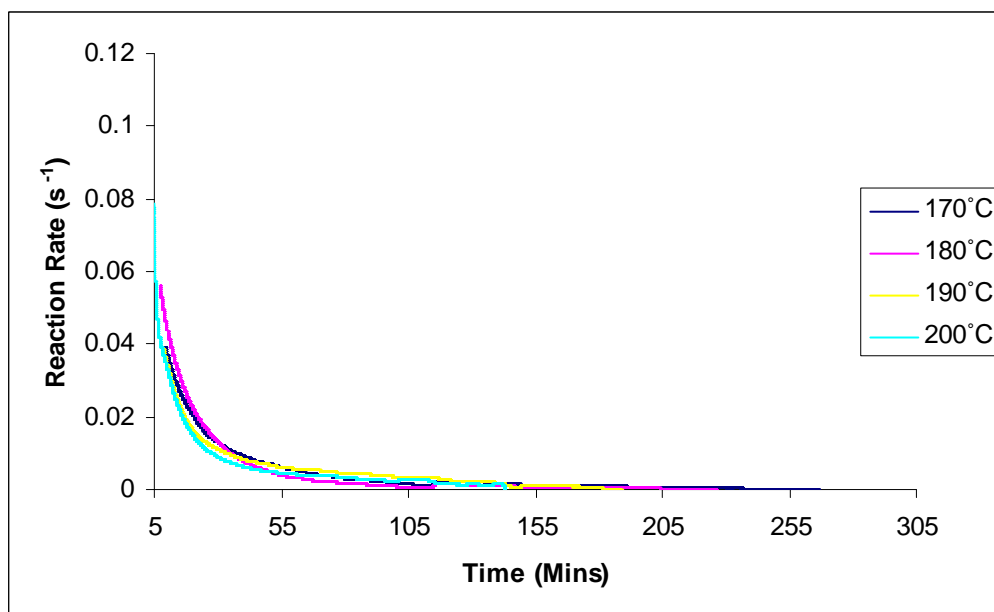


Figure 4.94 Reaction rates for isothermal cure of Araldite LY 5052 / 4 4' DDS epoxy system with an amine / epoxy ratio of 1.0 at different isothermal temperatures using microwave heating.

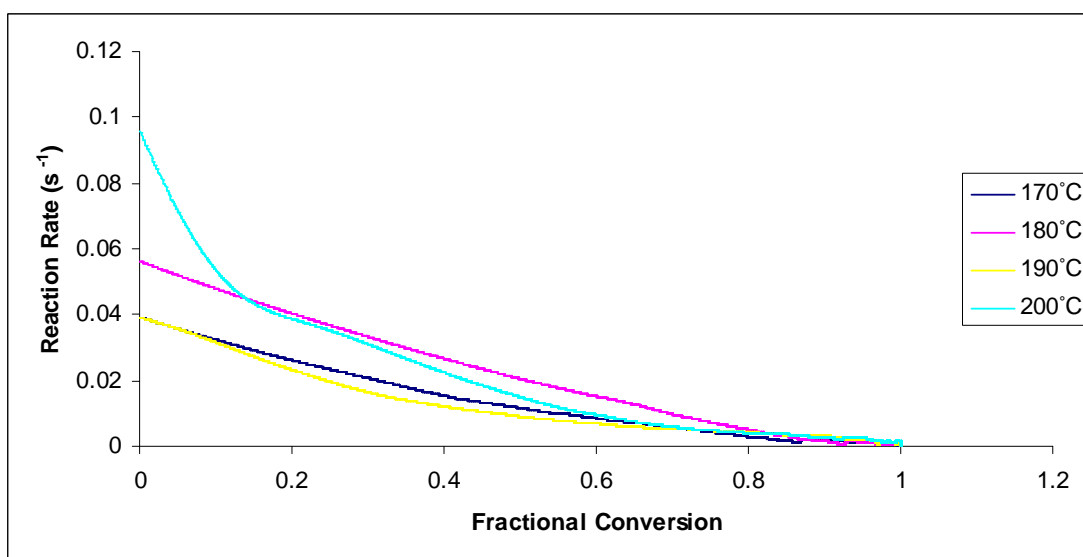


Figure 4.95 Plot of reaction rates against fractional conversion for the microwave cure reaction of Araldite LY 5052 / 4 4' DDS epoxy system with an amine / epoxy ratio of 1.0 at different isothermal temperatures.

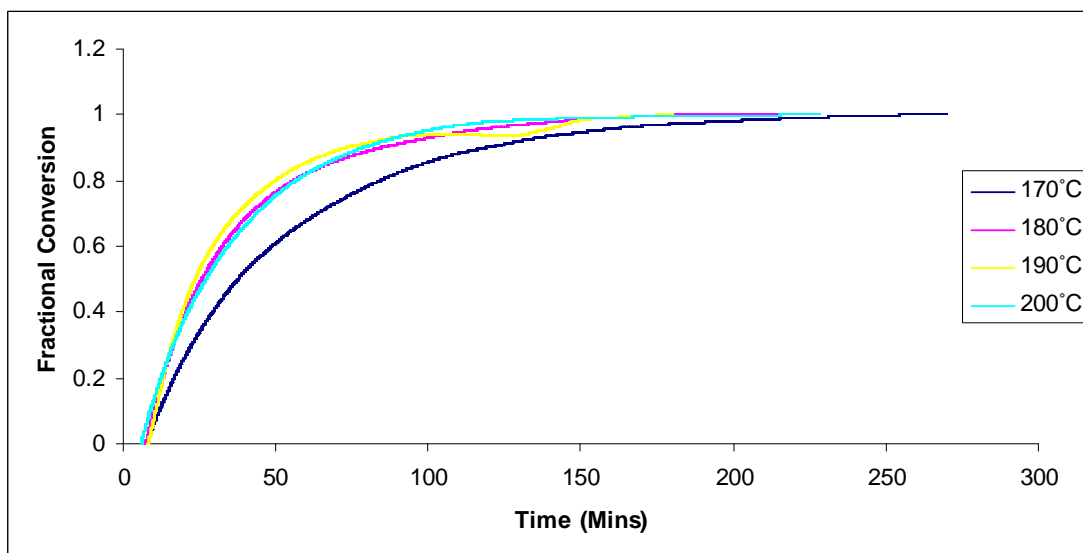


Figure 4.96 Fractional conversion for isothermal cure of 0.8M amine / epoxy ratio for Araldite DLS 772 / 4 4' DDS epoxy system at different isothermal temperatures using microwave heating.

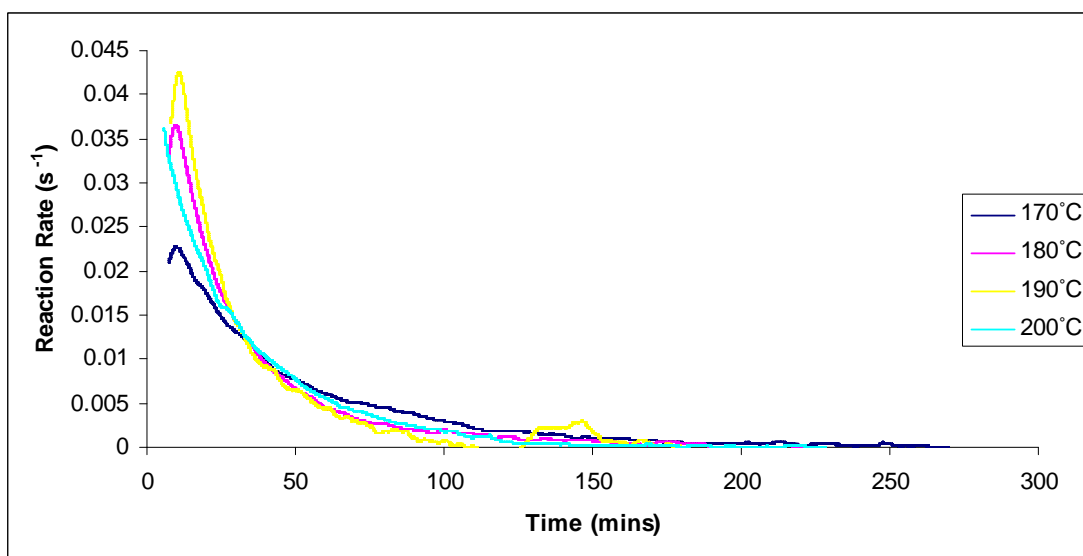


Figure 4.97 Reaction rates for dynamic cure of Araldite DLS 772 / 4 4' DDS epoxy system with an amine / epoxy ratio of 0.8 at different isothermal temperatures using microwave heating.

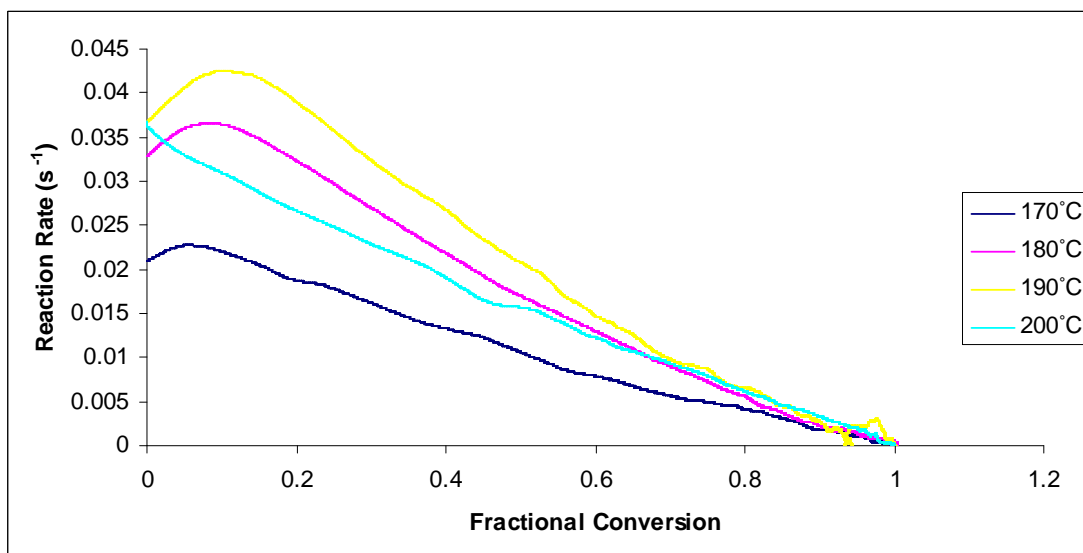
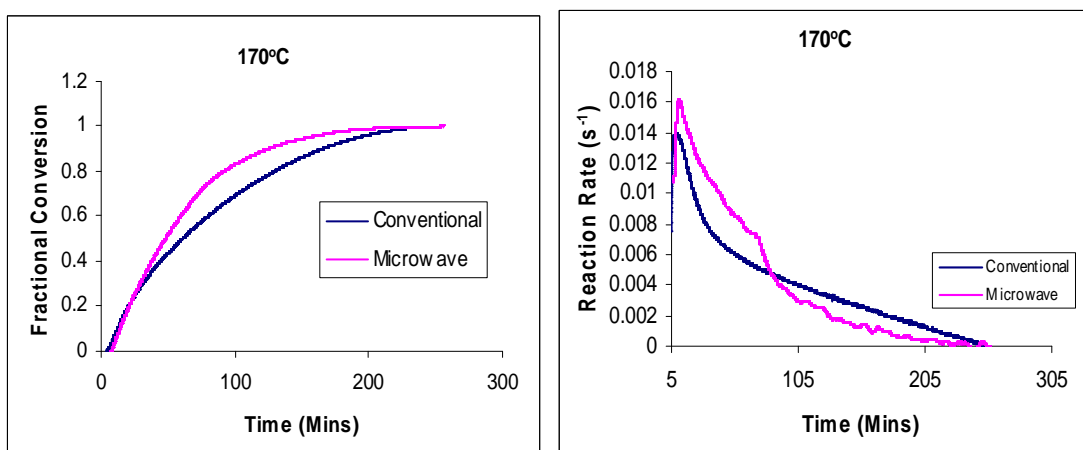


Figure 4.98 Plot of reaction rates against fractional conversion for the microwave cure reaction of Araldite DLS 772 / 4 4' DDS epoxy system with an amine / epoxy ratio of 0.8 at different isothermal temperatures.

Plots of the time dependence of fractional conversion and reaction rate for the microwave and conventional curing of Araldite LY 5052 / 4 4 DDS epoxy system are shown in the figures 4.99 and 4.100 below



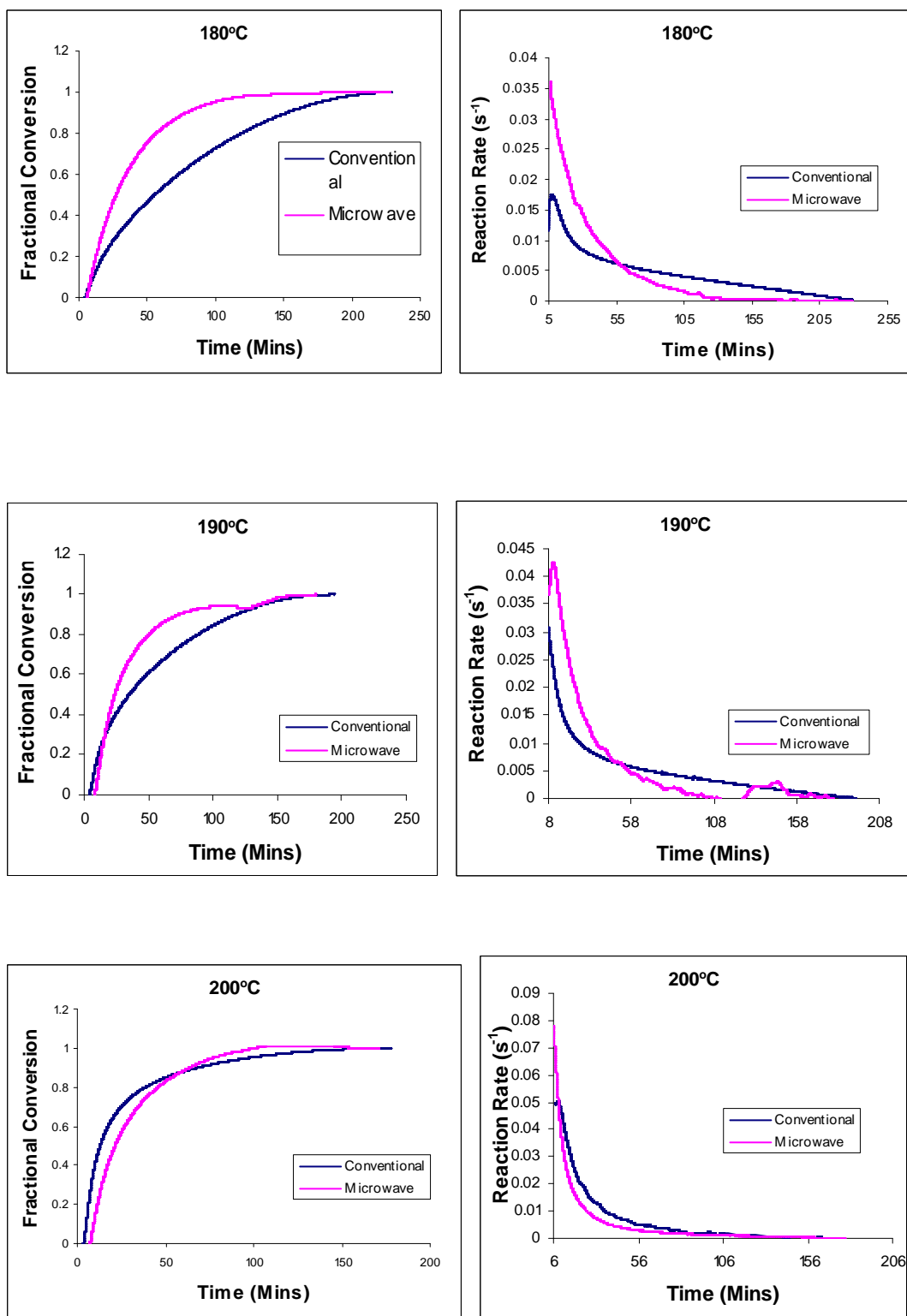
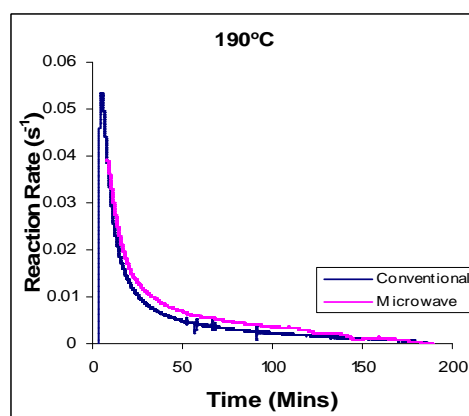
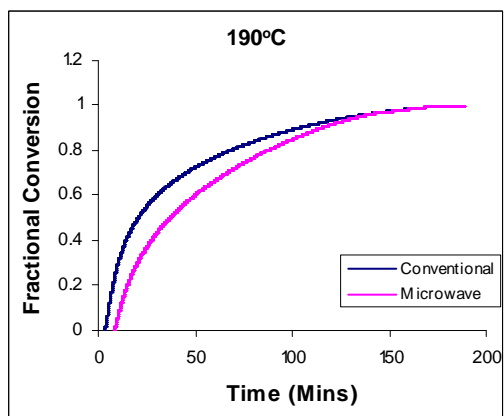
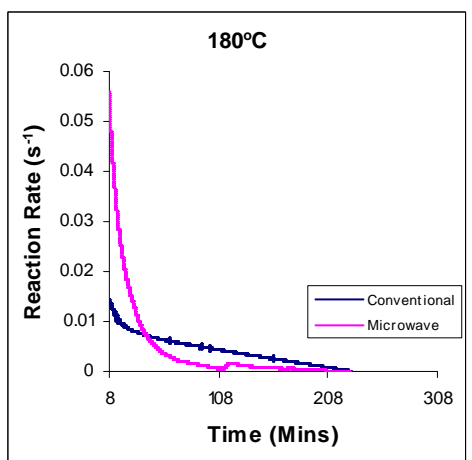
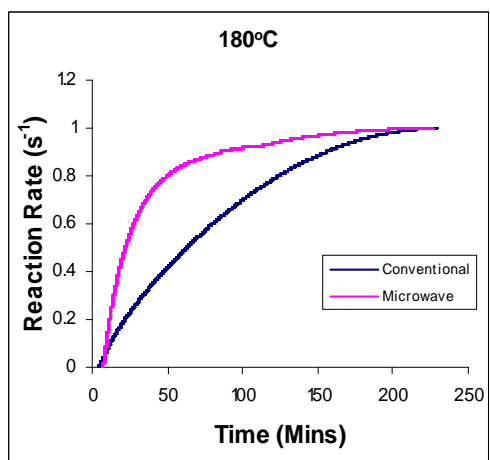
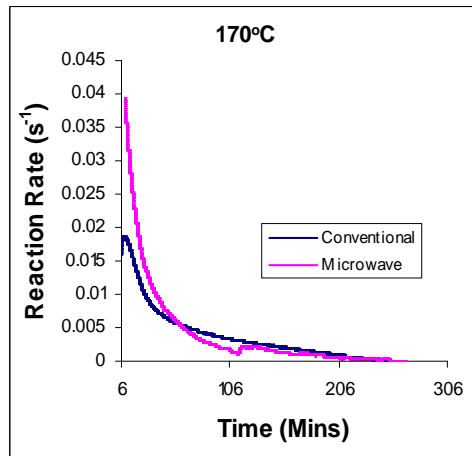
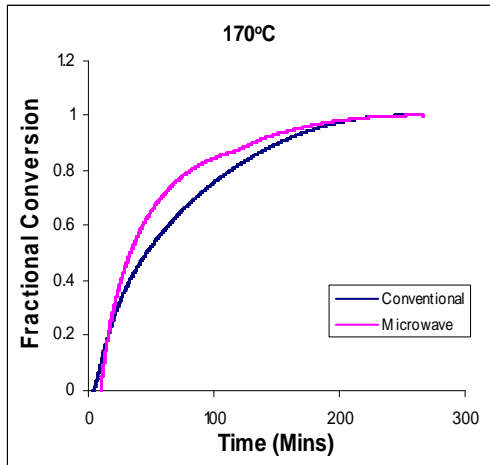


Figure 4.99 Time dependence of the fractional conversion (right) and the reaction rate (right) for Araldite LY 5052 / 4 4' DDS epoxy system with an amine / epoxy ratio of 0.85 under conventional and microwave curing, at different isothermal temperatures.



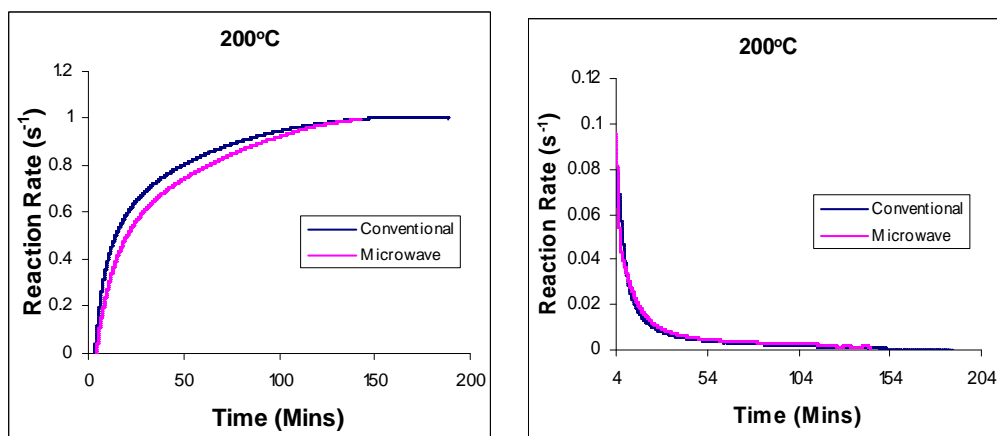


Figure 4.100 Time dependence of the fractional conversion (left), and reaction rate (right) for the curing of Araldite LY 5052 / 4 4' DDS epoxy system with an amine / epoxy ratio of 1.0 under conventional and microwave curing, at different isothermal temperatures.

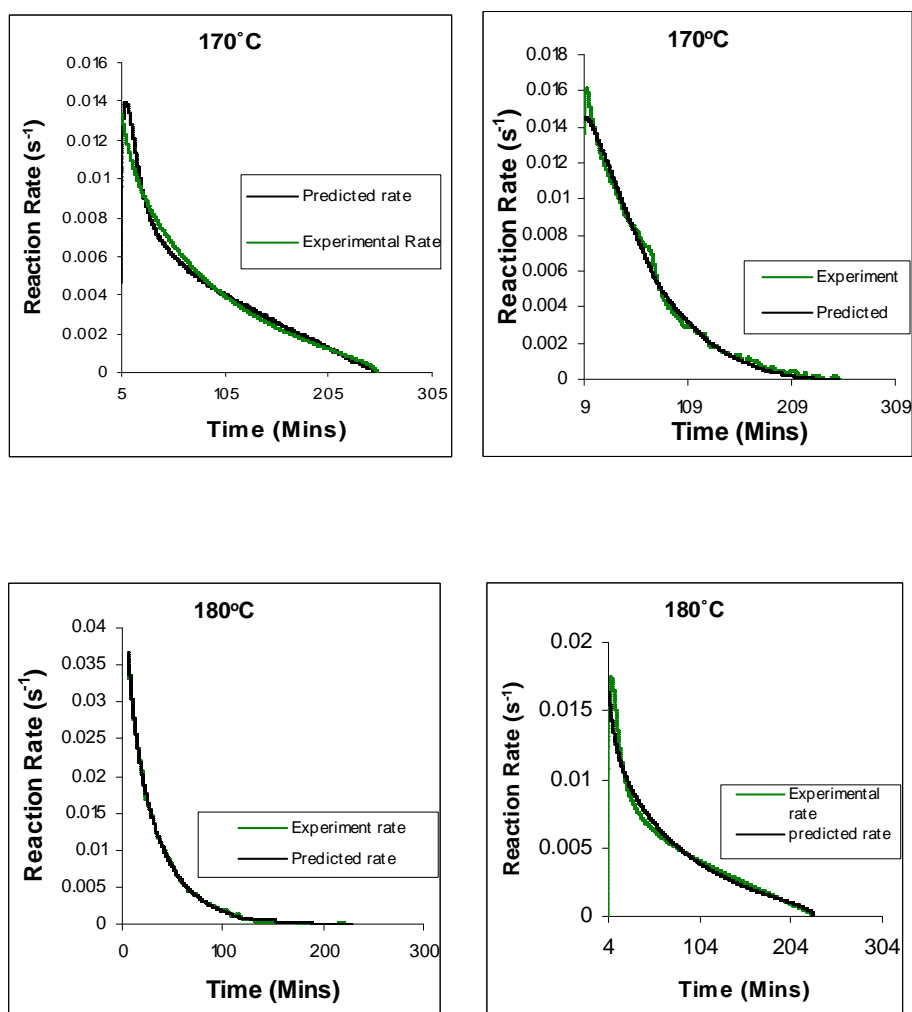
Figures 4.99 and 4.100 show the comparison of the time dependence of the fractional conversion and the reaction rates at different heating rates for both conventional and microwave cured Araldite LY 5052 / 4 4' DDS epoxy system. The microwave heated samples had a higher peak rate of reaction than the conventionally cured samples. When compared to the conventionally cured samples, there was a significant increase in the reaction rate of the microwave cured samples. For all the heating rates, higher reaction rates were observed in microwave cured samples.

As explained earlier during the dynamic curing of both epoxy systems, These differences between the conventional and microwave cured systems are all as a result of an improved efficiency in the transfer of energy for the microwave heating because microwave heating involves a direct interaction with the molecules with the electromagnetic field causing heat to be generated internally throughout the volume of the material [26], unlike conventional heating where energy is transferred from the surface of the material into the material via conduction or convection. Polymer molecules are heated in the microwave field directly as a result of the relaxation of the dipole polarization along the electromagnetic field. While conventional heating requires the entire molecule to first be heated, Microwave heating enable the reactive polar molecules to selectively absorb the microwave, and this enhances the reaction [26]. The

higher fractional conversion for the microwave cured samples can be as a result of an increase in the reactant mobility after gelation. This is as a result of the induced polarization of the polymer and monomer molecules along the applied electromagnetic field [13], enabling more reactants to be consumed to form a more rigid network.

4.12 Modelling of cure kinetics

The reaction rate profile obtained from both the conventional and microwave isothermal cured samples were fitted to a kinetic model (Equation 2.24). The figures 4.101 to 4.104 below compares the reaction rate profile of both conventionally cured (Left) and microwave cured (Right) Araldite LY 5052 / 4 4' DDS epoxy system with an amine / epoxy ratio of 0.85 obtained experimentally and the reaction rate profile predicted by the autocatalytic model.



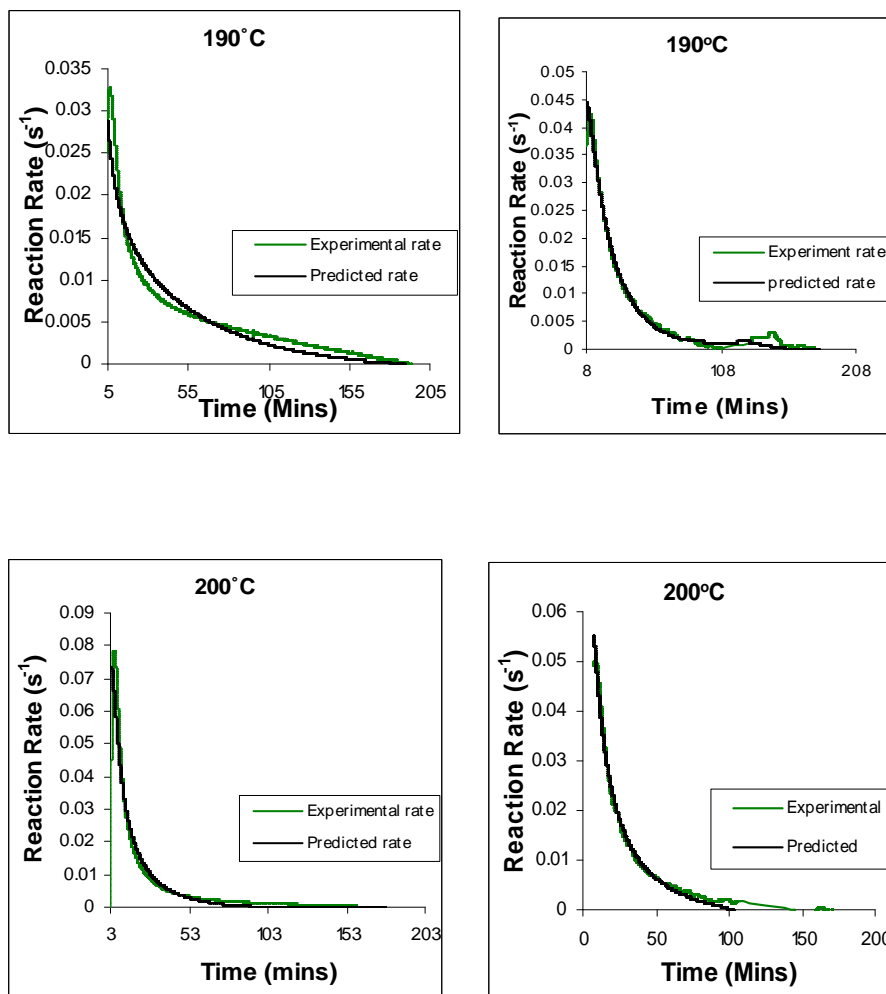
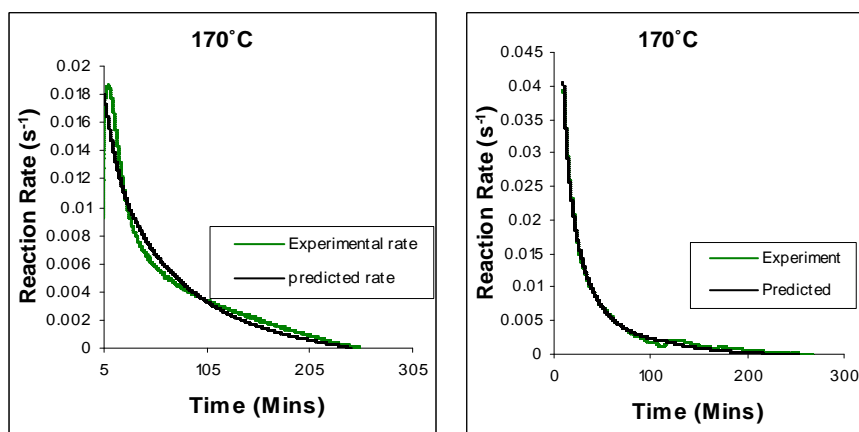


Figure 4.101 Comparison between time dependence of experimental reaction rate curves and the curves predicted by means of autocatalytic adjustment for conventional heating of Araldite LY 5052 / 4 4' DDS epoxy system with an amine / epoxy ratio of 0.85 on the left, and microwave heating on the right.



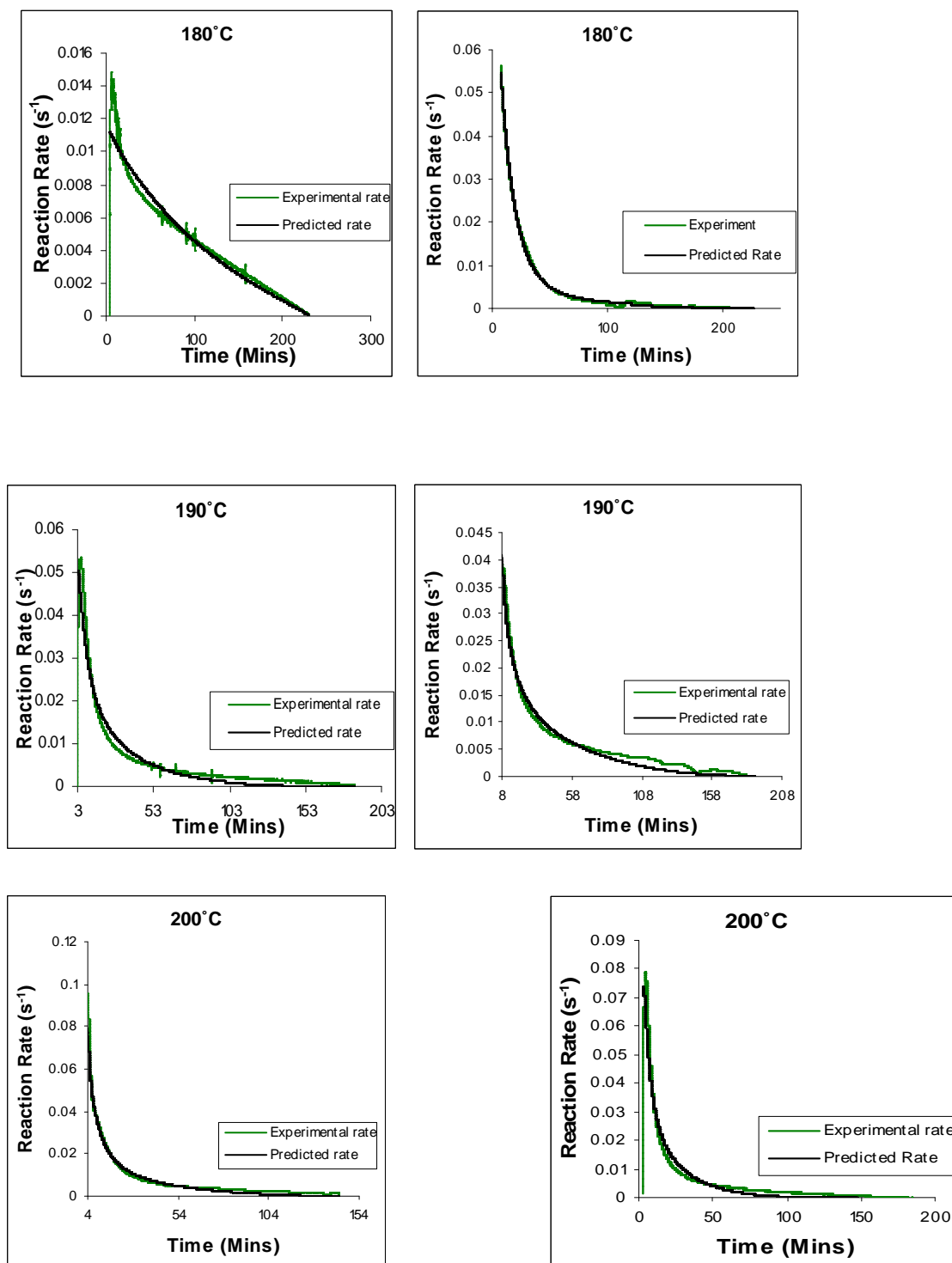
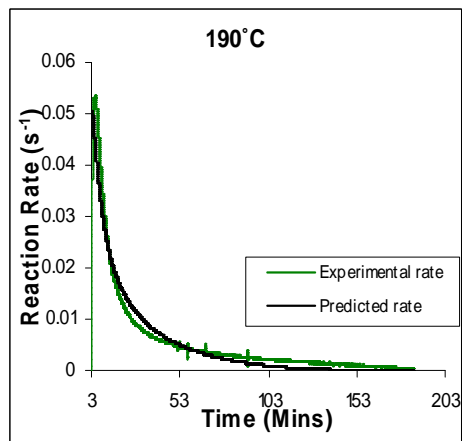
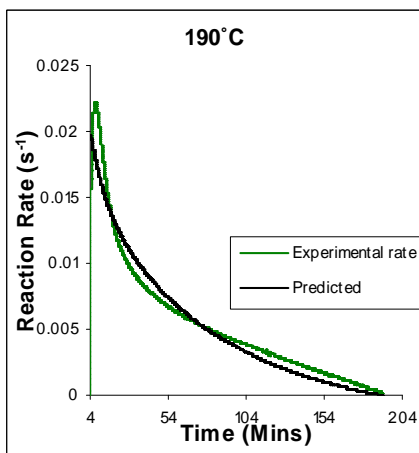
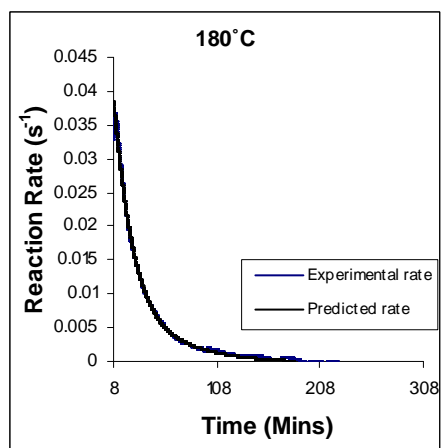
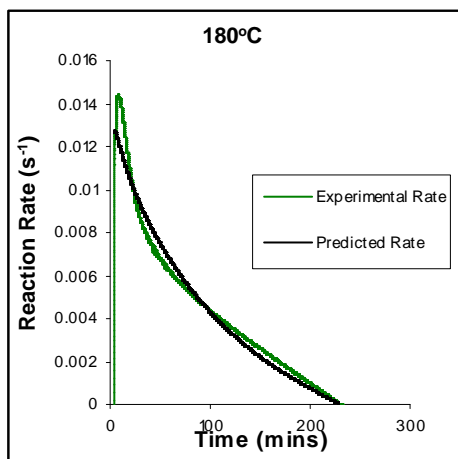
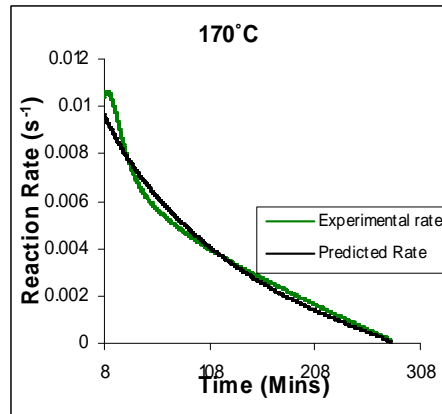
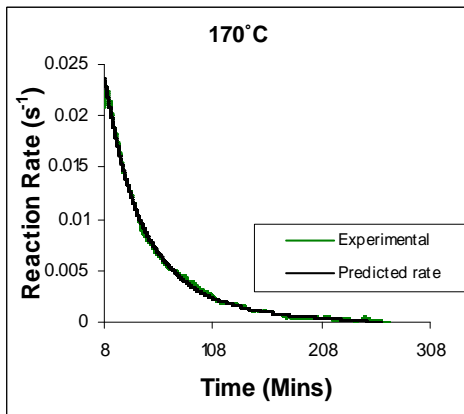


Figure 4.102 Comparison between time dependence of experimental reaction rate curves and the curves predicted by means of autocatalytic adjustment for conventional heating of Araldite LY 5052 / 4 4' DDS epoxy system with an amine / epoxy ratio of 1.0 on the left, and microwave heating on the right.



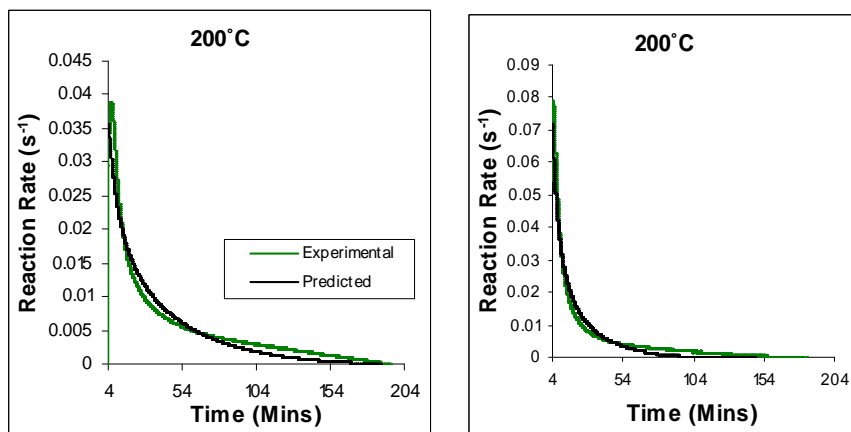
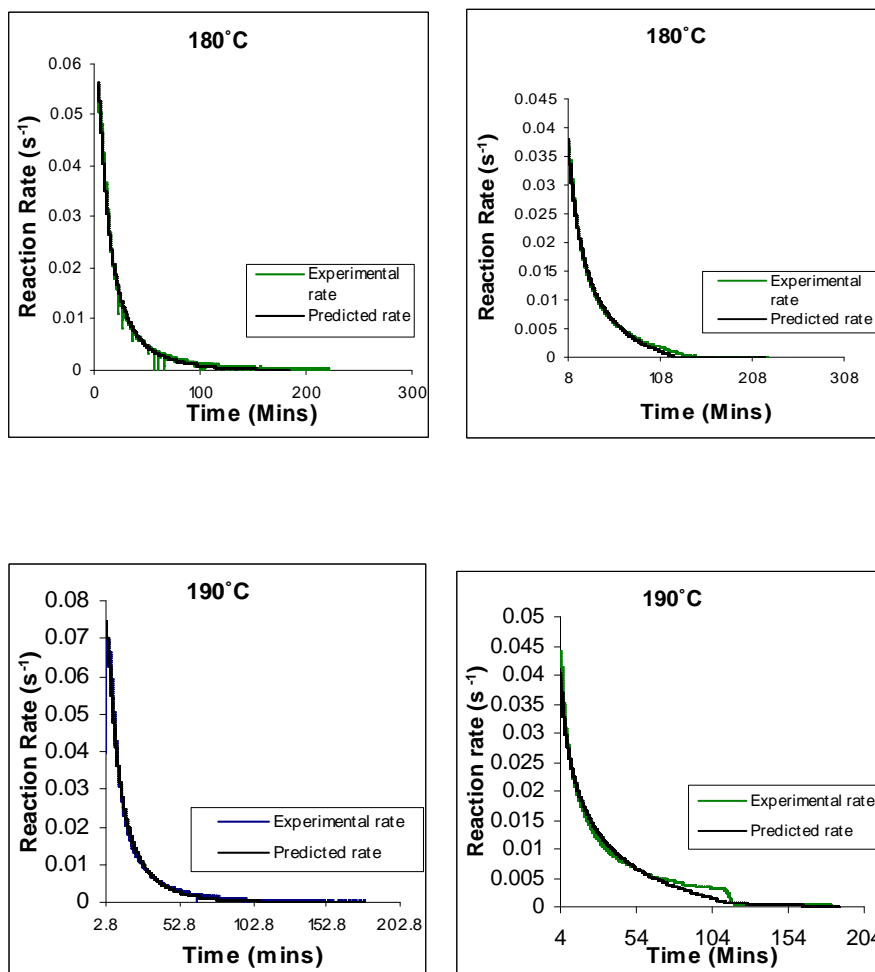


Figure 4.103 Comparison between time dependence of experimental reaction rate curves and the curves predicted by means of autocatalytic adjustment for conventional heating of Araldite DLS 772 / 4 4' DDS epoxy system with an amine / epoxy ratio of 0.8 on the left, and microwave heating on the right.



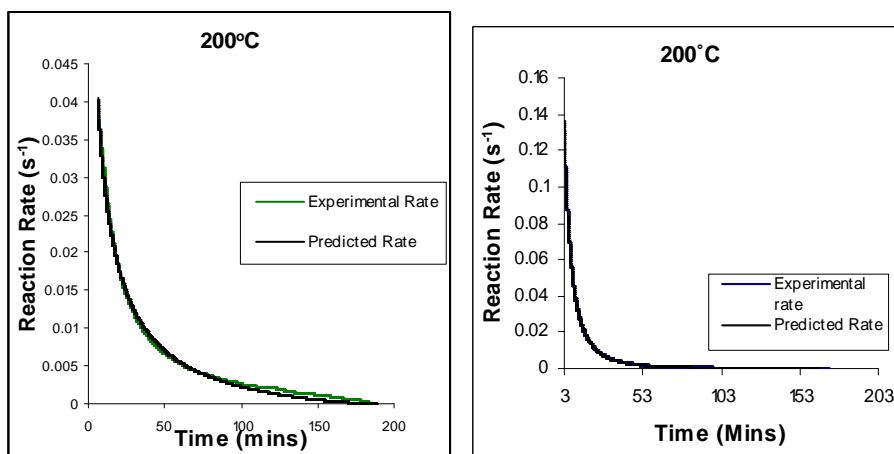


Figure 4.104 Comparison between time dependence of experimental reaction rate curves and the curves predicted by means of autocatalytic adjustment for conventional heating of Araldite DLS 772 / 4 4' DDS epoxy system with an amine / epoxy ratio of 1.1 on the left, and microwave heating on the right.

From the figures 4.101 to 4.104 above, we observe that the result of the mathematical simulations compare well with experimental results. There are good agreements between the experimental and the model results, proving that the autocatalytic model is able to predict the curing path of the epoxy system.

The kinetic parameters obtained from fitting the autocatalytic model with the experimental reaction rate are tabulated in tables 4.26 to 4.32 below.

Table 4.26 Kinetic parameters for isothermal cure of Araldite LY 5052 / 4 4' DDS epoxy system with an amine epoxy ratio of 0.85 using conventional heating.

Temperature (°C)	K_1	K_2	$k = \frac{K_1}{K_2}$	m	n	$m+n$
170	0.001592	0.0125	0.127	0.867	0.381	1.248
180	0.001849	0.0147	0.125	0.723	0.413	1.136
190	0.003665	0.03151	0.116	1.09	0.805	1.895

200	0.00659	0.0658	0.100	1.227	0.656	1.883
-----	---------	--------	-------	-------	-------	-------

Table 4.27 Kinetic parameters for isothermal cure of Araldite LY 5052 / 4 4' DDS epoxy system with an amine / epoxy ratio of 0.85 using microwave heating.

Temperature (°C)	K_1	K_2	$k = \frac{K_1}{K_2}$	m	n	$m+n$
170	0.0014	0.00607	0.096	0.575	0.933	1.508
180	0.00367	0.0137	0.108	0.701	0.863	1.564
190	0.00445	0.041	0.096	1.865	0.661	2.526
200	0.00553	0.083	0.066	1.049	1.03	2.079

Table 4.28 Kinetic parameters for isothermal cure of Araldite LY 5052 / 4 4' DDS epoxy system with an amine / epoxy ratio of 1.0 using conventional heating.

Temperature (°C)	K_1	K_2	$k = \frac{K_1}{K_2}$	m	n	$m+n$
170	0.001213	0.0160	0.1011	1.06	0.465	1.525
180	0.00255	0.0289	0.088	1.17	0.484	1.654
190	0.00328	0.0305	0.107	1.11	0.645	1.755
200	0.00595	0.0578	0.103	1.00	0.814	1.814

Table 4.29 Kinetic parameters for isothermal cure of Araldite LY 5052 / 4 4' DDS epoxy system with an amine / epoxy ratio of 1.0 using microwave heating.

Temperature (°C)	K_1	K_2	$k = \frac{K_1}{K_2}$	m	n	$m+n$
170	0.04097	0.043	0.09527	0.775	0.895	1.67

180	0.445	0.061	0.0729	1.312	0.741	2.053
190	0.0516	0.0715	0.07216	0.979	0.887	1.363
200	0.072	0.0892	0.0876	1.121	0.955	2.076

Table 4.30 Kinetic parameters for isothermal cure of Araldite DLS 772 / 4 4' DDS epoxy system with an amine / epoxy ratio of 0.8 using microwave heating.

Temperature (°C)	K ₁	K ₂	$k = \frac{K_1}{K_2}$	<i>m</i>	<i>n</i>	<i>m+n</i>
170	0.023705	0.0317	0.0747	1.025	0.673	1.698
180	0.03848	0.0526	0.073	1.294	0.589	1.883
190	0.04185	0.0617	0.0678	1.163	0.769	1.932
200	0.00595	0.0779	0.0763	0.924	0.995	1.919

Table 4.31 Kinetic parameters for isothermal cure of Araldite DLS 772 / 4 4' DDS epoxy system with an amine / epoxy ratio of 1.1 using conventional heating

Temperature (°C)	K ₁	K ₂	$k = \frac{K_1}{K_2}$	<i>m</i>	<i>n</i>	<i>m+n</i>
170	0.002053	0.0153	0.1341	1.036	0.677	1.713
180	0.003548	0.0376	0.09436	0.853	0.822	1.675
190	0.007876	0.0883	0.0891	0.678	0.759	1.437
200	0.009325	0.09339	0.09985	1.074	0.488	1.562

Table 4.32 Kinetic parameters for isothermal cure of Araldite DLS 772 / 4 4' DDS epoxy system with an amine / epoxy ratio of 1.1 using microwave heating.

Temperature (°C)	K_1	K_2	$k = \frac{K_1}{K_2}$	m	n	$m+n$
170	0.00436	0.0441	0.0988	0.724	0.769	1.493
180	0.005678	0.0592	0.082	0.914	0.883	1.797
190	0.00854	0.0986	0.086	0.697	0.913	1.61
200	0.00946	0.124	0.0763	0.973	0.828	1.801

Tables 4.26 to 4.32 display the kinetic parameters obtained for the isothermal curing of both the microwave and the conventional curing of Araldite LY 5052 / 4 4' DDS and Araldite DLS 772 / 4 4' DDS epoxy systems. It is observed that K_1 and K_2 values increased with increasing temperature. The absolute values of K_1 and K_2 are greater in microwave cure than the values of K_1 and K_2 obtained from conventional cure. For all the systems, the K_2 values are much larger than the K_1 values. The ratio of K_1 / K_2 was larger in conventional curing than in microwave curing. Miyalovic *et al* attributed the lower values of K_1 / K_2 in the microwave cure to the enhancement of the catalytic reaction of the epoxy system more than the non catalytic reaction by microwave radiation [28]. This phenomenon was explained by the high activity of the [OH] group in the microwave field.

The reaction orders m and n are independent of temperature for both conventional and microwave heating. However, for all the epoxy systems, the microwave cured samples have a higher reaction order ($m+n$) than conventionally cured samples. This means that the microwave cured samples have a higher reaction rate [16]

The values of $k = K_1 / K_2$ for both conventional and microwave cured samples were less than unity for both Araldite LY 5052 / 4 4' DDS and Araldite DLS 772 / 4 4' DDS epoxy systems. This is an indication that both systems were characterized by a negative substitution effect. There was a higher rate of reaction of the primary amine with the epoxy group compared to the reaction of the secondary amine with the epoxy group [4].

Plots of rate constant (K_1 and K_2) against temperature for both microwave and conventional curing of both epoxy systems are displayed in figures 4.105 to 4.112. Activation energy values obtained are tabulated in table 4.33

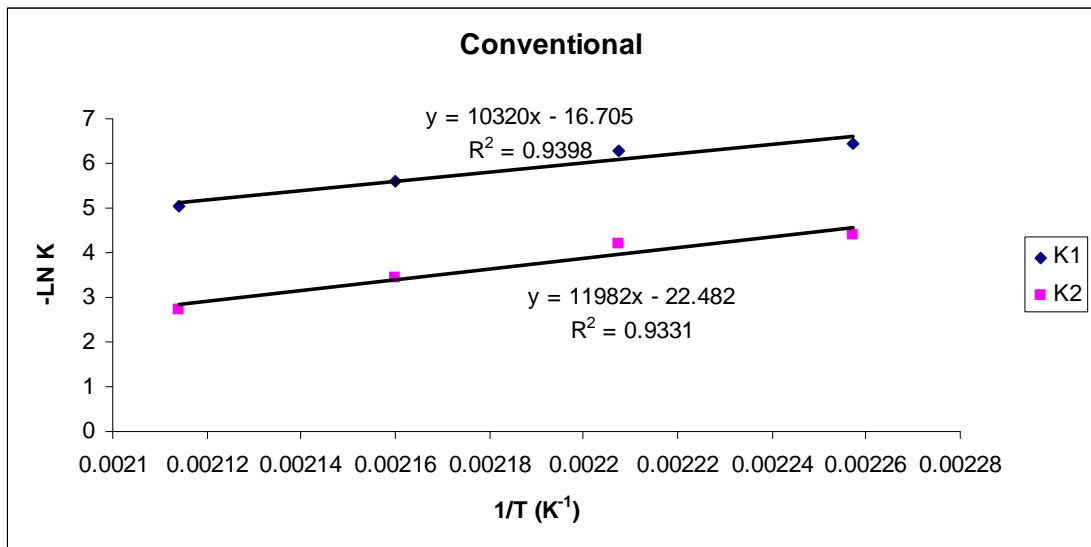


Figure 4.105 Rate constants of curing reaction against temperature for isothermal cure of Araldite LY 5052 / 4 4' DDS epoxy system with an amine / epoxy ratio of 0.85 under conventional curing.

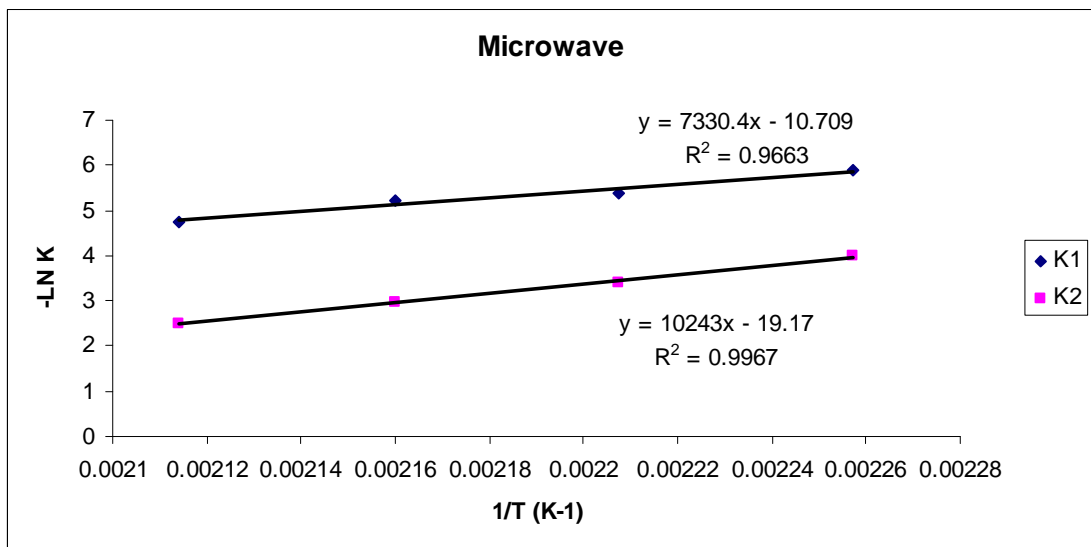


Figure 4.106 Rate constants of curing reaction against temperature for isothermal cure of Araldite LY 5052 / 4 4' DDS epoxy system with an amine / epoxy ratio of 0.85 under microwave curing.

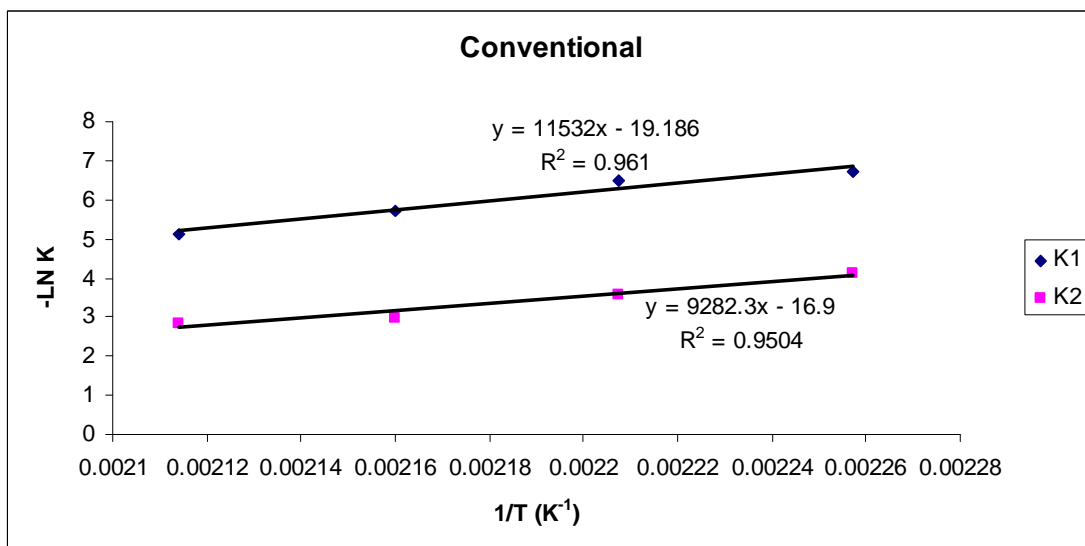


Figure 4.107 Rate constants of curing reaction against temperature for isothermal cure of Araldite LY 5052 / 4 4' DDS epoxy system with an amine / epoxy ratio of 1.0 under conventional curing.

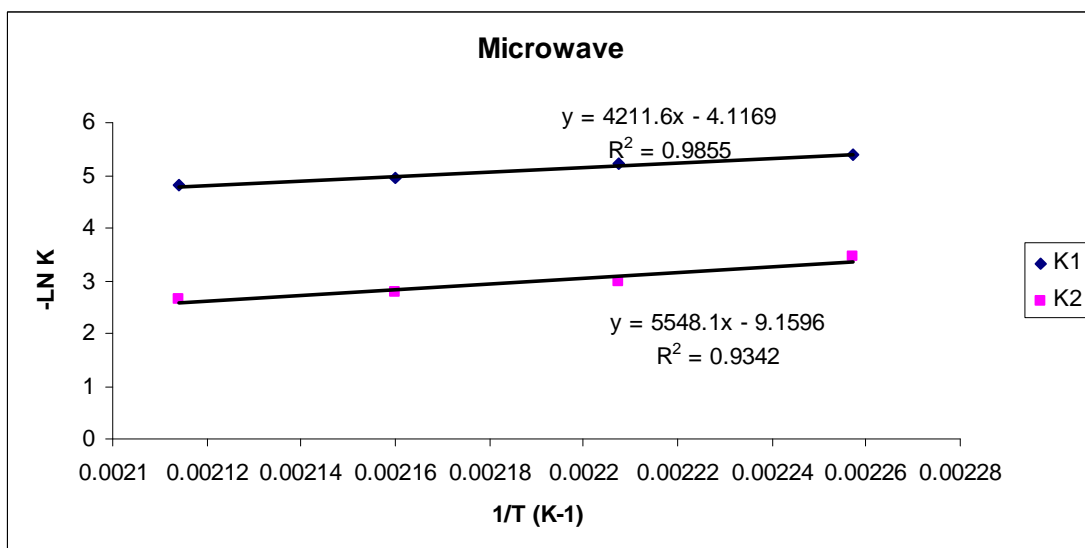


Figure 4.108 Rate constants of curing reaction against temperature for isothermal cure of Araldite LY 5052 / 4 4' DDS epoxy system with an amine / epoxy ratio of 1.0 under microwave curing.

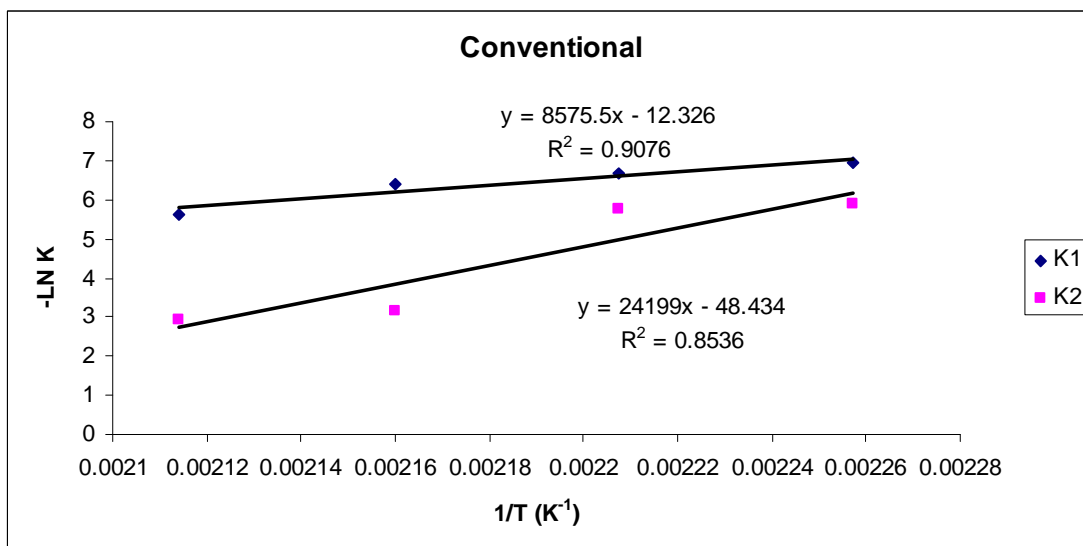


Figure 4.109 Rate constants of curing reaction against temperature for isothermal cure of Araldite DLS 772 / 4 4' DDS epoxy system with an amine / epoxy ratio of 0.8 under conventional curing.

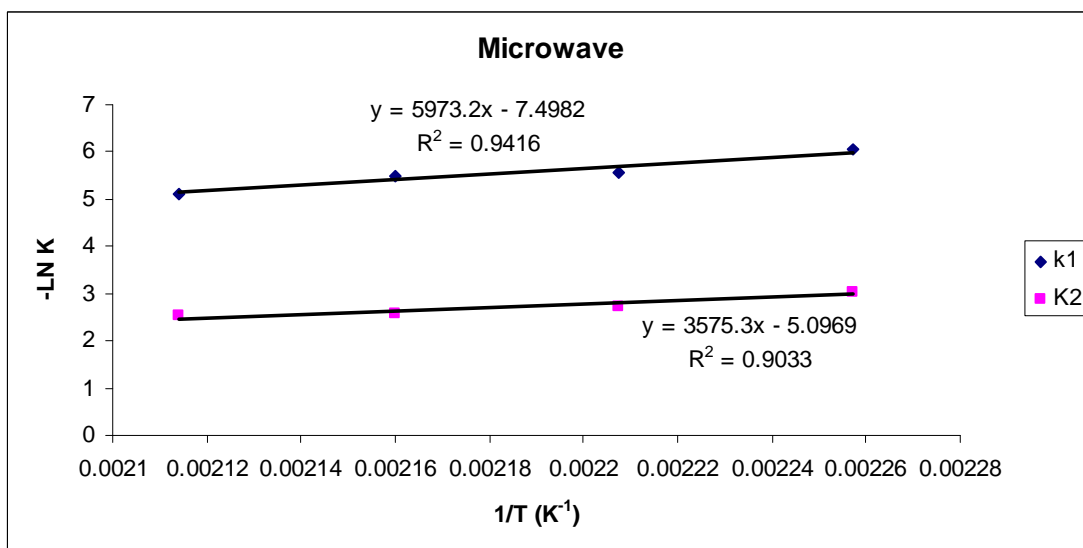


Figure 4.110 Rate constants of curing reaction against temperature for isothermal cure of Araldite DLS 772 / 4 4' DDS epoxy system with an amine / epoxy ratio of 0.8 under microwave curing.

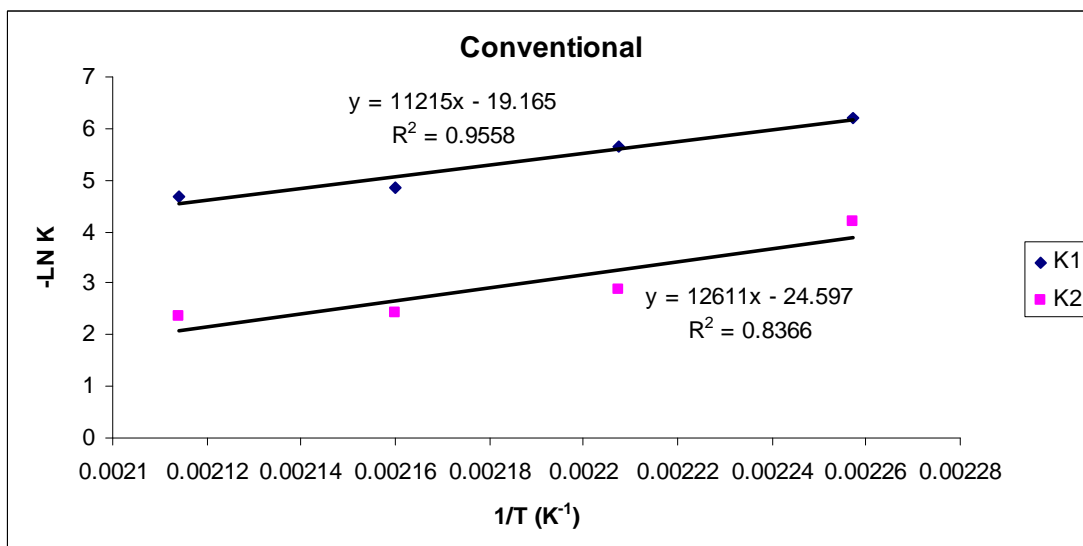


Figure 4.111 Rate constants of curing reaction against temperature for isothermal cure of Araldite DLS 772 / 4 4' DDS epoxy system with amine / epoxy ratio of 1.1 under conventional curing.

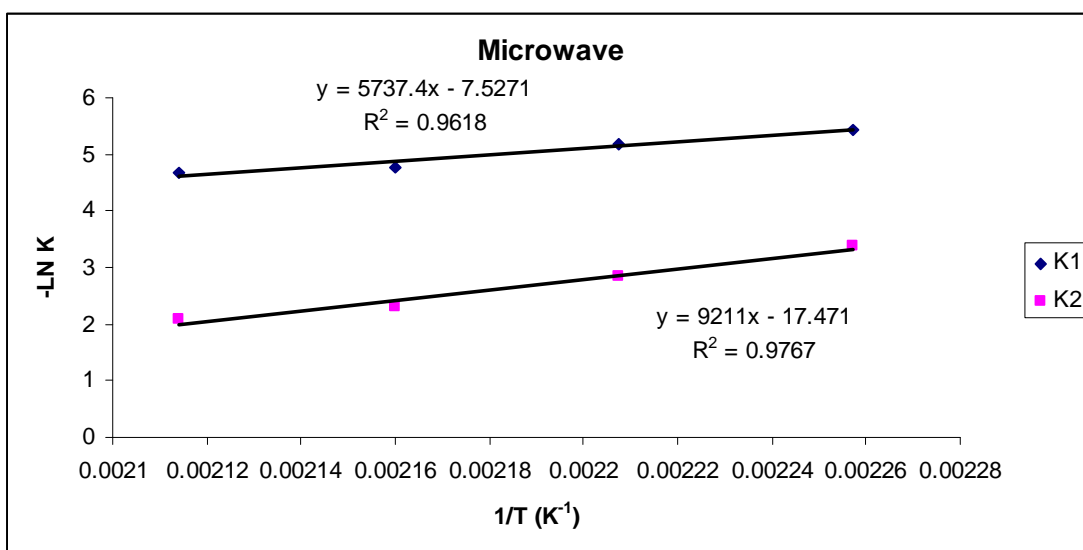


Figure 4.112 Rate constants of curing reaction against temperature for isothermal cure of Araldite DLS 772 / 4 4' DDS epoxy system with an amine / epoxy ratio of 0.85 under microwave curing.

Table 4.33 K_1 and K_2 activation energy values obtained from figures for both conventional and microwave heating for both Araldite LY 5052 / 4 4' DDS and Araldite DLS 772 / 4 4' DDS epoxy systems.

Epoxy System	Conventional Heating		Microwave Heating	
	K_1 E_a (KJ mol ⁻¹)	K_2 E_a (KJ mol ⁻¹)	K_1 E_a (KJ mol ⁻¹)	K_2 E_a (KJ /mol ⁻¹)
Araldite LY 5052 / 4 4' DDS with A/E ratio of 0.85	85.8	99.6	60.9	91.8
Araldite LY 5052 / 4 4' DDS with A/E ratio of 1.0	95.9	77.1	35.0	46.1
Araldite DLS 772 / 4 4' DDS with A/E ratio of 0.8	71.3	101.2	49.6	69.7
Araldite DLS 772 / 4 4' DDS with A/E ratio of 1.1	93.2	104.8	47.0	76.6

4.13 Summary

The results of the experiments show that for both isothermal and dynamic curing, there was a significant increase in the fractional conversion of the microwave cured samples compared to the conventionally cured samples. The curing reactions for the microwave cured samples took place over a smaller temperature range; and Higher reaction rates were observed in the samples cured using microwave heating.

During the non-isothermal curing of the samples, the microwave cured samples of Araldite LY 5052 / 4 4' DDS epoxy system had higher activation energy than the conventionally cured samples , while for Araldite DLS 772 / 4 4' DDS epoxy system,

the microwave cured samples had a lower activation energy than the conventionally cured samples.

During the isothermal curing, higher K_1 and K_2 kinetic parameters were observed in microwave cured samples. A lower K_1 / K_2 ratio was observed in microwave curing than in conventional curing. This is attributed to the enhancement of the catalytic reaction over the non-catalytic reaction by the microwave radiation which occurs as a result of the high activity of the [OH] group.

CHAPTER FIVE

5.0 FOURIER TRANSFORM INFRARED SPECTROSCOPY

5.1 Introduction

Fourier Transform Infrared Spectroscopy has been widely used to study crosslinked systems. It can provide detailed information on the chemical structure of the molecules. Fourier Transform Infrared spectroscopy also provides a quick and accurate means of determining the extent of conversion. For an epoxy system, the use of Fourier Transform Infrared Spectroscopy has mainly been limited to the investigation of the disappearance of epoxy and amine groups [92-95]. The reason for this limitation is because of several factors such as the complexity of the reactions, the difficulties associated with the characterization of the products during network formation, and the superimposition of the characteristic bands which make peak identification very difficult [1-4].

5.2 Araldite LY 5052 / 4 4' DDS and Araldite DLS 772 / 4 4 epoxy systems.

For this research, FT-IR was used to study the changes in the epoxy peaks which occur when the reaction took place. The spectrum of an uncured mixture of Araldite LY 5052 / 4 4' DDS epoxy system with an amine / epoxy ratio of 0.85 is shown in figure 5.1 below.

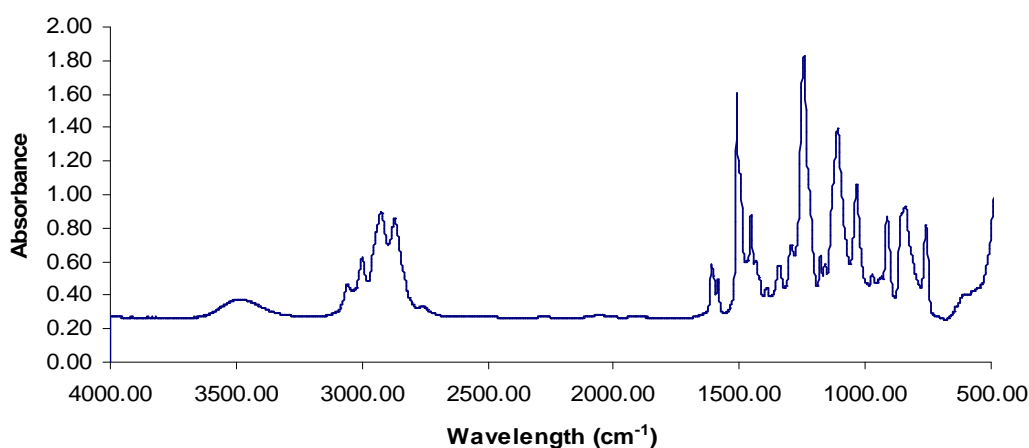


Figure 5.1 FT-IR Spectra of uncured Araldite LY 5052 / 4 4 ' DDS epoxy system with an amine / epoxy ratio of 0.85.

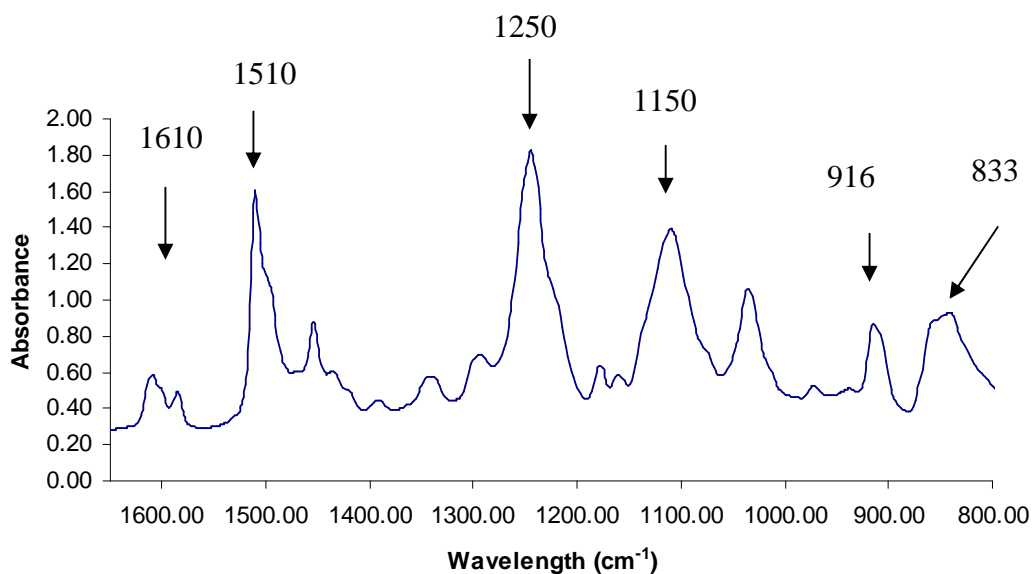


Figure 5.2 Expanded view of FT-IR Spectra of uncured 0.85M amine / epoxy ratio for Araldite LY 5052 / 4 4 ' DDS epoxy system .

The spectrum in figure 5.2 shows a noticeable oxirane ring (epoxy) peak at 916 cm⁻¹. This is the asymmetric ring stretching band of the epoxy ring [70, 96-98]. The spectrum also shows the symmetric stretching of the epoxy ring at 1250cm⁻¹. The bands at 1510cm⁻¹ and 833 cm⁻¹ are assigned to the p-phenylene groups [70, 97]. The aliphatic stretching vibration of -CH₂- groups is shown as a peak at 2920cm⁻¹ [70].The stretching vibration of the primary amino group (-NH₂) which is from the hardener (4 4' DDS) shows an absorption peak at 1610cm⁻¹ [70].The peaks at 1250cm⁻¹ and 1150 cm⁻¹ are the strong asymmetric and symmetric SO₂ stretching [70].

Figures 5.3 to 5.6 show the overlaid FT-IR spectra of Araldite LY 5052 / 4 4' DDS and Araldite DLS 772 / 4 4' DDS epoxy systems after conventional and microwave heating at 180 °C for 240 minutes

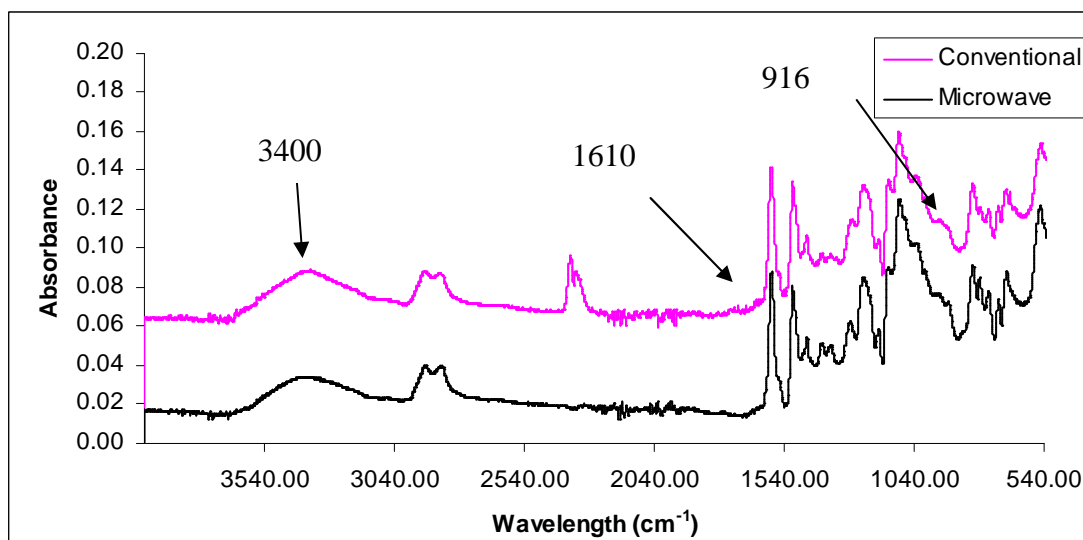


Figure 5.3 Overlaid FT-IR Spectra of Araldite LY 5052 / 4 4' DDS with an amine / epoxy ratio of 0.85 after conventional and microwave heating at 180°C for 240 minutes.

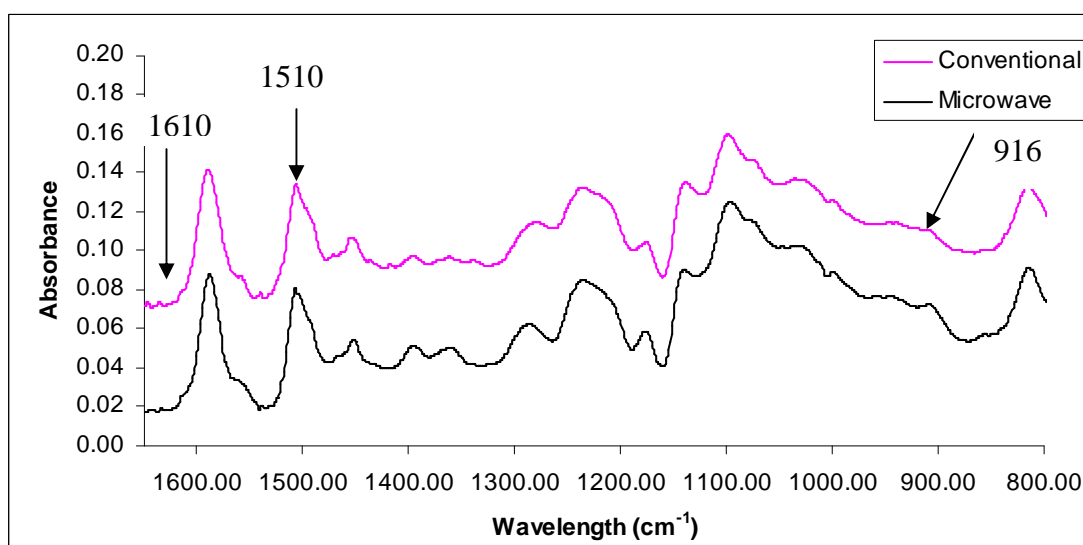


Figure 5.4 Expanded view of Overlaid FT-IR Spectra of Araldite LY 5052 / 4 4' DDS with an amine / epoxy ratio of 0.85 after conventional and microwave heating at 180 °C for 240 minutes

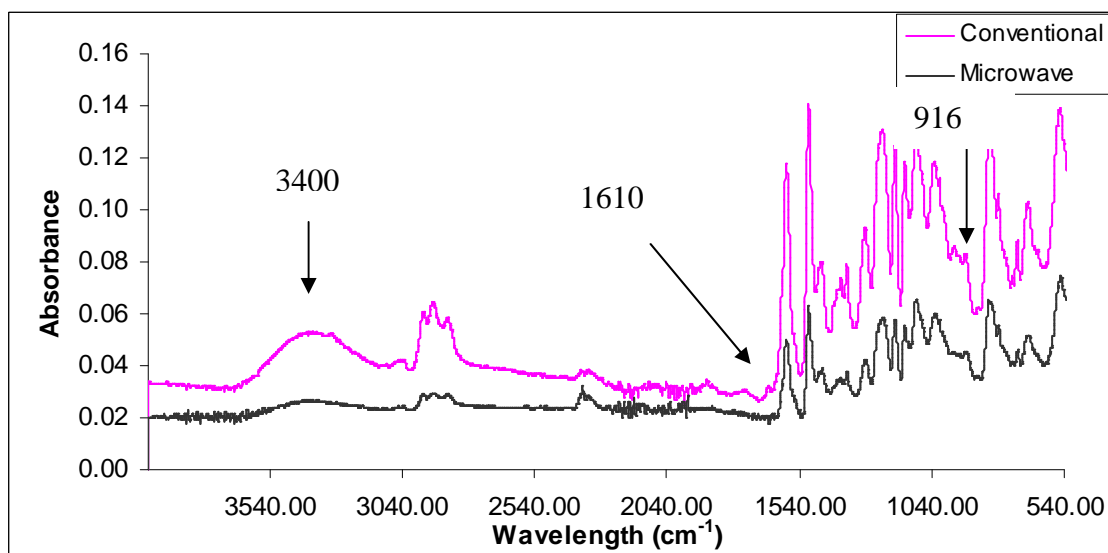


Figure 5.5 Overlaid FT-IR Spectra of Araldite DLS 772 / 4 4' DDS with an amine / epoxy ratio of 0.8 after conventional and microwave heating at 180 °C for 240 minutes.

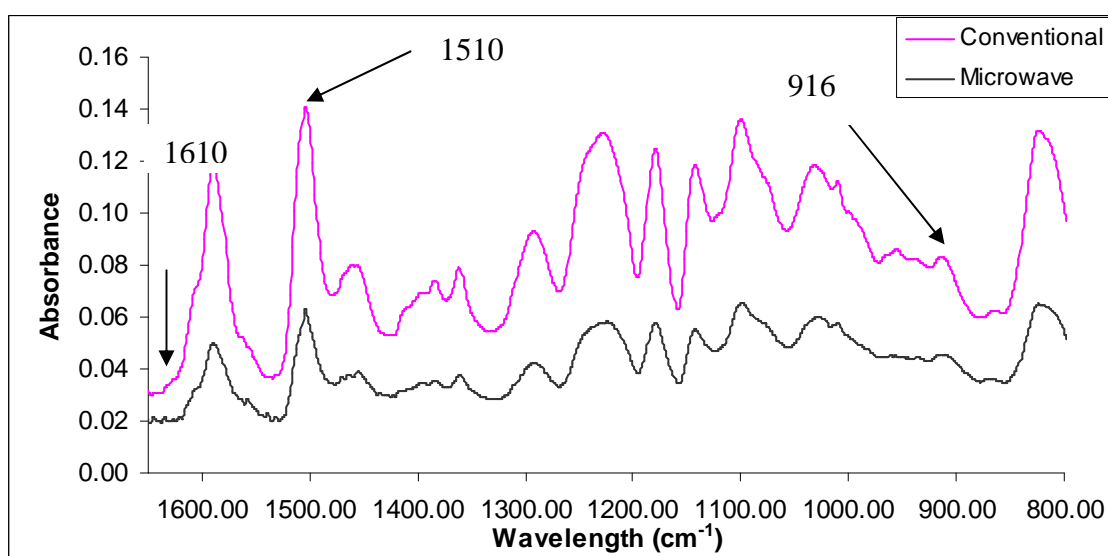


Figure 5.6 Expanded view of Overlaid FT-IR Spectra of Araldite DLS 772 / 4 4' DDS with an amine / epoxy ratio of 0.8 after conventional and microwave heating at 180 °C for 240 minutes.

For both epoxy systems (Araldite LY 5052 and Araldite DLS 772 / 4 4' DDS), the spectra of the specimen after they had been cured at 180°C for 240 minutes was noticeably different from the spectra of the uncured specimen. The prominent features

that occur during polymerization are the decreasing and almost complete disappearance of the epoxy ring at 915 cm^{-1} and 862 cm^{-1} [96, 98]. The N-H stretch band at 1610 cm^{-1} also decreases in size. The decrease in the epoxy and the amine bands is an indication of the consumption of the epoxy and the amine bands during the reaction. The curing reaction occurs by the reaction of the end epoxy groups with the hardener. The epoxy rings open out and the molecules become linked in a three dimensional network. New absorptions were formed around 3400 cm^{-1} . This was as a result of the formation of the secondary amine and the hydroxyl groups during cure. The bands at 833 and 1510 cm^{-1} were unaffected during cure and thus remained constant [96-98]. The almost complete disappearance of the epoxy and the amine peaks at the end of the spectra showed that most of the epoxy and the amine group reacted during the curing process. This is a pointer to the argument that a crosslinked network was formed.

Several samples of Araldite LY 5052 / 4 4' DDS with an amine / epoxy ratio of 0.85 and Araldite DLS 772 / 4 4' DDS with an amine / epoxy ratio of 0.8 were prepared and were cured using both a DSC and a microwave heated cavity at $180\text{ }^{\circ}\text{C}$. At intervals of 30 minutes up to 240 minutes, a specimen was removed. The reaction was quickly stopped by dipping it into liquid nitrogen for about ten minutes. An infrared spectrum was then taken.

The overlaid spectra for both the conventionally cured and microwave cured samples of both epoxy systems at different times at $180\text{ }^{\circ}\text{C}$ are shown in figures 5.7 to 5.12 below.

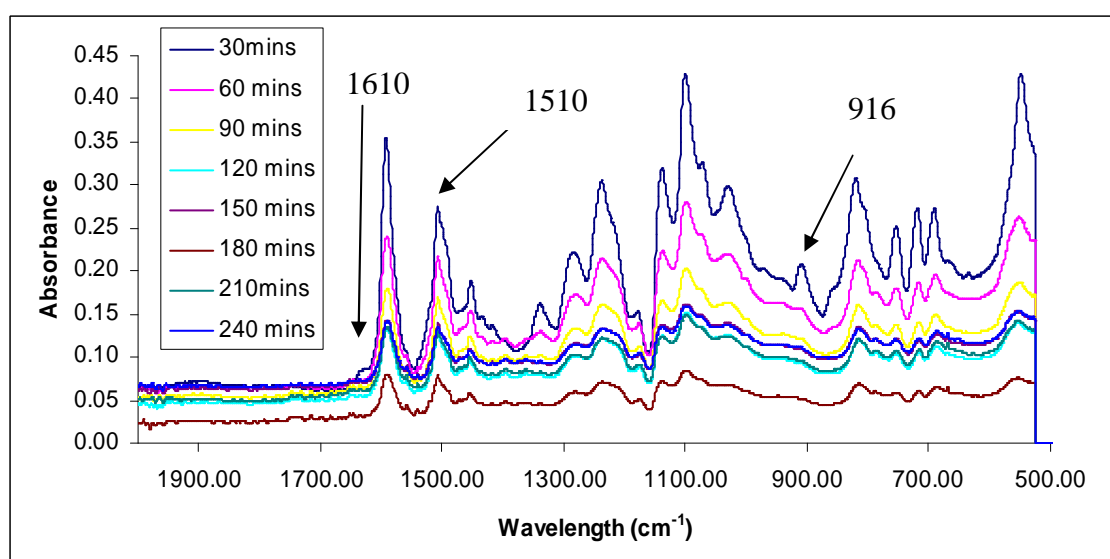


Figure 5.7 Overlaid spectra for conventionally cured Araldite LY 5052 / 4 4' DDS an amine / epoxy ratio of 0.85

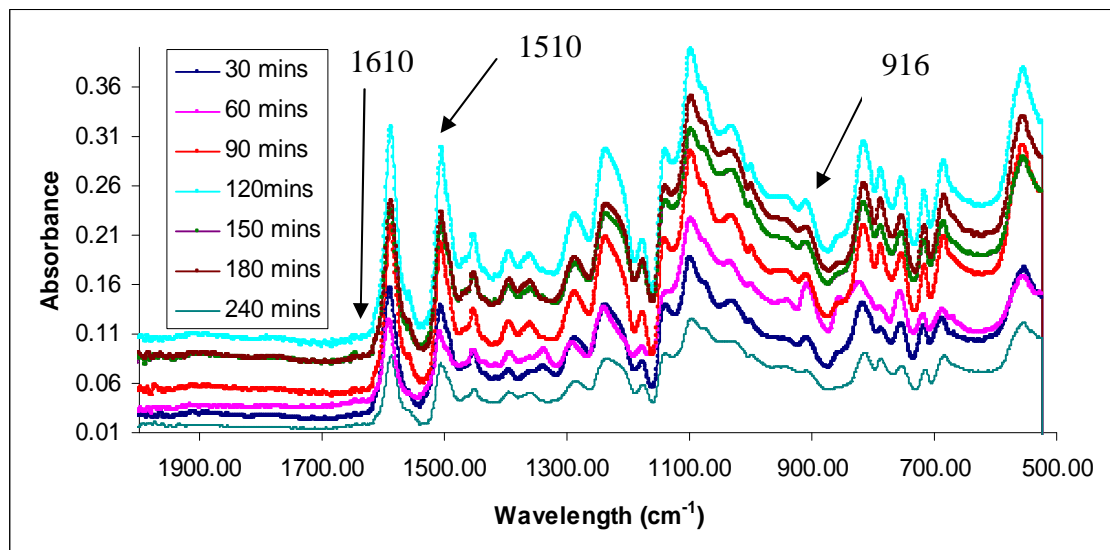


Figure 5.8 Overlaid spectra for microwave cured Araldite LY 5052 / 4 4' DDS an amine / epoxy ratio of 0.85

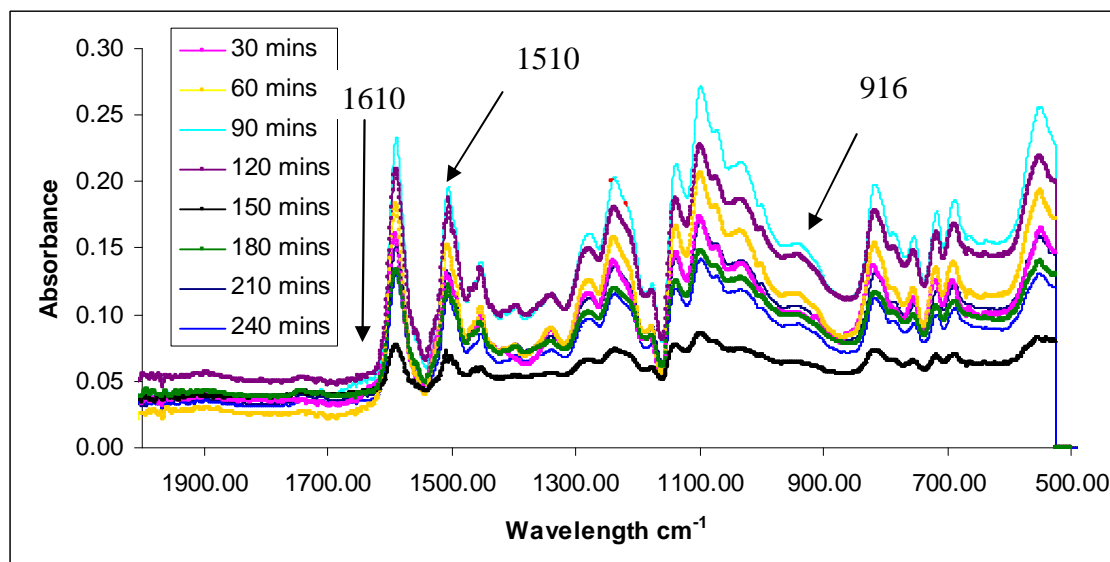


Figure 5.9 Overlaid spectra for conventionally cured Araldite LY 5052 / 4 4' DDS an amine / epoxy ratio of 1.0

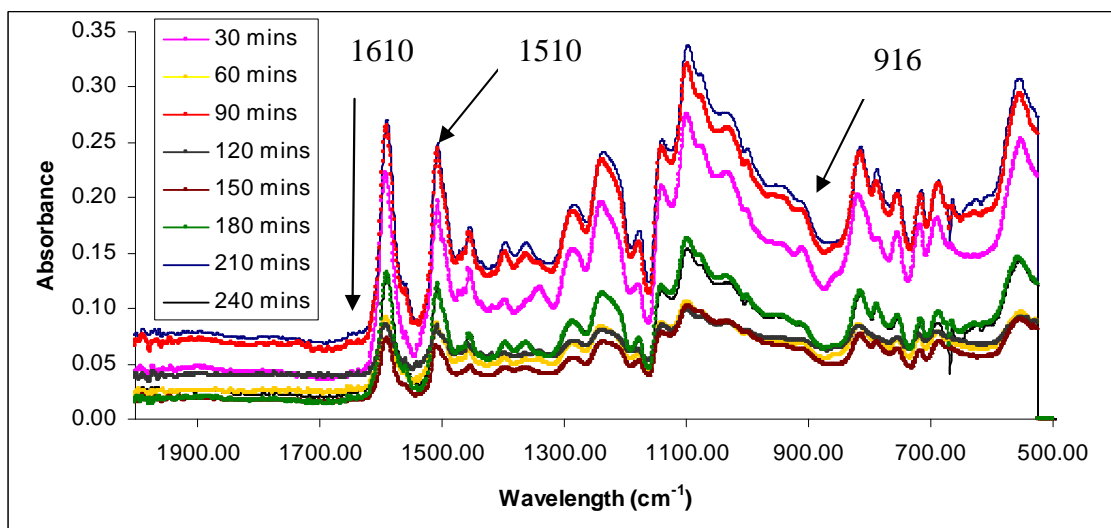


Figure 5.10 Overlaid spectra for microwave cured Araldite LY 5052 / 4 4' DDS an amine / epoxy ratio of 1.0

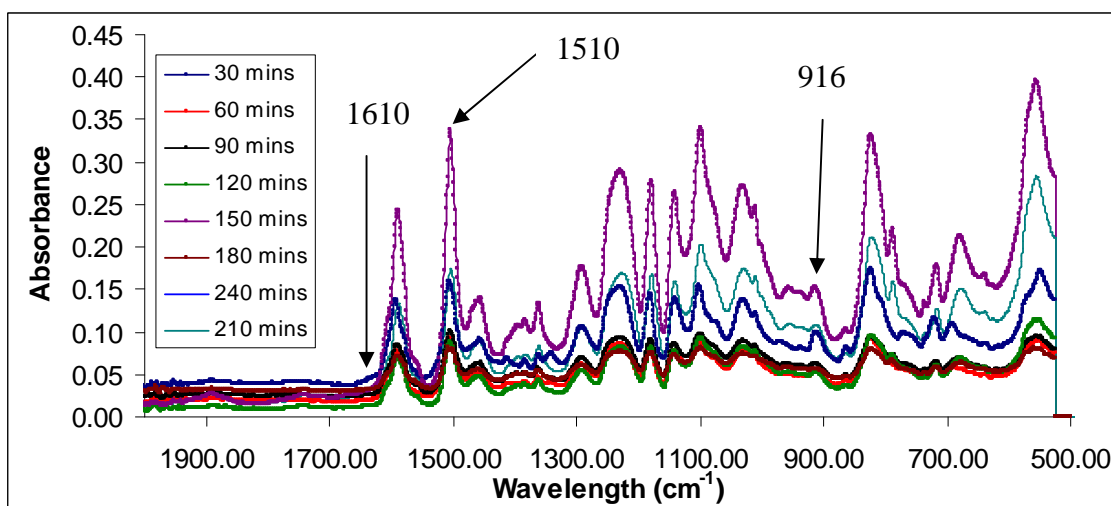


Figure 5.11 Overlaid spectra for conventional cured Araldite DLS 772 / 4 4' DDS an amine / epoxy ratio of 0.8.

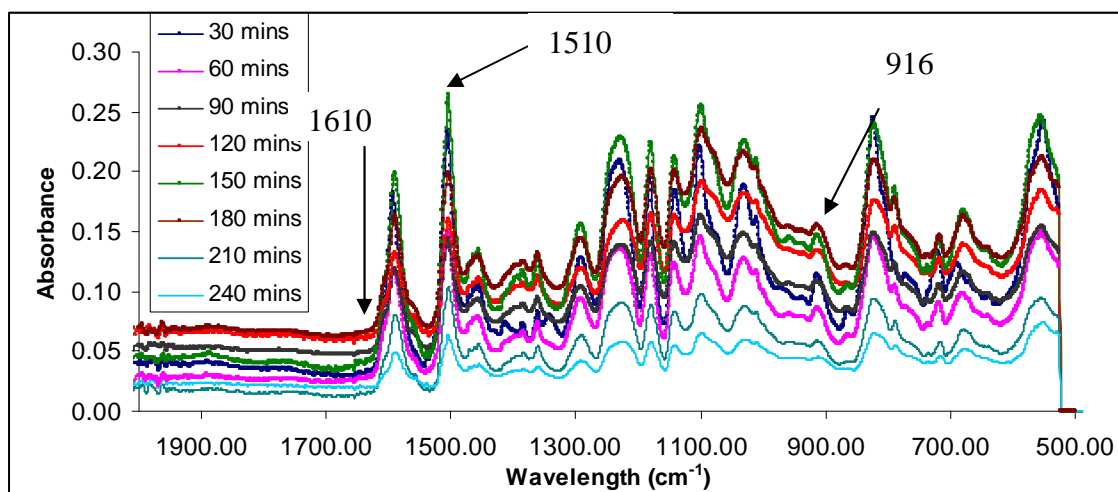


Figure 5.12 Overlaid spectra for microwave cured Araldite DLS 772 / 4 4' DDS an amine / epoxy ratio of 0.8.

The epoxide bands can be used to estimate the degrees of polymerization. The rate of polymerization can be estimated by following the loss of epoxide as the isothermal cure time increases. In order to estimate the changes in the epoxide concentrations during polymerization, the absorbance at 916 cm^{-1} is divided by the absorbance at 1510 cm^{-1} which was used as an internal standard [92, 99, 100]. The infrared spectra data used was in absorbance because as stated in Beer's Law, the absorbance is linearly proportional to concentration [101].

A comparison of polymerization rates is shown in figure 6.13 for conventional and microwave curing of Araldite LY 5052 / 4 4 DDS an amine/epoxy ratio of 0.8 at different times at an isothermal temperature of $180\text{ }^{\circ}\text{C}$.

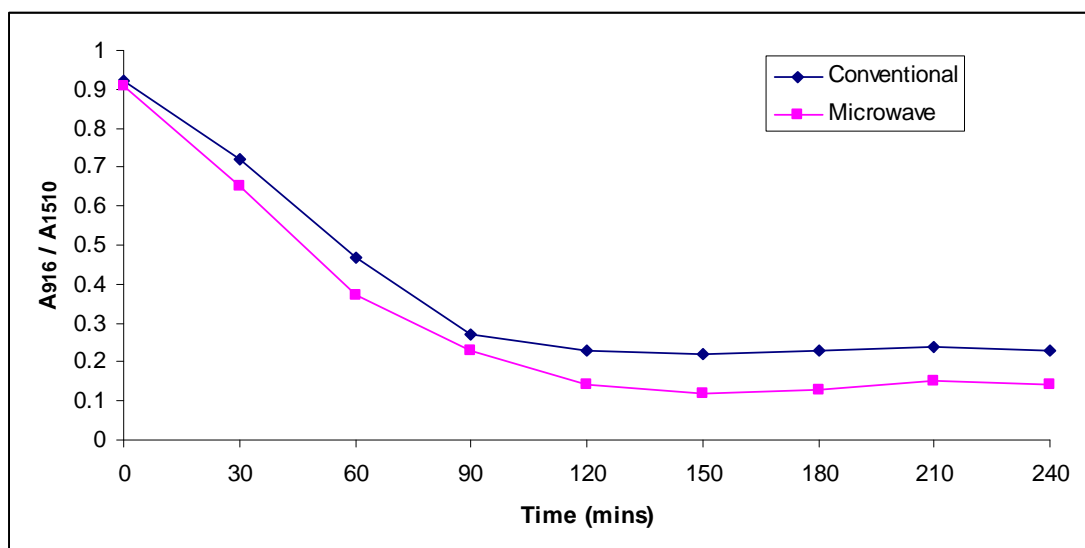


Figure 5.13 Epoxide absorbance normalised against the absorbance for phenyl for Araldite LY 5052 / 4 4' DDS an amine / epoxy ratio of 0.85 at different times at 180 °C during conventional and microwave heating.

It can be observed that there was an increase in the consumption of epoxide as the reaction time proceeded. Also, the rate of consumption of the epoxide was much faster in the microwave curing than in conventional curing at each measured time. Overall, there was a higher consumption of epoxy in the microwave curing than in the conventional curing. This enhancement in polymerization in the microwave region is very much anticipated because microwave heating directly heats the polymer molecules as a result of the relaxation of the polarized polymer dipoles along the electric field [9]. This allows more epoxy to be reacted with the amine in the curing reaction.

Epoxide absorbance ratios for Araldite LY 5052 / 4 4' DDS with an amine / epoxy ratio of 1.0 and Araldite DLS 772 / 4 4' DDS with an amine / epoxy ratio of 0.8 epoxy systems are shown 5.14 – 5.16 below. The results all show that a higher rate of epoxy was consumed in microwave heating than in conventional heating, and a higher rate of polymerization for microwave. As explained, this is because of the ability of microwave energy to selectively heat the localised hotspot in a molecule unlike the conventional heating which requires the entire material to be heated first.

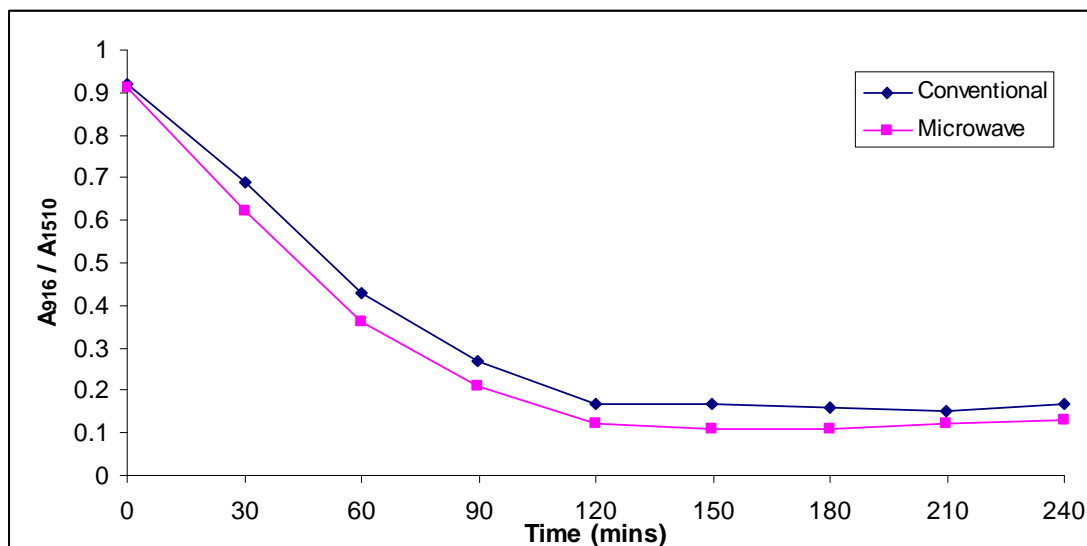


Figure 5.14 Epoxide absorbance normalised against the absorbance for phenyl for Araldite LY 5052 / 4 4' DDS with an amine / epoxy ratio of 1.0 at different times at 180 °C during conventional and microwave heating.

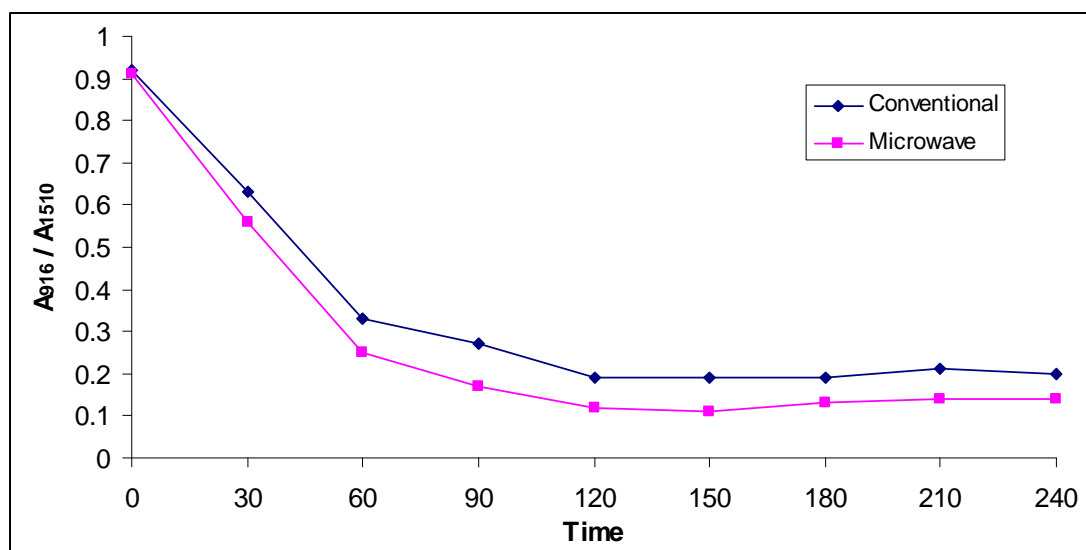


Figure 5.15 Epoxide absorbance normalised against the absorbance for phenyl for Araldite DLS 772 / 4 4' DDS with an amine / epoxy ratio of 0.8 at different times at 180 °C during conventional and microwave heating.

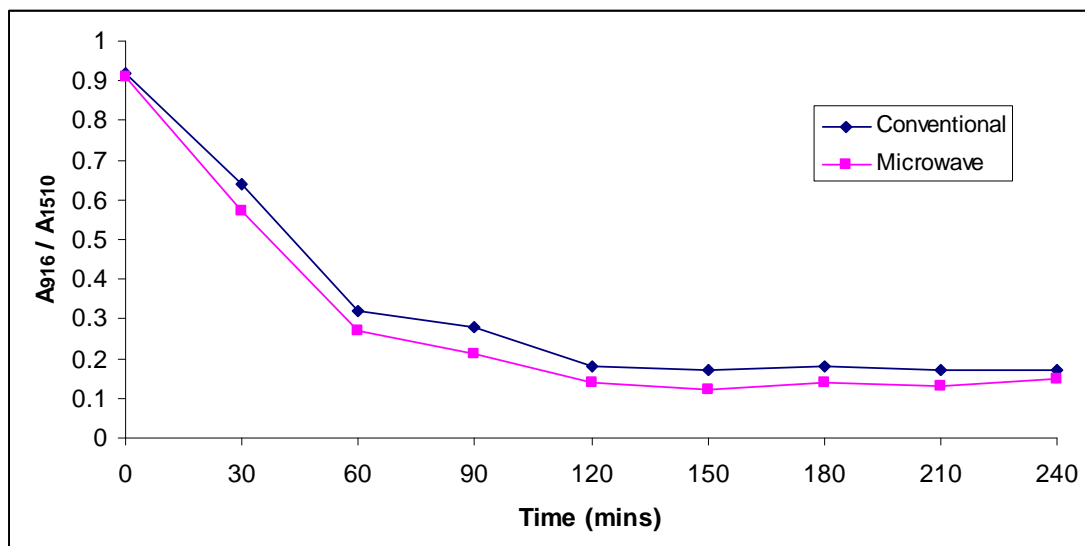


Figure 5.16 Epoxide absorbance normalised against the absorbance for phenyl for Araldite DLS 772 / 4 4' DDS with an amine / epoxy ratio of 1.1 at different times at 180 °C during conventional and microwave heating.

The amine bands can be used to estimate the degrees of polymerization. The loss of the amine band can also be used to follow the rate of polymerization as the isothermal cure time increases. In order to estimate the changes in the amine concentrations during polymerization, the absorbance at 1610 cm^{-1} is divided by the internal standard, which is the absorbance at 1510 cm^{-1} [92, 99, 100].

A comparison of polymerization rates using the amine band is shown in figure 5.17 for conventional and microwave curing of Araldite LY 5052 / 4 4 DDS an amine / epoxy ratio of 0.85 at different times at an isothermal temperature of 180 °C.

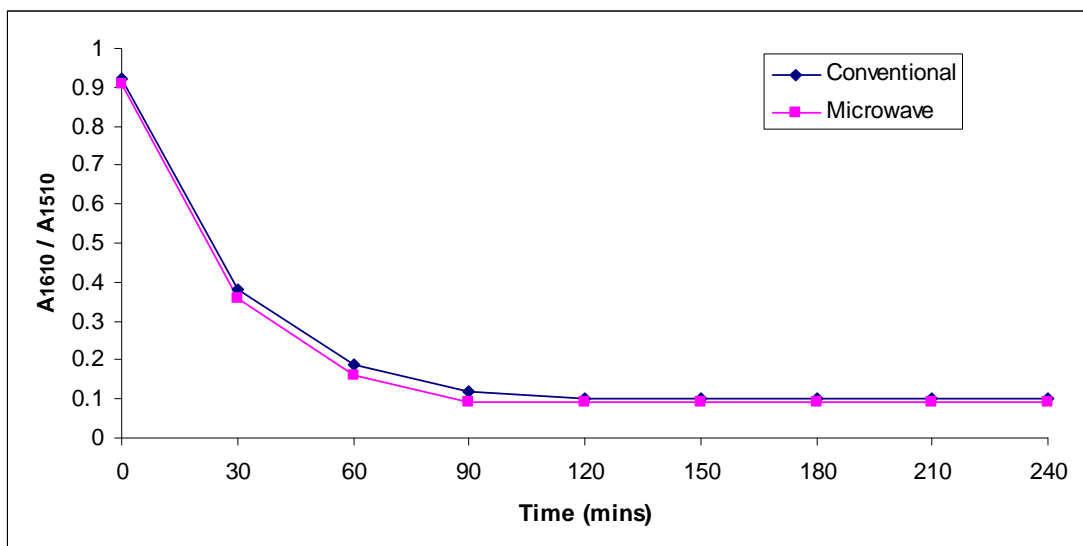


Figure 5.17 Amine absorbance normalised against the absorbance for phenyl for Araldite LY 5052 / 4 4' DDS with an amine / epoxy ratio of 0.85 at different times at 180 °C during conventional and microwave heating.

It can be observed from figure 5.17 that the rate of consumption of the amine was much faster in the microwave curing than in conventional curing at each measured time. A higher consumption of amine in the microwave curing than in the conventional curing was observed. As explained earlier, this enhancement in polymerization in the microwave region is very much anticipated because microwave heating directly heats the polymer molecules as a result of the relaxation of the polarized polymer dipoles along the electric field [26], allowing more amine to be consumed during the curing reaction.

The amine absorbance ratios Araldite LY 5052 / 4 4' DDS with an amine / epoxy ratio of 1.0 and Araldite DLS 772 / 4 4' DDS epoxy system with an amine / epoxy ratio of 0.8 are shown in figures 5.18 to 5.20 below. As with the figures 5.14 to 5.16, the results all show that a higher rate of amine was consumed in microwave heating than in conventional heating, and a higher rate of polymerization for microwave. This is because of the ability of microwave energy to selectively heat the localised hotspot in a molecule unlike the conventional heating which requires the entire material to be heated first.

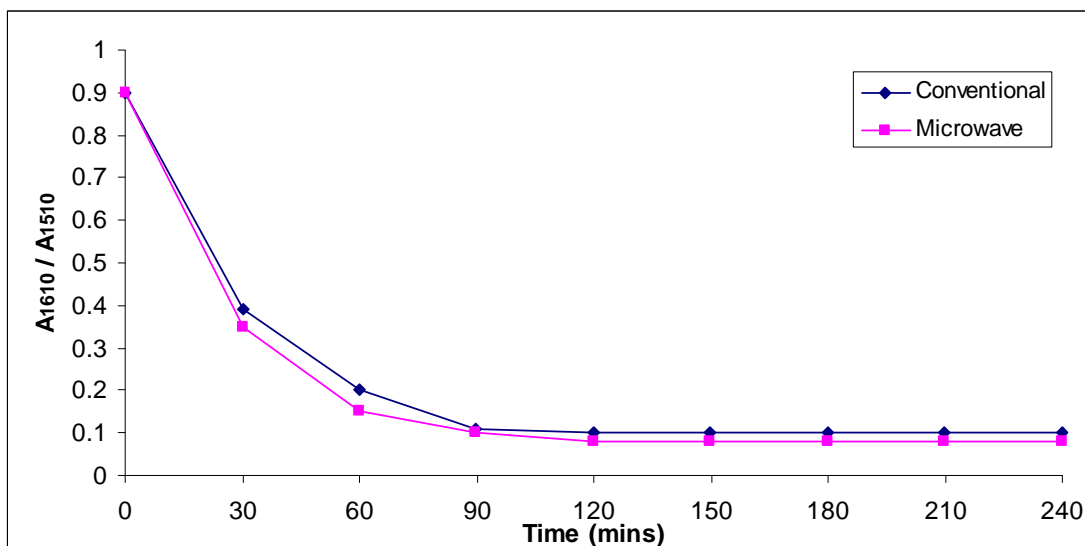


Figure 5.18 Amine absorbance normalised against the absorbance for phenyl for Araldite LY 5052 / 4 4' DDS with an amine / epoxy ratio of 1.0 at different times at 180 °C during conventional and microwave heating.

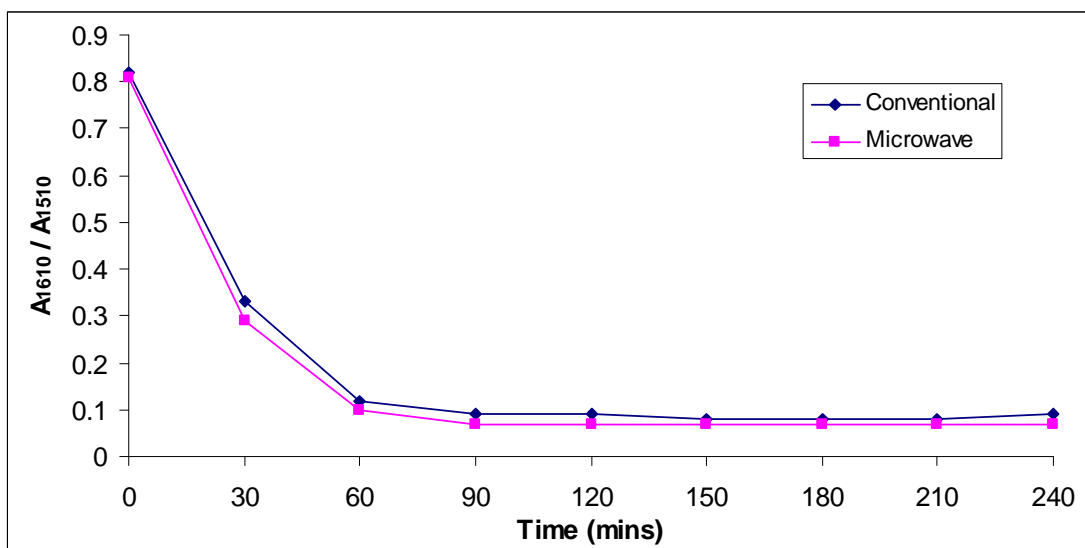


Figure 5.19 Amine absorbance normalised against the absorbance for phenyl for Araldite DLS 772 / 4 4' DDS with an amine / epoxy ratio of 0.8 at different times at 180 °C during conventional and microwave heating.

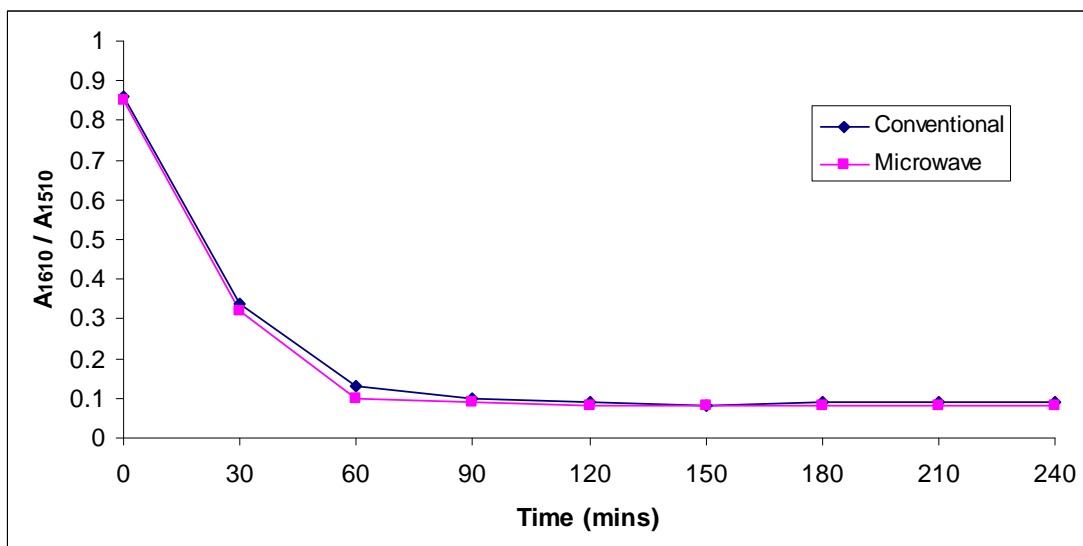


Figure 5.20 Amine absorbance normalised against the absorbance for phenyl for Araldite DLS 772 / 4 4' DDS with an amine / epoxy ratio of 1.1 at different times at 180 °C during conventional and microwave heating.

5.3 Summary

The similarity of the infrared spectra for both microwave and conventional curing of both epoxy systems is an indication that the curing reactions follows the same reaction pathway. For both Araldite LY 5052 / 4 4' DDS and Araldite DLS 772 / 4 4' DDS epoxy systems, the rate of consumption of the epoxy and amine groups was higher during the microwave curing reactions.

CHAPTER SIX

6.0 EFFECT OF CURING METHOD ON PHYSICAL AND MECHANICAL PROPERTIES

6.1 Introduction

During the curing of thermoset polymers, low molecular weight liquid monomers are transformed into a three-dimensional thermoset network by the means of chemical reactions. Hence, the structure of the network formed is affected by the way the resin reacts during polymerisation. The way the resin reacts during polymerisation also influences the physical and the mechanical properties of the polymer produced. The mechanical behaviour of the polymer materials in particular is important for the practical applications of these materials. The mechanical properties usually dictates when a given polymer material can be used for a particular purpose. Thus, the study these mechanical properties are vital so as to predict the performance of the polymer. Different network structures are anticipated for samples cured using conventional and microwave heating. This is because conventional and microwave samples are heated in different ways.

6.2 Effect of curing on Polymer density



Figure 6.0 Fully cured sample of Araldite LY 5052 / 4 4' DDS epoxy system with an amine / epoxy ratio of 0.85 with microwave heating at 180 °C for 240 minutes.

The density gives us an indication of how tightly or loosely packed the molecules are in the network structure. The difference in the network packing between the samples cured using conventional and microwave heating can be investigated through this method. A pycnometer was used to measure the density of the fully cured samples prepared as described in the previous section. Plots of average density as a function of the stoichiometric ratio content for the fully cured samples prepared using conventional and microwave curing for Araldite LY 5052 and DLS 772 are shown in the figures below.

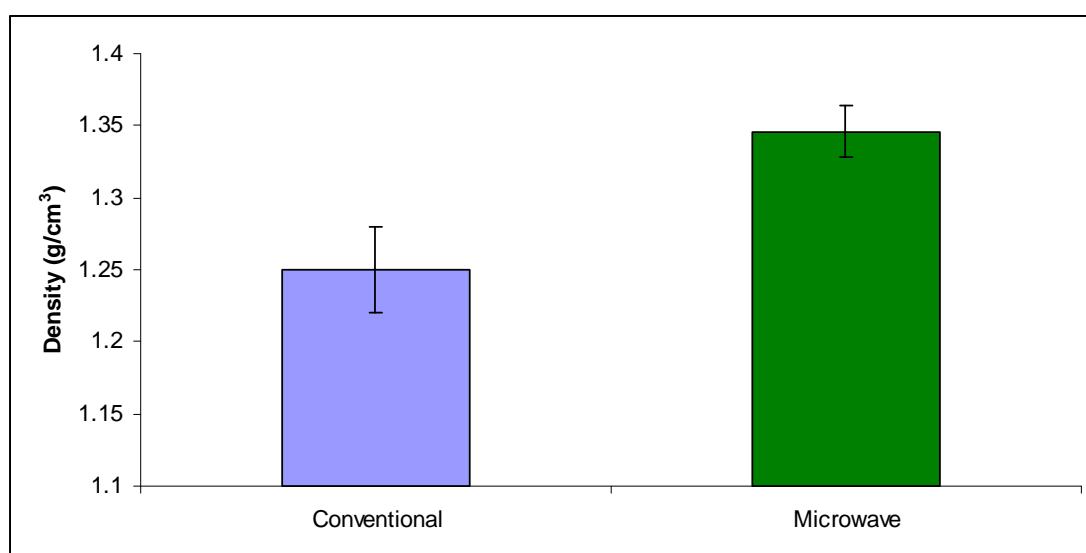


Figure 6.1 Plot of Average Density for conventionally and microwave cured samples of Araldite LY 5052 / 4 4' DDS epoxy system with an amine / epoxy ratio of 0.85.

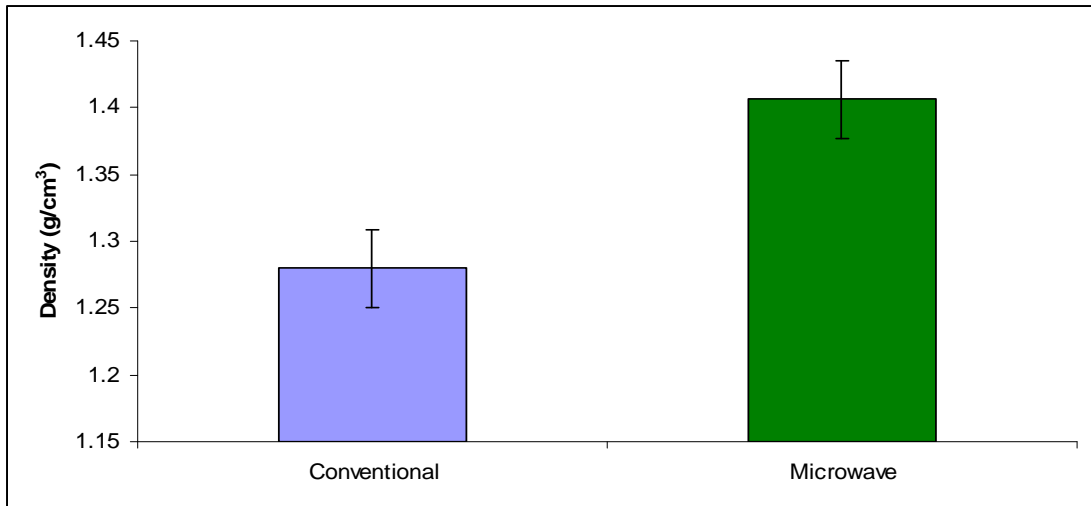


Figure 6.2 Plot of Average Density for conventionally and microwave cured samples of Araldite LY 5052 / 4 4' DDS epoxy system with an amine / epoxy ratio of 0.8

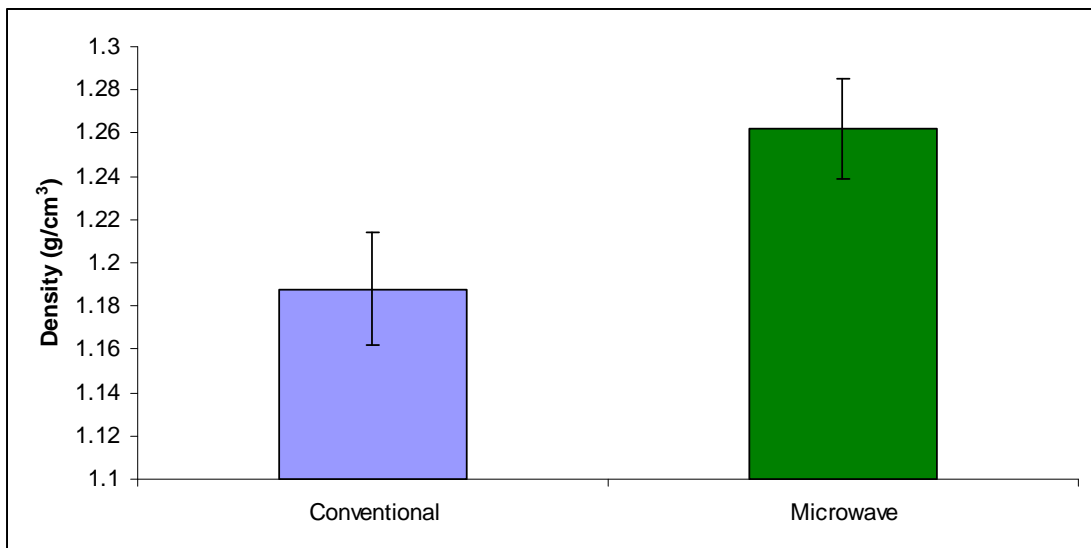


Figure 6.3 Plot of Average Density for conventionally and microwave cured samples of Araldite DLS 772 / 4 4' DDS epoxy system with an amine / epoxy ratio of 1.0

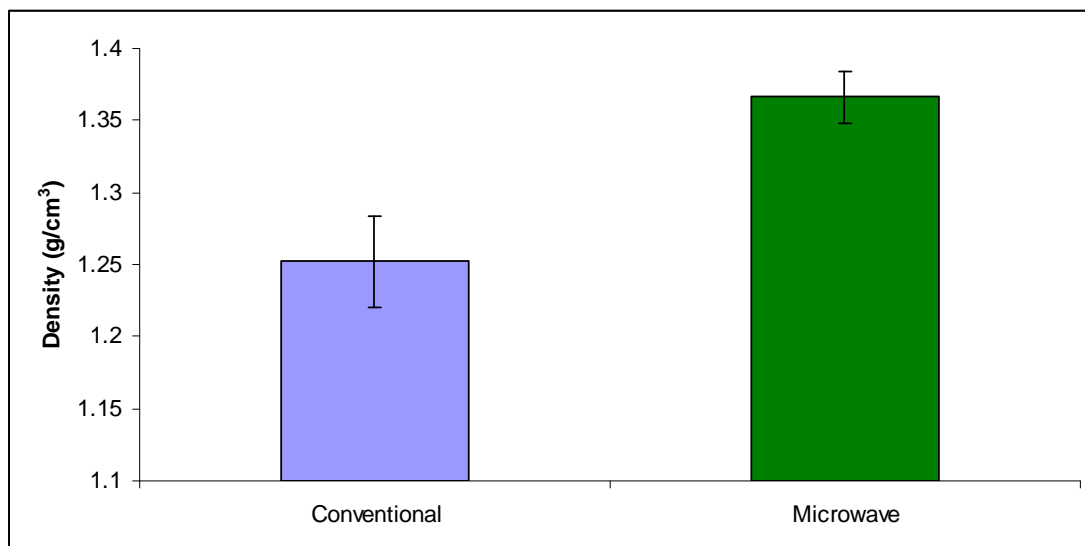


Figure 6.4 Plot of Average Density for conventionally and microwave cured samples of Araldite DLS 772 / 4 4' DDS epoxy system with an amine / epoxy ratio of 1.1.

Table 6.1 Table of abbreviations used for amine / epoxy ratios for both Araldite LY 5052 / 4 4' DDS and Araldite DLS 772 / 4 4' DDS epoxy systems.

CA85	Conventional cured Araldite LY 5052 /4 4 DDS epoxy system with an amine / epoxy ratio of 0.85
MA85	Microwave cured Araldite LY 5052 /4 4 DDS epoxy system an amine / epoxy ratio of 0.85
CA 100	Conventional cured Araldite LY 5052 /4 4 DDS epoxy system an amine / epoxy ratio of 1.0
MA100	Microwave cured Araldite LY 5052 /4 4 DDS epoxy system an amine / epoxy ratio of 100
CD80	Conventional cured Araldite DLS 772 /4 4 DDS epoxy system an amine / epoxy ratio of 0.8
MD80	Microwave cured Araldite DLS 772 /4 4

	DDS epoxy system an amine / epoxy ratio of 0.8
CD110	Conventional cured Araldite DLS 772 /4 4 DDS epoxy system an amine / epoxy ratio of 1.1
MD110	Microwave cured Araldite DLS 772 /4 4 DDS epoxy system an amine / epoxy ratio of 1.1

Table 6.2 shows the density values of fully cured samples of Araldite LY 5052 / 4 4' DDS and Araldite DLS 772 / 4 4' DDS epoxy systems.

Table 6.2 Density values of fully cured samples of Araldite LY 5052 / 4 4' DDS and Araldite DLS 772 / 4 4' DDS epoxy systems.

	Density 1 (g cm ⁻³)	Density 2 (g cm ⁻³)	Density 3 (g cm ⁻³)	Density 4 (g cm ⁻³)	Density 5 (g cm ⁻³)	Average (g cm ⁻³)	St. Dev
CA85	1.25	1.29	1.21	1.24	1.26	1.25	0.029
MA85	1.35	1.35	1.32	1.37	1.34	1.35	0.018
CA100	1.24	1.29	1.26	1.30	1.31	1.28	0.029
MA100	1.37	1.42	1.43	1.38	1.43	1.41	0.028
CD80	1.21	1.17	1.18	1.16	1.22	1.19	0.026
MD80	1.24	1.25	1.28	1.26	1.29	1.26	0.022
CD110	1.26	1.20	1.25	1.27	1.28	1.25	0.031
MD110	1.39	1.35	1.37	1.36	1.38	1.36	0.018

From figures 6.1 and 6.2 above, the density of the microwave cured samples for the epoxy system Araldite LY 5052 / 4 4' DDS were slightly higher than the densities of the conventionally cured samples, meaning that the molecules are more tightly packed. This reveals that the network structure in the microwave-cured samples were more

compact than the conventionally cured samples. This suggests a different morphology in microwave compared to conventionally prepared samples. A different morphology was also observed in the samples of Araldite DLS 772 / 4 4' DDS epoxy system. The densities of the microwave cured samples for Araldite DLS 772 / 4 4' DDS epoxy system with amine / epoxy ratios of 0.8 and 1.1 were higher than the conventionally cured samples, indicating a more compact network structure for the microwave cured samples.

6.3 Effect of curing on Dynamic Mechanical Properties

Dynamic Mechanical Thermal Analysis was used to study the morphology of the network structure of the polymer materials. The effect of curing method on the dynamic mechanical properties such as the loss tangent ($\tan \delta$) and the storage modulus (G') of the microwave and conventionally cured samples was determined and compared.

Figures 6.5 to 6.8 show the typical DMA results for conventionally and microwave-cured samples of Araldite LY 5052 / 4 4' DDS epoxy system.

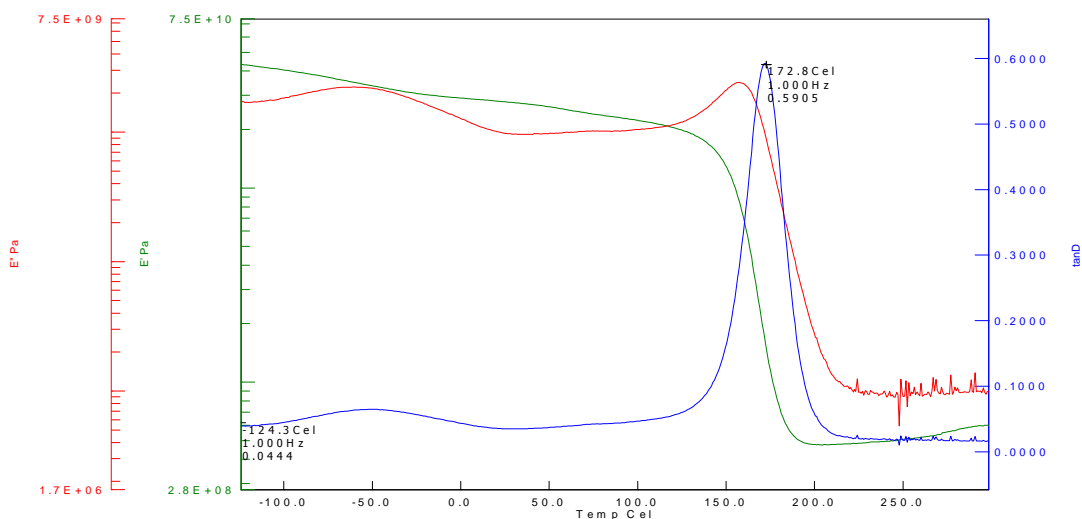


Figure 6.5 Dependence of storage modulus (G'), Loss modulus (G'') and $\tan \delta$ with temperature for a fully cured sample of Araldite LY 5052 / 4 4' DDS epoxy system with an amine / epoxy ratio of 0.85 prepared using microwave heating at 180°C for 240 mins

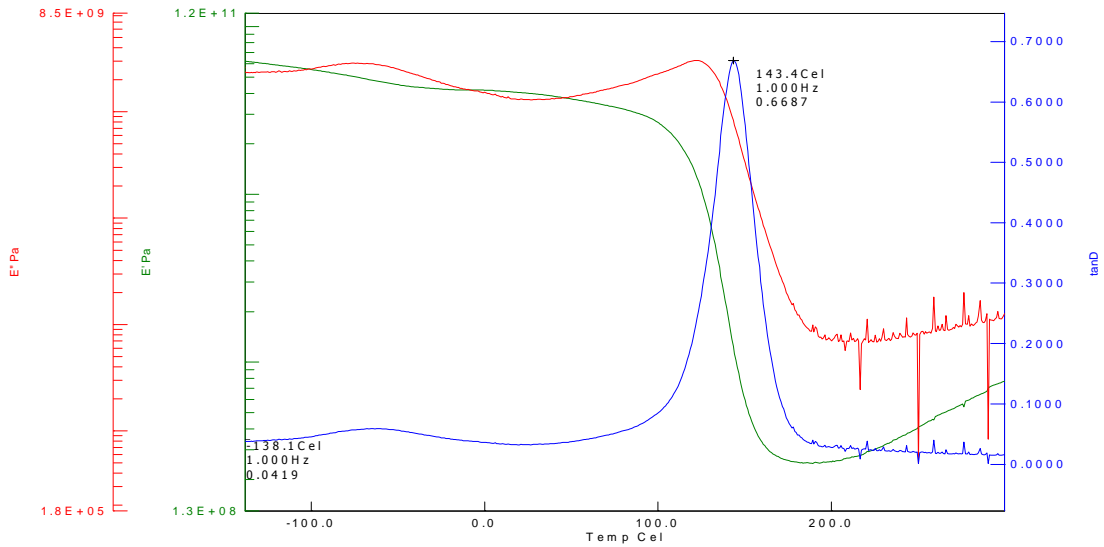


Figure 6.6 Dependence of storage modulus (G'), Loss modulus (G'') and $\tan \delta$ with temperature for a fully cured sample of Araldite LY 5052 / 4 4' DDS epoxy system with an amine / epoxy ratio of 0.85 prepared using conventional heating at 180°C for 240 mins.

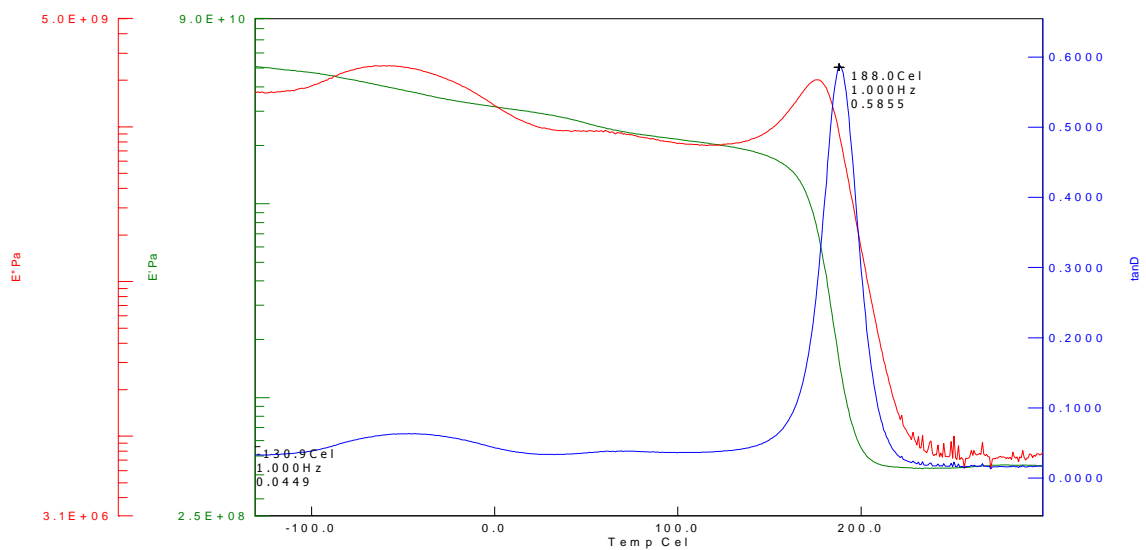


Figure 6.7 Dependence of storage modulus (G'), Loss modulus (G'') and $\tan \delta$ with temperature for a fully cured sample of Araldite LY 5052 / 4 4' DDS epoxy system with an amine / epoxy ratio of 1.0 prepared using conventional heating at 180 °C for 240 mins.

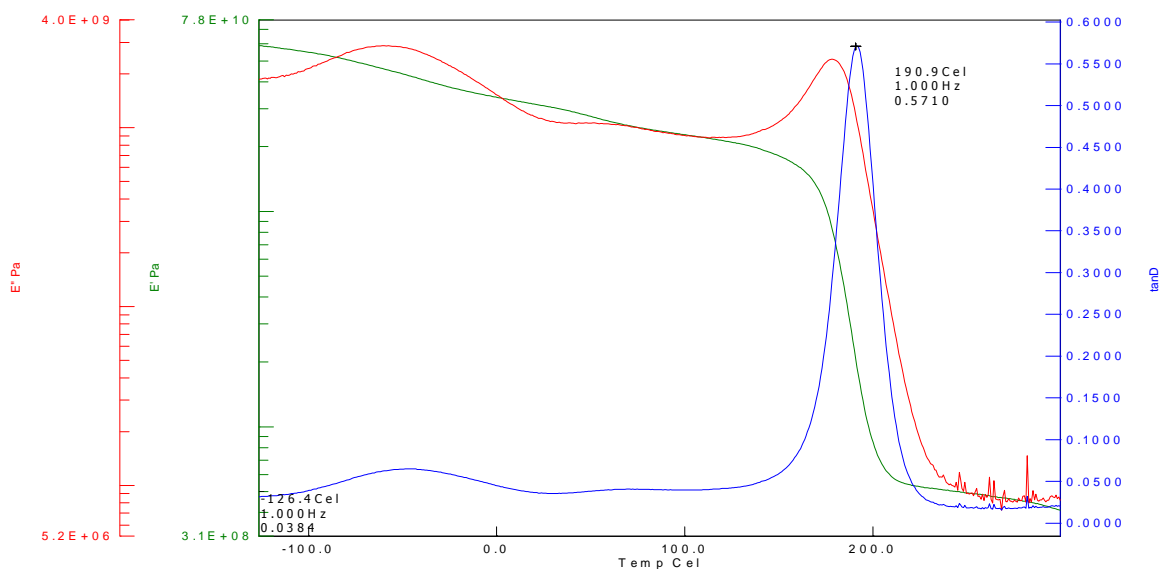


Figure 6.8 Dependence of storage modulus (G'), Loss modulus (G'') and $\tan \delta$ with temperature for a fully cured sample of Araldite LY 5052 / 4 4' DDS epoxy system with an amine / epoxy ratio of 1.0 prepared using microwave heating at 180 °C for 240 mins.

From the figures 6.5 to 6.8 above, we notice that the temperature dependence of the dynamic mechanical thermal analysis properties for the conventional and microwave cured Araldite LY 5052 / 4 4' DDS epoxy system follow the same course. The shear modulus (G') decreased as the temperature increased. At the point where the storage modulus decreased sharply, the damping curve ($\tan \delta$) went through a maximum. The loss modulus also went through a maximum, but its peak was not as striking as the damping curve peak. The peak in the loss modulus curve occurred at a temperature slightly lower than the peak in the $\tan \delta$ curve.

Usually, the $\tan \delta$ is the most sensitive indicator of the molecular motions which are occurring in the material. The $\tan \delta$ peak is associated with the main glass-to-rubber transition. The temperature at the maximum of this $\tan \delta$ peak is known as the glass transition temperature, T_g of the material.

Two peaks were observed in the $\tan \delta$ curve in both conventional and microwave-cured epoxy systems as shown in figures 6.5 to 6.8. A smaller peak was observed below 0 °C in all the plots. The presence of two peaks means that a secondary transition occurred in the samples during the thermal analysis. The secondary transition is attributed to the crankshaft motion of the hydroxyl-ether group [102]. The crankshaft motion is usually

found in amine crosslinked systems [102]. The width of the $\tan \delta$ peaks for all the figures appeared to be similar. However, the $\tan \delta$ peak temperature was found to be higher in the microwave cured samples. The difference in the T_g values was attributed by Wei *et al* [56] to the existence of different network structures and cross-links within the conventional and microwave cured samples. The higher T_g in the microwave cured samples also suggested that the cross-link density was probably higher in the microwave cured samples than conventionally cured samples.

The DMTA plots for conventionally and microwave cured Araldite DLS 772 / 4 4' DDS epoxy systems are shown in the figures below. Just as with the Araldite LY 5052 / 4 4' DDS epoxy system, higher $\tan \delta$ peak temperatures were observed for microwave cured samples, also indicating that there are different network structures in the microwave and conventionally cured samples. During the analysis, a secondary transition occurred in the material as evidenced by the two peaks in the $\tan \delta$ curve. The width of the $\tan \delta$ peak was also found to be similar for all the materials.

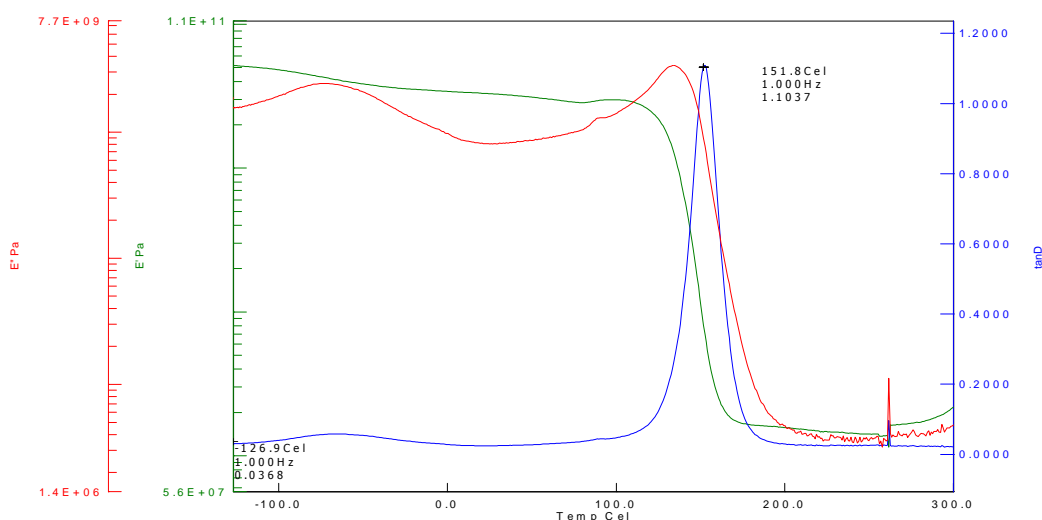


Figure 6.9 Dependence of storage modulus (G'), Loss modulus (G'') and $\tan \delta$ with temperature for a fully cured sample of Araldite DLS 772 / 4 4' DDS epoxy system with an amine / epoxy ratio of 0.8 prepared using microwave heating at 180 °C for 240 mins.

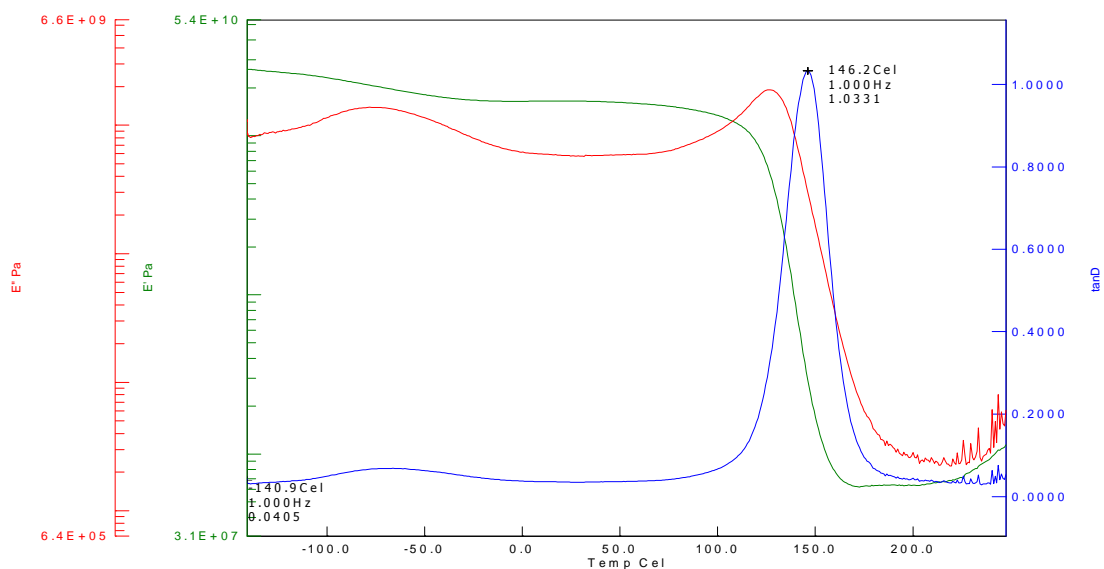


Figure 6.10 Dependence of storage modulus (G'), Loss modulus (G'') and $\tan \delta$ with temperature for a fully cured sample of Araldite DLS 772 / 4 4' DDS epoxy system with an amine / epoxy ratio of 0.8 prepared using conventional heating at 180 °C for 240 mins.

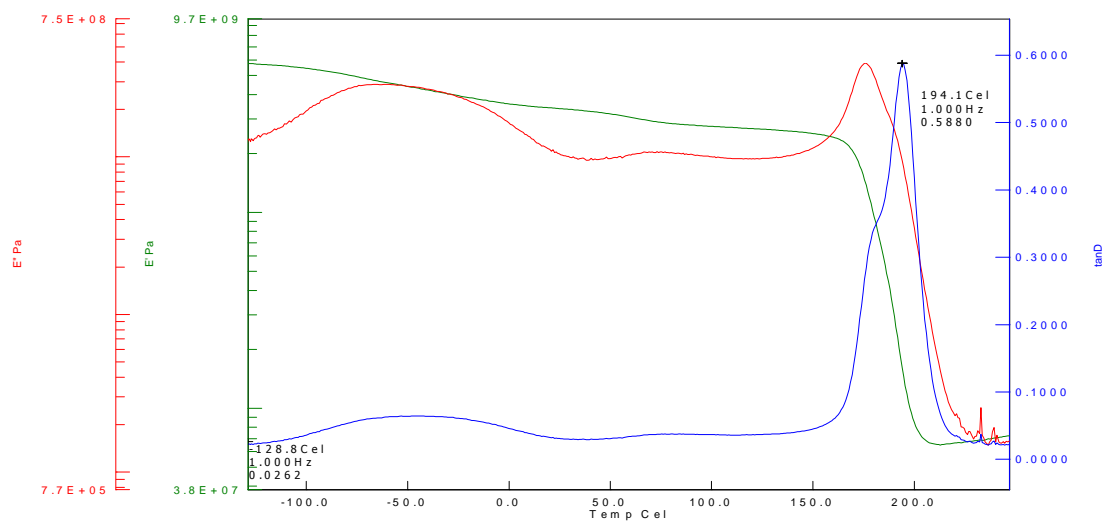


Figure 6.11 Dependence of storage modulus (G'), Loss modulus (G'') and $\tan \delta$ with temperature for a fully cured sample of Araldite DLS 772 / 4 4' DDS epoxy system an amine / epoxy ratio of 1.1 prepared using microwave heating at 180 °C for 240 mins.

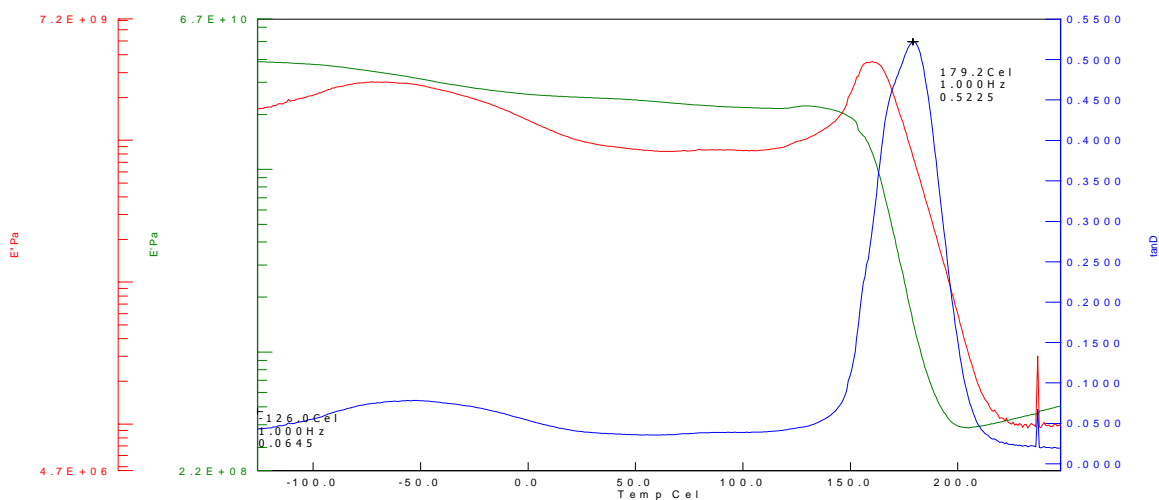


Figure 6.12 Dependence of storage modulus (G'), Loss modulus (G'') and $\tan \delta$ with temperature for a fully cured sample of Araldite DLS 772 / 4 4' DDS epoxy system an amine / epoxy ratio of 1.1 prepared using conventional heating at 180 °C for 240 mins.

Table 6.3 Glass transition values for fully cured samples of Araldite LY 5052 / 4 4' DDS and Araldite DLS 772 / 4 4' DDS epoxy systems at different stoichiometric ratios.

Epoxy System	Tg 1 (°C)	Tg 2 (°C)	Tg 3 (°C)	Tg 4 (°C)	Tg 5 (°C)	Average Tg (°C)	Standard Deviation
CA85	153.4	148.3	154.6	155.7	154.9	153.4	2.96
MA85	169.9	170.5	172.8	171.4	172.7	171.46	1.29
CA100	187.7	188.0	185.4	186.3	188.8	187.24	1.37
MA100	188.2	190.9	195.2	194.9	193.9	192.6	2.68
CD80	146.2	143.3	144.5	146.2	143.1	144.6	1.50
MD80	149.1	151.8	156.4	154.6	155.8	153.5	2.73
CD110	178.6	179.2	177.5	175.6	172.8	177.7	1.57
MD110	197.3	194.1	192.3	195.7	197.6	195.4	2.30

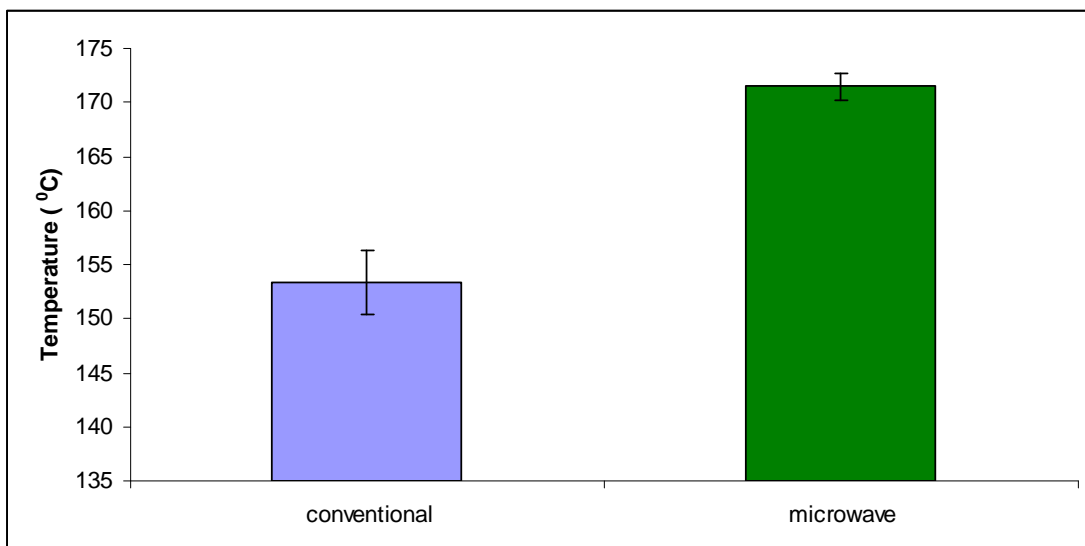


Figure 6.13 Bar chart of Average T_g values of conventional and microwave cured samples of Araldite LY 5052 / 4 4' DDS epoxy system with an amine / epoxy ratio of 0.85.

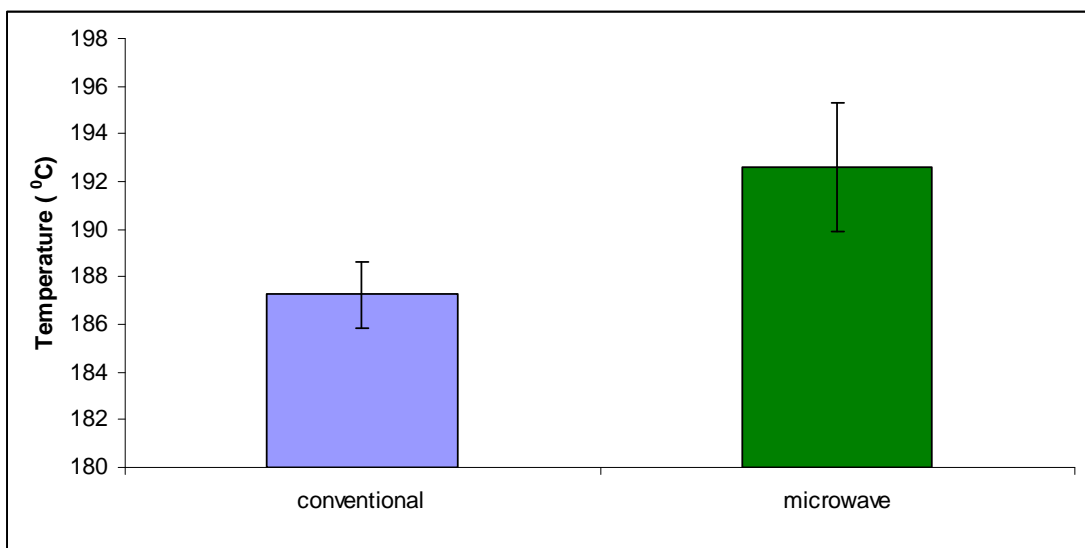


Figure 6.14 Bar chart of Average T_g values of conventional and microwave cured samples of Araldite LY 5052 / 4 4' DDS epoxy system with an amine / epoxy ratio of 1.0.

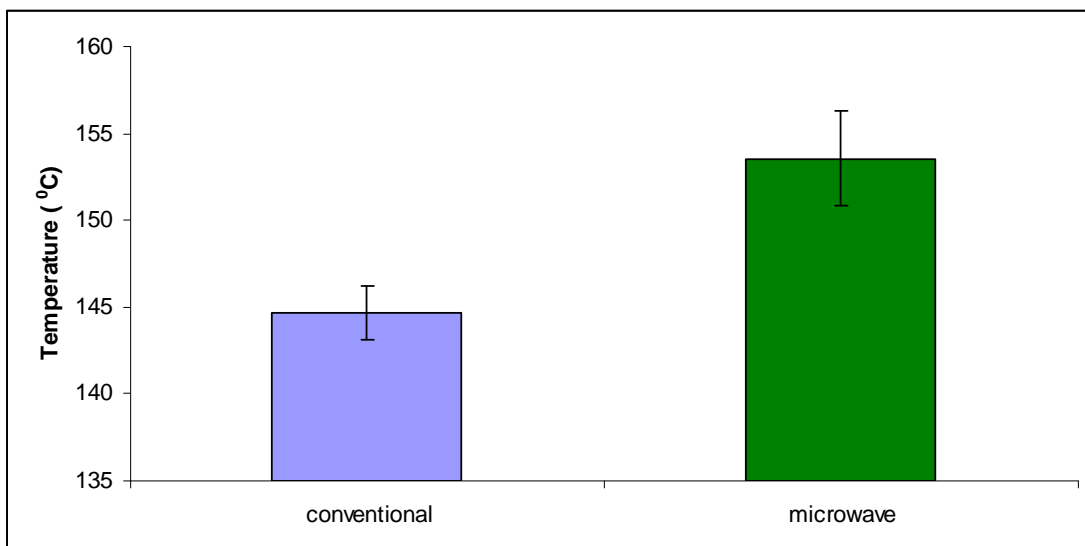


Figure 6.15 Bar chart of Average Tg values of conventional and microwave cured samples of Araldite DLS 772 / 4 4' DDS epoxy system with an amine / epoxy ratio of 0.8.

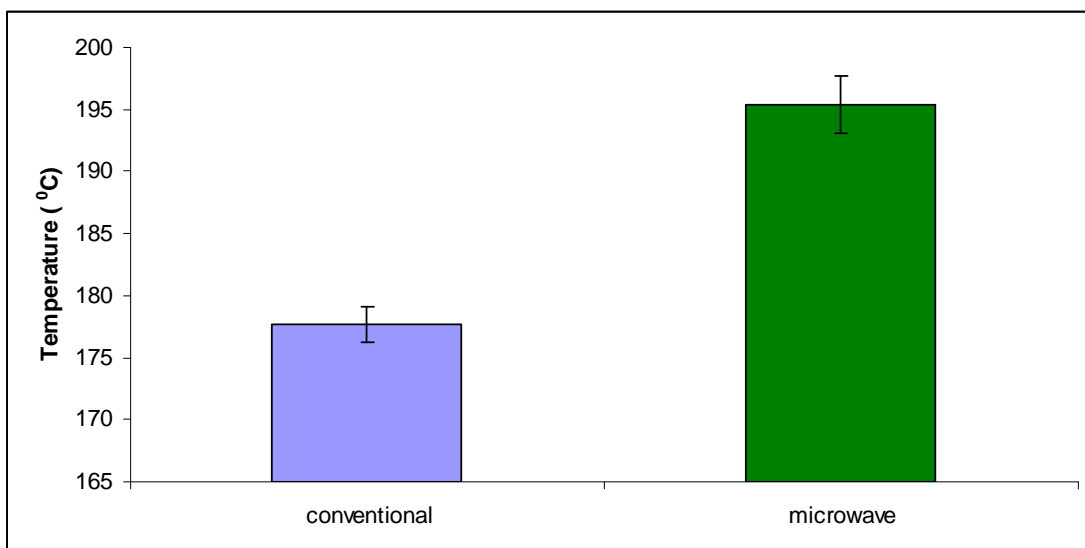


Figure 6.16 Bar chart of Average Tg values of conventional and microwave cured samples of Araldite DLS 772 / 4 4' DDS epoxy system with an amine / epoxy ratio of 1.1.

6.4 Cross- Link density

It is necessary to determine the cross-link density of the fully cured samples. This will enable us to investigate the variations in the structure of the materials produced by microwave and conventional heating.

The Cross-link density (ν) is defined as the number of moles of cross-linked chains per cubic centimetre of polymer [109]. The cross-link density can be determined by modulus measurements in the rubbery plateau. The relationship between rubbery plateau modulus and the crosslink density is given by [147]

$$\nu = \frac{G'}{RT} \quad 7.1$$

G' is the shear storage modulus which is obtained in the rubbery plateau. R is the gas constant, while T is the temperature in Kelvin which corresponds to the storage modulus value. The shear storage modulus is defined in the rubbery region at the temperature of $T_g + 50$ [103]

Bar chart plots of the cross-link density for both conventionally and microwave cured samples for both epoxy systems are shown in the figures below. The overall results reveal that microwave cured samples have a higher cross-link density than conventionally cured samples. This is an indication of a more compact network structure within the microwave cured samples.

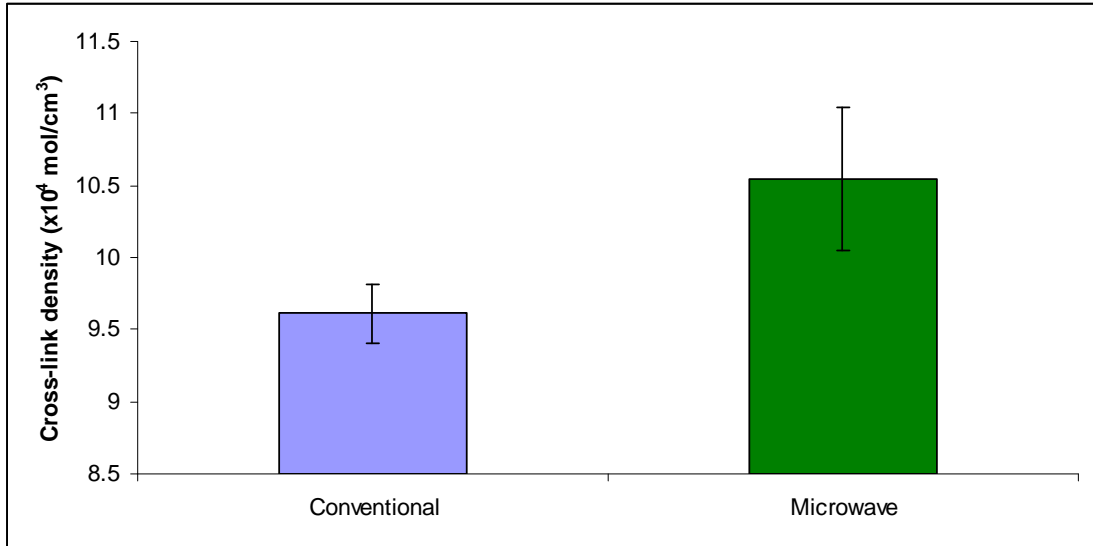


Figure 6.17 Plot of Bar chart of cross-link density values of conventional and microwave cured samples of Araldite LY 5052 / 4 4' DDS epoxy system with an amine / epoxy ratio of 0.85.

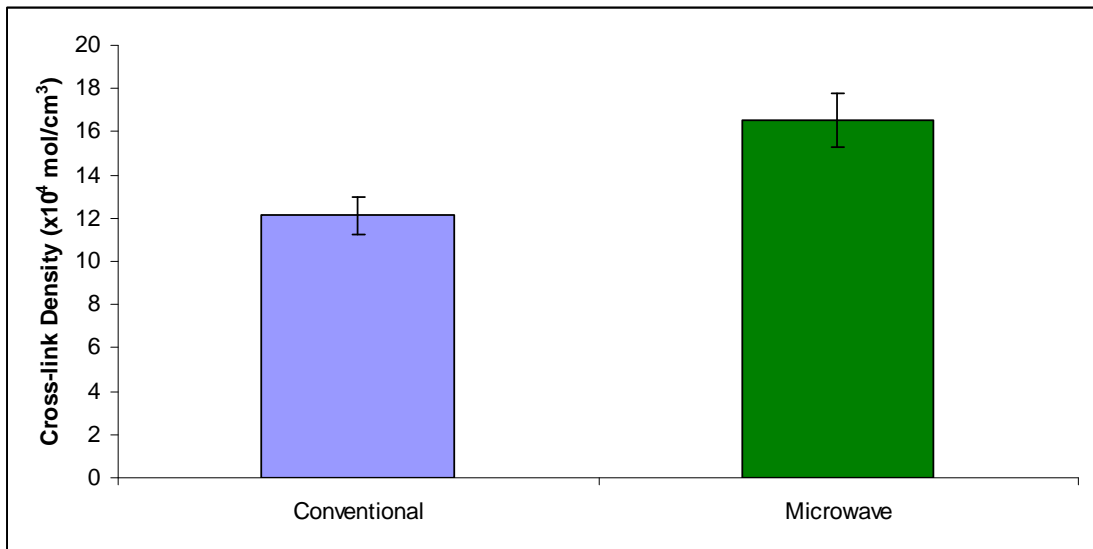


Figure 6.18 Plot of Bar chart of cross-link density values of conventional and microwave cured samples of Araldite LY 5052 / 4 4' DDS epoxy system with an amine / epoxy ratio of 1.0.

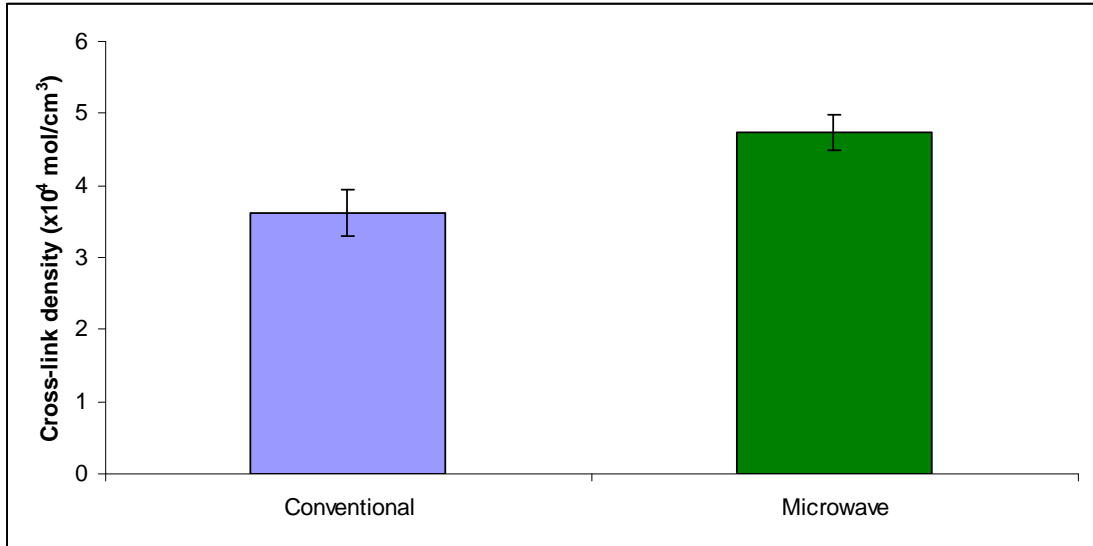


Figure 6.19 Plot of Bar chart of cross-link density values of conventional and microwave cured samples of 0.8M amine / epoxy ratio of Araldite DLS 772 / 4 4' DDS epoxy system.

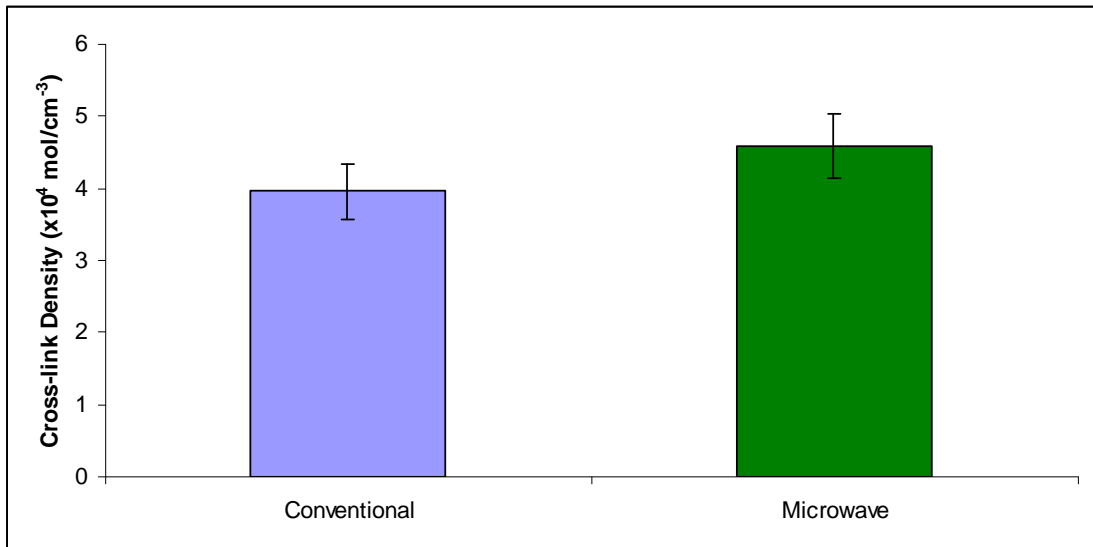


Figure 6.20 Plot of Bar chart of cross-link density values of conventional and microwave cured samples of Araldite DLS 772 / 4 4' DDS epoxy system with an amine / epoxy system of 1.1.

Table 6.4 Cross-link density values for fully cured microwave and conventionally cured samples of Araldite LY 5052 / 4 4' DDS and Araldite DLS 772 / 4 4' DDS epoxy systems.

	Value 1	Value 2	Value 3	Value 4	Value 5	Average	St. Dev
CA85	9.54	9.31	9.63	9.86	9.71	9.61	0.20
MA85	10.24	10.34	10.13	11.35	10.67	10.55	0.49
CA100	11.48	11.32	11.56	12.57	13.68	12.12	0.89
MA100	17.44	15.67	16.68	17.98	14.98	16.55	1.23
CD80	3.82	3.76	3.56	3.87	3.09	3.62	0.32
MD80	4.75	4.56	4.44	5.08	4.86	4.74	0.25
CA110	3.89	4.56	3.79	3.54	4.01	3.96	0.38
MA110	4.27	5.31	4.21	4.63	4.50	4.58	0.44

6.5 Average molecular weight between cross-links

The difference in the network structure formed by conventional and microwave heating can be investigated from the average molecular weight between cross-links (M_c) of each sample. As the cross-link density represents the ‘tightness’ of the network structure, the average molecular weight between cross-links characterise the ‘looseness’ of the network.

The average molecular weight between cross-links (M_c) is defined as the total sample weight that contains one mole of effective network chains. The determination of M_c is based on the simple rubber elasticity theory and can be calculated from [104, 105];

$$M_c = \frac{\rho RT}{G'} \quad 7.2$$

where ρ is the density, R is the gas constant, T is the temperature in Kelvin and G' is the shear storage modulus in the rubbery region. The unit of M_c is the same as for molecular weight, g/mol.

Comparison of Equations 6.1 and 6.2 shows that M_c is the proportional to cross-link density and can be expressed as follows.

$$M_c = \frac{\rho}{\nu} \quad 7.3$$

Nielsen, however, claimed the equations of the kinetic theory of rubber predict moduli far too small for extremely highly cross-linked materials [104]. He has proposed an empirical equation that agrees much better than equation 7.2 with the experimental results at very high degrees of cross-linking.

$$\log G' = 7.0 + \frac{293\rho}{M_c} \quad 7.4$$

The average molecular weight between cross-links for conventionally and microwave-cured samples were calculated using equations 7.3 and 7.4. The results both suggest that the M_c value of conventionally cured samples was generally higher than of microwave-cured samples. Bar chart plots of the average molecular weight between cross-links of microwave and conventionally cured samples of both epoxy systems are shown in figures 7.21 to 7.24. These results suggest that conventionally cured samples had larger ‘free volume’ between polymer chains. This result is consistent with the lower density observed in the conventionally cured samples.

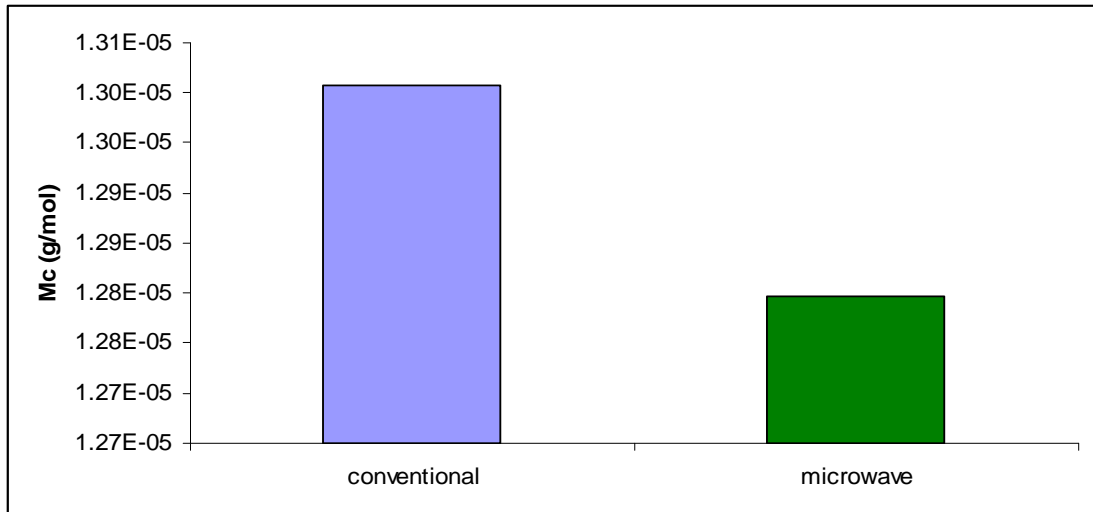


Figure 6.21 Plot of average molecular weight between cross-links (M_c) of conventional and microwave cured samples of Araldite LY 5052 / 4 4' DDS epoxy system with an amine / epoxy ratio of 0.85 using Nielsen's equation.

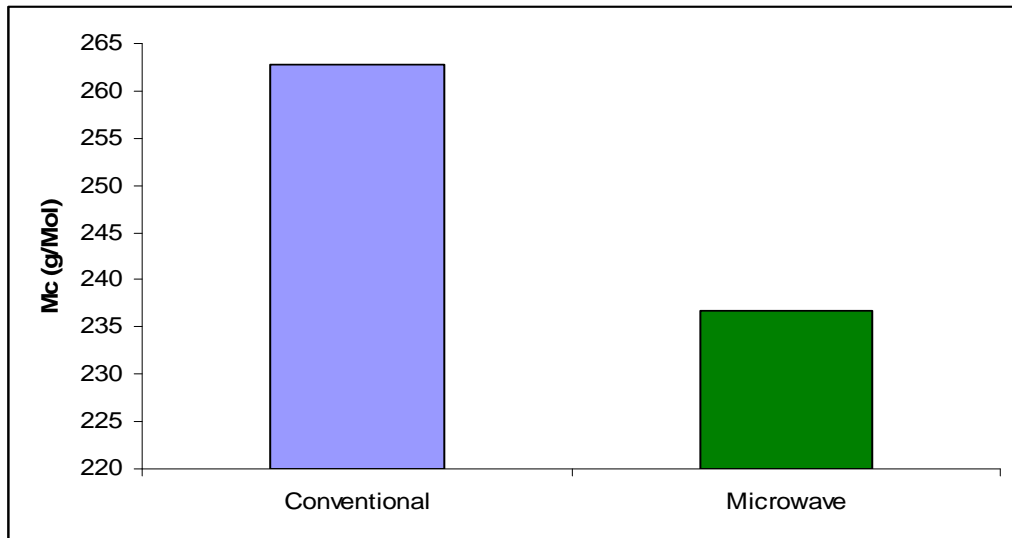


Figure 6.22 Plot of average molecular weight between cross-links (M_c) of conventional and microwave cured samples of Araldite LY 5052 / 4 4' DDS epoxy system with an amine / epoxy ratio of 0.85 using Nielsen's equation.

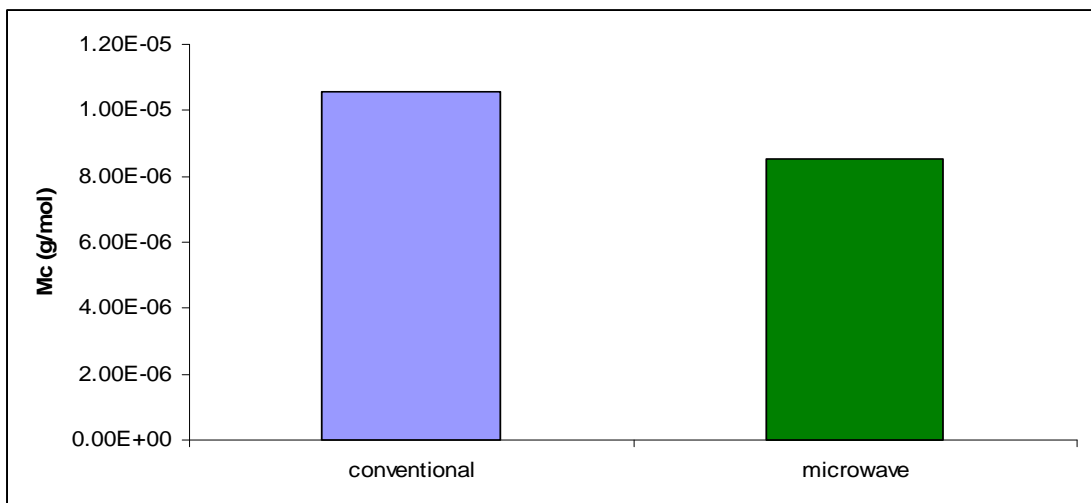


Figure 6.23 Plot of average molecular weight between cross-links (M_c) of conventional and microwave cured samples of Araldite LY 5052 / 4 4' DDS epoxy system with an amine / epoxy ratio of 1.0 using Nielsen's equation.

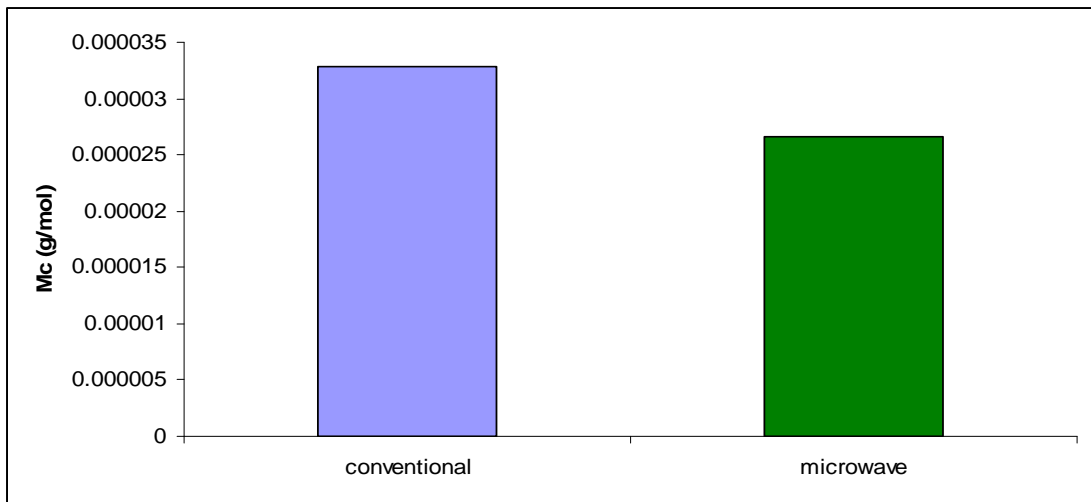


Figure 6.24 Plot of average molecular weight between cross-links (M_c) of conventional and microwave cured samples of Araldite DLS 772 / 4 4' DDS epoxy system with an amine / epoxy ratio of 0.8 using Nielsen's equation.

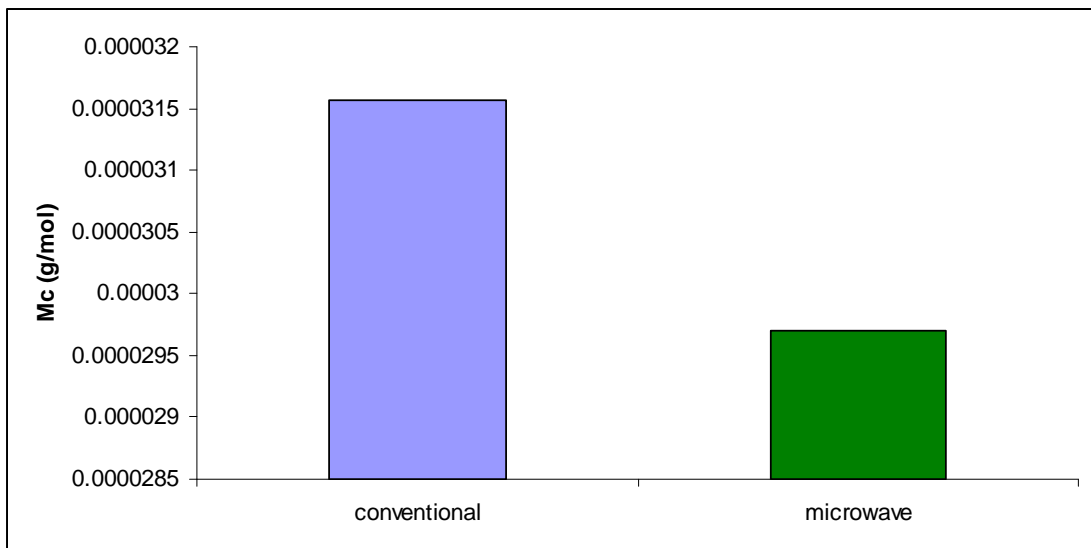


Figure 6.25 Plot of average molecular weight between cross-links (M_c) of conventional and microwave cured samples of Araldite LY 5052 / 4 4' DDS epoxy system with an amine / epoxy ratio of 1.1 using Nielsen's equation

6.6 Effect of curing on flexural properties

A 3-point bending test was used to determine the flexural mechanical properties of the fully cured samples. The 3 point bending test is a stress-strain test whereby the specimen is deformed under bending conditions. For this research, fully cured samples of Araldite LY 5052 / 4 4' DDS and Araldite DLS 772 / 4 4' DDS epoxy systems were subjected to three point bending tests. The figures below show flexural stress-strain curves obtained from conventional and microwave cured samples. The flexural load-displacement plots for the conventionally and microwave cured samples show similar patterns.

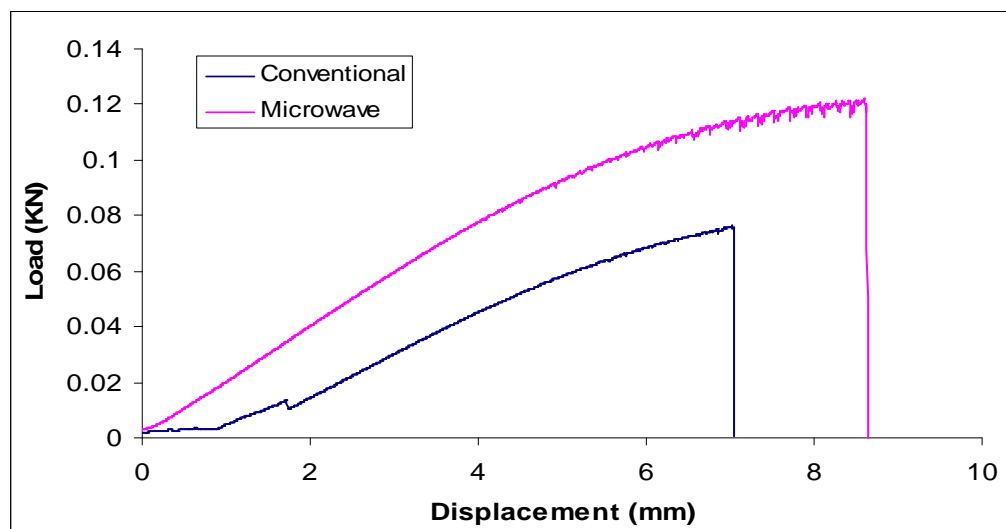


Figure 6.26 Load vs Displacement plot for conventional and microwave cured samples of Araldite LY 5052 / 4 4' DDS epoxy system with an amine / epoxy ratio of 0.85.

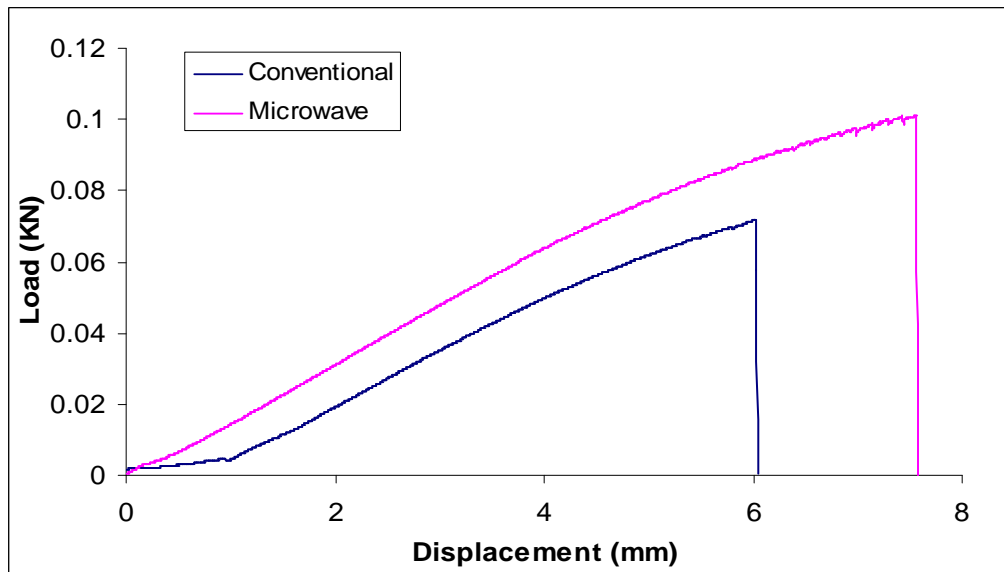


Figure 6.27 Load vs Displacement plot for conventional and microwave cured samples of Araldite LY 5052 / 4 4' DDS epoxy system with an amine / epoxy ratio of 1.0.

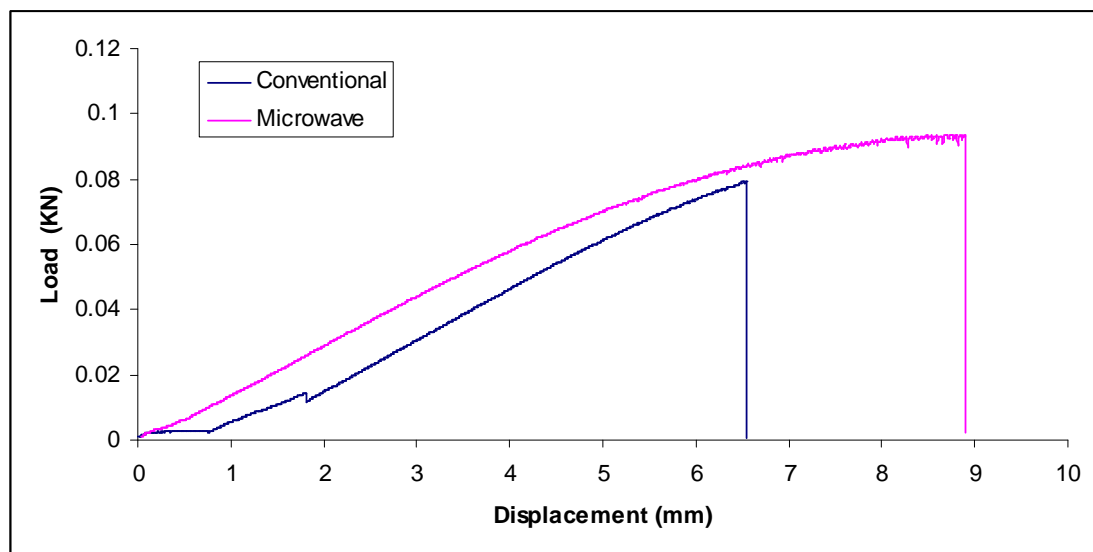


Figure 6.28 Load vs Displacement plot for conventional and microwave cured samples of Araldite DLS 772 / 4 4' DDS epoxy system with an amine / epoxy ratio of 0.8.

Table 6.5 Flexural Strength values for fully cured samples of Araldite LY 5052 / 4 4' DDS and Araldite DLS 772 / 4 4' DDS epoxy systems at different stoichiometric ratios.

	Flexural Strength 1	Flexural Strength 2	Flexural Strength 3	Flexural Strength 4	Flexural Strength 5	Average	St.Dev
CA85	98.5	96.3	100.8	101.9	90.4	97.6	4.55
MA85	129.6	133.5	136.5	124.7	139.4	132.7	5.77
CA100	114.5	121.3	110.1	115.0	107.7	113.8	5.15
MA100	144.1	152.4	143.1	148.7	145.9	146.8	3.78
CD80	107.3	113.6	117.9	105.3	110.6	110.9	5.01
MD80	147.6	140.7	139.7	143.8	134.6	144.2	4.85
CD110	121.5	117.3	129.7	127.1	115.7	122.3	6.06
MD110	155.0	163.3	157.4	152.1	155.3	156.3	4.19

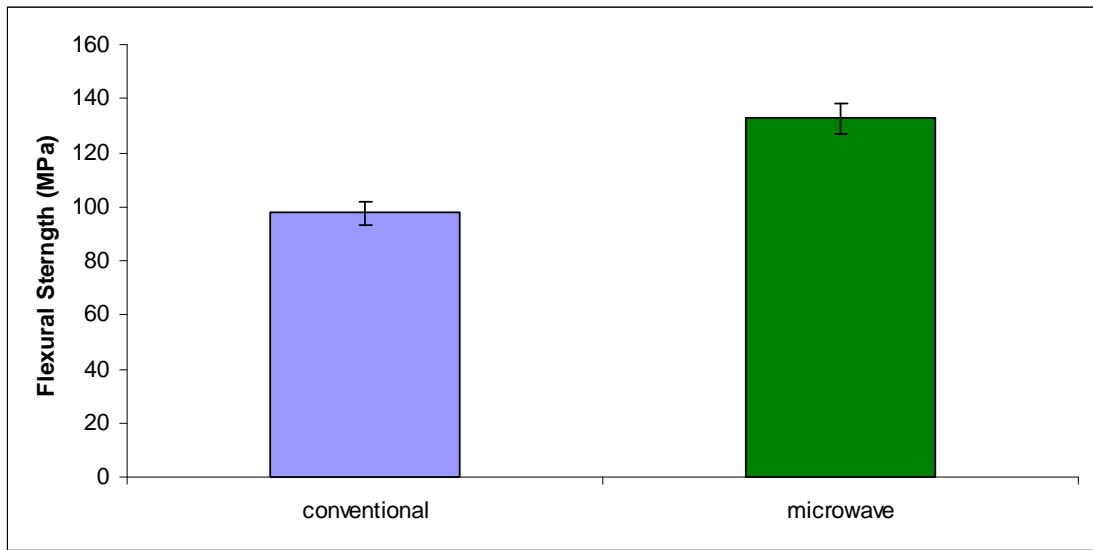


Figure 6.29 Bar chat of Average flexural strength values of conventional and microwave cured samples of Araldite LY 5052 / 4 4' DDS epoxy system with an amine / epoxy ratio of 0.85.

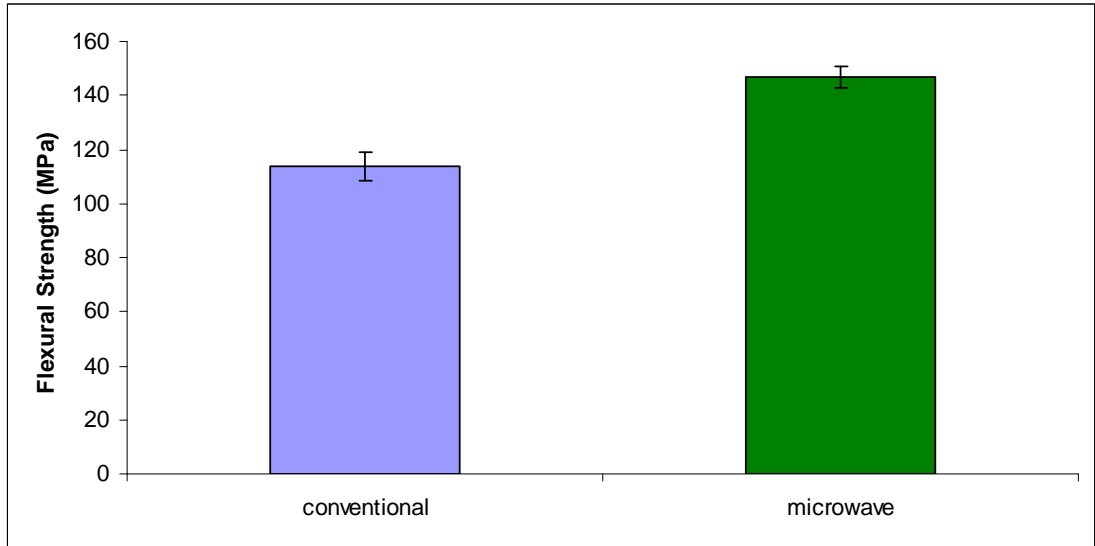


Figure 6.30 Bar chart of Average flexural strength values of conventional and microwave cured samples of Araldite LY 5052 / 4 4' DDS epoxy system with an amine / epoxy ratio of 1.0.

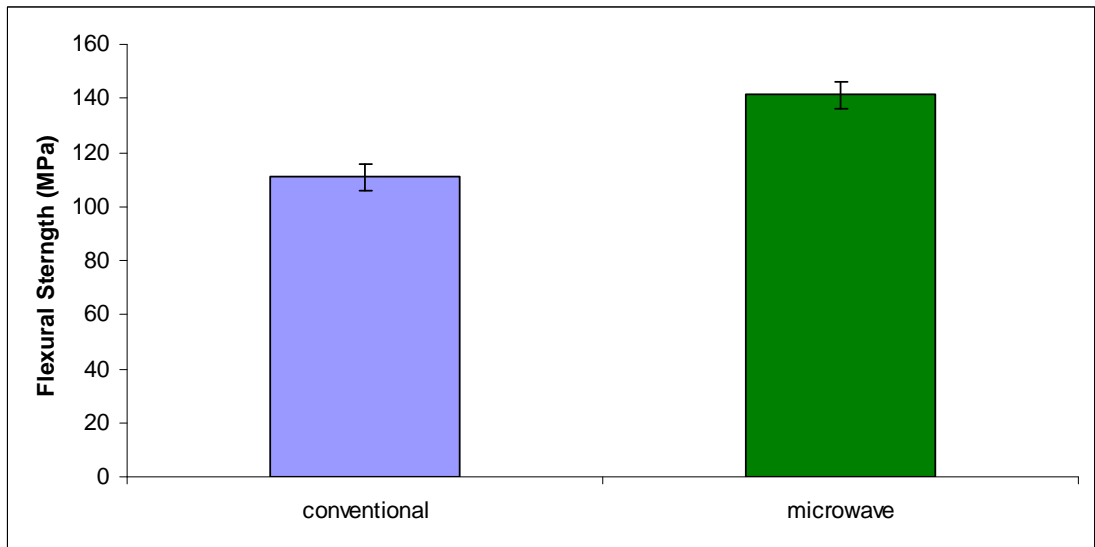


Figure 6.31 Bar chart of Average flexural strength values of conventional and microwave cured samples of Araldite DLS 772 / 4 4' DDS epoxy system with an amine / epoxy ratio of 0.8.

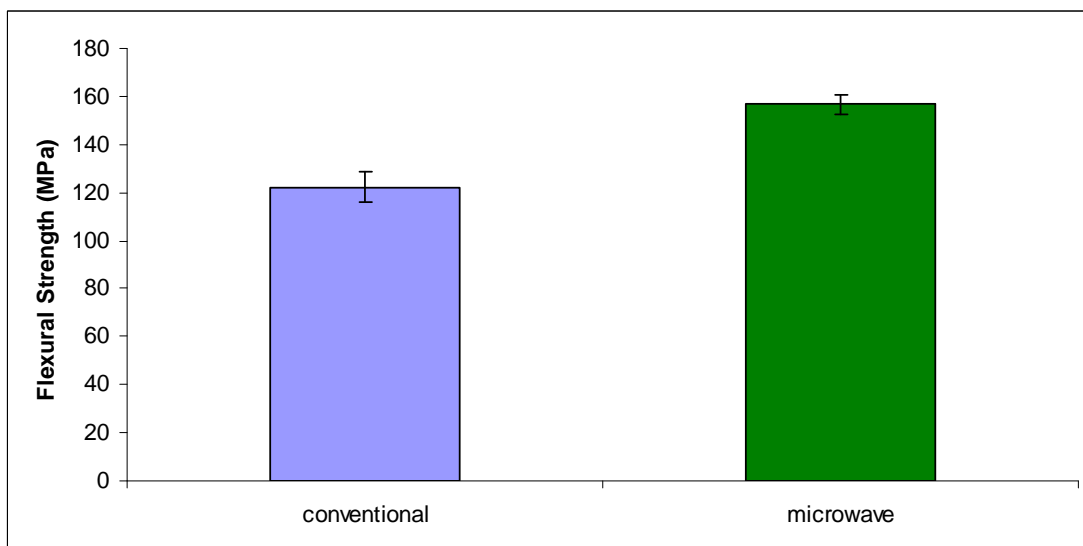


Figure 6.32 Bar chart of Average flexural strength values of conventional and microwave cured samples of Araldite DLS 772 / 4 4' DDS epoxy system with an amine / epoxy ratio of 1.1.

The results showed that the microwave cured samples had higher flexural strengths and modulus than conventionally cured samples. This suggests that microwave cured samples are stronger and stiffer than conventional cured samples, giving more credence to the argument that the molecular network structure are more packed in microwave cured samples. These results are in good agreement with the higher T_g and higher cross-link density. Singer *et al* [106] attributed their findings to a better alignment of the molecules exposed to the electric field. This alignment may produce a higher molecular packing with lower free volume and higher density resulting in a higher modulus for microwave-cured samples. Bai *et al* [107] suggested that the differences in tensile properties could be attributed to a greater homogeneity of the microwave cured resin. Navabnour *et al* [54, 55] observed a fifteen percent increase in the flexural modulus and the flexural strength of microwave cured samples, suggesting that this enhancement was as a result of a reduction in the residual stresses in the microwave cured samples brought upon as a result of a better temperature control associated with microwave heating.

6.7 Summary

In this chapter, we observed that for both Araldite LY 5052 / 4 4 DDS and Araldite DLS 772 / 4 4' DDS epoxy systems,

- i) The density of the fully cured microwave samples was higher than the density of the conventionally cured samples.
- ii) The glass transition temperature for the microwave cured samples were higher than the glass transition temperature of conventionally cured samples.
- iii) The microwave cured samples had higher cross-link densities and lower average molecular weight between crosslinks than the conventionally cured samples. This indicated that the microwave cured samples were more compact.
- iv) The microwave cured samples had a higher flexural strength and modulus than conventionally cured samples.

CHAPTER SEVEN

7.0 DECOMPOSITION AND CHEMICAL ANALYSIS OF CURED EPOXY SYSTEM USING MICROWAVE REACTION SYSTEM

7.1 Introduction

Fully cured epoxy samples of conventional and microwave cured Araldite DLS 772 / 4 4' DDS with an amine to epoxy ratio of 0.8M were dissolved in 4M nitric acid in a microwave reaction system at a temperature of 120 °C for a total of 75 minutes. The dissolved compound was collected and dried. High Performance Liquid Chromatography was used to analyse and separate the components in the compound. Infrared spectroscopy, nuclear magnetic resonance spectroscopy and electrospray ionization mass spectrometry was used to identify the dissolved product.

7.2 Decomposition of fully cured Araldite DLS 772 / 4 4' DDS with amine / epoxy ratio of 0.8

Fully cured samples of Araldite DLS 772 / 4 4' DDS with an amine / epoxy ratio of 0.8 were cut into small rectangular pieces of between 1 – 2 grammes. They were put in reaction vessels described in section 3.18. 20 ml of 4M HNO₃ was added to each reaction vessel. The vessels were then placed in the microwave reaction system. The samples were heated in the reaction vessels to a temperature of 120 °C and held at this temperature for about 25 minutes. This experiment was repeated three times. It took a total of 75 minutes for the sample to be completely dissolved in the nitric acid.

Figures 7.1 and 7.2 show the fully cured samples of microwave cured Araldite DLS 772 / 4 4' DDS with amine / epoxy ratio of 0.8 at 180 °C for 240 minutes before and after decomposition in the microwave reaction system.

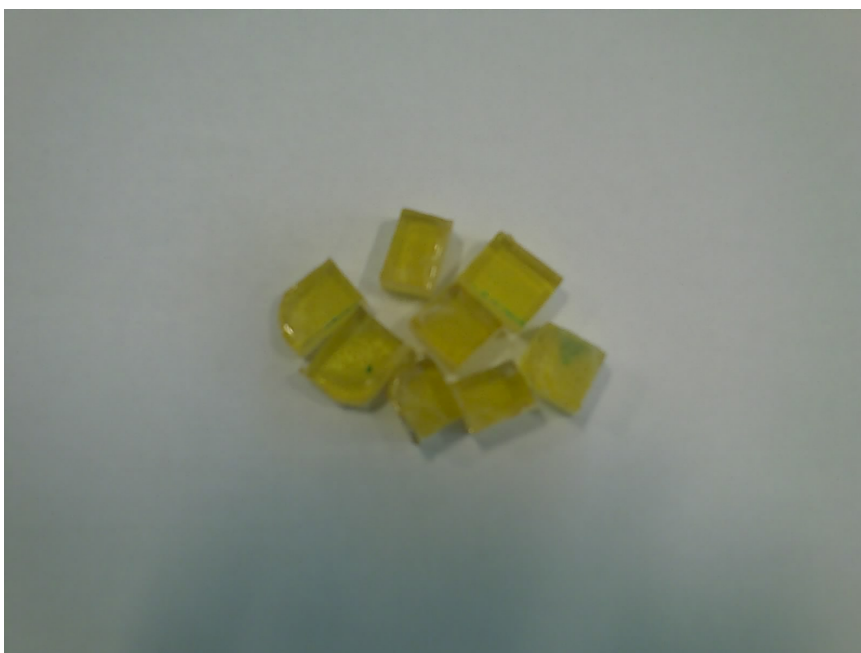


Figure 7.1 Fully cured sample of Araldite DLS 772 / 4 4' DDS with an amine / epoxy ratio of 0.8 before decomposition in Microwave Reaction System



Figure 7.2 Product obtained after decomposition of fully cured samples of Araldite DLS 772 / 4 4' DDS with an amine / epoxy ratio of 0.8 after decomposition at 120 °C for a total of 75 minutes in Microwave Reaction System.

The compounds which made up the decomposed epoxy system were determined. High Performance Liquid Chromatography HPLC was used to separate the peaks. Infrared spectroscopy, nuclear magnetic resonance spectrometry and mass spectrometry were used to identify the decomposed compound.

10 micro-litres of 10mg / mol concentration of the decomposed product was injected through the HPLC analytical system to test for purity and the constituents in the product. The analytical results for the dissolved epoxy systems are shown in the figures 7.3 and 7.4.

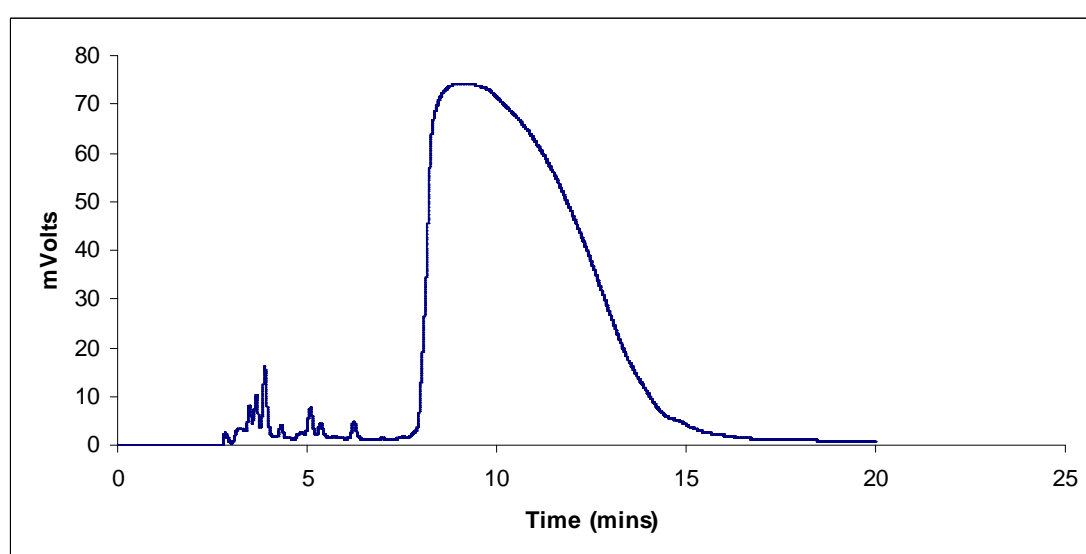


Figure 7.3 HPLC trace results of decomposed product of fully conventionally cured Araldite DLS 772 / 4 4'DDS epoxy system with an amine / epoxy ratio of 0.8 passed through a silica column using 50 : 50 Hexane / Ethyl acetate as solvents and detected at 254 nm.

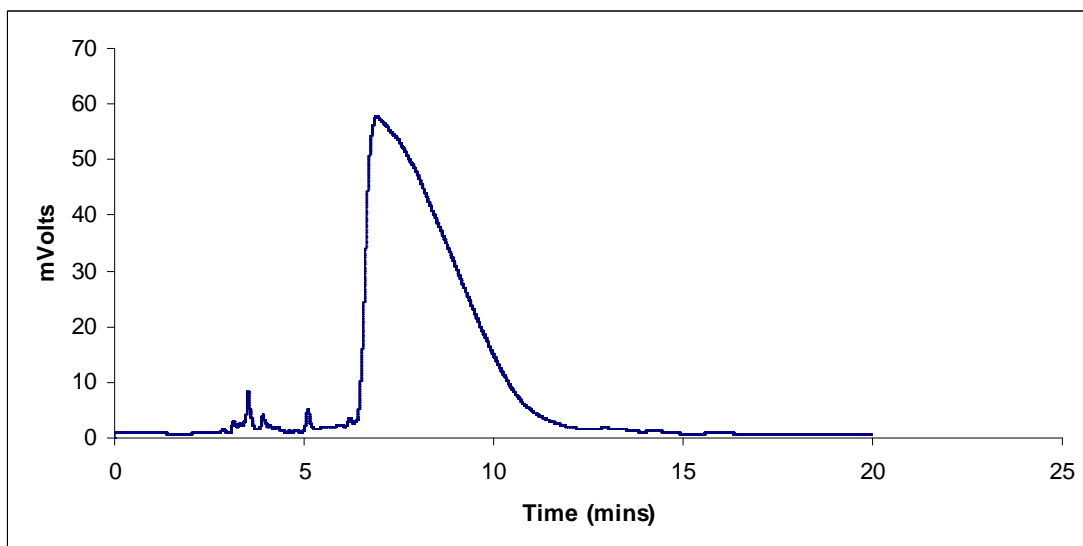


Figure 7.4 HPLC trace results of decomposed product of fully microwave cured Araldite DLS 772 / 4 4'DDS epoxy system with an amine / epoxy ratio of 0.8 passed through a silica column using 50 : 50 Hexane / Ethyl acetate as solvents and detected at 254nm.

The figures 7.3 and 7.4 above show a broad peak. This broad peak suggests that a range of similar compounds were probably eluted. The broadness of the peak also occurs when the compound is strongly absorbed on the silica column. This is usually the case when the compound is polar. Some of the end groups of the compound stuck longer to the silica as it was being forced through the pump. Polar compounds attach themselves chemically to the silica column

In order to collect and analyse the major peak, a much stronger concentration of about 100 mg / mol was prepared. 100 microlitres was injected into the pump controlled HPLC system. The chart recorder was used to monitor the elution of the sample to be collected.

The collected sample was rerun by analytical HPLC to confirm the purity of the collected peak.

The results of the rerun analytical HPLC test for purity for each epoxy system are shown in the figures 7.5 and 7.6 below.

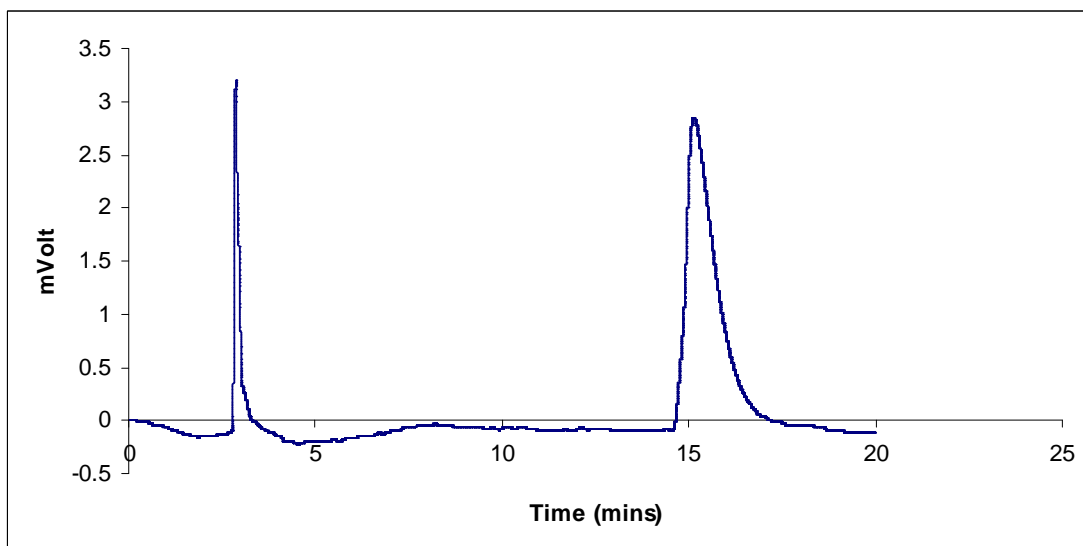


Figure 7.5 Analytical HPLC trace results of collected isolated compound of decomposed conventional cured Araldite DLS 772 / 4 4'DDS epoxy system with an amine / epoxy ratio of 0.8.

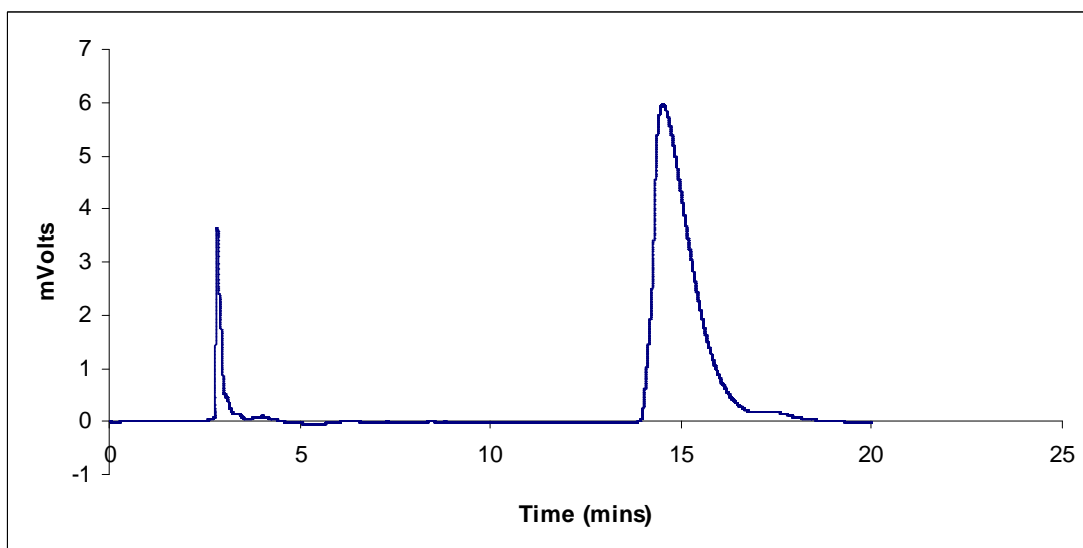


Figure 7.6 Analytical HPLC trace results of collected isolated compound of decomposed conventional cured Araldite DLS 772 / 4 4'DDS epoxy system with an amine / epoxy ratio of 0.8.

The figure above shows two peaks. The first peak is the solvent front. It usually comes out about two minutes after the sample is injected in the HPLC instrument machine using 50 : 50 hexane/ethyl acetate solvent mixture. This solvent front is probably ethyl

acetate. It absorbs at about the same UV at 254 nm. The second peak also shows that isolated compound seem to consist of a range of similar compounds in the solvent collected from the HPLC pump system.

A rotary evaporator was used to dry the collected compound, leaving the just the residue.

7.3 Fourier Transform Infrared Spectroscopy

Infra red spectra were taken of the residue samples. The spectra of the samples are shown in figures 7.7 and 7.8 below.

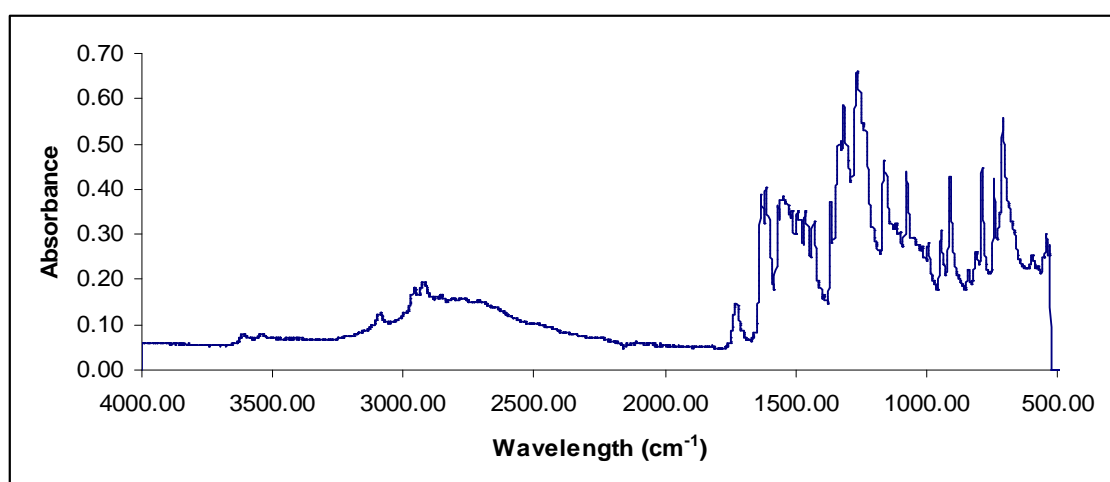


Figure 7.7 Infrared spectra of dried isolated compound collected from the decomposed product of cured Araldite DLS 772 / 4 4' DDS with an amine / epoxy ratio of 0.8

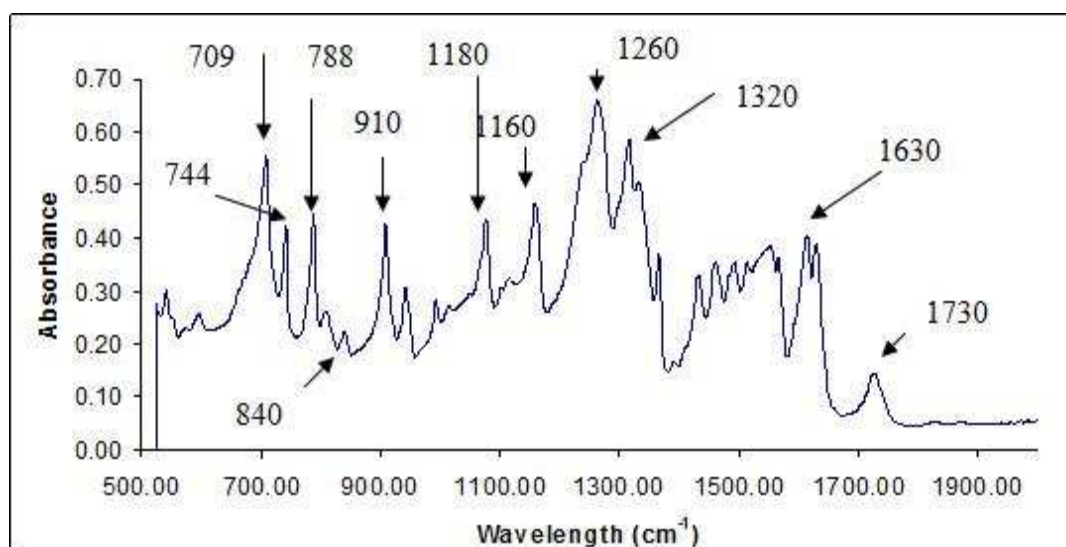


Figure 7.8 Expanded view of Infrared spectra of dried isolated compound collected from the decomposed product of cured Araldite DLS 772 / 4 4' DDS with an amine / epoxy ratio of 0.8

Figure 7.8 above shows the infrared spectra for the isolated compound of the dissolved microwave cured Araldite DLS 772 / 4 4 DDS. The peaks at 709 cm^{-1} and 788 cm^{-1} correspond to the monosubstituted benzene and meta-disubstituted benzene bands respectively. The peak at 1430 cm^{-1} is the aromatic C=C bond [70, 108, 109]. The absorption peaks at 1020 cm^{-1} and 1080 cm^{-1} correspond to the aliphatic amine band. The aromatic ethers C-O bond is represented by the absorption peak at 1260 cm^{-1} , while there is also an aromatic nitro bond N-O at 1320 cm^{-1} [110, 111]. A tertiary alcohol which is represented in the band 1160 cm^{-1} . The absorption peak at 1730 cm^{-1} signifies an ester or a carboxylic acid C=O bond [70, 108]. The FT-IR spectrum reveals that the compound contains some benzene rings, aromatics, amine and an ester or carboxylic acid.

7.4 Nuclear Magnetic Resonance

^1H -NMR and ^{13}C -NMR spectroscopy were used to determine the chemical structure of the unknown compound. The ^1H -NMR and ^{13}C -NMR spectroscopy measurements are described in section 3.19. The ^1H nucleus is the most commonly observed nucleus in NMR spectroscopy. This is because hydrogen is found throughout most organic molecules. The proton has high intrinsic sensitivity [112, 113]. It is also almost 100% abundant in nature. These factors make it a favourable nucleus to observe. The proton spectrum contains a wealth of chemical shifts and coupling information. This is a starting point for most structure determinations [114]. The ^1H -NMR spectra of the unknown compound is shown in figure 8.9 below

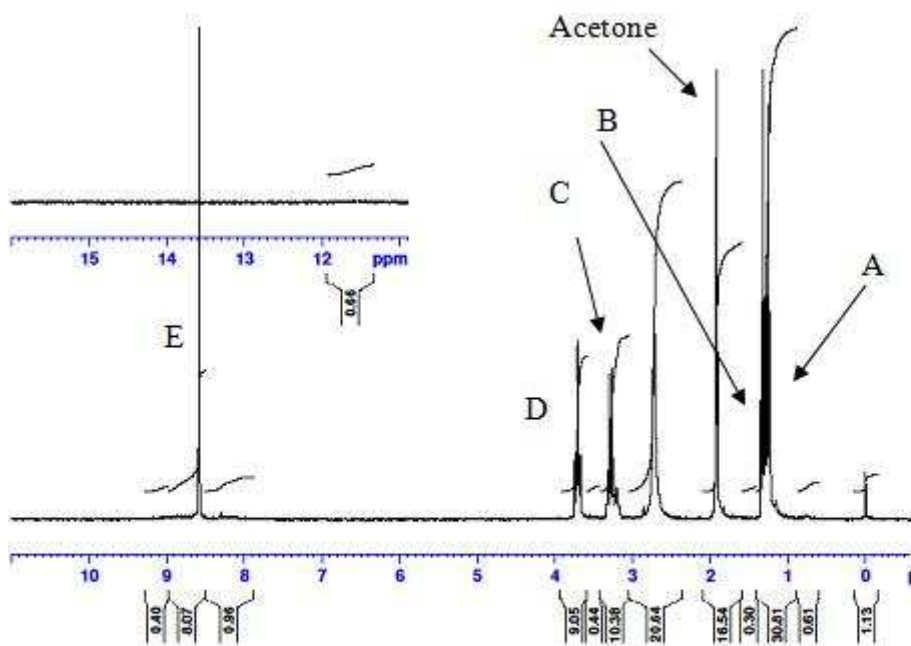


Figure 7.9 $^1\text{H-NMR}$ spectra of dried isolated compound collected from the decomposed product of cured Araldite DLS 772 / 4 4' DDS with an amine / epoxy ratio of 0.8

The $^1\text{H-NMR}$ spectrum of the unknown compound is shown in figure 7.9. The compound was dissolved in deuterated acetone before the NMR analysis. The deuterated acetone solvent gave rise to a peak at 2.09 parts per million (ppm). Two triplet absorbances at areas of 1.38 and 1.45 ppm were attributed to the methyl groups present in the compound [70, 113, 115]. Two quartet absorbances at areas of 3.40 and 3.85 ppm due to the presence of methylene groups in the compound which are separately connected with nitrogen and oxygen [70, 75]. There is a quartet as a result of spin-spin splitting which creates one more peak than the number of hydrogens adjacent to it. The quartet means that they are next to 3 hydrogens or a terminal CH_3 group. One methylene quartet is attached to a nitrogen atom, while the other methylene quartet at 3.85 ppm is directly bonded to the strongly deshielding O_2 or a carbonyl atom [116]. The more electronegative an atom is, the more electron time it will draw away from the nucleus. This will make the atom more deshielded, making the chemical shift move further downfield [74, 113]. There is a single sharp peak at 8.71 ppm. This peak is generated from the resonance of the aromatic protons. The presence of this single peak is an indication that the aromatic ring is symmetric. Another reason for this single peak is because the proton is next to no other hydrogen. Due to an absence of other hydrogens, the local magnetic field induced by the nucleus of other protons will not

cause a multiplet of peaks. Rather, there is just a single peak [70, 113]. The downfield shift of the aromatic peak is as a result of the nitration of the aromatic ring during the decomposition of the cured resin causes a downward shift in the aromatic peak. Nitrogen, being an electronegative atom, withdraws electron density. This consequently reduces the magnitude of the local magnetic field. The nitrogen atom deshields the aromatic proton from the applied magnetic field. As a result of this, the aromatic proton experiences a slightly weaker magnetic field and resonance occurs at a higher ppm [116]

7.5 ¹³C-NMR and Distortion Enhancement by Polarization Transfer (DEPT)

¹³C-NMR and DEPT were used to obtain more information about the backbone structure of the unknown compound. The ¹³C-NMR spectrum of the compound is shown in figure 7.10. The ¹³C-NMR spectrum is usually recorded with broadband decoupling of all protons. This removes multiplicity in carbon resonances. As a result, the doublet, triplet and quartet patterns which are indicative of CH, CH₂ and CH₃ groups are not seen, and each carbon resonance appears as a singlet, increasing sensitivity[117, 118]. Each peak identifies a carbon atom in a different environment within the molecule. There are different ranges of chemical shifts for different carbon environments.

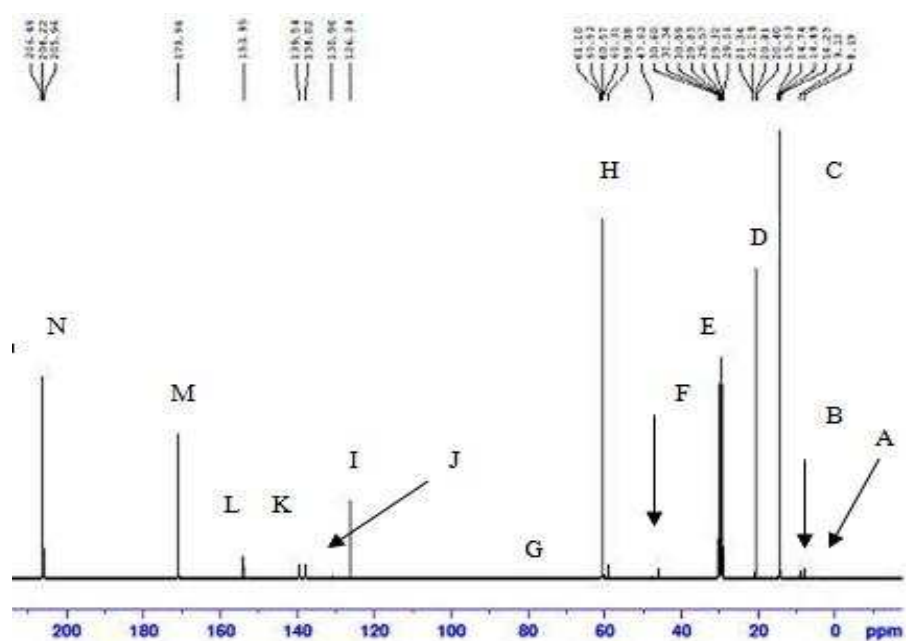


Figure 7.10 ^{13}C -NMR spectra of dried isolated compound collected from the decomposed product of microwave cured Araldite DLS 772 / 4 4' DDS with an amine / epoxy ratio of 0.8

Each chemically distinct carbon atom gave rise to a single peak in its normal ^{13}C NMR spectrum. The peaks at 47.6 and 60 ppm arose as a result of different carbons singly bonded to an oxygen atom. The external magnetic field experienced by the carbon nuclei is affected by the electronegativity of the atoms attached to them. The effect of this is that the chemical shift of the carbon increases if an atom like oxygen is attached to it [74, 119]. This is because the electronegative oxygen pulls electrons away from the carbon nucleus thereby leaving it more exposed to any external magnetic field. This means that a smaller external magnetic field will be needed to bring the nucleus into the resonance condition than if it was attached to less electronegative atoms [119, 120]. The peak at 170 ppm is a carbonyl resonance which is due to a carbon in a carbon – oxygen double bond in an acid or ester. The peaks at 126.3, 130.9, 139.5, and 153 ppm are typical for carbons in an aromatic benzene ring [70, 117, 121]. The triplet peak around 30 and 206 ppm are as a result of the carbon atoms present in the solvent.

7.6 Distortion Enhancement Polarisation Transfer

There are four possible types of carbon atoms. They are methyl (CH_3), methylene (CH_2), methane (CH) and quaternary carbon (C) [116]. The carbon type depends on the number of hydrogens directly attached to a particular carbon atom. The ^{13}C NMR does not give any information as to the types of carbon present in the spectrum [116].

Distortion Enhancement by Polarization Transfer (DEPT) is used to differentiate the carbon types. In DEPT with $\theta = 90^\circ$ spectrum, only CH carbons appear as positive signals. In DEPT with $\theta = 135^\circ$ spectrum, CH and CH_3 carbons produce positive peaks while CH_2 carbons produce negative peaks. Quaternary carbons do not appear in the DEPT spectra. Any extra peaks found in the normal ^{13}C spectrum are due to quaternary carbons. The DEPT with $\theta = 90^\circ$ and DEPT with $\theta = 135^\circ$ spectrum of the unknown compound are shown in figures 7.11 and 7.12 below

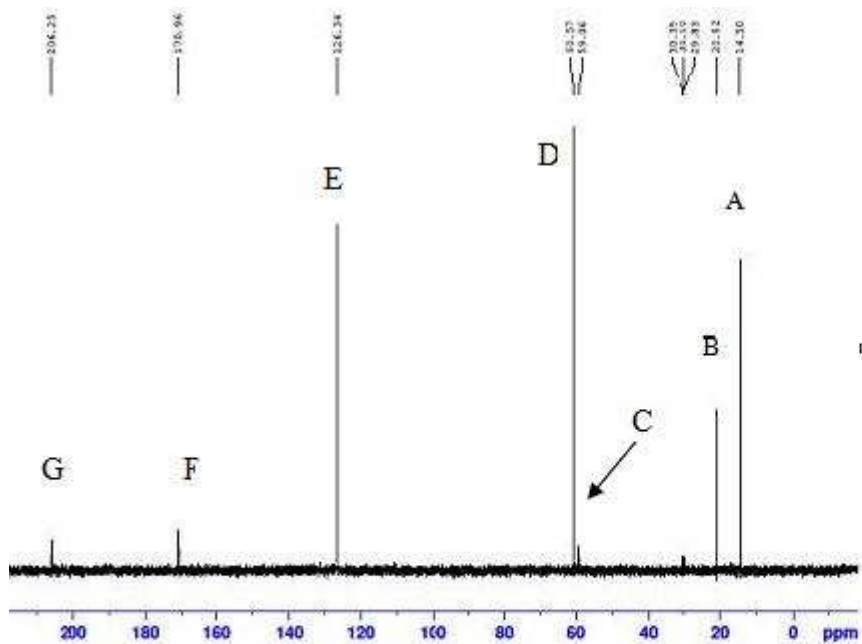


Figure 7.11 DEPT with $\theta = 90^\circ$ spectra of dried isolated compound collected from the decomposed product of microwave cured Araldite DLS 772 / 4 4' DDS with an amine / epoxy ratio of 0.8.

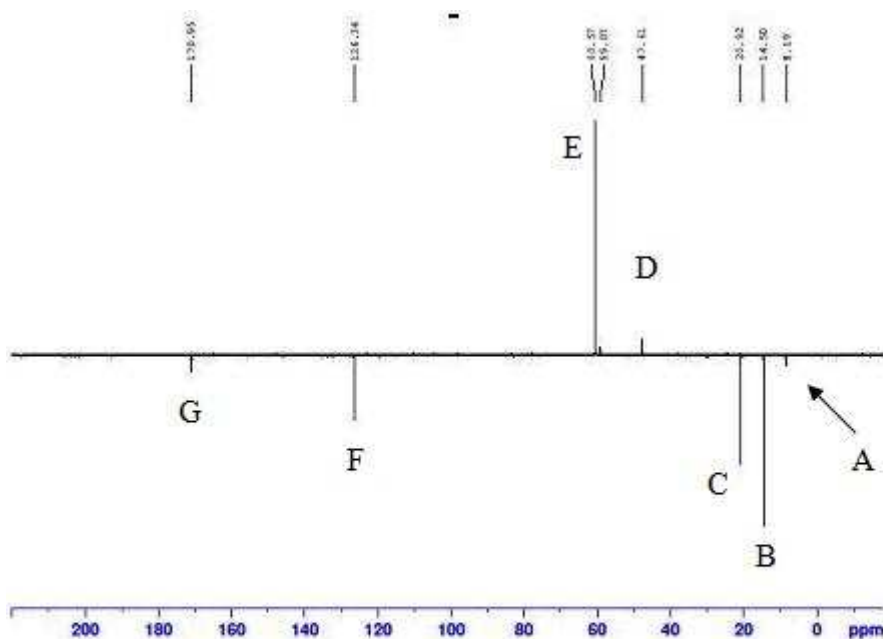


Figure 7.12 DEPT with $\theta = 135^\circ$ spectra of dried isolated compound collected from the decomposed product of microwave cured Araldite DLS 772 / 4 4' DDS with an amine / epoxy ratio of 0.8.

The DEPT with $\theta = 90^\circ$ spectra in figure 7.11 identifies CH resonances at 170.9, 126.3, 60.57, 20.82 and 14.5 ppm. The DEPT with $\theta = 135^\circ$ spectra in figure 7.12 identifies the CH₂ resonance as negative peaks at 126.3, 20.8, and 14.5 ppm. Since the DEPT with $\theta = 135^\circ$ spectra shows both CH₃ and CHs as positive peaks, the peaks at 47.6 and 8.19 ppm can be quickly identified as CH₃ resonances by comparing it to figure 7.11 which only shows CHs as positive peaks. The absence of the peaks 153 and 139 ppm in the DEPT spectra indicates that they are quaternary carbons. The peaks 29-31 ppm and 206 ppm arise from the carbon atoms present in the solvent (acetone) used for the NMR analysis.

7.7 Heteronuclear Multiple-Quantum Correlation

In Heteronuclear Multiple-Quantum Correlation experiment, two different types of nuclei (¹H and ¹³C) are correlated into a 2-dimensional experiment by the evolution and transfer of single quantum coherence [122, 123]. It offers a means of identifying 1-bond H-C activities within a molecule. One dimension represents the ¹H chemical shift, while the other represents the ¹³C chemical shift. Crosspeaks indicate a one-bond ¹H-¹³C connectivity. The HSQC technique relies on magnetisation transfer from the proton to its directly attached atom, and back on to the proton. As a result of this magnetisation transfer, no responses are expected for non-protonated carbons, or for protons bound to other heteroatoms [122-124].

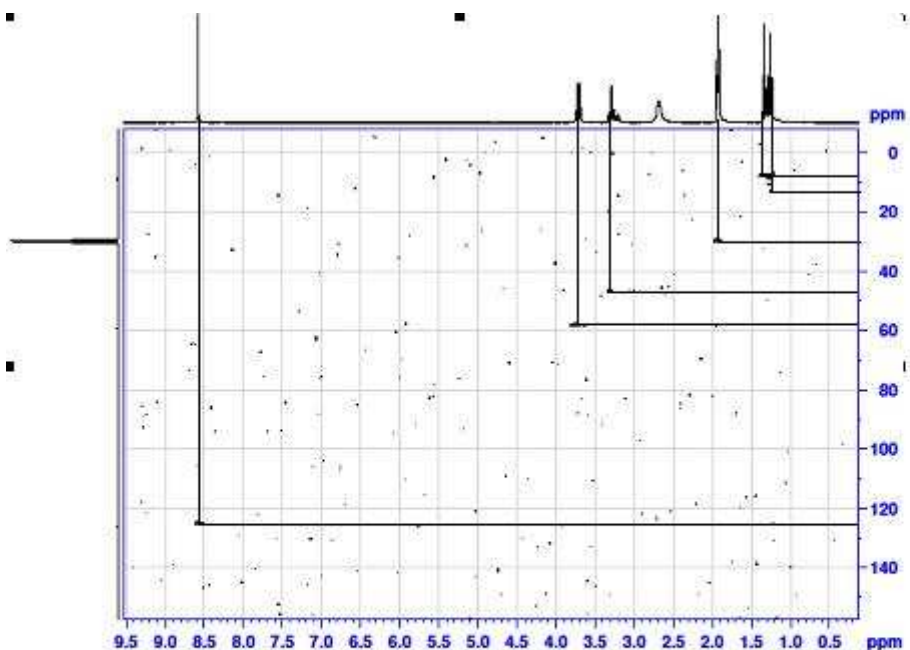


Figure 7.13 HSQC spectra of dried isolated compound collected from the decomposed product of microwave cured Araldite DLS 772 / 4 4' DDS with an amine / epoxy ratio of 0.8.

Figure 7.13 shows the HSQC spectra for the unknown compound. Here the ^1H protons from the ^1H -NMR spectra are related to the carbon atoms from the ^{13}C -NMR spectra. From the figure above, the aromatic proton indicated at peak 8.7 ppm is directly bonded to the aromatic carbon atom at about 126 ppm. The signals at 3.85 ppm which are characteristic for the methylene protons attached to O_2 is directly bonded to the carbon atoms of the methylene group at 60 ppm in the ^{13}C -NMR spectra. The methylene quartet at 3.4 ppm is bonded to the carbon atoms of methylene at 47 ppm. The signals appearing at 1.38 and 1.45 ppm which indicate methyl groups are bonded to the carbon atoms of the methyl groups at 9.1 ppm and 11 ppm.

From the above ^1H -NMR, ^{13}C -NMR, DEPT with $\theta = 90^\circ$, DEPT with $\theta = 135^\circ$ and the infrared spectra of the isolated compound, it is observed that there are two ethyl ester groups and an amine bound to the benzene ring. The analysis suggests the unknown compound is identified as 1, 3 – di(ethyl ester)-5-(diethyl amino)-2-hydroxybenzene. Its chemical structure is shown in the figure 7.14 below.

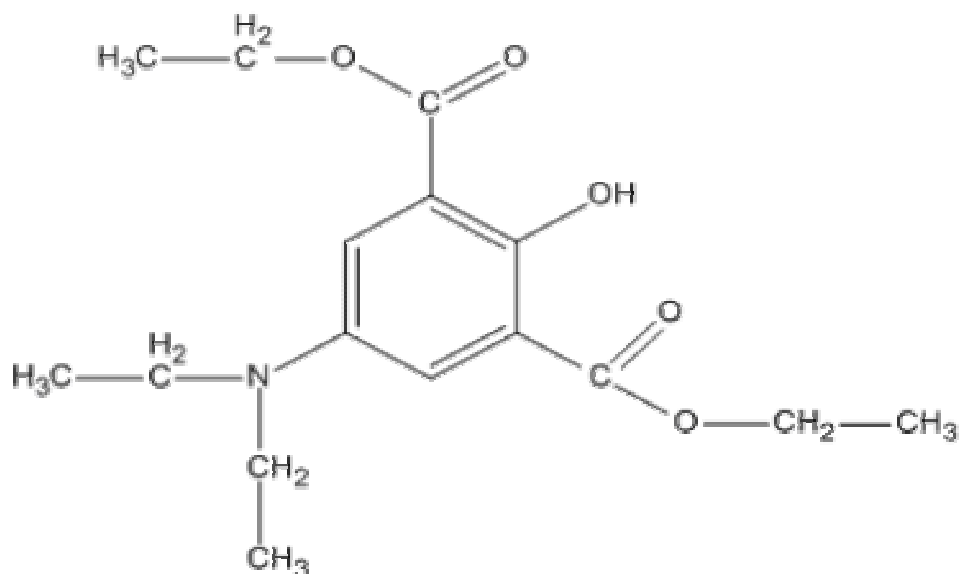


Figure 7.14 Structure of 1, 3 – di(ethyl ester)-5-(diethyl amino)-2-hydroxybenzene.

The assignment of the peaks of the $^1\text{H-NMR}$ spectrum of 1, 3 – di(ethyl ester)-5-(diethyl amino)-2-hydroxybenzene from figure 7.9 is tabulated in table 7.1 below.

Table 7.1 Assignment of peaks of the $^1\text{H-NMR}$ spectrum of 1, 3 – di(ethyl ester)-5-(diethyl amino)-2-hydroxybenzene

Peak	Chemical Shift, ppm	Assignment
A	1.38 Methyl CH_3	
B	1.45 Methyl CH_3	

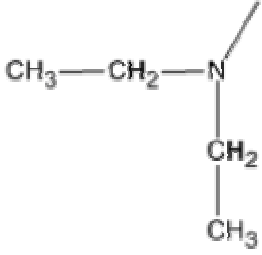
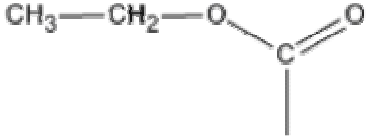
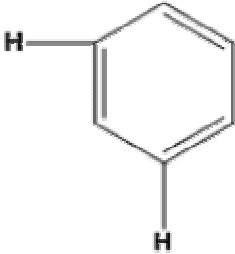
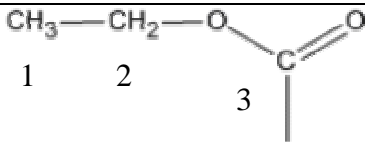
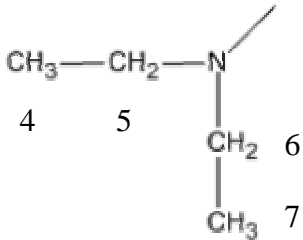
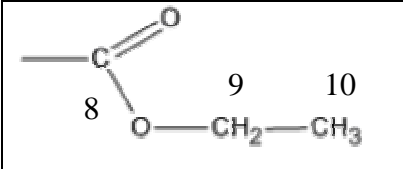
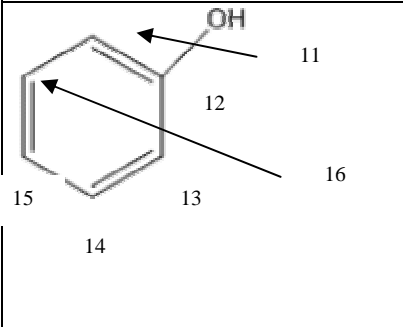
C	3.41 Methylene CH ₂	
D	3.85 Methylene CH ₂	
E	8.71 Benzene	

Table 7.2 below shows the assignment of peaks in the ¹³C NMR spectrum of 1, 3 – di(ethyl ester)-5-(diethyl amino)-2-hydroxybenzene from figure 8.10.

Table 7.2 Assignment of peaks of the ¹H-NMR spectrum of 1, 3 – di(ethyl ester)-5-(diethyl amino)-2-hydroxybenzene

Assignment	Peak	Chemical shift (ppm)
	C1	9.1
	C2	59.0
	C3	170.9
	C4	11.5
	C5	47.6
	C6	47.6
	C7	11.5

	C8 C9 C10	170.9 47.6 9.1
	C11 C12 C13 C14 C15 C16	126.3 153.9 126.3 138.0 139.5 138.0

7.8 Electrospray Ionization Mass Spectroscopy

Electrospray Ionization was used to confirm the molecular weight of the compound which was identified as 1, 3 – di(ethyl ester)-5-(diethyl amino)-2-hydroxybenzene. The electrospray ionization spectrum is shown in figure 7.15. A base peak of 332 is identified.

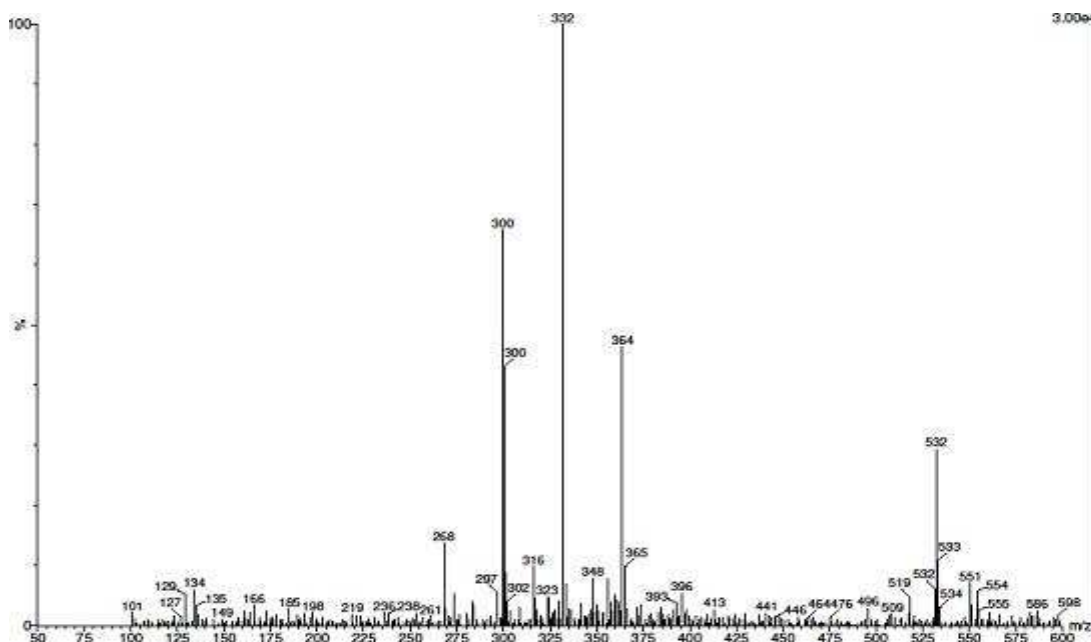


Figure 7.15 Electrospray ionization spectra of 1, 3 – di(ethyl ester)-5-(diethyl amino)-2-hydroxybenzene.

The molecular formula of 1, 3 – di(ethyl ester)-5-(diethyl amino)-2-hydroxybenzene is $C_{16}H_{23}O_5N$. This gives a molecular mass of 309 g mol^{-1} . There is a presence of sodium ion in the electrospray chamber. This sodium ion adds a unit mass of 23 to the molecular ion of the compound. Adding 23 to the molecular mass of 1, 3 – di(ethyl ester)-5-(diethyl amino)-2-hydroxybenzene gives us 332. This value corresponds to the molecular ion peak at m/z 332 which also corresponds to the base peak of the electrospray ionization spectra in figure 7.15. The electrospray ionization mass spectra confirms the molecular mass of 1, 3 – di(ethyl ester)-5-(diethyl amino)-2-hydroxybenzene.

7.9 Summary

Conventional and Microwave cured samples of Araldite DLS 772 / 4 4' DDS were successfully decomposed by a microwave reaction system. The chemical structure of the decomposed product was determined.

CHAPTER EIGHT

8.0 CONCLUSIONS AND SUGGESTIONS FOR FUTURE WORK

The aims of this study were to compare the curing kinetics, the reaction pathways, the physical and mechanical properties of two epoxy systems prepared by conventional and microwave heating; and also to explore the possibility of the use of microwave energy to decompose fully cured epoxy materials and identify the decomposed products with a view to then exploring potential reuses of these materials.

8.1 Conclusions

Araldite LY 5052 and DLS 772 epoxy resins (supplied by Huntsman, UK) were used for this research. 4,4'-Diaminodiphenyl sulfone was used as a hardener for this study. The curing kinetics of Araldite LY 5052 / 4,4'-DDS and Araldite DLS 772 / 4,4'-DDS epoxy systems were studied "in situ" by means of differential scanning calorimetry (DSC) and a microwave calorimeter under non-isothermal and isothermal conditions. The differences in the curing characteristics of the samples undergoing microwave and conventional heating were observed.

During the non-isothermal curing, the samples cured with conventional heating had a higher onset temperature and a higher exothermic peak temperature than the samples cured using microwave heating. Curing during microwave heating occurred over a smaller temperature range. The reaction rate of microwave-cured samples was higher than the reaction rate of conventionally cured samples. This was indicated by a higher slope of the fractional conversion curve. It took a shorter time for the microwave cured samples to reach the maximum final conversion, suggesting that the curing reaction occurred at a lower temperature. These results can be ascribed to a better efficiency in the energy transfer for microwave heating. An increase was observed in the fractional conversion for microwave-cured samples. This was due to the increase in the mobility of the reactants after gelation. This is caused by the induced polarization of the polymer and monomer molecules along the applied electromagnetic field, causing the consumption of more reactants leading to the formation of a more rigid network.

Kinetic analysis was carried out on the samples cured using conventional and microwave energy. Ozawa's method was used to determine the activation energy for a given fractional conversion, which shows the different stages through which the curing reaction proceeds. The activation energy of the conventionally and the microwave cured samples showed different patterns. For samples cured using conventional heating, the activation energy had a minimum value at the beginning of the reaction, and then increased as the reaction proceeded to a maximum, and then showed a tendency to decrease. The samples cured using microwave energy had a maximum value at the beginning of the reaction, which then decreases as the reaction proceeded until it reached a minimum value after which it began to show a tendency to increase.

Ozawa's method was also applied to the exothermic peak for the determination of activation energy. The results show that for Araldite LY 5052 / 4 4' DDS epoxy system, the activation energy of the microwave-cured samples were higher than the conventionally cured samples, while for the Araldite LY 5052 / 4 4' DDS epoxy system, the activation energy of the conventionally cured samples were higher than the activation energies of the microwave cured samples.

Kissinger's method was also used to study the kinetic analysis in this research. As with the Ozawa method, the activation energies of all the microwave-cured samples were found to be higher than the activation energies of conventionally cured samples for the Araldite LY 5052 / 4 4' DDS epoxy system, while the activation energies for the microwave cured samples were lower than those of the conventionally cured samples for Araldite DLS 772 / 4 4' DDS epoxy system.

A cavity perturbation technique was used to follow the dielectric properties of the microwave cured samples "*in situ*" as the curing reactions proceeded. It was found that the dielectric properties increased as the curing temperature increased until they reached a maximum value, after which it started to decrease. This pattern suggests that the microwave curing reactions of the epoxy systems occur in three phases. The dipoles rotate freely in the initial phase. This rotation leads to an increase in dielectric properties as the temperature increases. In the second phase, there is a decrease in the dielectric properties. This decrease occurs as a result of the formation of a cross-linked network.

This is as a consequence of the reduction in the molecular mobility and the functional polar group during the curing reaction. The formation of a highly cross-linked structure occurs in the third phase, leading to a further reduction in the dielectric properties.

The curing kinetics was also studied for the conventional and microwave curing of Araldite LY 5052 / 4 4' DDS and Araldite DLS 772 / 4 4' DDS epoxy systems under isothermal conditions. Higher rates of reaction were observed for samples cured with microwave heating. The microwave cured samples also had a steeper slope of fractional conversion than the conventionally cured samples.

The kinetic parameters of the isothermal curing reactions of Araldite LY 5052 / 4 4' DDS and Araldite DLS 772 / 4 4' DDS epoxy systems using conventional and microwave heating was determined. The rate constants K_1 and K_2 increased with temperature for both conventional and microwave cured samples. The values of K_1 and K_2 were greater in the microwave cured samples. However, the ratio of K_1 / K_2 was found to be lower in microwave curing than in conventional curing. These lower values have been attributed to the enhancement of the catalytic reaction over the non-catalytic reaction by microwave radiation which occurs as a result of the high activity of the [OH] group in the microwave field [26].

The activation energies of the rate constants were also determined. For Araldite LY 5052 / 4 4' DDS and Araldite DLS 772 / 4 4' DDS epoxy systems, it was found that the microwave cured samples had lower activation energy values compared to conventionally cured samples.

The infrared spectra of microwave and conventionally cured samples were found to be similar. This suggested that the curing reaction for conventional and microwave heating follow the same reaction pathway. More epoxide and amine were consumed during the microwave curing than during the conventional curing.

The density of fully cured microwave samples of both Araldite LY 5052 / 4 4' DDS and Araldite DLS 772 / 4 4' DDS epoxy systems were higher than the density of conventionally cured samples. This indicated that the network structure of microwave

cured samples was more packed than conventionally cured samples. This suggested different morphologies in the network structures.

The morphologies of the network structures were also studied with dynamic mechanical thermal analysis. The glass transition temperature for the microwave cured samples was found to be higher than the glass transition temperature of the conventionally cured samples for both Araldite LY 5052 / 4 4' DDS and Araldite DLS 772 / 4 4' DDS epoxy systems. The microwave cured samples also had higher cross-link densities and lower molecular weight between cross-links than the conventionally cured samples. This meant that the network structure in the conventionally cured samples was more loosely packed than the network structure in microwave cured samples.

The results of the flexural tests for the fully cured samples show that the microwave cured samples of Araldite LY 5052 / 4 4' DDS and Araldite DLS 772 / 4 4' DDS epoxy resins have a higher flexural strength and modulus than conventionally cured samples, suggesting a better stiffness and strength in the microwave cured samples. This improved stiffness is ascribed to a better molecular alignment and a greater homogeneity which is found in the microwave cured samples.

A microwave reaction system was used to successfully dissolve conventional and microwave cured samples of Araldite DLS 772 / 4 4' DDS epoxy system. The chemical structure of the decomposed product was determined.

8.2 Suggestions for further work

1. Although the TM_{010} microwave was designed so the maximum strength of the electromagnetic field was at the centre of the cavity, the presence of PTFE mould affected the distribution of the electromagnetic field in the TM_{010} microwave cavity, reducing the strength of the electromagnetic field at the centre of the cavity. This had an effect on the preparation of plaques for mechanical and physical testing because the electromagnetic field strength in the centre of the cavity, leaving the centre of the sample not fully cured. However, this problem was overcome by the use of very low heating rates ($1-2 \text{ K min}^{-1}$).

The cavity should be redesigned or modified so that the presence of the PTFE mould would not affect the distribution of the electromagnetic field.

2. A technique which can make dielectric measurements during conventional curing needs to be purchased. This will enable comparative data to be obtained.
3. Studies should be carried out on the possibility of converting 1,3 di(ethylester)-5-(diethylamino)-2-hydroxybenzene into an epoxy novolak resin, or a compound with epoxide or ethylene oxide groups for reuse in materials processing.
4. Attempts should be made on incorporating 1,3 di(ethylester)-5-(diethylamino)-2-hydroxybenzene in the formulation of new epoxy systems. Cure kinetics reaction study should be carried out on these epoxy systems and the kinetic parameters should be explored. The physical and mechanical properties of the epoxy systems should be studied.

REFERENCES

1. <http://www.azom.com/details.asp?ArticleID=1098>. [cited 2010 October 06].
2. Boey, F.Y.C. and B.H. Yap, *Microwave curing of an epoxy-amine system: effect of curing agent on the glass-transition temperature*. *Polymer testing*, 2001. **20**(8): p. 837-845.
3. Ayats, J.C., *MICROWAVE CURING OF A*.
4. Hill, D.J.T., G.A. George, and D.G. Rogers, *A systematic study of the microwave and thermal cure kinetics of the DGEBA/DDS and DGEBA/DDM epoxy-amine resin systems*. *Polymers for Advanced Technologies*, 2002. **13**(5): p. 353-362.
5. Dang, W., et al., *An approach to chemical recycling of epoxy resin cured with amine using nitric acid*. *Polymer*, 2002. **43**(10): p. 2953-2958.
6. Dilafruz, K., et al. *Chemical recycling bisphenol A type epoxy resin based on degradation in nitric acid*. 2003.
7. Yoshioka, T., T. Sato, and A. Okuwaki, *Hydrolysis of Waste PET by Sulfuric Acid at 150 for a Chemical Recycling*. *Journal of Applied Polymer Science*, 1994(52): p. 1353-1355.
8. Zhang, Z., et al., *Chemical recycling of waste polystyrene into styrene over solid acids and bases*. *Industrial & Engineering Chemistry Research*, 1995. **34**(12): p. 4514-4519.
9. Lee, H. and K. Neville, *Epoxy Resins: Their Applications and Technology*. First Edition ed. 1957.
10. Brydson, J.A., *Plastic Materials*. Sixth ed. 1995.
11. Lee, H. and K. Neville, *Handbook of Epoxy Resins*. 1967.
12. May, C.A., *Epoxy Resins: Chemistry And Technology*. 1987: CRC Press.
13. Bruins, P., *Epoxy Resin Technology*. 1968: Interscience Publishers.
14. in *Three Bond Technical News*. 1990, 32. p. 1-5.
15. Ghoul, C., *Microwave Curing of Diglycidyl Ether of Bisphenol A / Dicyandiamide Resin System*, in *Materials Science*. 2003, University of Manchester.
16. Costa, M., L. Pardini, and M. Rezende, *Influence of Aromatic Hardeners in the cure kinetics*. *Materials Research*, 2005. **8**: p. 65-70.

17. Baden Fuller, A.J., *Microwaves: An Introduction to Microwave Theory and Techniques*. Third Edition ed. 1990.
18. Hammond, P., *Electromagnetism for Engineers*. Third ed. 1986: Pergamon.
19. Hammond, P., *Applied Electromagnetism*. 1971: Pergamon.
20. Collin, R.E., *Foundations for Microwave Engineering*. 1966: McGraw-Hill.
21. Metaxas, A.C. and R.J. Meredith, *Industrial Microwave Heating*. 1988: Peter Peregrinus Ltd.
22. Ramo, S., J.R. Whinnery, and T. Van Duzzer, *Field and Waves in Communication Electronics*. Second ed. 1984: Wiley.
23. Stratton, J.A., *Electromagnetic Theory*. 1941: McGraw-Hill.
24. Mingos, D.M. and D.R. Baghurst, *Application of Microwave Dielectric Heating Effects to Synthetic Problems in Chemistry*. Chemical Society Reviews, 1991. **20**: p. 1-47.
25. Decareau, R.V. and R.A. Peterson, *Microwave Processing and Engineering*. Ellis Horwood Series in Food Science and Technology. 1986.
26. Wei, J., M.C. Hawley, and M.T. Demeuse, *Kinetics modeling and time-temperature-transformation diagram of microwave and thermal cure of epoxy resins*. Polymer Engineering and Science, 1995. **35**(6): p. 461-470.
27. Crosby, P.A., et al., Smartmaster Structures, 1996. **5**: p. 415-428.
28. Mijovic, J. and J. Wijaya, *Comparative calorimetric study of epoxy cure by microwave vs thermal energy*. Macromolecules, 1990. **23**(15): p. 3671-3674.
29. De Meuse, M.T. and C.L. Ryan, *The microwave processing of polymeric materials*. Advances in polymer technology, 1993. **12**(2): p. 197-203.
30. Atkins, P.W., *The Elements of Physical Chemistry*. Third Edition ed. 2000.
31. Sichina, W.J., *Better DSC Isothermal Cure Kinetic Studies Using Power Compensation DSC*, P.E. Instruments, Editor.
32. Turi, E.A., *Thermal characterization of polymeric materials(Book)*. New York, Academic Press, 1981. 985 p, 1981.
33. Halley, P.J. and M.E. Mackay, *Chemorheology of thermosets-an overview*. Polymer Engineering and Science, 1996. **36**(5): p. 593-609.
34. Salla, J.M. and X. Ramis, *Comparative study of the cure kinetics of an unsaturated polyester resin using different procedures*. Polymer Engineering and Science, 1996. **36**(6): p. 835-851.

35. Karkanias, P.I., I.K. Partridge, and D. Attwood, *Modelling the cure of a commercial epoxy resin for applications in resin transfer moulding*. Polymer International, 1996. **41**(2): p. 183-191.
36. Kenny, J.M., *Determination of autocatalytic kinetic model parameters describing thermoset cure*. Journal of Applied Polymer Science, 1994. **51**(4): p. 761-764.
37. Ivankovi, M. cacute, and N. zcaron, *DSC study on simultaneous interpenetrating polymer network formation of epoxy resin and unsaturated polyester*. Journal of Applied Polymer Science, 2002. **83**(12): p. 2689-2698.
38. de la Caba, K., et al., *Comparative study by DSC and FTIR techniques of an unsaturated polyester resin cured at different temperatures*. Polymer International, 1998. **45**(4): p. 333-338.
39. Vilas, J.L., et al., *Unsaturated polyester resins cure: Kinetic, rheologic, and mechanical dynamical analysis. I. Cure kinetics by DSC and TSR*. Journal of Applied Polymer Science, 2001. **79**(3): p. 447-457.
40. Zhou, S. and M.C. Hawley, *A study of microwave reaction rate enhancement effect in adhesive bonding of polymers and composites*. Composite Structures, 2003. **61**(4): p. 303-309.
41. Sarrionandia, M., et al., *Analysis of kinetic parameters of an urethane-acrylate resin for pultrusion process*. Journal of Applied Polymer Science, 2000. **77**(2): p. 355-362.
42. Haines, P.J., *Thermal Methods of Analysis : Principles, Applications and Problems*. 1995.
43. Horie, K., et al., *Calorimetric investigation of polymerization reactions. III. Curing reaction of epoxides with amines*. Journal of Polymer Science Part A 1: Polymer Chemistry, 1970. **8**(6): p. 1357-1372.
44. Kamal, M.R. and S. Sourour, *Kinetics and thermal characterization of thermoset cure*. Polymer Engineering & Science, 1973. **13**(1): p. 59-64.
45. Sourour, S. and M.R. Kamal, SPE Technical Papers, 1972. **18**.
46. Málek, J. and J.M. Criado, *Empirical kinetic models in thermal analysis*. Thermochemica Acta, 1992. **203**: p. 25-30.
47. Málek, J. and J.M. Criado, *The shape of a thermoanalytical curve and its kinetic information content*. Thermochemica Acta, 1990. **164**: p. 199-209.

48. Kissinger, H.E., *Reaction kinetics in differential thermal analysis*. Analytical Chemistry, 1957. **29**(11): p. 1702-1706.
49. Ramis, X. and J.M. Salla, *Effect of the initiator content and temperature on the curing of an unsaturated polyester resin*. Journal of Polymer Science Part B: Polymer Physics, 1999. **37**(8): p. 751-768.
50. Ramis, X. and J.M. Salla, *Time-temperature transformation (TTT) cure diagram of an unsaturated polyester resin*. Journal of Polymer Science Part B: Polymer Physics, 1997. **35**(2): p. 371-388.
51. Salla, J.M. and X. Ramis, *A kinetic study of the effect of three catalytic systems on the curing of an unsaturated polyester resin*. Journal of Applied Polymer Science, 1994. **51**(3): p. 453-462.
52. Doyle, C.D., *Kinetic analysis of thermogravimetric data*. Journal of Applied Polymer Science, 1961. **5**(15): p. 285-292.
53. Ozawa, T., *Kinetic analysis of derivative curves in thermal analysis*. Journal of thermal analysis and calorimetry, 1970. **2**(3): p. 301-324.
54. Navabpour, P., et al., *Comparison of the curing kinetics of the RTM6 epoxy resin system using differential scanning calorimetry and a microwave-heated calorimeter*. Journal of Applied Polymer Science, 2006. **99**(6): p. 3658-3668.
55. Navabpour, P., et al., *Comparison of the curing kinetics of a DGEBA/acid anhydride epoxy resin system using differential scanning calorimetry and a microwave-heated calorimeter*. Journal of Applied Polymer Science, 2007. **104**(3): p. 2054-2063.
56. Wei, J., et al., *Comparison of microwave and thermal cure of epoxy resins*. Polymer Engineering and Science, 1993. **33**(17): p. 1132-1140.
57. Marand, E., K.R. Baker, and J.D. Graybeal, *Comparison of reaction mechanisms of epoxy resins undergoing thermal and microwave cure from in situ measurements of microwave dielectric properties and infrared spectroscopy*. Macromolecules, 1992. **25**(8): p. 2243-2252.
58. Wallace, M., et al., *Investigation of the microwave curing of the PR500 epoxy resin system*. Journal of Materials Science, 2006. **41**(18): p. 5862-5869.
59. Rabek, J.F., *Experimental methods in polymer chemistry: physical principles and application*. 1980: John Wiley & Sons New York.
60. Zainol, I., *Microwave Processing of Bismaleimide Resins*. 2001, UMIST.

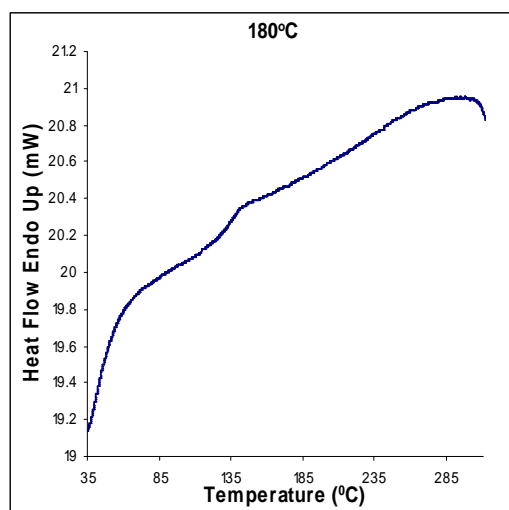
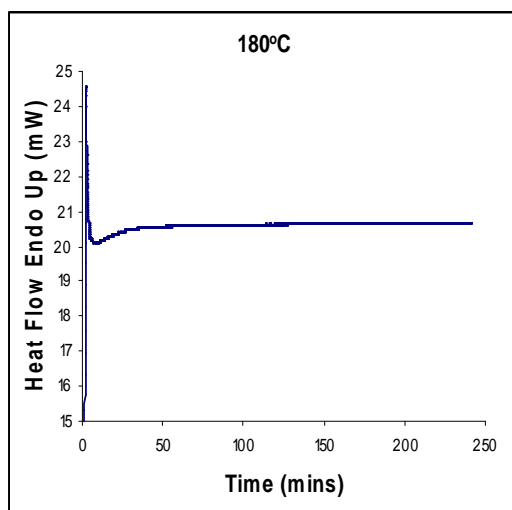
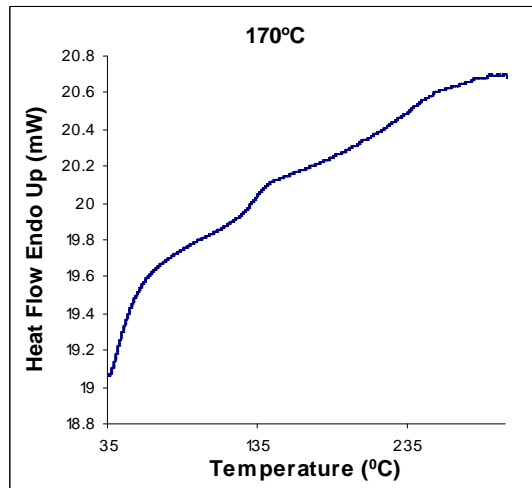
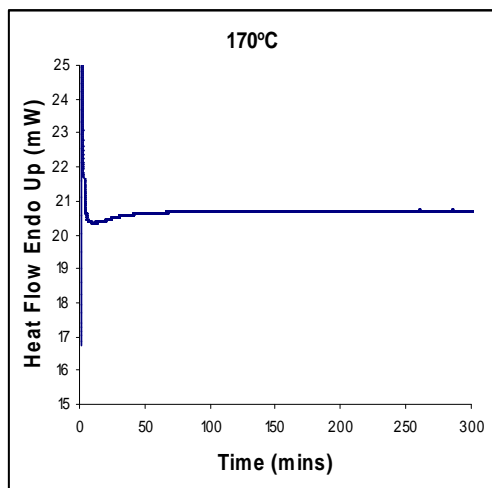
61. Petchuay, S., *The effect of microwave curing on the structure and properties of polymer resins and their blends*, in *Materials Science*. 2004, University of Manchester.
62. Yang, Y.S. and L.J. Lee, *Comparison of thermal and infrared spectroscopic analyses in the formation of polyurethane, unsaturated polyester, and their blends*. *Journal of Applied Polymer Science*, 1988. **36**(6): p. 1325-1342.
63. Prime, R.B., *Thermal Characterization of Polymeric Materials*. 1981: Academic Press.
64. Karkanis, P.I. and I.K. Partridge, *Cure modeling and monitoring of epoxy/amine resin systems. I. Cure kinetics modeling*. *Journal of Applied Polymer Science*, 2000. **77**(7): p. 1419-1431.
65. Bandara, U., *A systematic solution to the problem of sample background correction in DSC curves*. *Journal of thermal analysis and calorimetry*, 1986. **31**(5): p. 1063-1071.
66. Nesbitt, A., et al., *Development of a microwave calorimeter for simultaneous thermal analysis, infrared spectroscopy and dielectric measurements*. *Measurement Science and Technology*, 2004. **15**: p. 2313.
67. Cross, A.D., *Introduction to Practical Infra-Red Spectroscopy*. Second Edition ed.
68. Hsu, C.P., *Infrared spectroscopy*. *Handbook of Instrumental Techniques for Analytical Chemistry*, 1997: p. 247–83.
69. Young, R.J. and P.A. Lovell, *Introduction to polymers*. 1991: CRC.
70. Silverstein, R.M., G. Clayton Bassler, and T.C. Morrill, *Spectrometric Identification Of Organic Compounds*. Fifth ed. 1991.
71. Campbell, D. and J.R. White, *Polymer Characterization: Physical Techniques*. Second Edition ed. 2001.
72. Skoog, D.A., F.J. Holler, and T.A. Nieman, *Principles of instrumental analysis*. 1985.
73. Koenig, J.L., *Spectroscopy of polymers*. 1999: Elsevier Science Ltd.
74. Schoolery, J.N., *A Basic Guide to NMR*. 1972: Varian Associates.
75. Sanders, J.K. and B.K. Hunter, *Modern NMR Spectroscopy*. 1987: Oxford University Press.
76. John, V.B., *Testing of Materials*. 1992: Macmillan.

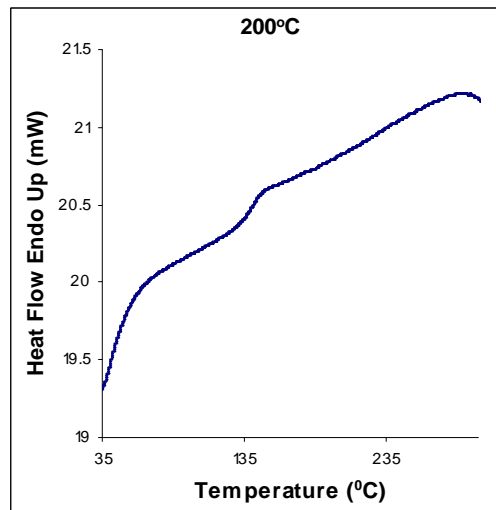
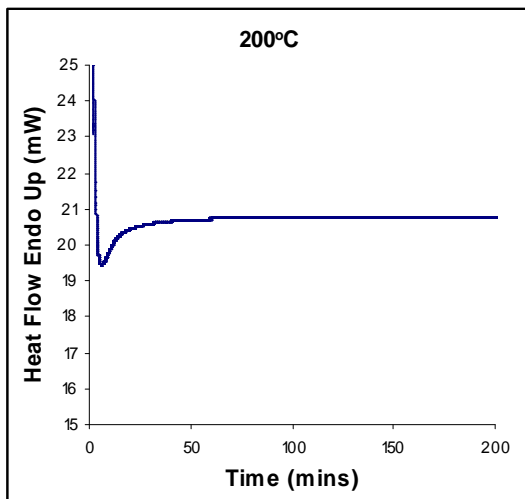
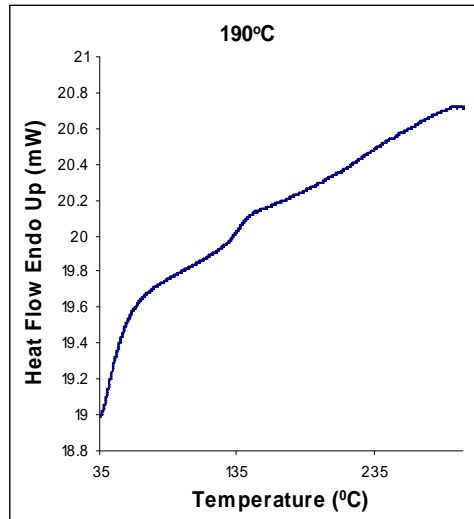
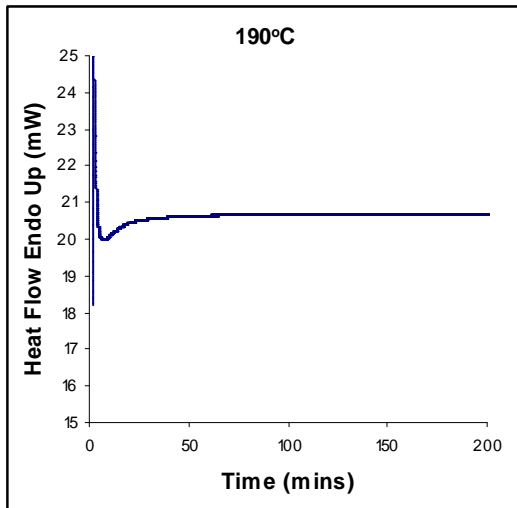
77. Lough, W.J. and I.W. Wainer, *High Performance Liquid Chromatography: Fundamental Principles and Practice*. 1995.
78. Wikipedia. [cited 2010 September]; Available from: http://en.wikipedia.org/wiki/High-performance_liquid_chromatography.
79. Provder, T., *Chromatography of Polymers: Characterization by Sec and Fff* 1993: Amer Chemical Society.
80. Montuado, G. and R.P. Lattimer, *Mass Spectrometry of Polymers*. 2002.
81. Garcia, F.G. and B.G. Soares, *Determination of the epoxide equivalent weight of epoxy resins based on diglycidyl ether of bisphenol A (DGEBA) by proton nuclear magnetic resonance*. Polymer testing, 2003. **22**(1): p. 51-56.
82. Garea, S.A., et al., *Determination of the epoxide equivalent weight (EEW) of epoxy resins with different chemical structure and functionality using GPC and ¹H-NMR*. Polymer testing, 2006. **25**(1): p. 107-113.
83. Dorsey, J.G., et al., *Determination of the epoxide equivalent weight of glycidyl ethers by proton magnetic resonance spectrometry*. Analytical Chemistry, 1977. **49**(8): p. 1144-1145.
84. Hunstman, *MSDS: Araldite LY 5052 / Aradur 5052*. 2007, Hunstman.
85. Carrozzino, S., et al., *Calorimetric and microwave dielectric monitoring of epoxy resin cure*. Polymer Engineering & Science, 1990. **30**(6): p. 366-373.
86. Thostenson, E.T. and T.W. Chou, *Microwave processing: fundamentals and applications*. Composites Part A: Applied Science and Manufacturing, 1999. **30**(9): p. 1055-1071.
87. Jacob, J., L.H.L. Chia, and F.Y.C. Boey, *Thermal and non-thermal interaction of microwave radiation with materials*. Journal of Materials Science, 1995. **30**(21): p. 5321-5327.
88. Eloundou, J.P., et al., *Modeling complex permittivity of an epoxy-amine system using simultaneous kinetic and microdielectric studies*. Macromolecular chemistry and physics, 2002. **203**(13): p. 1974-1982.
89. Jow, J., et al., *IEEE Transactions on Microwave Theory and Techniques*. MTT-35, 1987. **12**: p. 1435-1443.
90. Stutz, H., *Lifetime assessment of epoxies by the kinetics of thermal degradation*. Journal of Applied Polymer Science, 2004. **91**(3): p. 1881-1886.
91. Berglund, L. and J. Kenny, *Processing science for high performance thermoset composites*. Sampe Journal, 1991. **27**: p. 27-37.

92. Mertz, E. and J.L. Koenig, *Application of FTIR and NMR to epoxy resins*. Advances in polymer science, 1986. **74**: p. 75.
93. Allen, R.O. and P. Sanderson, *Characterization of Epoxy Glues with FTIR*. Applied Spectroscopy Reviews, 1988. **24**(3): p. 175-187.
94. Rozenberg, B., *Kinetics, thermodynamics and mechanism of reactions of epoxy oligomers with amines*. Epoxy resins and composites II, 1986: p. 113-165.
95. Oleinik, E.F., Advances in polymer science, 1986. **80**: p. 49.
96. Smith, R.E., F.N. Larsen, and C.L. Long, *Epoxy resin cure. II. FTIR analysis*. Journal of Applied Polymer Science, 1984. **29**(12): p. 3713-3726.
97. Cole, K.C., et al., *Comparison of infrared spectroscopic methods for the quantitative analysis of epoxy resins used in carbon-epoxy composite materials*. Applied Spectroscopy, 1988. **42**(5): p. 761-769.
98. Cañavate, J., et al., *Study of the curing process of an epoxy resin by FTIR spectroscopy*. Polymer-Plastics Technology and Engineering, 2000. **39**(5): p. 937-943.
99. Feazel, C.E. and E.A. Verchot, *A simple technique for use with infrared spectroscopy to study the curing of epoxy resins*. Journal of Polymer Science, 1957. **25**(110): p. 351-353.
100. Schiering, D.W., et al., *An infrared spectroscopic investigation of the curing reactions of the EPON 828/meta-phenylenediamine system*. Journal of Applied Polymer Science, 1987. **34**(7): p. 2367-2375.
101. Smith, B.C., *Fundamentals Of Fourier Transform Infrared Spectroscopy*. First ed. 1996.
102. Menczel, J.D. and R.B. Prime, *Thermal analysis of polymers: fundamentals and applications*. 2009: Wiley.
103. Cook, W.D. and O. Delatycki, *Relaxations in the transition region of crosslinked polyesters. II. The glass transition*. Journal of Polymer Science: Polymer Physics Edition, 1974. **12**(9): p. 1925-1937.
104. Nielsen, L.E. and R.F. Landel, *Mechanical properties of polymers and composites*. 1994: Marcel Dekker Inc.
105. Zhang, Y. and J. Cameron, *The Evaluation of the Flexural Strength of Cured Epoxy Resins from Heat Capacity Data*. International Journal of Polymeric Materials, 1992. **17**(1): p. 103-111.

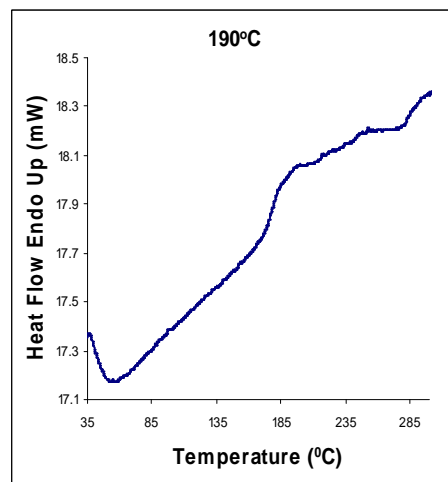
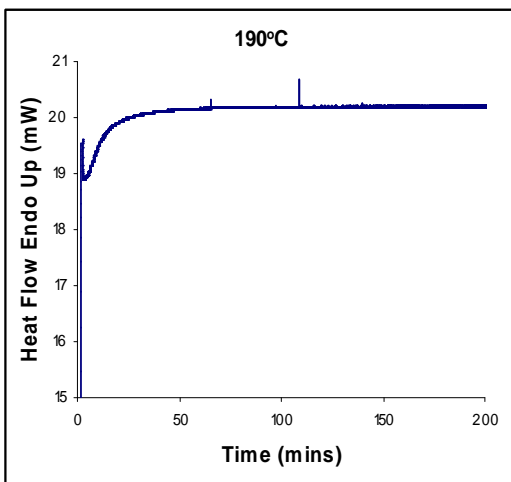
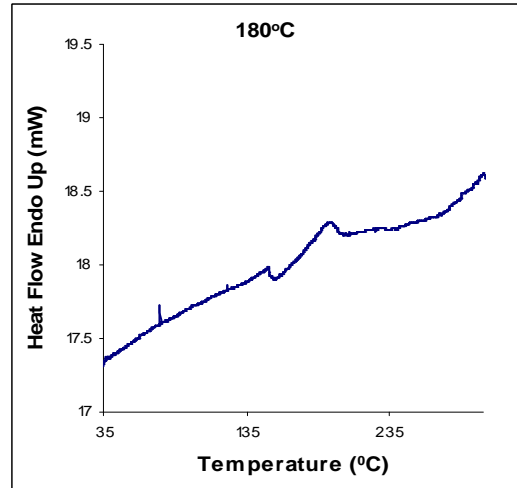
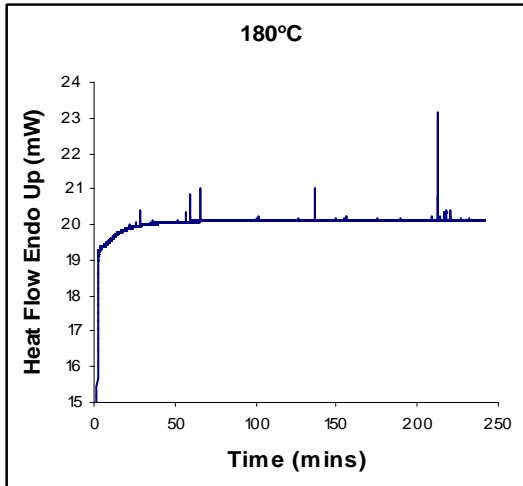
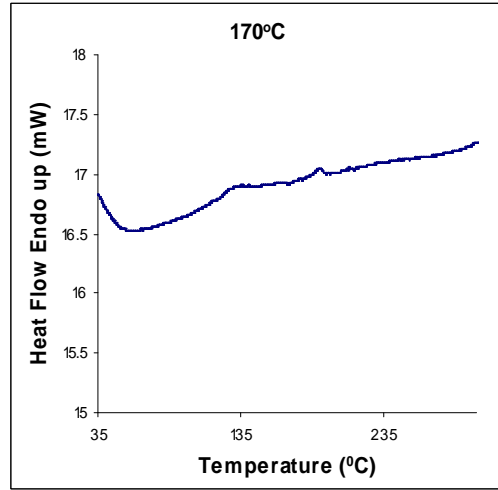
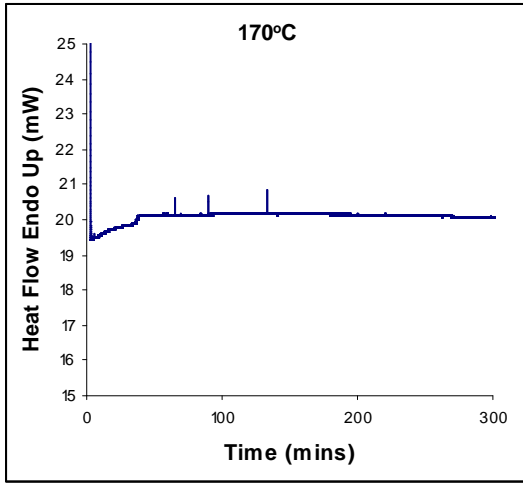
106. Singer, S.M., et al., *Polymeric Materials Science and Engineering*, 1989. **60**: p. 869-873.
107. Bai, S.L., et al., *European Polymer Journal*, 1995. **31**(9): p. 875-884.
108. Lin-Vien, D., et al., *The handbook of infrared and Raman characteristic frequencies of organic molecules*. 1991: Academic Press Boston.
109. Dyer, J.R., *Applications of Absorption Spectroscopy of Organic Compounds*. 1965.
110. Nakanishi, K. and P.H. Solomon, *Infrared Absorption Spectroscopy-Practical*. Second ed. 1977.
111. Stace, B.C. and K.G.J. Miller, *Laboratory Methods in Infrared Spectroscopy*. Second ed. 1972.
112. Paudler, W.W., *Nuclear Magnetic Resonance*. 1987.
113. Ault, A. and G.O. Dudek *NMR, An Introduction to Proton Nuclear Magnetic Resonance Spectrometry* 1976.
114. Bovey, F.A., *Nuclear Magnetic Resonance Spectroscopy*. Second Edition ed. 1988.
115. Atta-ur-Rahman, *Nuclear Magnetic Resonance*. 1986, New York: Springer-Verlag.
116. LeFevre, J.W. and S. Oswego, *Using Nuclear Magnetic Resonance Spectroscopy to Identify an Unknown Compound*.
117. Levy, G.C., R.L. Lichter, and G.L. Nelson, *Carbon-13 Nuclear Magnetic Resonance for Organic Chemists*. Second ed. 1980, New York: Wiley.
118. Breitmaier, E. and W. Voelter, *Carbon-13 NMR Spectroscopy*. Third ed. 1987, New York: VCH Publishers.
119. Wehrli, F.W., A.P. Marchand, and S. Wehrli, *Interpretation of Carbon-13 NMR Spectra*. Second ed. 1988.
120. Fuchs, P.L. and C.A. Bunnell, *Carbon-13 NMR-Based Organic Spectral Problems*. 1979, New York: Wiley.
121. Bates, R.B. and W.A. Beavers, *C-13 NMR Problems*. 1981: Humana Press.
122. Schraml, J. and J.M. Bellama, *Two-Dimensional NMR Spectrometry*. 1988.
123. Croasmum, W.R. and R.M.K. Carlson, *Two-Dimensional NMR Spectroscopy*. 1987, New York: VCH.
124. Freibolen, H., *Basic one and Two Dimensional Spectroscopy*: VCH.

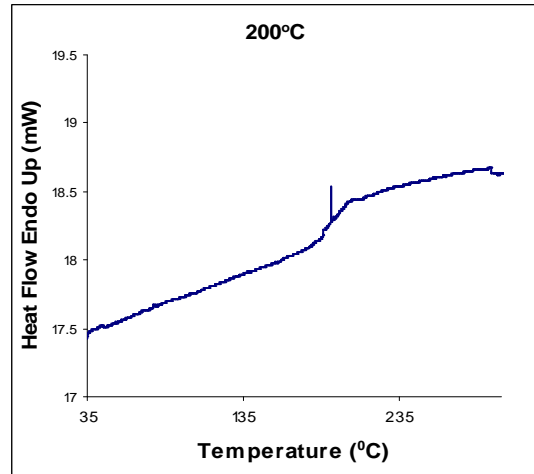
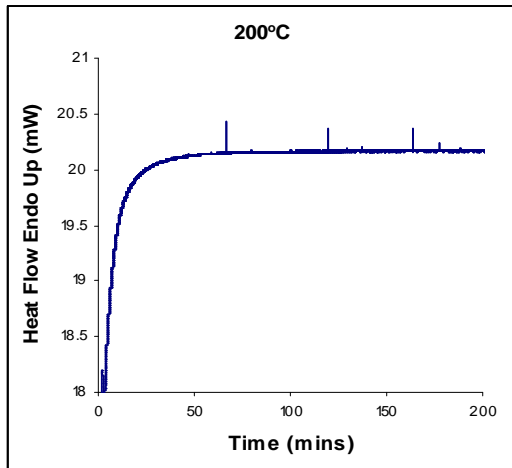
APPENDIX



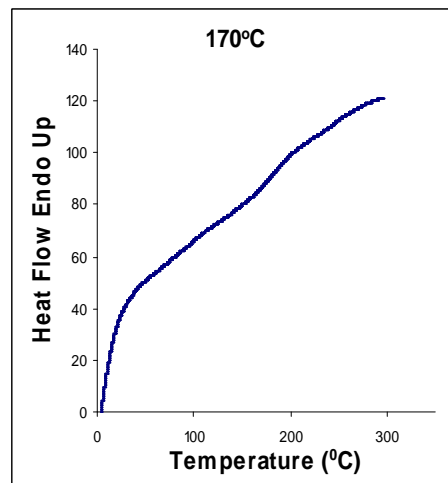
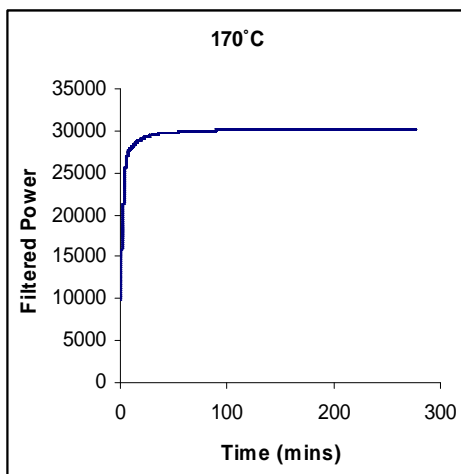


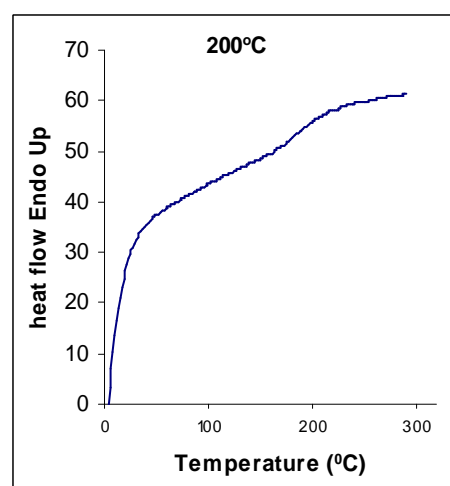
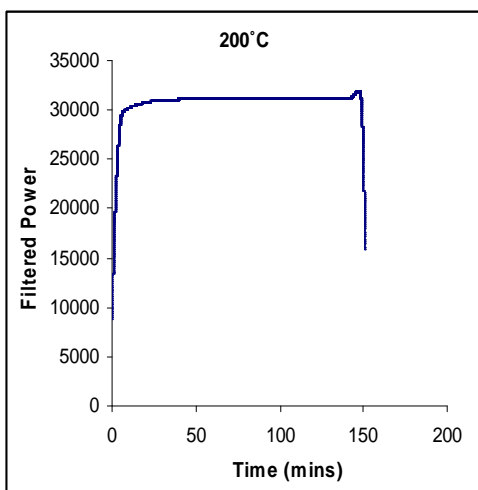
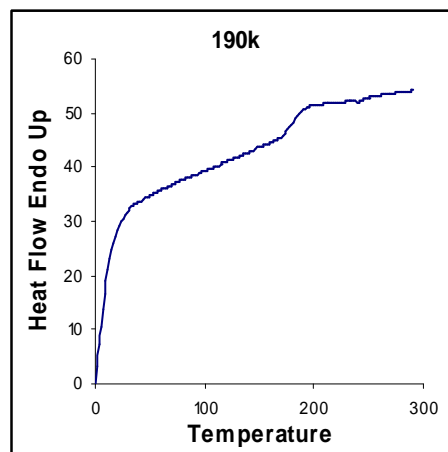
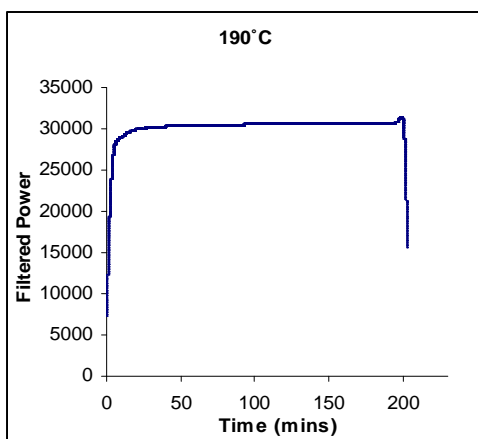
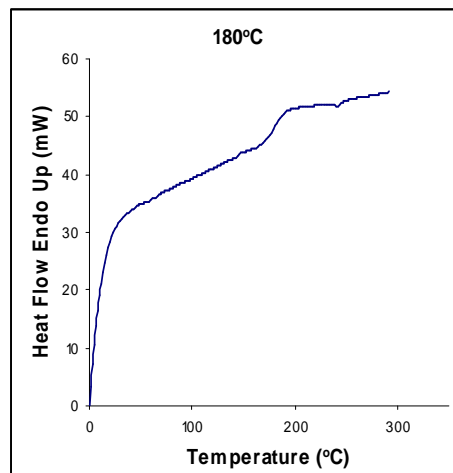
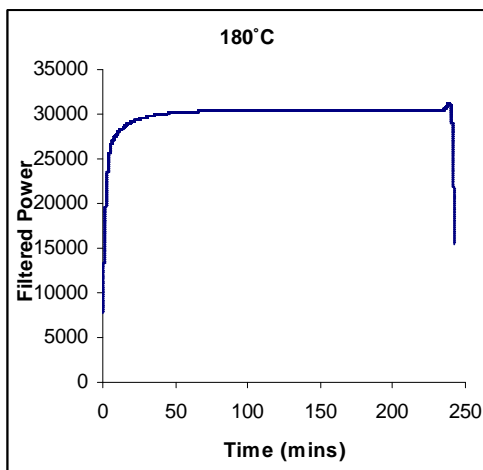
Appendix 1 Figure DSC thermograms of conventional isothermal cure (left) and subsequent DSC run to test for exotherm for 0.8M amine / epoxy ratio for Araldite DLS 772 / 4 4' DDS epoxy system



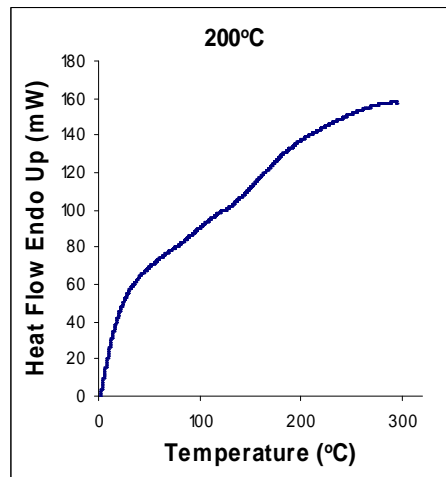
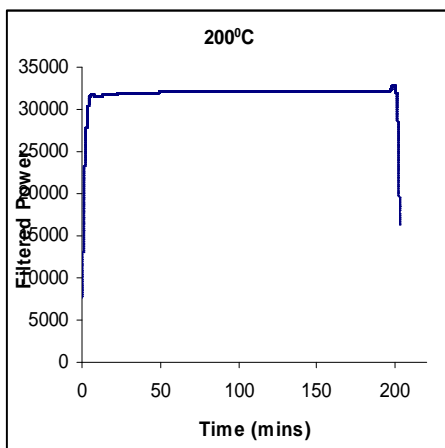
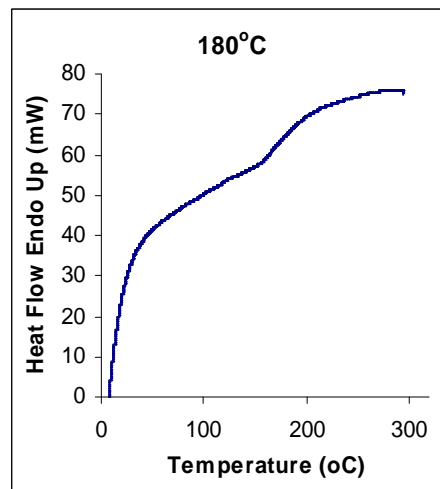
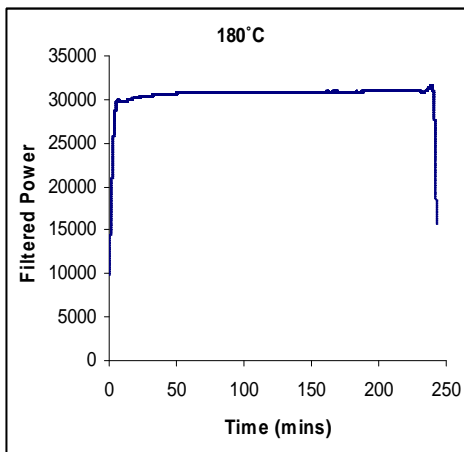
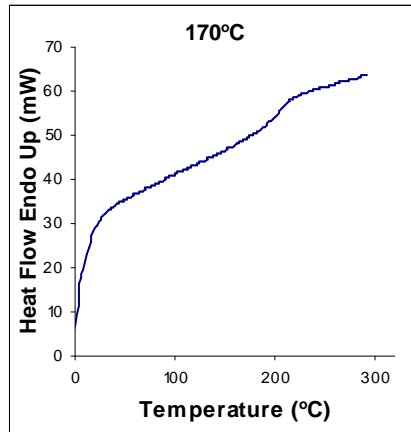
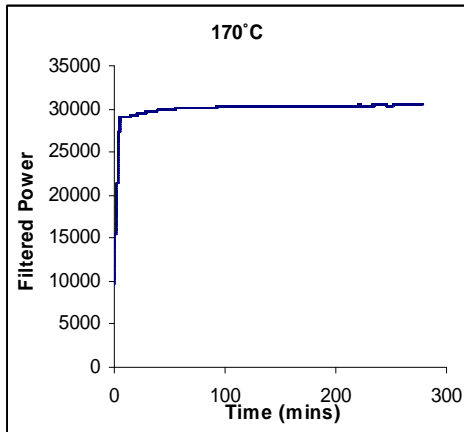


Appendix 2 DSC thermograms of conventional isothermal cure (left) and subsequent DSC run to test for exotherm for 1.1M amine / epoxy ratio for Araldite DLS 772 / 4 4' DDS epoxy system

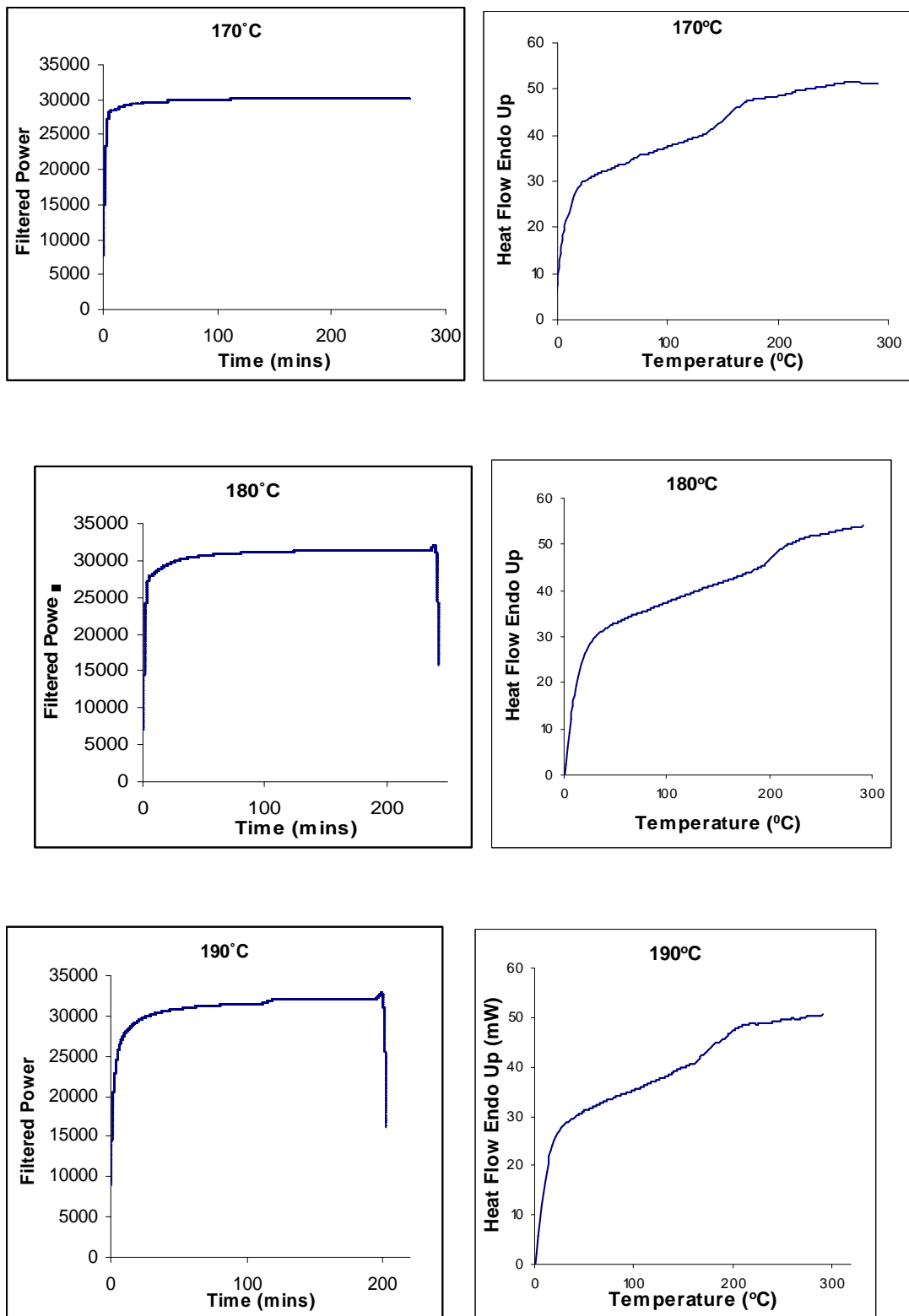




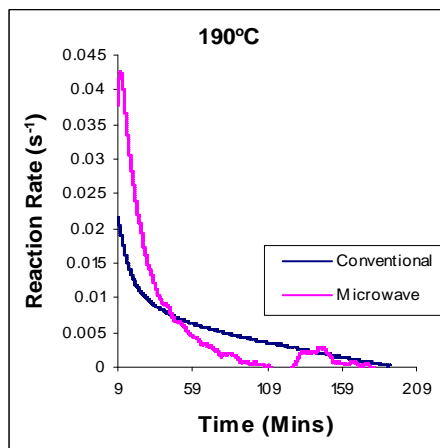
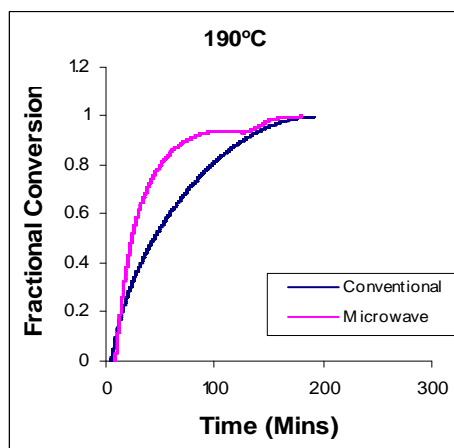
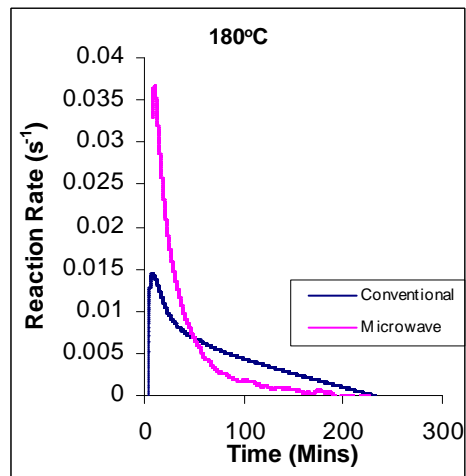
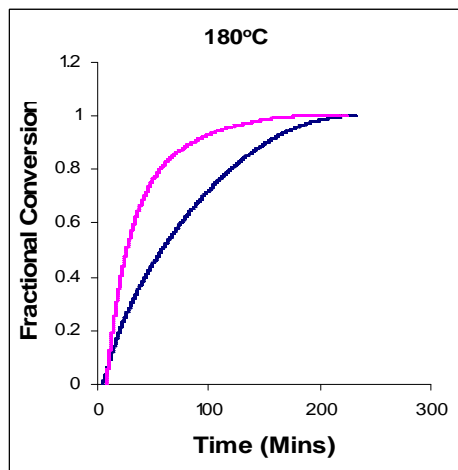
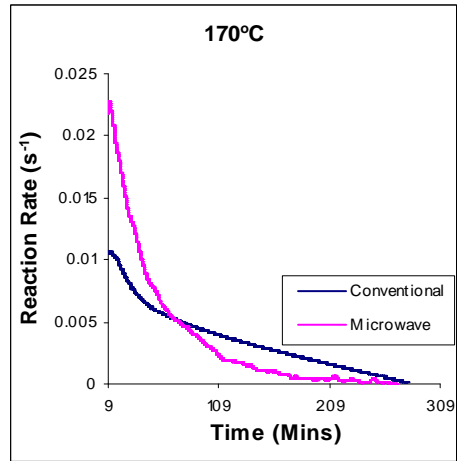
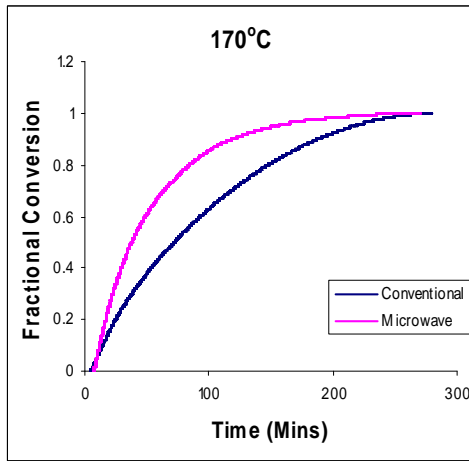
Appendix 3 Isothermal thermograms of microwave isothermal cure (left) and subsequent DSC run at 10 K min^{-1} from 30 to 300 °C (right) to test for exotherm Araldite LY 5052 / 4 4' DDS epoxy system with an amine / epoxy ratio of 1.0

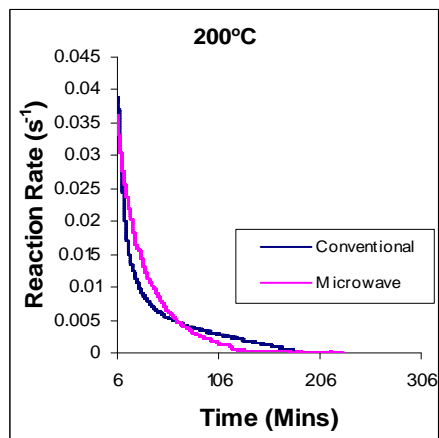
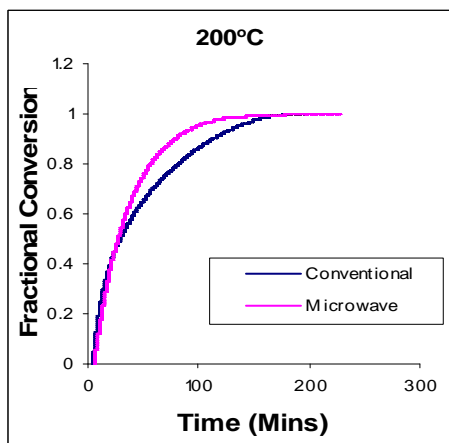


Appendix 3 DSC thermograms of conventional isothermal cure (left) and subsequent DSC run (right) to test for exotherm for Araldite DLS 772 / 4 4' DDS epoxy system with an amine / epoxy ratio of 0.8

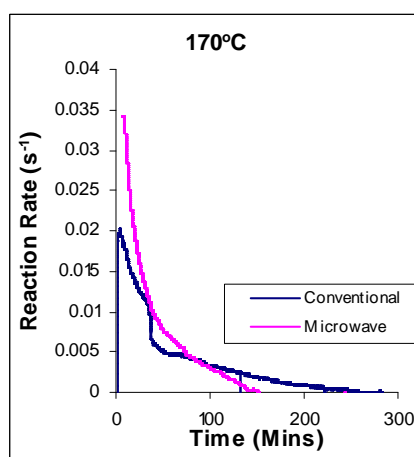
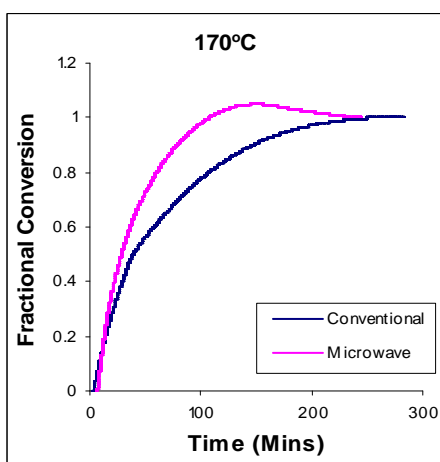


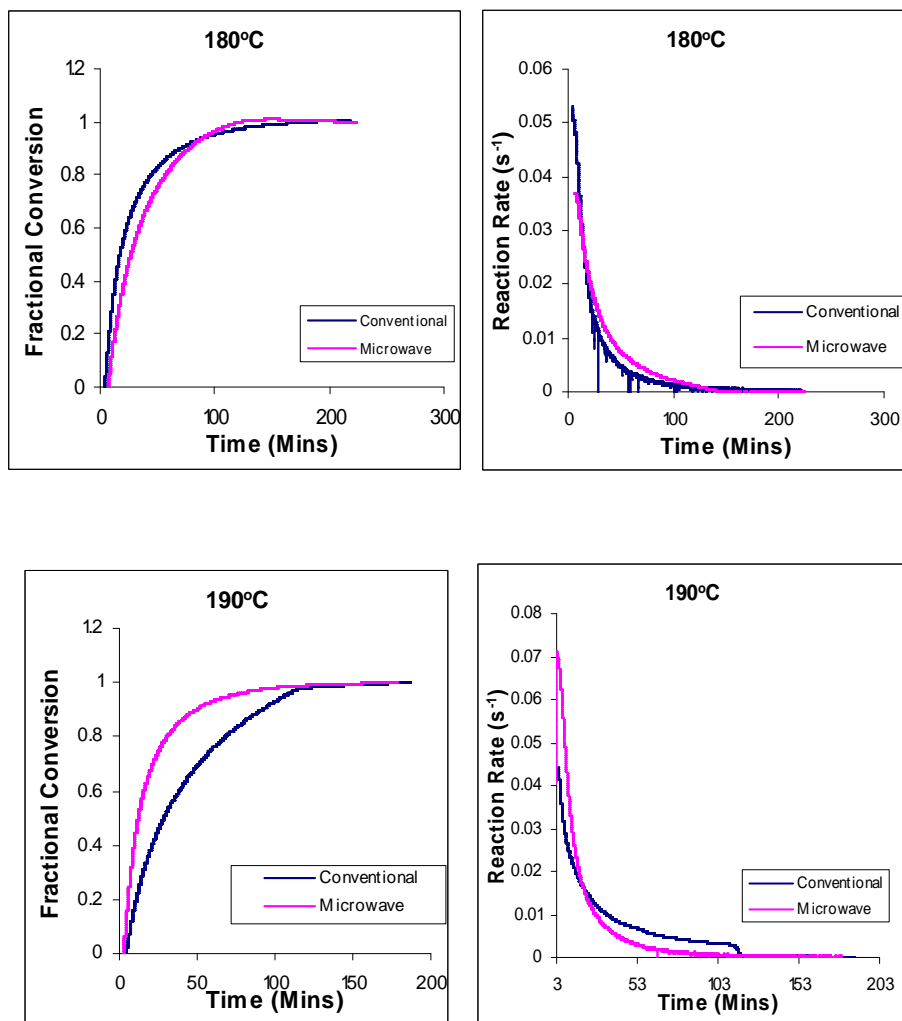
Appendix 4 DSC thermograms of isothermal cure (left) and subsequent DSC run (right) to test for exotherm for Araldite DLS 772 / 4 4' DDS epoxy system with an amine / epoxy ratio of 1.1



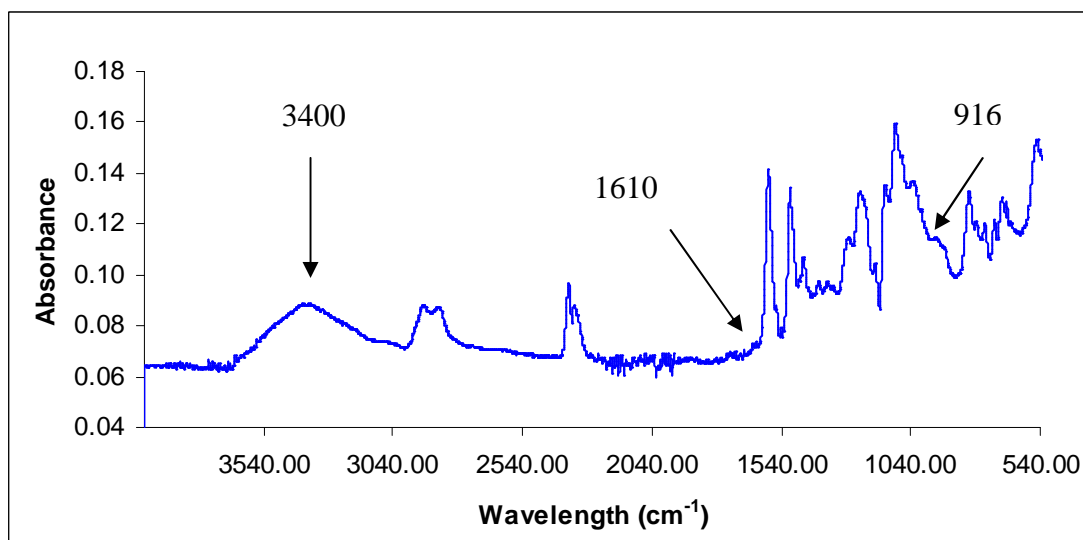


Appendix 5 Temperature dependence of the fractional conversion (left), and reaction rate (right) for the curing of Araldite DLS 772 / 4 4' DDS epoxy system with an amine / epoxy ratio of 0.8 under conventional and microwave curing, at different isothermal temperatures.

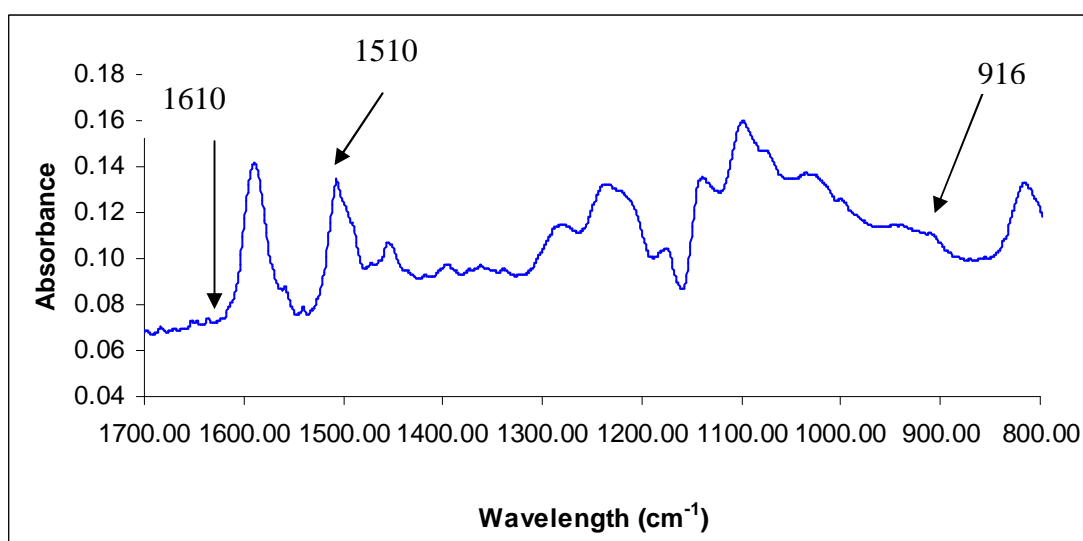




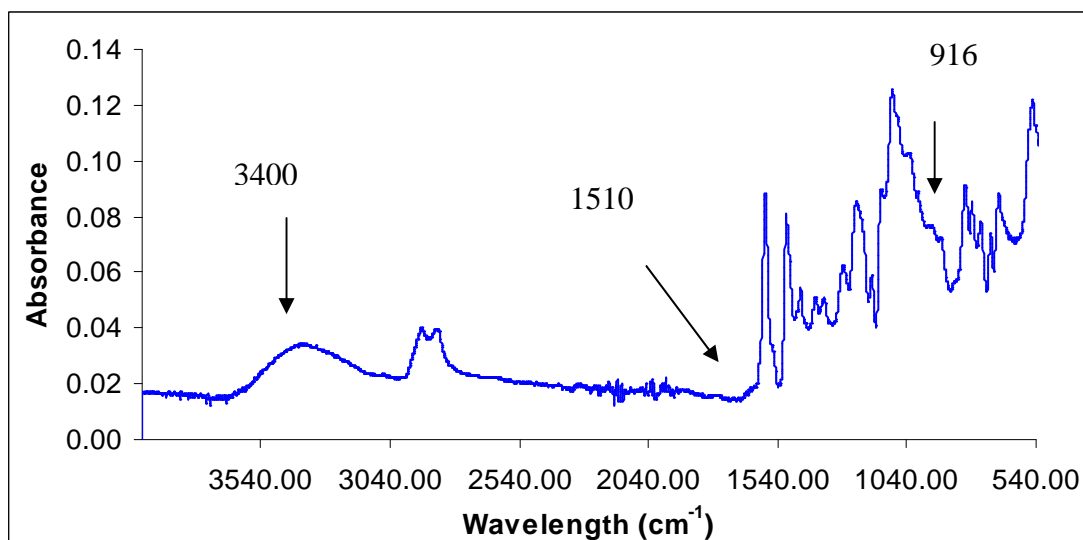
Appendix 6 Temperature dependence of the fractional conversion (left), and reaction rate (right) for the curing of Araldite DLS 772 / 4 4' DDS epoxy system with an amine / epoxy ratio of 1.1 under conventional and microwave curing, at different isothermal temperatures.



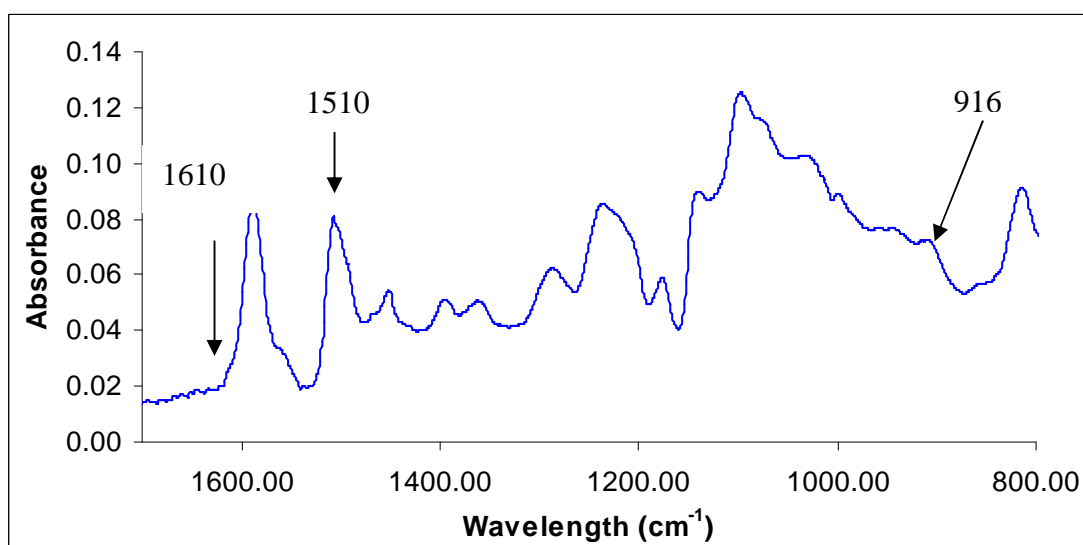
Appendix 7 FT-IR Spectra of Araldite LY 5052 / 4 4' DDS with an amine / epoxy ratio of 0.85M after conventional heating at 180°C for 240 minutes



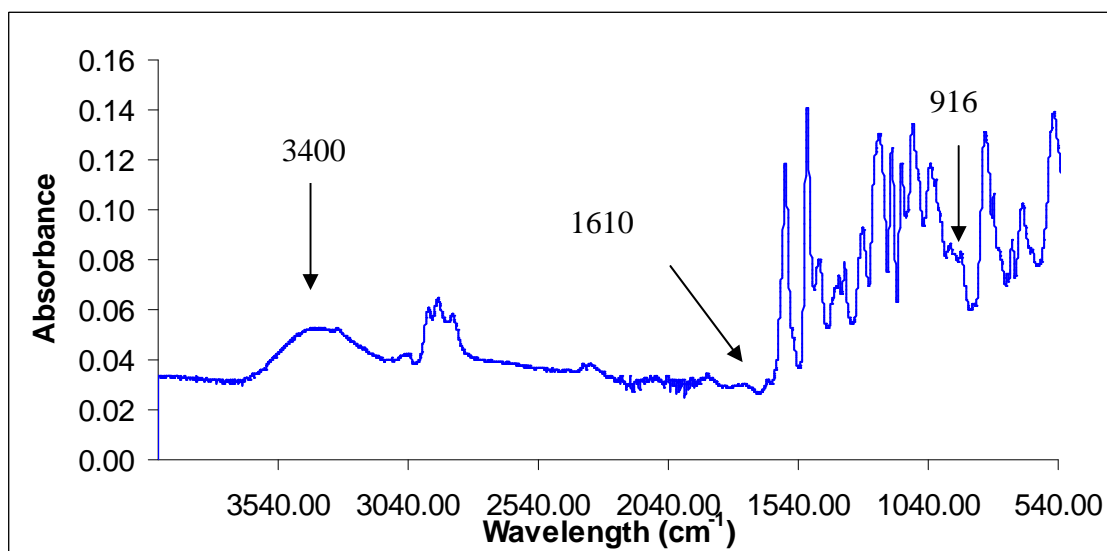
Appendix 8 Expanded view of FT-IR Spectra of Araldite LY 5052 / 4 4' DDS with an amine / epoxy ratio of 0.85M after conventional heating at 180°C for 240 minutes.



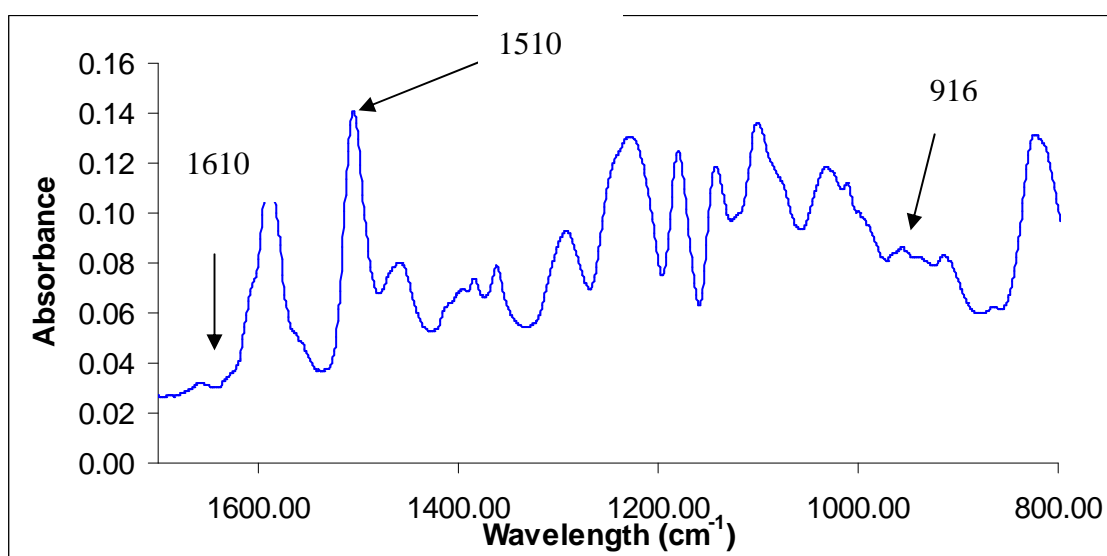
Appendix 9 FT-IR Spectra of Araldite LY 5052 / 4 4' DDS with an amine / epoxy ratio of 0.85M after microwave heating at 180°C for 240 minutes.



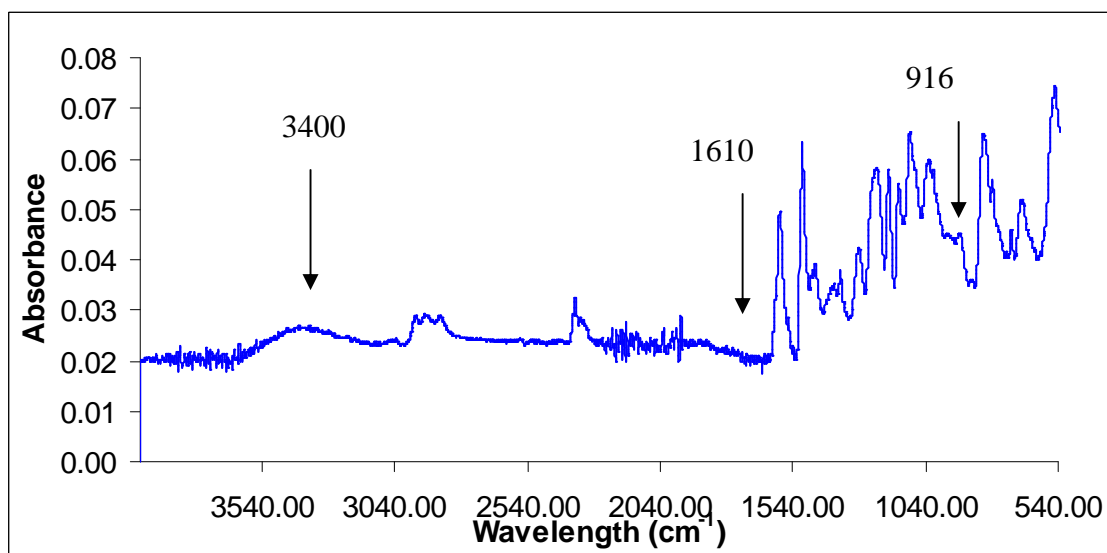
Appendix 10 Expanded view of FT-IR Spectra of Araldite LY 5052 / 4 4' DDS with an amine / epoxy ratio of 0.85M after microwave heating at 180°C for 240 minutes.



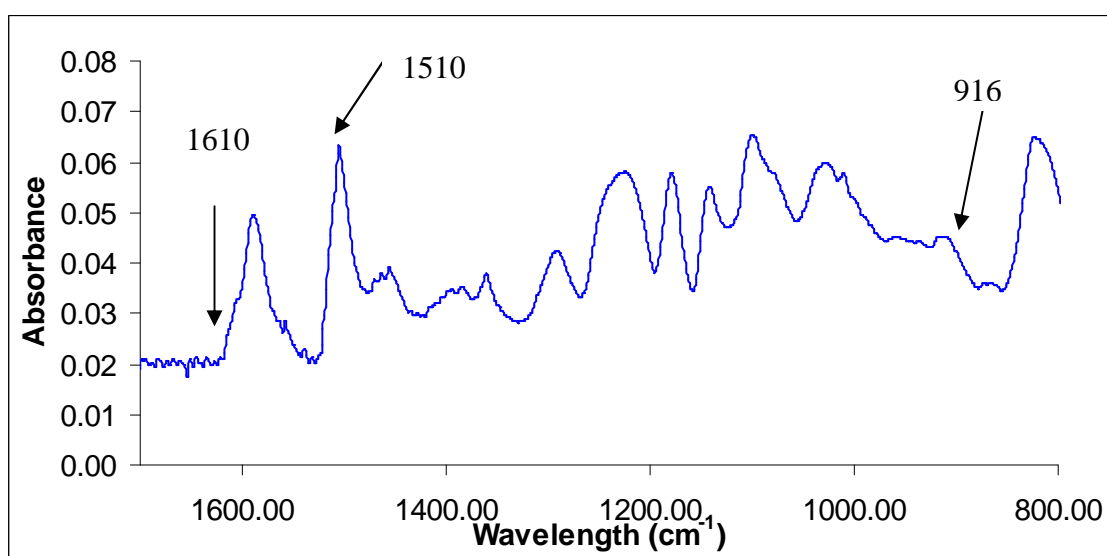
Appendix 11 FT-IR Spectra of Araldite DLS 772 / 4 4' DDS with an amine / epoxy ratio of 0.8 after conventional heating at 180°C for 240 mins



Appendix 12 Expanded view of FT-IR Spectra of Araldite DLS 772 / 4 4' DDS with an amine / epoxy ratio of 0.8 after conventional heating at 180°C for 240 minutes.



Appendix 13 FT-IR Spectra of Araldite DLS 772 / 4 4' DDS with an amine / epoxy ratio of 0.8 after microwave heating at 180°C for 240 minutes.



Appendix 14 Expanded view of FT-IR Spectra of Araldite DLS 772 / 4 4' DDS with an amine / epoxy ratio of 0.8 after microwave heating at 180°C for 240 minutes.